CUESTA & ASOCIADOS, ABOGADOS
Calle 72 # 10 – 07 Of. 603
Phone: 2113097 Fax: 2554538
Bogotá, D.C., Colombia
www.cuestalawyers.com
Respuesta Requerimiento
EXP: **NC2018/0013689**

Señora
Edna Marcela Ramírez Orozco
Directora de Nuevas Creaciones
Superintendencia de Industria y Comercio
E. S. D.

Referencia: Solicitud de PCT Patente de Invención denominada **Una Formulación Farmacéutica Líquida Estable, que Contiene un Anticuerpo o su Fragmento de Unión a Antígeno; un Tensioactivo; un Azúcar o su Derivado; y un Tampón que Comprende Acetato o Histidina.**

Asunto: Respuesta al Requerimiento No. 1031 del 29 de enero de 2021.

Expediente No. NC2018/0013689

Juan Carlos Cuesta Quintero, mayor de edad, identificado como aparece al pie de mí firma, obrando en mi calidad de apoderado de la sociedad **Celltrion Inc,** doy respuesta al Oficio No. 1031 del 29 de enero de 2021, en los siguientes términos:

1. **Título:**

De acuerdo a las objeciones expuestas acerca del título de la invención, solicitamos respetuosamente se tenga como título para la invención el siguiente:

Formulación Farmacéutica Líquida Estable, que Contiene un Anticuerpo o su Fragmento de Unión a Antígeno; un Tensioactivo; un Azúcar o su Derivado; y un Tampón que Comprende Acetato o Histidina

2. **Reivindicaciones:**

- Las nuevas reivindicaciones 1, 2 y 14 (antiguas reivindicaciones 1, 8 y 23, respectivamente) se han limitado al anticuerpo infliximab. Soporte para dicha modificación, puede encontrarse, por ejemplo, en las reivindicaciones originales 1 y 3.

- Adicionalmente, las nuevas reivindicaciones 1 y 15 (antiguas reivindicaciones 1 y 23, respectivamente) se han sido modificadas para limitar cada una de las características técnicas (componentes) que describe. En concreto, un anticuerpo o

su fragmento de unión a antígeno se ha limitado a un infliximab, tal y como se ha mencionado anteriormente.

El tensioactivo se ha limitado a una lista específica de compuestos: "éster de ácido graso de sorbitán polioxietilenado, éter alquílico de polioxietileno, éter alquilfenílico de polioxietileno, copolímeros de polioxietileno-polioxipropileno, dodecil sulfato sódico, o una mezcla de dos o más de ellos". Soporte para dicha modificación, puede encontrarse, por ejemplo, en la página 12, último párrafo y página 13 primer párrafo, de la solicitud originalmente presentada.

El azúcar o su derivado se ha limitado a comprender: "sorbitol, manitol, trehalosa, sacarosa, o una mezcla de dos o más de ellos". Soporte para dicha modificación, puede encontrarse, por ejemplo, en la reivindicación 14 original, así como en la página 13, tercer párrafo de la solicitud originalmente presentada.

- Las antiguas reivindicaciones 2 a 7, 13 a 14, y 22 se han eliminado. El resto de reivindicaciones se han renumerado y las dependencias se han adaptado en consonancia con las modificaciones aquí mencionadas.

- El Examinador indica que la reivindicación 1 no es concisa cuando menciona: *"(…) un anticuerpo o su fragmento de unión a antígeno (…) un tensioactivo (…) un azúcar o su derivado (…)"*, ya que con estos términos tan generales se podrían presentar múltiples opciones de diferentes composiciones que no encuentran sustento en el capítulo descriptivo. Dicha objeción aplica también para las reivindicaciones originales 9 a 11, 13, 14, 20, 21 y 23. Se sugiere delimitar los términos ambiguos e imprecisos.

  Las nuevas reivindicaciones 1 y 14, respectivamente, se han modificado limitando cada una de los componentes/ingredientes que forman dicha formulación. Más concretamente, la formulación farmacéutica líquida estable de la presente invención comprende ahora:

(A) Infliximab, como único anticuerpo;
(B) un tensioactivo que comprende éster de ácido graso de sorbitán polioxietilenado, éter alquílico de polioxietileno, éter alquilfenílico de polioxietileno, copolímeros de polioxietileno-polioxipropileno, dodecil sulfato sódico, o una mezcla de dos o más de ellos;
(C) un azúcar o su derivado; en donde el azúcar o su derivado (C) comprende sorbitol, manitol, trehalosa, sacarosa o una mezcla de dos o más de ellos, y
(D) un tampón que comprende acetato o histidina.

Por lo tanto, todas estas limitaciones hacen que las nuevas reivindicaciones 1 y 14 sean claras y precisas y definan claramente la formulación descrita en la invención por sus elementos concretos. Es más, incluso en la nueva reivindicación 14 se mencionan los rangos de concentraciones en las que se encuentran cada uno de los ingredientes de la formulación en la mezcla.

El Solicitante desea poner en conocimiento del Examinador que las correspondientes patentes hermanas en Korea (**KR10-2229274 B1**) y Australia (**AU2017287743 B2**) han sido **concedidas** con un conjunto de reivindicaciones que presentan un **alcance de protección similar** (KR) **e incluso mayor** (AU) al alcance de protección incluido en el nuevo conjunto de reivindicaciones modificadas que acompaña al presente escrito. La traducción al español de la reivindicación 1 concedida en la patente KR10-2229274 B1 es la siguiente:

1. Una formulación farmacéutica líquida estable, que contiene
(A) un infliximab;
(B) un tensioactivo que comprende éster de ácido graso de sorbitán polioxietilenado, éter alquilíco de polioxietileno, éter alquilfenílico de polioxietileno, copolímeros de polioxietileno-polioxipropileno, dodecil sulfato sódico o una mezcla de dos o más de ellos;
(C) un azúcar o su derivado, donde el azúcar o su derivado (C) comprende sorbitol, manitol, trehalosa, sacarosa o una mezcla de dos o más de ellos; y
(D) un tampón que comprende acetato o histidina.

Como puede observar el Examinador, la reivindicación 1 de la patente KR concedida presenta un alcance de protección idéntico al de la nueva reivindicación 1 modificada, por lo tanto, dicha reivindicación es clara y está soportada por la descripción originalmente presentada.

Por otro lado, la correspondiente reivindicación 1 concedida para la patente AU, describe incluso un alcance de protección más amplio que la presente reivindicación 1 modificada. Dicha reivindicación 1 australiana fue también por tanto considerada clara y soportada en la descripción ya que dicha patente está concedida. La traducción al español de la reivindicación 1 australiana concedida es la siguiente:

1. Una formulación farmacéutica líquida estable, que contiene
(A) un infliximab;
(B) un tensioactivo;
(C) uno o más azúcares y/o derivados del azúcar seleccionados del grupo que consiste en sorbitol, manitol, sacarosa y trehalosa; y
(D) un tampón que comprende acetato o histidina.

Así teniendo en cuenta que las patentes hermanas en KR y AU se han concedido con un alcance idéntico o incluso mayor al que presenta ahora el nuevo conjunto de reivindicaciones modificadas que acompaña al presente escrito, el Solicitante respetuosamente afirma que esta objeción ha quedado solventada.

- El Examinador indica que la reivindicación 22 no es clara cuando menciona: "*que tiene una viscosidad de 0,5 cp a 10 cp después de 1 mes de almacenamiento a 40 ºC ± 2 ºC, o una viscosidad de 0,5 cp a 5 cp después de 6 meses de almacenamiento a 5 ºC ± 3 °C.*", al considerarse un resultado a alcanzar y por tanto se sugiere eliminarla del pliego reivindicatorio.

  La reivindicación 22 e ha eliminado del nuevo set de reivindicaciones adjunto. Por lo tanto, dicha objeción no aplica.

- El Examinador indica que las reivindicaciones 26 y 27 no son claras cuando reclaman: "*Una jeringa precargada llenada (…) y un auto-inyector que incluye en el mismo la jeringa precargada de la reivindicación 26*", que son dispositivos externos, alejados de la invención que es la formulación farmacéutica. Se sugiere eliminar cualquier reivindicación que se aleje del objeto de la invención.

  El Solicitante respetuosamente difiere de la conclusión del Examinador. Como se ha explicado en el apartado de Novedad y Actividad Inventiva que aparece más adelante en el presente documento, la formulación de la nueva reivindicación 1 es nueva e inventiva a la luz de los documentos del estado de la técnica citados. Teniendo en cuenta que las nuevas reivindicaciones 17 y 18 (reivindicaciones 26 y 27 originales) comprenden todas las características técnicas nuevas e inventivas de la nueva reivindicación 1, dichas reivindicaciones 17 y 18 están dentro del alcance de la presente invención al comprender dicha formulación y por lo tanto no se les puede considerar dispositivos externos alejados de la invención, ya que comprenden el núcleo de la invención, la formulación farmacéutica líquida estable.

  Por todas las razones expuestas, el Solicitante respetuosamente considera que las nuevas reivindicaciones 17 y 18 presentan claridad al comprender las características técnicas esenciales de la invención. En consecuencia, dicha objeción no aplica.

Teniendo en cuenta todo lo anterior, el Solicitante respetuosamente considera que no se añade materia al nuevo pliego de reivindicaciones enmendadas que acompaña al presente escrito.

3. **Listado de secuencias:**

El Examinador indica que dado que la presente solicitud se refiere a secuencias de aminoácidos, deben presentarse las listas en un documento independiente, bajo el título: "Listado de secuencias" de acuerdo con el estándar ST. 25.

El Solicitante adjunta el "Listado de Secuencias" cumpliendo con los requisitos exigidos en el Estándar ST.25.

4. **Unidad de Invención:**

El Examinador indica que el concepto común de la presente invención es la composición farmacéutica que comprende un anticuerpo o su fragmento de unión a antígeno y los excipientes que la componen. Dicho concepto común se encuentra divulgado en el estado de la técnica, específicamente en los documentos WO2015177057 (**D1**) y US2006018903 (**D2**). Por lo tanto, según el Examinador existen 2 grupos de invenciones en el set de reivindicaciones originalmente presentado:

- Grupo 1: Composición farmacéutica que comprende un anticuerpo o su fragmento de unión a antígeno, un tensioactivo, un azúcar o su derivado y un tampón (reivindicaciones originales 1 a 25 – nuevas reivindicaciones modificadas 1 a 16).

- Grupo 2: Una jeringa precargada llenada y un auto-inyector que incluye en el mismo la jeringa precargada de la reivindicación 26 (reivindicaciones originales 26 y 27 – nuevas reivindicaciones modificadas 17 y 18).

Como se ha explicado anteriormente, y se detalla en el apartado de novedad y actividad inventiva descrito a continuación, la reivindicación 1 modificada incluye ahora características técnicas nuevas e inventivas respecto de los documentos del estado de la técnica citados, particularmente los documentos, D1 y D2.

Teniendo en cuenta ahora que el **concepto común** de la presente invención es la nueva **reivindicación 1 modificada**:

1. Una formulación farmacéutica líquida estable, que contiene:
(A) infliximab;
(B) un tensioactivo que comprende éster de ácido graso de sorbitán polioxietilenado, éter alquílico de polioxietileno, éter alquilfenílico de polioxietileno, copolímeros de polioxietileno-polioxipropileno, dodecil sulfato sódico, o una mezcla de dos o más de ellos;
(C) un azúcar o su derivado; en donde el azúcar o su derivado (C) comprende sorbitol, manitol, trehalosa, sacarosa o una mezcla de dos o más de ellos, y
(D) un tampón que comprende acetato o histidina.

Y que dicho concepto común es nuevo e inventivo a la luz de **D1** y **D2** (ver a continuación), está claro en el nuevo set de reivindicaciones modificadas que las nuevas reivindicaciones 1, 17 y 18 comparten dicho concepto inventivo común, que es la composición descrita arriba. Por lo tanto, las nuevas reivindicaciones 1 a 18, que acompañan al presente escrito, presentan unidad de invención.

5. Examen de Patentabilidad:

En primer lugar, el Solicitante desea insistir en el presente escrito y para conocimiento del Examinador, que tanto la Oficina de Patentes Coreana (**KR10-2229274 B1**), como la Oficina de Patentes Australiana(**AU2017287743 B2**) han concedido las respectivas solicitudes hermanas en dichos países, con un alcance de protección similar al de las reivindicaciones presentadas aquí, para el caso de la patente coreana **KR10-2229274 B1,** mientras que en el caso de la patente australiana, el alcance de protección dela reivindicación 1 es incluso mucho más amplio que el presentado por las presentes reivindicaciones modificadas (ver apartado 1 del epígrafe Reivindicaciones).

Por tanto, tal y como hemos mencionado anteriormente, tanto la Oficina de Patentes Coreana, como la australiana han considerado que las nuevas reivindicaciones presentadas junto con el presente escrito, presentan novedad y actividad inventiva a la luz del estado del mismo estado de la técnica, **D1** y **D2**, por lo que respetuosamente consideramos que dichas reivindicaciones también presentan novedad y actividad inventiva en Colombia, a la luz del mismo estado de la técnica citado, **D1** y **D2**.

El Examinador ha objetado la novedad y actividad inventiva de la presente solicitud en vista de los documentos **D1 (**WO 2015-177057 A1) y **D2 (**US 2006018903).

El Solicitante respetuosamente difiere de la opinión del Examinador, y considera que a la luz de la información descrita en cualquiera de las referencias identificadas como **D1** ya **D2**, un experto en la materia no podría predecir el efecto técnico demostrado en la presente invención, con el nuevo pliego de reivindicaciones que acompaña al presente escrito.

Se indican a continuación los argumentos a favor de la novedad y actividad inventiva del nuevo pliego de reivindicaciones adjunto.

Tal y como se ha mencionado anteriormente, la nueva reivindicación 1 va dirigida a:

> *1. Una formulación farmacéutica líquida estable, que contiene:*
> *(A) infliximab;*
> *(B) un tensioactivo que comprende éster de ácido graso de sorbitán polioxietilenado, éter alquílico de polioxietileno, éter alquilfenílico de*

polioxietileno, copolímeros de polioxietileno-polioxipropileno, dodecil sulfato sódico, o una mezcla de dos o más de ellos;

(C) un azúcar o su derivado; en donde el azúcar o su derivado (C) comprende sorbitol, manitol, trehalosa, sacarosa o una mezcla de dos o más de ellos, y

(D) un tampón que comprende acetato o histidina.

Independientemente de la concentración de infliximab en la formulación – ya sea alta o baja – la formulación farmacéutica líquida de la invención, se caracteriza porque tiene baja viscosidad; una estabilidad durante el almacenamiento a largo plazo ejemplar debido a su excelente estabilidad en condiciones aceleradas y severas; y además puede administrarse por vía subcutánea.

D1 se refiere a una formulación líquida que contiene el anticuerpo adalimumab. Específicamente, **D1** divulga una formulación farmacéutica líquida que comprende adalimumab o un biosimilar del mismo, un agente/sistema tampón de acetato y un azúcar estabilizante.

D2 se refiere a una composición polipeptídica que se une al factor alfa de necrosis tumoral humano (TNF-α), y al método de preparación de la misma. **D2** divulga una secuencia de aminoácidos de infliximab, pero no divulga ninguna información sobre una formulación líquida capaz de estabilizar el infliximab.

En resumen, **D1 sólo divulga y ejemplifica específicamente una formulación que contiene *adalimumab*,** entre otros anticuerpos TNF-α, mientras que no revelan ni describen una formulación dirigida a otros anticuerpos que se unen al TNF-α. Es decir, y para concretar, **D1** divulga una **formulación líquida que comprende adalimumab**.

Adicionalmente, **D2 no divulga una formulación farmacéutica que comprenda infliximab**.

5.1. Las características técnicas (constitución) de la formulación farmacéutica líquida estable de la invención con el anticuerpo infliximab es completamente diferente de las formulaciones descritas en cualquiera de los documentos D1 a D2.

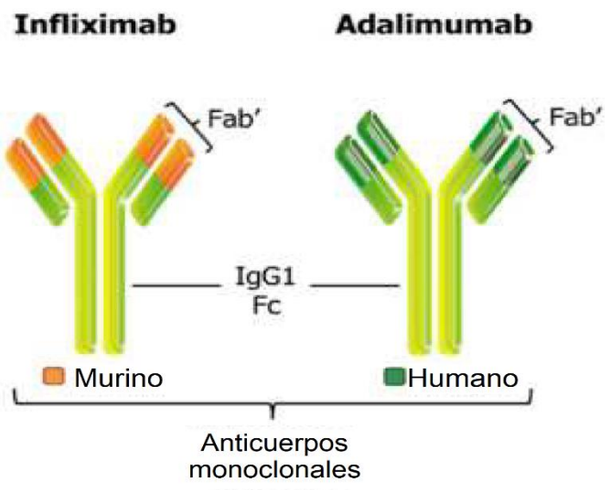
5.1.1. Diferencia en el anticuerpo.

El nuevo pliego de reivindicaciones de la presente solicitud de patente se ha limitado a una formulación líquida que contiene **infliximab**, entre otros ingredientes. Por el contrario, **D1** se refiere a una formulación que comprende **adalimumab**.

Aunque tanto infliximab como adalimumab inhiben al TNF-α, éstos son **anticuerpos esencial y completamente diferentes,** tanto en su estructura como en su secuencia.

La región Fab de un anticuerpo tiene una influencia importante en la estabilidad de las formulaciones. Se requieren condiciones específicas y únicas para obtener estabilidad dependiendo del origen de la región Fab. En particular, el infliximab de la nueva reivindicación 1 modificada tiene la región Fab de **origen murino**, mientras que el adalimumab descrito en **D1** tiene la región Fab de **origen humano**. Por consiguiente, las regiones Fab de estos dos anticuerpos tienen **orígenes diferentes** (ver Figura 1, a continuación).

[Figura 1] Diferentes orígenes de las regiones Fab entre infliximab y adalimumab.



Es decir, las formulaciones –consideradas adecuadas– pueden diferir por completo dependiendo de los anticuerpos.

Por tanto, **es imposible determinar si una formulación optimizada para un anticuerpo concreto también será adecuada para otros anticuerpos**. Una formulación adecuada para un determinado anticuerpo debe seleccionarse de manera individual y por separado teniendo en cuenta las características propias de cada anticuerpo.

Además, infliximab y adalimumab tienen **secuencias de aminoácidos en la región CDR completamente diferentes**. Específicamente, el Anexo 1 (Lee et al., Int. J. Mol. Sci. 2017, 18(1), 228), indica la diferencia en las secuencias de aminoácidos entre los anticuerpos infliximab y adalimumab tal y como se puede observar en la Figura 2, mostrada a continuación:

[Anexo 1. Figura 2]



(Comparación de las secuencias de aminoácidos entre infliximab y adalimumab)

Es decir, infliximab y adalimumab no solo tienen secuencias de aminoácidos completamente diferentes en la región Fab, sino también en la región CDR.

Por otro lado, como hemos mencionado anteriormente, **D2 no** divulga una formulación farmacéutica que comprenda **infliximab.**

Por lo tanto, la formulación de la nueva reivindicación 1 enmendada y las formulaciones descritas en **D1** comprende un tipo completamente diferente de anticuerpo.

5.2. Es difícil llegar a diseñar y concebir las características técnicas (constitución) de la formulación concreta de la presente invención a partir del estado de la técnica citado (D1 y D2).

5.2.1. La estabilidad de una formulación difiere dependiendo del tipo de anticuerpo y, por lo tanto, el estado de la técnica citado no permite tener expectativas razonables de éxito respecto a que la formulación reivindicada sea estable.

El solicitante ha llevado a cabo **experimentos adicionales para demostrar que la estabilidad de la formulación varía dependiendo del tipo de anticuerpo utilizado en la misma**.

Específicamente, se prepararon por separado dos formulaciones, una primera formulación que comprende adalimumab y una segunda formulación que comprende infliximab, basándose ambas en la formulación de la presente invención (acetato de sodio 10 mM, sorbitol al 5,0 %, polisorbato 80 al 0,1 % y 100 mg/ml de anticuerpo). Cada formulación se ensayó a 40℃ para verificar cualquier cambio en la estabilidad de la formulación

dependiendo del tipo de anticuerpo. Los resultados obtenidos se muestran en la Tabla 2, a continuación.

[Tabla 2] Prueba de estabilidad en las formulaciones que comprenden adalimumab o infliximab

Ensayo	Anticuerpo	0 semanas	2 semanas	4 semanas	Variación
IEC-HPLC (% de pico ácido)	Infliximab	19,60	27,20	33,90	14,30
	Adalimumab	12,51	23,77	32,48	28,83
IEC-HPLC (% del pico principal)	Infliximab	38,70	34,40	31,80	6,90
	Adalimumab	67,15	56,35	48,64	25,52
SEC-HPLC (% de APM)	Infliximab	1,09	1,04	1,04	-0,05
	Adalimumab	0,29	0,45	0,64	0,53
SEC-HPLC (% del pico principal)	Infliximab	98,91	98,54	98,14	0,77
	Adalimumab	99,67	96,33	95,80	4,30
SEC-HPLC (% de BPM)	Infliximab	0,00	0,43	0,82	0,82
	Adalimumab	0,04	3,23	3,56	3,77

* APM: alto peso molecular / PBM: bajo peso molecular

Como se muestra en la Tabla 2 anterior, el aumento en el porcentaje del pico ácido y la reducción en el porcentaje del pico principal fueron más pronunciadas en la formulación de adalimumab de acuerdo con los resultados de la IEC-HPLC. Además, el aumento en el porcentaje de APM y el aumento en el porcentaje de BPM fueron más pronunciados en la formulación de adalimumab de acuerdo con los resultados de la SEC-HPLC. La reducción en el porcentaje del pico principal también fue más pronunciada en la formulación de adalimumab.

Por consiguiente, los **resultados mostrados en la Tabla 2 anterior demuestran claramente que las formulaciones que tienen la misma composición pueden tener propiedades completamente diferentes dependiendo del tipo de anticuerpo que comprendan**. En particular, la formulación de la presente invención mostró propiedades superiores cuando contenía infliximab en lugar de adalimumab.

Dichos resultados experimentales respaldan aún más el argumento de que las referencias citadas no permiten tener una expectativa razonable de que una formulación que comprenden infliximab será estable sin llevar a cabo, previamente, una ardua verificación experimental.

5.2.2. Es difícil preparar una formulación optimizada para un anticuerpo

El Examinador indica en la acción oficial que la combinación específica de componentes de la formulación reivindicada puede concebirse fácilmente debido a que el estado de la técnica citado ya describe formulaciones similares con características técnicas similares (constitución técnica similar).

Sin embargo, cabe destacar que, una **formulación de anticuerpos optimizada y estable con características técnicas específicas, solo puede llevarse a cabo después de numerosos y repetidos ensayos y errores**. En este sentido, aunque el estado de la técnica citado describe formulaciones similares con una constitución técnica similar y un alcance similar, la formulación de la nueva reivindicación 1 no puede concebirse fácilmente, por las razones que se exponen a continuación.

Específicamente, el Anexo 2 (Wang et al., International Journal of Pharmaceutics 185 (1999) 129–188), valida el enfoque actual de los expertos en la materia en el campo técnico de la formulación de proteínas y respalda el argumento de que para una patente de invención relativa a una formulación de proteínas que comprende un anticuerpo u otras proteínas, es difícil predecir qué tipo de efecto puede tener.

[Anexo 2, p.175, columna de la izquierda]

Although significant progress has been made in recent years, there is still no single pathway to follow in formulating proteins due to their structural diversities and complexities. There are several stages that require careful consideration and extensive experimentation in formulating a stable protein product. First, the route of drug adminis-

Y la traducción al castellano de dicho párrafo es:

Aunque en los últimos años se han hecho progresos significativos, todavía no existe un único camino a seguir en la formulación de proteínas debido a su diversidad y complejidad estructural. Hay varias etapas que requieren un examen cuidadoso y una amplia experimentación en la formulación de un producto proteínico estable.

En el Anexo 2 se indica que diversos excipientes, tales como azúcar, poliol, aminoácido, amina, sal, polímero y agente tensioactivo, pueden utilizarse como estabilizadores para las formulaciones líquidas de proteínas. También describe que **el nivel de estabilización varía considerablemente en función de las proteínas**.

[Anexo 2, p. 165, Tabla 4]

Table 4
Examples of protein stabilization by excipients in liquid state

Proteins	Formulation compositions	Study conditions	Remaining activity (or as stated)	References
Baker's yeast ADH	50 μg/ml in 20 mM potassium phosphate, pH 7.6	50°C for 10 min	50%	Ramos et al., 1997
	Control + 500 mM KCl	50°C for 10 min	~90%	Ramos et al., 1997
	Control + 500 mM trehalose	50°C for 10 min	~70%	Ramos et al., 1997
	Control + 500 mM mannosylglycerate	50°C for 10 min	~90%	Ramos et al., 1997
GDH	50 μg/ml in 20 mM potassium phosphate, pH 7.5	50°C for 10 min	0%	Ramos et al., 1997
	Control + 500mM KCl	50°C for 10 min	~90%	Ramos et al., 1997
	Control + 500 mM trehalose	50°C for 10 min	~2%	Ramos et al., 1997
	Control + 500 mM mannosylglycerate	50°C for 10 min	~90%	Ramos et al., 1997
Rabbit muscle LDH	50 μg/ml in 20 mM potassium phosphate, pH 7.6	50°C for 10 min	5%	Ramos et al., 1997
	Control + 500 mM KCl	50°C for 10 min	~20%	Ramos et al., 1997
	Control + 500 mM trehalose	50°C for 10 min	~25%	Ramos et al., 1997
	Control + 500 mM mannosylglycerate	50°C for 10 min	~90%	Ramos et al., 1997

Específicamente, en términos de estabilización por trehalosa (azúcar estabilizador), la levadura de panadería ADH (alcohol deshidrogenasa) mantuvo el 70% de la actividad, la GDH (glutamato deshidrogenasa) mantuvo sólo el 2% de la actividad, y el músculo de conejo LDH (lactato deshidrogenasa) mantuvo el 25% de la actividad con la misma concentración de trehalosa bajo las mismas condiciones.

En consecuencia, se ha demostrado que **el nivel de estabilización varía significativamente según el tipo de proteína, incluso si se utiliza el mismo estabilizante**.

Además, dicho hallazgo también se ha confirmado consistentemente por un documento más reciente publicado en 2015 (Anexo 3, Challener, "Excipient Selection for Protein Stabilization" Pharmaceutical Technology APIS, EXCIPIENTS, & MANUFACTURING 2015, s35-s39). Por lo tanto, a la vista de dicha información, **es ampliamente aceptado y compartido por los expertos en la materia que el nivel de estabilización (efecto) difiere dependiendo del tipo de proteína (anticuerpo) utilizada**.

[Anexo 3, p. s38, columna de la izquierda]

Because every protein is different and reacts differently with different types of excipients, the selection of the proper excipients for a given formulation is a complex and challenging task. Some excipients may be effective in one formulation and cause protein degradation and aggregation in another.

(omitido)

The choice of the right excipients for stabilization of a desired protein must take into account the very complex physical and chemical degradation behaviors and the potential multifunctional influences that each excipient can have on protein stability, according to Kemter. "The formulation scientist must have

(omitido)

Unfortunately, the structural differences among different proteins are so significant that generalization of universal stabilization strategies has not been successful to date. In addition,

Y la traducción al castellano de dichos párrafos es:

Debido a que cada proteína es diferente y reacciona de manera distinta con diferentes tipos de excipientes, la selección de los excipientes adecuados para una determinada formulación es una tarea compleja y difícil. Algunos excipientes pueden ser eficaces en una formulación y causar degradación y agregación de proteínas en otra.

(omitido)

La elección de los excipientes adecuados para la estabilización de una proteína deseada, debe tener en cuenta los comportamientos complejos de degradación física y química, así como las posibles influencias multifuncionales que cada excipiente puede tener en la estabilidad de la proteína, según Kemter.

(omitido)

Lamentablemente, las diferencias estructurales entre las diferentes proteínas son tan importantes que la generalización de las estrategias de estabilización universal no ha tenido éxito hasta la fecha.

En este sentido, el experto en la materia que intente preparar una composición para estabilizar una formulación que comprenda una proteína (anticuerpo) concreta, puede tener dificultad para predecir qué estabilizante o qué combinación de estabilizantes, entre los diversos estabilizantes de proteínas conocidos para para su uso en formulaciones que comprenden anticuerpos u otras proteínas, pueden en última instancia, ser eficaces para la estabilización.

En resumen, **es sabido entre los expertos en la materia que no es fácil estabilizar proteínas y que no hay una sola vía o método para hacerlo**. Por consiguiente, el argumento de que la formulación de proteína estable reivindicada que comprende infliximab puede predecirse en vista de **D1 y D2**, donde dichos documentos divulgan un anticuerpo completamente diferente al anticuerpo de la invención, dalimumab, no se alinea con la perspectiva general compartida por los expertos en el presente campo técnico.

El Anexo 4 (US2009-0208492), divulga que el comportamiento y la eficacia de los anticuerpos en una formulación pueden diferir entre sí debido a características diferentes, tales como el pI y la solubilidad.

[Anexo 4, párrafo [0004]]

[0004] Antibodies, including monoclonal antibodies, all differ from one another in ways relevant to their behavior and efficacy in a formulation. For example, monoclonal antibodies differ from one another with regard to isoelectric points, solubility, and conditions at which the monoclonal antibodies will aggregate. Proteins differ from one another with regard to their behavior and efficacy in a formulation, making it difficult to predict if a formulation will be stable for a particular antibody. Three common problems in protein formulations include protein degradation, aggregation, deamidation, and oxidation. Further, many different reactions affecting formulation stability may occur simultaneously, making it difficult to determine which reaction is causing which result. See Cleland et al, "The Development of Stable Protein Formulations: A Close Look at Protein Aggregation, Deamidation, and Oxidation", *Critical Reviews in Therapeutic Drug Carrier Systems*, 10(4):307-377 (1993)).

Y la traducción al castellano de dichos párrafos es:

Los anticuerpos, incluidos los anticuerpos monoclonales, difieren entre sí en cuanto a su comportamiento y eficacia en una formulación. Por ejemplo, los anticuerpos monoclonales difieren entre sí en cuanto a los puntos isoeléctricos, la solubilidad y las condiciones en las que se agregan los anticuerpos monoclonales. Las proteínas difieren entre sí en cuanto a su comportamiento y eficacia en una formulación, lo que hace difícil predecir si una formulación será estable para un anticuerpo en particular. Tres problemas comunes en las formulaciones de proteínas son la degradación proteica, la agregación, deamidación y la oxidación de las proteínas. Además, pueden producirse simultáneamente muchas reacciones diferentes que afectan a la estabilidad de la formulación, lo que hace difícil determinar qué reacción está causando qué resultado. Véase Cleland y otros, "The Development of Stable Protein Formulations": A Close Look at Protein Aggregation, Deamidation, and Oxidation", Critical Reviews in Therapeutic Drug Carrier Systems, 10(4):307-377 (1993)].

Es decir, **es difícil preparar formulaciones debido a las diferentes características de los anticuerpos.**

Además, en el momento de determinar una formulación estable, debe llevarse a cabo una prueba específica para confirmar si es óptima o no y se tendrán que llevar a cabo numerosos ensayos y errores en el transcurso de este proceso. Además, diversos documentos, como se ha ilustrado anteriormente, indican claramente que es difícil hacer predicciones relativas a las formulaciones de anticuerpo. Asimismo, el experto en la materia

puede encontrar dificultad a la hora de usar documentos relativos a otras formulaciones de anticuerpo como referencia/guía cuando intenta preparar una formulación estable adaptada a un anticuerpo concreto.

Las referencias citadas divulgan únicamente una formulación que comprende adalimumab como anticuerpo y por lo tanto, es difícil concebir la formulación óptima y estable reivindicada en la presente invención, que comprende infliximab, a partir de la información descrita en los mismos.

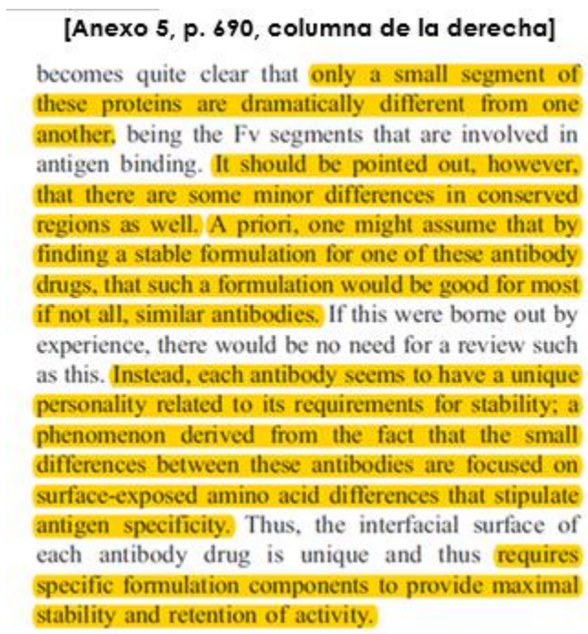
5.2.3. A la hora de preparar una formulación estable de anticuerpos, es difícil sustituir adalimumab por infliximab

Como se ha mencionado a lo largo del presente documento, la formulación de la presente invención contiene infliximab, mientras que **D1** se refiere a un anticuerpo diferente - adalimumab.

En cuanto a la estabilidad de una formulación, los tipos de anticuerpo (que sirven como principio activo) tienen una influencia importante en dicha estabilidad. En resumen, **la estabilidad de las formulaciones puede diferir dependiendo en las características únicas de los anticuerpos individuales, tales como aminoácidos de la superficie o aminoácidos en la región Fv o el dominio Fc**. Por consiguiente, es necesario preparar una formulación específica para el anticuerpo.

Concretamente, el Anexo 5 (Daugherty et al., Advanced Drug Delivery Reviews, 58, 2006, p. 690), describe que hay requisitos únicos para la estabilidad que proceden de las **diferencias en las secuencias de aminoácidos de los anticuerpos que determinan la especificidad de antígeno**.

[Anexo 5, p. 690, columna de la derecha]



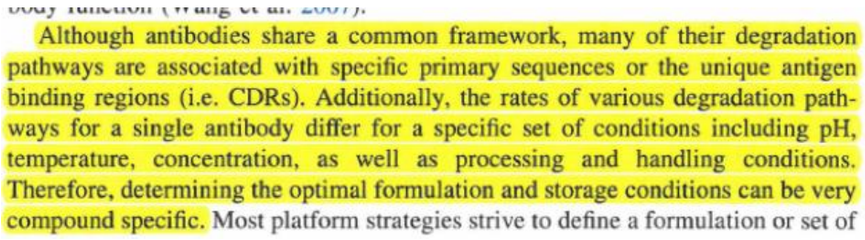
becomes quite clear that only a small segment of these proteins are dramatically different from one another, being the Fv segments that are involved in antigen binding. It should be pointed out, however, that there are some minor differences in conserved regions as well. A priori, one might assume that by finding a stable formulation for one of these antibody drugs, that such a formulation would be good for most if not all, similar antibodies. If this were borne out by experience, there would be no need for a review such as this. Instead, each antibody seems to have a unique personality related to its requirements for stability; a phenomenon derived from the fact that the small differences between these antibodies are focused on surface-exposed amino acid differences that stipulate antigen specificity. Thus, the interfacial surface of each antibody drug is unique and thus requires specific formulation components to provide maximal stability and retention of activity.

Y la traducción al castellano de dichos párrafos es:

queda bastante claro que sólo un pequeño segmento de estas proteínas son dramáticamente diferentes entre sí, siendo los segmentos Fv los que están involucrados en la unión de los antígenos. Sin embargo, cabe señalar que también hay algunas diferencias menores en las regiones conservadas. A priori, se podría suponer que al encontrar una formulación estable para uno de estos anticuerpos, dicha formulación sería buena para la mayoría, si no para todos, los anticuerpos similares. Si esto se confirmara por la experiencia, no habría necesidad de un examen como éste. En cambio, cada anticuerpo parece tener una personalidad única relacionada con sus requisitos de estabilidad; un fenómeno derivado del hecho de que las pequeñas diferencias entre estos anticuerpos se centran en las diferencias de aminoácidos expuestos a la superficie que estipulan la especificidad del antígeno. Así pues, la superficie interfacial de cada medicamento de anticuerpos es única y, por lo tanto, requiere componentes de formulación específicos para proporcionar la máxima estabilidad y retención de la actividad.

Asimismo, el Anexo 6 (Mohamad et al., Development of Antibody-Based Therapeutics), y el Anexo 7 (Helms y Wetzel, Protein Science (1995), 4:2073-2081), describen que la **estabilidad difiere dependiendo de las secuencias individuales, tales como las secuencias de los CDR de los anticuerpos**.

[Anexo 6, p. 362, párrafo 3]



body function (Wang et al. 2007).

Although antibodies share a common framework, many of their degradation pathways are associated with specific primary sequences or the unique antigen binding regions (i.e. CDRs). Additionally, the rates of various degradation pathways for a single antibody differ for a specific set of conditions including pH, temperature, concentration, as well as processing and handling conditions. Therefore, determining the optimal formulation and storage conditions can be very compound specific. Most platform strategies strive to define a formulation or set of

Y la traducción al castellano de dichos párrafos es:

Aunque los anticuerpos comparten un marco común, muchas de sus vías de degradación están asociadas a secuencias primarias específicas o a las regiones únicas de unión al antígeno (es decir, las CDR). Además, las tasas de las diversas vías de degradación de un solo anticuerpo difieren para un conjunto específico de condiciones, incluyendo pH, temperatura,

concentración, así como las condiciones de procesamiento y manipulación.

Por lo tanto, la determinación de las condiciones óptimas de formulación y almacenamiento pueden ser muy específicas de cada compuesto.

[Anexo 7, p. 2079, columna inferior izquierda]

antibody CDR loops. Although canonical CDR structures are usually discussed in terms of the role of CDRs in antigen binding, our results suggest an additional important role of CDR sequence and structure: their contribution to domain stability. Given this possibility, it will be interesting to see the frequency with which new "canonical" CDR structures arise in antibodies generated through the emerging use of CDR sequence randomization methods (Barbas et al., 1993; Fisch et al., 1994).

Y la traducción al castellano de dichos párrafos es:

Aunque las estructuras canónicas de los CDR suelen discutirse en términos del papel de los CDR en la unión de antígenos, nuestros resultados sugieren un importante papel adicional de la secuencia y estructura de los CDR: su contribución a la estabilidad de los dominios.

Dada esta posibilidad, será interesante ver la frecuencia con que surgen nuevas estructuras "canónicas" de CDR en los anticuerpos generados mediante el uso emergente de métodos de aleatorización de la secuencia de CDR (Barbas et al., 1993; Fisch et al., 1994).

Es decir, cabe destacar a partir de lo anterior que las características técnicas (constitución) de una formulación para optimizar la estabilidad difiere dependiendo del tipo de anticuerpo.

Por tanto, es **difícil y no es obvio diseñar una formulación óptima tomando en consideración los diferentes tipos de anticuerpo y por consiguiente, no es obvio sustituir adalimumab por infliximab, tal y como se ha hecho en la presente invención.**

5.3. Efectos técnicos sorprendentes de la formulación de la presente invención

5.3.1. <u>Excelente estabilidad no solo a baja concentraciones de anticuerpo, sino también a una elevada concentración de anticuerpo.</u>

Es sabido y resulta evidente en la técnica que es difícil mantener la estabilidad de las formulaciones con una elevada concentración de anticuerpos en comparación con formulaciones con una baja concentración de anticuerpos (por ejemplo, 50 mg/ml).

En este sentido, el Solicitante describió que han de llevarse a cabo numerosas etapas de ensayo, optimización y validación para concebir la formulación líquida reivindicada de la presente invención, especialmente usando anticuerpos a altas concentraciones mientras que se mantiene un nivel altamente estable para el almacenamiento a largo plazo.

Específicamente, se llevaron a cabo varias pruebas para medir la forma, la turbidez, el contenido de componentes de alto peso molecular, el contenido de inmunoglobulina G intacta, el contenido de cadena pesada y cadena ligera intactas, la velocidad de oxidación, las variantes de carga y el número de partículas sub-visibles. Como resultado, se ha confirmado que no solo a una baja concentración de infliximab, sino también a una alta concentración de infliximab, puede prepararse una formulación estable para la combinación específica de:

(i) un tensioactivo (Ejemplo experimental 4, etc., de la solicitud de patente),
(ii) sorbitol, manitol, trehalosa o sacarosa como un azúcar o su derivado (Ejemplos experimentales 1, 2, etc., de la solicitud de patente) y
(iii) acetato o histidina como tampón (Ejemplo experimental 1, etc., de la solicitud de patente).

Además, en cuanto a la prueba de estabilidad a largo plazo, en donde la formulación se almacenó durante 3 y 6 meses a una temperatura de 40±2ºC o 5±3ºC en condiciones cerradas, la formulación de la invención que contiene una alta concentración de infliximab mantuvo una excelente estabilidad (Ejemplo experimental 5 de la presente solicitud de patente).

Para resumir, **no solo a una baja concentración de anticuerpos, sino también a una alta concentración de anticuerpos, la formulación de infliximab reivindicada en la presente invención mostró baja viscosidad y una excelente estabilidad durante el almacenamiento a largo plazo**. **Además, dicho efecto en la excelente estabilidad de dicha formulación no puede concebirse, inferirse ni derivarse, de la información descrita en el estado de la técnica citado.**

Por lo tanto, ninguno de los documentos **D1 a D2**, solos o combinados, enseñan, ni sugieren la formulación farmacéutica líquida altamente estable de la nueva reivindicación 1, que comprende como principio activo infliximab, entre otros ingredientes.

Por tanto, la nueva reivindicación 1 y sus reivindicaciones dependientes, directa o indirectamente, son novedosas e inventivas en vista de los documentos del estado de la técnica citados.

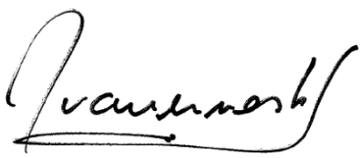
Por todos los motivos anteriormente mencionados, el Solicitante respetuosamente considera que la materia objeto de las reivindicaciones 1-18 que acompañan al presente escrito cumplen con los requisitos de novedad, nivel inventivo y aplicación industrial y, en consecuencia, solicita que se conceda una patente para la presente invención.

En caso de que el Examinador considere que la presente solicitud de patente no reúne todos los requisitos establecidos por la legislación de patentes de Colombia para la

concesión de una patente, respetuosamente se solicita la emisión de una nueva comunicación para dar la oportunidad al solicitante a solventar dicha objeción.

En vista de todo lo anterior, ruego a usted estudiar nuevamente la solicitud con base en las modificaciones realizadas y proceder de conformidad.

Cordialmente,



Juan Carlos Cuesta Quintero.
C.C. 79.339.809 de Bogotá
T.P. 43.273 del C.S. de la J.

International Journal of
Molecular Sciences

MDPI

Article

Molecular Basis for the Neutralization of Tumor Necrosis Factor α by Certolizumab Pegol in the Treatment of Inflammatory Autoimmune Diseases

Jee Un Lee, Woori Shin, Ji Young Son, Ki-Young Yoo and Yong-Seok Heo *

Department of Chemistry, Konkuk University, 120 Neungdong-ro, Gwangjin-gu, Seoul 05029, Korea; jaspersky@naver.com (J.U.L.); woolishin@nate.com (W.S.); jieyson@hanmail.net (J.Y.S.); kiyoung123@daum.net (K.-Y.Y.)

* Correspondence: ysheo@konkuk.ac.kr; Tel.: +82-2-450-3408; Fax: +82-2-3436-5382

Academic Editors: Silvio Danese and Laurent Peyrin-Biroulet
Received: 28 December 2016; Accepted: 17 January 2017; Published: 23 January 2017

Abstract: Monoclonal antibodies against TNFα, including infliximab, adalimumab, golimumab, and certolizumab pegol, are widely used for the treatment of the inflammatory diseases such as rheumatoid arthritis and inflammatory bowel disease. Recently, the crystal structures of TNFα, in complex with the Fab fragments of infliximab and adalimumab, have revealed the molecular mechanisms of these antibody drugs. Here, we report the crystal structure of TNFα in complex with the Fab fragment of certolizumab pegol to clarify the precise antigen-antibody interactions and the structural basis for the neutralization of TNFα by this therapeutic antibody. The structural analysis and the mutagenesis study revealed that the epitope is limited to a single protomer of the TNFα trimer. Additionally, the DE loop and the GH loop of TNFα play critical roles in the interaction with certolizumab, suggesting that this drug exerts its effects by partially occupying the receptor binding site of TNFα. In addition, a conformational change of the DE loop was induced by certolizumab binding, thereby interrupting the TNFα-receptor interaction. A comprehensive comparison of the interactions of TNFα blockers with TNFα revealed the epitope diversity on the surface of TNFα, providing a better understanding of the molecular mechanism of TNFα blockers. The accumulation of these structural studies can provide a basis for the improvement of therapeutic antibodies against TNFα.

Keywords: certolizumab pegol; TNFα; inflammatory bowel diseases; rheumatoid arthritis; therapeutic antibody; crystal structure

1. Introduction

Tumor necrosis factor superfamily (TNFSF) proteins mediate a diverse range of signaling events, including cell growth, survival, and apoptosis, and modulate inflammation, host defense, and organogenesis of the immune, ectodermal, and nervous systems [1–3]. The binding of TNFSF proteins to their receptors (TNFRSF) initiates many pro-inflammatory immune responses. It has been known that there are more than 35 specific ligand-receptor pairs between TNFSF and TNFRSF [4]. Among them, TNFα is a major inflammatory cytokine with a crucial role in the pathogenesis of inflammatory autoimmune diseases via interactions with its cognate receptors, TNFR1 and TNFR2 [5–7]. TNFα is a trimeric transmembrane protein; it can be cleaved to release a soluble trimer [8,9]. Both a mature form of soluble TNFα as well as a precursor form of transmembrane TNFα can mediate various inflammatory responses [10,11]. Each protomer of a TNFα trimer is formed by a sandwich of an inner and outer β-sheet with all 10 strands [12].

Biological agents against TNFα have been developed for the treatment of inflammatory diseases, including rheumatoid arthritis, psoriatic arthritis, axial spondyloarthritis, and inflammatory bowel

diseases, such as Crohn's disease and ulcerative colitis [13–16]. The USA Food and Drug Administration (FDA) has approved five TNFα blockers. Four are antibody-based drugs, i.e. infliximab, adalimumab, certolizumab-pegol, and golimumab, and the other drug, etanercept, is a fusion protein composed of two extracellular domains of TNFR2 and the Fc region of IgG1 [17–21]. All of these TNFα blockers bind to both a soluble and a transmembrane form of TNFα, thereby interrupting the TNFα–TNFR interaction [22,23].

Certolizumab pegol has a unique structure compared to those of the other approved therapeutic antibodies against TNFα. It is a monovalent Fab fragment of a humanized anti-TNFα antibody and lacks the Fc region [24]. The hinge region of certolizumab is attached to two cross-linked chains of a 20-kDa polyethylene glycol (PEG) and is therefore named the certolizumab pegol [25]. The lack of the IgG Fc region can result in the fast degradation of biologics because the binding of the Fc region to the neonatal Fc receptor (FcRn) in the endosome is important for regulating antibody homeostasis by protecting IgG from degradation, thereby contributing to the long plasma half-life of IgG [26,27]. However, the plasma half-life of certolizumab pegol is prolonged by the presence of the covalently linked PEG moiety, as PEGylation increases the plasma half-life and solubility and reduces immunogenicity and protease sensitivity [28]. Indeed, the serum half-life of certolizumab pegol (14 days) is comparable to those of other IgG1 drugs, including infliximab (8–10 days), adalimumab (10–20 days), and golimumab (9–15 days), despite its inability to bind to FcRn [29,30]. The distribution of certolizumab pegol in the inflamed joint is greater than those of infliximab and adalimumab [31], and this is probably due to the unique structure of certolizumab pegol. The lack of the Fc region in certolizumab pegol results in no activity of complement-dependent cytotoxicity (CDC) and antibody-dependent cell-mediated cytotoxicity (ADCC), whereas other TNFα blockers can induce potent CDC and ADCC [32,33].

The crystal structures of TNFα-TNFR2 and TNFβ-TNFR1 complexes have established the foundations of the ligand-receptor interactions between TNFSF and TNFRSF, providing invaluable information for understanding the molecular mechanisms of TNF signaling [34,35]. Recently, the crystal structures of TNFα in complex with the Fab fragments of infliximab and adalimumab have been reported, clarifying their epitopes and inhibitory mechanisms by overlap with the TNFα–TNFR interface [36,37]. In the TNFα-infliximab structure, the Fab fragment interacts with only one TNFα protomer in the TNFα trimer, and the EF loop plays a pivotal role in infliximab recognition by TNFα. In the TNFα-adalimumab complex structure, the epitope consists of two adjacent TNFα molecules in the homotrimer of TNFα and is highly similar to the interface of the TNFα–TNFR2 complex. To elucidate the molecular mechanism and epitope of another anti-TNFα agent, certolizumab pegol, we determined the crystal structure of TNFα in complex with the Fab fragments of certolizumab pegol. We examined the binding mode of the complex and the conformational changes induced by antibody binding, thereby clarifying the molecular basis by which certolizumab pegol effectively blocks TNFα-TNFR interactions, despite the monovalency originating from its unique structure.

2. Results

2.1. Crystal Structure of TNFα in Complex with Certolizumab Fab Fragment

We determined and refined the crystal structure of human TNFα in complex with the certolizumab Fab fragment at a resolution of 2.89 Å with R/R_{free} = 0.225/0.265. The crystallographic asymmetric unit contained 3 copies of TNFα-certolizumab Fab complex with a non-crystallographic 3-fold symmetry (Figure 1A). The gel filtration results also indicated a 3:3 molar ratio for TNFα and certolizumab Fab fragment in the complex (data not shown). Almost all residues of TNFα, except those in the EF loop region, were well defined in the electron density map. The dimensions of the trimeric complex of the TNFα-certolizumab Fab fragment were 130 × 130 × 75 $Å^3$. When viewed along the 3-fold axis, the trimeric complex had a shape that resembles a three-bladed propeller, with one protomer representing one blade. It consisted of three certolizumab Fab fragments radially bound

to a single TNFα homotrimer. The root mean square (rms) deviations between equivalent residues from the protomers of TNFα or the certolizumab Fab molecules in the complex were less than 0.25 Å, as non-crystallographic symmetry restraints were applied during most of the refinement process. The pseudo 2-fold axes of the bound certolizumab Fab fragments relating the heavy and light chains intersected the 3-fold axis of the TNFα homotrimer and had an approximate angle of 40° downward from a plane that was perpendicular to the 3-fold axis. When we consider a cell with a TNFα precursor attached, this plane represents the cell membrane (Figure 1A). In this binding orientation, certolizumab not only can bind to soluble TNFα, but also to a TNFα precursor that is not released from the cell membrane. This structural feature is quite consistent with the drug characteristics, which targets both soluble TNFα and transmembrane TNFα [23]. Each TNFα protomer of the trimeric complex adopted a typical β-sandwich with jellyroll topology composed of two five-stranded antiparallel β-sheets [12]. Superimposing TNFα in the TNFα-certolizumab Fab complex with its receptor-bound form (PDB code 3ALQ) yielded an rms deviation of 0.38 Å for all Cα atoms and indicated no significant overall structural changes, except for the conformational change of the DE loop region due to the interaction with certolizumab, which will be described later.

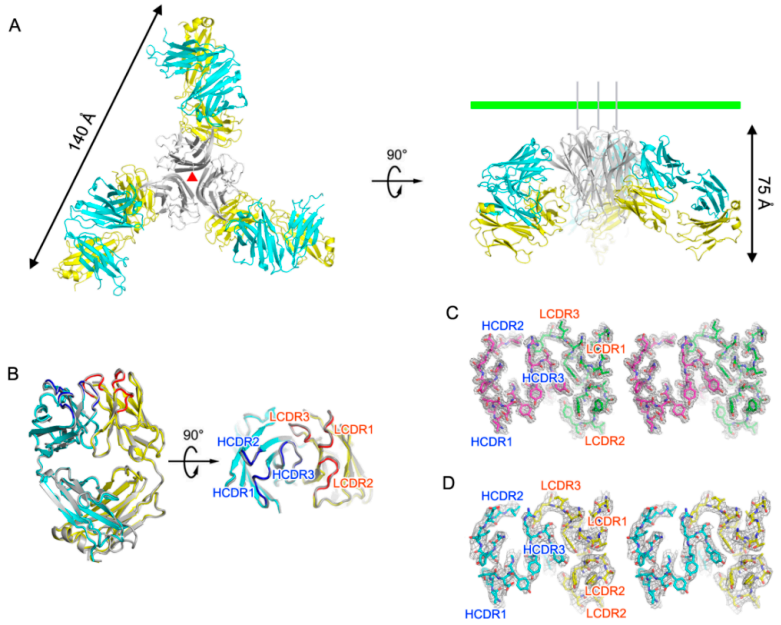


Figure 1. Overall structure of TNFα in complex with the certolizumab Fab fragment. (**A**) Ribbon representation of TNFα (gray) in complex with the certolizumab Fab fragment (heavy chain: cyan; light chain: yellow) in two orientations. The 3-fold axis in the trimeric complex is indicated as a red triangle. The green bar indicates a putative membrane of a TNFα-producing cell if the TNFα trimer is a precursor form of transmembrane TNFα; (**B**) Superposition of the free certolizumab Fab fragment (gray) onto the Fab fragment extracted from the TNFα-certolizumab complex (heavy chain: cyan; light chain: yellow; heavy chain complementary-determining regions: blue; light chain complementary-determining regions: red); (**C**) Cross-eyed stereoview of the 2fo-fc composite omit map (1.2 σ contour level) at the complementary-determining regions (CDRs) of the free certolizumab Fab fragment, calculated at 1.95 Å resolution (heavy chain: purple; light chain: green); (**D**) Cross-eyed stereoview of the 2Fo-Fc composite omit map (1.2 σ contour level) at the CDRs of the Fab fragment in the TNFα-certolizumab complex, calculated at 2.89 Å resolution (heavy chain: cyan; light chain: yellow).

The crystal structure of the uncomplexed certolizumab Fab fragment was also determined and refined to a resolution of 1.95 Å with R/R_{Free} = 0.147/0.179. The certolizumab Fab presented a canonical immunoglobulin fold and four intramolecular disulfide bonds in the structures of both its uncomplexed form and its TNFα-bound form, as expected. The elbow angle of the certolizumab

Fab fragment, defined as the angle subtended by the two pseudo-dyad axes relating the variable and constant domains of the Fab fragment, did not differ between the TNFα-bound and the free certolizumab, despite the intrinsic flexibility of the Fab elbow (Figure 1B). The electron density of the structure of the uncomplexed Fab fragment was clear throughout the entire structure, including in the complementary-determining regions (CDRs) (Figure 1C). Additionally, all CDRs of the structure of the uncomplexed certolizumab Fab fragment had the same conformation as those of this antibody in complex with TNFα, implying that this antibody drug maintains the CDRs in productive binding conformations prior to interactions with TNFα, thereby contributing to the high binding affinity to TNFα (Figure 1B–D).

2.2. Interaction between TNF-α and Certolizumab Fab

The interaction of a single Fab fragment of certolizumab with TNFα buried a total solvent-accessible area of 1887 Å^2, which was larger than a typical protein–protein interface (1560–1700 Å^2) [38], and thereby contributed to the high affinity between TNFα and certolizumab (Figure 2) [39]. Although TNFα exists as a trimer, the epitope of certolizumab was composed of only residues from a single protomer of TNFα. The certolizumab epitope of TNFα consisted of a number of residues, including $_{TNF\alpha}$G24, $_{TNF\alpha}$D45, $_{TNF\alpha}$Q47, $_{TNF\alpha}$T77, $_{TNF\alpha}$I83, $_{TNF\alpha}$V85, $_{TNF\alpha}$S86, $_{TNF\alpha}$Q88, $_{TNF\alpha}$T89, $_{TNF\alpha}$K90, $_{TNF\alpha}$R131, $_{TNF\alpha}$E135, $_{TNF\alpha}$N137, $_{TNF\alpha}$R138, $_{TNF\alpha}$P139, and $_{TNF\alpha}$D140, and most were located in the DE loop and GH loop regions of TNFα. Several residues on the epitope of certolizumab were also involved in the TNFα–TNFR interaction [35], indicating the mechanism by which certolizumab competitively blocks the TNFα–TNFR interaction.

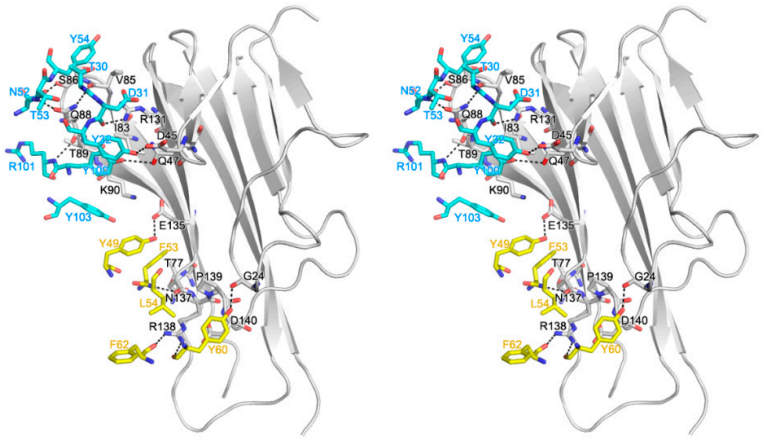


Figure 2. TNFα-certolizumab Fab fragment interface. Cross-eyed stereoview of the detailed TNFα-certolizumab Fab fragment interface. The carbon atoms from TNFα and the heavy and light chains of certolizumab are colored gray, cyan, and yellow, respectively. Hydrogen bonds are indicated with dashed lines.

While all three CDRs from the heavy chain of certolizumab participated in the interaction with TNFα, only one CDR from the light chain, LCDR2, was involved in the TNFα interaction. The interaction of the light chain of certolizumab mediated only by the LCDR2 loop was quite unique; it is generally observed that the LCDR2 region of antibodies is frequently not involved in antigen binding [40]. The paratope of certolizumab consisted of $_{heavy}$T30, $_{heavy}$D31, $_{heavy}$Y32 of HCDR1, $_{heavy}$N52, $_{heavy}$T53, and $_{heavy}$Y54 of HCDR2; $_{heavy}$Y100 $_{heavy}$R101, and $_{heavy}$Y103 of HCDR3; and $_{light}$Y49, $_{light}$F53, $_{light}$L54, $_{light}$Y60, and $_{light}$F62 of LCDR2.

There were 12 hydrogen bonds and no salt bridge interaction between a single protomer of TNFα and the certolizumab Fab fragment, and several residues of TNFα contributed to van der Waals contacts with the certolizumab. The heavy chain of certolizumab interacted with the B′B loop and the G strand as well as the DE loop. The side chain atoms of $_{TNF\alpha}$D45 and $_{TNF\alpha}$Q47 in the B′B loop formed

hydrogen bonds with the hydroxyl groups of $_{heavy}$Y32 and $_{heavy}$Y100, respectively. The residues $_{TNF\alpha}$I83, $_{TNF\alpha}$V85, $_{TNF\alpha}$S86, $_{TNF\alpha}$Q88, $_{TNF\alpha}$T89, and $_{TNF\alpha}$K90 of the DE loop were involved in the interaction with certolizumab. The backbone carbonyl groups of $_{TNF\alpha}$S86 and $_{TNF\alpha}$Q88 formed hydrogen bonds with the side chain of $_{heavy}$N52 and the backbone amide group of $_{heavy}$R101, and the side chain of $_{TNF\alpha}$Q88 made two hydrogen bonds with the backbone atoms of $_{heavy}$T30 and $_{heavy}$T53. The side chains of $_{TNF\alpha}$I83, $_{TNF\alpha}$V85, $_{TNF\alpha}$T89, and $_{TNF\alpha}$K90 made van der Waals contacts with the side chains of $_{heavy}$Y100, $_{heavy}$Y54, $_{heavy}$R101, and $_{heavy}$Y103, respectively. The side chain of $_{TNF\alpha}$R131 in the G strand also made a hydrogen bond with the backbone carbonyl group of $_{heavy}$D31. The interaction between the light chain of certolizumab and TNFα was primarily attributed to the GH loop. Several residues in the D strand and AA" loop also contributed to the interaction with certolizumab. The residues in the GH loop of TNFα involved in the interaction with certolizumab were $_{TNF\alpha}$E135, $_{TNF\alpha}$N137, $_{TNF\alpha}$R138, $_{TNF\alpha}$P139, and $_{TNF\alpha}$D140. The side chain atom of $_{TNF\alpha}$E135 and the backbone carbonyl group of $_{TNF\alpha}$N137 made hydrogen bonds with the side chain atom of $_{light}$Y49 and the backbone amide group of $_{light}$L54, respectively. $_{TNF\alpha}$R138 made two hydrogen bonds with the backbone carbonyl groups of $_{light}$Y60 and $_{light}$F62. In addition, the backbone carbonyl groups of $_{TNF\alpha}$G24 in the AA" loop made a hydrogen bond with the side chain atom of $_{light}$Y60. The residues $_{light}$F53, $_{light}$L54, and $_{light}$Y60 of LCDR2 contributed to van der Waals contacts with the side chains of $_{TNF\alpha}$T77 in the D strand and $_{TNF\alpha}$N137, $_{TNF\alpha}$R138, $_{TNF\alpha}$P139, and $_{TNF\alpha}$D140 in the GH loop.

Interestingly, the bidentate hydrogen bond mediated by $_{TNF\alpha}$Q88 induced a conformational change of the DE loop of TNFα (Figure 3A,B). In the structure of TNFα in complex with TNFR2, $_{TNF\alpha}$Y87 of the DE loop was optimally accommodated into a small pocket on the surface of TNFR2 and thereby contributed to the energetics of the TNFα-TNFR2 interaction (Figure 3C) [35]. However, the structural change of the DE loop induced by certolizumab binding was incompatible with TNFR2 binding, as the positional change of $_{TNF\alpha}$Y87 would cause steric collision with TNFR2 (Figure 3B,C). Thus, the neutralizing effect of certolizumab appears to be a consequence of the partial overlap of the epitope with the TNFα-TNFR interface and an antibody-induced conformational change of the DE loop.

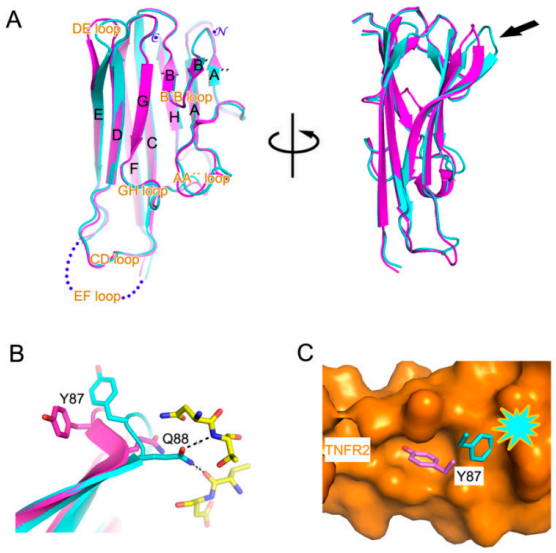


Figure 3. Conformational change of the DE loop. (**A**) Superposition of the TNFα protomers extracted from the TNFα-certolizumab complex (cyan) and the TNFα–TNFR2 complex (purple) in two orientations. The strands, loops, N-, and C-terminus of TNFα are labelled. The arrow indicates the discrepancy of the DE loop conformation; (**B**) Conformational change of the DE loop induced by certolizumab binding. The bidentate hydrogen bond by $_{TNF\alpha}$Q88 with certolizumab (yellow) changes the DE loop conformation; (**C**) Steric collision of $_{TNF\alpha}$Y87 with TNFα is represented in the case of the DE loop conformation altered by certolizumab binding. The surface of TNFR2 is colored orange.

2.3. Mutagenesis Study of the TNFα-Certolizumab Interface

For the mutagenesis analysis, we selected 6 residues of TNFα whose side chains were involved in the hydrogen bonds with certolizumab; i.e., $_{TNF\alpha}$D45, $_{TNF\alpha}$Q47, $_{TNF\alpha}$Q88, $_{TNF\alpha}$R131, $_{TNF\alpha}$E135, and $_{TNF\alpha}$N137. Each residue was replaced by alanine and the binding affinities of each mutant with certolizumab were measured by surface plasmon resonance to evaluate the effects of these replacements on the interaction with certolizumab (Figure 4). The substitutions of $_{TNF\alpha}$D45, $_{TNF\alpha}$Q47, and $_{TNF\alpha}$R131 with alanine did not substantially affect the binding affinity of TNFα to certolizumab, with decreases in the on-rate constants k_{on} of 3–5-fold and similar off-rate constant k_{off} values. These results imply that the hydrogen bonds mediated by these residues would only facilitate fast associations between TNFα and certolizumab, but are not important for slow dissociation in order to maintain the stable TNFα-certolizumab complex (Table 1). The replacement of $_{TNF\alpha}$Q88 resulted in a drastic decrease in binding affinity, with an 18-fold higher dissociation constant, K_D, implying that the hydrogen bonds by $_{TNF\alpha}$Q88 play a critical role in the interaction between the DE loop of TNFα and the heavy chain of certolizumab. The substitution of $_{TNF\alpha}$R138 also dramatically increased K_D by 20-fold, implying the importance of this residue for the interaction between the GH loop of TNFα and the light chain of certolizumab. The critical contribution of the residues $_{TNF\alpha}$Q88 and $_{TNF\alpha}$R138 to the binding affinity can be easily predicted from the structural features of the TNFα-certolizumab interaction, as the side chains of only these two residues made bidentate hydrogen bonds with certolizumab (Figure 2). The hydrogen bond between $_{TNF\alpha}$E135 and $_{light}$Y49 may also play a supplementary role in the energetics of the TNFα-certolizumab interaction as the mutation $_{TNF\alpha}$E135A increased K_D by 11-fold. Nonetheless, the mutation of a single residue side chain did not result in the complete loss of the TNFα-certolizumab interaction but slightly decreased the binding affinity. This indicates that the interaction surface is very extensive, involving a molecular network rather than individual residues.

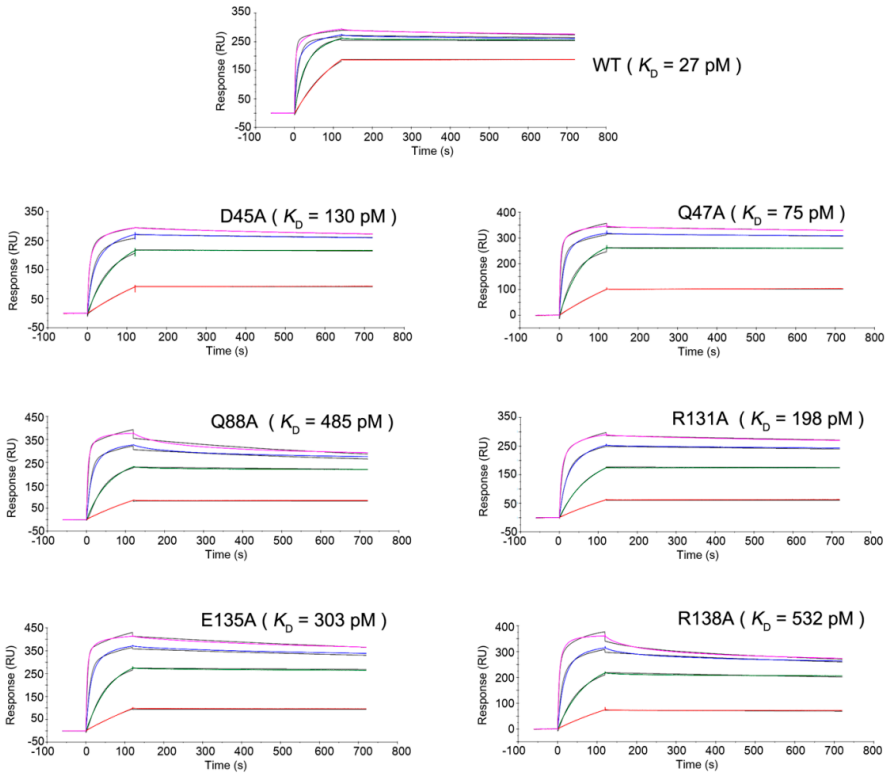


Figure 4. Sensorgrams for the binding kinetics of the TNFα mutants. Surface plasmon resonance analyses of wild-type and mutant TNFα, demonstrating their binding affinities to certolizumab Fab fragments. The concentrations of the wild-type and mutant TNFα for each experiment are 2 (red), 10 (green), 50 (blue), 250 nM (purple).

Table 1. Binding kinetics of the TNFα mutants with certolizumab Fab fragments. WT: Wild-type.

TNFα	K_{on} ($M^{-1} \cdot s^{-1}$)	K_{off} (s^{-1})	K_D (M)
WT	1.97×10^6	5.40×10^{-5}	2.74×10^{-11}
D45A	5.86×10^5	7.64×10^{-5}	1.30×10^{-10}
Q47A	5.83×10^5	4.39×10^{-5}	7.53×10^{-11}
Q88A	4.76×10^5	2.31×10^{-4}	4.85×10^{-10}
R131A	3.74×10^5	7.42×10^{-5}	1.98×10^{-10}
E135A	4.60×10^5	1.40×10^{-4}	3.04×10^{-10}
R138A	4.52×10^5	2.41×10^{-4}	5.32×10^{-10}

3. Discussion

TNFα is an important target for the treatment of inflammatory diseases, such as rheumatoid arthritis and inflammatory bowel diseases. Accordingly, five biological agents against TNFα have been approved by the FDA including three monoclonal anti-TNFα full IgG1 antibodies, infliximab, adalimumab, and golimumab; the PEGylated Fab fragment of the anti-TNFα antibody certolizumab pegol; and the extracellular domain of the TNFR2/IgG1-Fc fusion protein etanercept (Table 2). Each shows excellent efficacy, with similar rates of response, although the similarity is somewhat controversial owing to the lack of a head-to-head comparative studies [41].

Table 2. Approved biologics against TNF-α.

Drug	Trade Name	Type	Approval Date	
			FDA	EMA
Etanercept	Enbrel	TNFR2 extracellular portion Fc fusion	1998	2000
Infliximab	Remicade	Chimeric murine/human IgG1	1998	1999
Adalimumab	Humira	Fully Human IgG1	2005	2003
Certolizumab-pegol	Cimzia	Humanized, PEGylated Fab′	2008	2009
Golimumab	Simponi	Fully Human IgG1	2009	2009

FDA, Food and Drug Administration; EMA, European Medicine Agency.

Comparison of the TNFα interactions of each TNFα blocker can provide a better understanding of the neutralizing mechanism of these anti-TNFα drugs. The structural features of the TNFα-etanercept interface can be deduced from the crystal structure of TNFα in complex with TNFR2, as the TNFα binding part of etanercept is the extracellular domain of TNFR2, implying that the drug exerts neutralizing effects by occupying the receptor binding site of TNFα [35]. The crystal structures of TNFα in complex with infliximab and adalimumab have revealed the epitopes of each antibody drug, showing that they bind to TNFα efficiently and outcompete TNFRs for binding to TNFα, thereby preventing TNFα from functioning in inflammatory diseases [36,37]. However, structural studies of certolizumab pegol and golimumab have not been reported, despite many biochemical and clinical analyses of them. In this study, we report the crystal structure of the soluble trimer of human TNFα in complex with the Fab fragment of the therapeutic antibody certolizumab pegol to understand the antigen-antibody interface and the neutralizing mechanism of this drug. The structure showed that three Fab fragments bind symmetrically to a TNFα trimer. Certolizumab neutralizes TNFα function by partially overlapping with the TNFα-TNFR interface and preventing the conformational rearrangement of the DE loop, which is necessary for TNFR binding.

The CDRs of certolizumab have a typical length without an unusual amino acid sequence, according to a Kabat antibody sequence database search [42], which is similar to the other antibodies infliximab and adalimumab (Figure 5). However, comparison of the interactions of certolizumab with other TNFα blockers shows that the epitopes are very different from each other (Figure 6). In the TNFα-adalimumab Fab complex, one Fab fragment of adalimumab interacts with two adjacent TNFα protomers, similar to the TNFα-TNFR2 complex [37]. By contrast, the interactions mediated by the infliximab and certolizumab Fab fragments involve only one protomer of the TNFα homotrimer [36].

The EF loop of TNFα is involved in the interaction with the adalimumab and infliximab Fab fragments. In particular, in the TNFα-infliximab Fab complex, the residues in the EF loop play a crucial role in the antigen-antibody interaction. However, this region in the TNFα-certolizumab Fab complex is completely unobservable in the crystal structure, indicating that the EF loop is flexible and not involved in the interaction with certolizumab, as observed in the structure of the TNFα–TNFR2 complex [35]. It has been reported that the TNFα homotrimer is non-stable at physiological concentrations and slowly dissociates into a monomeric form with reversible trimerization, although the details of this process are not fully elucidated [43–45]. Etanercept, adalimumab, and infliximab were found to completely abrogate this monomer exchange reaction in the TNFα homotrimer, whereas certolizumab and golimumab could not prevent it but did slow down the monomer exchange process [39]. In other words, the former three anti-TNFα drugs stabilize the trimeric form of TNFα, whereas the others exhibit no or only slight stabilization. The differences in the monomer exchange behavior of the TNFα blockers are not likely correlated with their binding affinities to TNFα [39]. In the experiment, to measure the affinity of the Fab fragments of the TNFα blockers, the adalimumab Fab fragment, which inhibits the monomer exchange reaction and stabilizes the TNFα homotrimer, had the lowest affinity, whereas the certolizumab Fab fragment had the highest affinity to TNFα [39]. This high affinity of certolizumab Fab may lead to an excellent therapeutic efficacy, similar to those of other bivalent biologics, despite its monovalency originating from the shape of the PEGylated Fab fragment. The differences in TNFα homotrimer stabilization can be explained by the structural features of TNFα in complex with the biologics, described above (Figure 6). Adalimumab and etanercept interact with two neighboring protomers of TNFα simultaneously [35,37], thereby stabilizing interactions between the protomers in the TNFα homotrimer. Although the epitope of infliximab consists of the residues from only one protomer, the antigen-antibody interaction involves the EF loop and leads to its unique conformation [36], which may contribute to the stabilization of the trimeric form of TNFα via the productive communication between the EF loops of the unique conformation in the trimer. On the contrary, the binding of certolizumab is limited to only a single protomer and does not involve the EF loop without influencing its conformation or the interactions between the protomers in the TNFα homotrimer. Based on the monomer exchange behavior of golimumab, which is similar to that of certolizumab, golimumab is expected to bind to an epitope composed of only a single protomer without interacting with the EF loop of TNFα.

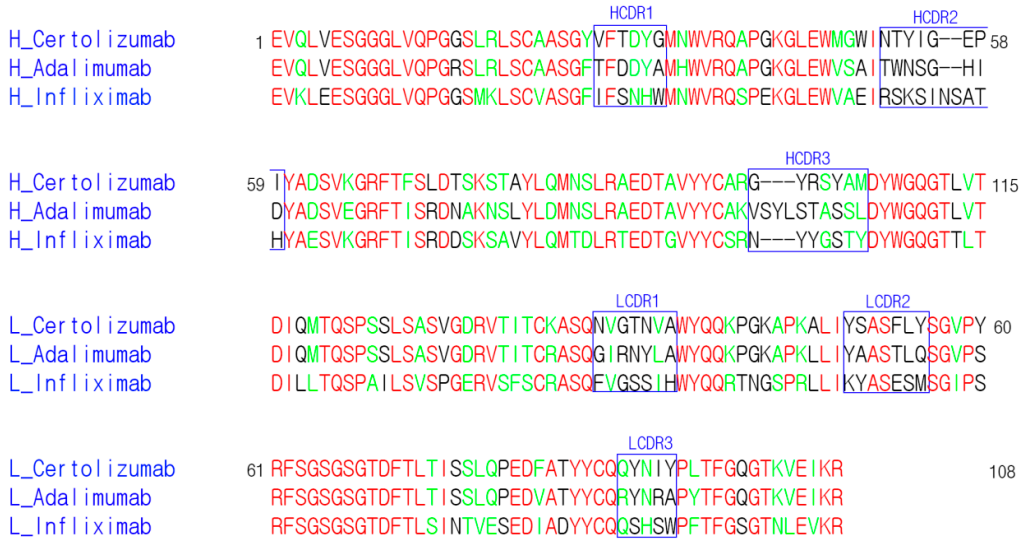


Figure 5. Sequence comparison of the antibodies against TNFα. The CDRs are indicated with boxes and labeled. The residue numbers refer to those in certolizumab. The identical and homologous residues are colored red and green, respectively.

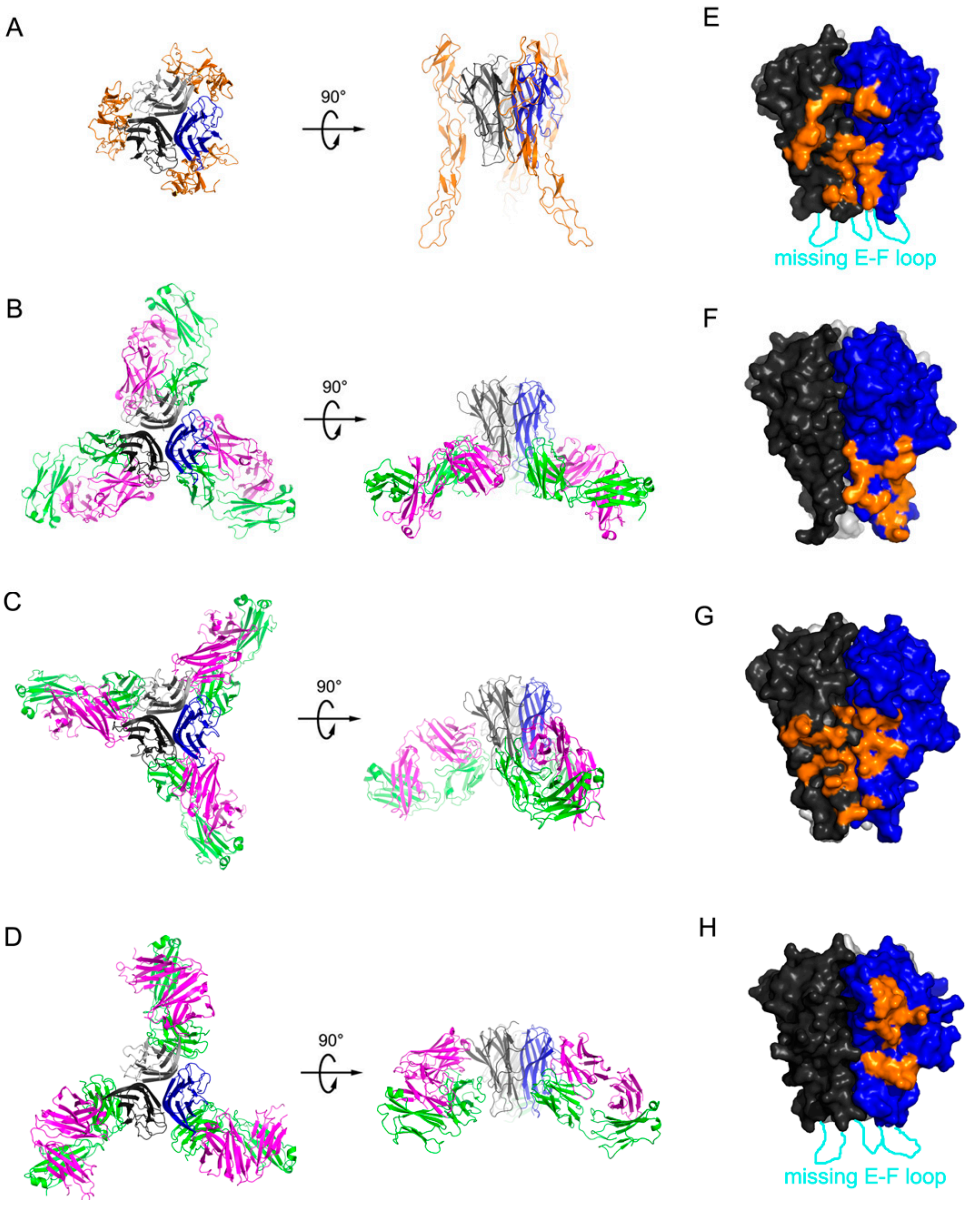


Figure 6. A comparison of the interface between TNFα and the TNFα blockers. (**A**) The structure of the TNFα trimer (black, gray, and blue) in complex with TNFR2 (orange); (**B**) The structure of the TNFα trimer (black, gray, and blue) in complex with the infliximab Fab fragment (heavy chain: purple; light chain: green); (**C**) The structure of the TNFα trimer (black, gray, blue) in complex with the adalimumab Fab fragment (heavy chain: purple; light chain: green); (**D**) The structure of the TNFα trimer (black, gray, blue) in complex with the certolizumab Fab fragment (heavy chain: purple; light chain: green); (**E**) The TNFR2 binding site on the surface of the TNFα trimer (black and blue for each protomer) is colored orange; (**F**) The infliximab epitope on the surface of the TNFα trimer (black and blue for each protomer) is colored orange; (**G**) The adalimumab epitope on the surface of the TNFα trimer (black and blue for each protomer) is colored orange; (**H**) The certolizumab epitope on the surface of the TNFα trimer (black and blue for each protomer) is colored orange. The EF loop, which is missing in the structures of TNFα–TNFR2 and the TNFα-certolizumab complex owing to a lack of interactions, is labeled.

4. Materials and Methods

4.1. Expression and Purification of TNFα

Genes encoding the soluble form of human TNFα (aa 77–233) were subcloned into pET-21a (Addgene, Cambridge, MA, USA). The protein was overexpressed with a C-terminal 6His-tag using plasmid-transformed *E. coli* BL21 (DE3) competent cells. The cells were first grown at 37 °C in Luria-Bertini (LB) medium supplemented with 50 μg·mL^{-1} ampicilin. Protein expression was induced by adding 0.5 mM isopropyl β-D-1-thiogalactopyranoside (IPTG) when the cells reached an optical density at 600 nm of about 0.6, and the cells were grown for 16 h at 18 °C prior to harvesting by centrifugation (3000× *g* for 0.5 h at 4 °C). The cell pellet was resuspended in a lysis buffer (20 mM Tris pH 8.0, 300 mM NaCl, 5 mM β-mercaptoethanol) and disrupted by sonication on ice. After the crude lysate was centrifuged (25,000× *g* for 1 h at 4 °C), the supernatant containing soluble was applied to the HisTrap HP column (GE Healthcare Life Sciences, Marlborough, MA, USA) and washed with five column volumes of wash buffer (20 mM Tris pH 8.0, 300 mM NaCl, 5 mM β-mercaptoethanol, 50 mM imidazole). The protein was then eluted with elution buffer (20 mM Tris pH 8.0, 300 mM NaCl, 5 mM β-mercaptoethanol, 400 mM imidazole). The eluted protein was concentrated for gel filtration chromatography using a HiLoad 16/60 Superdex 200 pg column (GE Healthcare Life Sciences). The column had previously been equilibrated with gel filtration buffer (20 mM Tris pH 8.0, 300 mM NaCl). The protein purity was evaluated by SDS–PAGE.

4.2. Expression and Purification of the Certolizumab Fab

The DNA sequence for the Fab fragment of certolizumab was synthesized after codon-optimization for expression in *E. coli* (Bioneer, Inc., Daejon, Korea). The sequences for the heavy chain and the light chain were cloned into a modified pBAD vector, containing the STII signal sequence in each chain for periplasmic secretion and a C-terminal 6His-tag in the heavy chain [46]. The plasmid pBAD-certolizumab Fab fragment was transformed into *E. coli* Top10F (Invitrogen, Carlsbad, CA, USA). The cells were grown at 37 °C in LB medium supplemented with 50 μg·mL^{-1} ampicillin. At an OD600 of 1.0, the protein expression was induced with 0.2% arabinose and cells were grown at 30 °C for 15 h. The cells were harvested by centrifugation, re-suspended in a lysis buffer (20 mM Tris, pH 8.0, 200 mM NaCl), and lysed by sonication on ice. After removing cell debris by centrifugation (25,000× *g* for 0.5 h at 4 °C), the supernatant containing soluble protein was applied to the HisTrap HP column (GE Healthcare Life Sciences) and washed with five column volumes of wash buffer (20 mM Tris, pH 8.0, 300 mM NaCl, 50 mM imidazole). The protein was then eluted with elution buffer (20 mM Tris pH 8.0, 300 mM NaCl, 400 mM imidazole). The eluted protein was concentrated for gel filtration chromatography using a HiLoad 16/60 Superdex 200 pg column (GE Healthcare Life Sciences). The column had previously been equilibrated with gel filtration buffer (20 mM Tris pH 8.0, 300 mM NaCl). The elution profile of the protein showed a single major peak and the protein quality was evaluated by reducing and nonreducing SDS–PAGE.

4.3. Crystallization and Structure Determination of the Certolizumab Fab

Gel-filtration fractions containing the certolizumab Fab fragment were concentrated to 10 mg·mL^{-1} in 20 mM Tris, pH 8.0, and 300 mM NaCl. Crystals were grown using a hanging-drop vapor diffusion with a reservoir solution containing 0.1 M Bis-Tris, pH 5.5, 0.2 M ammonium sulfate, and 25% PEG3350 at 20 °C within a week. Crystals were cryoprotected by brief immersion in a well solution, supplemented with 20% glycerol, and flash frozen in liquid nitrogen. X-ray diffraction data were collected at 100 K on beamline 5C of the Pohang Light Source (PLS) (Pohang, Korea). The crystals belonged to space group $P2_12_12_1$ (a = 58.33, b = 63.70, c = 161.41 Å) with one copy in the asymmetric unit. X-ray diffraction data were collected to a resolution of 1.95 Å, integrated, and scaled using HKL2000 (HKL Research, Charlottesville, VA, USA). The structure was solved by molecular replacement using a Phaser [47] with a structure of the Fab fragments that has high sequence identities with certolizumab Fab fragments

(PDB code 4DKF, chains H and L). Due to the intrinsic elbow flexibility of a Fab fragment, the Fv region and the other region including the CH1 and CL domains were separated when used as a search model. At this point, the electron density corresponding certolizumab was prominent. Iterative rounds of refinement were done using PHENIX [48] with manual inspection using COOT [49]. Statistics for data collection and refinement can be found in Table 3. All structure figures were prepared using PyMOL [50].

Table 3. Data collection and refinement statistics.

	Certolizumab Fab	**TNFα-Certolizumab Fab**
Data Collection		
X-ray source	PLS 5C	PLS 7A
Wavelength (Å)	1.0000	1.0000
Space group	$P2_12_12_1$	$C2$
Cell dimensions		
a, *b*, *c* (Å)	58.33, 63.70, 161.41	148.59, 207.22, 112.63
α, β, γ (°)	90, 90, 90	90, 118.81, 90
Resolution (Å)	1.95 (1.98–1.95) *	2.89 (2.95–2.89)
R_{sym} (%)	7.8 (29.7)	8.1 (48.6)
$I/\sigma I$	58.1 (3.1)	19.6.1 (2.3)
Completeness (%)	98.2 (85.6)	95.2 (94.5)
Redundancy	5.9 (2.5)	2.9 (2.6)
Refinement		
Resolution (Å)	1.95	2.89
No. reflections	43749	63355
R_{work}/R_{free} (%)	14.7/17.9	22.5/26.5
No. atoms		
Protein	3290	12793
Water	607	0
R.m.s. deviation		
Bond lengths (Å)	0.007	0.006
Bond angles (°)	1.060	1.278
Ramachandran		
Favored (%)	98.37	95.04
Allowed (%)	1.63	4.47
Outlier (%)	0.00	0.49
PDB code	5WUV	5WUX

* Values in parentheses are for the outer resolution shell.

4.4. Crystallization and Structure Determination of the TNFα-Certolizumab Fab Complex

Purified TNFα and certolizumab Fab were mixed in a 1:1 molar ratio and incubated for 1 h at 4 °C before being subjected to size exclusion chromatography using a HiLoad 16/60 Superdex 200 pg column equilibrated with 20 mM Tris, pH 8.0, and 300 mM NaCl. Gel-filtration fractions containing the TNFα-certolizumab Fab complex were concentrated to 7 mg·mL^{-1} in 20 mM Tris, pH 8.0, and 300 mM NaCl. Crystals were grown using hanging-drop vapor diffusion with a reservoir solution containing 0.1 M 3-(cyclohexylamino)-1-propanesulfonic acid pH 5.6, 0.2 M lithium sulfate, and 1.5 M ammonium sulfate at 20 °C within 20 days. Crystals were cryoprotected by brief immersion in the well solution, supplemented with 25% ethylene glycol, and flash frozen in liquid nitrogen. X-ray diffraction data were collected at 100 K on beamline 7A of the Pohang Light Source (PLS) (Pohang, Korea). The crystals belonged to space group *C*2 (a = 148.59, b = 207.22, c = 112.63 Å, β = 118.81°) with three copies in the asymmetric unit. X-ray diffraction data were collected to a resolution of 2.89 Å, integrated, and scaled using HKL2000 (HKL Research, Charlottesville, VA, USA). The structure was solved by molecular replacement using Phaser with a structure of the free certolizumab Fab fragment

and human TNFα (PDB code 1TNF). Due to the intrinsic elbow flexibility of a Fab fragment, the Fv region and the other regions, including the CH1 and CL domains, were separated when the structure of the free certolizumab Fab fragment was used as a search model. At this point, the electron density corresponding to the TNFα-certolizumab Fab Complex was prominent. Iterative rounds of refinement were done using PHENIX with manual inspection using COOT. Statistics for data collection and refinement can be found in Table 1.

4.5. Binding Kinetics of the TNFα WT and Mutants

Site-directed mutants of TNFα, including $_{TNF\alpha}$D45A, $_{TNF\alpha}$Q47A, $_{TNF\alpha}$Q88A, $_{TNF\alpha}$R131A, $_{TNF\alpha}$E135A, and $_{TNF\alpha}$R138A, were created with the QuickChange Kit (Agilent Technologies, Santa Clara, CA, USA) and confirmed by DNA sequencing. The mutant proteins were expressed and purified as described for wild-type TNFα. Approximately 1000 response units of the certolizumab Fab fragment were immobilized on the surface of a CM-5 chip (GE Healthcare Life Sciences) via amine coupling reactions, as described in the manufacturer's instructions. Purified wild-type and the mutants of TNFα were serially diluted to concentrations ranging from 2 nM to 250 nM using PBS buffer and flowed through the chip. A BIAcore T100 instrument (GE Healthcare Life Sciences, Marlborough, MA, USA) was operated at 25 °C using PBS buffer as a running buffer. The bound TNFα was removed with 10 mM glycine (pH 2.0) at the end of each cycle while retaining the surface integrity for chip regeneration. Sensorgrams were locally fitted and the dissociation constants (K_d) were calculated with the analysis software, BIAevaluation (GE Healthcare Life Sciences, Marlborough, MA, USA).

4.6. Accession Number

The coordinates and structure factors for the crystal structures of the free certolizumab Fab fragments and the complex of TNFα-certolizumab Fab fragments have been deposited in the Protein Data Bank under accession codes 5WUV and 5WUX, respectively.

5. Conclusions

In summary, the elucidation of the crystal structure of TNFα in complex with the Fab fragments of certolizumab pegol sheds light on the molecular mechanism underlying the therapeutic activity of this antibody drug. In addition, the precise epitope revealed by the present complex structure could provide useful information for the improvement of the current biological agents against TNFα for the treatment of inflammatory autoimmune diseases.

Acknowledgments: We are grateful to the staffs of beamline 7A and 5C at Pohang Accelerator Laboratory for help with the X-ray diffraction experiments. This paper was supported by Konkuk University in 2013.

Author Contributions: Jee Un Lee and Yong-Seok Heo designed the study. Jee Un Lee, Woori Shin, Ji Young Son, and Ki-Young Yoo performed the experiments, including expression, purification, crystallization, SPR analysis, and X-ray data collection. Jee Un Lee and Yong-Seok Heo determined and analysed the structures. Yong-Seok Heo wrote the manuscript. All authors discussed the results and commented on the manuscript.

Conflicts of Interest: The authors declare no conflict of interest.

References

1. Bodmer, J.L.; Schneider, P.; Tschopp, J. The molecular architecture of the TNF superfamily. *Trends Biochem. Sci.* **2002**, *27*, 19–26. [CrossRef]
2. Locksley, R.M.; Killeen, N.; Lenardo, M.J. The TNF and TNF receptor superfamilies: Integrating mammalian biology. *Cell* **2001**, *104*, 487–501. [CrossRef]
3. Wiens, G.D.; Glenney, G.W. Origin and evolution of TNF and TNF receptor superfamilies. *Dev. Comp. Immunol.* **2011**, *35*, 1324–1335. [CrossRef] [PubMed]
4. Bossen, C.; Ingold, K.; Tardivel, A.; Bodmer, J.L.; Gaide, O.; Hertig, S.; Ambrose, C.; Tschopp, J.; Schneider, P. Interactions of tumor necrosis factor (TNF) and TNF receptor family members in the mouse and human. *J. Biol. Chem.* **2006**, *281*, 13964–13971. [CrossRef] [PubMed]

5. Idriss, H.T.; Naismith, J.H. TNFα and the TNF receptor superfamily: Structure-function relationship(s). *Microsc. Res. Tech.* **2000**, *50*, 184–195. [CrossRef]
6. Aggarwal, B.B. Signalling pathways of the TNF superfamily: A double-edged sword. *Nat. Rev. Immunol.* **2003**, *3*, 745–756. [CrossRef] [PubMed]
7. Chen, G.; Goeddel, D.V. TNF-R1 signaling: A beautiful pathway. *Science* **2002**, *296*, 1634–1635. [CrossRef] [PubMed]
8. Aggarwal, B.B.; Gupta, S.C.; Kim, J.H. Historical perspectives on tumor necrosis factor and its superfamily: 25 years later, a golden journey. *Blood* **2012**, *119*, 651–665. [CrossRef] [PubMed]
9. Marušič, J.; Podlipnik, Č.; Jevševar, S.; Kuzman, D.; Vesnaver, G.; Lah, J. Recognition of human tumor necrosis factor α (TNF-α) by therapeutic antibody fragment: Energetics and structural features. *J. Biol. Chem.* **2012**, *287*, 8613–8620. [CrossRef] [PubMed]
10. Pennica, D.; Lam, V.T.; Weber, R.F.; Kohr, W.J.; Basa, L.J.; Spellman, M.W.; Ashkenazi, A.; Shire, S.J.; Goeddel, D.V. Biochemical characterization of the extracellular domain of the 75-kilodalton tumor necrosis factor receptor. *Biochemistry* **1993**, *32*, 3131–3138. [CrossRef] [PubMed]
11. Loetscher, H.; Gentz, R.; Zulauf, M.; Lustig, A.; Tabuchi, H.; Schlaeger, E.J.; Brockhaus, M.; Gallati, H.; Manneberg, M.; Lesslauer, W. Recombinant 55-kDa tumor necrosis factor (TNF) receptor. Stoichiometry of binding to TNFα and TNFβ and inhibition of TNF activity. *J. Biol. Chem.* **1991**, *266*, 18324–18329. [PubMed]
12. Eck, M.J.; Sprang, S.R. The structure of tumor necrosis factor-α at 2.6 Å resolution. Implications for receptor binding. *J. Biol. Chem.* **1989**, *264*, 17595–17605. [PubMed]
13. Elliott, M.J.; Maini, R.N.; Feldmann, M.; Kalden, J.R.; Antoni, C.; Smolen, J.S.; Leeb, B.; Breedveld, F.C.; Macfarlane, J.D.; Bijl, H.; et al. Randomised double-blind comparison of chimeric monoclonal antibody to tumour necrosis factor α (cA2) versus placebo in rheumatoid arthritis. *Lancet* **1994**, *344*, 1105–1110. [CrossRef]
14. Hanauer, S.B.; Sandborn, W.J.; Rutgeerts, P.; Fedorak, R.N.; Lukas, M.; MacIntosh, D.; Panaccione, R.; Wolf, D.; Pollack, P. Human anti-tumor necrosis factor monoclonal antibody (adalimumab) in Crohn's disease: The CLASSIC-I trial. *Gastroenterology* **2006**, *130*, 323–333. [CrossRef] [PubMed]
15. Murdaca, G.; Colombo, B.M.; Cagnati, P.; Gulli, R.; Spanò, F.; Puppo, F. Update upon efficacy and safety of TNF-α inhibitors. *Expert Opin. Drug Saf.* **2012**, *11*, 1–5. [CrossRef] [PubMed]
16. Weinblatt, M.E.; Keystone, E.C.; Furst, D.E.; Moreland, L.W.; Weisman, M.H.; Birbara, C.A.; Teoh, L.A.; Fischkoff, S.A.; Chartash, E.K. Adalimumab, a fully human anti-tumor necrosis factor α monoclonal antibody, for the treatment of rheumatoid arthritis in patients taking concomitant methotrexate: The ARMADA trial. *Arthritis Rheum.* **2003**, *48*, 35–45. [CrossRef] [PubMed]
17. De Simone, C.; Amerio, P.; Amoruso, G.; Bardazzi, F.; Campanati, A.; Conti, A.; Gisondi, P.; Gualdi, G.; Guarneri, C.; Leoni, L.; et al. Immunogenicity of anti-TNFα therapy in psoriasis: A clinical issue? *Expert Opin. Biol. Ther.* **2013**, *13*, 1673–1682. [CrossRef] [PubMed]
18. Ducharme, E.; Weinberg, J.M. Etanercept. *Expert Opin. Biol. Ther.* **2008**, *8*, 491–502. [CrossRef] [PubMed]
19. Taylor, P.C. Pharmacology of TNF blockade in rheumatoid arthritis and other chronic inflammatory diseases. *Curr. Opin. Pharmacol.* **2010**, *10*, 308–315. [CrossRef] [PubMed]
20. Cohen, M.D.; Keystone, E.C. Intravenous golimumab in rheumatoid arthritis. *Expert Rev. Clin. Immunol.* **2014**, *10*, 823–830. [CrossRef] [PubMed]
21. Deeks, E.D. Certolizumab Pegol: A Review in inflammatory autoimmune diseases. *BioDrugs* **2016**, *30*, 607–617. [CrossRef] [PubMed]
22. Kaymakcalan, Z.; Sakorafas, P.; Bose, S.; Scesney, S.; Xiong, L.; Hanzatian, D.K.; Salfeld, J.; Sasso, E.H. Comparisons of affinities, avidities, and complement activation of adalimumab, infliximab, and etanercept in binding to soluble and membrane tumor necrosis factor. *Clin. Immunol.* **2009**, *131*, 308–316. [CrossRef] [PubMed]
23. Lis, K.; Kuzawińska, O.; Bałkowiec-Iskra, E. Tumor necrosis factor inhibitors—State of knowledge. *Arch. Med. Sci.* **2014**, *10*, 1175–1185. [CrossRef] [PubMed]
24. Rivkin, A. Certolizumab pegol for the management of Crohn's disease in adults. *Clin. Ther.* **2009**, *31*, 1158–1176. [CrossRef] [PubMed]
25. Bourne, T.; Fossati, G.; Nesbitt, A. A PEGylated Fab' fragment against tumor necrosis factor for the treatment of Crohn disease: Exploring a new mechanism of action. *BioDrugs* **2008**, *22*, 331–337. [CrossRef] [PubMed]

26. Suzuki, T.; Ishii-Watabe, A.; Tada, M.; Kobayashi, T.; Kanayasu-Toyoda, T.; Kawanishi, T.; Yamaguchi, T. Importance of neonatal FcR in regulating the serum half-life of therapeutic proteins containing the Fc domain of human IgG1: A comparative study of the affinity of monoclonal antibodies and Fc-fusion proteins to human neonatal FcR. *J. Immunol.* **2010**, *184*, 1968–1976. [CrossRef] [PubMed]
27. Junghans, R.P.; Anderson, C.L. The protection receptor for IgG catabolism is the β2-microglobulin-containing neonatal intestinal transport receptor. *Proc. Natl. Acad. Sci. USA* **1996**, *93*, 5512–5516. [CrossRef] [PubMed]
28. Pasut, G. Pegylation of biological molecules and potential benefits: Pharmacological properties of certolizumab pegol. *BioDrugs Suppl.* **2014**, *1*, S15–S23. [CrossRef] [PubMed]
29. Tracey, D.; Klareskog, L.; Sasso, E.H.; Salfeld, J.G.; Tak, P.P. Tumor necrosis factor antagonist mechanisms of action: A comprehensive review. *Pharmacol. Ther.* **2008**, *117*, 244–279. [CrossRef] [PubMed]
30. Mahadevan, U.; Wolf, D.C.; Dubinsky, M.; Cortot, A.; Lee, S.D.; Siegel, C.A.; Ullman, T.; Glover, S.; Valentine, J.F.; Rubin, D.T.; et al. Placental transfer of anti-tumor necrosis factor agents in pregnant patients with inflammatory bowel disease. *Clin. Gastroenterol. Hepatol.* **2013**, *11*, 286–292. [CrossRef] [PubMed]
31. Palframan, R.; Airey, M.; Moore, A.; Vugler, A.; Nesbitt, A. Use of biofluorescence imaging to compare the distribution of certolizumab pegol, adalimumab, and infliximab in the inflamed paws of mice with collagen-induced arthritis. *J. Immunol. Methods* **2009**, *348*, 36–41. [CrossRef] [PubMed]
32. Nesbitt, A.; Fossati, G.; Bergin, M.; Stephens, P.; Stephens, S.; Foulkes, R.; Brown, D.; Robinson, M.; Bourne, T. Mechanism of action of certolizumab pegol (CDP870): In vitro comparison with other anti-tumor necrosis factor alpha agents. *Inflamm. Bowel Dis.* **2007**, *13*, 1323–1332. [CrossRef] [PubMed]
33. Ueda, N.; Tsukamoto, H.; Mitoma, H.; Ayano, M.; Tanaka, A.; Ohta, S.; Inoue, Y.; Arinobu, Y.; Niiro, H.; Akashi, K.; et al. The cytotoxic effects of certolizumab pegol and golimumab mediated by transmembrane tumor necrosis factor α. *Inflamm. Bowel Dis.* **2013**, *19*, 1224–1231. [CrossRef] [PubMed]
34. Banner, D.W.; D'Arcy, A.; Janes, W.; Gentz, R.; Schoenfeld, H.J.; Broger, C.; Loetscher, H.; Lesslauer, W. Crystal structure of the soluble human 55 kD TNF receptor-human TNFβ complex: Implications for TNF receptor activation. *Cell* **1993**, *73*, 431–445. [CrossRef]
35. Mukai, Y.; Nakamura, T.; Yoshikawa, M.; Yoshioka, Y.; Tsunoda, S.; Nakagawa, S.; Yamagata, Y.; Tsutsumi, Y. Solution of the structure of the TNF–TNFR2 complex. *Sci. Signal* **2010**, *3*, ra83. [CrossRef] [PubMed]
36. Liang, S.; Dai, J.; Hou, S.; Su, L.; Zhang, D.; Guo, H.; Hu, S.; Wang, H.; Rao, Z.; Guo, Y.; et al. Structural basis for treating tumor necrosis factor α (TNFα)-associated diseases with the therapeutic antibody infliximab. *J. Biol. Chem.* **2013**, *288*, 13799–13807. [CrossRef] [PubMed]
37. Hu, S.; Liang, S.; Guo, H.; Zhang, D.; Li, H.; Wang, X.; Yang, W.; Qian, W.; Hou, S.; Wang, H.; et al. Comparison of the inhibition mechanisms of adalimumab and infliximab in treating tumor necrosis factor α-associated diseases from a molecular view. *J. Biol. Chem.* **2013**, *288*, 27059–27067. [CrossRef] [PubMed]
38. Jones, S.; Thornton, J.M. Principles of protein-protein interactions. *Proc. Natl. Acad. Sci. USA* **1996**, *93*, 13–20. [CrossRef] [PubMed]
39. Van Schie, K.A.; Ooijevaar-de Heer, P.; Dijk, L.; Kruithof, S.; Wolbink, G.; Rispens, T. Therapeutic TNF inhibitors can differentially stabilize trimeric TNF by inhibiting monomer exchange. *Sci. Rep.* **2016**, *6*, 32747. [CrossRef] [PubMed]
40. Wilson, I.A.; Stanfield, R.L. Antibody-antigen interactions: New structures and new conformational changes. *Curr. Opin. Struct. Biol.* **1994**, *4*, 857–867. [CrossRef]
41. Mitoma, H.; Horiuchi, T.; Tsukamoto, H.; Ueda, N. Molecular mechanisms of action of anti-TNF-α agents—Comparison among therapeutic TNF-α antagonists. *Cytokine* **2016**. [CrossRef] [PubMed]
42. Martin, A.C. Accessing the Kabat antibody sequence database by computer. *Proteins* **1996**, *25*, 130–133. [CrossRef]
43. Narhi, L.O.; Arakawa, T. Dissociation of recombinant tumor necrosis factor-α studied by gel permeation chromatography. *Biochem. Biophys. Res. Commun.* **1987**, *147*, 740–746. [CrossRef]
44. Corti, A.; Fassina, G.; Marcucci, F.; Barbanti, E.; Cassani, G. Oligomeric tumour necrosis factor α slowly converts into inactive forms at bioactive levels. *Biochem. J.* **1992**, *284*, 905–910. [CrossRef] [PubMed]
45. Hlodan, R.; Pain, R.H. The folding and assembly pathway of tumour necrosis factor TNFα, a globular trimeric protein. *Eur. J. Biochem.* **1995**, *231*, 381–387. [CrossRef] [PubMed]
46. Lee, J.Y.; Lee, H.T.; Shin, W.; Chae, J.; Choi, J.; Kim, S.H.; Lim, H.; Heo, T.W.; Park, K.Y.; Lee, Y.J.; et al. Structural basis of checkpoint blockade by monoclonal antibodies in cancer immunotherapy. *Nat. Commun.* **2016**, *7*, 13354. [CrossRef] [PubMed]

47. McCoy, A.J.; Grosse-Kunstleve, R.W.; Adams, P.D.; Winn, M.D.; Storoni, L.C.; Read, R.J. Phaser crystallographic software. *J. Appl. Crystallogr.* **2007**, *40*, 658–674. [CrossRef] [PubMed]
48. Adams, P.D.; Afonine, P.V.; Bunkóczi, G.; Chen, V.B.; Davis, I.W.; Echols, N.; Headd, J.J.; Hung, L.W.; Kapral, G.J.; Grosse-Kunstleve, R.W.; et al. PHENIX: A comprehensive Python-based system for macromolecular structure solution. *Acta Crystallogr. D Biol. Crystallogr.* **2010**, *66*, 213–221. [CrossRef] [PubMed]
49. Emsley, P.; Cowtan, K. Coot: Model-building tools for molecular graphics. *Acta Crystallogr. D Biol. Crystallogr.* **2004**, *60*, 2126–2132. [CrossRef] [PubMed]
50. DeLano, W.L. *The PyMOL Molecular Graphics System*; Schrödinger, LLC: New York, NY, USA, 2002.



© 2017 by the authors; licensee MDPI, Basel, Switzerland. This article is an open access article distributed under the terms and conditions of the Creative Commons Attribution (CC BY) license (http://creativecommons.org/licenses/by/4.0/).

ELSEVIER

International Journal of Pharmaceutics 185 (1999) 129–188

international journal of pharmaceutics

www.elsevier.com/locate/promis

Review

Instability, stabilization, and formulation of liquid protein pharmaceuticals

Wei Wang *

Biotechnology, Bayer Corporation, 800 Dwight Way, Berkeley, CA 94701, USA

Received 21 January 1999; received in revised form 26 April 1999; accepted 28 April 1999

Abstract

One of the most challenging tasks in the development of protein pharmaceuticals is to deal with physical and chemical instabilities of proteins. Protein instability is one of the major reasons why protein pharmaceuticals are administered traditionally through injection rather than taken orally like most small chemical drugs. Protein

Abbreviations: ADA, adenosine deaminase; ADH, alcohol dehydrogenase; AcP, acylphosphatase; BDNF, brain-derived neurotrophic factor; BGG, bovine γ-globulin; BSA, bovine serum albumin; BSF, bovine serum fetuin; CD, circular dichroism spectroscopy; CE, capillary electrophoresis; CMC-Na, carboxymethyl cellulose sodium; rhCNTF, recombinant human ciliary neurotrophic factor; rConIFN, recombinant consensus α-interferon; DGK, diacylglycerol kinase; DMSO, dimethylsulfoxide; rhDNase, recombinant human deoxyribonuclease; DSC, differential scanning calorimetry; hEGF, human epidermal growth factor; aFGF, acidic fibroblast growth factor; bFGF, basic fibroblast growth factor; rFVIII, recombinant factor VIII; pdFIX, plasma-derived factor IX; rFIX, recombinant factor IX; rFXIII, recombinant factor XIII; FTIR, Fourier transform infrared spectroscopy; GA, glucoamylase; GAPDH, glyceraldehyde-3-phosphate dehydrogenase; G-CSF, granulocyte colony-stimulating factor; GDH, glutamate dehydrogenase; met-hGH, methionyl human growth hormone; pGH, porcine growth hormone; GRF, growth hormone releasing factor; GdnHCl, guanidine hydrochloride; HP-β-CD, hydroxypropyl-β-cyclodextrin; IFN-β, interferon-β; IFN-γ, interferon-γ; hIGF-I, recombinant human insulin-like growth factor I; IL-1β, interleukin-1β; IL-1R, interleulin-1 receptor; IL-2, interleukin-2; rhIL-1ra, recombinant human interleukin-1 receptor antagonist; IR, infrared spectroscopy; rhKGF, recombinant human keratinocyte growth factor; LDH, lactate dehydrogenase; *phm*-MDH, pig heart mitochondrial malate dehydrogenase; LMW-UK, low molecular weight urokinase; rhM-CSF, recombinant human macrophage colony-stimulating factor; rhMGDF, recombinant human megakaryocyte growth and development factor; MS, mass spectroscopy; rhNGF, recombinant human nerve growth factor; NMR, nuclear magnetic resonance spectroscopy; tPA, tissue plasminogen activator; PAGE, polyacrylamide gel electrophoresis; hPAH, human phenylalanine hydroxylase; PE40, 40 kD segment of *Pseudomonas* exotoxin (PE); PEG, polyethylene glycol; *ml*-PEPC, maize leaf phosphoenolpyruvate carboxylase; PFK, phosphofructokinase; huPrP(90-231), recombinant protein corresponding to the human prion protein domain (residues 90-231); PVA, polyvinylalcohol; PVP, polyvinylpyrrolidone; rhPTH, recombinant human parathyroid hormone; RP-HPLC, reversed phase HPLC; RNase A, ribonuclease A; SDS, sodium dodecyl sulfate; SEC-HPLC, size exclusion HPLC; TGF, transforming growth factor; TMAO, trimethylamine *N*-oxide; TP40, Cys-replaced (with Ala in PE40) mutant of TGF-α-PE40; rhTPO, recombinant human thrombopoietin; YEI, yeast external invertase.

* Tel.: +1-510-705-4755; fax: +1-510-705-5629.

E-mail address: wei.wang.b@bayer.com (W. Wang)

0378-5173/99/$ - see front matter © 1999 Elsevier Science B.V. All rights reserved.

PII: S0378-5173(99)00152-0

pharmaceuticals usually have to be stored under cold conditions or freeze-dried to achieve an acceptable shelf life. To understand and maximize the stability of protein pharmaceuticals or any other usable proteins such as catalytic enzymes, many studies have been conducted, especially in the past two decades. These studies have covered many areas such as protein folding and unfolding/denaturation, mechanisms of chemical and physical instabilities of proteins, and various means of stabilizing proteins in aqueous or solid state and under various processing conditions such as freeze-thawing and drying. This article reviews these investigations and achievements in recent years and discusses the basic behavior of proteins, their instabilities, and stabilization in aqueous state in relation to the development of liquid protein pharmaceuticals. © 1999 Elsevier Science B.V. All rights reserved.

Keywords: Denaturation; Unfolding; Melting; Aggregation; Degradation; Preferential interaction

1. Introduction

The advent of recombinant DNA technology has led to a worldwide zeal to develop protein pharmaceuticals in the past two decades. These protein pharmaceuticals or pharmaceutical candidates include functional regulators and supplements, enzyme activators and inhibitors, poly- and monoclonal antibodies, and various vaccines. In comparison with small chemical drugs, protein pharmaceuticals have high specificity and activity at relatively low concentrations. These features have made protein pharmaceuticals indispensable in combating human diseases.

Due to advances in analytical separation technology, recombinant proteins can now be purified to an unprecedented level (Bond et al., 1998). Highly purified protein pharmaceuticals significantly reduce the known and unknown potential side or even toxic effects. However, one of the most challenging tasks remains in the development of protein pharmaceuticals: dealing with physical and chemical instabilities of proteins. Protein instability is one of the two major reasons why protein pharmaceuticals are administered traditionally through injection rather than taken orally like most small chemical drugs (Wang, 1996). Protein pharmaceuticals usually have to be stored under cold conditions or even freeze-dried to a solid form to achieve an acceptable shelf life.

In search for ways of stabilizing proteins, scientists turned their attention to nature for an answer. It is well known that certain natural organisms can grow well at extreme temperatures. Hyperthermophilic organisms (hyperthermophiles) such as anaerobic, methanogenic, or sulfate-reducing archaebacteria grow at temperatures near or above 100°C (Huber et al., 1989; Adams, 1993, 1994). Proteins in these organisms function normally at high temperatures. For example, enolase and α-glucosidase in hyperthermophilic *Pyrococcus furiousus* have optimum activity, at >90 and >105°C, respectively (Costantino et al., 1990; Peak et al., 1994). The most thermostable proteins found so far have half-lives in excess of 10 min at 130°C (Daniel et al., 1996). The mechanisms responsible for the high molecular stability of thermophilic proteins include increased hydrophobic interactions, greater molecular packing, more H-bonds, more salt-bridging, loss of surface loops, more helix-forming amino acids, restricted N-terminus mobility, etc. (Vieille and Zeikus, 1996; Cowan, 1997; Vogt and Argos, 1997). Extrinsic factors (not primary structure-related) have also contributed to protein stabilization. One of these is the high cellular content of sugars, salts, or other organic solutes/osmolytes, such as α-glutamate, di-myo-inositol-phosphate and its isomer, β-mannosylglycerate, and diglycerol-phosphate (Huber et al., 1989; Rupley and Careri, 1991; Martins and Santos, 1995; Martins et al., 1997; Ramakrishnan et al., 1997).

The identification of intrinsic and extrinsic factors that contribute to the stabilization of thermophilic proteins has provided valuable information for stabilizing protein pharmaceuticals and for designing more stable mutant proteins. Yet the structural differences among different proteins are so significant that generalization of universal stabilization strategies has not been successful. Very often, proteins have to be evaluated individually and stabilized on a trial-and-error basis.

To understand and maximize the stability of protein pharmaceuticals or any other usable proteins such as various catalytic enzymes, many studies have been conducted in the past few decades. These studies have been reviewed with emphasis on general protein stability (Jaenicke, 1991; Kristjánsson and Kinsella, 1991), mechanisms of chemical and physical instabilities of proteins (Manning et al., 1989), mechanisms and prevention of major protein degradation pathways (Cleland et al., 1993), and various means of stabilizing proteins in aqueous or solid state and under various processing conditions such as freeze-thawing or drying (Gianfreda and Scarfi, 1991; Arakawa et al., 1993; Timasheff, 1993; Manning et al., 1995; Wong and Parascrampuria, 1997). This article reviews these investigations and achievements in recent years and discusses the basic behavior of proteins, their instabilities, and stabilization in aqueous state in relation to the development of liquid protein pharmaceuticals.

2. Basic protein behavior and properties

Protein pharmaceuticals, unlike small drug molecules, have high molecular weight (>5 kD). Their large size, compositional variety, and amphipathic characteristics constitute specific behavior such as folding, conformational stability, and unfolding/denaturation. Understanding proteins' basic behavior may help toward their stabilization.

2.1. Protein folding and its related forces and stability

Biologically active proteins are properly folded. The number of possible conformations of a folded polypeptide chain with an average domain size is about 10^{80} (Jaenicke, 1991). The three-dimensional folded state of a protein is a fluctuating state of a limited number of preferred conformations (Tang and Dill, 1998). The most stable (least energy) conformation of a protein is usually the native state (Darnell et al., 1986). Under native conditions the vast majority of protein molecules exist in their unique native state (N). A tiny fraction must also occupy all possible higher energy states as dictated by the Boltzmann relationship (Bai and Englander, 1996).

2.1.1. Protein Folding Process

Folding of newly-synthesized polypeptides in cells requires the assistance of so-called molecular chaperone proteins (Hendrick and Hartl, 1995). These proteins bind unfolded or partially folded polypeptides in their central cavity and promote folding by ATP-dependent cycles of release and rebinding. The molecular chaperone GroEL facilitates protein folding by preventing protein aggregation and correcting protein misfolding (Golbik et al., 1998). Protein folding is generally a highly cooperative process, in which only the native and unfolded states are stable (Goto and Fink, 1989).

When a protein folds, about 80% of nonpolar side chains (Ala, Val, Ile, Leu, Met, Phe, Trp, Cys) are buried in the interior of protein molecules out of contact with water. For example, folding of RNase T1, a compact globular protein (104 aa), removes about 85% of nonpolar residues from contact with water (Thomson et al., 1989). More than 80% of amino acids in globular proteins exist in α-helix/β-sheet or in the turns connecting them (Pace et al., 1996).

The rate of protein folding is usually high. Many small proteins can fold in milliseconds or less (Dobson and Hore, 1998). Some may fold at a slower rate. For example, the folding of a bacteria protein MerP (72 aa) by diluting the protein solution containing 3 M guanidine hydrochloride (GdnHCl) shows two exponential phases. The initial phase is fast with a rate constant of 1.2/s, but the second phase is slow with a rate constant of 0.053/s, accounting for about 20% of the folding signal (Aronsson et al., 1997). Folding of proteins involving Pro isomerization is also relatively slow.

2.1.2. Major forces involved in protein folding

Many forces are involved in protein folding. These include hydrophobic interactions, electrostatic interactions (charge repulsion and ion pairing), hydrogen bonding, intrinsic propensities, and van der Waals forces. Hydrophobic interactions are repulsive interactions between water and

non-polar residues in proteins, leading to minimal hydration of the hydrophobic core. These interactions are strongly disfavored and associated with a large increase in heat capacity (Dill, 1990). A hydrogen bond is the strong dipole–dipole attraction between covalently-bonded hydrogen atoms and other strongly electronegative atoms such as oxygen and nitrogen. It is primarily a linear arrangement of donor, hydrogen, and acceptor. Hydrogen bonds between amide hydrogen and carbonyl oxygen make up 68% of the total hydrogen bonds in globular proteins (Pace et al., 1996).

Among all the forces involved in protein folding, the apparent dominant force is hydrophobic interaction (Jaenicke, 1990; Kristjánsson and Kinsella, 1991). The dominant opposing force is the loss of non-local conformational entropy (Dill et al., 1989; Dill, 1990). The difference in heat capacity of a protein in the native folded and denatured states (ΔC_p) is a measure of hydrophobic stabilization of the protein, and the large ΔC_p on thermal denaturation of proteins supports the major role of hydrophobic interactions in protein stabilization (Wang et al., 1996a). Recently, it was found that the contribution of electrostatic interactions in proteins at neutral conditions to the free energy difference between the folded and unfolded states is close to 0, indicating that the main driving forces for protein folding under these conditions are hydrophobic and hydrogen-bonding interactions (Dimitrov and Crichton, 1997).

Hydrophobic interaction, albeit dominant, needs to be balanced to maintain protein activity. In studying the stability of mutant Rop proteins, Munson et al. (1996) demonstrated that underpacking the hydrophobic core with small amino acids like Ala not only loses protein activity but also decreases protein stability. On the other hand, overpacking the hydrophobic core with only large amino acids like Leu stabilizes proteins but protein activity is lost. This indicates that both favorable steric interaction and burial of sufficient hydrophobic volume and surface area are important to stabilize a protein.

Protein molecular packing may be the most applicable factor that leads to the unique structures of most globular proteins (Richards, 1997). The packing in native proteins is so well arranged that all solvent molecules are essentially excluded and the protein interior is more like a crystalline solid than a non-polar liquid (Jaenicke, 1991). Glu, Lys, and Arg, with three or four rotatable bonds, are almost invariably located on the protein surface and use their flexibility to help ensure exposure of their charged groups to the solvent. However, buried polar residues do not necessarily destabilize a protein if they can form stable hydrogen bonds (Pace et al., 1996) and/or form stable intramolecular salt bridges, enhancing the structural rigidity (Vieille and Zeikus, 1996).

Interaction forces in proteins can also be divided into two types: local (short-ranged or secondary) and non-local (long-ranged or tertiary) (Chan and Dill, 1991). Long-range interactions happen between two residues that are separated by at least ten residues (Dosztányi et al., 1997). Long-range interactions such as parallel and antiparallel sheets are mainly responsible for polymer collapse to compact states whereas local forces are mainly responsible for helix formation such as hydrogen bonding. It seems that long-range interactions (non-local forces) control overall protein stability. The dominant role of long-range interactions in protein stability is supported by recent identification of so-called elements of stabilization center (SC) in proteins. By long-range interactions, these SCs, mainly consisting of hydrophobic residues that are less flexible, tend to connect more sheets to each other, and are primarily responsible for stabilization of protein structures (Dosztányi et al., 1997). If different proteins have similar structural folds, their conformational stability may still be very different due to the difference in their primary sequences (Chiti et al., 1998).

2.1.3. Protein folding and free energy change

The folded state of proteins has conformational stability, which is defined as the free energy change, $\Delta G_{f\rightarrow u}$ (or simply ΔG), for the unfolding/denaturation reaction under physiological conditions (Pace, 1990). The larger the $\Delta G_{f\rightarrow u}$, the more stable the protein. The folded state of proteins is only marginally more stable than the unfolded state since its $\Delta G_{f\rightarrow u}$ is small. The $\Delta G_{f\rightarrow u}$

for proteins has been reported in the following ranges: 21–63 kJ/mol (Kristjánsson and Kinsella, 1991); 5–20 kcal/mol (Volkin and Klibanov, 1989); or 5–10 kcal/mol (Jaenicke, 1990; Pace et al., 1996).

The low $\Delta G_{f\rightarrow u}$ values indicate that conformational stability of a protein in aqueous solution is equivalent to a few H-bonds or ion pairs. A single hydrogen bond can lower the protein's free energy by 0.5–2 kcal/mol and an ion pair by 0.4–1.0 kcal/mol (Vogt and Argos, 1997). After analyzing more than a dozen mutant proteins, Pace et al. (1996) found that average free energy gain is 1.1–1.6 kcal/mol per hydrogen bond and 1.18 kcal/mol per -CH_2- for hydrophobic effect. These values suggest significant contribution of hydrogen bonding to $\Delta G_{f\rightarrow u}$ relative to that from hydrophobic effect, however, if the polar groups must be buried to form intramolecular hydrogen bonds, the net gain is only about 0.6 kcal/mol per hydrogen bond. In comparison, the strength of a hydrogen bond in water is about 5 kcal/mol, and the energy of van der Waals interaction amounts to about 1 kcal/mol at 25°C (Darnell et al., 1986).

2.2. Protein unfolding/denaturation

In solution, the folded state of any protein is not infinitely stable (Shortle, 1996). It may unfold/denature into an inactive form—a process of protein conformational changes. These conformational changes are due to predominant intermolecular protein–solvent interactions over intramolecular interactions, which keeps the folded state (Jaenicke, 1990). On the other hand, solvent-induced inactivation of proteins may occur without disruption of protein conformation (tertiary structure) (Cowan, 1997).

2.2.1. Protein unfolding process

Protein unfolding can be described generally by a single transition step between the completely folded and unfolded states since any intermediate state is highly unstable and only exists in negligible amounts (Chan and Dill, 1991; Jaenicke, 1991). This is true at least for small globular proteins (Kristjánsson and Kinsella, 1991). Others may have more than one unfolding process such as human placental alkaline phosphatase (Hung and Chang, 1998).

The following equation describes the two-state model:

$$\mathrm{N\ (native)} \leftrightharpoons \mathrm{U\ (unfolded/denatured)} \Rightarrow \mathrm{A\ (aggregated)}$$

or

$$\mathrm{P_{folded}} \leftrightharpoons \mathrm{P_{unfolded}} \Rightarrow \mathrm{A}.$$

For most proteins, the unfolded state (U) is insoluble and favors aggregation. Under certain conditions, a particular U state exists, which is highly compact and has significant amounts of residual secondary structures such as thermally-unfolded RNase T1 (Pancoska et al., 1996) and acid-unfolded apomyoglobin (Staniforth et al., 1998). This particular U state is termed molten globule (Goto and Fink, 1989; Shortle, 1996).

The N state may unfold reversibly or, depending on the condition, irreversibly to the U state. For example, unfolding of wild-type barnase and some of its mutants are reversible based on the repeatability of DSC endotherms or CD transitions on rescanning (Johnson et al., 1997). Thermal treatment of IFN-β-1a (Runkel et al., 1998) and β-galactosidase (Yoshioka et al., 1994a) causes irreversible denaturation of both proteins and eventually leads to formation of aggregates (A).

Proteins unfold locally and globally. Local and global unfolding occur concurrently and independently. Increasing denaturant concentration or temperature can selectively promote global unfolding because global unfolding exposes more surface and gives rise to higher chain entropy and enthalpy (at high temperatures) than local unfolding (Bai et al., 1994).

An important thermodynamic parameter in two-state transition is the change in heat capacity, ΔC_p. The large and positive ΔC_p observed in protein denaturation is due primarily to exposure of nonpolar groups (Pace et al., 1996; Johnson et al., 1997). The molar enthalpy of protein denaturation, ΔH, at low temperatures may be either positive or negative but increases markedly with temperature. Since the driving force for protein unfolding is the increased conformational entropy

in aqueous solution, $\Delta S_{f\rightarrow u}$ is expected to be positive.

2.2.2. Protein unfolding/melting temperature

Proteins unfold above certain temperatures. During a thermal unfolding process, the temperature at which 50% of protein molecules are unfolded ($\Delta G = 0$ at this time) is defined as the unfolding (or melting/denaturation/transition) temperature (T_m). Thermal unfolding of a protein is usually endothermic. The T_m of many proteins have been determined (Table 1) and appear mostly in the range of 40–80°C. When the level of protein hydration decreases, T_m may increase sharply due to destabilization of the unfolded state (Rupley and Careri, 1991).

The higher the T_m, the greater the thermal resistance of a protein. For example, glyceraldehyde-3-phosphate dehydrogenase (GAPDH) from hyperthermophilic bacterium *Thermotoga maritima* has a melting temperature of 109°C (Jaenicke, 1996). However, there is no particular relationship between T_m and protein stability as measured by $\Delta G_{f\rightarrow u}$ (Dill et al., 1989). For example, the T_m of serum albumin from different sources has the following order: human (59.7°C) > dog (59.5°C) > rabbit (57.8°C) > rat (57.6°C) > bovine (56.8°C), yet their temperatures of maximum stability (ΔG) are all similar at about 20°C (Kosa et al., 1998). The ΔGs of three SH3 domains of the Tec family of tyrosine kinases are below 12–16 kJ/mol, but their melting temperatures are relatively high between 69 and 80°C (Knapp et al., 1998).

A protein may have two or more melting temperatures, depending on the experimental conditions and analytical techniques used (Table 1). For example, Kosa et al. (1998) demonstrated that dog and rabbit albumin have one transition, but human, bovine, and rat albumin have two transitions, suggesting the presence of a stable intermediate. The apical domain (residues 191–376) of GroEL protein shows two reversible melting temperatures at 35 and 67°C by far UV CD, which are attributed to unfolding of the C-terminal helices and the domain core, respectively. Protein huPrP(90–231) has one melting temperature in the presence of GdnHCl at pH 5.0 and 7.2, but shows two transition temperatures at pH 3.6 and 4.0 with a stable unfolding intermediate (Swietnicki et al., 1997). By DSC, interleukin-1 receptor (IL-1R, 50 kD) shows two unfolding transitions near 48°C and 65°C, but after deconvolution, three melting transition peaks are identified, representing three different domains in the protein (Remmele et al., 1998).

Multimeric, chimeric, or modular proteins often have more than one melting temperature. For example, native recombinant human placental factor XIII (rFXIII) is a non-covalent dimer and each subunit consists of 3 thermolabile domains (56 kD, N-terminal) and two thermostable domains (24 kD, C-terminal). The intact protein melts in two distinct temperature regions by DSC: 69°C at pH 8.6, representing three thermolabile domains; and 90°C in 2 M GdnHCl, representing two thermostable domains (Kurochkin et al. 1995). The chimeric protein toxin sCD4(178)-PE40 (sCD4-PE40), consisting of HIV binding domains of the T-cell membrane protein (CD4) and the cytotoxic domains of *Pseudomonas* exotoxin A (PE-40), has two transition temperatures originating from both components. In addition, unfolding of the less stable PE-40 induces unfolding of the more stable CD4 component because the free form of CD4 denatures at a higher temperature (56°C) than that in the protein complex (46°C) at pH 6.5 (Davio et al., 1995).

2.3. Mesophilic versus thermophilic proteins

In describing basic properties of proteins, it is necessary to mention thermophilic proteins, a different class of proteins having much higher thermostability than that of mesophilic counterparts like those in humans. Mesophilic proteins usually retain their native structures over a narrow range of temperatures from about 5 to 50°C. For thermophilic proteins, the upper limit of thermostability is usually 20 to 30°C higher, corresponding to an increase in protein stability by 5–7 kcal/mol. A ΔG of this order may be achieved by 1 or 2 additional salt bridges inside the protein globule, several additional hydrogen bonds, or 7–10 additional CH_3- groups in the hydrophobic nucleus of the protein (Mozhaev and Martinek, 1984).

Table 1
Melting temperatures (T_m) of proteins

Proteins	Protein solution compositions	Methods	T_m (°C)	References
AcP (98 aa)	0.4 mg/ml in 50 mM acetate, pH 5.5	CD (222 nm)	57	Chiti et al., 1998
HSA (66 kD)	20 μM in 100 mM phosphate, pH 7.4	Fluorescence (λ_{em} = 345 nm)	62	Farruggia et al., 1997
	88 μM in 100 mM phosphate, pH 7.4	DSC	63	Picó, 1995
	0.1 mM in 67 mM phosphate, pH 7.4	DSC	60	Kosa et al., 1998
BSF (48 kD)	2.5 mg/ml in 50 mM phosphate, pH 6	DSC	60	Wang et al., 1996a
	2.5 mg/ml in 50 mM phosphate, pH 7	DSC	54	Wang et al., 1996a
	2.5 mg/ml in 50 mM phosphate, pH 8	DSC	48	Wang et al., 1996a
α-Chymotrypsin	0.3 mg/ml in 10 mM phosphate, pH 6.0	UV (281 nm)	47	Lozano et al., 1997
	0.3 mg/ml in 10 mM phosphate, pH 7.0	UV (281 nm)	44	Lozano et al., 1997
	0.3 mg/ml in 10 mM phosphate, pH 8.0	UV (281 nm)	42	Lozano et al., 1997
Cytochrome c	2 mg/ml in 600 mM NaCl	DSC	77	Lo and Rahman, 1998
rhDNase	10 mg/ml in water, pH 6.8	DSC	67	Chan et al., 1996
Elastase	20 mg/ml in 10 mM acetate, pH 5.0	DSC	66	Chang et al., 1993
aFGF	100 μg/ml in PBS, pH 7.2	CD (228 nm)	45	Volkin et al., 1993
bFGF	1 mg/ml in phosphate-citrate-borate, pH 4	DSC	50	Wang et al., 1996b
	1 mg/ml in phosphate-citrate-borate, pH 9	DSC	64	Wang et al., 1996b
GA (82 kD)	1.8 mg/ml in 50 mM phosphate, pH 6	DSC	64	Wang et al., 1996a
	1.8 mg/ml in 50 mM phosphate, pH 7	DSC	62	Wang et al., 1996a
	1.8 mg/ml in 50 mM phosphate, pH 8	DSC	58	Wang et al., 1996a
rhGH (22 kD)	0.18 mg/ml in 10 mM citrate, pH 6.0	CD (222 nm)	89	Bam et al., 1998
	1 mg/ml in 10 mM citrate, pH 6.0	CD (222 nm)	81	Bam et al., 1998
	3 mg/ml in 10 mM citrate, pH 6.0	CD (222 nm)	79	Bam et al., 1998
IgG (mouse)	3.3 mg/ml in 5 mM phosphate, pH 6.0	DSC	74	Vermeer et al., 1998
Recombinant IFN-β-1a	100 μg/ml in 100 mM Na_2HPO_4, 200 mM NaCl, pH 7.2	UV (280 nm)	67	Runkel et al. 1998
Recombinant IFN-β-1a, deglycosylated	100 μg/ml in 100 mM Na_2HPO_4, 200 mM NaCl, pH 7.2	UV (280 nm)	63	Runkel et al. 1998
Lysozyme	In 0.1 M NaCl, 0.1 M acetate, pH 5.4	CD	66	Shoichet et al., 1995
	In 50 mM citrate, pH 4.0	DSC	74	Liu and Sturtevant, 1996
	In 50 mM citrate and 1 M sucrose, pH 4.0	DSC	80	Liu and Sturtevant, 1996

Table 1 (continued)

Proteins	Protein solution compositions	Methods	T_m (°C)	References
M-CSF	1.2 mg/ml in 20 mM PolyB buffer	DSC	87	Schrier et al., 1993
wt-hPAH (452 aa)	14-18 mg/ml in 20 mM HEPES buffer, pH 7.4	IR, peak ratio of 1619 to 1650 cm^{-1}	57	Chehin et al. 1998
RNase A	In 0.04 M glycine, pH 2.8	UV (287 nm)	41	Lin and Timasheff, 1996
	In 0.03 M MES, pH 5.8	UV (287 nm)	60	Lin and Timasheff, 1996
	In 0.03 potassium phosphate, pH 6.7	UV (287 nm)	64	Lin and Timasheff, 1996
	2 mg/ml in 600 mM NaCl	DSC	62	Lo and Rahman, 1998
	0.1 mg/ml in water	CD (222 nm)	65	Tsai et al., 1998a
	0.2 mg/ml in 20 mM citric acid, pH 2.3	CE	36	McIntosh et al., 1998
	0.2 mg/ml in 20 mM citric acid, pH 3.1	CE	49	McIntosh et al., 1998
	0.2 mg/ml in 20 mM citric acid, pH 3.1	CD (222 nm)	50	McIntosh et al., 1998
	About 2 mg/ml in 50 mM glycine, pH 2.8	DSC	48	Liu and Sturtevant, 1996
	About 2 mg/ml in 50 mM citrate, pH 6.0	DSC	65	Liu and Sturtevant, 1996
	About 2 mg/ml in 50 mM citrate and 1 M sucrose, pH 6.0	DSC	70	Liu and Sturtevant, 1996
	About 2 mg/ml in 50 mM citrate and 1 M glycine, pH 6.0	DSC	68	Liu and Sturtevant, 1996
RNsae H	25 μg/ml in 5 mM HEPES and 0.8 M GdnHCl, pH 8	CD (222 nm)	30	Goedken and Marqusee, 1998
	25 μg/ml in 5 mM HEPES, 0.8 M GdnHCl, and 1 mM $MnCl_2$, pH 8	CD (222 nm)	41	Goedken and Marqusee, 1998
wt-RNase T1	About 1 mg/ml in 30 mM MOPS, pH 7	Optical rotation (295 nm)	48	Shirley et al., 1989
	About 0.2 mg/ml in 30 mM MOPS, pH 7	UV (286 nm)	48	Thomson et al. 1989
	About 0.2 mg/ml in 30 mM MOPS, pH 7	CD (238 nm)	47	Thomson et al., 1989
	About 0.2 mg/ml in 30 mM MOPS, pH 7	CD (284 nm)	48	Thomson et al., 1989
Thrombin	1 mg/ml in 25 mM phosphate and 400 mM NaCl, pH 6.5	DSC	57	Boctor and Mehta, 1992
	1 mg/ml in 25 mM phosphate and 400 mM NaCl, pH 7.9	DSC	54	Boctor and Mehta, 1992
	1 mg/ml in 25 mM phosphate and 400 mM NaCl, pH 9.9	DSC	48	Boctor and Mehta, 1992
TP40 (40kD)	0.1mg/ml, pH 7.2	Fluorescence	42	Sanyal et al., 1996
	0.1mg/ml, pH 7.2	CD	55	Sanyal et al., 1996
	1 mg/ml, pH 7.2	DSC	48	Sanyal et al., 1996
Trypsin	1.5 mg/ml in HCl solution, pH 2.5	DSC	52	Boctor and Mehta, 1992
YEI (240 kD)	2 mg/ml in 50 mM phosphate, pH 6.0	DSC	63	Wang et al., 1996a
	2 mg/ml in 50 mM phosphate, pH 7.0	DSC	52	Wang et al., 1996a
	2 mg/ml in 50 mM phosphate, pH 8.0	DSC	48	Wang et al., 1996a

There are seemingly two basic mechanisms responsible for enhanced thermal stability of thermophilic proteins. First, thermophilic proteins may possess structural characteristics different from those of mesophilic proteins. These structural characteristics include (1) increased hydrophobic interactions; (2) formation of extra hydrogen bonds and/or salt bridges; (3) more compact protein structures (may have crystal-like density); and (4) presence of few Cys, high content of Arg, and low content of Lys (Mozhaev and Martinek, 1984; Vieille and Zeikus, 1996; Vogt and Argos, 1997). The second mechanism of stabilization is favorable interactions of proteins with other cellular components or accumulated low-molecular-weight compounds/osmolytes as thermoprotectants. The interaction reduces the contact area of nonpolar fragments in proteins with water, leading to a decrease in free energy of the system and stabilization of proteins. These osmolytes include potassium salt, sugars, α-glutamate, cyclic 2, 3-diphosphoglycerate (DPG), 2-*O*-β-mannosylglycerate, di-glycerol-phosphate, and di-myo-inositol-1,1′(3,3′)-phosphate (Mozhaev and Martinek, 1984; Huber et al., 1989; Rupley and Careri, 1991; Martins and Santos, 1995; Martins et al., 1997).

Is there a major force that contributes the most to stability of thermophilic proteins? Many thermophilic proteins show good correlation between stability and high hydrophobicity as measured by the hydrophobic index, a ratio of the volumes of polar to nonpolar amino acids (Mozhaev and Martinek, 1984). Detailed analysis indicates that protein stability depends not on total content of hydrophobic amino acid residues but on those inside the protein. Recent findings suggest that hydrogen bonding may play a major role in stabilizing thermophilic proteins. By comparing a group of thermostable proteins, Vogt and Argos (1997) recently concluded that increasing hydrogen bonding density at the protein surface is a major factor for increased thermal stability. After analyzing 16 protein families containing a total of 56 proteins from thermophilic, mesophilic, and thermophobic sources, Vogt et al. (1997) found that hydrogen bonding can provide the most general explanation for thermal stability in proteins because over 80% of the protein families show correlation between thermostability and an increase in the number of hydrogen bonds.

Secondary structure also contributes to enhanced stability of thermophilic proteins (Vogt and Argos, 1997). The α-helix and loops/turns are stabilized in thermophilic proteins. Ala residues (with high helix propensity) are prevalent in helical structures, and loops are often shorter in thermozymes (Vieille and Zeikus, 1996). Two facets of intrahelical interactions—the intrinsic helical propensities of amino acids and side chain interactions, are found to be the main contributors to protein thermostability, and an enhanced total stability of α-helices is a general feature of many thermophilic proteins (Petukhov et al., 1997).

3. Protein instability and its influencing factors and analytical monitoring

One of the most troubling and challenging tasks in the development of liquid protein pharmaceuticals is to deal with their physical and chemical instabilities. The most common physical instability is protein aggregation, which can be induced and/or affected by a variety of factors and chemical transformations. Careful examination of these stability-influencing factors may help to prevent or mitigate certain stability problems. In addition, selection of proper and adequate analytical methods for efficient and accurate monitoring of protein instability may ensure successful development of quality protein products.

3.1. Protein aggregation—a major event of physical instability

Under certain conditions (or simply with time), the secondary, tertiary, and quaternary structure of a protein may change and lead to protein unfolding and/or aggregation, a major event of physical instability. Protein aggregates may have no or reduced activity, reduced solubility, and altered immunogenicity. Presence of any insoluble aggregates in a protein pharmaceutical is generally not acceptable for product release.

3.1.1. Mechanisms of protein aggregation

Protein aggregation in many cases results from intermolecular association of partially denatured protein chains (Fields et al., 1992). Recent evidence suggests that aggregation may occur by specific interaction of certain conformations of protein intermediates rather than by nonspecific coaggregation (Speed et al., 1996). The aggregation process can be roughly divided into three steps: initiation, propagation, and termination (Roefs and De Kruif, 1994).

Proteins aggregate to minimize thermodynamically unfavorable interactions between solvent and exposed hydrophobic residues of proteins. Hydrophobic interaction, the reluctance of nonpolar groups to be exposed to water, is considered to be the major driving force for both protein folding and aggregation. Both protein aggregation and folding represent a balance of exposed and buried hydrophobic surface areas (Patro and Przybycien, 1996). The balance is so delicate that a change of one amino acid in a protein may substantially change its aggregation behavior (Fields et al., 1992).

Protein aggregation may be induced by a variety of physical factors, such as temperature, ionic strength, vortexing, surface/interface adsorption, etc. These factors can increase the hydrophobic surface area of proteins, causing aggregation. For example, recombinant human keratinocyte growth factor (rhKGF) undergoes slow unfolding at elevated temperatures, leading to immediate aggregation and precipitation (Chen et al., 1994a). Recombinant porcine growth hormone (pGH) at 0.5 mg/ml precipitates with time at 63°C (Charman et al., 1993). Vortexing hGH (22 kD) solutions (0.5 mg/ml at pH 7.4) for 1 min denature 67% as insoluble aggregates (Katakam et al., 1995). These influencing factors will be discussed in detail in Section 3.3.

Protein aggregation may result from chemical degradations or modifications and subsequent exposure of the hydrophobic surface(s). Proteins can directly form covalent aggregates such as insulin (Strickley and Anderson, 1997) or aggregate indirectly such as human relaxin after oxidation of His and Met residues (Li et al., 1995a). Both physical and chemical aggregations may occur simultaneously. For example, bFGF in citrate buffer (pH 5) forms intact and truncated dimers and trimers after storage at 25°C for 7 weeks (Shahrokh et al., 1994a). Freeze-dried β-galactosidase aggregates and forms insoluble precipitates via covalent disulfide bonding during storage, while non-covalent interaction causes aggregation but forms soluble precipitates in solution (Yoshioka et al., 1993). Protein aggregates, like proteins, may have isomeric forms such as IL-1ra dimers (Chang et al., 1996a).

Protein aggregation may start from a single protein molecule (unimolecular/intramolecular process) or more than one protein molecule (multimolecular/intermolecular process). Unimolecular processes include β-elimination and intrachain disulfide scrambling or formations such as IL-1ra in aqueous solution (Chang et al., 1996a). Examples of multimolecular aggregation include thiol-disulfide interchange for bovine serum albumin, thiol-catalyzed disulfide exchange for insulin, other covalent aggregation such as ribonuclease A, and non-covalent aggregation such as tetanus toxoid (Costantino et al., 1994a). If the percentage of precipitates/aggregates increases with increasing protein concentrations, multimolecular aggregation/precipitation processes may be involved such as aggregation of hIGF-I (Charman et al., 1993; Fransson et al., 1996).

Protein aggregation may or may not follow first-order kinetics (Pikal et al., 1991). The formation of IL-1ra dimers in aqueous solution during storage follows first-order kinetics (Chang et al., 1996a). Both heat and denaturant-induced aggregations of recombinant human interferon-γ (IFN-γ) apparently follow first-order kinetics (Kendrick et al., 1998a,b). At 60°C, the aggregation/precipitation of IL-1β follows apparent first-order behavior to 30% drug remaining, but at or below 55°C, it deviates and becomes biphasic (slow and fast) (Gu et al., 1991). Biphasic aggregation has also been observed for aFGF in phosphate buffer (pH 7.4) at 50°C.

Many agents can be used to probe possible mechanisms of protein aggregation. Denaturants such as sodium dodecyl sulfate (SDS), GdnHCl, and urea can be used to determine whether protein aggregation is covalent in nature. If

protein aggregates can be dissolved in these agents, formation of these aggregates is probably non-covalent. Otherwise, covalent/chemical aggregation is suggested. Examples of non-covalent aggregation evidenced by this method include chymotrypsinogen (Allison et al., 1996), insulin (Sluzky et al., 1991), and IL-1β (Gu et al., 1991). Similarly, reducing agents such as DTT or β-mercaptoethanol can be used to determine any involvement of disulfide bonds in protein aggregation. Since these reducing agents may have limited dissolution capability, denaturants are often included for complete dissolution of protein aggregates.

Nevertheless, there are cases in which experimental results may lead to inaccurate or even incorrect interpretation. For example, the insoluble aggregates of hGH can be completely dissolved in either 1 or 2% SDS. SEC-HPLC analysis of the solubilized aggregates indicates presence of both protein monomers and dimers in 1% SDS, suggesting possible covalent aggregation, but only monomers are found in 2% SDS, suggesting non-covalent aggregation (Katakam et al., 1995). This example illustrates that denaturants may not be able to dissolve non-covalent protein aggregates depending on their concentrations. As a matter of fact, non-covalent insulin fibrils cannot be dissolved in 7 M urea from pH 2 to 8, 5 M GdnHCl, 50% acetonitrile, or detergents (Brange et al., 1997). The failure of these agents to dissolve insulin fibrils suggests that these substances do not have access to the interfaces of insulin molecules due to strong hydrophobic interactions in fibrils.

Protein aggregation may be probed by computer simulation. Agitation or hydrophobic surface-induced aggregation of insulin has been modeled by computer simulation and the model predicts rather reliably the effect of protein concentration, agitation rate, and hydrophobic surface area on insulin aggregation (Sluzky et al., 1991, 1992). Recently, the colloid aggregation process has been simulated by a cluster–cluster aggregation (CCA) process. The heat-induced aggregation of BSA at pH 7.0 seems to fit the reaction-limited CCA model; at pH 5.1, it fits diffusion-limited CCA model (Hagiwara et al., 1996).

3.1.2. Reversibility of Protein Aggregation

Protein aggregation can be reversible or irreversible. Generally speaking, aggregation is irreversible if the aggregates cannot be resolubilized in denaturing and reducing agents. The aggregation and precipitation of apomyoglobin formed in 0.5–4 M urea is reversible, as the precipitates can be dissolved in 8 M urea and further dilution leads to protein refolding (De Young et al., 1993). Thermally-induced protein aggregation is often irreversible. Thrombin in solution aggregates and loses its clotting activity irreversibly when heated to 85°C (Boctor and Mehta, 1992). Thermally-induced precipitation of recombinant pGH is irreversible (Charman et al., 1993).

What determines reversibility of protein aggregation? Patro and Przybycien (1996) simulated the structure of reversible protein aggregates as a function of protein surface characteristics and protein–protein interactions. They demonstrated that the structure and morphology of protein aggregates are profoundly affected by the surface characteristics of protein monomers. Both the extent and distribution of hydrophilic and hydrophobic sites on protein surface affect aggregate properties kinetically and thermodynamically. Although physical properties of reversible and irreversible aggregates are similar, reversible aggregates are more stable energetically, more ordered (or crystal-like), and less dense than irreversible counterparts. An increase in the extent of monomer hydrophobic surface area can result in decreased solvent-exposed hydrophobic surface area and lower free energy, forming preferably reversible aggregates.

3.1.3. Activity of protein aggregates

Protein aggregates usually have no or reduced activity. Bovine pancreas ribonuclease A (RNase A, 13.7 kD) at 1.5 mg/ml forms soluble aggregates in 0.1 M phosphate buffer (pH 10) during storage at 45°C, and the amount of aggregates corresponds qualitatively to loss of enzyme activity (Townsend and DeLuca, 1990). The specific antiviral activity of interferon-β-1b (IFN-β-1b) aggregates is three times lower than that of the intact protein (Runkel et al., 1998).

Table 2
Favored pH conditions for some degradation reactions in proteins/peptides

Degradations	Proteins/peptides	Reaction sites	Favored pH conditions	References
Cleavage	bFGF	Asp-X, esp.X = Pro	Very acidic	Shahrokh, et al., 1994a
Deamidation	hEGF	Asn^{1}	Neatral to alkaline	Son and Kwon, 1995
Deamidation	bFGF	Asn-X	Neutral to alkaline	Shahrokh, et al., 1994a
Deamidation	Insulin	Asn^{A21}	pH < 5	Strickley and Anderson, 1997
Deamidation	RNase A Lysozyme	Asn-X, Gln-X	High pHs	Kristjánsson and Kinsella, 1991
Oxidation (by H_2O_2)	rhPTH	Met^{8} and Met^{18}	10	Nabuchi et al., 1995
Oxidation (by ascorbic acid/$CuCl_2$ /O_2)	Relaxin	His^{A12}, Met^{B4}, Met^{B25}, etc.	5 > 6 > 7 > 8	Li et al., 1995a
Oxidation (by ascorbic acid/$FeCl_3$ /O_2)	His-Met	Met	7–8	Li et al., 1993
Succinimidation	bFGF	Asx-Gly	4–5	Shahrokh et al., 1994a

Protein aggregation may or may not accompany major conformational changes. Interleukin-1 receptor antagonist (IL-1ra) in solution can form non-covalent but irreversible dimers during storage, and the activity of the non-covalent dimer is about one-third of the native monomer, even though the dimer has almost the same structure as the native form by CD and IR spectroscopy (Chang et al., 1996a).

3.2. Chemical instabilities of proteins

Many chemical reactions are responsible for inactivation of protein drugs. In many cases, a couple of reactions can happen simultaneously in proteins, making separation and identification of protein degradation products very difficult. For example, bFGF undergoes multiple degradations in solution, including multimerization, succinimidation, hydrolysis, and aggregation (Wang et al., 1996b). Lyophilized insulin, after forming a cyclic anhydride intermediate at low pH, may react with water to form desamido insulin or react with other amino acids to form two different dimers (Asp^{A21}-Phe^{B1} and Asp^{A21}-Gly^{A1}) (Strickley and Anderson, 1997). The eventual degradation product distribution (between desamido insulin or covalent dimers) may depend on water content of the formulation, pH of the reconstituted solution, and nature of the excipients in the formulation. Many proteins show changes in degradation pathways at different pHs and temperatures. The degradation products (aggregates and C-terminal fragments) of recombinant human macrophage colony-stimulating factor (M-CSF) change significantly at different pHs (Schrier et al., 1993). Recombinant human thrombopoietin (rhTPO) shows different shapes of k_{obs}-pH profiles and different patterns of bands on SDS-PAGE at 5, 30, and 37°C (Senderoff et al., 1996). Therefore, to prevent proteins from chemical inactivation, the dominant reaction should first be identified and inhibited. This can be achieved to a certain degree by adjusting the formulation pH away from favorable ranges (Table 2).

The location of labile amino acids in a protein is critical in determining their chemical reactivity. Since a very limited number of water molecules exist inside a protein, presence of chemically labile amino acids may not be a problem if they are localized inside and have limited mobility (Mozhaev and Martinek, 1984). Chemical reactions of many amino acids in proteins require certain local molecular flexibility; and thus the rate of reaction may be higher in denatured proteins or small peptides with high flexibility

than in native proteins. For example, the reactivity (disulfide exchange) of the sulphydryl group in β-lactoglobulin-A is very slow in its native state but increases significantly when the protein gradually unfolds with increasing urea concentration from 4 to 8 M (Apenten, 1998). Native protein conformation, therefore, needs to be protected to prevent or inhibit potential chemical degradations.

Powell (1996) tried to correlate the reactivity of protein deamidation, hydrolysis, and oxidation in aqueous solutions with protein sequence structure by analyzing the hydropathy/flexibility (hydroflex) plots for 73 proteins. The analysis shows that the primary reaction in proteins at pH 4.5–7.5 occurs largely at Asn and Asp within these motifs: -Asn-Gly-, -Asn-Ser-, -Asp-Gly-, and, to a lesser extent, -Gln-Gly-, -Asp-Pro-, and -Met- (the hot-spot sites). Reactions at non-hot-spot sites can also occur if the site conformation is favorable (hydrophilicity and flexibility) or if the reaction is catalyzed by contaminating proteases. Hydropathy appears to be a better predictor of protein degradation than does calculated flexibility.

Chemical reactions may not always affect protein conformation or activity depending on the location of transformed residues. Due to the terminal location of Met^{B4} and Met^{B25} in recombinant human relaxin, oxidation at these two residues does not change the protein bioactivity (Nguyen et al., 1993). The Met^{1} mono-oxidized recombinant human leptin (16 kD) does not show any detectable changes in tertiary structure and retains its full potency as compared to native form (Liu et al., 1998). Similarly, when 63% of human epidermal growth factor (hEGF, 6 kD) is deamidated, its mitogenic activity is completely unchanged, indicating that the deamidation site is not critical in determining the mitogenic activity. Other deamidated products having essentially the same biological activity as the intact proteins include insulin (Brange et al., 1992b) and rIL-2 (Sasaoki et al., 1992). In some cases, degraded proteins may have even higher activities such as rhTPO during storage at 5, 30, and 37°C (Senderoff et al., 1996).

3.2.1. Deamidation

Deamidation appears to be the most common degradation in protein pharmaceuticals. In many cases, it is a major degradation pathway in proteins, such as recombinant human deoxyribonuclease (rhDNase) (Shire, 1996; Chen et al., 1998) and rhVEGF at pH 5–6 (Goolcharran et al., 1998). The deamidated rhDNase has only about 40–50% of the original activity.

Several deamidation mechanisms have been reported and discussed (Cleland et al., 1993; Xie and Schowen, 1999). Asn and Gln are the two amino acids susceptible to deamidation in proteins and Asn is much more labile (Powell, 1994; Li et al., 1995b; Daniel et al., 1996). Deamidation of Asn in proteins and peptides in an aqueous solution can proceed at a much higher rate than hydrolysis of a peptide bond (Daniel et al., 1996).

The rate, mechanism, and location of deamidation in peptides or proteins are pH-dependent. Deamidation of Asn-X appears favored mostly at neutral or alkaline conditions (Son and Kwon, 1995; Daniel et al., 1996). Maximum stability of Asn residues within peptides is found between pH 2-5. Between pH 5 and 12, the reaction proceeds rapidly and entirely through a cyclic imide (succinimide) intermediate, while slow deamidation at pH 1–2 seems to bypass the succinimide intermediate (Daniel et al., 1996). The rate of deamidation at Asn^{74} in bovine pancreatic DNase increases with increasing pH from 5.0 to 7.7 (Shire, 1996). In insulin, however, deamidation originates from a rate-limiting intramolecular nucleophilic attack at the C-terminal Asn^{A-21} with a cyclic anhydride intermediate to form desamido insulin (Brange et al., 1992b; Darrington and Anderson, 1995; Strickley and Anderson, 1997). Since the unionized carboxyl group at the C terminal is the catalyzing group, increasing solution pH inhibits deamidation of Asn^{A-21}. Therefore, the reaction is favored at low pH (< 5). In neutral solutions, deamidation in insulin takes place predominantly at Asn^{B-3} residue (Brange et al., 1992b; Darrington and Anderson, 1995).

The relative position of Asn and/or Gln in proteins may determine their relative rate of deamidation. hEGF has three deamidation

residues (Asn^{1}, Asn^{32}, and Gln^{43}) and Asn^{1} is the most labile one in neutral and alkaline pH due to its relatively high mobility in the protein (Son and Kwon, 1995). In tPA, only three Asn-X sequences (Asn^{58}-Gly^{59}, Asn^{77}-Ser^{178}, and Asn^{37} -Ser^{38}) are deamidated; and all three sites are located on the protein surface and have more-than-average local sequence mobility (Paranandi et al., 1994).

Neighboring amino acids at deamidation sites in peptides or proteins may affect the rate of deamidation. Cross and Schirch (1991) have studied the rate of non-enzymatic deamidation of a series of pentapeptides. They have found that in neutral and alkaline solutions, amino acid residues on the amino side of Asn have little or no effect on the rate of deamidation regardless of its charge or size, but residues on the carboxyl side of Asn affect the rate significantly. Increasing the size and branching in the side chain of the residue decreases the rate of deamidation as much as 70-fold relative to Gly. Therefore, the most labile sequence seems to be Asn-Gly (Powell, 1994, 1996). However, under acidic conditions, the rate of deamidation of Asn residue is not affected by neighboring amino acids in these pentapeptides (Cross and Schirch, 1991). In tPA, 7 Asn-X sequences are identified to have more-than-average local sequence mobility, but only three of them show detectable deamidation, suggesting possible influence of neighboring amino acids on the rate of deamidation in addition to local flexibility (Paranandi et al., 1994). Local flexibility/mobility of proteins can be plotted for comparison based on hydrophobicity–volume product for consecutive quintuplets of amino acid residues (Ragone et al., 1989).

The rate of deamidation in proteins is also influenced by secondary structure of proteins. Xie and Schowen (1999) recently reviewed secondary structure and protein deamidation and indicated that both α-helical and β-turn secondary structures tend to stabilize Asn residues against deamidation. A good example is the deamidation of Asn^{8} in several growth hormone releasing factor (GRF) analogues, which decreases with increasing helical content in aqueous methanol solutions (Stevenson et al., 1993).

3.2.2. Oxidation

The side chains of His, Met, Cys, Trp, and Tyr residues are potential sites of oxidation (Manning et al., 1989; Li et al., 1995b,c; Daniel et al., 1996). Oxidation at these sites can be catalyzed by trace amount of transition metal ions (site-specific process) or enhanced by oxidants or upon exposure to light (non-site-specific process). The site specificity is due to generation of and oxidation by reactive oxygen species at specific metal-binding sites (Li et al., 1995a; Zhao et al., 1997). The complicated oxidation mechanisms and related major oxidation products have been reviewed elsewhere (Cleland et al., 1993; Stadtman, 1993; Li et al., 1995c).

The most easily oxidizable sites are thio groups on Met and Cys. Met residues in proteins can be easily oxidized by atmospheric oxygen such as hGH in a vial containing only 0.4% oxygen. The easy oxidation of Met residue occurs probably because Met (also Gln) is one of the most flexible of nonpolar or mildly polar residues in proteins (Richards, 1997). Nevertheless, it was concluded that oxidation at Met residues in most proteins is not as significant as deamidation and hydrolysis (Powell, 1996).

The thioether group of Met can be oxidized into two possible forms: sulfoxide and sulfone. Met is first oxidized reversibly to sulfoxide, which can be further oxidized irreversibly to sulfone under harsh conditions. Like deamidation, the rate of oxidation depends on the position of oxidizable groups in a protein. For example, Met sulfoxides can form at both Met^{18} and Met^{8} in recombinant human parathyroid hormone (rhPTH) in the presence of H_2O_2, but Met^{18} is more susceptible to oxidation (Nabuchi et al., 1995). There are four oxidizable Met residues in recombinant human leptin, and their relative reactivity is $Met^{1} > Met^{69} > > Met^{55} \cong Met^{137}$ (Liu et al., 1998).

The formulation pH may affect the rate of oxidation by changing the oxidation potential of oxidants, the affinity of binding between catalytic metal ions and the ionizable amino acids, and the stability of oxidation intermediates. In a few cases, the rate of oxidation is enhanced at alkaline pHs. rhPTH is oxidized most at pH 10 by H_2O_2

(Nabuchi et al., 1995). The relative rate of oxidation of human relaxin in ascorbate/Cu (II) solution is pH $8 > 7 > 6 > 5$ (Li et al., 1995a). The oxidation rate of human insulin-like growth factor I (hIGF-I, 7.65 kD) in solution increases as the solution pH is increased from 6.0 to 7.5. The pH dependence of hIGF-I oxidation was attributed to formation of a phosphorylated sulfonium ion between Met and phosphate as an oxidation intermediate (Fransson and Hagman, 1996). In a different case, changing the solution pH in the range of 3–8 fails to change significantly the rate of oxidation of recombinant human relaxin by H_2O_2 (Nguyen et al., 1993).

Oxidation could dominate other degradation pathways in a protein. There are several potential degradation reactions in hIGF-I, including oxidation of Met^{59}, deamidation of Asn^{26} and Gln^{15}, and reduction of three disulfide bridges (Cys^{6}-Cys^{48}, Cys^{47}-Cys^{52}, and Cys^{18}-Cys^{61}) and oxidation of Met is found to be the major degradation pathway (Fransson et al., 1996). Similarly, oxidation is the major degradation pathway for KGF-2 (Kaushal et al., 1998).

3.2.3. Disulfide bond breakage and formation

Disulfide bonds are often critical in controlling both protein activity and stability. α-Interferon has two disulfide crosslinks between 1 and 98 and between 29 and 138. Selective breaking of the 1–98 crosslink results in no loss of activity, while breaking of the other results in almost complete loss of activity (Evans and Grassam, 1986). Ribonuclease T1 has two disulfide bonds, which stabilize the protein. When the two disulfide bonds are broken, its T_m is reduced by about 40°C and its conformational stability is decreased by over 9 kcal/mol (Thomson et al., 1989).

Free Cys residues in proteins can be oxidized easily to form disulfide bond linkages or cause thio-disulfide exchanges, causing protein aggregation or polymerization, such as basic fibroblast growth factor (bFGF) (Shahrokh, et al. 1994a; Wang et al., 1996b). However, if these cysteinyl residues are buried within the tertiary structure of proteins, they are much less reactive without much concern. Thio-disulfide exchange in a protein is a reaction between an ionized thiol group (thiolate anion) and a disulfide bond. The rate of thiol-disulfide exchange depends on the extent of ionization of the nucleophilic thiol, and therefore, generally increases as the reaction pH increases until pK of the nucleophilic thiol group is exceeded (Darby and Creighton, 1997).

Even though a protein does not have free Cys residues, disulfide bond scrambling may still occur, causing protein aggregation. This is the case for lyophilized insulin, which has only three disulfide bonds but still forms disulfide-scrambled aggregates via β-elimination of an intact disulfide during storage (Costantino et al., 1994b). β-Elimination was also observed for IL-1ra in aqueous solution (Chang et al., 1996a).

3.2.4. Hydrolysis

Amino acids, the components of proteins, are subject to acid and base hydrolysis. Most peptide bonds are stable except those in -X-Asp-Y- sequence (Manning et al. 1989; Li et al., 1995b; Vieille and Zeikus, 1996). The Asp-Y bond may be at least 100 times more labile than other peptide bonds in dilute acid (Li et al., 1995b). Cleavage is particularly rapid at Asp-Gly and Asp-Pro (Powell, 1994, 1996). A major degradation pathway of rhM-CSF in an acidic solution is peptide cleavage at two sites: Asp^{169}-Pro^{170} and Asp^{213}-Pro^{214} (Schrier et al., 1993). During hydrolysis, Asp forms succinimide intermediate, which is similar to that for Asn (Daniel et al., 1996). In addition, formation of cyclic anhydride intermediate is also possible, especially when the C-flanking residue of Asp is Pro such as bFGF (Shahrokh et al., 1994a).

In many cases, hydrolysis is a continuation after deamidation of Asn residues. Insulin first forms *iso*-Asp and Asp derivatives at $Asn^{A\text{-}21}$ and/or $Asn^{B\text{-}3}$ depending on the solution pH during storage. These derivatives are further hydrolyzed and the rate of hydrolysis at B3 position is independent of the insulin strength between 40 and 400 IU/ml (Brange et al., 1992b).

3.2.5. Isomerization

All amino acids have the potential of racemization except Gly. Natural or deamidation-derived

Asp-X peptide bonds can easily undergo a reversible isomerization between Asp and *iso*-Asp via a cyclic imide (succinimide) intermediate. The succinimide intermediate is usually not stable, and significant hydrolysis may occur in hours such as tissue plasminogen activator (tPA) (Paranandi et al., 1994).

Many cases of protein isomerization have been reported, such as bFGF (Shahrokh et al., 1994a), insulin (Brange et al., 1992b), and tPA (Paranandi et al., 1994). Incubation of tPA at pH 7.3 and 37°C for 14 days can result in formation of 0.77 mol of *iso*-aspartate derivative per mol of tPA due to multiple deamidations at Asn^{58}-Gly^{59}, Asn^{177}-Ser^{178}, and Asn^{37} -Ser^{38} (Paranandi et al., 1994).

Like deamidation, the rate of Asp isomerization is strongly influenced by its location and mobility in a protein. The *iso*-aspartate formation is most likely to occur in relatively unstructured domains of intact proteins or in domains susceptible to transient unfolding (Johnson et al., 1989). Methionyl recombinant human growth hormone (met-hGH) at pH 7.4 forms isoaspartate derivatives only at Asp^{130} (Asp-Gly) and Asn^{149} (Asn-Ser) during storage at 37°C, even though a couple of Asn and Asp residues exist in the protein. The selective *iso*-aspartate formation at Asp^{130} occurs because Asp^{130} resides in a domain, which has conformational flexibility similar to that of a short synthetic peptide (Johnson et al., 1989).

3.2.6. Succinimidation

Formation of succinimide intermediates may precede deamidation of Asn and isomerization of Asp in proteins and peptides. In fact, formation of succinimide is the cause of *iso*-aspartate derivative formation in proteins. Asn deamidates via succinimide formation at neutral and alkaline conditions, but formation of succinimide at Asp-Gly linkages in proteins may occur at an optimum pH of 4–5, such as bFGF (Shahrokh et al., 1994a).

Like other chemical degradations, the rate of succinimide formation is strongly influenced by neighboring groups of the labile residue(s) and protein conformation. Stephenson and Clarke (1989) studied the rate of succinimide formation in a series of synthetic peptides (Val-Tyr-Pro-X-Y-Ala) at pH 7.4. They demonstrated that the rate of succinimide formation of the asparaginyl (X) peptides is 13.1–35.6 times faster than those of the aspartyl peptides when Y is glycyl, seryl, or alanyl residue. The relative rate of succinimide formation is glycyl > seryl > alanyl peptides. Recently, Gietz et al. (1998) identified two degradation products in hirudin, which are succinimides at Asp^{53} and Asp^{33}. Both of these two sites are located in two flexible segments of the molecule.

3.2.7. Non-disulfide crosslinking

Proteins may form covalent dimers or polymers by non-disulfide pathways. Insulin has been shown to form such dimers and polymers during storage (Brange et al., 1992a). The rate-limiting generation of a cyclic anhydride intermediate is involved in formation of both dimeric and deamidated insulin (Darrington and Anderson, 1995). The covalent insulin dimer appears to form mainly through transamidation reactions involving Asn^{A-21} and Phe^{B-1} residues. The relative amounts of the two insulin reaction products (deamidated and dimeric insulin) changes with pH between 2.0 and 5.5. Increasing the pH decreases the formation of [desamido $^{A-21}$] insulin with a concurrent increase in desamido^{A-21}-Phe^{B-1} dimer. The formation of insulin dimer is negligible below pH 4 at insulin concentration of about 10 μM, increases sharply with increasing pH, and becomes dominant near pH 5. Recently, it has been found that the C-terminal Asn in insulin, after forming a cyclic anhydride intermediate, may form two different dimers with either Phe (Asp^{A21}-Phe^{B1}) or Gly (Asp^{A21}-Gly^{A1}) in both aqueous and lyophilized formulations (Strickley and Anderson, 1997).

Another non-disulfide pathway is the formaldehyde-mediated crosslinking proposed by Schwendeman et al. (1995). This crosslinking pathway apparently causes significant aggregation of lyophilized tetanus and diphtheria toxoids during storage and thus raises concerns for storing formalin-treated vaccines in both liquid and solid forms.

3.2.8. Deglycosylation

One of the functions of carbohydrate moieties in proteins is to protect proteins from thermal and hydrolytic inactivation (Lis and Sharon, 1993). The effect of glycosylation on stability of proteins is highly protein-dependent. Wang et al. (1996a) studied the effect of deglycosylation on the stability of five glycoproteins, including yeast external invertase, bovine serum fetuin, glucoamylase from *Aspergillus niger*, chicken egg white ovotransferrin, and avidin. The amounts of saccharides in these proteins vary from 2.2 to 50%. Deglycosylation of the five model glycoproteins decreases the protein stability as evidenced by decreased T_m and denaturation enthalpy (ΔH), even though protein conformations are not significantly affected.

Natural IFN-β is a 166 amino acid glycoprotein and has multiple functions. Runkel et al. (1998) demonstrated that deglycosylation of recombinant IFN-β-1a with PNGase F decreases the protein activity, and the loss of activity is primarily due to formation of insoluble aggregates upon carbohydrate removal. Deglycosylation also makes the protein more sensitive to thermal denaturation. At a protein concentration of 100 μg/ml, deglycosylated IFN-β-1a denatures at 63°C while glycosylated IFN-β-1a denatures at 67°C. Similarly, RNase A at 85 μM in 50 mM Tris–HCl buffer (pH 8.0) unfolds at 60.4°C while RNase B, a carbohydrated derivative at Asn^{34}, unfolds at 61.9°C under the same condition (Arnold and Ulbrich-Hofmann, 1997).

3.2.9. Maillard reaction

Sugars are often used as protein stabilizers in both liquid and solid formulations (see Section 4.2). Unfortunately, reducing sugars may react with amino groups in proteins forming carbohydrate adduct, especially at high temperatures. This extremely complex browning pathway is known as the Maillard reaction (Paulsen and Pflughaupt, 1980).

Maillard reactions are widely present in the food industry (Chuyen, 1998). Thermal treatment of milk easily leads to formation of β-lactoglobulin-lactose adduct via Lys residues (Fogliano et al., 1998). Although there have not been many reports on Maillard reactions in the development of liquid protein pharmaceuticals, this reaction may present potential formulation issues. Tarelli et al. (1994) demonstrated that lysine vasopressin undergoes rapid glycation in the presence of reducing sugars in both aqueous and solid formulations and that the N-terminal adduct can form rapidly even at −20°C.

3.3. Factors affecting protein stability

Protein stability is a result of balancing between destabilizing and stabilizing forces. The destabilizing forces are mainly due to the large increase in entropy of unfolding, and the stabilizing forces are provided by a few non-covalent interactions as discussed in Section 2.1. Disruption of any of these interactions will shift the balance and destabilize a protein. Many factors can disrupt this delicate balance.

3.3.1. Temperature

The most important factor affecting protein stability is temperature. Unfortunately, there is no general mechanism to describe the effect of temperature on the structure and function of proteins due to their structural complications. In general, the higher the temperature, the lower the protein stability.

Proteins are usually stable in a certain temperature range. Several globular proteins, including basic pancreatic trypsin inhibitor, α-chymotrypsin, cytochrome c, lysozyme, metmyoglobin, RNase A, and trypsin, have maximum free energy change $\Delta G_{f\rightarrow u}$ (8–17 kcal/mol) in a temperature range between 10 and 40°C, indicating that both high and low temperatures outside this range may destabilize or denature the proteins (Jaenicke, 1991). Under 3000 bar (to prevent freezing), RNase undergoes both cold (−22°C) and heat (40°C) denaturation (Zhang et al., 1995). Similarly, two extreme denaturation temperatures, lower than 0°C and higher than 50°C, exist for serum albumin in solution (Kosa et al., 1998).

Thermodynamically, protein stability comes from two large but opposing forces: enthalpic and entropic forces. Both are temperature-dependent. The enthalpic forces (the intramolecular interac-

tions) are stabilizing, and the entropic forces (the dissipative forces, loss of conformational entropy of native state) are destabilizing (Kristjánsson and Kinsella, 1991). High temperature-induced loss of protein stability ($\Delta\Delta G < 0$) seems to result from a decrease in free energy of the denatured state instead of an increase in free energy of the native state (Shortle, 1996). The free energy of the denatured state decreases rapidly with increasing temperature mainly due to increased entropy ($-T\Delta S$). When temperature increases, electrostatic interactions are not affected much, hydrogen bonding is weakened, and hydrophobic interactions are strengthened (to a certain point) due to its entropic origin (Jaenicke, 1990). Hydrophobic interaction increases until the temperature reaches about 110°C, when water does not solvate non-polar groups in proteins (Jaenicke, 1990; Kristjánsson and Kinsella, 1991). The ΔH of protein unfolding also increases with increasing temperature and changes from negative to positive (Jaenicke, 1990). Therefore, low temperature denaturation is mainly enthalpy-driven (Jaenicke, 1991; Shortle, 1996).

High temperatures cause denaturation of many protein pharmaceuticals. Examples include the rapid formation of bovine insulin fibrils (Brange et al., 1997), aggregation/precipitation of rhKGF (Chen et al., 1994a), and precipitation of pGH (Charman et al., 1993). High temperature is also responsible for almost complete aggregation of recombinant consensus α-interferon (rConIFN) at 0.5 mg/ml after ultrasonic nebulization in a Microstat device for 10 min (Ip et al., 1995).

Protein denaturation at high temperatures can be reversible depending on experimental conditions. Both thermal and chemical (urea) denaturation of muscle acylphosphatase (AcP, 98 aa) are reversible (Chiti et al., 1998). Patatin, the major potato tuber protein (40 kD), unfolds at a high temperature (91°C) but refolds partially upon cooling (20°C). Heating native serum albumin to 85°C causes reversible denaturation (approximately 80–90% recovery), but heating for a longer period (10 h) at 60°C (pasteurization condition) causes irreversible denaturation (Kosa et al., 1998).

High temperatures also accelerate chemical degradations, such as increased hydrolysis of Asp residues, deamidation of Asn or Gln residues in RNase A and lysozyme at high temperatures (Kristjánsson and Kinsella, 1991), and formation of covalent insulin oligo- and polymers at temperatures ≥ 25°C (Brange et al., 1992a). Degradation mechanisms in proteins easily change with temperature. At 60°C, the aggregation of interleukin 1β (IL-1β) in aqueous solution follows apparent first-order behavior to 30% drug remaining, but at or below 55°C, the aggregation deviates from apparent first-order and becomes biphasic (slow and fast) (Gu et al., 1991).

3.3.2. Formulation pH

At extreme pHs, far away from p*I* of proteins, electrostatic repulsions between like charges in proteins increase, resulting in a tendency to unfold (Goto and Fink, 1989; Volkin and Klibanov, 1989; Dill, 1990). The process of unfolding leads to a reduction of charge density, thus lowering electrostatic free energy (Chan and Dill, 1991). A minor factor contributing to the unfolding tendency is the decreased capability of salt bridge formation at extreme pHs. In addition, the pKa values of charged groups in the folded state are different from those in the unfolded state. Changes in pH lead to titration of groups only in the unfolded form, which causes destabilization of overall native protein structure (Chiti et al., 1998). pH-dependent unfolding has been found to be due only to a small number of groups with anomalous pKa's (Dimitrov and Crichton, 1997). These ionizable groups with anomalous pKa's may stabilize or destabilize a protein in different pH ranges, as those in hen egg-white lysozyme (Yang and Honig, 1993).

Proteins are often stable in a narrow pH range such as pH 6.5–7.0 for recombinant factor VIII SQ (FVIII SQ) (Fatouros et al. 1997a); 6–7 for low molecular weight urokinase (LMW-UK, 33 kD) (Vrkljan et al., 1994); and 4.5–5 for relaxin (Nguyen and Shire, 1996). Protein refolding to a wrong conformation is often seen at a pH close to its p*I* (Kristjánsson and Kinsella, 1991). pH-induced denaturation of proteins can be reversible, such as porcine pancreatic elastase, which dena-

tures on lowering the pH to less than 5.0 but renatures completely by immediately adjusting the pH back to 5.0 (Chang et al., 1993).

Certain proteins may have stable folded structures at extreme pHs. Apomyoglobin has five conformational states: native (N), acidic (A), acid-unfolded (U_A), basic (B), and base-unfolded (U_B) (Goto and Fink, 1989). Apomyoglobin starts to unfold at pH 5 with loss of helical structure and exposure of Trp residues as monitored by CD and fluorescence. At pH 2, the protein is maximally unfolded (U_A) to an extent similar to that unfolded in 6 M GdnHCl. Further increase in HCl concentration results in refolding to A state. The conformation of U_A state varies from fully unfolded to a partially folded structure (Goto and Fink, 1994). The acidic transition under low salt conditions is reversible ($N \leftrightharpoons U \leftrightharpoons N$), while reversibility of the alkaline transition depends on the length of time under high-pH conditions (Goto and Fink, 1989).

The rate of protein aggregation can be strongly affected by pH, such as the aggregation of bFGF (Wang et al., 1996b), deoxy hemoglobin (Kerwin et al., 1998), IL-1β (Gu et al., 1991), human relaxin (Li et al., 1995a), and bovine pancreas RNase A (Townsend and DeLuca, 1990; Tsai et al., 1998a). At pH 2.5, bovine insulin forms a significant amount of fibrils within a few hours at 37°C but is very stable without agitation for many months at pH 7. As pH increases from <2 to 7, monomeric insulins gradually form dimeric, tetrameric, and eventually hexameric insulins. The monomeric form has the highest tendency to form fibrils due to its large exposed hydrophobic area as compared with other forms (Brange et al., 1997).

Formulation pH, like temperature, may affect both physical and chemical stability of proteins. Different chemical degradations may be facilitated at different pHs (Table 2). This explains why degradation products are different at different pHs for the same protein, such as hirudin (Gietz et al., 1998). Hydrolysis can easily occur at Asp residues under mild acidic condition (Volkin and Klibanov, 1989). Deamidation of Asn and Gln residues readily takes place under strongly acidic, neutral, and basic conditions. Under basic conditions, many reactions can occur, such as peptide bond hydrolysis, deamidation, hydrolysis of Arg to ornithine, β-elimination and racemization, and double bond formation. The pH effect on chemical stability may depend on the presence of other excipients. For example, a V-shaped chemical (oxidation and deamidation) degradation-pH profile has been demonstrated for hGH with minimum degradation at a pH of about 7.5, but the minimum is shifted to a pH of about 7 when formulated with dextran 40 (Pikal et al., 1991).

The destabilizing effect of pH on proteins can be estimated by determining of a variety of parameters. These parameters include (1) $\Delta G_{f\rightarrow u}$ of proteins such as RNase T1 (Thomson et al., 1989), (2) hydrodynamic radius of proteins such as β-lactamase (28.5 kD) (Goto and Fink, 1989), and (3) T_m of proteins such as yeast external invertase (YEI), bovine serum fetuin, glucoamylase (Wang et al., 1996a), myoglobin (Chan and Dill, 1991), rhDNase (Chan et al., 1996), bFGF (Wang et al., 1996b), RNase A (Liu and Sturtevant, 1996; McIntosh et al., 1998), and thrombin (Boctor and Mehta, 1992). The pH effect on protein function and stability can also be probed by computerized molecular dynamics simulation (Baptista et al., 1997).

3.3.3. Adsorption

Proteins can be adsorbed to many surfaces and interfaces, such as container surfaces, and air/water interfaces. Protein adsorption in air/water interfaces starts with creation of an area for anchoring the protein molecule, followed by subsequent reorientation and rearrangement of the adsorbed molecules at the interface (Damodaran and Song, 1988). The severity of adsorption is protein-dependent and does not seem to depend on the size and p*I* of proteins (Burke et al., 1992). Evidence suggests that secondary structure of a protein may change significantly at the adsorption surface such as IgG (Vermeer et al., 1998). Therefore, surface adsorption may result in loss and/or destabilization of proteins. At 1 μg/ml, the adsorptive loss of aFGF to surfaces of several containers (untreated glass, siliconized glass, sulfur-treated glass, Purcoat glass, polyester,

polypropylene, and nylon) are in the range of 20–40% or 0.2–0.8 μg protein/cm^2 (Volkin and Middaugh, 1996). Interleukin-2 (IL-2), at 0.1 mg/ml in 10 mM phosphate buffer (pH 7.4) containing 150 mM NaCl, has been shown to lose about 90% of its activity after being pumped through silicone rubber catheter tubing (60 × 0.1 cm) in 24 h (Tzannis et al., 1996). The majority (> 80%) of the activity loss is due to adsorption-induced protein denaturation (Tzannis et al., 1997).

Protein surface adsorption is usually concentration-dependent and may reach a maximum (at least for certain proteins) above certain protein concentrations. The adsorption of bovine serum albumin (BSA) is linearly proportional to its concentration (up to 0.5%) in membrane filters made of pleated nylon, polyvinylidene difluoride, or cellulose acetate. Burke et al. (1992) examined surface adsorption of six proteins, including alcohol dehydrogenase (ADH), β-amylase, lactate dehydrogenase (LDH), α-chymotrypsinogen A, thyroglobulin, and IgG. Except LDH, adsorption of all other proteins to surfaces of containers (untreated glass, nylon, polyester + 0.3%, and polypropylene) appears saturated at approximately 5 μg/ml at a surface/solution volume ratio of 2.4 cm^2/ml. At this concentration, the amount of protein adsorbed is less than 0.5–1 μg/ml (about 10–15% of the total protein).

The type of container or membrane significantly influences protein adsorption to its surface. The adsorption of 14 model proteins has been examined in a variety of containers made of untreated glass, siliconized glass, sulfur-treated glass, Purcoat-treated glass, nylon, polypropylene, polyester 5X0, and polyester + 0.3%. Among these different containers, the untreated glass, silicone-treated glass, and polypropylene seem to have the least protein binding to their surfaces, and sulfur-treated glass and polyester containers seem to have higher adsorption for certain proteins (Brose and Waibel, 1996). Storing 1 ml of transforming growth factor-β_1 (TGF-β_1) at 1.0 μg/ml in 30 mM citrate buffer (pH 2.5) at 4°C for 11 days drops the protein concentration to 0.39, 0.37, and < 0.10 μg/ml, respectively, in polypropylene, siliconized glass, and untreated glass containers due to surface adsorption (Gombotz et al., 1996). BSA can be adsorbed to pleated nylon filter at 220 μg/cm^2/wt%, but at 120 μg/cm^2/wt% to filters made of polyvinylidene difluoride (PVDF) and cellulose acetate (CA).

The rate of protein adsorption can be very rapid. At 22 and 45°C, the percentages of recombinant human granulocyte colony-stimulating factor (rhG-CSF) adsorbed to PVC surface are, respectively, 93 and 97% of maximum after 10 min of equilibration (Johnston, 1996).

3.3.4. Salts

The effect of salts on protein stability is complex, partly because of the complex ionic interactions on fully exposed surfaces, and in fully or partially buried interior of proteins. Salts may stabilize, destabilize, or have no effect on protein stability depending on the type and concentration of salt, nature of ionic interactions, and charged residues in proteins (Kohn et al., 1997). For example, the T_m (67.4°C) of recombinant human deoxyribonuclease (rhDNase) decreases to 65.3°C in the presence of 75 mg/ml of NaCl but increases to 70.1°C at 200 mg/ml (Chan et al., 1996). Increasing $(NH)_2SO_4$ concentration from 50 to 200 mM increases aggregation of KGF during storage at 45°C, but NaCl has the opposite effect within the same concentration range (Zhang et al., 1995).

Salts can affect electrostatics in a protein in two ways: by non-specific (Debye-Hückel) electrostatic shielding, and by specific ion binding to the protein. At low concentrations, salts affect electrostatic shielding and weaken ionic repulsion/attractions as counterions. Therefore, this shielding effect may be either stabilizing when there are major repulsive interactions leading to protein unfolding, or destabilizing when there are major stabilizing salt bridges or ion pairs in the protein. At high concentrations, electrostatic shielding is saturated; the dominant effect of salt, like other additives, is on solvent properties of the solution. The net effect on stability of a protein would be determined by the relative effect on free energy of unfolded and native states (Goto and Fink, 1989). The stabilizing salts seem to increase surface tension at water-protein interface and strengthen hydrophobic interaction by keeping hydrophobic groups away from water molecules, inducing pref-

erential hydration of proteins (Kristjánsson and Kinsella, 1991; Kohn et al., 1997).

The salt effect strongly depends on the solution pH, which dictates charged state of ionizable groups. Recently, in a study on stability of de novo designed two-stranded α-helical coiled coils, it has been found that stability of a designed protein (QQx), which has no intra or interhelical ionic interaction but contains 5 Lys residues for maintaining solubility, increases gradually with increasing KCl concentration (up to 1 M) against urea-induced denaturation (Kohn et al., 1997). The effect is the same at both pH 3 and 7, since there is no ionized state in this pH range. However, stability of another designed protein (KEx), which contains Glu and Lys at positions that form interhelical ionic interactions, increases drastically with increasing KCl concentration at pH 3. This is because at this pH, Lys is the only charged residue at interaction positions, and KCl can electrostatically shield the destabilizing repulsion by interacting with charged Lys. Addition of 50 mM $LaCl_3$ increases slightly the stability of QQx at both pH 3 and 7 but decreases the stability of KEx due to La^{3+} binding to glutamate residues and disrupting interhelical ion pairs at pH 7. However, at pH 3, $LaCl_3$ stabilizes KEx since Glu residues are largely protonated at this pH and can not bind to La^{3+}. The destabilizing effect of salts on proteins has been reported in many cases. Increasing ionic strength of insulin solution from 0.04 to 0.11 by addition of NaCl increases insulin fibrillation, possibly by shielding repulsive forces between similarly charged groups (Brange et al., 1997). Probably by similar shielding effect, NaCl causes thermal aggregation of RNase at pH 3 (Tsai et al., 1998b). Increasing NaCl concentration from 120 to 360 mM also increases the mean particle (aggregate) size of hepatitis A virus (HAV) in solution from about 30 nm to greater than 120 nm in 24 h at room temperature (Volkin et al., 1996).

In many cases, salts do not play a major role in altering chemical instability of proteins or peptides based on a limited number of studies. It has been found that the rate of deamidation of Asn residues in a series of pentapeptides is not affected by ionic strength (Cross and Schirch, 1991). The rate of oxidation of Met in hIGF-I at 0.13 mM does not change whether or not sodium chloride (145 mM) is included at pH 6.0 (Fransson and Hagman, 1996). Similarly, the rate of oxidation of recombinant human relaxin by hydrogen peroxide does not change significantly at NaCl concentrations ranging from 0.007 to 0.21 M in 0.01 M acetate buffer at pH 5.0 (Nguyen et al., 1993). However, addition of 0.1 M KCl inhibits intracellular SH and S-S exchange in bovine mercaptalbumin at pH 8.6 (Kuwata et al., 1994).

3.3.5. Metal ions

Depending on the type and concentration, metal ions may destabilize or stabilize a protein. Since the negative counter ions may also significantly affect protein stability either positively or negatively, contribution of metal ions to protein stability should be carefully interpreted.

Some proteins are stable only in the presence of certain metal ions. The number of stabilizing metal ions required in each protein molecule is protein-dependent, and the metal ions may or may not be mutually replaceable for protein stability. It has been found that maximum activity of murine adenosine deaminase (ADA) is at 1:1 molar ratio of zinc (Zn^{2+}) or cobalt (Co^{2+}) to ADA. Both higher and lower ratios can inhibit the protein activity, and no measurable activity of ADA is left in the presence of other metals ions (at 1:1, 10:1 or 100:1 ratio), including Ca^{2+}, Cd^{2+}, Cu^{2+}, Cu^{+}, Mn^{2+}, Fe^{2+}, Fe^{3+}, Pb^{2+}, or Mg^{2+} (Cooper et al., 1997). While Ca^{2+} (up to 100 mM) stabilizes rhDNase, other metal ions such as Mg^{2+}, Mn^{2+} and Zn^{2+} destabilize it (Chan et al., 1996). The stabilizing effect of Ca^{2+} on rhDNase is presumably due to direct binding of Ca^{2+} to the protein and preventing breaking of a disulfide bridge (Chen et al., 1998). A number of metal ions have been tested for stabilization of FVIII SQ, including Ca^{2+}, Sr^{2+}, Cu^{2+}, Mg^{2+}, Fe^{2+}, Zn^{2+}, and Mn^{2+}. While Ca^{2+} or Sr^{2+} increases the stability of the protein, Fe^{+2} at 1 or 10 mM and Cu^{+2} or Zn^{+2} at 10 mM sharply destabilize FVIII SQ (Fatouros et al., 1997a).

Metal ions may significantly affect protein stability without affecting much of its secondary structure. Although ADA (apoenzyme) is not ac-

tive (less than 0.1% of the holoenzyme activity) in the absence of Zn^{2+} or Co^{2+}, CD analysis of the protein indicates that secondary structures are the same with or without these metal ions (Cooper et al., 1997). Similarly, removal of exogenous Ca^{2+} by EGTA-treatment has little effect on the secondary structure of rhDNase based on IR determination in the amide III region in either aqueous or lyophilized state (Chen et al., 1998).

Trace amount of metal ions in protein formulation may catalyze oxidation in proteins mainly via the Fenton pathway (Stadtman, 1993). These labile residues include Met, Cys, His, Trp, Tyr, Pro, Arg, Lys, or Thr (Stadtman, 1993; Li et al., 1995b,c). The catalysis depends on concentration of the metal ions. For example, addition of 0.15 ppm (w/w) chloride salts of Fe^{3+}, Ca^{2+}, Cu^{2+}, Mg^{2+}, or Zn^{2+} does not affect the oxidation rate of Met in hIGF-I at 0.13 mM in 50 mM sodium phosphate (pH 6.0) at room temperature, but when the salt concentration increases to 1 ppm, Fe^{3+} causes a significant increase in oxidation (Fransson and Hagman, 1996). The metal-catalyzed oxidation can be facilitated in the presence of a reducing agent such as ascorbate or RSH (Stadtman, 1993; Li et al., 1995c). Metal ions, oxygen, and reducing agents can generate reactive oxygen species (ROS) to oxidize proteins. The ascorbate/Cu(II)/O_2 system easily oxidizes papain (Kanazawa et al., 1994), brain-derived neurotrophic factor (BDNF) (Jensen et al., 1998), His in hGH (Zhao et al., 1997), His and Met in human relaxin (Li et al., 1995a), and the His-containing fragment of relaxin (Khossravi and Borchardt, 1998). The dual effect of ascorbic acid might explain why it slightly inhibits oxidation of recombinant human nerve growth factor (rhNGF) but destabilizes FVIII SQ (Österberg and Fatouros, 1994) and increases oxidation of recombinant human ciliary neutotrophic factor (rhCNTF) in the presence of peroxides (Knepp et al., 1996).

3.3.6. Chelating agents

In close relation to metal ions, chelating agents such as EDTA and citric acid may destabilize a protein by binding to the protein and/or its critical metal ions or stabilize the protein by binding to any harmful metal ions.

Since transition metal ions can catalyze protein oxidation, metal ion-chelating agents should be able to protect a protein from metal-catalyzed oxidation. EDTA at 0.1 mM can completely inhibit oxidation of relaxin induced by the ascorbic acid/$CuCl_2$/O_2 system (Li et al., 1995a). At 0.15 mM and 1 mM, it also effectively inhibits oxidation of Cys in aFGF (Wang et al., 1996b) and bFGF (Volkin and Middaugh, 1996).

In many cases, however, the effect of chelating agents is more complex. The net effect depends on the metal ions, oxidation mechanism, and type and concentration of the chelating agent (Stadtman, 1993). It has been found that EDTA at 0.02 mM suppresses formation of Met sulfoxide in His-Met catalysed by the ascorbic acid/$FeCl_3$/O_2 system at pH 7.4 but increases the overall degradation (Li et al., 1993). In a recent study, some polyaminocarboxylate metal chelators including EDTA failed to inhibit oxidation of Met- or His-containing heptapeptides induced by the dithiothreitol/Fe_3Cl/O_2 system but significantly changed the distribution of oxidation products (Zhao et al., 1996).

3.3.7. Shaking and shearing

Proteins can be denatured by shaking or shearing. Shaking creates hydrophobic air/water interface, which results in alignment of protein molecules at the interface, unfolding to maximize exposure of hydrophobic residues to air and to initiate aggregation (Volkin and Klibanov, 1989). The hydrophobic surfaces causing protein aggregation during shaking can be either gaseous or solid (Sluzky et al., 1991, 1992). Similarly, shearing also exposes hydrophobic areas of proteins, initiating aggregation.

Examples of shaking-induced protein instability include aggregation of rFXIII (Kreilgaard et al., 1998), hGH (Katakam et al., 1995; Katakam and Banga, 1997; Bam et al., 1998), hemoglobin (Kerwin et al., 1998), and insulin (Thurow and Geisen, 1984; Sluzky et al., 1991; Brange et al., 1997). More than 50% of urease activity is lost at 0.33 mg/ml in phosphate buffer (pH 7.0) after shaking for 24 h, and 77% of rIL-2 activity is lost at 0.2 μg/ml in PBS (pH 7.0) after shaking for 8 h at 4°C (Wang and Johnston, 1993a). Air-jet nebu-

lization of rConIFN at pH 6.3 for 25 min at 40 psig causes 70% aggregation (Ip et al., 1995).

Proteins may tolerate shearing inactivation to a different degree. Catalase loses about 50% of its activity after exposure to a shear of 7×10^6, but plasma fibrinogen loses the same amount of its clotting activity after exposure to a shear of 5×10^8 (Charm and Wong, 1970a,b). Similarly, about 30% of rhGH forms aggregates at a shear of 10^5, while rhDNase is stable at a shear of 2×10^7 when these proteins are homogenized (Maa and Hsu, 1997). This is because rhGH is more surface active and may easily accumulate at the homogenization-induced air/water interface, accelerating aggregation. Other factors such as the rigidity of protein structure and the number of hydrophobic residues exposed on the protein surface might have contributed to the different level of shear tolerance.

The effect of shear can be evaluated by pumping a protein solution through a capillary tube. The amount of shear experienced by the protein can be expressed as the product of shear rate (S) and residence time (t): $S*t = (8/3)(L/r)$, where L is the length and r is the radius of the tube (Charm and Wong, 1970a).

3.3.8. Protein denaturants

GdnHCl, urea, NaSCN (thiocyanate), and SDS are often-used denaturants. These denaturants bind preferentially to proteins, disrupting both hydrophobic interaction and hydrogen bonds, and reducing protein chemical potential and free energy of denaturation (Darnell et al., 1986; Volkin and Klibanov, 1989; Timasheff, 1993; Allison et al., 1996). While GdnHCl and urea may interact weakly with the hydrophobic surface of a protein, SDS probably interacts strongly with it, causing protein denaturation, since a denatured state exposes more hydrophobic surface for binding (Shortle, 1996). The denaturant concentration for complete protein denaturation is usually 6 M for GdnHCl and 8 M for urea, although lower concentrations can be as effective depending on the protein.

GdnHCl is a more potent denaturant than urea. RNase H can be completely denatured in 2 M GdnHCl, but 4 M urea is needed for complete denaturation (Goedken and Marqusee, 1998). For rhDNase, 0.5 M GdnHCl lowers its T_m from 67.4 to 61°C, but 2 M urea is needed to achieve the same effect (Chan et al., 1996). The denatured proteins by GdnHCl or urea may be reversible, such as diacylglycerol kinase (DGK) (Clarke and Waltho, 1997).

Denatured proteins are usually soluble in a denaturant solution because of increased solvation of nonpolar amino acids (Chan and Dill, 1991). Exceptions do exist. For example, the rate and extent of horse apomyoglobin aggregation increase with increasing urea concentrations (up to 2.4 M) (De Young et al., 1993). This may be due to the possible effect of protein-dependent preferential exclusion of urea at low concentrations (Timasheff, 1998). In fact, protein activation or stabilization by low concentrations of a denaturant has been reported. GdnHCl at concentrations up to 0.6 M stimulates activity of human placental alkaline phosphatase (Hung and Chang, 1998) and at concentrations up to 0.3 M stabilizes RNase T1 against thermal and urea-induced unfolding (Mayr and Schmid, 1993). The stabilizing effect of GdnHCl is apparently due to the contribution of stabilizing effect of Cl^- as observed for apomyoglobin (Staniforth et al., 1998).

It should be noted that cyanate may spontaneously form from urea, and an 8 M urea solution contains approximately 0.02 M cyanate, which can react with both amino and sulphydryl groups in proteins, causing irreversible inactivation (Volkin and Klibanov, 1989). Therefore, urea should be prepared fresh or cyanate ions should be removed when used in probing protein stability. In IR studies NaSCN is a preferable denaturant since it does not absorb in the amide I region (Allison et al., 1996).

3.3.9. Non-aqueous solvents

A folded protein in an aqueous solution has hydrophobic regions sequestered from and hydrophilic areas in contact with the aqueous environment. When the polarity of an aqueous solvent decreases by adding a non-aqueous solvent, protein hydrophobic cores tend to dissipate in contact with the solvent, and the protein hydration shell may be disrupted, leading to destabiliza-

tion and unfolding of the protein. For example, addition of 60% (v/v) glycerol in 10 mM Tris–HCl buffer (pH 7.4) decreases $\Delta G_{f\rightarrow u}$ of ferric horse heart myoglobin by about 10 kcal/mol (Barteri et al., 1996). Therefore, non-aqueous solvents reduce free energy of the unfolded state by solvating the exposed nonpolar residues (Dill, 1990). In two-phase organic/aqueous systems, proteins unfold/denature predominantly at the interface, which depends on both the interfacial tension and interfacial surface area (Cowan, 1997).

Non-aqueous solvent-induced inactivation of proteins by disruption of water residues at the active site may occur without disruption of the tertiary structure. Therefore, protein inactivation by non-aqueous solvents may be reversible. For instance, inactivation of certain proteins by dimethylsulfoxide (DMSO) is fully reversible upon immediate dilution with aqueous solution (Chang et al., 1991).

While non-aqueous solvents generally destabilize proteins, some at low concentrations may have the opposite (stabilizing) effect, such as polyhydric alcohol and some polar, aprotic solvents like DMSO and dimethylformamide (DMF) (Volkin and Klibanov, 1989). Four organic solvent additives, polyethylene glycol (PEG), 2-methyl-2,4-pentanediol (MPD), DMSO, and trimethylamine N-oxide (TMAO), have been found to induce preferential hydration of lysozyme and BSA (Kita et al., 1994). The T_m of IL-1R is increased from 48.1 to 48.6°C in the presence of 5.1 mg/ml ethanol but decreased to 43.8°C at 50 mg/ml (Remmele et al., 1998). The stabilization effect by low concentrations of non-aqueous solvents is probably due to the mixed solvent system more resembling the protein's cellular environment (Butler, 1979a,b).

Proteins suspended in certain non-aqueous solvents may be as stable as in solid state. Recently, it has been found that plasma-derived factor IX (pdFIX) suspended in perfluorodecalin with 0.0003% moisture does not lose protein activity within 24 weeks as observed in a lyophilized formulation at 37°C, while that suspended in soybean oil, methoxyflurane, octanol, or PEG 400 rapidly loses activity to a different degree within the same period (Knepp et al., 1998). When pdFIX powder containing 10% moisture is suspended in perfluorodecalin, the resultant suspension is not as stable. This may be explained as the strong dependency of non-aqueous solvent-induced denaturation on availability of free water. In the absence of free water, protein conformation is highly rigid and compact, and resists unfolding processes (Cowan, 1997). Due to the inflexibility, certain proteins in non-aqueous solvents can resist thermal denaturation as well as chemical degradation (Tuena de Gómez-Puyou and Gómez-Puyou, 1998).

3.3.10. Protein concentration

Protein aggregation is generally concentration-dependent. The mean-field lattice model predicts that proteins will aggregate/precipitate at sufficiently high concentrations (Fields et al., 1992). It has been suggested that increasing protein concentration to higher than 0.02 mg/ml may facilitate potential protein aggregation (Ruddon and Bedows, 1997).

Accelerated aggregation of proteins at high concentrations has been reported in many cases. Examples include aFGF (Won et al., 1998), β-lactoglobulin (Roefs and De Kruif, 1994), IL-1β in the range of 0.1–0.5 mg/ml (Gu et al., 1991), LMW-UK in the range of 0.2–0.9 mg/ml (Vrkljan et al., 1994), and apomyoglobin in the range of 4–12 mg/ml in the presence of 2.4 M urea (De Young et al., 1993). The size of protein aggregates may also increase with increasing protein concentrations such as β-lactoglobulin (Roefs and De Kruif, 1994).

The effect of protein concentration on its aggregation may depend on the mechanism of aggregation and the experimental conditions. The formation of bovine insulin fibrils increases with increasing protein concentrations from 0.75 to 5% during storage at pH 2.5 and 21°C, and it takes less than 10 h to produce the same amount of fibrils at 5% as that in 15 days at 0.75% (Brange et al., 1997). In contrast, bovine insulin at 0.1 mg/ml at pH 7.4 aggregates more readily than at 0.6 mg/ml during shaking (Sluzky et al., 1991, 1992). This is attributable to the more favorable formation of insulin hexamers at 0.6 mg/ml, which are less susceptible to hydrophobic surface-

induced adsorption/aggregation than insulin monomers.

In some cases, protein concentration also affects chemical degradations to a certain degree. Increasing insulin concentration increases formation of covalent insulin oligomers and polymers in neutral solution at 37 or 45°C (Brange et al., 1992a). However, the rate constant for oxidation of Met in hIGF-I (k_{ox}) decreases when the protein concentration is increased from 0.26 to 1.4 mM at either 30 or 50°C, presumably due to the limited amount of oxygen available for oxidation in the solution.

On the other hand, concentrated protein solutions can be more resistant against freezing-induced protein aggregation and loss of activity such as labile LDH (Carpenter et al., 1990, 1997). There are at least three explanations. First, the amount of protein accumulated at ice-water interface is finite and therefore, interface-induced protein denaturation is limited in concentrated protein solutions. Second, protein unfolding may be inhibited by steric repulsion of neighboring protein molecules (Allison et al., 1996). Last, protein–protein interactions may change monomers to active and more stable dimers or multimers (Mozhaev and Martinek, 1984).

3.3.11. Source and purity of proteins

Stability of proteins may be significantly different depending on the manufacturer and source of proteins. The rate of formation of high-molecular-weight products in human insulin preparations in neutral solutions can differ up to 100% among different manufacturers (Brange et al., 1992a). One of the major influencing factors is the purity of proteins. Any presence of trace amount of enzymes, metal ions, or other contaminants can potentially affect protein stability. Thus, protein purification is one of the most critical steps in controlling protein quality.

Very often, the extent and mechanism of protein degradation is different depending on the purification scheme such as rhTPO (Senderoff et al., 1996). Recombinant and plasma-derived proteins may require different purification schemes, which may influence protein stability. Recombinant factor IX (rFIX) is essentially free of contamination from non-factor IX products, but many high-purity pdFIX preparations exhibit significant amounts of non-factor IX contaminants, including other coagulation proteins, which may potentially affect the protein stability (Bond et al., 1998).

3.3.12. Protein morphism

Protein morphism is also a factor influencing protein stability. Crystalline drugs are generally more stable chemically than amorphous forms, especially for small molecules. The formation of high-molecular-weight insulin in a suspension of amorphous zinc insulin appears faster than that in crystalline zinc insulin at 37°C (Brange et al., 1992a). The total hydrolytic transformation at B3 position of the amorphous (or soluble) insulin is considerably higher than that of the crystalline form (Brange et al., 1992b). On the contrary, freeze-dried amorphous insulin is far more stable than crystalline insulin against deamidation and dimerization at all water content up to 15%. While the rate of degradation of crystalline insulin increases with increasing water content, the rate of amorphous form is essentially independent of water content change in the same range (Pikal and Rigsbee, 1997).

3.3.13. High pressure

High pressure can cause protein unfolding because the volume of protein–solvent systems is smaller in the unfolded state. In other words, unfolded proteins are more compressible than folded ones. For example, 40% of staphylococcal nuclease at < 10 μM unfolds under 1000 bar in 10 mM Bis–Tris buffer (pH 4.5) containing 1.25% xylose (Frye and Royer, 1997). Bovine pancrease RNase A unfolds completely under 4000 bar (Zhang et al., 1995; Prehoda et al., 1998). Increasing the pressure from 0 to 2000 bar significantly inhibits activity of H^+-ATPase and increases its aggregation (Tsai et al., 1998c).

3.4. Analytical techniques in monitoring protein instability

To monitor protein instability, a protein activity assay is indispensable. Often, a bioassay is

needed based on the protein's function, such as the clot lysis assay for tissue plasminogen activator (tPA) (Hsu et al. 1995). A good activity assay should be reproducible and sensitive enough to detect small changes in protein activity. In reality, a protein activity assay is often variable, unable to detect small activity changes, labor-intensive, and unable to reveal any intricate changes in the structure of proteins. Therefore, other analytical techniques are used, preferably in conjunction with an activity assay, to characterize a protein and monitor its instability. The available analytical methods for assessing protein formulations have been discussed elsewhere (Jones, 1994). Table 3 lists the major analytical techniques and their applications in monitoring protein instability.

3.4.1. Monitoring the protein unfolding process

Proteins can be unfolded chemically or thermally. The often-used chemicals for protein unfolding studies include urea and GdnHCl. The denaturant-induced unfolding process can be slow depending on the protein, and on the type and concentration of denaturant. It has been reported that at least 6 h are needed to unfold human placental alkaline phosphatase (Hung and Chang, 1998). Different denaturants may also unfold a protein differently. Apomyoglobin from *Aplysia limacina* shows two transitions on titration with GdnHCl but only one with urea as monitored by far-UV CD (Staniforth et al., 1998).

Many physical techniques can be used to monitor an unfolding event, including circular dichroism (CD), fluorescence, optical rotation, or UV (Thomson et al., 1989; Lau and Bowie, 1997; Swietnicki et al., 1997). The signal of hydrogen exchange (HX) in proteins, as monitored by nuclear magnetic resonance spectroscopy (NMR), can also be used in these studies (Bai et al., 1994; Zhang et al., 1995). These techniques are based on signal differences between the folded and unfolded states. Two useful parameters in chemical unfolding studies can be determined: C_{half}, the concentration of a denaturant causing unfolding of 50% protein molecules, and $\Delta G_{\text{f}\rightarrow\text{u}}$, the free energy change of unfolding. Both parameters can be used to examine the effect of formulation excipients on protein stability (Barteri et al., 1996; Foord and Leatherbarrow, 1998). To obtain $\Delta G_{\text{f}\rightarrow\text{u}}$, the fraction of unfolded protein, F_{u}, is first calculated using the following equation, assuming a two-state transition:

$$F_{\text{u}} = (y_{\text{f}} - y_{\text{obs}})/(y_{\text{f}} - y_{\text{u}}).$$

In this equation, y_{obs} is the observed variable signal in the presence of different denaturant concentrations, and y_{f} and y_{u} are, respectively, the signal of completely folded and unfolded conformations. ΔG at the equilibrium state can be calculated using the following equation (Thomson et al., 1989; Pace, 1990):

$$\Delta G = -RT \ln[(F_{\text{u}})/(1 - F_{\text{u}})]$$
$$= -RT \ln[(y_{\text{f}} - y_{\text{obs}})/(y_{\text{obs}} - y_{\text{u}})],$$

where R is the gas constant and T is the absolute temperature. The $\Delta G_{\text{f}\rightarrow\text{u}}$ is obtained by extrapolating the unfolding curve (ΔG versus denaturant concentration) at 0 denaturant concentration.

What causes the signal difference between the folded and unfolded states of proteins? Protein unfolding exposes hydrophobic amino acid residues. Solvent exposure of these residues such as Tyr or Trp changes their environment and often results in a signal change. The change in UV or fluorescence signal can be negative or positive depending on protein sequence and solution properties. For example, unfolding of α-chymotrypsin at 0.3 mg/ml at pH 7.0 decreases its UV absorption by about 10% at 281 nm and fluorescence intensity by about 70% with a shift of fluorescence λ_{max} from 331 to 347 nm (Lozano et al., 1997). The signal decrease results from an increase in polarity of the environment of Trp in the protein upon unfolding as observed for apomyoglobin (Staniforth et al., 1998). The intrinsic fluorescence of human albumin decreases substantially upon unfolding due to loss of energy transfer (several Tyr residues transferring excitation energy to Trp residues in the native state) (Farruggia et al., 1997). However, exposure of buried Tyr to solvent upon unfolding of cutinase increases its UV absorbance significantly at 250 nm at pH 9.6 due to ionization of Tyr (Melo et al., 1997). Positive change in fluorescence signal has also been reported. The fluorescence intensity of soluble protein MerP (72 aa) increases about 10 times at

Table 3
Analytical techniques in protein characterization and instability monitoring

Analytical techniques	Major applications	Protein examples	References
Analytical centrifugation	Protein aggregation	Rop proteins	Munson et al., 1996
CE	Protein degradation	Hirudin	Gietz et al., 1998
	Determination of T_m	RNase	McIntosh et al., 1998
CD	Estimation of secondary structures	α-Spectrin	Prieto et al., 1997
	Determination of T_m	AcP	Chiti et al. 1998
	Probing protein conformation	β-lactoglobulin	Matsuura and Manning, 1994
	Determination of multimers	Fragment of ribosomal protein L9	Kuhlman et al., 1997
DSC	Determination of T_g	hGH	Pikal et al., 1991
	Determination of T_m	aFGF	Tsai et al., 1993
	Protein unfolding	BSA	Giancola et al., 1997
Electron paramagnetic resonance (EPR)	Ligand-protein interactions	rhGH, rhIFN-γ	Bam et al., 1995
Fluorescence	Protein unfolding/interaction	MerP	Aronsson et al., 1997
	Determination of T_m	HSA	Farruggia et al., 1997
	Probing protein conformation	α-Antitrypsin	Kwon and Yu, 1997
HPLC-ion exchange	Protein degradation and aggregation	hGH	Zhao et al., 1997
HPLC-reversed phase	Protein degradation and aggregation	hGH	Pikal et al., 1991
	Estimation of contamination	rhPTH	Nabuchi et al., 1995
HPLC-size exclusion	Protein degradation and aggregation	hGH	Pikal et al., 1991
	Estimation of contamination	β-Galactosidase	Yoshioka et al., 1993
IR	Estimation of secondary structures	Chymotrysinogen	Allison et al., 1996
	Determination of T_m	hPAH	Chehin et al. 1998
	Probing protein confirmation	IL-1ra	Chang et al., 1996b
Karl Fischer	Water determination	Insulin formulation	Strickley and Anderson, 1996, 1997
Light scattering	Protein aggregation	Human relaxin	Li et al., 1995a
MS	Determination of molecular weight, degradation products and contaminants	bFGF	Shahrokh et al., 1994a
NMR	Determination of 3-D and secondary structures	IL-6	Xu et al., 1997
	Protein relaxation and softening	BSA, BGG	Yoshioka et al., 1997, 1998
	Protein unfolding	RNase	Zhang et al., 1995
Raman spectroscopy	Determination of secondary structures	Insulin	Yeo et al. 1994
Refractometry	Ligand–protein interactions	rhGH, rhIFN-γ	Bam et al., 1995
UV/visible spectroscopy	Determination of T_m	RNase	Thomson et al., 1989
	Protein aggregation	aFGF	Tsai et al., 1993
	Estimation of contamination	hGH	Perlman and Nguyen, 1992
	Probing protein conformation	IL-2, Insulin	Butler, 1979a,b; Brewster et al., 1991

300 nm upon unfolding (Aronsson et al., 1997). Similar increase in fluorescence signal was also observed for Trp RNase A mutant at 350 nm (Sendak et al., 1996). Effective quenching of Tyr and Trp in the folded proteins causes the large signal increase upon unfolding. Sometime the signal change is due to a simple solute effect rather than conformational change. A 30% drop in fluorescence intensity of DGK at 330 nm is observed upon SDS denaturation, and the same extent of signal change is also seen for free Trp (Lau and Bowie, 1997). To maximize detection sensitivity, a signal ratio may be used, such as the ratio of fluorescence intensity at 350 nm to that at 330 nm in the study of rFXIII unfolding (Kurochkin et al., 1995).

Proteins may have more than one unfolding process if there is a stable protein intermediate, which may not be detectable depending on the techniques used. Two unfolding processes are observed for human, bovine, rat, dog, and rabbit albumin when they are denatured by GdnHCl and monitored by CD, but only human, bovine, or rat albumin shows two transitions when monitored by fluorescence (Kosa et al., 1998). Similarly, the UV absorption of DGK drops biphasically with increasing concentration of denaturant SDS, suggesting two unfolding transitions, but CD measurement at 222 nm only shows a single denaturation phase (Lau and Bowie, 1997). The failure of CD to detect an intermediate is probably due to a variety of factors affecting CD determination, such as protein concentration (causing improportional changes in secondary structure), pH, solvent property, and ionic strength (Farnsworth et al., 1997; Hu et al., 1997).

Fluorescence spectroscopy is often used to probe protein unfolding (Eftink, 1994). A red shift in fluorescence spectroscopy is commonly observed during protein unfolding because Trp or Tyr residues are in less hydrophobic environments (De Young et al., 1993; Volkin et al., 1996). An often-used agent in the investigation of protein unfolding is Bis-ANS, whose fluorescence is pH-independent and very weak in water but increases greatly upon binding to unfolding-exposed hydrophobic sites in proteins. Due to this property, Bis-ANS has been used recently to probe the mechanism of α_1-antitrypsin polymerization (James and Bottomley, 1998).

Both primary and second-derivative amide I IR spectra can be used to probe pH or temperature-induced protein unfolding or conformational changes in proteins such as hemoglobin (Dong and Caughey, 1994) and insulin (Pikal and Rigsbee, 1997). By monitoring changes in band intensity of native β-sheet structure at 1638 cm^{-1} and an aggregate band at 1619 cm^{-1}, human FXIII has been found to denature irreversibly as the temperature increases from 25 to 85°C (Dong et al., 1997). IR spectra of proteins in solution can be significantly different from those obtained in solid state. Insulin in solution shows a sharper and stronger IR helix band than solid insulin, and the spectrum of denatured insulin (spectrum at 85°C) resembles that of solid insulin (Pikal and Rigsbee, 1997).

3.4.2. Determination of protein melting/unfolding temperature (T_m)

Those physical methods used to determine $\Delta G_{f\rightarrow u}$ can be used similarly to determine protein melting/unfolding temperature (T_m), such as CD, fluorescence, optical rotation, or UV. T_m can be easily located at $\Delta G = 0$ on the ΔG versus T curve or directly determined from the signal–temperature curve (Farruggia et al., 1997).

Differential scanning calorimetry (DSC) is one of the frequently-used techniques to determine protein T_m. Proteins unfold with an endothermic peak, but aggregation is exothermic by DSC. If the two events happen approximately at the same time, a peak would be the sum of the two events. The first event may be overwhelmed by the second, such as the single exothermic peak observed for rhKGF unfolding and aggregation (Chen et al., 1994a). In this case, modulated DSC may be considered as a way to differentiate overlapping thermal events due to its higher resolution (Craig and Royall, 1998; Royall et al., 1998).

There are several other factors that can potentially affect determination of T_m. The first factor is the determination method to be used. Different methods can give significantly different T_m values

for the same protein. Detailed examples are listed in Table 1. Temperature-ramping rate during determination of T_m may have a significant effect. For example, lowering the temperature-ramping rate reduces the T_m of rhKGF, suggesting a kinetically controlled denaturation process (Chen et al., 1994a). Vermeer et al. (1998) recently demonstrated that at 0.5°C/min, mouse IgG shows both a melting and an aggregation peak by DSC but at 0.1°C/min, only the melting peak can be observed. Protein concentration may or may not affect determination of T_m. While the initial unfolding temperature of rhKGF is independent of protein concentration (Chen et al., 1994a), that of IFN-β-1a decreases from about 77 to 68°C when the protein concentration is increased from 10 to 100 μg/ml (Runkel et al., 1998). The T_m independence on protein concentration may imply a rate-limiting protein unfolding.

Recently, infrared spectroscopy (IR) and capillary electrophoresis (CE) have also found their application in determination of T_m. By IR, the T_m of human phenylalanine hydroxylase (hPAH) has been estimated based on temperature-induced changes in the intensity ratio of the amide I band at 1619 and 1650 cm^{-1} (Chehin et al., 1998). Similarly, the T_m of RNase has been determined by CE based on changes in the protein's electrophoretic mobility at different temperatures (McIntosh et al., 1998).

3.4.3. Estimation of protein secondary structures

IR is one of oldest methods and remains the most extensively-used technique today for studying secondary structure of proteins (Susi and Byler, 1986; Dong et al., 1995b; Allison et al., 1996; D'Auria et al., 1997). The commonly-used band for determination of protein secondary structure is the amide I region (1620–1690 cm^{-1}), although the amide III band (1200–1330 cm^{-1}) has also been used in this regard. The amide I region covers different C=O stretching frequencies arising from different secondary structures (α-helix, β-sheet, turn, and unordered structures) and has no major interfering bands from other structures in proteins, whereas the amide III band has better resolution for secondary structures and no water interference (Cooper and Knutson, 1995). A good example of using the amide III band is the estimation of secondary structure of some dozen different proteins in both liquid and solid states by Griebenow and Klibanov (1995).

IR absorption bands are generally broad and consist of overlapping components representing different structures. Two methods have been used for resolution enhancement: Fourier self-deconvolution and second or fourth derivation (Goormaghtigh et al., 1994b). Both techniques work equally well in resolving overlapping components (Dong et al., 1995b). However, some believe that analysis of derivative spectra should be discouraged because derivation does not preserve the integrated areas of individual components (Surewicz et al., 1993). Nevertheless, the two resolution-enhancing methods can be conveniently used on modern instruments of Fourier transform infrared spectroscopy (FTIR), which also offer high sensitivity (high S/N ratio), greater accuracy, and higher speed (Susi and Byler, 1986; Surewicz et al. 1993). Secondary structure estimation after resolution enhancement seems rather accurate. Dong et al. (1990) determined the second-derivative IR spectra of 12 globular proteins in aqueous solutions, and the relative amounts of different secondary structures in all proteins were nearly identical (mostly $\pm 5\%$) to those obtained by crystallography.

Unfortunately, water molecules absorb strongly in the amide I region (about 1640 cm^{-1}), interfering with data interpretation. There are two ways to overcome this obstacle: careful subtraction of water absorption or use of D_2O as the solvent (Goormaghtigh et al., 1994a). To make reliable subtraction, higher protein concentrations (>10 mg/ml) are recommended to increase the protein signal and a CaF_2 (or BaF_2) cell with a path length of 10 μm or less should be used to control the total sample absorbance within 1 unit (Cooper and Knutson, 1995). Replacing water with D_2O as the solvent not only eliminates water interference in the amide I region but also stabilizes proteins in some cases (Bai et al., 1994). For example, human FXIII is apparently more stable in D_2O than in H_2O (Dong et al., 1997). The higher stability of proteins in D_2O is believed to be due to stronger hydrogen bonds formed by deuterium

than those formed by hydrogen. This suggests that IR spectra of proteins in D_2O may not be the same as those in water. As a matter of fact, subtle differences in the secondary structure in bovine β-lactoglobulin variants are found in the two solvents (Dong et al., 1995a).

Another often-used method to determine the relative composition and changes of secondary structure in a protein is CD. A broad negative peak at about 218 nm is characteristic of a β-sheet structure, and two negative peaks at 208 and 222 nm are characteristic of a α-helix structure (Chen et al., 1994a; Farnsworth et al., 1997; Hu et al., 1997; Swietnicki et al., 1997). Although CD is generally less sensitive than IR, the two methods are highly complementary and, if possible, should be used together (Surewicz et al., 1993). Their relative contribution can be illustrated in the following examples. In the comparison of the secondary structures of two generic bovine β-lactoglobulin variants in D_2O solution, the CD spectra of the two proteins are nearly identical, but the IR spectra are significantly different (Dong et al., 1995a). In a different investigation, about 20–35% random or unordered elements in human FXIII in an aqueous solution are detected by CD but not observed by FTIR, although detailed analysis indicates that the secondary structures determined by the two methods are very similar (Dong et al., 1997).

Several factors can affect the appearance of the characteristic peaks in CD spectra, such as protein concentration, temperature, pH, and ionic strength. Increasing protein concentration may be associated with increased content of β-sheet (Matsuura and Manning, 1994). High ionic strength may reduce helicity of a protein (destabilization), if charge–charge interactions make a net favorable contribution to helix stability (Kuhlman et al., 1997). Although a double ellipticity minima at 208 and 222 nm is of a typical helical conformation, this may not be obvious if the helical content is very low and/or there are interfering aromatic residues such as Tyr (Prieto et al., 1997).

Lastly, NMR can also be used to determine secondary structures of proteins. It can provide accurate estimation of both the extent and location of the secondary structures (Reid et al., 1997). A particular use of NMR is the determination of secondary structural propensities of residues in unfolded or partially-folded proteins (Dyson and Wright, 1998).

3.4.4. Protein aggregation

In addition to polyacrylamide gel electrophoresis (PAGE) and analytical centrifugation, size exclusion HPLC (SEC-HPLC) is an often-used method in monitoring protein aggregation. Unfortunately, the size of a protein or its aggregates can be overestimated by SEC-HPLC if the protein is not spherical (such as highly-coiled proteins) and its Stokes radius is greater than that of a globular protein (Kuhlman et al., 1997). In addition, if a protein has carbohydrates or interacts with the column, the elution profile of the protein may change, leading to erroneous estimation of its molecular weight. To solve these issues, SEC-HPLC can be coupled with both light scattering and refractive index detectors to determine the size of a protein or its aggregates. The size calculated by the signal ratio of the two detectors is not affected by the above factors (Wen et al., 1996).

While SEC-HPLC can only determine the total amount of aggregates based on size, reversed phase HPLC (RP-HPLC) may detect both covalent and non-covalent aggregates such as hGH (Perlman and Nguyen, 1992) or different isoforms of protein aggregates such as bFGF dimers (Shahrokh et al. 1994b). Since a protein sample is usually filtered through a 0.2 μm filter to remove any particulates before analysis, the HPLC method is limited for determination of soluble aggregates. In addition, a protein may unfold or refold during HPLC analysis depending on the protein and the nature of the mobile phase, which may change the retention time of the protein. For example, denatured bFGF partially refolds into native protein during analysis, which changes the retention time and peak shape of the denatured protein (Shahrokh et al. 1994b). Therefore, prevention of unfolding/refolding by addition of certain modifiers in the mobile phase may be needed in these cases.

The turbidimetric method is often used to estimate the amount of protein aggregates by measuring optical density of samples based on light scattering in near UV or visible region, where

proteins do not have any absorption (Eckhardt et al., 1994). A variety of wavelengths has been chosen and used, including 300 nm for urokinase (Vrkljan et al., 1994), 350 nm for aFGF (Tsai et al., 1993; Volkin et al., 1993), average optical density between 340 and 360 nm for met-hGH and tPA (Hsu et al. 1991, 1995), 450 nm for pGH (Charman et al. 1993), and 500 nm for IL-1ra (Chang et al., 1996b). This method has been proved to be more sensitive than HPLC in detecting early formation of aggregates (Wang et al., 1996b). In addition, the turbidity of a protein solution can be linear in a narrow concentration range for accurate quantitation, such as IL-1ra in the range of 0.1–0.3 mg/ml (Chang et al., 1996b). On the other hand, this method can be variable. For example, it has been found that the turbidimetric variation in determination of LMW-UK aggregation in phosphate buffer (pH 6.5) upon heat treatment is usually less than 10% but increases up to 30% when the LMW-UK solution contains other polymer additives (Vrkljan et al., 1994).

A simpler method for estimation of the extent of protein aggregation is to compare visually the level of sample cloudiness using seven categories of visual appearance: clear, slightly opalescent, opalescent, very opalescent, slightly cloudy, cloudy, and very cloudy (Eckhardt et al., 1994). The requirement of using this method is a uniform distribution of all the aggregates.

Recently, IR has been used extensively in protein denaturation/aggregation studies. A common feature of thermally-induced (or lyophilization-induced) protein aggregation is the formation of an intermolecular hydrogen-bonded antiparallel β-sheet structure, which is represented by a low-frequency band around 1620 cm^{-1} and an associated weaker high-frequency band around 1685 cm^{-1} (Dong et al., 1995b). For example, an aggregation band has been found at 1619 cm^{-1} for human FXIII (Dong et al., 1997) and hPAH (Chehin et al., 1998), and at 1620 cm^{-1} for recombinant human IFN-γ (Kendrick et al., 1998b). This structural transition occurs regardless of the initial composition of the secondary structure of native proteins. Therefore, these bands can be used to monitor and quantify aggregation in both aqueous and solid states. Similarly, reversibility of protein aggregation may be determined by monitoring an aggregate band. By this method, the temperature-induced aggregation of human FXIII in both D_2O and H_2O was found irreversible (Dong et al., 1997).

Another IR method for estimating protein aggregation is to compare overall spectral change of proteins, as the change may correlate with protein aggregation. The overall spectral change can be measured by fractional area overlapping of the second-derivative spectrum of a protein sample with that of a reference. Using this method, Allison et al. (1996) demonstrated that any decrease in fractional spectral area overlap of freeze-dried chymotrypsinogen directly correlates with the amount of aggregates formed after rehydration of the solid.

3.4.5. Determination of protein degradation products

A variety of analytical methods is available to determine protein degradation products. Both SEC-HPLC and PAGE can detect protein degradation products or certain fragments but these methods are usually inadequate in detecting subtle structural changes in proteins such as oxidation and deamidation. Generally, RP-HPLC is the preferred method in these cases. RP-HPLC has been widely used to separate and quantitate deamidated proteins such as GRF (Stevenson et al., 1993), insulin (Darrington and Anderson, 1995), and tPA (Paranandi et al., 1994), oxidized proteins such as hIGF-1 (Fransson et al., 1996), human leptin (Liu et al., 1998), and rhPTH (Nabuchi et al., 1995), hydrolyzed proteins such as bFGF (Shahrokh et al., 1994a), insulin (Brange et al. 1992b) and rhM-CSF (Schrier et al., 1993), isomerized and oxidized (Met^{125}) hGH (Johnson et al., 1989; Perlman and Nguyen, 1992), and succinimidated bFGF (Shahrokh et al., 1994a).

However, RP-HPLC itself is usually not capable of identifying protein degradation products. To achieve identification, RP-HPLC-separated degradation products have to be collected and further analyzed by other analytical methods such as mass spectroscopy (MS), peptide mapping and sequencing, and amino acid analysis (Johnson et

al., 1989; Schrier et al., 1993; Shahrokh et al., 1994a; Nabuchi et al., 1995; Liu et al., 1998). A more efficient technique in use is the coupled RP-HPLC and MS (LC-MS). This technique has been used in the identification of hydrolyzed bFGF (Shahrokh et al., 1994a), and different mono-, di- and tri-oxidized human leptin (Liu et al., 1998). In addition to HPLC, capillary electrophoresis has also been coupled to MS (CE-MS) for highly sensitive analysis of proteins and peptides (Figeys and Aebersold, 1998). MS alone has been a very powerful tool in identification of protein degradation products as well as molecular weight determination (Nguyen et al., 1995). The use of tandem MS (MS–MS) may allow direct identification of partial to complete sequence for peptides up to 25 amino acids, sites of deamidation, and isomerization (Carr et al., 1991).

3.4.6. Probing protein tertiary/quaternary structure

The ultimate goal of structural studies on proteins is to gain insight into the protein's three-dimensional structure at a high-resolution level. Two delicate techniques can be used to probe protein structures: X-ray crystallography and NMR. Both methods have advantages and shortcomings. X-ray crystallography has more accuracy but needs highly-ordered crystals and a large amount of material in solid state. NMR can be applied for solutions containing an adequate amount of protein (typically millimolar) but is usually limited to small proteins (< 20 kD) (Middaugh, 1990). Recent advances in multidimensional NMR methodology can now permit structural determination of larger proteins up to 60 kD (Clore and Gronenborn, 1998). Other indirect techniques for probing structures of large proteins by NMR include determination of the rate of hydrogen exchange (Raschke and Marqusee, 1998) or structures of 'dissected' protein subunits or domains (Campbell and Downing, 1998).

Other methods of probing protein tertiary structure include CD in the near UV region, fluorescence spectroscopy, and second-derivative UV spectroscopy. However, these methods generally do not provide detailed information about structure. Nevertheless, CD has been used to demonstrate destabilization of methionyl pGH in the presence of either poloxamer 407 (Pluronic F127) or 188 (Pluronic F68) (Charman et al., 1995), and to monitor changes in the tertiary structure of β-lactoglobulin upon heating (Matsuura and Manning, 1994). Second-derivative UV spectroscopy in combination of SEC-HPLC has been used to monitor the relative solvent exposure of Tyr residues in IL-2 mutants (Ackland et al., 1991).

4. Stabilization and formulation of liquid protein pharmaceuticals

Proteins in extremophilic organisms can tolerate one or more of the following stresses: low or high temperatures, high hydrostatic pressure, high salinity, and extreme pHs, even though their building blocks are exclusively the canonical 20 natural amino acids. Therefore, significant room exists to stabilize any unstable protein pharmaceuticals. The central issue in protein stabilization is preservation of the functional state of proteins under various stressful conditions.

4.1. Means and mechanisms of protein stabilization

Proteins may be stabilized either by changing their structural characteristics (internally) or by changing the properties of solvent in contact with them (externally). Structural changes may increase the protein's unfolding free energy change (ΔG_{mut}), leading to its stabilization with a free energy change $\Delta\Delta G = \Delta G_{\mathrm{mut}} - \Delta G_{\mathrm{nat}}$. Since the difference between mesophilic and thermophilic proteins is small in terms of $\Delta\Delta G$ (5–7 kcal/mol), stabilization of mesophilic proteins to the level of thermophilic proteins is feasible (Querol et al., 1996). To estimate the degree of internal or external stabilization, the change in the protein's unfolding temperature (T_{m}) is often used as an indicator. A minimum increase of 1°C in T_{m} is considered as the threshold of thermostability increase (Querol et al., 1996).

4.1.1. Mechanisms of internal protein stabilization

As discussed in Section 2.1, native proteins are stabilized by many forces. Any structural change

that increases any of the stabilizing forces without changing the overall protein conformation generally stabilizes proteins (Jaenicke, 1991). Protein thermal stability usually increases if amino acid substitution/modification results in increased internal and decreased external (or surface) hydrophobicity (Kristjánsson and Kinsella, 1991). Increasing internal hydrophobicity often correlates with increased packing efficiency and protein stability (Mozhaev and Martinek, 1984; Vieille and Zeikus, 1996). This positive correlation was demonstrated recently in a study on a series of hydrophobic mutants of human lysozyme (Takano et al., 1998). Protein stability also positively correlates with the content of hydrogen bond-forming amino acids and the ability of these amino acids to maintain these bonds, especially at critical locations (Kristjánsson and Kinsella, 1991). However, no direct correlation has been found between protein thermal stability and protein volume (Querol et al., 1996). Increasing charge density apparently destabilizes a protein (Sindelar et al., 1998).

Local interactions of amino acids are indispensable in native proteins. The interactions may come from residues close in sequence and contribute to the secondary structure propensities. Enhancement of native local interactions makes proteins more resistant to thermal and chemical denaturation, and introduction of non-native local interactions destabilizes proteins because non-native/denatured conformations are stabilized (Prieto et al., 1997). The α-helix can be stabilized by introducing residues of high helix propensity (such as Ala), which eventually stabilizes proteins (Querol et al., 1996; Vieille and Zeikus, 1996).

Thermostable proteins are less flexible than thermolabile ones (Daniel et al., 1996). Protein stability inversely correlates with its flexibility (Tang and Dill, 1998). The flexible regions in proteins are typically the labile areas (Vieille and Zeikus, 1996). Some inactivation processes, such as oxidation of Cys and sensitive Met, hydrolysis of peptide bonds at Asp residues, and deamidation of Asn and Gln residues, are more likely to occur in flexible (or solvent-accessible) areas of the protein (Powell, 1996; Querol et al., 1996). These areas should be considered first for structural modification/stabilization.

4.1.2. Mechanisms of external protein stabilization

There are two mechanisms of solvent-induced stabilization of proteins: (1) strengthening protein-stabilizing forces; and (2) destabilizing the denatured state. This is to say that any change in solvent property that enhances a native interaction or perturbs a non-native interaction increases stability of proteins (Wrabl and Shortle, 1996). Under non-native conditions, proteins may still be stabilized as long as the condition favors strengthening of non-covalent interactions, especially hydrophobic interactions. These non-native conditions, such as concentrated solutions of salt, polyols, or certain organic solvents can enhance hydrophobic interactions and stabilize proteins by altering the structure of water and reducing protein interaction with the solutes (Mozhaev and Martinek, 1984; Kristjánsson and Kinsella, 1991; Brange et al. 1997). Although an excipient(s) stabilizes a protein mostly by changing solvent property, some may interact favorably with charged sites on the protein surface and minimize electrostatic protein–protein interactions to achieve protein stabilization (Remmele et al., 1998).

4.1.3. Preferential Interaction—a major stabilization mechanism of excipients

The most tenable and widely-accepted mechanism of protein stabilization in aqueous solution is preferential interaction of proteins. Preferential interaction means that a protein prefers to interact with either water or an excipient (co-solute/co-solvent). In the presence of a stabilizing excipient, a protein prefers to interact with water (preferential hydration) and the excipient is preferentially excluded from the protein domain (preferential exclusion). In this case, proportionally more water molecules and fewer excipient molecules are found at the surface of the protein than in the bulk (Arakawa et al., 1991, 1993; Timasheff, 1993, 1998; Lin and Timasheff, 1996).

Preferential interaction of a protein with an excipient has been defined as:

$$(\partial g_3/\partial g_2)_{T,\mu_1,\mu_3} \text{ or } (\partial m_3/\partial m_2)_{T,\mu_1,\mu_3}$$

in which 1, 2, and 3 represent water, protein, and excipient, respectively, and μ is the chemical po-

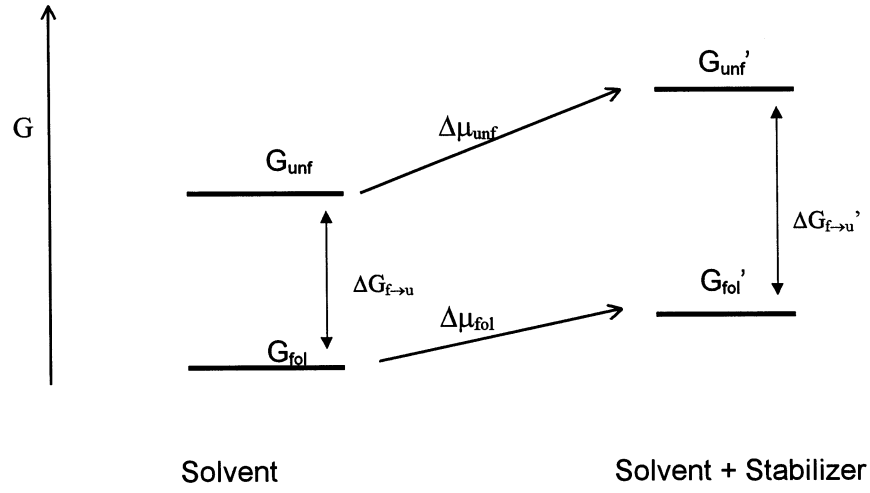


Fig. 1. Diagram of free energy change of a protein in the presence of a protein stabilizer

tential (Timasheff, 1992, 1993, 1998). The interaction can be expressed on a gram basis (g) or on a molar basis (m). Preferential interaction of a protein with either water or an excipient is the consequence of a difference in affinity of a protein for water or an excipient. If there is a preference for an excipient, the measured interaction is positive, preferential binding. In the opposite case, the measured interaction is negative, preferential hydration and the protein is stabilized. Sucrose is a commonly-used protein stabilizer, and the preferential interaction of rhIL-1ra and α-chymotrypsin in 1 M sucrose is, respectively, -0.164 g sucrose/g protein (Kendrick et al., 1997) and -7.6 mol sucrose/mol protein (Timasheff, 1993). In a recent study on stabilization of RNase by sucrose, Liu and Bolen (1995) have found that the protein side chains actually favor exposure to sucrose relative to water, facilitating protein unfolding, and that it is the highly unfavorable exposure of polypeptide backbone on unfolding that leads to protein stabilization by sucrose. In contrast, peptide backbone exposure is favorable in the presence of strong denaturants such as urea and GdnHCl because they preferentially bind to the backbone.

Stabilizing preferential interaction of a protein with an excipient is usually associated with an increase in chemical potential of the protein, which is thermodynamically unfavorable (Carpenter et al., 1990; Timasheff, 1993; Kendrick et al., 1997). This means that protein interaction with the excipient is unfavorable relative to water; hence, the protein is preferentially hydrated and the excipient is preferentially excluded from the protein surface. The positive change in chemical potential is marginal at low excipient concentrations and becomes more positive at higher concentrations. The increase in chemical potential is directly proportional to the surface area of the protein exposed to solvent. Since a denatured protein has a greater surface area than a native protein, preferential exclusion of the excipient from the surface of the denatured protein is more unfavorable than from that of the native protein. Therefore, protein stabilization arises from destabilization of the denatured state by the excipient, leading to a larger free energy change ($\Delta G_{f\rightarrow u}$). Fig. 1 shows the free energy changes associated with this type of protein stabilization; a stabilizer destabilizes the unfolded state to a greater degree than the native state.

Stabilization of proteins in solution by a variety of excipients appears to correlate positively with their capability of increasing the surface tension of water. Introduction of a protein molecule into water must form additional protein–water interface, and the interfacial tension is equal to the surface tension of water after proper correction

for curvature of the protein surface (Kita et al., 1994). Substances lowering the surface tension of water accumulate at the protein surface; those raising it are kept away from the protein surface. It has been found that most stabilizers for lysozyme and BSA increase the surface tension of water, which also correlates with the increase in chemical potentials of the two proteins (Kita et al., 1994).

However, the surface tension effect of an excipient is not the sole factor involved in the protein–solvent interactions. Increasing the surface tension of water by an excipient does not necessarily mean automatic protein stabilization. Surface tension-derived stabilization can be overcome by weak binding of these excipients to proteins. For example, Arg hydrochloride (ArgHCl) increases the surface tension of water but destabilizes RNase A because ArgHCl binds to the protein, as indicated by a decreasing preferential hydration, $(\partial g_1/\partial g_2)_{T,\mu_1,\mu_3}$, with increasing ArgHCl concentration (Lin and Timasheff, 1996). Urea and $MgCl_2$ increase the surface energy of water but are preferentially bound to proteins at high concentrations (Kita et al., 1994). On the other hand, excipients decreasing surface tension of water may still stabilize a protein. Betaine and glycerol decrease the surface energy of water but induce protein preferential hydration (Kita et al., 1994). Four organic solvents, PEG, 2-methyl-2,4-pentanediol (MPD), DMSO, and TMAO, decrease the surface tension of water but induce preferential hydration of lysozyme and BSA (Kita et al., 1994). This has been attributed to the presence of two types of agents which are preferentially excluded: (1) those that are totally independent of the chemical nature of protein surface and excipient concentration; and (2) those that are not (Timasheff, 1993, 1998). The first-type agents achieve preferential exclusion either by increasing the surface free energy of water or by steric exclusion. The second-type agents rely on the solvophobic effect such as glycerol, PEG, 2-methyl-2,4-pentanediol (MPD), and may stabilize or destabilize a protein depending on its concentration and solvent conditions (Kita et al., 1994; Frye and Royer, 1997).

Alternative explanations for excipient-induced protein stabilization have been offered recently through studies on hydrogen exchange (HX) in proteins by NMR. Different types of protons have different rates of HX in a protein, including slow-exchanging amide protons mainly from the compact unfolded state and the fast and intermediate amide protons mainly from the native state (Wang et al., 1995). Sucrose at 1 M decreases the HX rate of slow-exchanging amide protons by decreasing the population of unfolded protein, suggesting that sucrose may favor protein folding (Wang et al., 1995). An increased rate of folding is also the primary reason for stabilization of staphylococcal nuclease by xylose (Frye and Royer, 1997).

The H-D exchange rate and solvent accessibility are considered a measurement of protein flexibility, which inversely correlates protein stability (Tang and Dill, 1998). It has been found that both the H-D exchange rate in IL-1ra and the reactivity of Cys (free thiol groups) with 7-chloro-4-nitrobenzo-2-oxa-1,3-diazole (NbdCl) are reduced by increasing sucrose concentrations, suggesting reduction of solvent accessibility and conformational mobility of rhIL-1ra by sucrose (Kendrick et al., 1997). The apparent hydrodynamic diameter of the protein also decreases gradually with increasing sucrose concentration, which indicates increased packing of the protein structure and decreased solvent accessibility.

4.2. Stabilization of proteins by excipients

The most common method for stabilizing liquid protein pharmaceuticals is the use of a formulation excipient(s), which should be at least soluble and nontoxic. These excipients are also referenced as chemical additives (Li et al., 1995c), co-solutes (Arakawa et al. 1993) or co-solvents (Timasheff, 1993, 1998; Lin and Timasheff, 1996). These excipients can also retard certain chemical degradations in proteins. Their stabilizing effects are usually concentration- and protein-dependent, although high concentrations of excipients may not be necessarily more effective, and in some cases, can have negative effects. For example, sorbitol reduces heat-induced aggregation of aFGF at

55°C effectively at concentrations below 0.5 M but is less effective at higher concentrations (Tsai et al., 1993).

Protein-stabilizing excipients can be broadly divided at least into the following types: sugars and polyols, amino acids, amines, salts, polymers, and surfactants. Their stabilizing effects can be significantly different (Table 4). For example, the amounts of excipients required to reduce 50% of heat-induced aggregation of aFGF are 0.55 mM for sodium sulfate, 1.6 mM for His, 180 mM for Gly, 155 mM for trehalose, 250 mM for dextrose and 310 mM for sorbitol (Tsai et al., 1993).

4.2.1. Stabilizing buffer

Usually, a protein is stable only in a very narrow pH range, such as recombinant FVIII SQ, whose stable pH range is between 6.5 and 7 in 0.1 or 1 M NaCl solution (Fatouros et al., 1997a). Accurate control of the pH of a protein formulation is the first step toward protein stabilization. Unfortunately, no general rules have been reported for buffer selection. In a few cases, phosphate buffer has been shown to be detrimental. About 38% of hEGF at 0.5 μg/ml are deamidated in Tris–HCl at pH 7.0 on incubation at 60°C for 2 days, and the amounts of deamidated hEGF increase to 83, 63, 52, 51, and 49%, respectively, in buffers of PBS, sodium phosphate, sodium borate, sodium citrate, and sodium acetate (Son and Kwon, 1995). Similarly, at 37°C, rhKGF in 100 mM phosphate buffer (pH 7.0) has a half-life of 15 days, but the half-life increases to 25 and 88 days, respectively, in 100 and 500 mM sodium citrate buffers (Chen et al., 1994a). The better stability of rhKGF in citrate buffer may be due to the favorable interaction of citrate with positively charged residues in rhKGF as hypothesized in the stabilization of pig heart mitochondrial malate dehydrogenase (*phm*-MDH) (Jensen et al., 1996). In a different study, however, increasing citrate buffer concentrations increase the formation of bFGF particles at pH 5, and the citrate buffer also causes aggregation of bFGF at pH 3.7, whereas acetate buffer at pH 3.8 does not (Wang et al., 1996b). On the other hand, phosphate has been shown to stabilize certain proteins. Increasing phosphate buffer concentration from 4.6 to 9.2 mg/ml significantly decreases the rate of aFGF aggregation (Won et al., 1998). In the presence of 0.1 or 1 mM phosphate, the GdnHCl concentration for unfolding 50% alkaline phosphatase molecules is increased from 2.46 to 2.67 and 2.72 M, respectively (Hung and Chang, 1998). Phosphate at 0.05 M can also stabilize maize leaf phosphoenolpyruvate carboxylase (*ml*-PEPC) upon incubation at 40°C, although it is not as effective as citrate at the same concentration (Jensen et al., 1996).

Both buffer species and concentration may affect physical and chemical stability of a protein. Pikal et al. (1991) examined the effect of three phosphate buffer concentrations (0.11, 0.23 and 0.45 mg sodium phosphate/mg hGH) on the stability of hGH. While maximum aggregation occurs at 0.23 mg sodium phosphate/mg hGH, chemical degradations (oxidation and deamidation) are less significant at both 0.23 and 0.45 mg sodium phosphate/mg hGH. At a lower buffer concentration of 0.11 mg sodium phosphate/mg hGH, chemical degradation is relatively high. Therefore, a balanced buffer concentration should be selected to maximize protein stability. An ideal buffer should be able to inhibit both physical and chemical instabilities simultaneously.

4.2.2. Sugars and polyols

Sugars and polyols represent often-used nonspecific protein stabilizers. Their stabilizing effect is demonstrated and widely interpreted as the result of preferential exclusions, weak and nonspecific (Xie and Timasheff, 1997a,b; Timasheff, 1998). Among various sugars, sucrose and trehalose appear to be the most often-used stabilizers. Sucrose has been shown to effect concentration-dependent stabilization of rhDNase at pH 6.8 (Chan et al., 1996), and inhibition of IL-1ra dimer formation (Chang et al., 1996a) and GdnHCl-induced rhIFN-γ aggregation (Kendrick et al., 1998a). Similarly, trehalose is able to increase the T_m of RNase A (Lin and Timasheff, 1996), to inhibit heat-induced aggregation of aFGF (Tsai et al., 1993), and to stabilize rhDNase in a concentration-dependent manner (Chan et al., 1996).

Table 4
Examples of protein stabilization by excipients in liquid state

Proteins	Formulation compositions	Study conditions	Remaining activity (or as stated)	References
Baker's yeast ADH	50 μg/ml in 20 mM potassium phosphate, pH 7.6	50°C for 10 min	50%	Ramos et al., 1997
	Control + 500 mM KCl	50°C for 10 min	~90%	Ramos et al., 1997
	Control + 500 mM trehalose	50°C for 10 min	~70%	Ramos et al., 1997
	Control + 500 mM mannosylglycerate	50°C for 10 min	~90%	Ramos et al., 1997
hEGF	0.5 μg/ml in 50 mM sodium phosphate, pH 8.0	60°C for 1 day	49%	Son and Kwon, 1995
	Control + 0.02% Triton X-100	60°C for 1 day	84%	Son and Kwon, 1995
	Control + 0.01% Tween 20	60°C for 1 day	75%	Son and Kwon, 1995
	Control + 0.05% fibronectin	60°C for 1 day	85%	Son and Kwon, 1995
	Control + 6 mM $ZnCl_2$	60°C for 1 day	76%	Son and Kwon, 1995
GDH	50 μg/ml in 20 mM potassium phosphate, pH 7.5	50°C for 10 min	0%	Ramos et al., 1997
	Control + 500mM KCl	50°C for 10 min	~90%	Ramos et al., 1997
	Control + 500 mM trehalose	50°C for 10 min	~2%	Ramos et al., 1997
	Control + 500 mM mannosylglycerate	50°C for 10 min	~90%	Ramos et al., 1997
rIL-2	0.2 μg/ml in PBS, pH 7.0	Moderate shaking at 4°C for 96 h	~30%	Wang and Johnston, 1993a
	+ 10% (w/w) Pluoronic F-127	Moderate shaking at 4°C for 96 h	100%	Wang and Johnston, 1993a
rhKGF	0.5 mg/ml in 140 mM NaCl and 10 mM sodium phosphate, pH 7.0	37°C	$T_{1/2}$ + 2 days (loss of soluble aggregates)	Chen et al., 1994a
	0.5 mg/ml in 100 mM sodium phosphate, pH 7.0	37°C	$T_{1/2}$ + 15 days	Chen et al., 1994a
	0.5 mg/ml in 100 sodium citrate buffer, pH 7.0	37°C	$T_{1/2}$ + 25 days	Chen et al., 1994a
	0.5 mg/ml in 500 sodium citrate, pH 7.0	37°C	$T_{1/2}$ + 88 days	Chen et al., 1994a
	0.5 mg/ml in 10 mM sodium phosphate, 140 mM NaCl, and 0.5% (w/v) heparin, pH 7.0	37°C	$T_{1/2}$ + 105 days	Chen et al., 1994a
Rabbit muscle LDH	50 μg/ml in 20 mM potassium phosphate, pH 7.6	50°C for 10 min	5%	Ramos et al., 1997
	Control + 500 mM KCl	50°C for 10 min	~20%	Ramos et al., 1997
	Control + 500 mM trehalose	50°C for 10 min	~25%	Ramos et al., 1997
	Control + 500 mM mannosylglycerate	50°C for 10 min	~90%	Ramos et al., 1997
Urease	0.33 mg/ml in phosphate buffer and 1 mM EDTA, pH 7.0	Moderate shaking at 4°C for 96 h	~40%	Wang and Johnston, 1993a
	Control + 10% (w/w) Pluoronic F-127	Moderate shaking at 4°C for 96 h	100%	Wang and Johnston, 1993a
Urease	0.33 mg/ml in phosphate buffer and 1 mM EDTA, pH 7.0	50°C for 96 h	AUC = 4868 (activity-time plot)	Wang and Johnston, 1993b
	Control + 1% Pluoronic F-127	50°C for 96 h	AUC = 6722	Wang and Johnston, 1993b

In all these examples, the stabilizing effect of sugars depends on their concentrations. A concentration of 0.3 M (or 5%) sugar or polyols has been suggested to be the minimum to achieve significant protein stabilization (Arakawa et al. 1993). This seems true in many cases. As high as 1 M sucrose or 10% glycerol have been commonly used to protect the activity of proteins during their isolation (Timasheff, 1993). Other examples include stabilization of thrombin by 20% dextrose or sorbitol or 50% glycerol (Boctor and Mehta, 1992) and rhG-CSF by 5% mannitol (Herman et al., 1996), inhibition of bFGF aggregation by $\geq 30\%$ sucrose (Wang et al., 1996b), IL-1ra dimer formation by 40% (w/v) sucrose (Chang et al., 1996a), and IgG aggregation by 33% sorbitol (Ganzález et al., 1995), and significant increase in the T_m of RNase A by 0.5–1 M sucrose or sorbitol (Liu and Sturtevant, 1996; McIntosh et al., 1998) and porcine pancreatic elastase by 20% sucrose, sorbitol, lactose, or mannitol (Chang et al., 1993).

Different sugars or polyols may stabilize a protein to a similar or different degree depending on the protein. It has been found that lactose, sucrose, trehalose, or mannitol stabilizes rhDNase at pH 6.8 to a similar degree based on their effect on the T_m (Chan et al., 1996). In a different case, while 0.55 M sucrose increases the T_m of RNase from 35.5 to 44.9°C, the same concentration of sorbitol only increases the T_m to 40.5°C (McIntosh et al., 1998). Similarly, different concentrations of excipients (155 mM trehalose, 250 mM dextrose, or 310 mM sorbitol) are required to reduce 50% of heat-induced aggregation of aFGF (Tsai et al., 1993). Sucrose at 10, 300, or 600 mg/ml is more effective than sorbitol or mannitol in the stabilization of FVIII SQ (Fatouros et al., 1997b).

Sugars and polyols can also protect proteins from chemical degradations. For example, Li et al. (1996a,b) studied the effect of sugars and polyols on the metal-catalyzed oxidation of human relaxin and found that sugars and polyols, such as glucose, mannitol, glycerol, and ethylene glycol, can significantly inhibit the oxidative degradation. The inhibitory effect was shown to be due to their complexation with metal ions instead of the commonly-accepted radical-scavenging mechanisms. Due to the weak complexation, as high as 50 mM mannitol is needed to have a significant protective effect.

Not all proteins can be stabilized by sugars or polyols. At 37°C, the half-life for the loss of soluble rhKGF in 10 mM phosphate buffer (pH 7.0) and 140 mM NaCl is 1.8 days and replacing NaCl with 9% (w/v) sucrose or 5% sorbitol does not improve its half-life (Chen et al., 1994a). Sorbitol does not show any effect against interfacial denaturation of pGH and is marginally effective to prevent precipitation by thermal and quanidine dilution denaturation (Charman et al., 1993). Mannitol at 5 mg/ml even destabilizes IL-1R by decreasing its T_m from 48.1 to 46.7°C (Remmele et al., 1998).

In the selection of sugars for protein stabilization, reducing sugars should be avoided whenever possible, as these sugars have the potential to react with amino groups in proteins via the Maillard reaction (see Section 3.2).

4.2.3. Surfactants

There are basically two types of surfactants—nonionic and ionic. These surfactants drop surface tension of protein solutions and decrease the driving force for protein adsorption and/or aggregation at hydrophobic surfaces.

Nonionic surfactants are generally preferred in protein stabilization. Low concentrations of nonionic surfactants are often sufficient to prevent or reduce protein surface adsorption and/or aggregation due to their relatively low critical micelle concentrations (CMC) (Bam et al. 1995). Complete or significant inhibition has been reported of surface adsorption loss of TGF-β_1 by Tween 80 at 0.01% (Gombotz et al., 1996), glass surface-induced rConIFN aggregation by Tween 20 or Tween 80 at 0.01% (Ip et al., 1995), shear (or shaking)-induced rhGH aggregation by Pluronic F88 or Tween 20 at 0.1 mg/ml (or at ≥ 4:1 Tween 20:rhGH molar ratio) (Maa and Hsu, 1997; Bam et al., 1998), shaking-induced hemoglobin aggregation by Tween 80 at 0.045% (Kerwin et al., 1998), vortex-induced hGH aggregation by Tween 80, Brij 35, or Pluoronic F68 at respective concentrations of 0.1%, 0.013%, and 0.1% (Katakam et al., 1995), refolding-induced rhGH aggregation by

Tween 20, 40, and 80 at a Tween:rhGH molar ratio of 10 (Bam et al., 1996), shaking-induced loss of urease and rIL-2 activity by poloxamer 407 (Pluoronic F-127) at 10% (w/w) (Wang and Johnston, 1993a), and agitation-induced rhFXIII aggregation by Tween 20 at around 0.007% (w/v) (Kreilgaard et al., 1998). Tween 20 seems to be relatively more effective in a few cases. The rank order of minimizing rhG-CSF adsorption to PVC surface is Tween 20 > Tween 80 > Pluronic F127 > Pluronic F68 (Johnston, 1996). Tween 20 is also more effective than Tween 80 or Tween 40 in the inhibition of shaking-induced aggregation of rhGH (Bam et al., 1998). Not all proteins can be stabilized by surfactants and Tween 80 at 0.1% has no effect on the aggregation of IL-1β at 100 μg/ml at pHs from 3 to 7 (Gu et al., 1991).

Nonionic surfactants can also inhibit chemical degradations in proteins. hEGF degrades mainly by deamidation and loses 51% of its mitogenic activity in 50 mM sodium phosphate buffer (pH 8.0) during storage at 60°C for 1 day, and in the presence of 0.02% Triton X-100 or 0.01% Tween 20, the remaining activity is, respectively, 84 and 75% (Son and Kwon, 1995). At the same time, surfactants may be contaminated with alkyl peroxides, which can accelerate oxidation of proteins. rhCNTF has been found to dimerize by alkyl peroxides present in Tween 80 (Knepp et al., 1996). Inclusion of certain antioxidants, such as Cys, Met, or glutathione, can significantly retard the reaction. A correlation between the peroxide level in Tween 80 and the degree of oxidation in rhG-CSF has also been reported, and the peroxide-induced oxidation appears more severe than that induced by atmospheric oxygen present in the vial headspace (Herman et al., 1996). For this reason, only 0.004% Tween 80 is formulated in the liquid rhG-CSF formulation.

Ionic surfactants are usually not used in stabilizing proteins because they can bind to both polar and nonpolar groups in proteins and cause denaturation (Giancola et al., 1997). Anionic surfactants such as SDS generally bind more effectively than cationic detergents such as decyltrimethyl ammonium chloride. The binding of ionic detergents such as SDS to a protein is a function of the free detergent concentration and may become saturated beyond the critical micelle concentration (Volkin and Klibanov, 1989). Nevertheless, these surfactants have been reported to have stabilizing effect on proteins. It has been found that SDS stabilizes BSA up to a SDS/protein molar ratio of 10 (Giancola et al., 1997) and reduces aggregation of aFGF in a concentration-dependent manner (Won et al., 1998). SDS at either 0.1 or 1% effectively prevents aggregation of heat-denatured RNase at pH 7.8, possibly by increasing repulsion of the added negative charges on the protein (Tsai et al., 1998b). Anionic detergents have also been used to increase thermal stability of proteins in non-aqueous solvents by stoichiometric formation of complexes with proteins (hydrophobic ion pairing) (Manning et al., 1995). In addition, certain ionic (including nonionic) surfactants in a limited concentration range may help protein refolding. Rhodanese at 1 mg/ml denatures in a mixture of 6 M GdnHCl and 200 mM β-mercaptoethanol, and the denatured enzyme at 50 μg/ml can be reactivated to various extents in the presence of 1 mg/ml ionic (sodium cholate, cetyltrimethylammonium bromide, sodium lauryl sulfate), zwiterionic (*N*-octyl-, *N*-decyl, *N*-dodecyl-, *N*-tetradecyl- and *N*-hexadecyl-*N*,*N*-dimethyl-3-ammonio-1-propanesulfonate), and nonionic surfactants (Tween 20, Triton X-100, dodecyl β-D-maltoside) (Tandon and Horowitz, 1987). The activity recovery of the denatured enzyme is bell-shaped as a function of cetyltrimethylammonium bromide concentration in the range of 0–5 mg/ml, indicating different effects at different concentrations.

Nonionic surfactants also bind weakly to proteins. The binding stoichiometry between Tween 20 and rhGH has been determined to be 2.5–3.5 (Tween 20/rhGH) by electron paramagnetic resonance (EPR) (Bam et al., 1995). A recent study shows that complete blocking of shaking-induced rhGH aggregation can be achieved only at a Tween 20:rhGH molar ratio of ≥4:1 (Bam et al., 1998). This molar ratio is close to the binding stoichiometry, suggesting that the inhibition of rhGH aggregation is probably due to Tween 20 binding to and blocking the aggregation-prone hydrophobic sites on the protein surface. Since the Tween 20 concentration required for complete

protection of the protein is much higher than the reported CMC of Tween 20 (59 μM), CMC does not appear to play a critical role. Therefore, the net effect of surfactants may depend on their concentrations relative to that of the protein (Katakam et al., 1995). In a different case, maximum protection of rhFXIII from agitation-induced aggregation is found at Tween 20 concentrations close to its CMC, independent of initial protein concentration (Kreilgaard et al., 1998). Therefore, additional mechanisms of protein protection by Tween 20 exist, which seem to arise from its competition with proteins for adsorption on denaturation interfaces.

Surfactant–protein interactions are hydrophobic in nature because proteins with more hydrophobicity bind more surfactants (Bam et al., 1995). Therefore, it has been suggested that surfactants should be avoided when formulating hydrophobic proteins (Dix et al., 1995). Since hydrophobic interaction increases with increasing temperature, a stronger hydrophobic protein–surfactant interaction is expected at high temperatures. This may explain why nonionic surfactants destabilize certain proteins, especially at higher temperatures or toward thermal denaturation. For example, poloxamer 407 at 1% significantly increases the stability of urease at 0.33 mg/ml in phosphate buffer (pH 7.0) at 37 or 50°C but decreases its stability at 75°C (Wang and Johnston, 1993b). This surfactant at 0.5% also decreases the stability of IL-2 at about 0.2 μg/ml in phosphate buffer (pH 7.0) at 50°C (Wang and Johnston, 1993b). rhCNTF, a hydrophobic and physically unstable protein, is destabilized by Tween 80 when subjected to thermal incubation (Dix et al., 1995). Either Pluoronic F68 at 0.1 mg/ml or Tween 80 at 1 mg/ml destabilizes IL-1R by decreasing its T_m (Remmele et al., 1998). Decreased T_m is also observed for rhGH at 3 mg/ml in the presence of Tween 80, Tween 40, or Tween 20 at a surfactant:rhGH molar ratio of 10:1 (Bam et al., 1998).

Poloxamers 407 and 188 (Pluronic F68) have been shown to inhibit thermally-induced aggregation/precipitation of recombinant hGH or methionyl pGH (Charman et al., 1995; Katakam and Banga, 1997). In comparison with Tweens, poloxamers may increase viscosity of a protein solution, restraining the motion of protein backbone to achieve thermal stabilization (Wang and Johnston, 1993a).

4.2.4. Salts

As discussed in Section 3.3, salts may stabilize, destabilize, or have no effect on protein stability depending on type and concentration of salt, nature of the ionic interactions, and the charged residues in a protein (Kohn et al., 1997). The net effect is a balance among non-specific (Debye-Hückel) electrostatic shielding, specific ion binding to a protein, and its effect on solvent properties.

The effect of salt at high concentrations correlates with the Hoffmeister lyotropic series both for anions and cations (Volkin and Klibanov, 1989; Timasheff, 1993, 1998):

$$(CH_3)_4N^+ > NH_4^+ > K^+,\ Na^+ > Mg^{2+} > Ca^{2+} > Ba^{2+} > GdnH^+$$

$$SO_4^{2-} > CH_3CO_2^- > Cl^- > Br^- > NO_3^- > ClO_4^- > SCN^-$$

in which anions and cations to the left of the series are the most stabilizing. By increasing ionic strength of a solution, these salts enhance hydrophobic interactions and reduce solubility of hydrophobic groups in proteins. In addition, they enhance accumulation of water molecules around proteins, leading to preferential hydration. The combination of these two effects makes proteins more compact and stable. Ions on the right are destabilizing by binding extensively to the charged groups or the dipoles (peptide bonds) of proteins.

NaCl, the often-used salt, has been found to play a critical role in stabilizing certain proteins. It increases both the denaturation temperature and enthalpy of BSA due to increased compactness of the protein structure resulting from an increase in ionic strength and possible reduction in long-range electrostatic repulsion between the net charges (Giancola et al., 1997). Recombinant factor VIII SQ (rFVIII SQ) at 125 IU/ml is not stable at low salt concentrations and precipitates at < 0.1 M NaCl at pH 7 (Fatouros et al., 1997a). A higher amount of rFVIII SQ needs higher NaCl concentrations to prevent precipitation. Increasing NaCl concentration (up to 1 M) also linearly increases the T_m of RNase T1 from 59 to 63°C (Mayr and Schmid, 1993). Recently, NaCl has been found to be the most effective in improving

the thermal stability of IL-1R among all the excipients tested, including ascorbic acid, sugars (mannitol, lactose, sucrose, glucose), polyols (PEGs, glycerol, ethanol), polymers (PVP 10k, dextran 40), salts ($CaCl_2$), amino acids (Gly, Lys, Cys, Ala, Arg) and surfactants (Pluoronic F68, Tween 80) (Remmele et al., 1998).

Another similar salt, KCl, is also a powerful protein stabilizer. It has been shown to protect the activity of yeast ADH and bovine liver glutamate dehydrogenase (GDH) against thermal inactivation more effectively than trehalose, a commonly-used nonspecific protein stabilizer (Ramos et al., 1997).

The separate contribution of anions and cations in salts to the stability of a protein can be significantly different or even in opposite direction (Timasheff, 1998). For example, GdnHCl at 3 M destabilizes RNase at pH 7.0 by decreasing its T_m from 60 to 25°C, but $(GdnH)_2SO_4$ at 3 M stabilizes the protein by increasing its T_m by 10°C due to the dominant contribution of stabilizing SO_4^{2-} (Timasheff, 1993). GdnHCl at low concentrations (up to 0.3 M) stabilizes RNase T1 against thermal and urea-induced unfolding, probably due to the significant contribution of the stabilizing effect of Cl^- (Mayr and Schmid, 1993). This also seems to be the case in the stabilization of *ml*-PEPC (Jensen et al., 1996),

4.2.5. Polyethylene glycols (PEGs)

PEGs are often used as protein cryoprotectants and precipitating/crystallizing agents in aqueous media at high concentrations. They are hydrophobic in nature and may interact with hydrophobic side chains in proteins, promoting unfolding, especially at high temperatures (Farruggia et al., 1997). Nevertheless, PEGs of different molecular weights have been demonstrated to stabilize certain proteins. For examples, PEG 300 at 0.5 or 2% inhibits the aggregation of rhKGF in 10 mM potassium phosphate buffer (pH 7.0) containing 5% mannitol at 45°C (Zhang et al., 1995). PEG 200, 400, 600, and 1000 stabilize lysozyme and BSA, even though they decrease the surface tension of water (Kita et al., 1994). PEG 4000 (up to 15%) inhibits the thermal aggregation of LMW-UK in a concentration-dependent manner (Vrkljan et al., 1994).

The stabilization mechanism of PEGs in solution has not been well established. Stabilization seems dependent on the protein and the size of PEGs. Liquid IL-1R is stabilized by PEGs, and the stabilization effect is PEG 300 > 1000 > 3350, possibly because PEG 300 is the least hydrophobic (Remmele et al., 1998). On the contrary, PEG 1000 and 4000 destabilize human albumin by decreasing its thermal transition temperature, while high-molecular-weight PEG 8000 and 10 000 stabilize the native state of the protein (negative preferential interaction with the protein) (Farruggia et al., 1997). Similarly, PEG 8000 at 1% significantly reduces the nebulization-induced aggregation and glass surface adsorption of rConIFN (Ip et al., 1995). Protein stabilization by high-molecular-weight PEGs is probably due to their steric hindrance of protein-protein interactions.

4.2.6. Polymers

Various kinds of polymers have been shown to stabilize proteins. Stabilization is generally due to one or more of these properties of polymers: surface activity, preferential exclusion, steric hindrance of protein–protein interactions, and increased viscosity limiting protein structural movement.

Serum albumin has been used often for inhibition of protein surface adsorption and general stabilization. However, its potential contamination with blood-borne pathogens limits its future applications. Among other polymers examined for protein stabilization, hydroxypropyl-β-cyclodextrin (HP-β-CD) appears to be one of the most valuable, partly because it is a good solubilizing agent and parenterally safe. HP-β-CD has been shown to prevent the thermal and interfacial denaturation and precipitation of pGH (Charman et al., 1993), to inhibit the aggregation of rhKGF (Zhang et al., 1995), and to stabilize IL-2 and bovine insulin (Brewster et al., 1991). Other polymers include dextran (51 and 18 kD) in increasing the T_m of thrombin (Boctor and Mehta, 1992), dextran (38 and 82 kD) in increasing the T_m of porcine pancreatic elastase (Chang, et al., 1993), PVP 10 k in increasing the T_m of IL-1R (Remmele et al., 1998), fibronectin (0.05%) in improving the

mitogenic activity of hEGF in 50 mM sodium phosphate (pH 8.0) at 60°C (Son and Kwon, 1995), heparin (0.5%) in the inhibition of rhKGF aggregation in 10 mM phosphate buffer (pH 7.0) at 37°C (Chen et al., 1994a), 16-kD heparin in the concentration-dependent inhibition ($IC_{50} = 2$ μg/ml) of the heat-induced aggregation of aFGF in PBS at pH 7.2 (Volkin et al., 1993), gelatin type A and B (up to 1%) and hydroxyethyl (heta) starch (up to 20%) in the concentration-dependent inhibition of the thermal aggregation of LMW-UK (Vrkljan et al., 1994; Manning et al., 1995). A variety of polymers has been found effective in inhibiting the aggregation of rhKGF in 10 mM phosphate buffer (pH 7.0) containing 5% mannitol, including heparin, dextran sulfate, polyphosphoric acid, poly-L-glutamic acid, poly-L-lysine, etc (Zhang et al., 1995).

The effect of polymers on protein stability is strongly protein-dependent, and in certain cases destabilization may occur. While α-CD and γ-CD do not affect the stability of hen-egg lysozyme (HEL), some of its derivatives including M-β-CD, HE-β-CD, HP-β-CD, and HB-β-CD lower the protein's T_m (Brunchu et al., 1996). Type A gelatin at 0.1% destabilizes LMW-UK but increases its stability at higher concentrations (Vrkljan et al., 1994). PVP at 2, 5, or 10% increases the heat-induced aggregation of LMW-UK (Vrkljan et al., 1994). The failure of PVP to protect the protein could be attributed to its relatively hydrophobic nature as temperature increases. The increased hydrophobicity may promote preferential binding to proteins and facilitate protein unfolding because the denatured state has more hydrophobic binding sites than the native state.

Proteins can be stabilized by polymers through multiple electrostatic interactions. A number of sulfated polysaccharides, sulfated polymers, and poly-amino acids have been shown to stabilize aFGF against aggregation, including low-MW heparin (5 kD), sulodexide, dextran sulfate, fucoidan, pentosan polysulfate, polyvivyl sulfate, keratan sulfate, poly-Asp, and poly-Glu (Volkin et al., 1993; Won et al., 1998). Increasing the sulfation level of both heparin and sulfated β-cyclodextrin results in dramatic enhancement of their ability against thermal inactivation of aFGF. It is the sulfate ions that bind to specific sites in aFGF (in the vicinity of $Lys^{118}/Lys^{112}/Arg^{22}$ region) to achieve stabilization. Poly-Arg, a positively charged polymer, destabilizes aFGF. Detailed discussion can be found elsewhere on the structure, interaction, and specificity of aFGF polyanion binding sites (Volkin and Middaugh, 1996). By similar stabilization mechanisms, the aggregation of rhKGF, another member of the FGF family, is significantly inhibited by polyanions, including poly(acrylic acid), poly(-methacrylic acid), heparin, dextran sulfate (8 and 500 kD), and pentosan polysulfate (Chen et al., 1994b). In a recent study, as many as 13 model proteins have been stabilized to a different degree against thermal inactivation by forming multiple electrostatic complexes with selected soluble polyelectrolytes (such as DEAE-dextran) and polyhydroxyl compounds (such as ethylene glycol) (Gibson, 1996). However, the protection against aggregation of heat-denatured RNase by dextran sulfate at 0.1 or 1% is apparently due to the increased repulsion of the added negative charges on the protein (Tsai et al., 1998b).

Polymers may inhibit chemical degradations in proteins. For example, dextran can inhibit the metal-catalyzed oxidation of human relaxin (Li et al., 1996a,b). All the polyanions that protect aFGF against heat-induced aggregation also protect the protein at least partially against copper-catalyzed oxidation (Volkin et al., 1993). Among the polymers, heparin is the most effective. The protection could be due to both the dominant interaction of polymers with the protein and chelation of divalent metal cations.

Polymers used for protein stabilization should be stable enough against chemical and/or enzymatic degradations so that they can keep their stabilizing effect during storage. Unfortunately, proteins may be contaminated with trace amounts of enzymes, which may degrade a polymer stabilizer and result in loss of formulation quality or even protein stability. For example, hydroxyethylcellulose (HEC) has been formulated with recombinant bFGF. The viscosity of the formulation decreases with time due to the presence of trace amounts of a cellulase-like activity that originates from the *E. coli* lysate in the production of the protein (Shahrokh et al., 1995).

4.2.7. Metal ions

Some metal ions (such as calcium, magnesium, and zinc) can be used as protein stabilizers as they bind to a protein and make the overall protein structure more rigid, compact, and stable (Kristjánsson and Kinsella, 1991). This is one of the mechanisms responsible for the high stability of thermophilic proteins (Mozhaev and Martinek, 1984). In addition to stabilization, metal ions may enhance the activity of a protein such as RNase H (Goedken and Marqusee, 1998). Among these metal ions, calcium is a well-known stabilizer for many enzymes at both high and low temperatures (Daniel et al., 1996).

Different metal ions may require different concentrations to achieve protein stabilization, and their specificity in protein stabilization varies. The effect of some divalent metal ions on rFVIII SQ has been investigated, including Ca^{+2}, Cu^{+2}, Mn^{+2}, Mg^{+2}, Zn^{+2}, Sr^{+2}, and Fe^{+2} at 1 and 10 mM (Fatouros et al., 1997a). At 1 mM, only Ca^{+2} and Sr^{+2} increase the stability relative to the control (0.1 mM Ca^{+2}) and Fe^{+2} sharply destabilizes rFVIII SQ. At 10 mM, Ca^{+2} and Sr^{+2} further increase the stability of rFVIII SQ up to about 50 mM. Cu^{+2}, Zn^{+2} and Fe^{+2} all sharply reduce the stability at 10 mM. Mn^{+2} and Mg^{+2} do not have any significant effect at both concentrations. In another study, the T_m of rhDNase increases with increasing Ca^{2+} ($CaCl_2$) concentrations and reaches a maximum at around 100 mM $CaCl_2$ (Chan et al., 1996). However, Mg^{2+}, Mn^{2+}, and Zn^{2+} destabilize the protein. The stabilizing effect of Ca^{2+} probably results from its binding to the protein and preventing the breaking of a disulfide bridge. Other examples of protein stabilization by metal ions include the inhibition of insulin fibrillation by calcium or zinc ions (Brange et al., 1997), the stabilization of 19 kD catalytic fragment of human fibroblast collagenase by calcium (Lowry et al., 1992), the stabilization of RNase H by Mn^{2+} (Goedken and Marqusee, 1998), the increase in T_m of porcine pancreatic elastase by 10 mM $CaCl_2$ (Chang, et al., 1993), the stability dependence of bovine pancreatic DNase on Ca^{2+} (Shire, 1996), and the increased hEGF mitogenic activity in the presence of 6 mM $ZnCl_2$ in 50 mM sodium phosphate buffer (pH 8.0) during storage at 60°C (Son and Kwon, 1995). Calcium or zinc stabilizes insulin probably by neutralizing negative charges in the center of insulin hexamer and enhancing native hydrophobic interaction. In a different case, $CaCl_2$, $MgCl_2$, and KSCN at concentrations below 0.5 M destabilize albumin and lysozyme by preferential binding to these proteins (Picó, 1996).

The effect of metal ions on protein stability can be significantly influenced by the negative counter ions. Picó (1996) studied the effect of sodium halides at 0.3 M on the stability of human serum albumin in 20 mM sodium phosphate (pH 7.4) and found that the negative ions increase the melting temperature and enthalpy of unfolding of albumin in the following order: $I^- > Br^- > Cl^- > F^-$.

4.2.8. Amino acids

Certain amino acids, either alone or in combination with other excipients, stabilize proteins most likely by preferential exclusion (Jensen et al., 1996). The aggregation of rhKGF in 10 mM potassium phosphate buffer (pH 7.0) containing 5% mannitol at 45°C can be inhibited to various degrees in the presence of the following amino acids: His, Gly, sodium aspartate, glutamate, and lysine hydrochloride (Zhang et al., 1995). Similarly, the stability of *ml*-PEPC can be significantly increased in the presence of 0.05 M sodium glycinate, sodium glutamate, sodium aspartate, or lysine hydrochloride upon incubation at 40°C (Jensen et al., 1996). Replacing 40 mM NaCl with 0.4% (w/v) L-Asp and 0.7% (w/v) L-Glu significantly increases the half-life of rhKGF from 1.8 to 2.6 and 2.4 days, respectively, for the loss of soluble protein at 37°C (Chen et al., 1994a). Gly at 1 M increases the T_m of RNase A from 65 to 68°C at pH 6.0 (Liu and Sturtevant, 1996) and at 2 M increases the $\Delta G_{f\rightarrow u}$ of cytochrome c by 17.3 kJ/mol (Foord and Leatherbarrow, 1998). Use of amino acids with propylene glycol improves the structural stability of rhCNTF (Dix et al., 1995). L-Lys and L-Arg increase the stability of IL-1R by increasing its T_m, although Gly and L-Ala decrease it (Remmele et al., 1998).

Certain chemical degradations in proteins can be reduced in the presence of certain amino acids.

Met is an effective antioxidant. His at 2.5 mM can completely inhibit the oxidation-induced inactivation of papain by the ascorbate/Cu(II)/O_2 system, possibly through the formation of Cu-His complex (Kanazawa et al., 1994).

4.2.9. Miscellaneous compounds/approaches

The identification of certain cellular accumulants in thermophilic organisms upon temperature or salinity increase has led to the choice of some of these compounds as protein stabilizers. For example, potassium salt of cyclic diphosphoglycerate can stabilize the thermolabile GADPH at 90°C (Hensel and König, 1988). Another compound is 2-*O*-β-mannosylglycerate in the stabilization of several mesophilic proteins, including rabbit muscle LDH, baker's yeast ADH, and bovine liver GDH, which is more effective than trehalose (Ramos et al., 1997). Specifically, this compound at 500 mM keeps 90% of LDH activity while trehalose (or KCl) at the same concentration keeps about 30% activity after incubation of the protein at 50 μg/ml in phosphate buffer at 50°C for 10 min.

A few other compounds have been reported to increase the thermal stability of proteins. These include dipalmitoylphosphatidylglycerol (DPPG, an anionic lipid) for RNase and cytochrome c (Lo and Rahman, 1998), 2-bromo-2-chloro-1,1,1-trifluoroethane for serum albumin (Tanner et al., 1999), and some anionic phosphate species such as ATP, inorganic phosphates, and phosphorylated inositols for aFGF (Volkin et al., 1993). Perfluorodecalin, a non-aqueous solvent, has recently been used to stabilize plasma-derived factor IX and recombinant human α-IFN in the absence of moisture ($< 0.001\%$) (Knepp et al., 1998). Its stabilization mechanism is briefly discussed in Section 3.3.

Another potential way of stabilizing proteins is the use of so-called molecular chaperones. Folding of newly synthesized polypeptides in cells requires the assistance of molecular chaperone proteins because of the tendency of folding intermediates to aggregate at relatively high protein concentrations (Hendrick and Hartl, 1995; Lewis and Cowan, 1996; Ruddon and Bedows, 1997). For example, the GroEL minichaperone in bacteria has been found to facilitate protein folding by preventing protein aggregation and correcting protein misfolding (Golbik et al. 1998). α-Crytallin exhibits chaperone-like properties and inhibits the aggregation of denatured-reduced lysozyme (Raman et al., 1997). Recombinant human protein disulfide isomerase (rhPDI) enhances folding of C125A rhIL-2 by accelerating thiol-disulfide interchange (Du et al., 1998). Therefore, inclusion of a molecular chaperone in a protein formulation is foreseeable but seems practical only if the chaperone can be easily obtained and is safe and stable.

Reduction of dissolved oxygen in protein solutions should decrease oxygen-initiated oxidation. It has been found that replacing the air in container headspace with nitrogen reduces the loss of rFVIII SQ activity from 69 to 19% during storage at 7°C (Fatouros et al., 1997a). To prevent potential oxidation of proteins, oxygen dissolved in protein solutions can be simply and effectively reduced by a few low-temperature cycles of normal-low-normal pressure changes (Fransson et al., 1996).

Computer graphics can be used to facilitate design of more effective protein stabilizers based on proteins' steric structures. Such a molecule, benzene-1,4-disulfonic acid, has been designed to fill the center space of insulin hexamer and appears to stabilize the hexamer (Manallack et al., 1985).

4.3. Stabilization of proteins by structural modification

Although proteins are very delicate molecules, they can be made more stable by careful modification of their amino acids either chemically or genetically. Again, the key issue is preservation of protein activity during and after the modification.

4.3.1. Modification of amino acid and site-directed mutagenesis

Site-directed mutagenesis or chemical modification can be used to modify protein stability by mutating or blocking specific amino acids. Structural characteristics of labile proteins may be changed toward those of thermophilic proteins (see Section 2.3).

After analyzing the effect of amino acid replacement on protein thermal stability, Querol et al. (1996) made the following recommendations for amino acid replacement: (1) maintaining or enhancing secondary structure propensity; (2) replacing preferentially solvent accessible residues; (3) replacing residues by introducing a negative charge at N-cap or a positive charge at the C-cap of the helix (same for β-stands); (4) substituting with residues of enhancing hydrogen bonding or van der Waals contacts; (5) favoring the formation of an additional disulfide bridge, metal binding site, or glycosylation site; and (6) substituting with Pro in loops.

Even with these clear-cut guidelines, it has not been always successful to increase protein stability simply by amino acid substitution because of the complexity of protein structure and the limited number of amino acids responsible for the extra protein stability (Daniel et al., 1996). For example, the higher thermostability of the novel bacillar ADH is apparently due to the replacement of only three amino acids ($Glu^{11} \rightarrow Lys$, $Lys^{14} \rightarrow Gln$, and $Pro^{242} \rightarrow Ala$) (Cannio et al., 1994). It is no surprise that amino acid substitution has been done often on a trial-and-error basis. Even after well-defined amino acid exchange(s), it is often difficult to predict the protein stability (Jaenicke, 1990, 1996; Lee and Vasmatzis, 1997). Recently, using tables of amino acid substitution and propensity, Topham et al. (1997) were able to correlate the predicted stability change after amino acid substitution with experimentally determined free energy difference ($\Delta\Delta G$) or difference in melting temperature between a mutant and the wild-type protein. A correlation coefficient of 0.80 is obtained for 83 staphylococcal nuclease and 68 barnase mutants. Also, mutations at the buried sites are more reliably predicted than those at the exposed or partially-buried positions, and better predictions are obtained with residues not engaged in hydrogen bonding interactions with neighboring residues than those that are.

Protein activity may change significantly after amino acid substitution. Both successful and unsuccessful examples exist in this regard. aFGF has three Cys residues (Cys-16, -83, -117), and all three single Ser mutants are as active as the wild type in the presence of heparin. In the absence of heparin, the triple mutant is the most active and stable (Volkin and Middaugh, 1996). However, substitution of Glu^{58} with Ala in the wild-type ribonuclease T1 not only destabilizes the protein by 0.8 kcal/mol ($\Delta\Delta G = -0.8$) but also removes the majority of the hydrolytic activity (Shirley et al., 1989). A more recent study on the stability of T4 lysozyme mutants shows that those mutants with increased protein stability have either abolished or reduced protein activity (Shoichet et al., 1995).

There are other concerns in modifying protein structure for increased stability. One of them is the immunogenicity of a protein, which may change significantly. Therefore, mutant proteins have to go through extensive toxicity studies if they are pharmaceutical candidates. Replacement of any hydrophilic amino acids with hydrophobic ones may change the solubility of a protein, presenting formulation challenges. Thus, any chemical or genetic modification of proteins should be carefully considered.

4.3.2. Glycosylation

Glycosylation can affect protein activity, antigenicity, solubility, proteolytic resistance, and stability (Liu, 1992). Different glycoforms frequently have different physical and chemical properties. Therefore, proteins can be properly glycosylated to increase their stability. Several stabilization mechanisms of protein glycosylation have been proposed. These include formation of hydrogen bonds with the polypeptide backbone or surface hydrophilic amino acids, and steric interaction with adjacent peptide residues (Baek and Vijayalakshmi, 1997; Runkel et al., 1998). Again, the key issue is preservation of protein activity after glycosylation.

There are many successful cases of protein stabilization by glycosylation. Glycosylation of RNase A dramatically increases its stability with its activity essentially unchanged (Baek and Vijayalakshmi, 1997). The native RNase A at 0.3 mg/ml in 10 mM phosphate buffer (pH 8.0) loses more than 90% of its original activity after incubation at 90°C for 15 min, while the glycosylated protein maintains about 75% of its activity under

the same condition. Glycosylated α_1-antitrypsin has been found to be more resistant to urea-induced unfolding and thermal denaturation (an aggregation process) than non-glycosylated form (Kwon and Yu, 1997).

Insulin may form fibrils in solution, probably due to the presence of insulin monomer and its conformational change at a hydrophobic interface. To examine the effect of glycosylation on insulin fibrillation, several *p*-succinamidophenylglucopyranoside-insulin conjugate (SAPG-insulin) have been synthesized, including monosubstituted, disubstituted, and trisubstituted insulins. It has been found that the tendency to form insulin dimers/hexamers decreases and the physical stability increases as the number of SAPG moieties increases (Baudyš et al., 1995). This is seemingly due to increased hydrophilicity of the monomer surface and/or steric hindrance by SAPG moieties, preventing fibril formation. These derivatives also significantly increase insulin stability against shaking-induced fibrillation. While native insulin starts to form insoluble aggregates (fibrils) in about 0.5 day upon shaking at 37°C, it takes 18.8 days for $(SAPG)_3$-insulin to form any aggregates. At the same time, the bioactivity for most of these derivatives is close to the native insulin ($\pm$ 20%) except the Gly^{A1}-Lys^{B29}-substituted derivative, which shows about 65% activity of the native insulin.

4.3.3. Formation of disulfide bonds

Naturally-occurring disulfide bonds generally increase thermodynamic stability of proteins (Jaenicke, 1991; Darby and Creighton, 1997; Johnson et al., 1997). This seems to result from a reduction in the configurational entropy (ΔS_{conf}) of the unfolded state.

Crosslinking proteins (formation of external 'braces') with bi(poly)-functional agents such as glutaraldehyde and imidoesters can prevent/reduce unfolding of tertiary structure and dissociation of oligomeric proteins (Mozhaev and Martinek, 1984; Kristjánsson and Kinsella, 1991). This is true especially when a disulfide bond (or other crosslink) is created connecting two groups that are sequentially far apart but spatially close, since this creates physical constraint to unfolding (reducing entropy of the unfolded state) (Lee and Vasmatzis, 1997). For example, Matsumura et al. (1989) found that single or multiple disulfide-bonded mutants of T4 lysozyme significantly increase the T_m of the wild type. Similarly, Johnson et al. (1997) demonstrated that introduction of a single or multiple disulfide bonds increases the thermodynamic stability of barnase.

On the other hand, the added disulfide bonds may have potential stability problems particularly at a higher pH and temperature due to possible β-elimination-induced disulfide scrambling (see Section 3.2). β-Elimination of disulfide bonds has been observed for more than a dozen unrelated proteins at 100°C in the pH range of 4–8 (Volkin and Klibanov, 1987).

4.3.4. Pegylation

Conjugation of PEGs to proteins is referred to as 'PEGylation' (Katre, 1993). PEGs are mostly attached to Lys amino groups in proteins. Generally, PEG-modified proteins exhibit increased stability, improved solubility, decreased immunogenicity, increased circulation half lives, and low toxicity (Li et al., 1995b). For example, conjugation of PEG_{20000} to insulin (insulin-Gly_1-PEG_{20000} or insulin-Lys_{29}-PEG_{20000}) increases the protein's enzymatic stability in blood (Caliceti and Veronese, 1998). Conjugation of recombinant human megakaryocyte growth and development factor (rhMGDF) with PEG increases the storage stability of the protein in phosphate buffer at pH 7 (Guerra et al., 1998).

Pegylation may or may not change protein activity. The activity of recombinant consensus interferon (IFN-Con_1) does not change after pegylation (Jensen-Pippo et al., 1995). However, the *in vitro* bioactivity of interleukin-6 (IL-6) decreases linearly with increasing degree of PEG-modification, while the thrombopoietic activity of PEG-modified IL-6, in which 54% of the Lys amino groups are coupled with PEG, is more than 10 times higher (Tsutsumi et al., 1995).

PEGs are generally considered safe and have very low toxicity. However, adverse reactions such as seizure and anaphylactic shock have been seen in humans after topical or oral administration of PEG-containing formulations (Katre, 1993).

4.4. Formulation of liquid protein pharmaceuticals

There are two major dosage forms for protein pharmaceuticals: liquid and freeze-dried solid. Generally, it is the protein stability that dictates selection of the final dosage form. Liquid formulation has advantages of simple processing, less manipulation, and easy application, whereas freeze-dried solid protein formulation is generally more stable, although lyophilization often causes significant protein instability. There are cases when proteins in a liquid formulation are as stable as or more stable than those in a solid state. For example, oxidation of Met^{59} in hIGF-I is a major modification pathway, and its rate in solution is roughly the same as that in a freeze-dried formulation in air-filled vials at either 25 or 30°C (Fransson et al., 1996). Liquid mannitol formulation of IFN-γ is more stable at 5°C than a freeze-dried formulation of the same composition during storage (Perlman and Nguyen, 1992).

The science of protein formulation had been primarily empirical in the past (Middaugh, 1990). Although significant progress has been made in recent years, there is still no single pathway to follow in formulating proteins due to their structural diversities and complexities. There are several stages that require careful consideration and extensive experimentation in formulating a stable protein product. First, the route of drug administration should be addressed based on proposed indications. The remaining critical stages in protein formulation include: (1) purification, in which a protein is satisfactorily purified such that no harmful contaminants (such as proteases) exist and the process yields reproducibly stable active drug; (2) preformulation, in which physicochemical properties (such as protein p*I* and solubility), excipient compatibility, aggregation, and/or decomposition pathways are performed; and (3) final formulation, in which several key issues should be addressed, including choice of buffer, pH, stabilizers, and other excipients, stability-indicating assays, decomposition pathways, and optimal storage conditions.

4.4.1. Route of drug administration

Bolus intravenous injection generally requires an aqueous protein solution. This solution, usually not exceeding 10 ml, can be either a liquid formulation or reconstituted freeze-dried formulation. The tonicity of the solution is not a great concern since the volume is small. Other types of solutions, such as suspensions, emulsions, and cosolvent or oleagenous systems, may be used for intramuscular (up to 3 ml) or subcutaneous (up to 2 ml) injection. The buffer and pH in these systems should be carefully adjusted to alleviate irritation and provide maximum protein solubility and stability.

4.4.2. Preformulation

To develop a protein formulation successfully, the basic properties of a protein should be understood thoroughly. These include protein purity, p*I*, and solubility at different pHs. Other critical issues can then be addressed, including the effect of different buffer systems, pH, tonicity modifiers, stabilizers, freeze/thaw cycles, and protein adsorption. Before conducting any preformulation studies, the purity of a protein should be adequate; usually a purity level of 95% or better is recommended (Berry, 1996).

4.4.3. Composition of a liquid protein formulation

Multiple excipients are often required in a liquid protein formulation, although a single-excipient protein formulation may be sufficient, such as tPA, which is formulated in 0.5 M arginine–phosphate buffer (pH 7.3) (Overcashier et al., 1997). Both the type and level of excipients can significantly affect protein stability. These excipients include buffering agents, stabilizers, tonicity modifiers, and antimicrobial agents. Solubilizers should be used if a protein has limited solubility, such as rIFN-β-1b, which has a solubility of < 0.05 mg/ml at neutral pH and is solubilized by SDS or Tween 80 (Lin et al., 1996c). To ensure adequate solubility of a protein, the formulation pH should be at least 0.5 unit below or above its p*I* (Cleland et al., 1993). When multiple excipients are used, they should not interact with one another, and, more importantly, should not adversely affect protein stability. Thus, compatibility studies should be conducted.

Almost without any exception, an optimum pH (or a range) is required for maximum protein stability, and this pH may shift depending on the presence of other excipients. The often-used buffering agents are phosphate for pHs between 6 and 8 and citrate for pHs below 6. If these two agents adversely affect protein stability, other buffering agents may be used such as acetate for rhG-CSF at pH 4.0 (Herman et al., 1996), Tris–HCl for hEGF at pH 7.0 (Son and Kwon, 1995), and succinate for IFN-γ at pH 5.0 (Lam et al., 1996).

In close relation to the selection of formulation excipients, a compatible container should be used. Type I borosilicate glass is usually the material of choice for containers due to its strong chemical resistance and low level of leachables. Closures should be carefully chosen based on their compatibility with protein formulation, resistance to formulation pH, excipients and sterilization, moisture/vapor transfer property, and resealability.

4.4.4. Rapid screening of protein formulations

Development of a liquid protein formulation often requires screening of many excipients and their combinations at different pHs, even under rigorous computer-aided formulation design. Therefore, use of an efficient method for screening these excipients is recommended to expedite excipient selection without undertaking time- and labor-extensive stability studies. A few screening methods are briefly described here, which should be used with caution as they may or may not lead to the identification of ideal formulations. These methods include: (1) comparison of protein unfolding temperature (T_m) in different formulations; (2) comparison of half denaturation concentration, $C_{half,}$ in the presence of a denaturant; and (3) comparison of IR spectra of different protein formulations with a reference spectrum.

Although T_m does not have a defined relationship with the free energy of protein unfolding (an indicator of protein stability), it is widely accepted that any increase in T_m should lead to an increase in protein stability (Dill et al., 1989). Therefore, a change in T_m may indicate whether a particular excipient has any stabilizing or destabilizing effect. For example, an increase in the amount of IL-1R aggregates correlates roughly with a gradual decrease in T_m in the presence of one of the three preservatives: phenol, m-cresol, and benzyl alcohol (Remmele et al., 1998). On the other hand, a protein stabilizer may not always increase T_m. EDTA and two reducing agents, dithiothreitol and β-mercaptoethanol, can protect aFGF from thermally-induced aggregation, but at low concentrations these agents do not affect the protein's T_m (Tsai et al., 1993). The T_m of a protein in the presence of two or more excipients can be roughly estimated without experimentation by calculating the algebraic sum of T_ms obtained in the presence of individual excipient. T_m estimation by this method seems rather reliable whether the excipients have the same or opposite effects (Allison et al., 1996).

C_{half} is the concentration of a denaturant at which 50% of protein molecules are unfolded or denatured. It can be estimated from a protein denaturation curve as discussed in Section 3.4. The effect of a formulation excipient on protein stability is reflected in the change in C_{half}. The higher the $C_{half,}$, the more stable the protein in the formulation. It should be noted that the time needed to unfold a protein by a denaturant may be very slow. Complete unfolding of the wide type Rop in 4 M GdnHCl takes 48 h (Munson et al., 1996).

IR has been used extensively to probe protein structural changes in liquid, frozen, and dried states (Dong et al. 1995b). The effect of excipients on protein stability can be examined by comparing the IR spectrum of a sample in the sensitive amide I region with that of a reference. Comparison can be based on the degree of spectral correlation (r) (Prestrelski et al., 1993a,b), or the extent of spectral area overlap (Heimburg and Marsh, 1993; Allison et al., 1996; Kendrick et al., 1996), although these parameters may not necessarily reflect changes in protein activity. Using the correlation coefficient (r), Prestrelski et al. (1995) successfully selected the formulation pH and stabilizers in designing a freeze-dried IL-2 formulation. Nevertheless, overlap comparison of area-normalized second-derivative or deconvo-

luted spectra is seemingly more reliable and objective. To overcome the interference of water absorption, protein IR spectra have to be determined either in D_2O or at higher protein concentrations (>10 mg/ml) as discussed in Section 3.4.

4.4.5. Stability studies

To accelerate formulation development, stability studies are often conducted under accelerated (stressed) conditions. These stressed conditions include high temperature, high humidity, intensive lighting, extreme pHs, increased air/water interfaces by vortexing or shaking, and repeated freeze/thaw cycles. These studies are usually short but very helpful in screening protein formulations. Parameters used in monitoring stability studies include protein activity, rate of protein degradation, product formation and aggregation/precipitation, solution color, pH and viscosity, sterility, and pyrogenicity.

Accelerated stability studies are often conducted at high temperatures. The key issue is whether and how well the data from accelerated stability studies can be extrapolated to those under real-time conditions. Extrapolation of stability data from high to lower temperature is usually limited to a temperature range over which the same degradation pathway is operative. Very often, protein stability results obtained at high temperatures do not reflect or predict what happens under real-time conditions. This is due to the complexity of multiple protein degradation pathways at different temperatures. For example, temperature-dependent degradation mechanisms have been reported for interleukin 1β (IL-1β) (Gu et al., 1991), and hGH (Pikal et al., 1991). Nonlinear Arrhenius relationships were observed for relaxin between 5 and 30°C (Nguyen and Shire, 1996) and for *phm*-MDH between 4 to 65°C in the presence of a variety of excipients, such as salts, salts of amino acids, and polyols (Jensen et al., 1997). The temperature nonlinearity may suggest at least two major degradation pathways in proteins.

Nevertheless, if the multiple degradation processes in proteins can be described separately, or the rate-limiting degradation step does not change with temperature, prediction of protein stability based on accelerated stability studies is very optimistic. For example, the following thermal denaturation model with two different reaction rates representing two isoenzymes of β-galactosidase has been used to describe the biphasic irreversible denaturation process, and linear Arrhenius plots are obtained for both k_1 and k_2 (Yoshioka et al., 1994b):

$$N_1 \overset{k_1}{\Rightarrow} N_2 \overset{k_2}{\Rightarrow} D.$$

Linear Arrhenius relationships have also been reported for a number of proteins in certain temperature ranges. Examples include the inactivation of *ml*-PEPC in the presence of 0.8 M sodium glutamate between 7.6 and 48°C (Jensen et al., 1997), thermal inactivation of recombinant hepatitis B surface antigen (HBsAg) between 60 and 90°C (Volkin et al., 1996), and second-order oxidation of hIGF-I between 7 and 37°C (Fransson et al., 1996).

5. Conclusions

Native proteins are properly folded, which involves many forces, including hydrophobic interactions, electrostatic interactions (charge repulsion and ion pairing), hydrogen bonding, intrinsic propensities, and van der Waals forces. Among these forces, hydrophobic interactions seem to be the dominant. Proteins are generally not very stable, as stabilization energy of the native state is mostly between 5 and 20 kcal/mol, which is equivalent to that of a few hydrogen bonds. Most mesophilic proteins such as those from human beings can be unfolded/denatured easily at temperatures between 50 to 80°C.

A common phenomenon of protein instability is formation of protein aggregates, which can be soluble or insoluble, chemical or physical, and reversible or irreversible. There are many factors affecting protein stability. These include at least temperature, pH, ionic strength, metal ions, surface adsorption, shearing, shaking, additives, solvents, protein concentration, purity, morphism, pressure, and freeze-thawing/drying. Chemical transformations that lead to protein instability include at least deamidation, oxidation, hydroly-

sis, isomerization, succinimidation, disulfide bond formation and breakage, non-disulfide crosslinking, and deglycosylation. Today, many analytical techniques are available to monitor protein instability. Even with the sophistication of present instrumentation, no single technique can satisfactorily provide sufficient information about a protein. Thus, a combination of analytical methods needs to be used to characterize a protein and to monitor protein instability.

To develop a liquid protein pharmaceutical, the basic properties of a protein need to be examined first. These include protein purity, p*I*, and solubility and stability at different pHs and in different buffer systems. With these data, protein formulation issues can then be addressed. These include the indication, route of drug administration, selection of proper formulation buffer and excipients, and finally, stability studies. To facilitate rapid development of a protein formulation, a formulation screening method may be used with caution, such as the determination of T_m, $C_{half,}$ or degree of IR spectral similarities. Alternatively, accelerated stability studies may be conducted under high-temperature conditions, but stability results obtained at high temperatures may not reflect or predict what happens under real-time conditions. For proteins, real-time stability studies are necessary for selection of the final formulation.

In the development of a protein formulation, the most challenging task is the stabilization of a protein to achieve an acceptable shelf life. Due to complication of structural modifications, proteins are commonly stabilized by excipients. The often-used protein stabilizers include sugars, polyols, surfactants, salts, PEGs, polymers, metal ions, and amino acids. Unfortunately, there is no single pathway to follow in selection of a suitable stabilizer(s), partly due to the lack of a clear and definitive understanding of protein-cosolute interactions and proteins' multiple inactivation mechanisms. Depending on the protein, these traditional protein stabilizers may increase protein stability only to a limited level. Therefore, new types of protein stabilizers need to be further explored. One obvious direction is to identify additional cellular components in hyperthermophilic organisms or cellular accumulants under various stressed conditions, which may have the potential to stabilize proteins.

In summary, the most formidable challenge in formulating a liquid protein pharmaceutical is to preserve the biological activity of the protein for an acceptable shelf life. Unfortunately, there is no single pathway to follow in formulating such a product. Usually, proteins have to be evaluated on a case-by-case basis. Much more effort is still needed to understand the basic behavior of proteins, their instability factors and mechanisms, and their stabilization mechanisms in a broader and clearer perspective. This further understanding will definitely depend on further advancement of sophisticated analytical instrumentation. Therefore, research activities directed toward a general solution to protein instability will continue for at least a few decades (Richards, 1997).

Acknowledgements

This manuscript would not be possible without the support of Drs Robert Kuhn and Rajiv Nayar. I am also indebted to Drs Rajiv Nayar and Mike Zachariou for the helpful discussions about the manuscript, the Editorial Services Department for careful editing, and especially, the two referees for their critical and valuable comments.

References

Ackland, C.E., Berndt, W.G., Frezza, J.E., Landgraf, B.E., Pritchard, K.W., Ciardelli, T.L., 1991. Monitoring of protein conformation by high-performance size-exclusion liquid chromatography and scanning diode array second-derivative UV absorption spectroscopy. J. Chromatogr. 540, 187–198.

Adams, M.W., 1993. Enzymes and proteins from organisms that grow near and above 100°C. Annu. Rev. Microbiol. 47, 627–658.

Adams, M.W., 1994. Biochemical diversity among sulfur-dependent, hyperthermophilic microorganisms. FEMS Microbiol. Rev. 15, 261–277.

Allison, S.D., Dong, A., Carpenter, J.F., 1996. Counteracting effects of thiocyanate and sucrose on chymotrypsinogen secondary structure and aggregation during freezing, drying and rehydration. Biophys. J. 71, 2022–2032.

Apenten, R.K.O., 1998. Protein stability function relations: β-lactoglobulin-A sulphydryl group reactivity and its rela-

tionship to protein unfolding stability. Int. J. Biol. Macromol. 23, 19–25.
Arakawa, T., Prestrelski, S.J., Kenney, W.C., Carpenter, J.F., 1993. Factors affecting short-term and long term stabilities of proteins. Adv. Drug Deliv. Rev. 10, 1–28.
Arakawa, T., Yoshiko, K., Carpenter, J.F., 1991. Protein-solvent interactions in pharmaceutical formulations. Pharm. Res. 8, 285–291.
Arnold, U., Ulbrich-Hofmann, R., 1997. Kinetic and thermodynamic thermal stabilities of ribonuclease A and ribonuclease B. Biochemistry 36, 2166–2172.
Aronsson, G., Brorsson, A.C., Sahlman, L., Jonsson, B.H., 1997. Remarkably slow folding of a small protein. FEBS Lett. 411, 359–364.
Baek, W.O., Vijayalakshmi, M.A., 1997. Effect of chemical glycosylation of RNase A on the protein stability and surface histidines accessibility in immobilized metal ion affinity electrophoresis (IMAGE) system. Biochim. Biophy. Acta 1336, 394–402.
Bai, Y., Englander, S.W., 1996. Future directions in folding: the multi-state nature of protein structure. Proteins Struc. Funct. Genet. 24, 145–151.
Bai, Y., Milne, J.S., Mayne, L., Englander, S.W., 1994. Protein stability parameters measured by hydrogen exchange. Proteins Struc. Funct. Genet. 20, 4–14.
Bam, N.B., Cleland, J.L., Randolph, T.W., 1996. Molten globule intermediate of recombinant human growth hormone: stabilization with surfactants. Biotechnol. Prog. 12, 801–809.
Bam, L., Cleland, J.L., Yang, J., Manning, M.C., Carpenter, J.F., Kelley, R.F., Randolph, T.W., 1998. Tween protects recombinant human growth hormone against agitation-induced damage via hydrophobic interactions. J. Pharm. Sci. 87, 1554–1559.
Bam, N.B., Randolph, T.W., Cleland, J.L., 1995. Stability of protein formulations: investigation of surfactant effects by a novel EPR spectroscopic technique. Pharm. Res. 12, 2–11.
Baptista, A.M., Martel, P.J., Petersen, S.B., 1997. Simulation of protein conformational freedom as a function of pH: constant-pH molecular dynamics using implicit titration. Proteins Struc. Funct. Genet. 27, 523–544.
Barteri, M., Gaudiano, M.C., Santucci, R., 1996. Influence of glycerol on the structure and stability of ferric horse heart myoglobin: a SAXS and circular dichroism study. Biochim. Biophys. Acta. 1295, 51–58.
Baudyš, M., Uchio, T., Mix, D., Wilson, D., Kim, S.W., 1995. Physical stabilization of insulin by glycosylation. J. Pharm. Sci. 84, 28–33.
Berry, A., 1996. In: Prince, N.C. (Ed.), Criteria of protein purity in Proteins. Labfax. Academic Press, San Diego, CA, pp. 73–84.
Boctor, A.M., Mehta, S.C., 1992. Enhancement of the stability of thrombin by polyols: microcalorimetric studies. J. Pharm. Pharmacol. 44, 600–603.
Bond, M., Jankowski, M., Patel, H., et al., 1998. Biochemical characterization of recombinant factor IX. Semin. Hematol. 35, 11–17.
Brange, J., Andersen, L., Laursen, E.D., Meyn, G., Rasmussen, E., 1997. Toward understanding insulin fibrillation. J. Pharm. Sci. 86, 517–525.
Brange, J., Havelund, S., Hougaard, P., 1992a. Chemical stability of insulin. 2. Formation of higher molecular weight transformation products during storage of pharmaceutical preparations. Pharm. Res. 9, 727–734.
Brange, J., Langkjær, L., Havelund, S., Vølund, A., 1992b. Chemical stability of insulin. 1. Hydrolytic degradation during storage of pharmaceutical preparations. Pharm. Res. 9, 715–726.
Brewster, M.E., Hora, M.S., Simpkins, J.W., Bodor, N., 1991. Use of 2–hydroxypropyl-β-cyclodextrin as a solubilizing and stabilizing excipient for protein drugs. Pharm. Res. 8, 792–795.
Brose, D.J., Waibel, P., 1996. Adsorption of proteins to commercial microfiltration capsules. Biopharmocology 9, 36–40.
Brunchu, S., Forbes, R.T., Nyqvist, H., York, P., 1996. A calorimetric study of the effect of cyclodextrins on the thermal stability of lysozyme. Pharm. Res. (Suppl.) 13, S94.
Burke, C.J., Steadman, B.L., Volkin, D.B., Tsai, P-K., Bruner, M.W., Middaugh, C.R., 1992. The adsorption of proteins to pharmaceutical container surfaces. Int. J. Pharm. 86, 89–93.
Butler, L.G., 1979a. Enzymes in non-aqueous solvents. Enzyme Microb. Technol. 1, 253–259.
Butler, W.L., 1979b. Fouth Derivative Spectra. Methods Enzymol. 56, 501–515.
Caliceti, P., Veronese, F.M., 1998. Successful insulin delivery by PEG conjugation. Proc. Intern. Symp. Control. Rel. Bioact. Mater. 25, 263–264.
Campbell, I.D., Downing, A.K., 1998. NMR of modular proteins. Nat. Struct. Biol. (Suppl.) 5, 496–499.
Cannio, R., Rossi, M., Bartolucci, S., 1994. A few amino acid substitutions are responsible for the higher thermostability of a novel NAD^+-dependent bacillar alcohol dehydrogenase. Eur. J. Biochem. 222, 345–352.
Carpenter, J.F., Crowe, J.H., Arakawa, T., 1990. Comparison of solute-induced protein stabilization in aqueous solution and in frozen and dried state. J. Dairy Sci. 73, 3627–3636.
Carpenter, J.F., Pikal, M.J., Chang, B.S., Randolph, T.W., 1997. Rational design of stable lyophilized protein formulations: some practical advice. Pharm. Res. 14, 969–975.
Carr, S.A., Hemling, M.E., Bean, M.F., Roberts, G.D., 1991. Integration of mass spectrometry in analytical biotechnology. Anal. Chem. 63, 2802–2824.
Chan, H.-K., Au-Yeung, K.-L., Gonda, I., 1996. Effects of additives on heat denaturation of rhDNase in solutions. Pharm. Res. 13, 756–761.
Chan, H.S., Dill, K.A., 1991. Polymer principles in protein structure and stability. Annu. Rev. Biophy. Chem. 20, 447–490.
Chang, B.S., Beauvais, R.M., Arakawa, T., Narhi, L.O., Dong, A., Aparisio, D.I., Carpenter, J.F., 1996a. Formation of an active dimer during storage of interleukin-1

receptor antagonist in aqueous solution. Biophy. J. 71, 3399–3406.

Chang, B.S., Reeder, G., Carpenter, J.F., 1996b. Development of a stable freeze-dried formulation of recombinant human interleukin-1 receptor antagonist. Pharm. Res. 13, 243–249.

Chang, B.S., Randall, C.S., Lee, Y.S., 1993. Stabilization of lyophilized porcine pancreatic elastase. Pharm. Res. 10, 1478–1483.

Chang, N., Hen, S.J., Klibanov, A.M., 1991. Protein separation and purification in neat dimethyl sulfoxide. Biochem. Biophys. Res. Commun. 176, 1462–1468.

Charm, S.E., Wong, B.L., 1970a. Enzyme inactivation with shearing. Biotechnol. Bioeng. 12, 1103–1109.

Charm, S.E., Wong, B.L., 1970b. Shear degradation of fibrinogen in the circulation. Science 170, 466–468.

Charman, S.A., Mason, M.L., Charman, W.N., 1993. Techniques for assessing the effects of pharmaceutical excipients on the aggregation of porcine growth hormone. Pharm. Res. 10, 954–962.

Charman, S.A., Ralph, C.E., Bakalova, M.V., Charman, W.N., 1995. The effects of poloxamers 407 and 188 on the conformational stability and aggregation of recombinant porcine growth hormone. Pharm. Res. (Suppl.) 12, S92.

Chehin, R., Thorolfsson, M., Knappskog, P.M., et al., 1998. Domain structure and stability of human phenylalanine hydroxylase inferred from infrared spectroscopy. FEBS Lett. 422, 225–230.

Chen, B., Costantino, H.R., Chung, J.L., Hsu, C., Shire, S.J., 1998. The influence of calcium ions on the structure and stability of recombinant human deoxyribonuclease I in the aqueous and lyophilized states. PharmSci (Suppl.) 1, S543.

Chen, B.-L., Arakawa, T., Hsu, E., Narhi, L.O., Tressel, T.J., Chien, S.L., 1994a. Strategies to suppress aggregation of recombinant keratinocyte growth factor during liquid formulation development. J. Pharm. Sci. 83, 1657–1661.

Chen, B-L., Arakawa, T., Morris, C.F., Kenney, W.C., Wells, C.M., Pitt, C.G., 1994b. Aggregation pathway of recombinant human keratinocyte growth factor and its stabilization. Pharm. Res. 11, 1581–1587.

Chiti, F., van Nuland, N.A.J., Taddei, N., Magherini, F., Stefani, M., Ramponi, G., Dobson, M., 1998. Conformational stability of muscle acylphosphatase: the role of temperature, denaturant concentration, and pH. Biochemistry 37, 1447–1455.

Chuyen, N.V., 1998. Maillard reaction and food processing. Application aspects. Adv. Exp. Med. Biol. 434, 213–235.

Clarke, A.R., Waltho, J.P., 1997. Protein folding pathways and intermediates. Curr. Opin. Biotechnol. 8, 400–410.

Cleland, J.L., Powell, M.F., Shire, S.J., 1993. The development of stable protein formulations: a close look at protein aggregation, deamidation, and oxidation. Crit. Rev. Ther. Drug Carrier Syst. 10, 307–377.

Clore, G.M., Gronenborn, A.M., 1998. Determining the structures of large proteins and protein complexes by NMR. Trends Biotechnol. 16, 22–34.

Cooper, B.F., Sideraki, V., Wilson, D.K., et al., 1997. The role of divalent cations in structure and function of murine adenosine deaminase. Protein Sci. 6, 1031–1037.

Cooper, E.A., Knutson, K., 1995. Fourier transform infrared spectroscopy investigations of protein structures. In: Herron, J.N., Jiskoot, W., Crommelin, D.J.A. (Eds.), Physical Methods to Chracterize Pharmaceutical Proteins. Plenum Press, New York, pp. 101–143.

Costantino, H.R., Brown, S.H., Kelly, R.M., 1990. Purification and characterization of an alpha-glucosidase from a hyperthermophilic archaebacterium, Prococcus furiosus, exhibiting a temperature optimum of 105 to 115°C. J. Bacteriol. 172, 3654–3660.

Costantino, H.R., Langer, R., Klibanov, A.M., 1994a. Solid-phase aggregation of proteins under pharmaceutically relevant conditions. J. Pharm. Sci. 83, 1662–1669.

Costantino, H.R., Langer, R., Klibanov, A.M., 1994b. Moisture-induced aggregation of lyophilized insulin. Pharm. Res. 11, 21–29.

Cowan, D.A., 1997. Thermophilic proteins: stability and function in aqueous and organic solvent. Comp. Biochem. Physiol. 118A, 429–438.

Craig, D.Q.M., Royall, P.G., 1998. The use of modulated temperature DSC for the study of pharmaceutical systems: potential uses and limitations. Pharm. Res. 15, 1152–1153.

Cross, R.T., Schirch, V., 1991. Effect of amino acid sequence, buffers, and ionic strength on the rate and mechanism of deamidation of asparagine residues in small peptide. J. Biol. Chem. 266, 22549–22556.

Damodaran, S., Song, K.B., 1988. Kinetics of adsorption of proteins at interfaces: role of protein conformation in diffusional adsorption. Biochim. Biophy. Acta 954, 253–264.

Daniel, R.M., Dines, M., Petach, H.H., 1996. The denaturation and degradation of stable enzymes at high temperature. Biochem. J. 317, 1–11.

Darby, N., Creighton, T.E., 1997. Probing protein folding and stability using disulfide bonds. Mol. Biotechnol. 7, 57–77.

Darnell, J., Lodish, H., Baltimore, D., 1986. Introduction: molecules, cells, and experimental technique. In: Molecular Cell Biology, Part I. Scientific American Books, New York, pp. 17–266.

Darrington, R.T., Anderson, B.D., 1995. Evidence for a common intermediate in insulin deamidation and covalent dimer formation: effects of pH and aniline trapping in dilute acidic solutions. J. Pharm. Sci. 84, 275–282.

D'Auria, S., Barone, S., Rossi, M., et al., 1997. Effects of temperature and SDS on the structure of β-glycosidase from the thermophilic archaeon *Sulfolobus solfataricus*. Biochem. J. 323, 833–840.

Davio, S.R., Kienle, K.M., Collins, B.E., 1995. Interchain interactions in the chimeric protein toxin sCD4(178)-PE40: a differential scanning calorimetry (DSC) study. Pharm. Res. 12, 642–648.

De Young, L.R., Dill, K.A., Fink, A.L., 1993. Aggregation and denaturation of apomyoglobin in aqueous urea solutions. Biochemistry 32, 3877–3886.

Dill, K.A., 1990. Dominant forces in protein folding. Biochemistry 29, 7133–7155.

Dill, K.A., Alonso, D.O.V., Hutchinson, K., 1989. Thermal stabilities of globular proteins. Biochemistry 28, 5439–5449.

Dimitrov, R.A., Crichton, R.R., 1997. Self-consistent field approach to protein structure and stability. 1. pH dependence of electrostatic contribution. Proteins Struc. Funct. Genet. 27, 576–596.

Dix, D.B., Carpenter, J.F., Halcome, J., Reeder, G., Chang, B.S., 1995. Increasing the physical stability of a hydrophobic protein: rhCNTF. Pharm. Res. (Suppl.) 12, S97.

Dobson, C.M., Hore, P.J., 1998. Kinetic studies of protein folding using NMR spectroscopy. Nat. Struct. Biol. 5, 504–507.

Dong, A., Caughey, W.S., 1994. Infrared methods for study of hemoglobin reactions and structures. Methods Enzymol. 232, 139–175.

Dong, A., Huang, P., Caughey, W.S., 1990. Protein secondary structures in water from second-derivative amide infrared spectra. Biochemistry 29, 3303–3308.

Dong, A., Kendrick, B., Kreilgård, L., Matsuura, J., Manning, M.C., Carpenter, J.F., 1997. Spectroscopic study of secondary structure and thermal denaturation of recombinant human factor XIII in aqueous solution. Arch. Biochem. Biophy. 347, 213–220.

Dong, A., Matsuura, J., Allison, S.D., Chrisman, E., Manning, M.C., Carpenter, J.F., 1995a. Infrared and circular dichroism spectroscopic characterization of structural differences between β-lactoglobulin A and B. Biochemistry 35, 1450–1457.

Dong, A., Prestrelski, S.J., Allison, S.D., Carpenter, J.F., 1995b. Infrared spectroscopic studies of lyophilization- and termperature-induced protein aggregation. J. Pharm. Sci. 84, 415–423.

Dosztányi, Z., Fiser, A., Simon, I., 1997. Stabilization centers in proteins: identification, characterization and predictions. J. Mol. Biol. 272, 597–612.

Du, C., Ye, J.M., Wolfe, J.L., 1998. Improved folding yields of a model protein using protien disulfide isomerase. Pharm. Res. 15, 1808–1815.

Dyson, H.J., Wright, P.E., 1998. Equilibrium NMR studies of unfolded and partially folded proteins. Nat. Struct. Biol. (Suppl.) 5, 499–503.

Eckhardt, B.M., Oeswein, J.Q., Yeung, D.A., Milby, T.D., Bewley, T.A., 1994. A turbidimetric method to determine visual appearance of protein solutions. J. Parent. Sci. Technol. 48, 64–70.

Eftink, M.R., 1994. The use of fluorescence methods to monitor unfolding transitions in proteins. Biophys. J. 66, 482–501.

Evans, S., Grassam, P., 1986. Considerations for parenteral dosage form development of natural alpha interferon. J. Par. Sci. Technol. 40, 83–87.

Farnsworth, P.N., Groth-Vasselli, B., Greenfield, N.J., Singh, K., 1997. Effects of temperature and concentration on bovine lens α-crystallin secondary structure: a circular dichroism spectroscopic study. Int. J. Biol. Macromol. 20, 283–291.

Farruggia, B., Garcia, G., D'Angelo, C., Picó, G., 1997. Destabilization of human serum albumin by polyethylene glycols studied by thermodynamical equilibrium and kinetic approaches. Int. J. Biol. Macromol. 20, 43–51.

Fatouros, A., Österberg, T., Mikaelsson, M., 1997a. Recombinant factor VIII SQ—influence of oxygen, metal ions, pH and ionic strength on its stability in aqueous solution. Int. J. Pharm. 155, 121–131.

Fatouros, A., Österberg, T., Mikaelsson, M., 1997b. Recombinant factor VIII SQ—inactivation kinetics in aqueous solution and the influence of disaccharides and sugar alcohols. Pharm. Res. 14, 1679–1684.

Fields, G., Alonso, D., Stiger, D., Dill, K., 1992. Theory for the aggregation of proteins and copolymers. J. Phys. Chem. 96, 3974–3981.

Figeys, D., Aebersold, R., 1998. High sensitivity analysis of proteins and peptides by capillary electrophoresis-tandem mass spectrometry: recent developments in technology and applications. Electrophoresis 19, 885–892.

Fogliano, V., Monti, S.M., Visconti, A., et al., 1998. Identification of a β-lactoglobulin lactosylation site. Biochim. Biophys. Acta 1388, 295–304.

Foord, R.L., Leatherbarrow, R.J., 1998. Effect of osmolytes on the exchange rates of backbone amide protons in proteins. Biochemistry 37, 2969–2978.

Fransson, J., Florin-Robertsson, E., Axelsson, K., Nyhlén, C., 1996. Oxidation of human insulin-like growth factor I in formulation studies: kinetics of methionine oxidation in aqueous solution and in solid state. Pharm. Res. 13, 1252–1257.

Fransson, J., Hagman, A., 1996. Oxidation of human insulin-like growth factor I in formulation sudies. II. Effect of oxygen, visible light, and phosphate on methionine oxidation in aqueous solution and evaluation of possible mechanisms. Pharm. Res. 13, 1476–1481.

Frye, K.J., Royer, C.A., 1997. The kinetic basis for the stabilization of staphylococcal nuclease by xylose. Protein Sci. 16, 789–793.

Ganzález, M., Murature, D.A., Fidelio, G.D., 1995. Thermal stability of human immunoglobulins with sorbitol. Vox Sang 68, 1–4.

Giancola, C., De Sena, C., Fessas, D., Graziano, G., Barone, G., 1997. DSC studies on bovine serum albumin denaturation: effects of ionic strength and SDS concentration. Int. J. Biol. Macromol. 20, 193–204.

Gianfreda, L., Scarfi, M.R., 1991. Enzyme stabilization: the state of art. Mol. Cell. Biochem. 100, 97–128.

Gibson, T.D., 1996. Protein stabilization using additives based on multiple electrostatic interactions. Dev. Biol. Stand. 87, 207–217.

Gietz, U., Alder, R., Langguth, P., Arvinte, T., Merkle, H.P., 1998. Chemical degradation kinetics of recombinant hirudin (HV1) in aqueous solution: effect of pH. Pharm. Res. 15, 1456–1462.

Goedken, E.R., Marqusee, S., 1998. Folding the ribonuclease H domain of Moloney murine leukemia virus reverse transcriptase requires metal binding or a short N-terminal extension. Proteins Struc. Funct. Genet. 33, 135–143.

Golbik, R., Zahn, R., Harding, S.E., Fersht, A.R., 1998. Thermodynamic stability and folding of GroEL minichaperones. J. Mol. Biol. 276, 505–515.

Gombotz, W.R., Pankey, S.C., Bouchard, L.S., Phan, D.H., MacKenzie, A.P., 1996. Stability, characterization, formulation and delivery system development for transforming growth factor-beta1. In: Pearlman, R., Wang, Y.J. (Eds.), Formulation, Characterization, and Stability of Protein Drugs. Plenum Press, New York, pp. 219–245.

Goolcharran, C., Borchardt, R.T., Keck, R., Cleland, J.L., 1998. Comparison of the rate of deamidation and diketopiperazine formation in rhVEGF and model peptides. PharmSci (Suppl.) 1, S535.

Goormaghtigh, E., Cabiaux, V., Ruysschaert, J.-M., 1994a. Determination of soluble and membrane protein structure by Fourier transform infrared spectroscopy II. Experimental aspects, side chain structure, and H/D exchange. Subcell. Biochem. 23, 363–404.

Goormaghtigh, E., Cabiaux, V., Ruysschaert, J.-M., 1994b. Determination of soluble and membrane protein structure by Fourier transform infrared spectroscopy III. Secondary structures. Subcell. Biochem. 23, 405–450.

Goto, Y., Fink, A.L., 1989. Conformational states of β-lactamase: molten-globule states at acidic and alkaline pH with high salt. Biochemistry 28, 945–952.

Goto, Y., Fink, A.L., 1994. Acid-induced folding of heme proteins. Methods Enzymol. 232, 3–15.

Griebenow, K., Klibanov, A.M., 1995. Lyophilization-induced reversible changes in the secondary structure of proteins. Proc. Natl. Acad. Sci. USA 92, 10969–10976.

Gu, L.C., Erdös, E.A., Chiang, H.-S., et al., 1991. Stability of interleukin 1β(IL-1β) in aqueous solution: analytical methods, kinetics, products, and solution formulation implications. Pharm. Res. 8, 485–490.

Guerra, P., Acklin, C., Kosky, A.A., Davis, J.M., Treuheit, M.J., Brems, D.N., 1998. PEGylation prevents the N-terminal degradation of megakaryocyte growth and development factor. Pharm. Res. 15, 1822–1827.

Hagiwara, T., Kumagai, H., Nakamura, K., 1996. Fractal analysis of aggregates formed by heating dilute BSA solutions using light scattering methods. Biosci. Biotechol. Biochem. 60, 1757–1763.

Heimburg, T., Marsh, D., 1993. Investigation of secondary and tertiary structural changes of cytochrome c in complexes with anionic lipids using amide hydrogen exchange measurements: an FTIR study. Biophys. J. 65, 2408–2417.

Hendrick, J.P., Hartl, F.-U., 1995. The role of molecular chaperones in protein folding. FASEB J. 9, 1559–1569.

Hensel, R., König, H., 1988. Thermoadaptation of methanogenic bacteria by intracellular ion concentration. FEMS Microbiol. Lett. 49, 75–79.

Herman, A.C., Boone, T.C., Lu, H.S., 1996. Characterization, formulation, and stability of Neupogen® (Filgrastim), a recombinant human granulocyte-colony stimulating factor. In: Pearlman, R., Wang, Y.J. (Eds.), Formulation, Characterization, and Stability of Protein Drugs. Plenum Press, New York, pp. 303–328.

Hsu, C.C., Nguyen, H.M., Yeung, D.A., et al., 1995. Surface denaturation at solid-void interface—a possible pathway by which opalescent particulates form during the storage of lyophilized tissue-type plasminogen activator at high temperatures. Pharm. Res. 12, 69–77.

Hsu, C.C., Ward, C.A., Pearlman, R., Nguyen, H.M., Yeung, D.A., Curley, J.G., 1991. Determining the optimum residual moisture in lyophilized protein pharmaceuticals. Develop. Biol. Stand. 74, 255–271.

Hu, H.Y., Lu, Z.X., Du, Y.C., 1997. Solution conformation of N-terminal fragments of trichosanthin small domain (TCS 182–200)—Circular dichroic studies. J. Pep. Res. 49, 113–119.

Huber, R., Kurr, M., Jannasch, H.W., Stetter, K.O., 1989. A novel group of abyssal methanogenic archaebacteria (*Methanopyrus*) growing at 110°C. Nature 342, 833–834.

Hung, H.C., Chang, G.G., 1998. Biphasic denaturation of human placental alkaline phosphatase in guanidinium chloride. Proteins Struc. Funct. Genet. 33, 49–61.

Ip, A.Y., Arakawa, T., Silvers, H., Ransone, C.M., Niven, R.W., 1995. Stability of recombinant consensus interferon to air-jet and ultrasonic nebulization. J. Pharm. Sci. 84, 1210–1214.

Jaenicke, R., 1990. Protein structure and function at low temperatures. Philos. Trans. R. Soc. London B 326, 535–551.

Jaenicke, R., 1991. Protein stability and molecular adaptation to extreme conditions. Eur. J. Biochem. 202, 715–728.

Jaenicke, R., 1996. Glyceraldehyde-3-phosphate dehydrogenase from *Thermotoga maritima*: strategies of protein stabilization. FEMS Microbiol. Rev. 18, 215–224.

James, E.L., Bottomley, S.P., 1998. The mechanism of α_1-antitrypsin polymerization probed by fluorescence spectroscopy. Arch. Biochem. Biophy. 356, 296–300.

Jensen, J.L., Roy, S.E., Hershenson, S.I., Schöneich, C., 1998. Metal-catalyzed degradation of brain-derived neurotrophic factor (BDNF): analytical and mechanistic challenges. PharmSci (Suppl.) 1, S536.

Jensen, W.A., Armstrong, J.M., De Giorgio, J., Hearn, M.T., 1996. Stability studies on pig heart mitochondrial malate dehydrogenase: the effect of salts and amino acids. Biochim. Biophys. Acta 1296, 23–34.

Jensen, W.A., Armstrong, J.M., De Giorgio, J., Hearn, M.T., 1997. Thermodynamic analysis of the stabilisation of pig heart mitochondrial malate dehydrogenase and maize leaf phosphoenolpyruvate carboxylase by different salts, amino acids and polyols. Biochim. Biophys. Acta 1338, 186–198.

Jensen-Pippo, K.E., Whitcomb, K.L., Woodward, M., Wilson, J., Reardon, P., Habberfield, A., 1995. Enteral bioavailability of pegylated IFN-Con1. Pharm. Res. (Suppl.) 12, S291.

Johnson, B.A., Shirokawa, J.M., Hancock, W.S., Spellman, M.W., Basa, L.J., Aswad, D.W., 1989. Formation of

isoaspartate at two distinct sites during in vitro aging of human growth hormone. J. Biol. Chem. 264, 14262–14271.
Johnson, C.M., Oliveberg, M., Clarke, J., Fersht, A.R., 1997. Thermodynamics of denaturation of mutants of barnase with disulfide crosslinks. J. Mol. Biol. 268, 198–208.
Johnston, T.P., 1996. Adsorption of recombinant human granulocyte colony stimulating factor (rhG-CSF) to polyvinyl chloride, polypropylene, and glass: effect of solvent additives. PDA J. Pharm. Sci. Technol. 50, 238–245.
Jones, A.J.S., 1994. Analytical Methods for the Assessment of Protein Formulations and Delivery Systems. In: Cleland, J.L., Langer, R. (Eds.), Formulation and Delivery of Proteins and Peptides. American Chemical Society, Washington DC, pp. 23–44.
Kanazawa, H., Fujimoto, S., Ohara, A., 1994. Effect of radical scavengers on the inactivation of papain by ascorbic acid in the presence of cupric ions. Biol. Pharm. Bull. 17, 476–481.
Katakam, M., Banga, A.K., 1997. Use of poloxamer polymers to stabilize recombinant human growth hormone against various processing stresses. Pharm. Dev. Technol. 2, 143–149.
Katakam, M., Bell, L.N., Banga, A.K., 1995. Effect of surfactants on the physical stability of recombinant human growth hormone. J. Pharm. Sci. 84, 713–716.
Katre, N.V., 1993. The conjugation of proteins with polyethylene glycol and other polymers altering properties of proteins to enhance their therapeutic potential. Adv. Drug Del. Rev. 10, 91–114.
Kaushal, P., Burducea, I, Hunt, S., Geblaoui, A., Gentz, R., Khan, F., 1998. Identification of chemical modifications in proteins, myeloid progenitor inhibitory factor-1 (MPIF-1) and keratinocyte growth factor-2 (KGF-2) by matrix-assisted laser desorption mass spectrometry. PharmSci (Suppl.) 1, S537.
Kendrick, B.S., Chang, B.S., Arakawa, T., et al., 1997. Preferential exclusion of sucrose from recombinant interleukin-1 receptor antagonist: role in restricted conformational mobility and compaction of native state. Proc. Natl. Acad. Sci. USA 94, 11917–11922.
Kendrick, B.S., Carpenter, J.F., Cleland, J.L., Randolph, T.W., 1998a. A transient expansion of the native state precedes aggregation of recombinant human interferon-gamma. Proc. Natl. Acad. Sci. USA 95, 14142–14146.
Kendrick, B.S., Cleland, J.L., Lam, X., et al., 1998b. Aggregation of recombinant human interferon gamma: kinetics and structural transitions. J. Pharm. Sci. 87, 1069–1076.
Kendrick, B.S., Dong, A., Allison, S.D., Manning, M.C., Carpenter, J.F., 1996. Quantitation of the area of overlap between second-derivative amide I infrared spectra to determine the structural similarity of a protein in different states. J. Pharm. Sci. 85, 155–158.
Kerwin, B.A., Alkers, M.J., Apostol, I., et al., 1998. Acute and long-term stability studies of deoxy hemoglobin and characterization of ascorbate-induced modifications. J. Pharm. Sci. 88, 79–88.
Khossravi, M., Borchardt, R.T., 1998. Chemical pathways of peptide degradation: IX. Metal-catalyzed oxidation of histidine in model peptides. Pharm. Res. 15, 1096–1102.
Kita, Y., Arakawa, T., Lin, T-Y., Timasheff, S.N., 1994. Contribution of the surface energy perturbation to protein–solvent interactions. Biochemistry 33, 15178–15189.
Knapp, S., Mattson, P.T., Christova, P., et al., 1998. Thermal unfolding of small proteins with SH3 domain folding pattern. Proteins: Struct. Funct. Gen. 31, 309–319.
Knepp, V.M., Whatley, J.L., Muchnik, A., Calderwood, T.S., 1996. Identification of antioxidants for prevention of peroxide-mediated oxidation of recombinant human ciliary neurotrophic factor and recombinant human nerve growth factor. J. Pharm. Sci. Technol. 50, 163–171.
Knepp, V.M., Muchnik, A., Oldmark, S., Kalashnikova, L., 1998. Stability of nonaqueous suspension formulation of plasma derived factor IX and recombinant human alpha interferon at elevated temperatures. Pharm. Res. 15, 1090–1095.
Kohn, W.D., Kay, C.M., Hodges, R.S., 1997. Salt effects on protein stability: two-stranded alpha-helical coiled-coils containing inter- or intrahelical ion pairs. J. Mol. Biol. 267, 1039–1052.
Kosa, T., Maruyama, T., Otagiri, M., 1998. Species differences of serum albumins: II chemical and thermal stability. Pharm. Res. 15, 449–454.
Kreilgaard, L, Jones, L.S., Randolph, T.W., et al., 1998. Effect of Tween 20 on freeze-thawing- and agitation-induced aggregation of recombinant human factor XIII. J. Pharm. Sci. 87, 1597–1603.
Kristjánsson, M.M., Kinsella, J.E., 1991. Protein and enzyme stability: structural, thermodynamic, and experimental aspects. Adv. Food Nutr. Res. 35, 237–316.
Kuhlman, B., Yang, H.Y., Boice, J.A., Fairman, R., Raleigh, D.P., 1997. An exceptionally stable helix from the ribosomal protein L9: implications for protein folding and stability. J. Mol. Biol. 270, 640–647.
Kurochkin, I.V., Procyk, R., Bishop, P.D., et al., 1995. Domain structure, stability and domain-domain interactions in recombinant factor XIII. J. Mol. Biol. 248, 414–430.
Kuwata, K., Era, S., Sogami, M., 1994. The kinetic studies on the intramolecular SH, S–S exchange reaction of bovine mercaptalbumin. Biophim. Biophys. Acta. 1205, 317–324.
Kwon, K-S., Yu, M-H., 1997. Effect of glycosylation on the stability of α_1-antitrypsin toward urea denaturation and thermal deactivation. Biophim. Biophys. Acta. 1335, 265–272.
Lam, X.M., Costantino, H.R., Overcashier, D.E., Nguyen, T.H., Hsu, C.C., 1996. Replacing succinate with glycolate buffer improves the stability of lyophilized interferon-γ. Int. J. Pharm. 142, 85–95.
Lau, F.W., Bowie, J.U., 1997. A method for assessing the stability of a membrane protein. Biochemistry 36, 5884–5892.
Lee, B., Vasmatzis, G., 1997. Stabilization of protein structures. Curr. Opin. Biotechnol. 8, 423–428.

Lewis, S.A., Cowan, N.J., 1996. Progress in understanding protein folding. Pharm. Technol. 20, 40–48.

Li, S., Schöneich, C., Wilson, G.S., Borchardt, R.T., 1993. Chemical pathways of peptide degradation. V. Ascorbic acid promotes rather than inhibits the oxidation of methionine to methionine sufoxide in small model peptides. Pharm. Res. 10, 1572–1579.

Li, S., Nguyen, T., Schöneich, C., Borchardt, R.T., 1995a. Aggregation and precipitation of human relaxin induced by metal-catalyzed oxidation. Biochemistry. 34, 5762–5772.

Li, S., Schöneich, C., Borchardt, R.T., 1995b. Chemical instability of proteins. Pharm. News 2, 12–16.

Li, S., Schöneich, C., Borchardt, R.T., 1995c. Chemical instability of protein pharmaceuticals: Mechanisms of oxidation and strategies for stabilization. Biotechnol. Bioeng. 48, 491–500.

Li, S., Patapoff, T.W., Nguyen, T.H., Borchardt, R.T., 1996a. Inhibitory effect of sugars and polyols on the metal-catalyzed oxidation of human relaxin. J. Pharm. Sci. 85, 868–872.

Li, S., Patapoff, T.W., Overcashier, D., Hsu, C., Nguyen, T.H., Borchardt, R.T., 1996b. Effects of reducing sugars on the chemical stability of human relaxin in the lyophilized state. J. Pharm. Sci. 85, 873–877.

Lin, L.S., Kunitani, M.G., Hora, M.S., 1996c. Interferon-β-1b (Betaseron®): a model for hydrophobic therapeutic proteins. In: Pearlman, R., Wang, Y.J. (Eds.), Formulation, Characterization, and Stability of Protein Drugs. Plenum Press, New York, pp. 275–301.

Lin, T.-Y., Timasheff, S.N., 1996. On the role of surface tension in the stabilization of globular proteins. Protein Sci. 5, 372–381.

Lis, H., Sharon, N., 1993. Protein glycosylation-structural and functional aspects. Eur. J. Biochem. 218, 1–27.

Liu, D.T-Y., 1992. Glycoprotein pharmaceuticals: scientific and regulatory considerations, and the US Orphan Drug Act. Trends Biotechnol. 10, 114–120.

Liu, J.L., Lu, K.V., Eris, T., et al., 1998. In vitro methionine oxidation of recombinant human leptin. Pharm. Res. 15, 632–640.

Liu, Y., Bolen, D.W., 1995. The peptide backbone plays a dominant role in protein stabilization by naturally occurring osmolytes. Biochemistry 34, 12884–12891.

Liu, Y., Sturtevant, J.M., 1996. The observed change in heat capacity accompanying the thermal unfolding of proteins depends on the composition of the solution and on the method employed to change the temperature of unfolding. Biochemistry 35, 3059–3062.

Lo, Y.L., Rahman, Y.E., 1998. Effect of lipids on the thermal stability and conformational changes of proteins: ribonuclease A and cytochrome c. Int. J. Pharm. 161, 137–148.

Lowry, C.L., McGeehan, G., LeVine, H., 1992. Metal ion stabilization of the conformation of a recombinant 19-kDa catalytic fragment of human fibroblast collagenase. Proteins 12, 42–48.

Lozano, P., De Diego, T., Iborra, J.L., 1997. Dynamic structure/function relationships in the alpha-chymotrypsin deactivation process by heat and pH. Eur. J. Biochem. 248, 80–85.

Maa, Y.-F., Hsu, C.C., 1997. Protein denaturation by combined effect of shear and air-liquid interface. Biotechnol. Bioeng. 54, 503–512.

Manallack, D.T., Andrews, P.R., Woods, E.F., 1985. Design, synthesis, and testing of insulin hexamer-stabilizing agents. J. Med. Chem. 28, 1522–1526.

Manning, M.C., Matsuura, J.E., Kendrick, B.S., et al., 1995. Approaches for increasing the solution stability of proteins. Biotechnol. Bioeng. 48, 506–512.

Manning, M.C., Patel, K., Borchardt, R.T., 1989. Stability of protein pharmaceuticals. Pharm. Res. 6, 903–917.

Martins, L.O., Huber, R., Huber, H., Stetter, K.O., Da Costa, M.S., Santos, H., 1997. Organic solutes in hyperthermophilic *Archaea*. Appl. Environ. Microbiol. 63, 896–902.

Martins, L.O., Santos, H., 1995. Accumulation of mannosylglycerate and di-myo-inositol-phosphate by *Pyrococcus furiosus* in response to salinity and temperature. Appl. Environ. Microbiol. 61, 3299–3303.

Matsumura, M., Signor, G., Matthews, B.W., 1989. Substantial increase of protein stability by multiple disulphide bonds. Nature 342, 291–293.

Matsuura, J.E., Manning, M.C., 1994. Heat-induced gel formation of β-lactoglobulin: a study on the secondary and tertiary structure as followed by circular dichroism spectroscopy. J. Agric. Food Chem. 42, 1650–1656.

Mayr, L.M., Schmid, F.X., 1993. Stabilization of a protein by guanidinium chloride. Biochemistry 32, 7994–7998.

McIntosh, K.A., Charman, W.N., Charman, S.A., 1998. The application of capillary electrophoresis for monitoring effects of excipients on protein conformation. J. Pharm. Biomed. Anal. 16, 1097–1105.

Melo, E.P., Aires-Barros, M.R., Costa, S.M., Cabral, J.M., 1997. Thermal unfolding of proteins at high pH range studied by UV absorbance. J. Biochem. Biophys. Methods 34, 45–59.

Middaugh, C.R., 1990. Biophysical approaches to the pharmaceutical development of proteins. Drug Dev. Ind. Pharm. 16, 2635–2654.

Mozhaev, V.V., Martinek, K., 1984. Structure-stability relationships in proteins: new approaches to stabilizing enzymes. Enzyme Microb. Technol. 6, 50–59.

Munson, M., Balasubramanian, S., Fleming, K.G., et al., 1996. What makes a protein a protein? Hydrophobic core design that specify stability and structural properties. Protein Sci. 5, 1584–1593.

Nabuchi, Y., Fujiwara, E., Ueno, K., Kuboniwa, H., Asoh, Y., Ushio, H., 1995. Oxidation of recombinant human parathyroid hormone: effect of oxidized position on the biological activity. Pharm. Res. 12, 2049–2052.

Nguyen, D.N., Becker, G.W., Riggin, R.M., 1995. Protein mass spectrometry: applications to analytical biotechnology. J. Chromatogr. A 705, 21–45.

Nguyen, T.H., Burnier, J., Meng, W., 1993. The kinetics of relaxin oxidation by hydrogen peroxide. Pharm. Res. 10, 1563–1571.

Nguyen, T.H., Shire, S.J., 1996. Stability and characterization of recombinant human relaxin. In: Pearlman, R., Wang, Y.J. (Eds.), Formulation, Characterization, and Stability of Protein Drugs. Plenum Press, New York, pp. 247–271.

Österberg, T., Fatouros, A., 1994. Oxygen-reduced aqueous solution of factor VIII. International patent WO94/26286.

Overcashier, D.E., Brooks, D.A., Costantino, H.R., Hsu, C.C., 1997. Preparation of excipient-free recombinant human tissue-type plasminogen activator by lyophilization from ammonium bicarbonate solution: an investigation of the two-stage sublimation phenomenon. J. Pharm. Sci. 86, 455–459.

Pace, C.N., 1990. Measuring and increasing protein stability. Trends Biotechnol. 8, 93–98.

Pace, C.N., Shirley, B.A., McNutt, M., Gajiwala, K., 1996. Forces contributing to the conformational stability of proteins. FASEB J. 10, 75–83.

Pancoska, P., Fabian, H., Yoder, G., Baumruk, V., Keiderling, T.A., 1996. Protein structural segments and their interconnections derived from optical spectra. Thermal unfolding of ribonuclease T1 as an example. Biochemistry. 35, 13094–13106.

Paulsen, H., Pflughaupt, K.-W., 1980. Glycosylamines. In: Pigman, W., Horton, D., Wander, J.D. (Eds.), The Carbohydrates Chemistry and Biochemistry. Academic Press, New York, pp. 881–921.

Picó, G., 1995. Thermodynamic aspects of the thermal stability of human serum albumin. Biochem. Mol. Biol. Int. 36, 1017–1023.

Picó, G.A., 1996. Thermal stability of human serum albumin by sodium halide salts. Biochem. Mol. Biol. Int. 38, 1–6.

Paranandi, M.V., Guzzetta, A.W., Hancock, W.S., Aswad, D.W., 1994. Deamidation and isoaspartate formation during in vitro aging of recombinant tissue plasminogen activator. J. Biol. Chem. 269, 243–253.

Patro, S., Przybycien, T.M., 1996. Simulations of reversible protein aggregate and crystal structure. Biophys. J. 70, 2888–2902.

Peak, M.J., Peak, J.G., Stevens, F.J., et al., 1994. The hyperthermophilic glycolytic enzyme enolase in the archaeon, *Pyrococcus furiosus*: comparison with mesophilic enolases. Arch. Biochem. Biophys. 313, 280–286.

Perlman, R., Nguyen, T., 1992. Pharmaceutics of protein drugs. J. Pharm. Pharmcol. 44 (Suppl 1), 178–185.

Petukhov, M, Kil, Y., Kuramitsu, S., Lanzov, V., 1997. Insights into thermal resistance of proteins from the intrinsic stability of their alpha-helices. Proteins: Struct. Func. Gen. 29, 309–320.

Pikal, M.J., Dellerman, K.M., Roy, M.L., Riggin, R.M., 1991. The effects of formulation variables on the stability of freeze-dried human growth hormone. Pharm. Res. 8, 427–436.

Pikal, M.J., Rigsbee, D.R., 1997. The stability of insulin in crystalline and amorphous solids: observation of greater stability for the amorphous form. Pharm. Res. 14, 1379–1387.

Powell, M.F., 1994. Peptide Stability in Aqueous Parenteral Formulations. In: Cleland, J.L., Langer, R. (Eds.), Formulation and Delivery of Proteins and Peptides. American Chemical Society, Washington DC, pp. 101–117.

Powell, M.F., 1996. A compendium and hydropathy/flexibility analysis of common reactive sites in proteins: Reactivity at Asn, Asp, Gln, and Met motifs in neutral pH solution. In: Pearlman, R., Wang, Y.J. (Eds.), Formulation, Characterization, and Stability of Protein Drugs. Plenum Press, New York, pp. 1–140.

Prehoda, K.E., Mooberry, E.S., Markley, J.L., 1998. Pressure denaturation of proteins: evaluation of compressibility effects. Biochemistry 37, 5785–5790.

Prestrelski, S.J., Arakawa, T., Carpenter, J.F., 1993a. Separation of freezing and drying-induced denaturation of lyophilized proteins using stress-specific stabilization. II. Structural studies using infrared spectroscopy. Arch. Biochem. Biophys. 303, 465–473.

Prestrelski, S.J., Tedeschi, N., Arakawa, T., Carpenter, J.F., 1993b. Dehydration-induced conformational transitions in proteins and their inhibition by stabilizers. Biophy. J. 65, 661–671.

Prestrelski, S.J., Pikal, K.A., Arakawa, T., 1995. Optimization of lyophilization conditions for recombinant human interleukin-2 by dried-state conformational analysis using Fourier-transform infrared spectroscopy. Pharm. Res. 12, 1250–1259.

Prieto, J., Wilmans, M., Jimenez, M.A., Rico, M., Serrano, L., 1997. Non-native local interactions in protein folding and stability: introducing a helical tendency in the all β-sheet α-spectrin SH3 domain. J. Mol. Biol. 268, 760–778.

Querol, E., Pervez-Pons, J.A., Mozo-Villarias, A., 1996. Analysis of protein conformational characteristics related to thermostability. Protein Eng. 9, 265–271.

Ragone, R., Facchiano, F., Facchiano, A., Facchiano, A.M., Colonna, G., 1989. Flexibility plot of proteins. Protein Eng. 2, 497–504.

Ramakrishnan, V., Verhagen, M.F.J.M., Adams, M.W.W., 1997. Characterization of di-myo-inositol-1,1′-phosphate in the hyperthermophilic bacterium *Thermotoga maritina*. Appl. Environ. Microbiol. 63, 347–350.

Raman, B., Ramakrishna, T., Rao, C.M., 1997. Effect of the chaperone-like alpha-crystallin on the refolding of lysozyme and ribonuclease A. FEBS Lett. 416, 369–372.

Ramos, A., Raven, N.D.H., Sharp, R.J., et al., 1997. Stabilization of enzymes against thermal stress and freeze-drying by mannosylglycerate. Appl. Environ. Microbiol. 63, 4020–4025.

Raschke, T.M., Marqusee, S., 1998. Hydrogen exchange studies of protein structure. Curr. Opin. Biotechnol. 9, 80–86.

Reid, D.G., MacLachlan, L.K., Edwards, A.J., Hubbard, J.A., Sweeney, P.J., 1997. Introduction to the NMR of proteins. Methods Mol. Biol. 60, 1–28.

Remmele Jr, R.L., Nightlinger, N.S., Srinivasan, S., Gombotz, W.R., 1998. Interleukin-1 receptor (IL-1R) liquid formula-

tion development using differential scanning calorimetry. Pharm. Res. 15, 200–208.
Richards, F.M., 1997. Protein stability: still an unsolved problem. Cell. Mol. Life Sci. 53, 790–802.
Roefs, S.P.F.M., De Kruif, K.G., 1994. A model for the denaturation and aggregation of β-lactoglobulin. Eur. J. Biochem. 226, 883–889.
Royall, P.G., Craig, D.Q.M., Doherty, C., 1998. Characterization of the glass transition of an amorphous drug using modulated DSC. Pharm. Res. 15, 1117–1121.
Ruddon, R.W., Bedows, E., 1997. Assisted protein folding. J. Biol. Chem. 272, 3125.
Runkel, L., Meier, W., Pepinsky, R.B., et al., 1998. Structural and functional differences between glycosylated and non-glycosylated forms of human interferon-β (IFN-β). Pharm. Res. 15, 641–649.
Rupley, J.A., Careri, G., 1991. Protein hydration and function. Adv. Protein Chem. 41, 37–173.
Sanyal, G., Marquis-Omer, D., Middaugh, C.R., 1996. Biological characterization and formulation of TP40: a chimeric protein that requires a pH-dependent conformational change for its biological activity. In: Pearlman, R., Wang, Y.J. Jr. (Eds.), Formulation, Characterization, and Stability of Protein Drugs. Plenum Press, New York, pp. 365–392.
Sasaoki, K., Hiroshima, T., Kusumoto, S., Nishi, K., 1992. Deamidation at asparagine-88 in recombinant human interleukin 2. Chem. Pharm. Bull. 40, 976–980.
Schrier, J.A., Kenley, R.A., Williams, R., Corcoran, R.J., Kim, Y., Northey, R.P. Jr., D'Augusta, D., Huberty, M., 1993. Degradation pathways for recombinant human macrophage colony-stimulating factor in aqueous solution. Pharm. Res. 10, 933–944.
Schwendeman, S.P., Costantino, H.R., Gupta, R.K., Siber, G.R., Klibanov, A.M., Langer, R., 1995. Stabilization of tetanus and diphtheria toxoids against moisture-induced aggregation. Proc. Natl. Acad. Sci. USA 92, 11234–11238.
Sendak, R.A., Rothwarf, D.M., Wedemeyer, W.J., Houry, W.A., Scheraga, H.A., 1996. Kinetic and thermodynamic studies of the folding/unfolding of a tryptophan-containing mutant of ribonuclease A. Biochemistry 35, 12978–12992.
Senderoff, R.I., Kontor, K.M., Heffernan, J.K., et al., 1996. Aqueous stability of recombinant human thrombopoietin as a function of processing schemes. J. Pharm. Sci. 85, 749–752.
Shahrokh, Z., Beylin, I., Eberlein, G., et al., 1995. Cellulose-cleaving activity contaminating *E.coli*-produced recombinant proteins. Biopharm 8, 32–38.
Shahrokh, Z., Eberlein, G., Buckley, D., et al., 1994a. Major degradation products of basic fibroblast growth factor: detection of succinimide and iso-aspartate in place of aspartate. Pharm. Res. 11, 936–944.
Shahrokh, Z., Strantton, P.R., Eberlein, G.A., Wang, Y.J., 1994b. Approaches to analysis of aggregates and demonstrating mass balance in pharmaceutical protein (basic fibroblast growth factor) formulations. J. Pharm. Sci. 83, 1645–1649.
Shire, S.J., 1996. Stability characterization and formulation development of recombinant human deoxyribonuclease I [Pulmozyme®, (dornase alpha)]. In: Pearlman, R., Wang, Y.J. (Eds.), Formulation, Characterization, and Stability of Protein Drugs. Plenum Press, New York, pp. 393–426.
Shirley, B., Stanssens, P., Steyaert, J., Pace, C.N., 1989. Conformational stability and activity of ribonuclease T1 and mutants. J. Biol. Chem. 264, 11621–11625.
Shoichet, B.K., Baase, W.A., Kuroki, R., Matthews, B.W., 1995. A relationship between protein stability and protein function. Proc. Natl. Acad. Sci. USA 92, 452–456.
Shortle, D., 1996. The denatured state (the other half of the folding equation) and its role in protein stability. FASEB J. 10, 27–34.
Sindelar, C.V., Hendsch, Z.S., Tidor, B., 1998. Effects of salt bridges on protein structure and design. Protein Sci. 7, 1898–1914.
Sluzky, V., Tamada, J.A., Klibanov, A.M., Langer, R., 1991. Kinetics of insulin aggregation in aqueous solutions upon agitation in the presence of hydrophobic surfaces. Proc. Natl. Acad. Sci. USA 88, 9377–9381.
Sluzky, V., Klibanov, A.M., Langer, R., 1992. Mechanism of insulin aggregation and stabilization in agitated aqueous solutions. Biotechnol. Bioeng. 40, 895–903.
Son, K., Kwon, C., 1995. Stabilization of human epidermal growth factor (hEGF) in aqueous formulation. Pharm. Res. 12, 451–454.
Speed, M.A., Wang, D.I.C., King, J., 1996. Specific aggregation of partially folded polypeptide chains: the molecular basis of inclusion body composition. Nature Biotechnol. 14, 1283–1287.
Stadtman, E.R., 1993. Oxidation of free amino acid residues in proteins by metal-catalyzed reactions. Annu. Rev. Biochem. 62, 797–821.
Staniforth, R.A., Bigotti, M.G., Cutruzzola, F., Allocatelli, C.T., 1998. Brunori M unfolding of apomyoglobin from *Aplysia limacina*: the effect of salt and pH on the cooperativity of folding. J. Mol. Biol. 275, 133–148.
Stephenson, R.C., Clarke, S., 1989. Succinimide formation from aspartyl and asparaginyl peptides as a model for the spontaneous degradation of proteins. J. Biol. Chem. 264, 6164–6170.
Stevenson, C.L., Friedman, A.R., Kubiak, T.M., Donlan, M.E., Borchardt, R.T., 1993. Effect of secondary structure on the rate of deamidation of several growth hormone releasing factor analogs. Int. J. Peptide Protein Res. 42, 497–503.
Strickley, R.G., Anderson, B.D., 1996. Solid-state stability of human insulin. I. Mechanism and the effect of water on the kinetics of degradation in lyophiles from pH 2–5 solutions. Pharm. Res. 13, 1142–1153.
Strickley, R.G., Anderson, B.D., 1997. Solid-state stability of human insulin. II. Effect of water on reactive intermediate partitioning in lyophiles from pH 2–5 solutions: stabilization against covalent dimer formation. J. Pharm. Sci. 86, 645–653.

Surewicz, W., Mantsch, H.H., Chapman, D., 1993. Determination of protein secondary structure by Fourier transform infrared spectroscopy: a critical assessment. Biochemistry 32, 389–393.

Susi, H., Byler, D.M., 1986. Resolution-enhanced Fourier transform infrared spectroscopy of enzymes. Methods Enzymol. 130, 290–311.

Swietnicki, W., Petersen, R., Gambetti, P., Surewicz, W.K., 1997. pH-dependent stability and conformation of the recombinant human prion protein PrP(90–231). J. Biol. Chem. 272, 27517–27520.

Takano, K, Yamagata, Y., Yutani, K., 1998. A general rule for the relationship between hydrophobic effect and conformational stability of a protein: Stability and structure of a series of hydrophobic mutants of human lysozyme. J. Mol. Biol. 280, 749–761.

Tandon, S., Horowitz, P.M., 1987. Detergent-assisted refolding of guanidinium chloride-denatured rhodanese. J. Biol. Chem. 262, 4486–4490.

Tang, K.E.S., Dill, K.A., 1998. Native protein fluctuations: The conformational-motion temperature and the inverse correlation of protein flexibility with protein stability. J. Biomol. Struct. Dyn. 16, 397–411.

Tanner, J.W., Eckenhoff, R.G., Liebman, P.A., 1999. Halothane, an inhalational anesthetic agent, increases folding stability of serum albumin. Biophim. Biophys. Acta. 1430, 46–56.

Tarelli, E., Corran, P.H., Bingham, B.R., Mollison, H., Wait, R., 1994. Lysine vasopressin undergoes rapid glycation in the presence of reducing sugars. J. Pharm. Biomed. Anal. 12, 1355–1361.

Thomson, J.A., Shirley, B., Grimsley, G.R., Pace, C.N., 1989. Conformational stability and mechanism of folding of ribonuclease T1. J. Biol. Chem. 264, 11614–11620.

Thurow, H., Geisen, K., 1984. Stabilization of dissolved proteins against denaturation at hydrophobic interfaces. Diabetologia 27, 212–218.

Timasheff, S.N., 1992. Water as ligand: preferential binding and exclusion of denaturants in protein unfolding. Biochemistry 31, 9857–9864.

Timasheff, S.N., 1993. The control of protein stability and association by weak interactions with water: how do solvents affect these processes? Annu. Rev. Biophy. Biomol. Struct. 22, 67–97.

Timasheff, S.N., 1998. Control of protein stability and reactions by weakly interacting cosolvents: the simplicity of the complicated. Adv. Protein Chem. 51, 355–432.

Topham, C.M., Srinivasan, N., Blundell, T.L., 1997. Prediction of the stability of protein mutants based on structural environment-dependent amino acid substitution and propensity tables. Protein. Eng. 10, 7–21.

Townsend, M.W., DeLuca, P.P., 1990. Stability of ribonuclease A in solution and the freeze-dried state. J. Pharm. Sci. 79, 1083–1086.

Tsai, P.K., Volkin, D.B., Dabora, J.M., et al., 1993. Formulation design of acidic fibroblast growth factor. Pharm. Res. 10, 649–659.

Tsai, A.M., van Zanten, J.H., Betenbaugh, M.J., 1998a. I. Study of protein aggregation due to heat denaturation: a structural approach using circular dichroism spectroscopy, nuclear magnetic resonance, and static light scattering. Biotechnol. Bioeng. 59, 273–280.

Tsai, A.M., van Zanten, J.H., Betenbaugh, M.J., 1998b. II. Electrostatic effect in the aggregation of heat-denatured RNase A and implications for protein additive design. Biotechnol. Bioeng. 59, 281–285.

Tsai, Y.R., Yang, S.J., Jiang, S.S., et al., 1998c. High-pressure effects on vacuolar H^+ -ATPase from etiolated mung bean seedlings. J. Protein Chem. 17, 161–172.

Tsutsumi, Y., Kihira, T., Tsunoda, S-I., et al., 1995. Polyethylene glycol modification of interleukin-6 enhances its thrombopoietic activity. J. Control. Release 33, 447–451.

Tuena de Gómez-Puyou, M., Gómez-Puyou, A., 1998. Enzymes in low water systems. Crit. Rev. Biochem. Mol. Biol. 33, 53–89.

Tzannis, S.T., Hrushesky, W.J.M., Wood, P.A., Przybycien, T.M., 1996. Irreversible inactivation of interleukin 2 in a pump-based delivery environment. Proc. Natl. Acad. Sci. USA 93, 5460–5465.

Tzannis, S.T., Hrushesky, W.J.M., Wood, P.A., Przybycien, T.M., 1997. Adsorption of a formulated protein on a drug delivery device surface. J. Colloid Interface Sci. 189, 216–228.

Vermeer, A.W., Bremer, M.G., Norde, W., 1998. Structural changes of IgG induced by heat treatment and by adsorption onto a hydrophobic Teflon surface studied by circular dichroism spectroscopy. Biochim. Biophys. Acta 1425, 1–12.

Vieille, C., Zeikus, J.G., 1996. Thermoenzymes: identifying molecular determinants of protein structural and functional stability. Trends Biotechnol. 14, 183–191.

Vogt, G., Argos, P., 1997. Protein thermal stability: hydrogen bonds or internal packing? Fold. Des. 2, S40–46.

Vogt, G., Woell, S., Argos, P., 1997. Protein thermal stability, hydrogen bonds, and ion pairs. J. Mol. Biol. 269, 631–643.

Volkin, D.B., Burke, C.J., Sanyal, G., Middaugh, C.R., 1996. Analysis of vaccine stability. Dev. Biol. Stand. 87, 135–142.

Volkin, D.B., Klibanov, A.M., 1987. Thermal destruction processes in proteins involving cystine residues. J. Biol. Chem. 262, 2945–2950.

Volkin, D.B., Klibanov, A.M., 1989. Minimizing protein inactivation. In: Creighton, T.E. (Ed.), Protein Function A Practical Approach. Information Press, Oxford, UK, pp. 1–24.

Volkin, D.B., Middaugh, C.R., 1996. The characterization, stabilization, and formulation of acidic fibroblast growth factor. In: Pearlman, R., Wang, Y.J. (Eds.), Formulation, Characterization, and Stability of Protein Drugs. Plenum Press, New York, pp. 181–217.

Volkin, D.B., Tsai, P.K., Dabora, J.M., et al., 1993. Physical stabilization of acidic fibroblast growth factor by polyanions. Arch. Biochem. Biophys. 300, 30–41.

Vrkljan, M., Foster, T.M., Powers, M.E., et al., 1994. Thermal stability of low molecular weight urokinase during heat treatment. Part 2. Effect of polymeric additives. Pharm. Res. 11, 1004–1008.

Wang, A., Robertson, A.D., Bolen, D.W., 1995. Effects of a naturally occurring compatible osmolyte on the internal dynamics of ribonuclease A. Biochemistry 34, 15069–15104.

Wang, C., Eufemi, M., Turano, C., Giartosio, A., 1996a. Influence of the carbohydrate moiety on the stability of glycoproteins. Biochemistry 35, 7299–7307.

Wang, P-L., Johnston, T.P., 1993a. Enhanced stability of two model proteins in an agitated solution environment using poloxamer 407. J. Parenter. Sci. Technol. 47, 183–189.

Wang, P-L., Johnston, T.P., 1993b. Thermal-induced denaturation of two model proteins: effect of poloxamer 407 on solution stability. Int. J. Pharm. 96, 41–49.

Wang, W., 1996. Oral protein drug delivery. J. Drug Target. 4, 195–232.

Wang, Y.J., Shahrokh, Z., Vemuri, S., Eberlein, G., Beylin, I., Busch, M., 1996b. Charaterization, stability, and formulation of basic fibroblast growth factor. In: Pearlman, R., Wang, Y.J. (Eds.), Formulation, Characterization, and Stability of Protein Drugs. Plenum Press, New York, pp. 141–180.

Wen, J., Arakawa, T., Philo, J.S., 1996. Size-exclusion chromatography with on-line light-scattering, absorbance, and refractive index detectors for studying proteins and their interactions. Anal. Biochem. 240, 155–166.

Won, C.M., Molnar, T.E., McKean, R.E., Spenlehauer, G.A., 1998. Stabilizers against heat-induced aggregation of RPR 114849, an acidic fibroblast growth factor (AFGF). Int. J. Pharm. 167, 25–36.

Wong, D., Parascrampuria, J., 1997. Pharmaceutical excipients for the stabilization of proteins. Pharm. Technol. 21, 34–50.

Wrabl, J.O., Shortle, D., 1996. Perturbations of the denatured state ensemble: modeling their effects on protein stability and folding kinetics. Protein. Sci. 5, 2343–2352.

Xie, G., Timasheff, S.N., 1997a. Mechanism of the stabilization of ribonuclease A by sorbitol: preferential hydration is greater for the denatured than for the native protein. Protein Sci. 6, 211–221.

Xie, G., Timasheff, S.N., 1997b. The thermodynamic mechanism of protein stabilization by trehalose. Biophys. Chem. 64, 25–43.

Xu, G.Y., Yu, H.A., Hong, J., et al., 1997. Solution structure of recombinant human interleukin-6. J. Mol. Biol. 268, 468–481.

Xie, M., Schowen, R., 1999. Secondary structure and protein deamidation. J. Pharm. Sci. 88, 8–13.

Yang, A-S., Honig, B., 1993. On the pH dependence of protein stability. J. Mol. Biol. 231, 459–474.

Yeo, S-D., Debenedetti, P.G., Patro, S.Y., Przybycien, T.M., 1994. Secondary structure characterization of microparticulate insulin powders. J. Pharm. Sci. 83, 1651–1656.

Yoshioka, S., Aso, Y., Izutsu, K., Terao, T., 1993. Aggregates formed during storage of β-galactosidase in solution and in the freeze-dried state. Pharm. Res. 10, 103–108.

Yoshioka, S., Aso, Y., Izutsu, K., Kojima, S., 1994a. Is stability prediction possible for protein drugs? Denaturation kinetics of β-galactosidase in solution. Pharm. Res. 11, 1721–1725.

Yoshioka, S., Aso, Y., Izutsu, K-I., Terao, T., 1994b. Application of accelerated testing for shelf-life prediction of commercial protein preparations. J. Pharm. Sci. 83, 454–456.

Yoshioka, S., Aso, Y., Kojima, S., 1997. Softening temperature of lyophilized serum albumin and γ-globulin as measured by spin-spin relaxation time of protein protons. J. Pharm. Sci. 86, 470–474.

Yoshioka, S., Aso, Y., Nakai, Y., Kojima, S., 1998. Effect of high molecular mobility of poly(vinyl alcohol) on protein stability of lyophilized γ-globulin formulations. J. Pharm. Sci. 87, 147–151.

Zhang, J., Peng, X., Jonas, A., Jonas, J., 1995. NMR study of the cold, heat, and pressure unfolding of ribonuclease A. Biochemistry 34, 8631–8641.

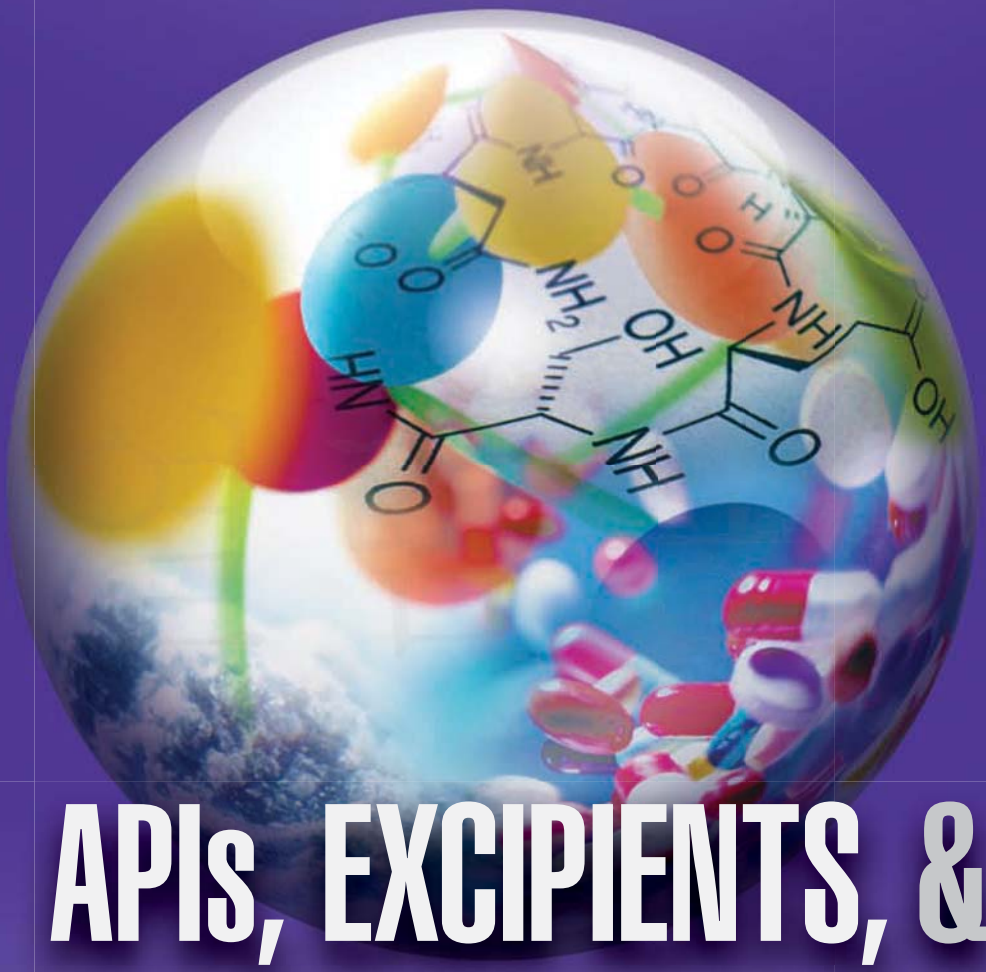
Zhao, F., Ghezzo-Schöneich, E., Aced, G.I., Hong, J., Milby, T., Schöneich, C., 1997. Metal-catalyzed oxidation of histidine in human growth hormone. J. Biol. Chem. 272, 9019–9029.

Zhao, F., Yang, J., Schöneich, C., 1996. Effects of polyaminocarboxylate metal chelators on iron-thiolate induced oxidation of methionine- and histidine-containing peptides. Pharm. Res. 13, 931–938.

Advancing Development & Manufacturing
Pharmaceutical Technology® PharmTech.com

2015

CPhI WORLDWIDE PLANNING GUIDE



APIs, EXCIPIENTS, & MANUFACTURING 2015

UBM
CPhI worldwide InnoPack icse P-mec

Pharmaceutical Technology
PharmTech.com

EDITORIAL
Editorial Director **Rita Peters** rpeters@advanstar.com
Senior Editor **Agnes Shanley** ashanley@advanstar.com
Managing Editor **Susan Haigney** shaigney@advanstar.com
Science Editor **Adeline Siew, PhD** asiew@advanstar.com
Manufacturing Editor **Jennifer Markarian** jmarkarian@advanstar.com
Science Editor **Randi Hernandez** rhernandez@advanstar.com
Art Director **Dan Ward**
Contributing Editors **Jill Wechsler** jwechsler@advanstar.com; **Jim Miller** info@pharmsource.com; **Hallie Forcinio** editorhal@cs.com; **Susan J. Schniepp** sue.schniepp@mac.com; **Eric Langer** info@bioplanassociates.com; and **Cynthia A. Challener, PhD** challener@vtlink.net
Correspondent **Sean Milmo** (Europe, smilmo@btconnect.com)
485 Route One South, Building F, Second Floor, Iselin, NJ 08830, USA
Tel. 732.596.0276, Fax 732.647.1235, **PharmTech.com**

SALES
Publisher **Mike Tracey** mtracey@advanstar.com
Director of Sales **Paul Milazzo** pmilazzo@advanstar.com
Mid-West Sales Manager **Irene Onesto** ionesto@advanstar.com
East Coast Sales Manager **Joel Kern** jkern@advanstar.com
European Sales Manager **Chris Lawson** clawson@advanstar.com
European Senior Sales Executive **Stephen Cleland** scleland@advanstar.com
Executive Assistant **Barbara Sefchick** bsefchick@advanstar.com
485 Route One South, Building F, Second Floor, Iselin, NJ 08830, USA
Tel. 732.596.0276, Fax 732.647.1235
PharmTech.com
Sr. Production Manager **Karen Lenzen**
International Licensing **Maureen Cannon** mcannon@advanstar.com, tel. 440.891.2742 or toll-free 800.225.4569 ext 2742, fax. 440.756.5255
Audience Development Manager **Rochelle Ballou** rballou@advanstar.com

UBM LIFE SCIENCES
Joe Loggia, Chief Executive Officer **Tom Ehardt,** Executive Vice-President, Life Sciences **Georgiann DeCenzo,** Executive Vice-President **Chris DeMoulin,** Executive Vice-President **Rebecca Evangelou,** Executive Vice-President, Business Systems **Julie Molleston,** Executive Vice-President, Human Resources **Mike Alic,** Executive Vice-President, Strategy & Business Development **Tracy Harris,** Sr Vice-President **Dave Esola,** Vice-President, General Manager Pharm/Science Group **Michael Bernstein,** Vice-President, Legal **Francis Heid,** Vice-President, Media Operations **Adele Hartwick,** Vice-President, Treasurer & Controller

UBM AMERICAS
Simon Foster, Chief Executive Officer **Brian Field,** Chief Operating Officer **Margaret Kohler,** Chief Financial Officer

UBM PLC
Tim Cobbold, Chief Executive Officer **Andrew Crow,** Group Operations Director **Robert Gray,** Chief Financial Officer **Dame Helen,** Alexander Chairman

Pharmaceutical Technology does not verify any claims or other information appearing in any of the advertisements contained in the publication and cannot take any responsibility for any losses or other damages incurred by readers in reliance on such content. **Pharmaceutical Technology** welcomes unsolicited articles, manuscripts, photographs, illustrations, and other materials but cannot be held responsible for their safekeeping or return. UBM Life Sciences provides certain customer contact data (such as customers' names, addresses, phone numbers and e-mail addresses) to third parties who wish to promote relevant products, services, and other opportunities which may be of interest to you. If you do not want UBM Life Sciences to make your contact information available to third parties for marketing purposes, simply call toll-free 866.529.2922 between the hours of 7:30 am and 5 pm CT and a customer service representative will assist you in removing your name from UBM Life Sciences' lists. Outside the United States, please phone 218.740.6477. **To subscribe**: Call toll-free 888.527.7008. Outside the US, call 218.740.6477. **Single issues, back issues:** Call toll-free 800.598.6008. Outside the US call 218.740.6480. **Reprints** of all articles in this issue and past issues of this publication are available. Call 877-652-5295 ext. 121 or email bkolb@wrightsmedia.com. Outside US, UK, direct dial: 281-419-5725. Ext. 121. **Direct mail lists:** Contact Tamara Phillips, Marketing Services, tel. 440.891.2773, tphillips@advanstar.com. **Permissions**: Contact Maureen Cannon, tel. 440.891.2742 or toll-free 800.225.4569 ext 2742, fax. 440.756.5255, mcannon@advanstar.com.

APIs, EXCIPIENTS, AND MANUFACTURING 2015

FROM THE EDITORS AND PUBLISHERS

s6 The PharmTech/CPhI Connection

REGULATORY COMPLIANCE

s8 Lessons Learned from FDA Inspections of Foreign API Facilities
Lisa Tung and Maria Eng

EXCIPIENT cGMP

s14 Certifying Excipient cGMPs
Agnes Shanley

IMPORT TESTING

s18 Import Testing of Pharmaceutical Products Has Limited Safety Benefits
Joerg H.O. Garbe, Karl Ennis, Guido M. Furer, Maria G. Jacobs, and Stephan K. Roenninger

REGULATORY CORRESPONDENCE

s27 Regulatory Considerations for Controlled Correspondence Related to Generic Drug Chemistry
Kristina Adams, Xiaochuan Yang, Min Li, Thomas O'Connor, Lane Christensen, Frank Holcombe Jr., Andre Raw, Susan Rosencrance, and Geoffrey Wu

PROCESS ANALYTICAL TECHNOLOGY

s33 PAT Paves the Way for Continuous Manufacturing
Sofia T. Santos, Francisca F. Gouveia, and Jose C. Menezes

PROTEIN STABILITY

s35 Excipient Selection for Protein Stabilization
Cynthia A. Challener

PROCESS CONTROLS

s44 Utilizing Run Rules for Effective Monitoring in Manufacturing
Aaron Spence

CLEANING VALIDATION

s48 Cleaning of Dedicated Equipment: Why Validation is Needed
Cristina Baccarelli, Paola Bernard, Teresa Cortellino, Oscar Cruciani, Rita Pacello, Chiara Parisi, Luisa Stoppa, and Isabella Marta

CPHI WORLDWIDE PLANNING GUIDE

s51 CPhI Worldwide Planning Guide

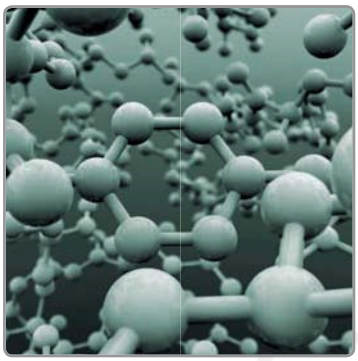
s66 Ad Index

Issue Editor: Rita Peters and Adeline Siew. Cover: Science Photo Library/ Science Photo Library-TEK IMAGE/Phil Ashley/Stockbyte Silver/Getty Images; Dan Ward

©2015 Advanstar Communications Inc. All rights reserved. No part of this publication may be reproduced or transmitted in any form or by any means, electronic or mechanical including by photocopy, recording, or information storage and retrieval without permission in writing from the publisher. Authorization to photocopy items for internal/educational or personal use, or the internal/educational or personal use of specific clients is granted by Advanstar Communications Inc. for libraries and other users registered with the Copyright Clearance Center, 222 Rosewood Dr. Danvers, MA 01923, 978-750-8400 fax 978-646-8700 or visit http://www.copyright.com online. For uses beyond those listed above, please direct your written request to Permission Dept. fax 440-756-5255 or email: mcannon@advanstar.com.

Excipient Selection for Protein Stabilization

Cynthia A. Challener



CHRIS DASCHER/E+/GETTY IMAGES

The complex task of stabilizing proteins is made more challenging due to the limited number of approved excipients.

Cynthia A. Challener, PhD, is a contributing editor to *Pharmaceutical Technology*.

Biopharmaceuticals, while highly effective medicines, are susceptible to aggregation upon manufacturing, distribution, and storage, which can result in immunogenicity and/or reduced efficacy. Stabilization of proteins and other biologic drugs is, therefore, crucial for ensuring both safety and efficacy.

The molecular structures of therapeutic proteins and the critical sites within these proteins that are prone to oxidation, deamidation, hydrolysis, etc., and can result in aggregation and fragmentation, are well known. The development process, therefore, begins with efforts to stabilize therapeutic proteins using protein engineering. However, the improvement in stability is generally limited because of the unstable nature of proteins; the stabilization energy for the native state is typically between 5 and 20 kcal/mol, which is equivalent to that of a few hydrogen bonds. Because the folded state is only marginally more stable than the unfolded state, any changes in the protein environment may trigger protein degradation, aggregation, and or inactivation.

The use of excipients is, therefore, common during the entire manufacturing process and in the final formulation to achieve protein stabilization through retardation of chemical degradation processes and prevention of aggregation, according to Kristina Kemter, project leader in the Research and Development department of Leukocare. Selection of appropriate stabilization agents, however, is challenging, and made more so by the limited choice of substances that have been approved for this use.

Aggregation and other stability issues

Protein stability is a result of achieving a balance between destabilizing and stabilizing forces. The destabilizing forces are mainly due to the large increase in entropy of unfolding; the stabilizing forces are provided by intra-protein and protein-solvent interactions. Disruption of these interactions will shift the balance and destabilize a protein, and many stress factors are known to disrupt this delicate balance and affect protein stability.

These stress parameters include temperature, pH, ionic strength, metal ions, surface adsorption, shearing, shaking, additives, solvents, protein concentration, purity, morphism, pressure, and freeze/thaw-drying, according to Kemter. As a

result, a variety of physical and chemical processes can lead to aggregation of proteins. She also notes that there are significant differences between freeze-dried and liquid protein products in terms of the stress exposures upon manufacturing (freeze drying) and during storage of the final products.

Liquid formulations in general have a higher risk for physical and chemical instability during storage than dried formulations due to their high mobility and the increased likelihood of chemical reactions and physical instability. For liquid-protein preparations, stability can be enhanced by selection of pH-buffering salts, and often amino acids can also be used. It is often interactions at the liquid/air interface or liquid/solid interface (with the packaging) that lead to aggregation following adsorption and unfolding of the protein, according to Jens T. Bukrinski, a formulation scientist with Novozymes. Shear stresses during spray drying can also lead to exposure of hydrophobic protein regions upon spray drying that allow initiation of aggregation, according to Kemter.

Stability, particularly thermal stability, can be increased greatly when the protein is dried. For example, lyophilized formulations are generally more shelf-life stable than liquid formulations; however, protein molecules can potentially form large amounts of aggregates during the lyophilization process, according to Jay Kang, director of analytical and formulation development at Patheon. In the freezing phase, the formation of numerous ice crystals creates a large water/solid surface, a highly concentrated solution, and often an altered pH environment. All these conditions can cause protein aggregation. During drying, removal of water puts significant stresses on protein molecules and can induce aggregate formation.

Mechanisms of destabilization

Temperature and pH have the greatest influence on both physical and chemical protein stability. High temperatures can lead to thermal denaturation and subsequent aggregation as well as accelerate chemical degradation pathways (i.e., side chain oxidation, hydrolysis, and deamidation) that may result in aggregation. In addition, most proteins are generally stable only in a narrow pH range, and physical and chemical pathways to aggregation are possible outside of that window, according to Kemter. Furthermore, the effect of pH on the chemical stability of a protein can be altered in the presence of excipients.

For instance, the effect of salts strongly depends on the pH of the solution, which dictates the charged state of ionizable groups in the protein. "Salts may stabilize, destabilize, or have no effect on proteins depending on the type and concentration of salt, the nature of ionic interactions, and the presence and amount of charged residues in proteins on fully exposed surfaces and/or in fully or partially buried interior sections," Kemter says.

Depending on the type and concentration, metal ions may also stabilize or destabilize a protein because their interactions with proteins are highly protein-dependent. Metal ions may also significantly affect protein stability without affecting much of its secondary structure. "Trace amounts of metal ions in protein formulations may catalyze the oxidation of proteins, namely via the Fenton pathway, targeting in particular the residues methionine, cysteine, histidine, tryptophan, tyrosine, proline, arginine, lysine, or threonine. The catalysis depends on the concentration of the metal ions, and the metal-catalyzed reaction can be facilitated in the presence of reducing agents such as ascorbate or sulfhydryl (RSH) compounds," Kemter explains. Oxidation of proteins by metal ions, oxygen, or reducing agents can lead to aggregation.

Similarly, chelating agents such as ethylenediaminetetraacetic acid (EDTA) and citric acid can bind and destabilize proteins or bind harmful metal ions and prevent oxidation. The net effect depends on the metal ions, oxidation mechanism, and the type of chelating agent, according to Kemter.

Protein concentration can also influence aggregation and in some cases chemical degradation, depending on the mechanism. "More biopharmaceuticals are being formulated at very high concentrations today. Higher concentrations create more chances for unwanted self-association, and consequently high viscosities, which can make both processing and injection more difficult," Bukrinski observes. High pressure can also cause protein unfolding during freeze-drying or spray-freeze drying.

Chemical degradation pathways include not only oxidation, hydrolysis, and deamidation, but also isomerization, succinimidation, disulfide bond formation and breakage, non-disulfide crosslinking, and deglycosylation, and often occur simultaneously, according to Kemter. She notes that deamidation of asparagine and glutamine residues is most common, and the rate, mechanism, and location of deamidation are all pH-dependent. Oxidation is another important chemical degradation mechanism, particularly the oxidation of the thio groups in methionine and cysteine residues. The formation of disulfide bond linkages or thio-disulfide exchanges can result in protein aggregation or polymerization.

"All of these influences can occur—either simultaneously or separately—when different types of stresses are applied to a protein, such as during isolation and purification of a protein; drying of a protein by lyophilization, spray-drying, spray-freeze drying or foam drying; storage of a protein in solution; after drying; as well as reconstitution after drying," states Kemter.

Types of stabilizing excipients

Stabilizing excipients are added to formulations to slow down or prevent protein aggregation through different mechanisms, including strengthening of protein-stabilizing forces, destabilization of the denatured state, and direct binding to the protein, which are applied during isolation and purification, drying (lyophilization, spray-drying, spray-freeze drying, foam-drying), storage in solution or after drying, and reconstitution after drying, according to Kemter.

Six categories of excipients are commonly used to stabilize proteins against aggregation, according to Kang: buffers, salts, amino acids, polyols/disaccharides/polysaccharides, surfactants, and antioxidants. These excipients prevent aggregation through several mechanisms. "First, pH is critical to protein

stability and must be controlled to an optimal value through the use of appropriate buffers. Salts and amino acids increase the ionic strength of solutions while minimizing electrostatic interactions between protein molecules."

Polyols/disaccharides/polysaccharides, on the other hand, stabilize protein molecules through preferential hydration or preferential exclusion, in which the excipient is excluded from the protein surface, allowing the rearrangement and stabilization of a stabilizing hydrate shell around the protein surface and preventing protein molecules from interacting. Surfactants, meanwhile, protect proteins against interaction with hydrophobic surfaces such as air/water interfaces and container surfaces, and antioxidants protect proteins against oxidation.

Specific examples include trehalose and sucrose (disaccharides); mannitol and sorbitol (sugar alcohols); histidine, glycine, and arginine (amino acids); polysorbate 20, polysorbate 80, and proteins like human serum albumin (surfactants); sodium chloride (salt); and dextran and polyethylene glycol (polymers). Each type has a completely different stabilizing mechanism.

Alkylsaccharides as alternatives to polysorbates

The quality of the excipients can have a dramatic impact on protein stability. For example, common surfactants such as polysorbates are well known to contain trace amounts of peroxides that can become significant during storage and consequently compromise protein stability through oxidation of susceptible amino acids, particularly exposed methionine, according to Kang. "A good practice is to use compendial excipients in the development study and control the quality/storage of the excipients from the very beginning, so no surprises are encountered in GMP manufacturing and subsequent long-term storage," he says.

The issues with polysorbates have been a focus of Aegis Therapeutics. "The oxidative damage to biotherapeutic proteins can directly reduce their efficacy, but perhaps more importantly introduce unwanted immunogenicity, which can give rise to neutralization of activity and in more serious cases, neutralization of any residual biological activity associated with the patient's own corresponding proteins," observes Edward T. Maggio, president and chief executive officer of the company.

The polysorbates do an excellent job of preventing aggregation and permitting the creation of high-concentration formulations of biotherapeutics, but even though they are ideally highly purified when first incorporated, Maggio notes that formation of chemically reactive species occurs immediately upon any contact with oxygen during manufacturing or storage of the final product.

Aegis has shown that alkylsaccharides are as effective, and in some cases, more effective than the polysorbates for the prevention of aggregation, and they are completely free of any oxidative damage problems. Comprising a sugar attached to a long chain fatty acid, alkylsaccharides break up rapidly in the body into a sugar, typically glucose, and a fatty acid. They are essentially nontoxic food components, and are considered generally recognized as safe (GRAS) for food purposes. Both Big Pharma and smaller biotech companies (e.g., Roche and Biodel) are investigating the use of alkylsaccharides as replacements for polysorbates, according to Maggio. He also notes that there is extensive safety and toxicity study data in the drug master file covering the alkylsaccharides to which licensees of the technology receive a right of reference for their regulatory filings.

A blending approach

To assist formulators of biologic drugs with the stabilization and protection of therapeutic proteins in dry and liquid formulations, Leukocare developed its Stabilizing and Protecting Solutions (SPS) platform of excipient formulations. The proprietary SPS platform has been proven to stabilize different biological macromolecules during freeze drying and spray drying, during storage at increased temperature in dry or liquid formulations, and even during sterilization processes, according to Kempter. She adds that the modular concept of the SPS facilitates the possibility to adjust excipient compositions to the specific requirements of the biomolecule to protect from various types of stress exposures.

SPS formulations solely comprise excipients (mainly based on amino acids) listed in pharmacopeia that are also in general listed by FDA as inactive ingredients. Interactions between multiple functional groups of the excipients in solution and particularly during drying result in a strong amorphous character of the dried product, according to Kemter. The osmolytic excipients of the compositions may also support stabilization of the hydration shell around proteins in liquid formulations according to the preferential exclusion theory. In dried formulations, and according to the theory of water replacement, the excipients may substitute the stabilizing hydrogen bonds between proteins and water through the formation of stabilizing electrostatic interactions or hydrogen bonds with the proteins upon drying.

Recombinant human serum albumin (rHSA)

rHSA is the most common protein found in human plasma and is known for ligand binding and colloidal stabilization, properties that are also ideal for the stabilization of proteins and other biologics. In addition, because rHSA is a natural protein in the body, it is safer than other alternative surfactant excipients, such as synthetic polymers, because it has a low risk for immunogenicity and there is a natural pathway for its elimination from the body.

In addition to preventing protein aggregation by blocking undesired adsorption onto vial surfaces or air/liquid interfaces, rHSA has also been shown to prevent self-association of protein drugs through preferential hydration or preferential exclusion effects and to prevent the formation of micrometer-sized particles to increase the solubility of poorly soluble peptide-based drugs. Furthermore, rHSA exhibits antioxidant properties used for the stabilization of radiolabeled drugs. "As a result of this multifunctionality, in some cases, it is possible to reduce the number of excipients required to stabilize a biologic drug," Bukrinski says. He also notes that through covalent linking of

a biologic API to rHSA or through encapsulation in albumin particles, it is possible to extend the circulatory half-life and control the release of drugs. Novozymes offers recombinant HSA products specifically produced for the biopharmaceutical industry.

Choosing the right stabilizing excipients

Because every protein is different and reacts differently with different types of excipients, the selection of the proper excipients for a given formulation is a complex and challenging task. Some excipients may be effective in one formulation and cause protein degradation and aggregation in another. "For instance, commonly used polysorbate detergents often disrupt the protein complexes in virus-like particles, and therefore an alternative such as recombinant human serum album or a carbohydrate-based polymer is needed," Bukrinski comments.

The choice of the right excipients for stabilization of a desired protein must take into account the very complex physical and chemical degradation behaviors and the potential multifunctional influences that each excipient can have on protein stability, according to Kemter. "The formulation scientist must have a thorough knowledge of several factors: how to optimize the physical and chemical stability of the active ingredient; how, rationally, to include specific excipients in the formulation; how to obtain the optimum conditions for stability; how to prevent stability issues during up-scaling; and, finally, how to design a formulation that is suitable for the intended route of administration, that is, one that allows the absorption barrier to be overcome."

Unfortunately, the structural differences among different proteins are so significant that generalization of universal stabilization strategies has not been successful to date. In addition, while it is desirable to keep the number of functional excipients as low as possible, the vast amount of potential destabilizing effects often necessitates the addition of several excipients.

Many scientists select excipients empirically, which takes a long time and puts a strain on resources, according to Kang. "It is more effective to perform a preformulation study to identify degradation pathways and stability-indicating analytical methods before testing major categories of excipients for their ability to protect protein molecules against specific degradations. Further study using a design-of-experiment (DoE) approach enables determination of the optimal levels of the most effective excipients and their interactions for the final formulation," he asserts. In fact, Patheon has been able to shorten the development timeline by designing formulations based on scientific rationale and the screening of large quantities of excipients using DoE.

Even so, Kemter believes that there remains a significant need for improved methods for the folding of proteins and the prevention of unfolding during production and storage and that can be generally applied to the majority of biopharmaceuticals. "Such technology would eliminate the need for so many individual investigations," she notes.

Evaluation of stability

Typical studies for determination of the stability of biopharmaceutical formulations include determination of the level of aggregates and insoluble particles of various sizes; detection of increased immunogenicity; determination of the level of amino acid oxidation, in particular, methionine and tryptophan; and evaluation of the fragmentation of polypeptide chains, all for samples subjected to both stressed and unstressed conditions, according to Maggio.

Most of the tests are accelerated aging studies, such as heating at elevated temperatures for 1 to 4 weeks, shaking at high temperature with an air/liquid interface for several days, and freezing and thawing for multiple cycles. Temperature ramping experiments are also common for determination of the melting and aggregation temperatures under different conditions, but Bukrinski has on several occasions observed that results from such studies do not always correlate well with shelf-life stability.

A whole host of advanced techniques are employed to analyze the results obtained in the above tests. Some examples include polyacrylamide-gel electrophoresis (PAGE), particle-size analysis using micro-flow imaging (MFI), dynamic and static light scattering, size-exclusion chromatography (SEC), ion-exchange chromatography (IEX), and reversed-phase (RP) high-pressure liquid chromatography (HPLC), liquid chromatography/mass spectrometry (LC/MS), peptide and glycan mapping, circular dichroism (CD), Fourier transform infrared spectroscopy, and other advanced MS methods.

A newer method that, according to Bukrinski, is increasingly used as an orthogonal method for the validation of SEC results is field flow fractionation (FFF). Instead of passing through a packed column, the fluid passes through a narrow channel and a force applied perpendicular to the channel causes separation of the particles based on their different mobilities.

Not all methods will work equally well for each biologic API. Therefore, the first step in any study is to determine which methods provide accurate results for the protein in question. "It is very important to first determine the appropriate methods for stability evaluation, followed by optimization of the pH and ionic strength for the formulation. It is only at that point that screening for appropriate excipients can be effective," Bukrinski says.

Because so many stability tests must be performed for the development of an effective biopharmaceutical formulation, he also notes that the ability to perform rapid, high-throughput screening is imperative. "We perform as many analytical methods as we can using robotics systems that can evaluate small quantities of samples in microplates. Often times, however, tight timelines will dictate a less optimal formulation development process," notes Bukrinski.

"Two of the most efficient screening tools include biophysical characterization and high-throughput degradation analysis under stressed conditions," adds Kang. "Biophysical tools, such as differential scanning calorimetry (DSC) and CD, directly measure the effect of excipients on the higher order structure of

the proteins, which is often a good indicator of protein stability. High-throughput methods such as plate-based dynamic light scattering (DLS) can screen a large amount of excipients in a short period time."

Compared to small molecules, however, protein degradation involves multiple pathways, and a simple Arrhenius equation is generally not applicable, according to Kang. It is, therefore, difficult to predict long-term real-time stability through stressed and accelerated stability studies. "New mathematical models are currently being developed to establish a correlation between protein stability at different storage temperatures, and if successful, will greatly enhance formulation development and shelf-life prediction for protein drugs," he states.

Automated stability determination using chemical denaturation

Because temperature has such a significant influence on protein aggregation, it is important to obtain accurate thermodynamic data on proteins. However, temperature denaturation is often irreversible and accompanied by aggregation and precipitation and, therefore, not suitable for thermodynamic analysis.

On the other hand, isothermal chemical denaturation is generally a reversible process for most biologic drugs and has been proven to provide reliable thermodynamic data of use for the evaluation of protein stability. AVIA Biosystems has developed an automated protein denaturation system for protein stability analysis that uses intrinsic (or extrinsic) fluorescence to monitor the protein conformational changes associated with protein unfolding (denaturation). Using the instrument, the identification of solvent conditions that maximize the structural stability of biologics can be completely automated, according to the company. Proteins and other compounds can also be ranked by their stability and propensity to aggregate.

Few approved excipients creates challenges

Although the large number of stability tests and analyses required for the development of stable protein formulation present difficulties for biopharmaceutical companies, one of the biggest challenges for formulators is the limited number of known and approved excipients for protein stabilization, according to Kemter. In addition, many biopharmaceutical manufacturers will only use excipients that are approved internally, and generally only consider other excipients that are approved but have not been previously used by the company if no solution is possible with the existing choices, according to Bukrinski. "New excipients—whether just new to the company or compounds that have not been used as excipients before—will only be used if they have significantly high value and can compensate for the extended approval process. There must be a justification for the additional cost and risk," he says.

Kang agrees that the biggest challenge in developing new stabilizing excipients for biologics is the additional safety data required to introduce a novel excipient to a pharmaceutical product, particularly a parenteral formulation, which is the form in which most protein drugs are formulated. "The resources and time associated with this requirement makes formulation scientists hesitant to try new excipients," he observes. **PT**

PROCESS ANALYTICAL TECHNOLOGY — *contin. from page 34*

Conclusion

The business strategy of both pharmaceutical and biopharmaceutical companies can benefit from the implementation of continuous manufacturing, because it enables more responsive and efficient supply-chain management. Lower production costs motivate smaller companies to start manufacturing earlier in their lifecycle, thus reducing their dependency on CMOs. Additionally, smaller plants permit establishing multipurpose facilities, and a standard production platform enables producing different products in the same unit, increasing operational flexibility, and allowing a better control of costs (6).

The coming years will certainly be exciting in the pharmaceutical industry, especially for those involved in manufacturing sciences and technologies, as the transformation from batch to continuous manufacturing takes root and allows faster and safer supply of new and more affordable drug products to patients.

References

1. FDA, *Guidance for Industry: PAT—a Framework for Innovative Pharmaceutical Development, Manufacturing, and Quality Assurance* (Rockville, MD, Sept. 2004).
2. C. Schaefer et al., *J. Pharm. Biomed. Anal.* 83, 194-201 (2013).
3. S. Kozlowski et al., "The CMC Strategy Forums, Celebrating a Decade of Collaborative Technical and Regulatory Interaction, Part 1: QbD and Risk Management," *BioProcess International* Special Report (2015).
4. FDA, "FDA Perspective on Continuous Manufacturing," www.fda.gov/downloads/AboutFDA/CentersOffices/OfficeofMedicalProductsandTobacco/CDER/UCM341197.pdf, accessed 21 July, 2015.
5. EMA, *Guideline on Process Validation for Finished Products—Information and Data to Be Provided in Regulatory Submissions* (London, Feb. 2014).
6. K.B. Konstantinov and C.L. Cooney, *J. Pharm. Sci.* online, DOI:10.1002/jps.24268, 21 Nov. 2014.
7. Z. Chen, D. Lovett, and J. Morris, *J. Process Control* 21 (10) 1467-1482 (2011).
8. R. Chen et al., *Pharma. Outsourcing* 12 (4) 1-7 (2011).
9. M. Roberto et al., *Processes* 2 (1) 24-33 (2013).
10. M.J. Pedersen et al., *Org. Process Res. Dev.* 17 (9) 1142-1148 (2013).
11. A.E. Cervera-Padrell et al., *Org. Process Res. Dev.* 16 (5) 901-914 (2012). **PT**

US 20090208492A1

(19) **United States**

(12) **Patent Application Publication**

(10) **Pub. No.: US 2009/0208492 A1**

(43) **Pub. Date: Aug. 20, 2009**

O'Connor et al.

(54) **LYOPHILIZED IMMUNOGLOBULIN FORMULATIONS AND METHODS OF PREPARATION**

(75) Inventors: **Barbara Horsey O'Connor**, San Carlos, CA (US); **Shaun E. Buckley**, San Francisco, CA (US); **David Burke**, Oakland, CA (US)

Correspondence Address:
CROWELL & MORING LLP
INTELLECTUAL PROPERTY GROUP
P.O. BOX 14300
WASHINGTON, DC 20044-4300 (US)

(73) Assignee: **Elan Pharmaceuticals, Inc.**, South San Francisco, CA (US)

(21) Appl. No.: **12/138,075**

(22) Filed: **Jun. 12, 2008**

Related U.S. Application Data

(60) Provisional application No. 60/929,133, filed on Jun. 14, 2007.

Publication Classification

(51) **Int. Cl.**
A61K 39/395 (2006.01)

(52) **U.S. Cl.** **424/133.1**

(57) **ABSTRACT**

The present invention relates generally to the field of pharmaceutical formulation of immunoglobulins. Specifically, the present invention relates to stable, lyophilized, high concentration immunoglobulin formulations. This invention is exemplified by a stabilized lyophilized formulation of the recombinant humanized anti-alpha-4 integrin antibody natalizumab.

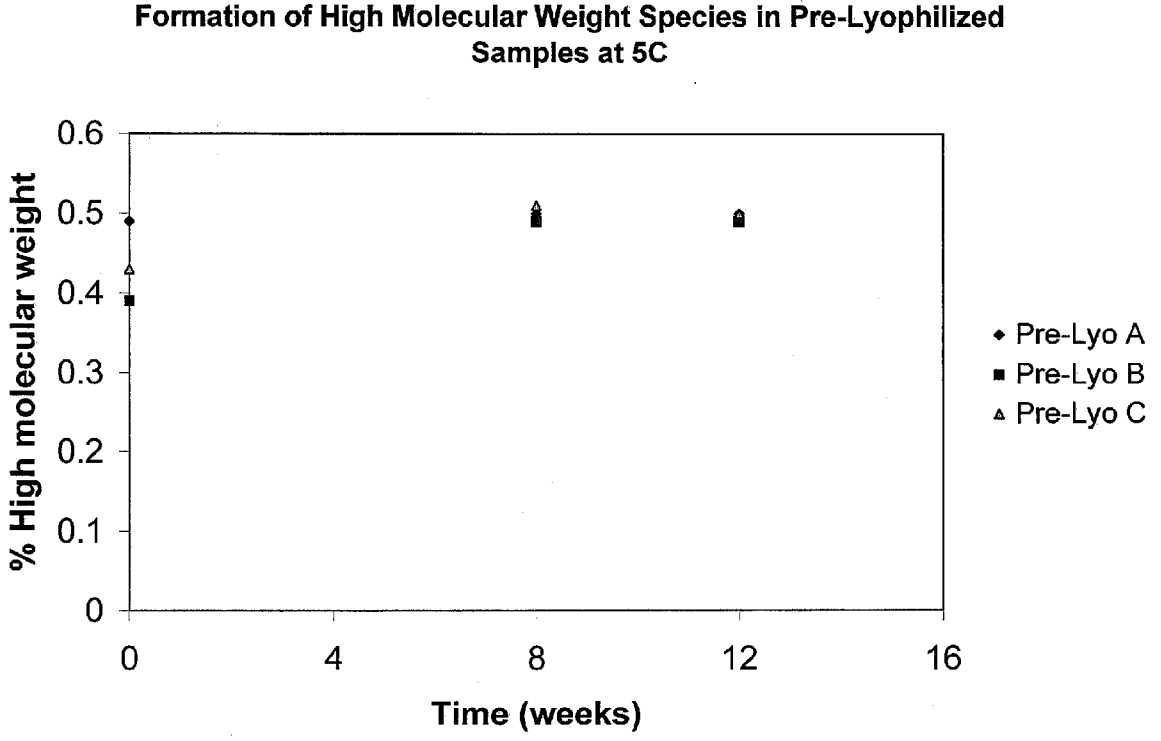


Figure 1

Formation of High Molecular Weight Species at 30°C in Pre- Lyophilized and Liquid Formulations

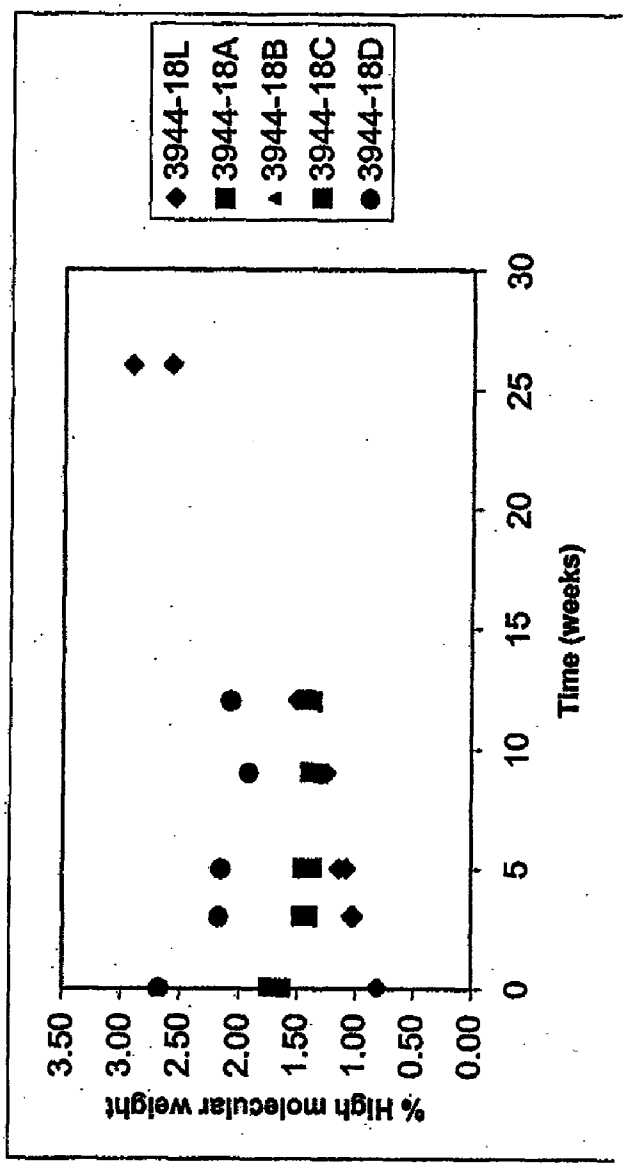


Figure 2: Formation of High Molecular Weight Species at 40°C in Pre-Lyophilized and Liquid Formulations

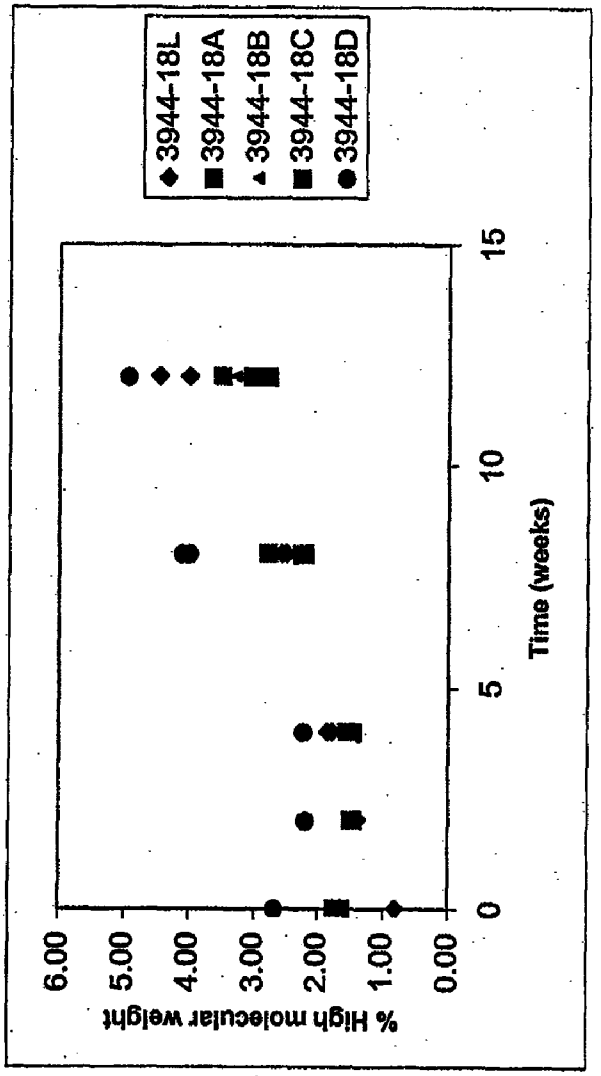


Figure 3: Formation of Low Molecular Weight Species at 30°C in Pre-lyophilized and Liquid Formulations

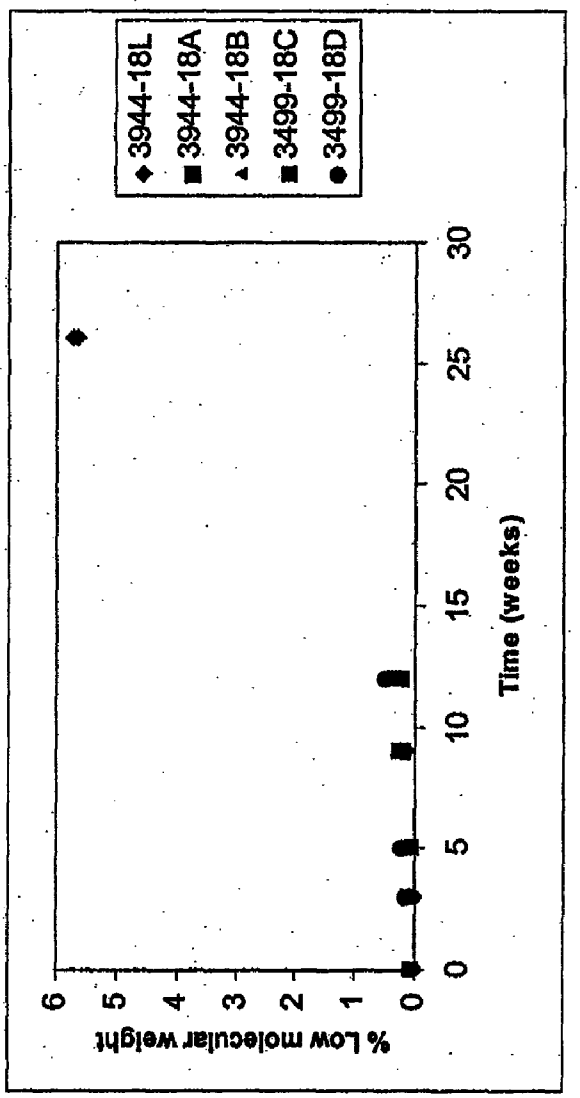


Figure 4: Formation of Low Molecular Weight Species at 40°C in Pre-lyophilized and Liquid Formulations

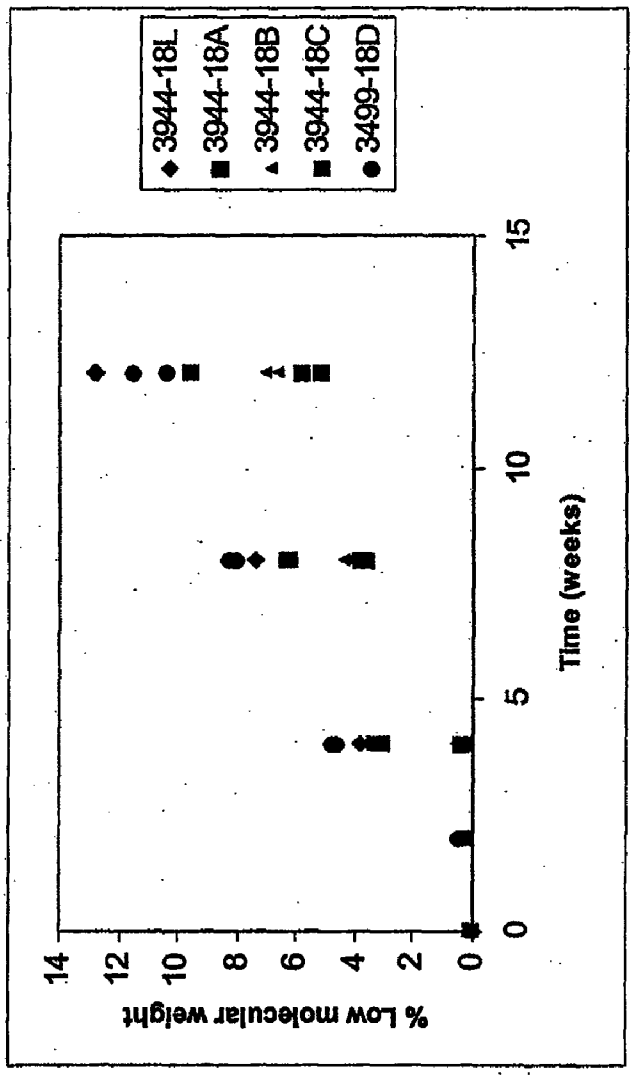


Figure 5: Loss of Monomer at 5°C in Pre-Lyophilized and Liquid Formulations

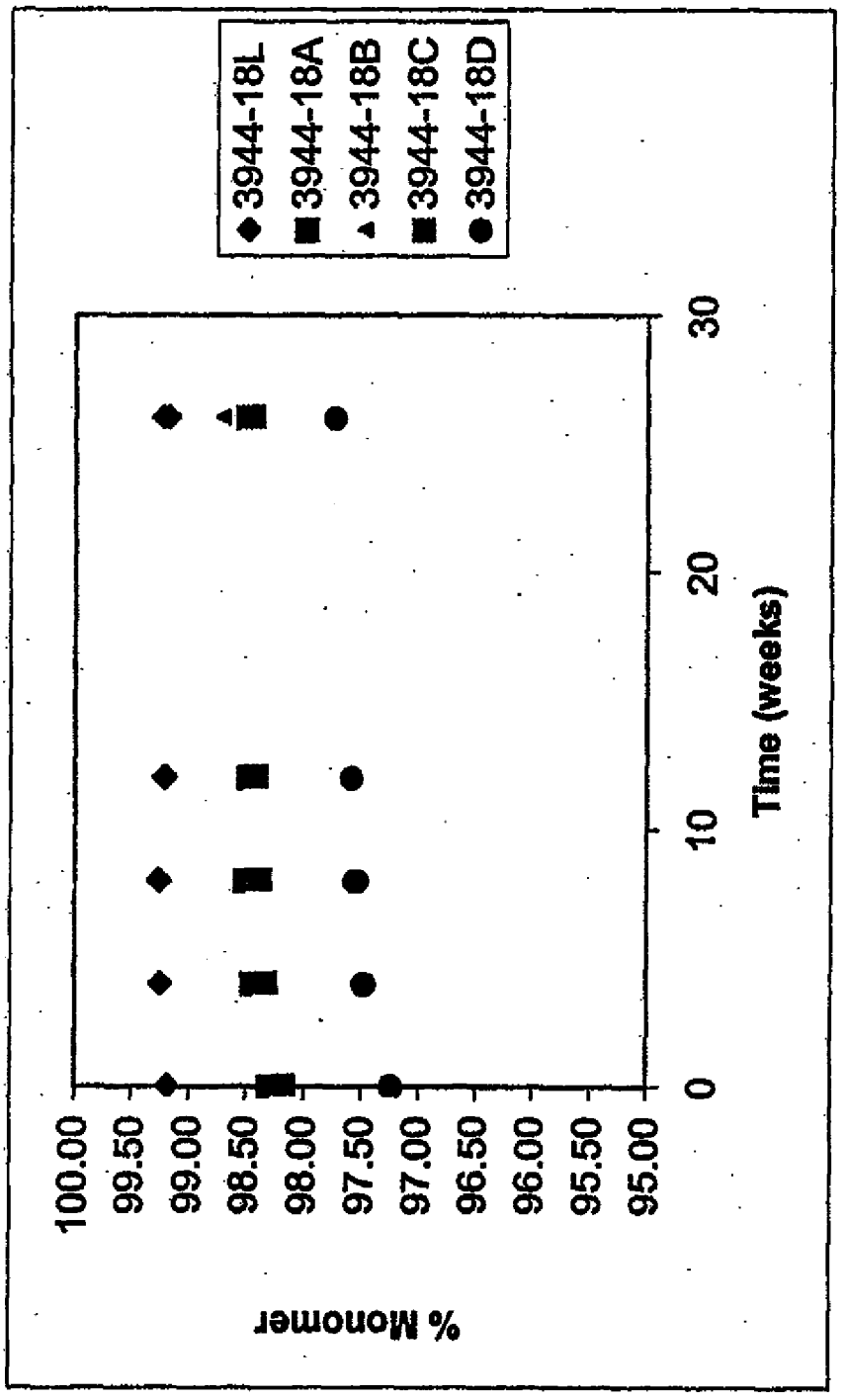


Figure 6: Loss of Monomer at 30°C in Pre-Lyophilized and Liquid Formulations

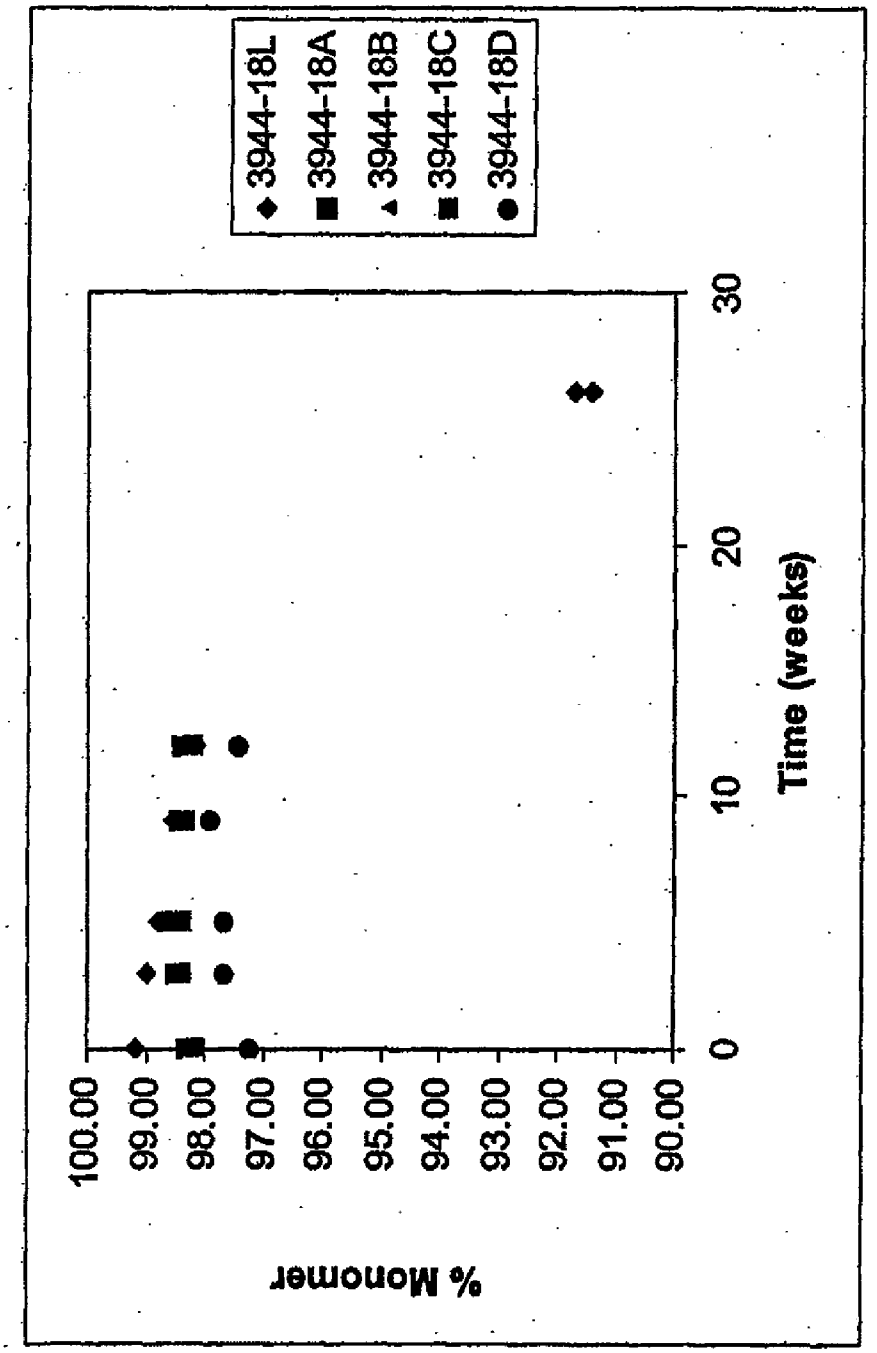


Figure 7: Loss of Monomer at 40°C in Pre-Lyophilized and Liquid Formulations

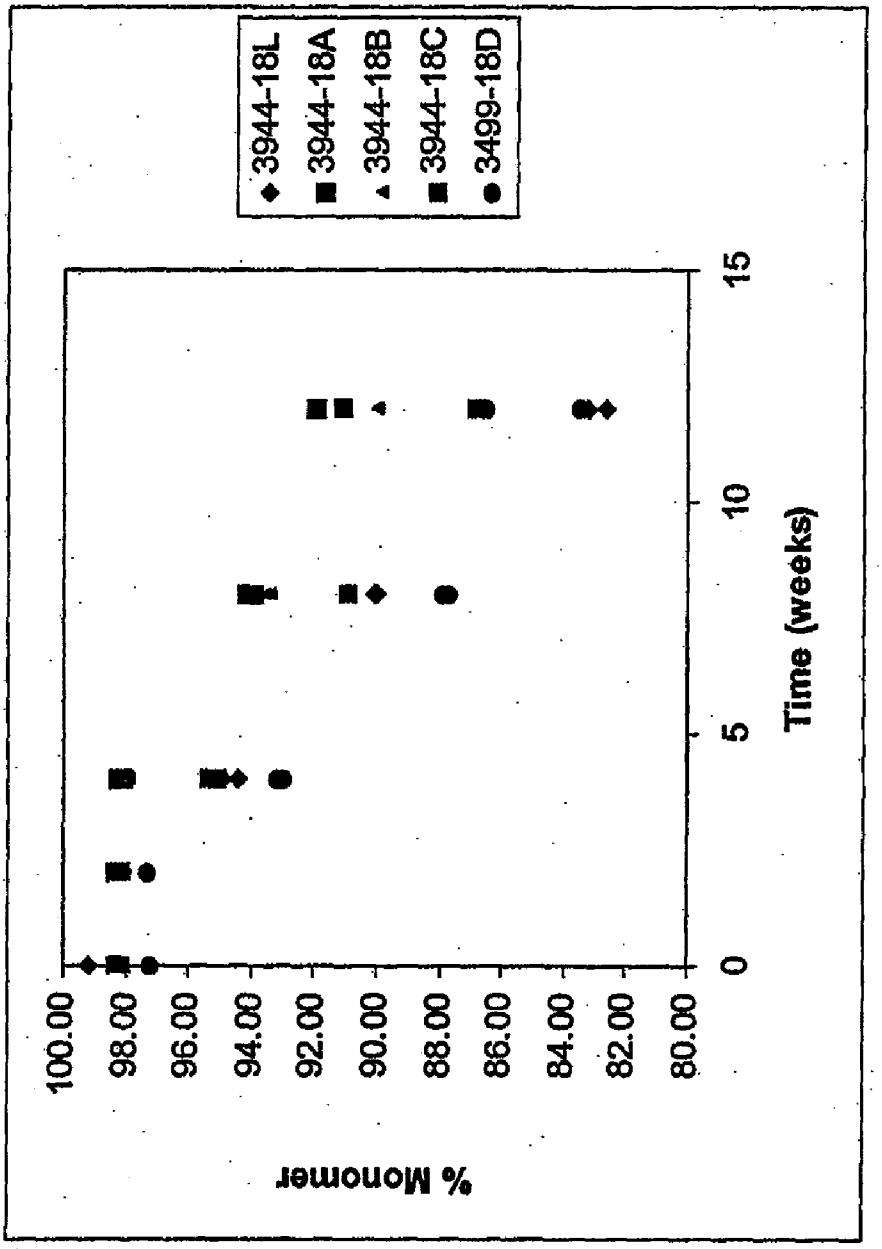


Figure 8: Loss of Monomer at 5°C in Lyophilized Formulations

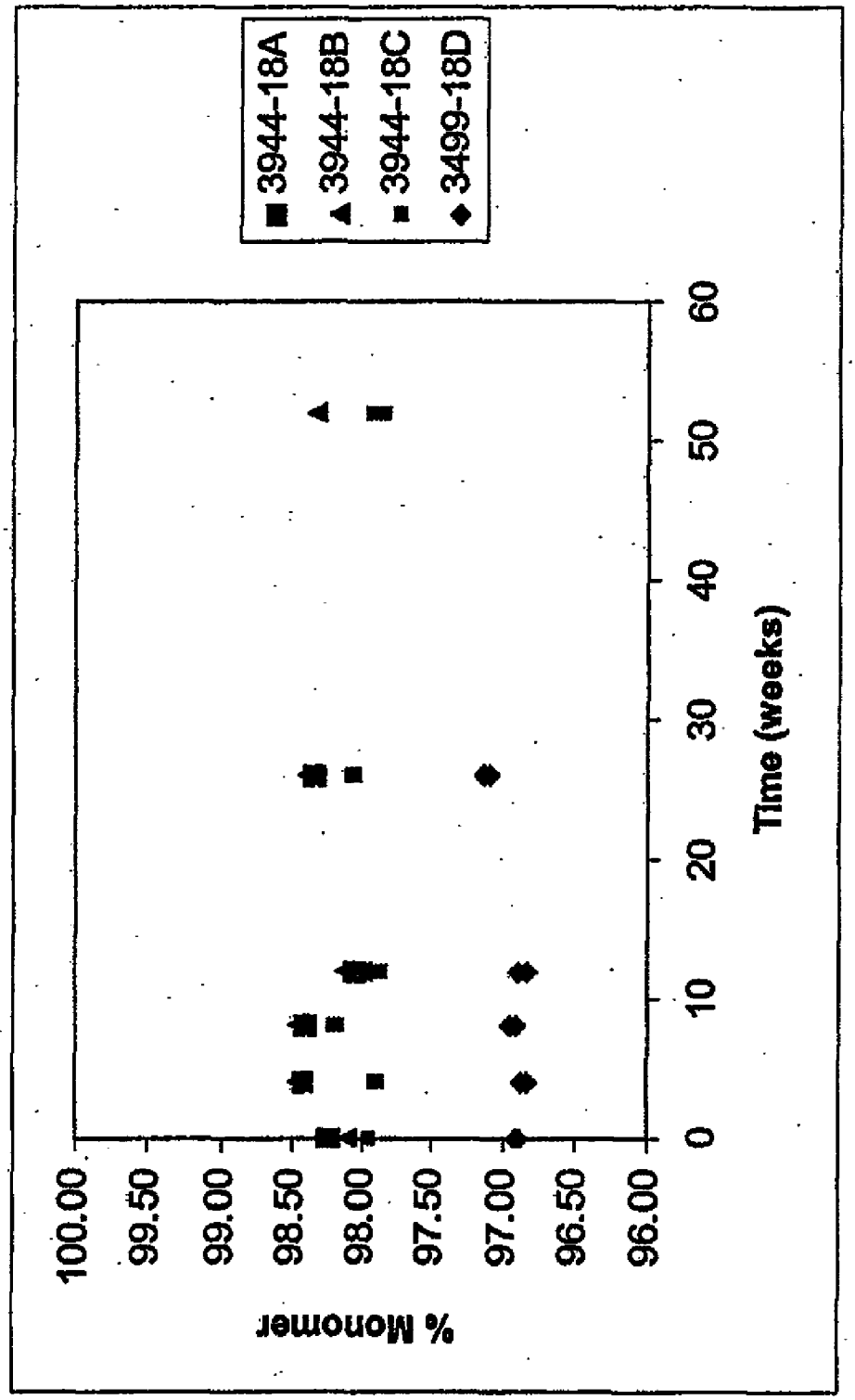


Figure 9: Loss of Monomer at 30°C in Lyophilized Formulations

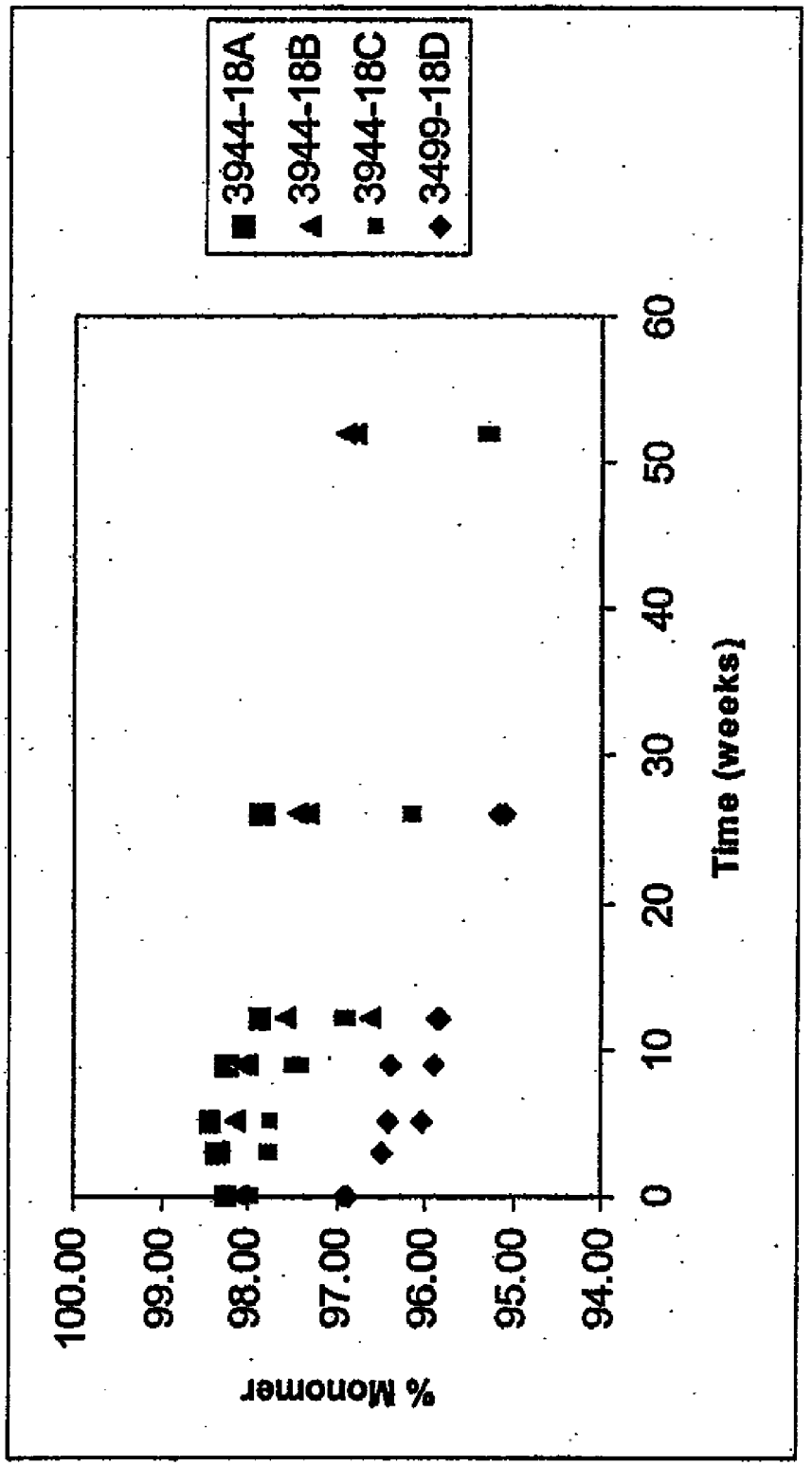


Figure 10: Loss of Monomer at 40°C in Lyophilized Formulations

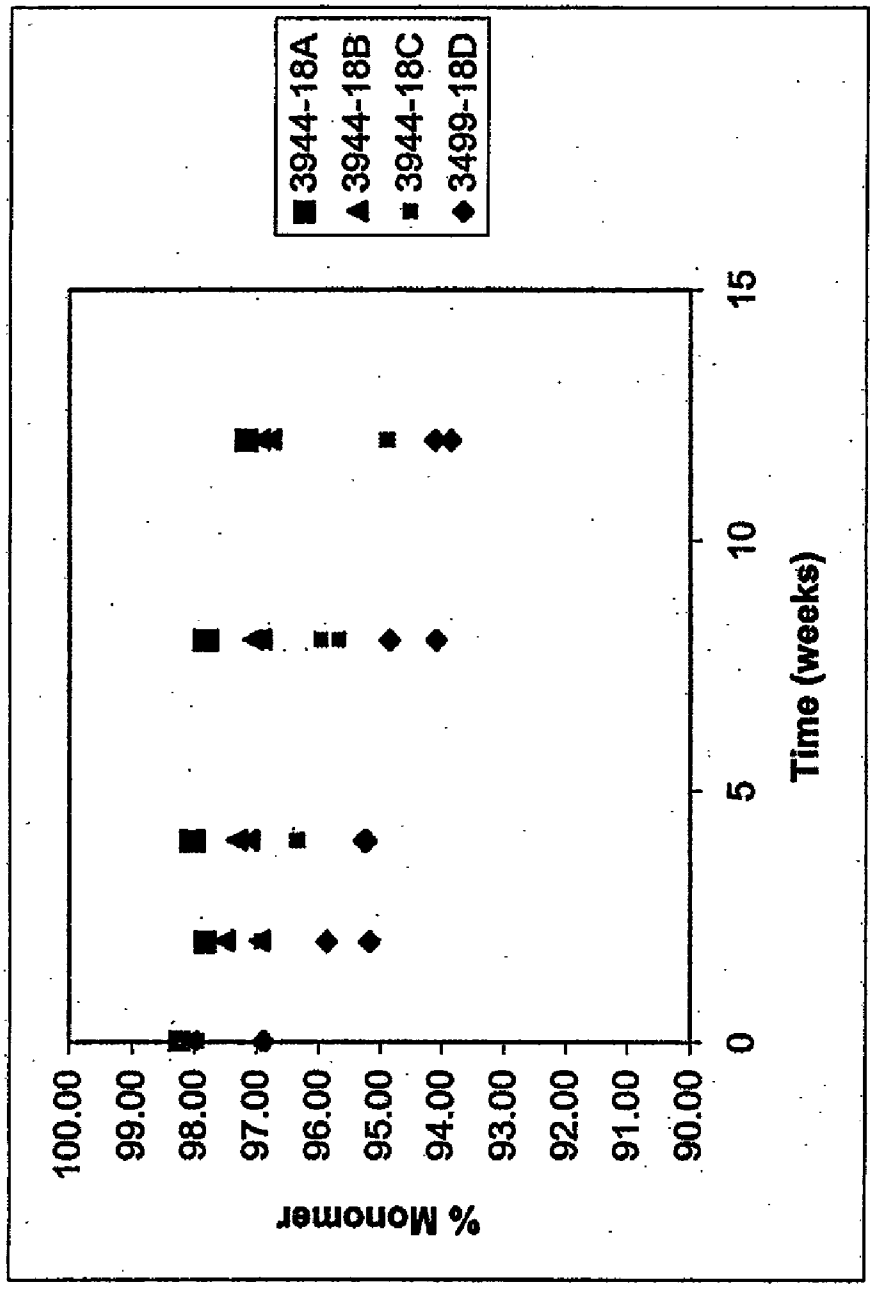


Figure 11: Formation of Low Molecular Weight Species at 30°C in Pre-Lyophilized Formulations

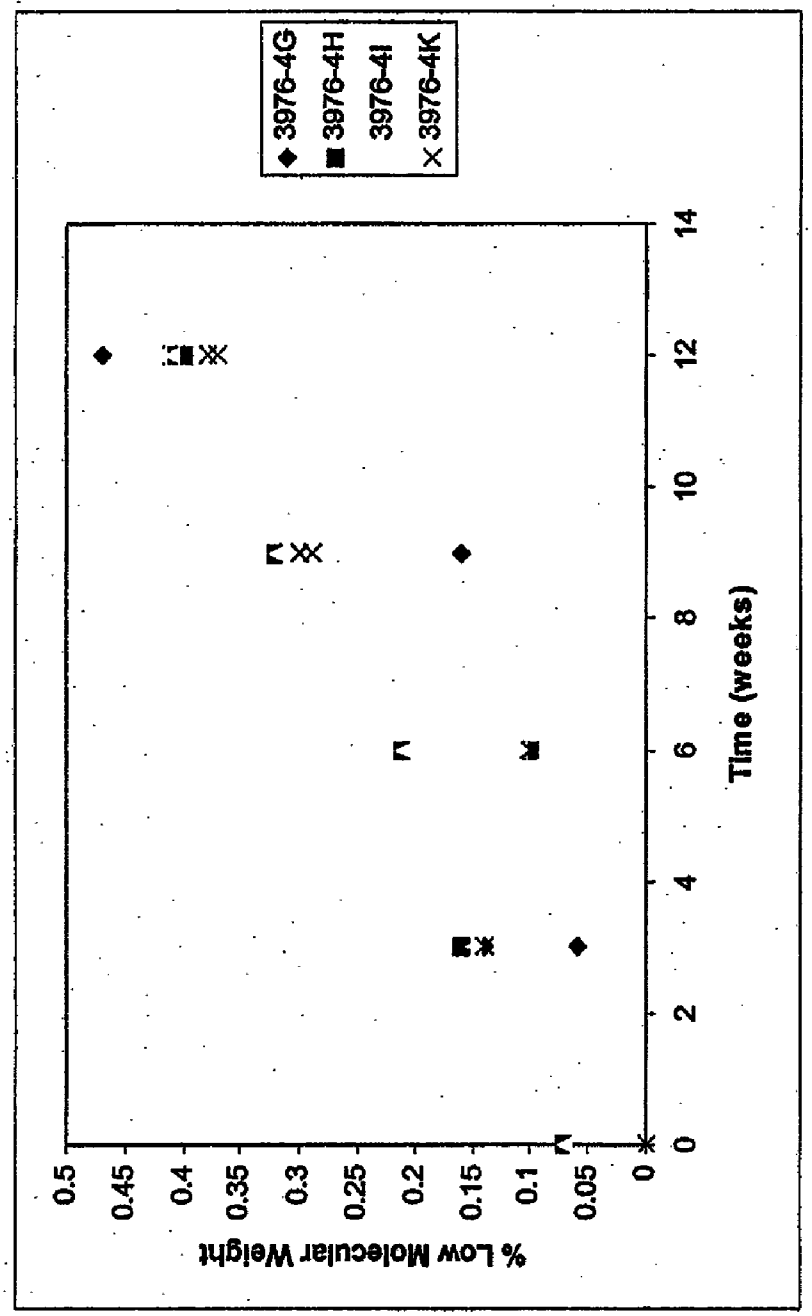


Figure 12: Formation of Low Molecular Weight Species at 40°C in Pre-Lyophilized Formulations

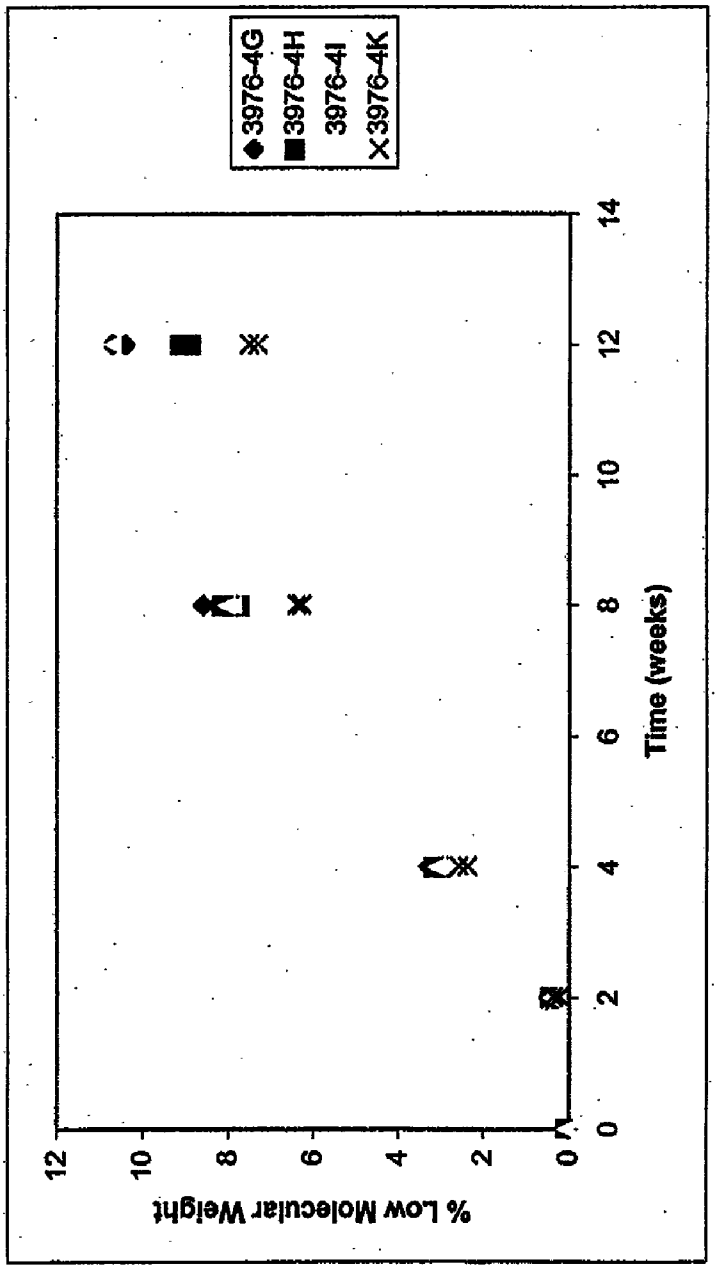


Figure 13: Formation of High Molecular Weight Species at 40°C in Pre-Lyophilized Formulations

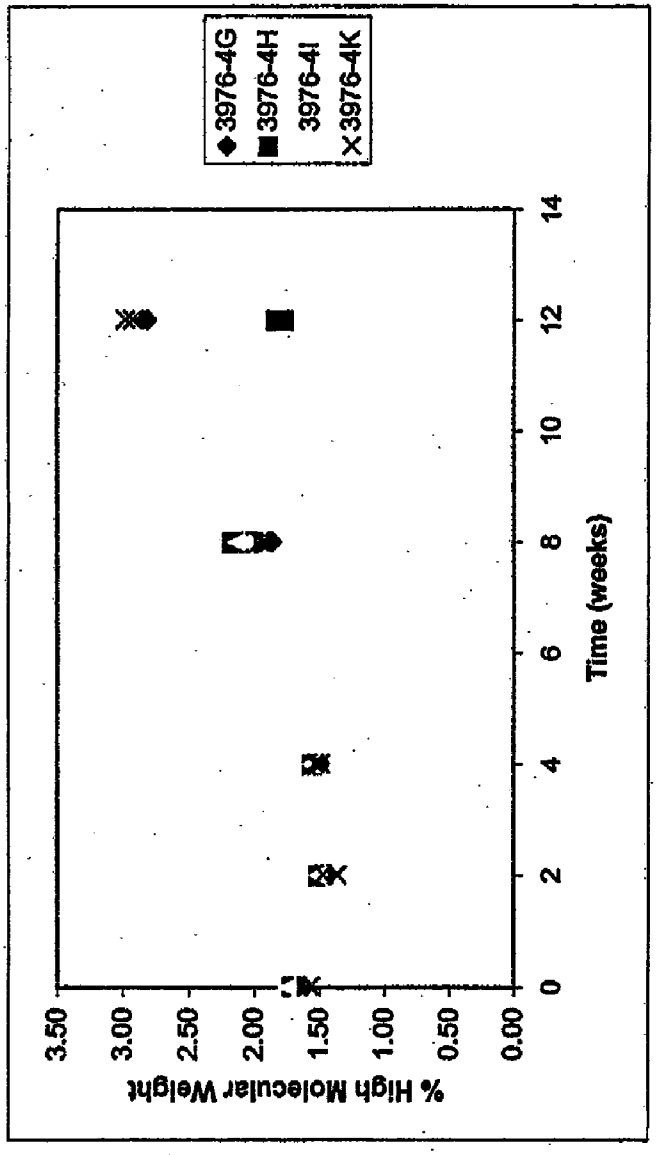


Figure 14: Loss of monomer at 5°C for Lyophilized Formulations

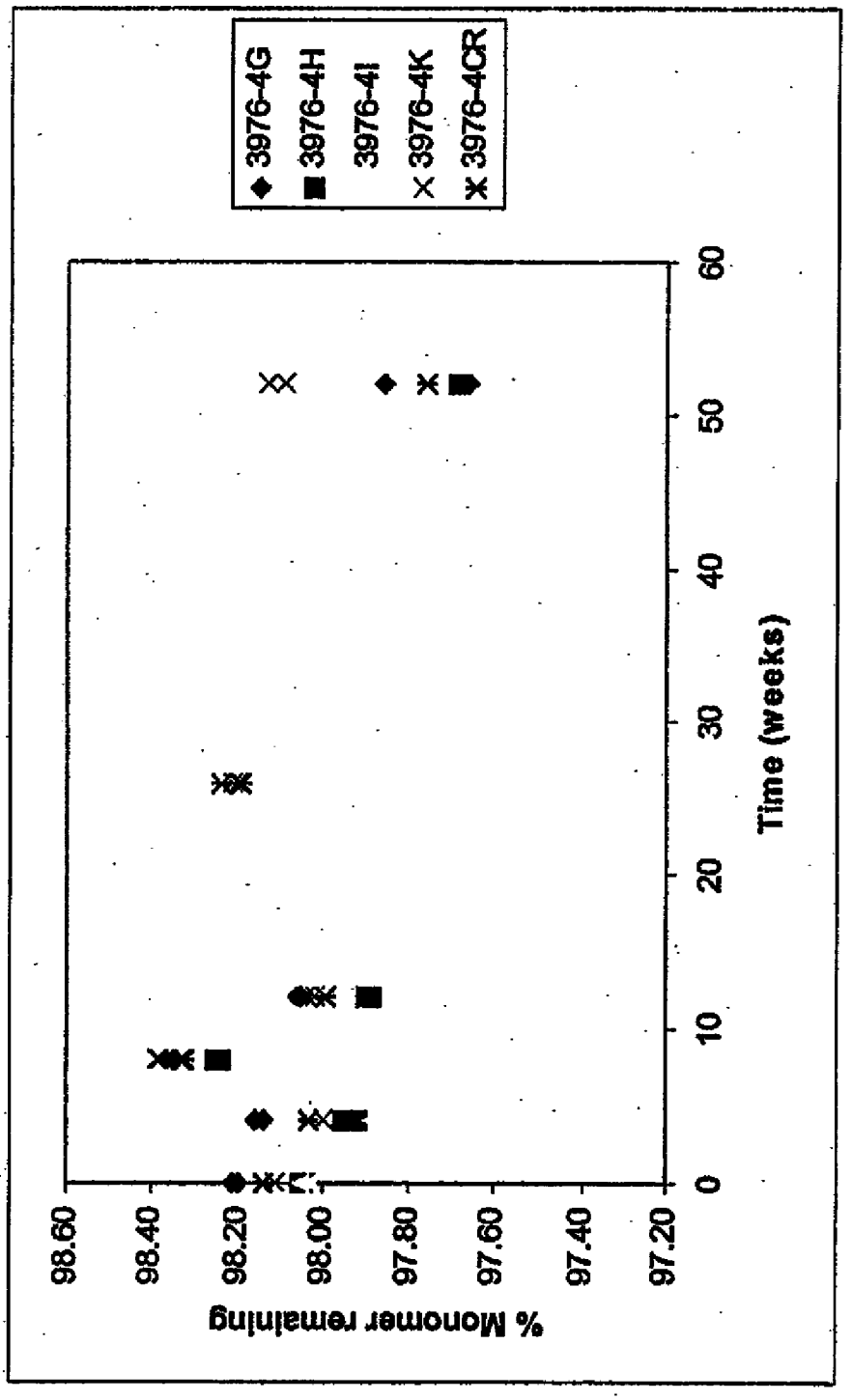


Figure 15: Loss of monomer at 30°C for Lyophilized Formulations

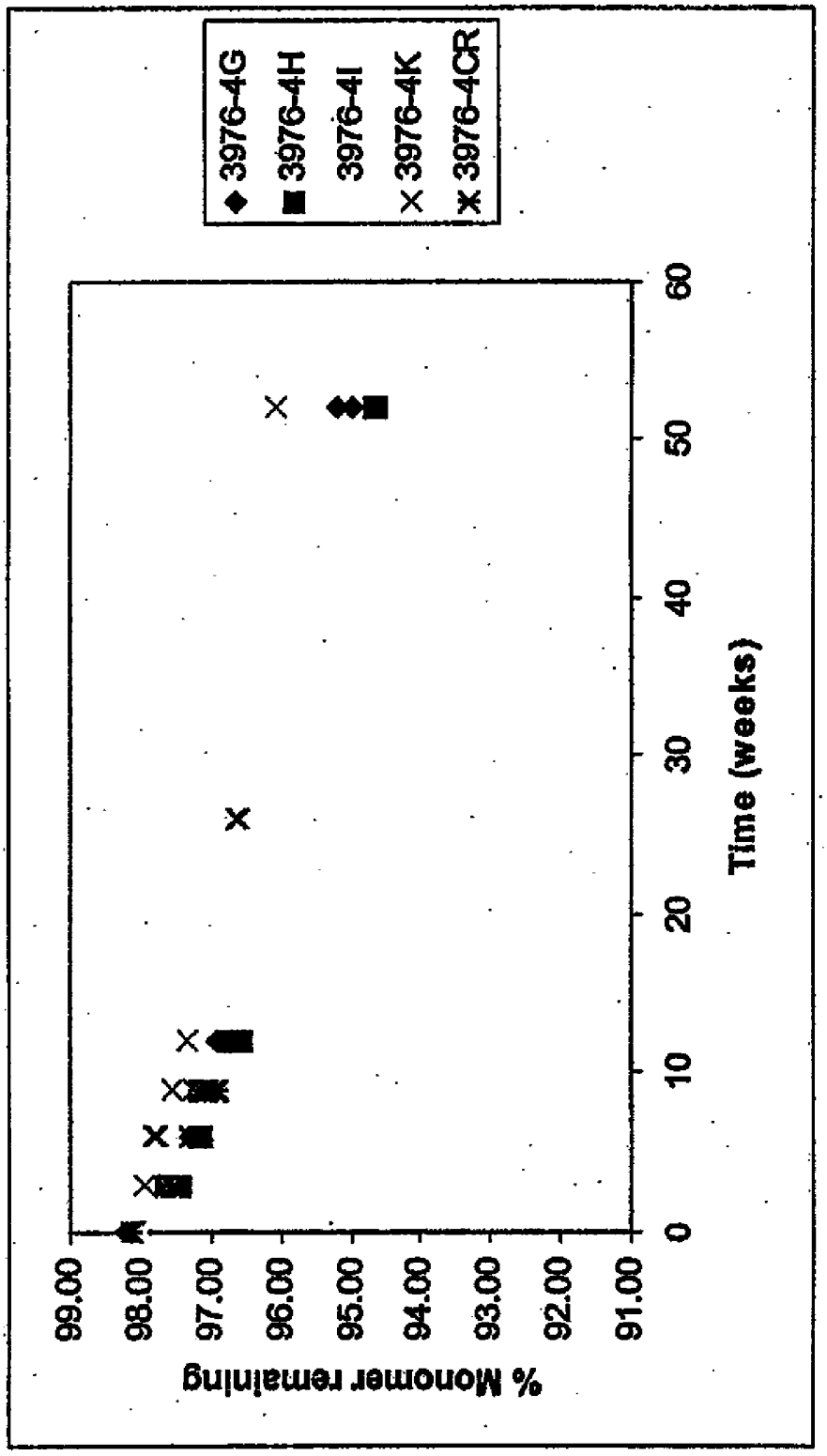


Figure 16: Loss of monomer at 40°C for Lyophilized Formulations

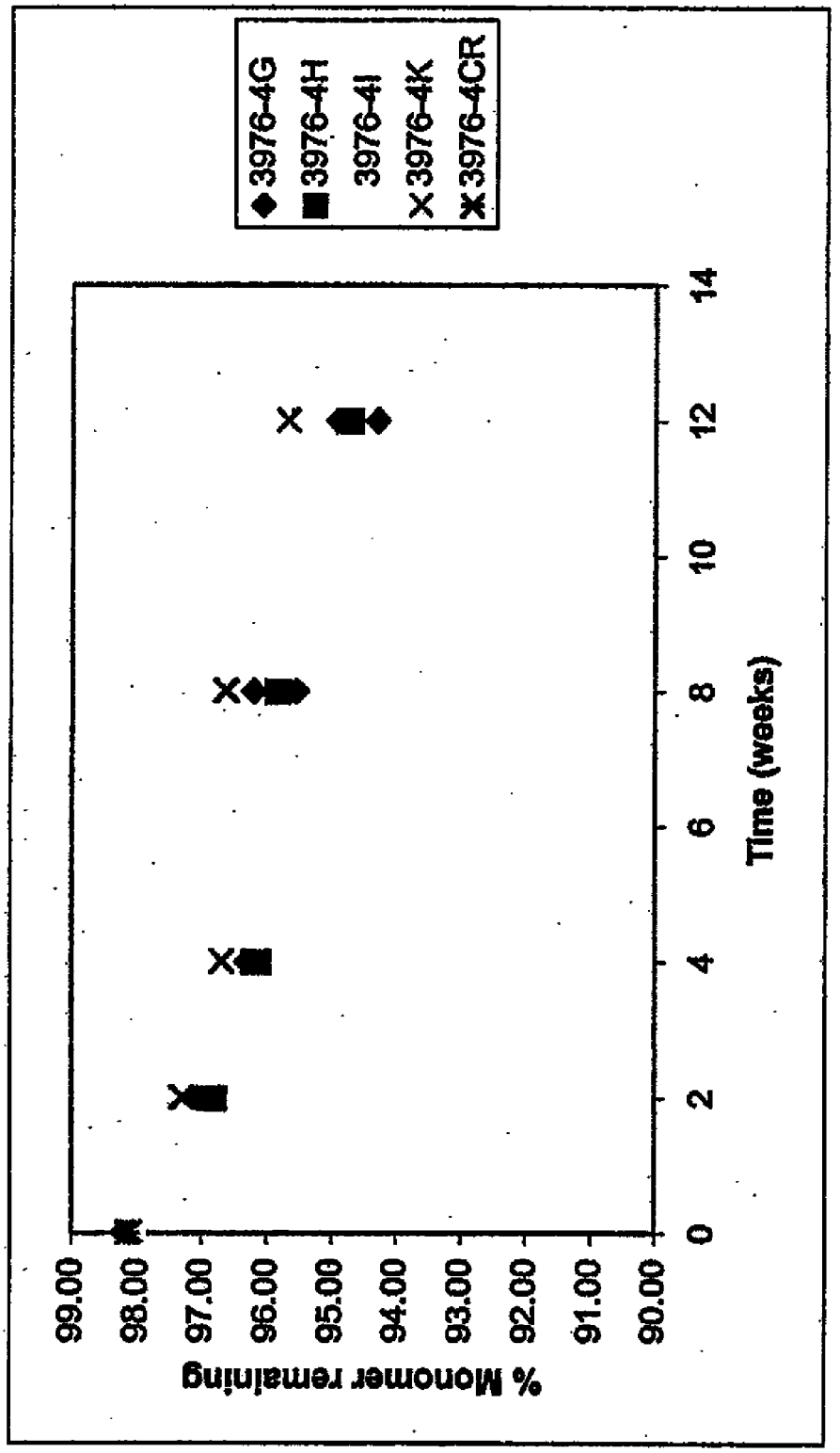


Figure 17: Formation of high molecular weight species in pre-lyophilized samples at 40°C

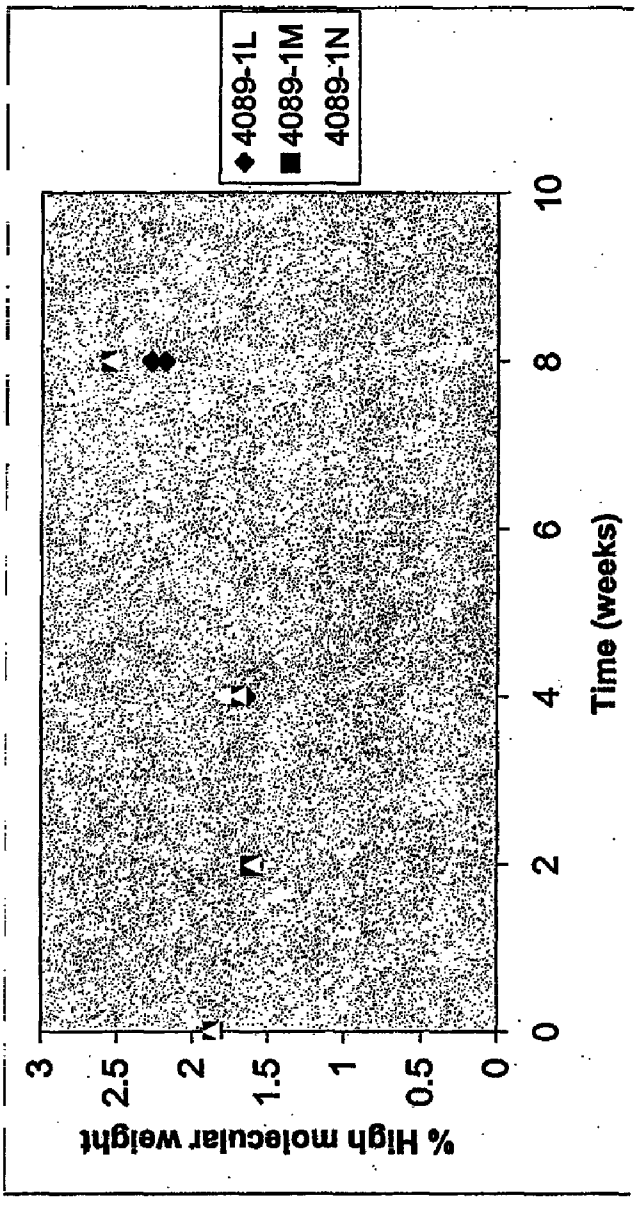


Figure 18: Formation of low molecular weight species in pre-lyophilized samples at 40°C

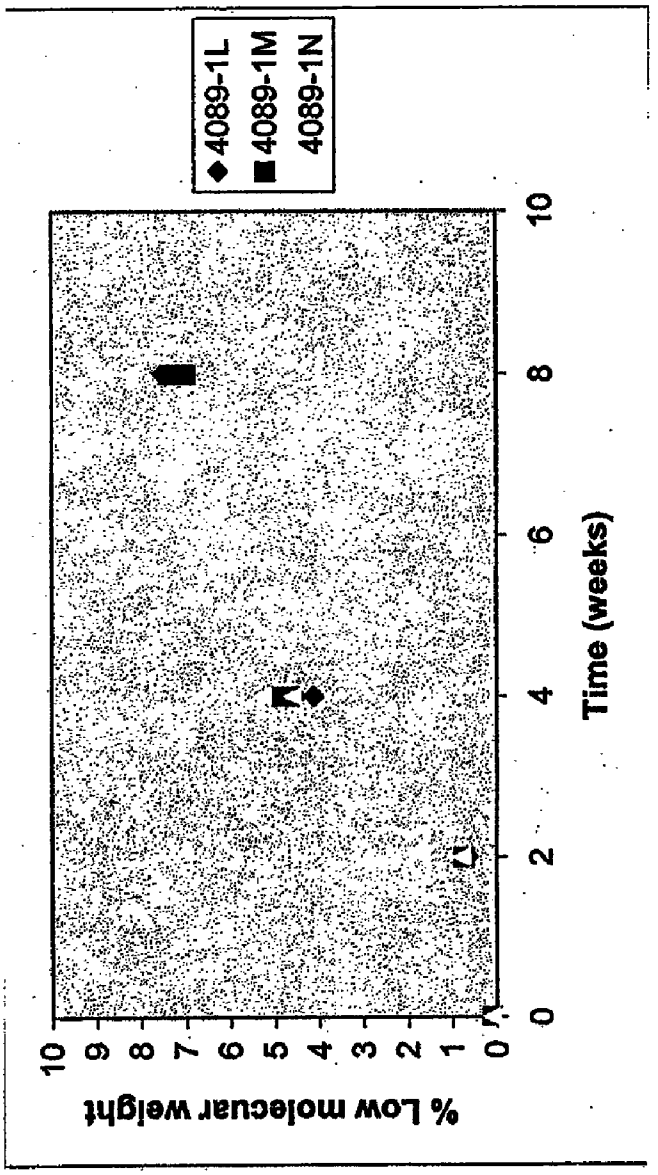


Figure 19: Loss of monomer in pre-lyophilized samples at 40°C

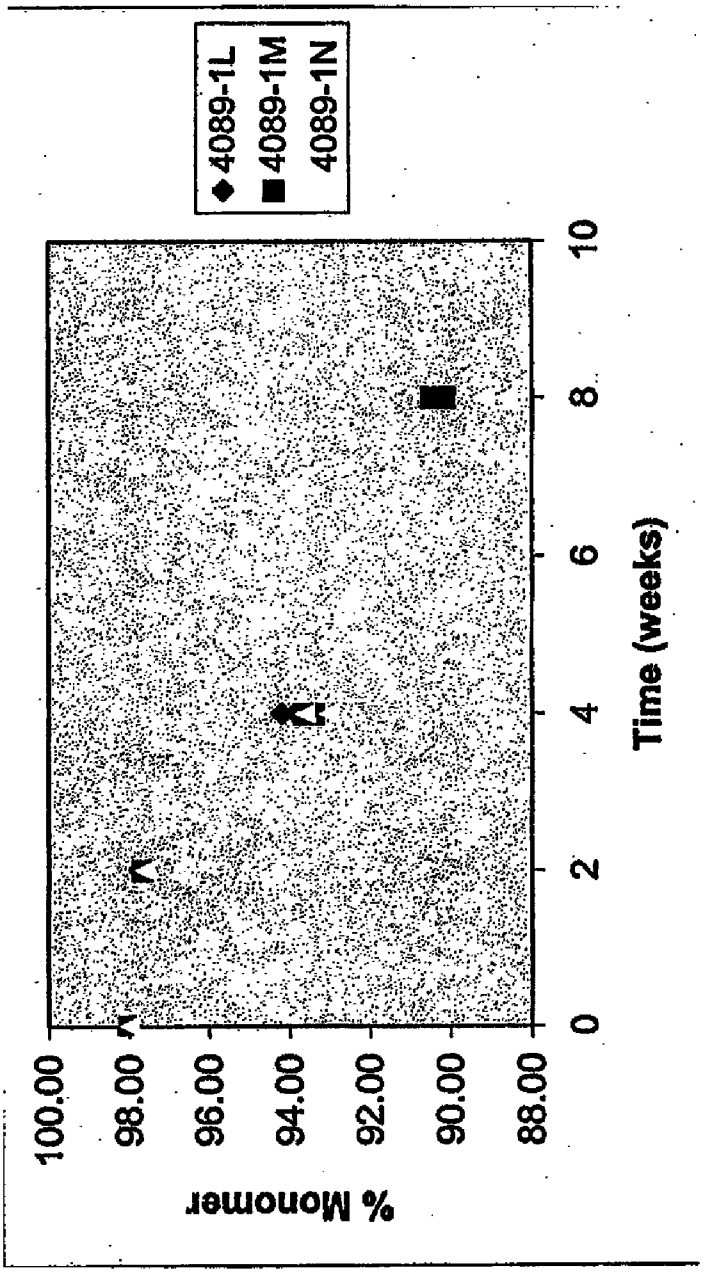


Figure 20: Reconstitution times at 40°C

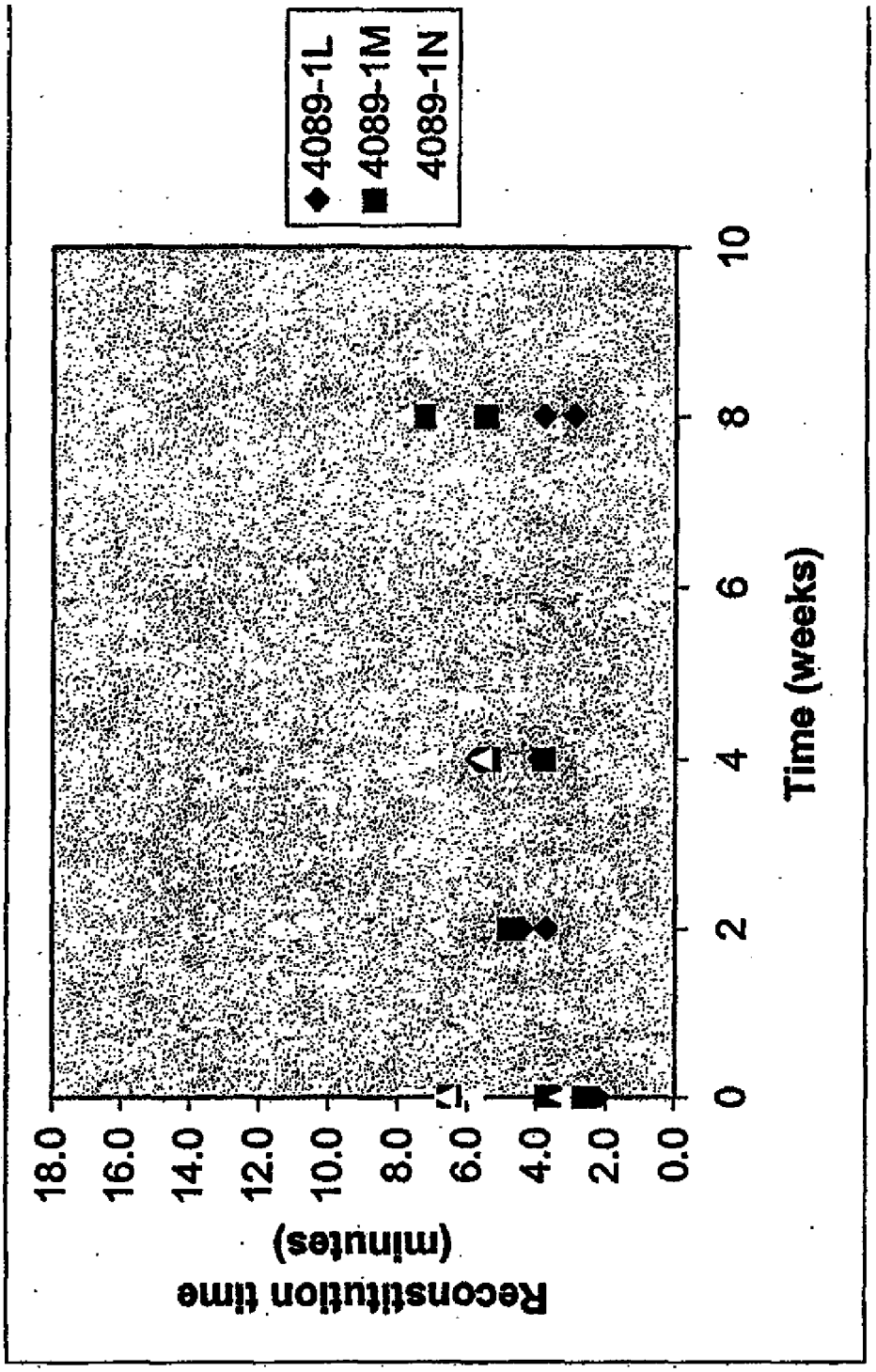


Figure 21: Formation of high molecular weight species in lyophilized samples at 40°C

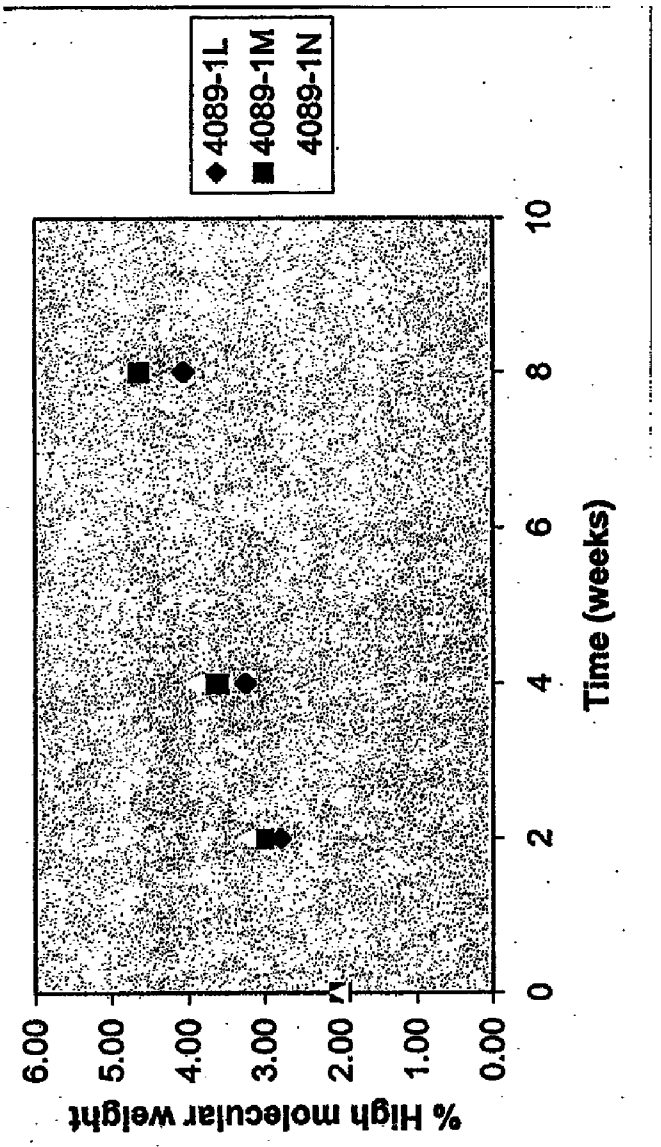


Figure 22: Formation of low molecular weight species in lyophilized samples at 40°C

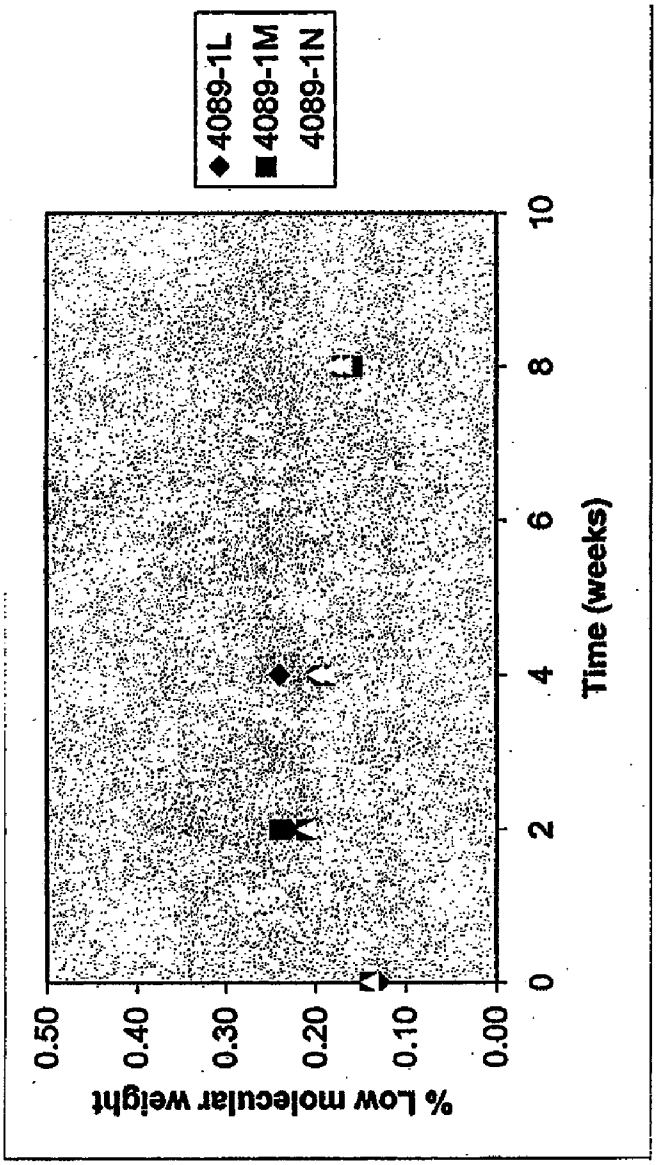


Figure 23: Loss of monomer in lyophilized samples at 40°C

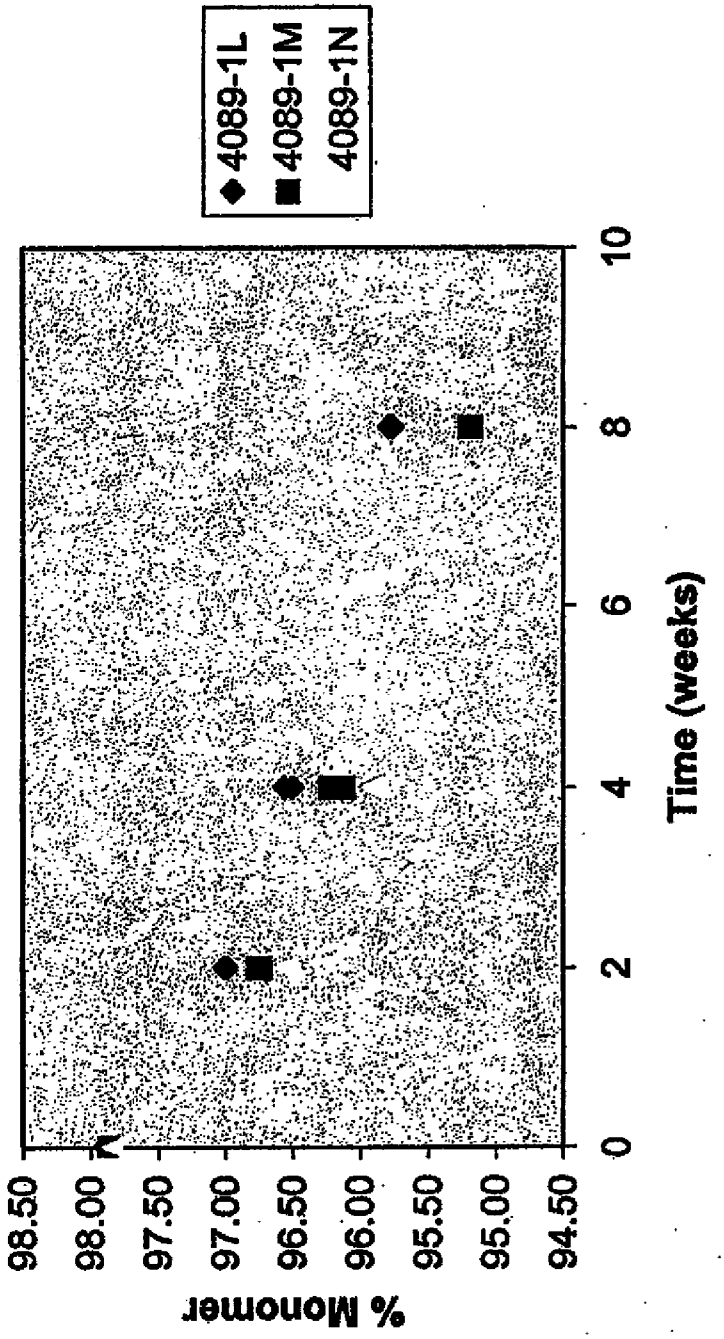


FIGURE 24A

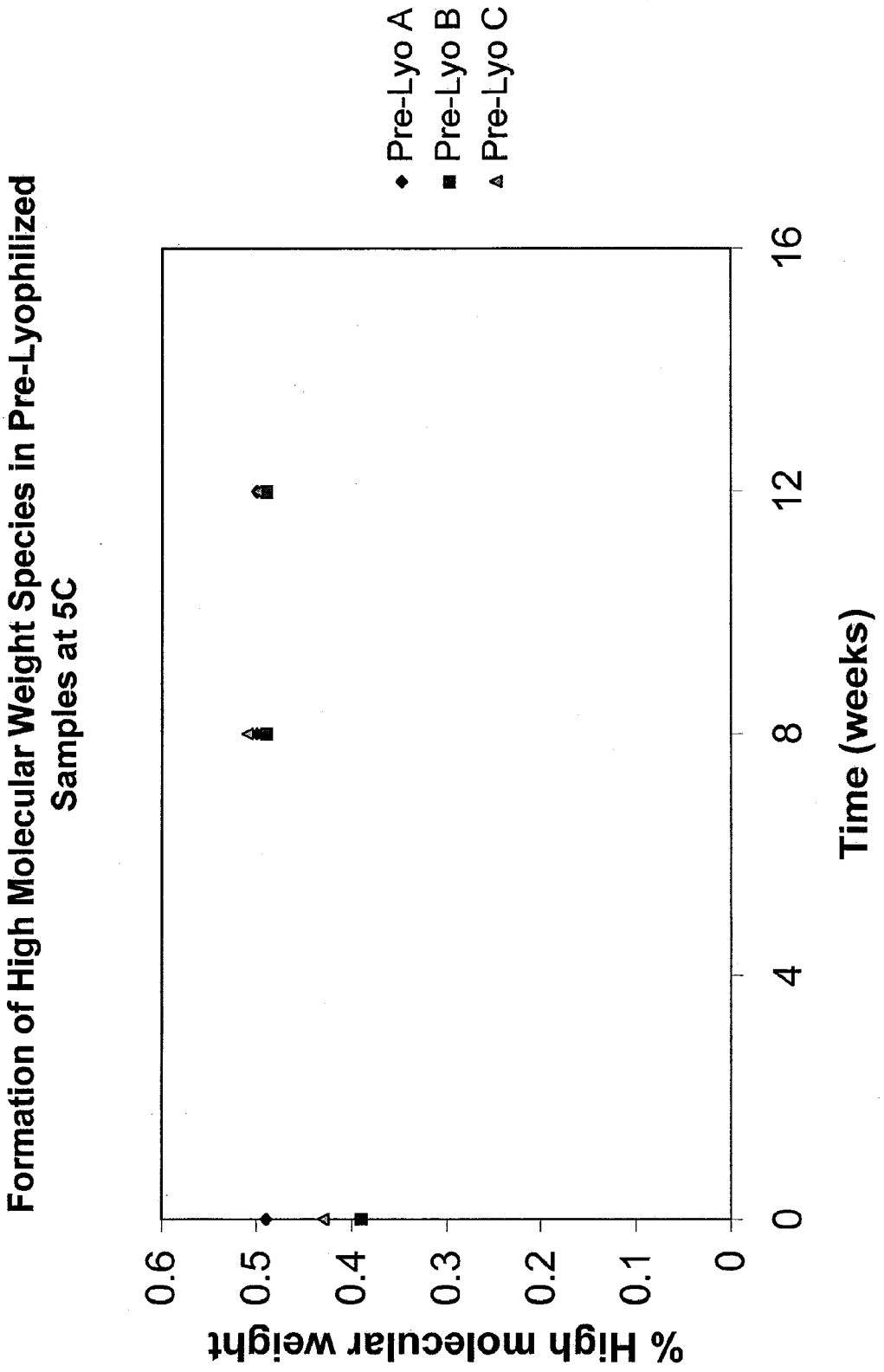

Formation of High Molecular Weight Species in Pre-Lyophilized Samples at 5C
Pre-Lyo A
Pre-Lyo B
Pre-Lyo C
% High molecular weight
0
0.1
0.2
0.3
0.4
0.5
0.6
Time (weeks)
0
4
8
12
16

FIGURE 24B

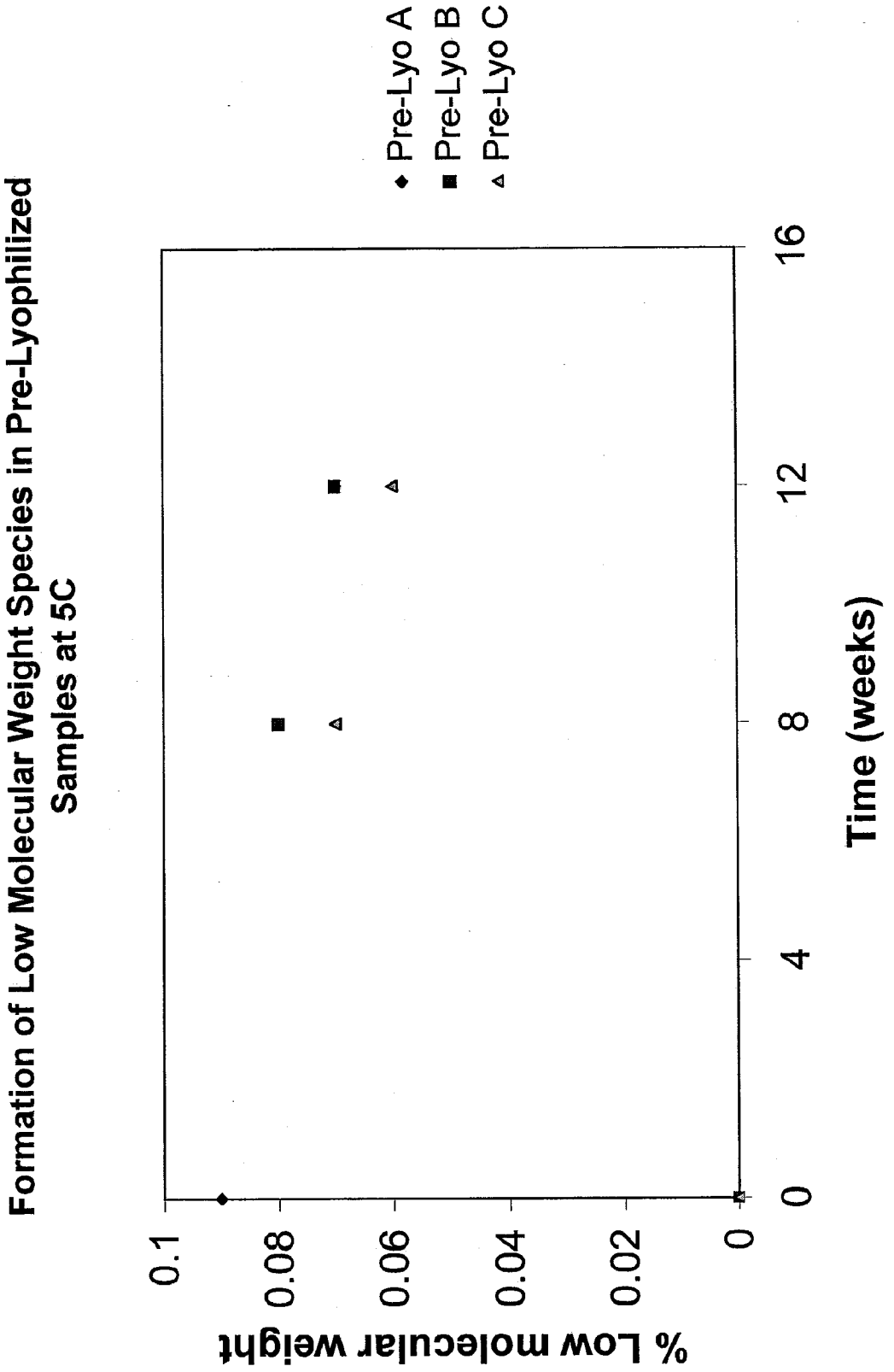
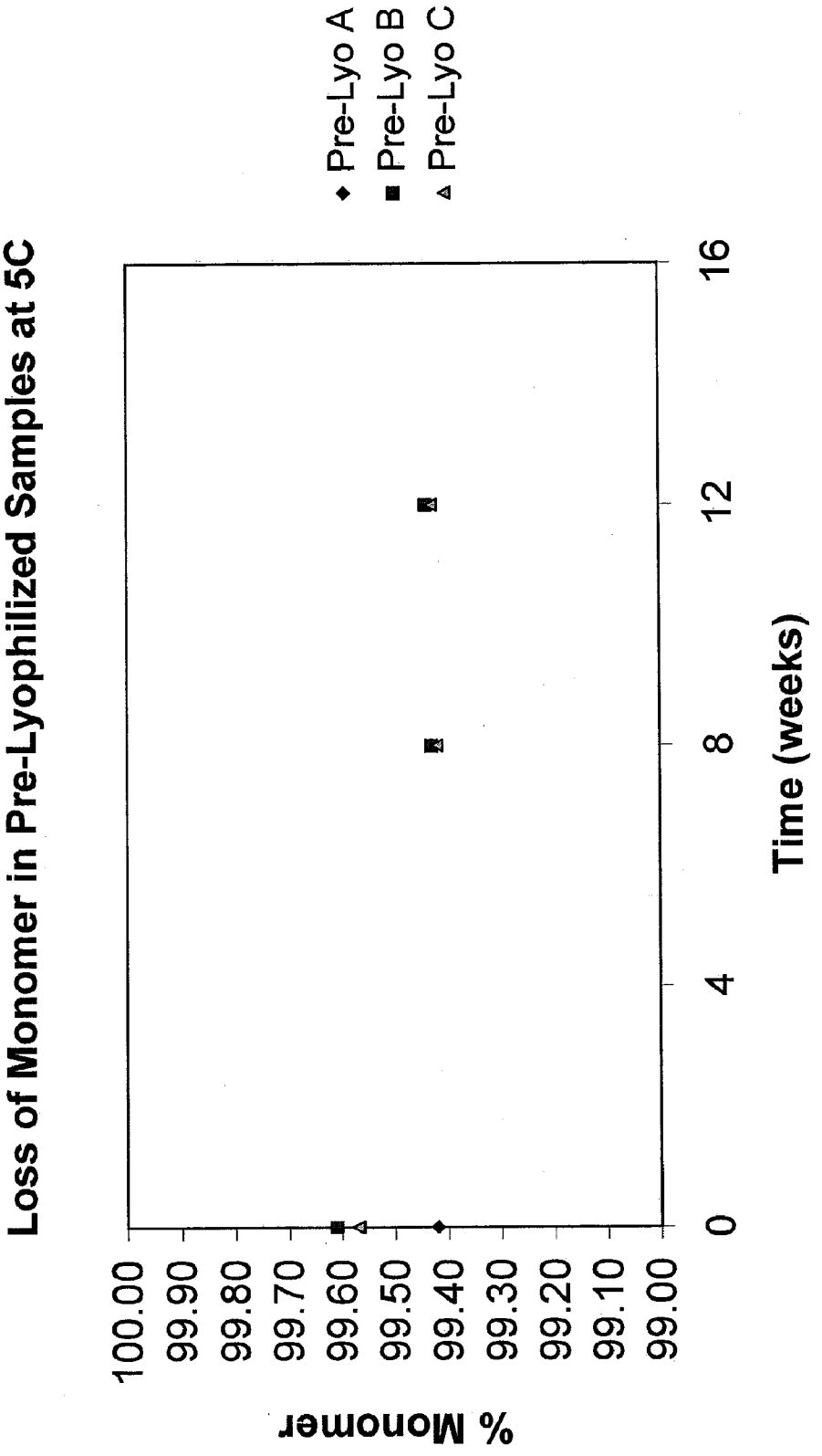

Formation of Low Molecular Weight Species in Pre-Lyophilized Samples at 5C
Pre-Lyo A
Pre-Lyo B
Pre-Lyo C
% Low molecular weight
0.1
0.08
0.06
0.04
0.02
0
0
4
8
12
16
Time (weeks)

FIGURE 24C


Loss of Monomer in Pre-Lyophilized Samples at 5C
Pre-Lyo A
Pre-Lyo B
Pre-Lyo C
% Monomer
100.00
99.90
99.80
99.70
99.60
99.50
99.40
99.30
99.20
99.10
99.00
0
4
8
12
16
Time (weeks)

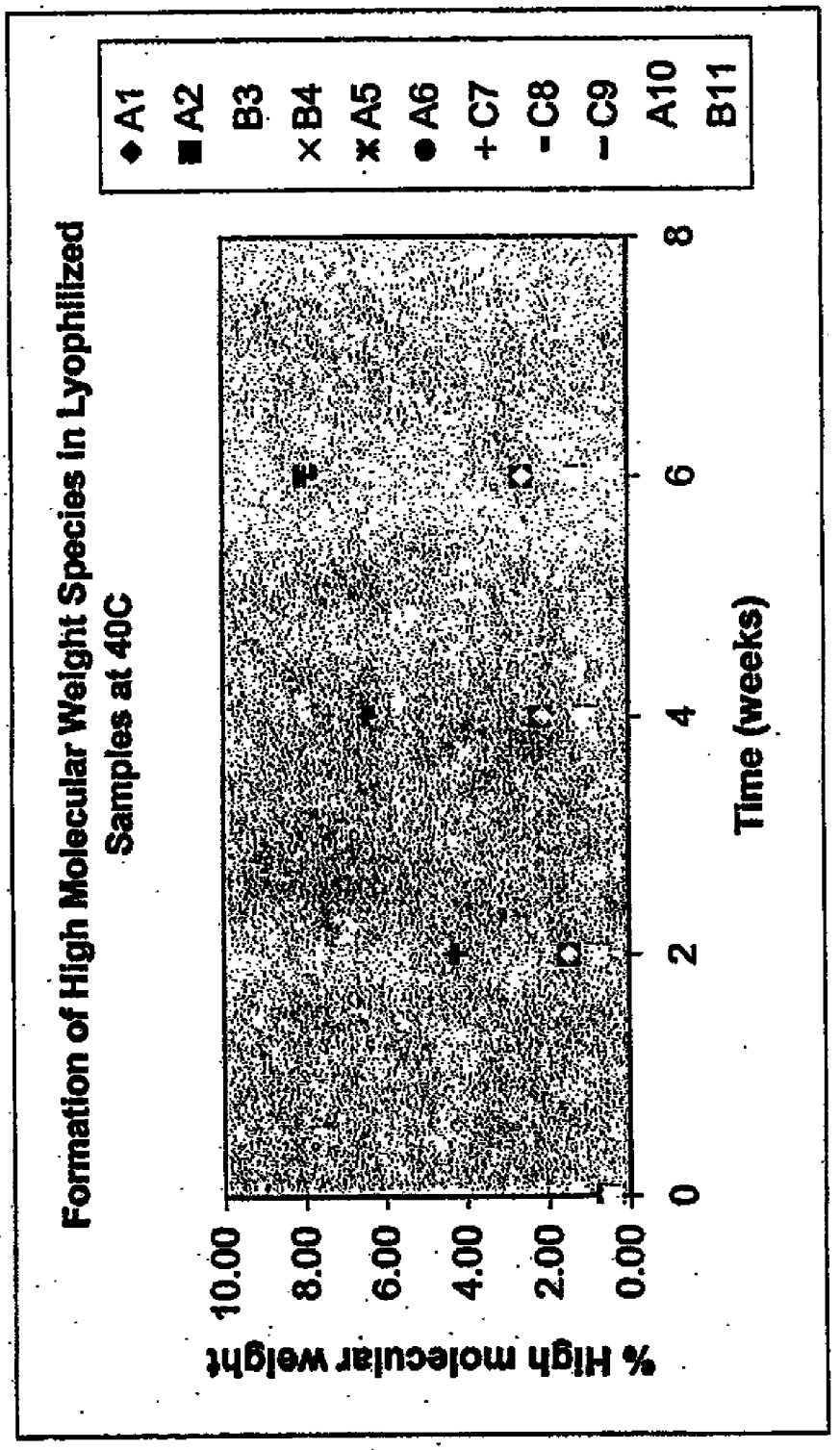

Formation of High Molecular Weight Species in Lyophilized Samples at 40C
% High molecular weight
10.00
8.00
6.00
4.00
2.00
0.00
0
2
4
6
8
Time (weeks)
A1
A2
B3
B4
A5
A6
C7
C8
C9
A10
B11

Figure 25

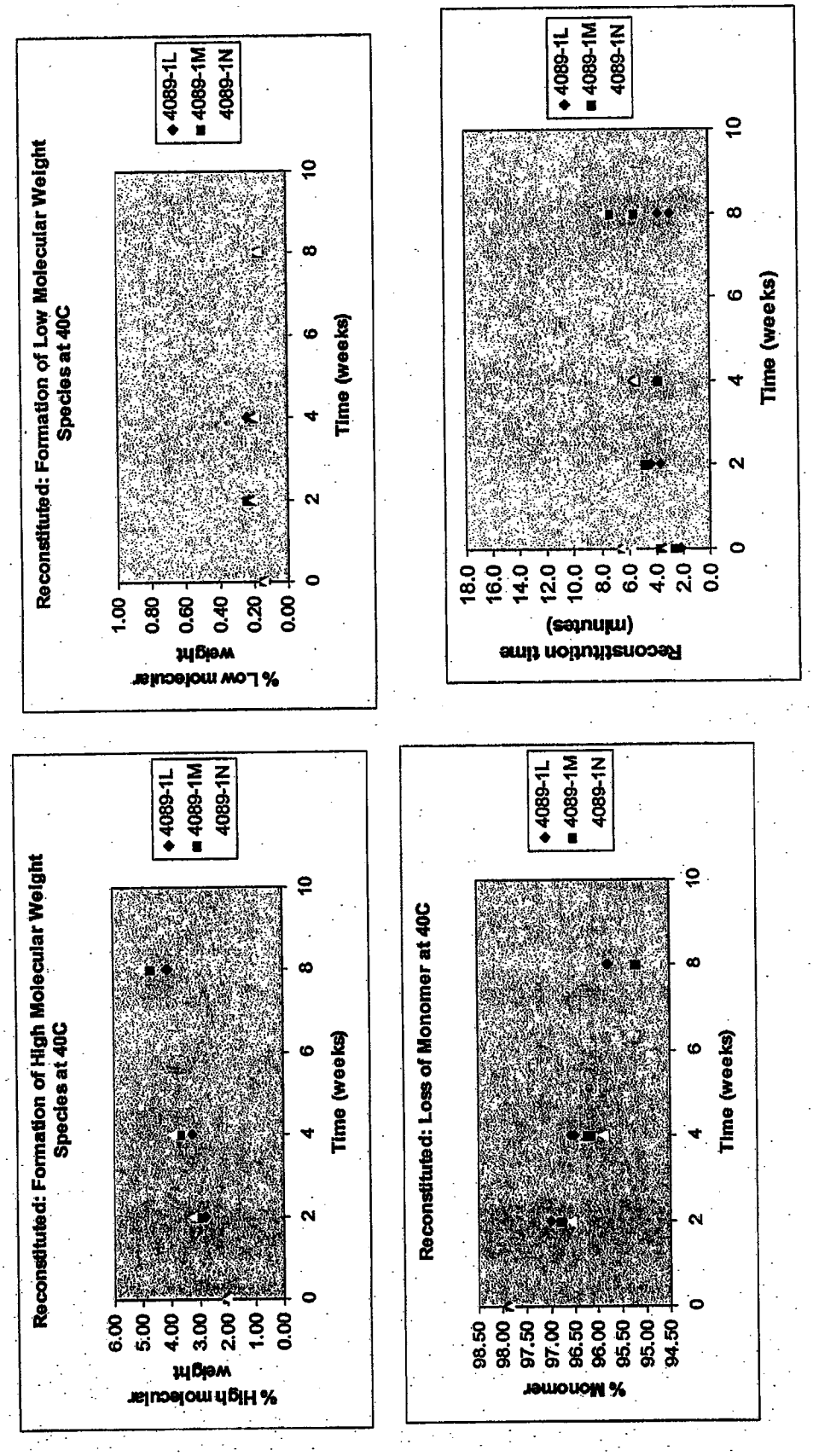


FIGURE 26A, B, C, D

LYOPHILIZED IMMUNOGLOBULIN FORMULATIONS AND METHODS OF PREPARATION

CROSS REFERENCE TO RELATED APPLICATIONS

[0001] This application claims priority under 35 U.S.C. § 119 to U.S. Provisional Application No. 60/929,133, filed Jun. 14, 2007, the entire content of which is hereby expressly incorporated by reference in its entirety.

[0002] The present invention relates generally to the field of pharmaceutical formulation of immunoglobulins. Specifically, the present invention relates to stable, lyophilized, high concentration immunoglobulin formulations. This invention is exemplified by a stabilized lyophilized formulation of the recombinant humanized anti-alpha-4 integrin antibody natalizumab.

BACKGROUND OF THE INVENTION

[0003] Drug preparations intended for administration to humans may require stabilizers to prevent alternations to the drugs prior to the use of the preparation. Because proteins are larger and more complex than traditional organic and inorganic drugs (i.e. proteins possess multiple functional groups in addition to complex three-dimensional structures), the formulation of proteins poses special problems. Degradation pathways for proteins can involve chemical instability (any process which involves modification of the protein by bond formation or cleavage resulting in a new chemical entity) or physical instability (changes in the higher order structure of the protein). Chemical instability can result from deamidation, racemization, hydrolysis, oxidation, beta elimination or disulfide exchange. Physical instability can result from denaturation, aggregation, precipitation or adsorption, for example. Many protein preparations are particularly unstable in very dilute or highly concentrated solutions, and this instability is often increased when the protein preparation is stored, or shipped. Thus, a major challenge that exists in the field of protein drugs is in the development of formulations that maintain both protein stability and activity.

[0004] Antibodies, including monoclonal antibodies, all differ from one another in ways relevant to their behavior and efficacy in a formulation. For example, monoclonal antibodies differ from one another with regard to isoelectric points, solubility, and conditions at which the monoclonal antibodies will aggregate. Proteins differ from one another with regard to their behavior and efficacy in a formulation, making it difficult to predict if a formulation will be stable for a particular antibody. Three common problems in protein formulations include protein degradation, aggregation, deamidation, and oxidation. Further, many different reactions affecting formulation stability may occur simultaneously, making it difficult to determine which reaction is causing which result. See Cleland et al, "The Development of Stable Protein Formulations: A Close Look at Protein Aggregation, Deamidation, and Oxidation", *Critical Reviews in Therapeutic Drug Carrier Systems,* 10(4):307-377 (1993)).

SUMMARY OF THE INVENTION

[0005] Specifically, the present invention relates to stable, lyophilized, high concentration immunoglobulin formulations. There are three steps in preparing the present formulations, including preparing an aqueous pre-lyophilized formulation, a lyophilization step, and a reconstitution step.

[0006] This invention is directed to a stable lyophilized formulation prepared by lyophilizing an aqueous formulation, wherein the aqueous formulation comprises about 40 mg/ml to about 50 mg/ml of an immunoglobulin in a buffer, polysorbate, and sucrose. In a preferred embodiment of the invention, the aqueous pre-lyophilized formulation comprises (a) about 30 mg/ml to about 60 mg/ml natalizumab; (b) a buffer having a pH of about 5.5 to about 6.5; (c) about 20 mg/ml to about 50 mg/ml sucrose; and (d) about 0.02% to about 0.08% polysorbate. In a more preferred embodiment, the aqueous pre-lyophilized formulation comprises (a) about 40 mg/ml natalizumab; about 6 mM histidine, pH about 6.0; about 41 mg/ml sucrose; and (d) about 0.04% polysorbate 80.

[0007] The lyophilized formulation retains the stability of the immunoglobulin, and prevents the immunoglobulins intended for administration to human subjects from forming aggregates and/or particulates in the final product. This lyophilized formulation is stable at room temperature for at least three months, preferably 6 months, and more preferably one year. The lyophilized formulation is also stable at 2-8° C. for 1 year, preferably 2 years. This lyophilized formulation has a short reconstitution time of less than 10 minutes, and after reconstitution is suitable for parenteral administration such as intramuscular, subcutaneous, intravenous, or intraperitoneal injection.

[0008] The lyophilized formulation is reconstituted with a liquid to a clarified solution containing about 80-160 mg/ml immunoglobulin concentration. In a preferred embodiment, the reconstituted formulation comprises (i) about 80 mg/ml to about 160 mg/ml natalizumab; (ii) about 18 mM histidine at a pH of about 6.0; (iii) about 123 mg/ml sucrose; and (iv) about 0.12% polysorbate 80. In a more preferred embodiment, the reconstituted formulation comprises about 120 mg/ml natalizumab.

[0009] The pre-lyophilized formulation of the present invention can be lyophilized using appropriate drying parameters. The following drying parameters are preferred: a primary drying phase temperature of about −25° C. and pressure between about 80 mTorr to about 120 mTorr; and a secondary drying phase at about 20° C., and pressure between about 80 mTorr to 120 mTorr.

[0010] This invention further provides methods for making and for using the reconstituted formulations.

BRIEF DESCRIPTION OF THE DRAWINGS

[0011] FIG. **1** shows the formation of high molecular weight species at 30°.

[0012] FIG. **2** shows the formation of high molecular weight species at 40° C.

[0013] FIG. **3** shows the formation of low molecular weight species at 30° C. in the prelyophilized solutions.

[0014] FIG. **4** shows the formation of low molecular weight species at 40° C. in the pre-lyophilized solutions.

[0015] FIG. **5** shows the total loss of monomer at 5° C. due to formation of both high and low molecular weight species.

[0016] FIG. **6** shows the total loss of monomer at 30° C. due to formation of both high and low molecular weight species.

[0017] FIG. **7** shows the total loss of monomer at 40° C. due to formation of both high and low molecular weight species.

[0018] FIG. **8** shows the loss of monomer in the lyophilized formulations with time at 5° C.

[0019] FIG. **9** shows the loss of monomer in the lyophilized formulations with time at 30° C.

[0020] FIG. **10** shows the loss of monomer in the lyophilized formulations with time at 40° C.

[0021] FIG. **11** shows the formation of low molecular weight species for each formulation at 30° C.

[0022] FIG. **12** shows the formation of low molecular weight species for each formulation at 40° C.

[0023] FIG. **13** shows the formation of high molecular weight species at 40° C. in pre-lyophilized formulations.

[0024] FIG. **14** shows the loss of monomer due to formation of aggregate at 5° C.

[0025] FIG. **15** shows the loss of monomer due to formation of aggregate at 30° C.

[0026] FIG. **16** shows the loss of monomer due to formation of aggregate at 40° C.

[0027] FIG. **17** shows the formation of high molecular weight species in pre-lyophilized samples at 40° C.

[0028] FIG. **18** shows the formation of low molecular weight species in pre-lyophilized samples at 40° C.

[0029] FIG. **19** shows the total loss of monomer at 40° C. due to formation of both high and low molecular weight species.

[0030] FIG. **20** shows reconstitution times at 40° C.

[0031] FIG. **21** shows the formation of high molecular weight species in lyophilized samples at 40° C.

[0032] FIG. **22** shows the formation of low molecular weight species in lyophilized samples at 40° C.

[0033] FIG. **23** shows the total loss of monomer at 40° C. due to formation of both high and low molecular weight species.

[0034] FIG. **24**A shows the formation of high molecular weight species in pre-lyophilized samples at 5° C. FIG. **24** B shows the formation of low molecular weight species in pre-lyophilized samples at 5° C. FIG. **24** C shows loss of monomer in pre-lyophilized samples at 5° C.

[0035] FIG. **25** shows formation of high molecular weight species in lyophilized samples at 40° C.

[0036] FIG. **26**A shows formation of high molecular weight species at 40° C. in reconstituted samples.

[0037] FIG. **26**B shows formation of low molecular weight species at 40° C. in reconstituted samples.

[0038] FIG. **26**C shows loss of monomer at 40° C. in reconstituted samples. FIG. **26**D shows reconstitution time.

DETAILED DESCRIPTION OF EMBODIMENTS OF THE INVENTION

1. Definitions

[0039] As used herein, the term "immunoglobulin" includes but is not limited to an antibody and antibody fragment (such as scFv, Fab, Fc, (Fab')2), and other genetically engineered portions of antibodies. Depending on the amino acid sequence of the constant domain of their heavy chains, immunoglobulin can be assigned to different classes. There are five major classes of immunoglobulins: IgA, IgD, IgE, IgG and IgM. Several of these may be further divided into subclasses (isotypes), e.g., IgG1, IgG2, IgG3, and IgG4; IgA1 and IgA2.

[0040] The term "antibody" is used in the broadest sense and specifically covers monoclonal antibodies (including agonist and antagonist antibodies), antibody compositions with polyepitopic specificity, and antibody fragments (e.g., Fab, (Fab')2, scFv and Fv), so long as they exhibit the desired biological activity. "Antibody" is meant to include polyclonal antibodies, monoclonal antibodies, humanized antibodies, human antibodies, primatized antibodies and other antibodies produced via genetic engineering.

[0041] The term "monoclonal antibody" as used herein refers to an antibody obtained from a population of substantially homogeneous antibodies, i.e., the individual antibodies comprising the population are identical except for possible naturally occurring modifications or glycosylation variants that may be present in minor amounts. The modifier "monoclonal" indicates the character of the antibody as being obtained from a substantially homogeneous population of antibodies, and is not to be construed as requiring production of the antibody by any particular method. The term "monoclonal antibodies" also includes "chimeric" antibodies (immunoglobulins) in which a portion of the heavy and/or light chain is identical with or homologous to corresponding sequences in antibodies derived from a particular species or belonging to a particular antibody class or subclass, while the remainder of the chain(s) is identical with or homologous to corresponding sequences in antibodies derived from another species or belonging to another antibody class or subclass, as well as fragments of such antibodies, so long as they exhibit the desired biological activity. "Humanized" forms of non-human (e.g., murine, rabbit, bovine, equine, porcine, and the like) antibodies are chimeric immunoglobulins, immunoglobulin chains or fragments thereof (such as Fv, Fab, Fab', F(ab')2 or other antigen-binding subsequences of antibodies), which contain minimal sequence derived from non-human immunoglobulin.

[0042] The term "natalizumab" refers to the antibody also known as AN100226 (antibody code number), and is the active ingredient in TYSABRI® (trade name; formerly ANTEGREN®). The term "natalizumab" is the United States Adopted Name (USAN) (the official non-proprietary or generic name given to a pharmaceutical substance). Natalizumab is a recombinant, humanized anti-alpha-4 integrin antibody. Natalizumab is an IgG4 antibody. U.S. Pat. No. 5,840,299, incorporated herein by reference, describes how to make a recombinant humanized anti-alpha-4 integrin antibody, including natalizumab, using routine synthetic and molecular biology methods.

[0043] The terms "lyophilization," "lyophilized," and "freeze-dried" refer to a process by which the material to be dried is first frozen and then the ice or frozen solvent is removed by sublimation in a vacuum environment. One or more excipients may be included in pre-lyophilized formulations to enhance stability of the lyophilized product upon storage.

[0044] The term "pharmaceutical formulation" refers to preparations which are in such form as to permit the active ingredients to be effective, and which contains no additional components which are toxic to the subjects to which the formulation would be administered.

[0045] "Pharmaceutically acceptable" excipients (vehicles, additives) are those which can reasonably be administered to a subject mammal to provide an effective dose of the active ingredient employed.

[0046] "Reconstitution time" is the time that is required to rehydrate a lyophilized formulation with a solution to a particle-free clarified solution.

[0047] A "stable" formulation is one in which the protein therein essentially retains its physical stability and/or chemical stability and/or biological activity upon storage. Various

analytical techniques for measuring protein stability are available in the art and are reviewed in Peptide and Protein Drug Delivery, 247-301, Vincent Lee Ed., Marcel Dekker, Inc., New York, N.Y., Pubs. (1991) and Jones, A. Adv. Drug Delivery Rev. 10:29-90 (1993). Stability can be measured at a selected temperature for a selected time period.

[0048] A "stable" lyophilized immunoglobulin formulation is a lyophilized antibody formulation with no significant changes observed at a refrigerated temperature (2-8° C.) for at least 12 months, preferably 2 years, and more preferably 3 years; or at room temperature (23-27° C.) for at least 3 months, preferably 6 months, and more preferably 1 year. The criteria for stability are as follows. No more than 10% of antibody monomer is degraded as measured by SEC-HPLC. Preferably no more than 5%, of antibody monomer is degraded as measured by SEC-HPLC. The rehydrated solution is colorless, or clear to slightly opalescent by visual analysis. The concentration, pH and osmolality of the formulation have no more than +/−10% change. Potency is within 70-130%, and preferably within 80-120%, of the control. No more than 10% of clipping is observed. Preferably, no more than 5% of clipping is observed. No more than 10% of aggregation is formed. Preferably, no more than 5% of aggregation is formed.

[0049] An immunoglobulin "retains its physical stability" in a pharmaceutical formulation if it shows no significant increase of aggregation, precipitation and/or denaturation upon visual examination of color and/or clarity, or as measured by LV light scattering, size exclusion chromatography (SEC) and dynamic light scattering. The changes of protein conformation can be evaluated by fluorescence spectroscopy, which determines the protein tertiary structure, and by FTIR spectroscopy, which determines the protein secondary structure.

[0050] An immunoglobulin "retains its chemical stability" in a pharmaceutical formulation, if it shows no significant chemical alteration. Chemical stability can be assessed by detecting and quantifying chemically altered forms of the protein. Degradation processes that often alter the protein chemical structure include hydrolysis or clipping (evaluated by methods such as size exclusion chromatography and SDS-PAGE), oxidation (evaluated by methods such as by peptide mapping in conjunction with mass spectroscopy or MALDI/TOF/MS), deamidation (evaluated by methods such as ion-exchange chromatography, capillary isoelectric focusing, peptide mapping, isoaspartic acid measurement), and isomerization (evaluated by measuring the isoaspartic acid content, peptide mapping, etc.).

[0051] An immunoglobulin "retains its biological activity" in a pharmaceutical formulation, if the biological activity of the immunoglobulin at a given time is within a predetermined range of the biological activity exhibited at the time the pharmaceutical formulation was prepared. The biological activity of an immunoglobulin can be determined, for example, by an antigen binding assay.

[0052] The term "isotonic" means that the formulation of interest has essentially the same osmotic pressure as human blood. Isotonic formulations will generally have an osmotic pressure from about 270-328 mOsm. Slightly hypotonic pressure is 250-269 and slightly hypertonic pressure is 328-350 mOsm. Osmotic pressure can be measured, for example, using a vapor pressure or ice-freezing type osmometer.

[0053] The term "buffer" encompasses those agents which maintain the solution pH in an acceptable range prior to lyophilization and may include histidine, succinate (sodium or potassium), phosphate (sodium or potassium), Tris (tris (hydroxymethyl) aminomethane), diethanolamine, citrate (sodium), gluconate, and other organic acid buffers.

[0054] "Tonicity Modifiers" include salts such as NaCl, KCl, MgCl2 CaCl2, etc. that can be used to control osmotic pressure. In addition, cryprotectants, lyoprotectants and/or bulking agents such as sucrose, mannitol, glycine etc. can serve as tonicity modifiers.

[0055] In the context of the present invention, a "therapeutically effective amount" of an immunoglobulin refers to an amount effective in the prevention or treatment of a disorder for the treatment of which the immunoglobulin is effective. A "disorder" is any condition that would benefit from treatment with the immunoglobulin. This includes chronic and acute disorders or diseases including those pathological conditions which predispose the mammal to the disorder in question. Preferably, the disorder is one that that can be treated and/or prevented by an immunoglobulin that recognizes and binds to alpha-4 integrin, such as natalizumab.

[0056] "Treatment" refers to both therapeutic treatment and prophylactic or preventative measures. Those in need of treatment include those already with the disorder as well as those in which the disorder is to be prevented.

[0057] A "preservative" is a compound which can be included in the formulation to essentially reduce bacterial action therein, thus facilitating the production of a multi-use formulation, for example. Examples of potential preservatives include octadecyldimethylbenzyl ammonium chloride, hexamethonium chloride, benzalkonium chloride (a mixture of alkylbenzyldimethylammonium chlorides in which the alkyl groups are long-chain compounds), and benzethonium chloride. Other types of preservatives include aromatic alcohols such as phenol, butyl and benzyl alcohol, alkyl parabens such as methyl or propyl paraben, catechol, resorcinol, cyclohexanol, 3-pentanol, and m-cresol.

[0058] The term "patient" or "subject" is meant to include any mammal. A "mammal," for purposes of treatment, refers to any animal classified as a mammal, including but not limited to humans, domestic and farm animals, and zoo, sports, or pet animals, such as dogs, horses, cats, cows, and the like. Preferably, the mammal is human. Preferably the disease or condition being treated in the mammal is one which is modulated when a therapeutically effective dose of natalizumab is administered.

2. Immunoglobulin Formulations

[0059] The compositions of this invention minimize the formation of aggregates and particulates and ensure that the immunoglobulin in solution maintains its immunoreactivity over time. The compositions comprise a sterile, pharmaceutically acceptable lyophilized formulation prepared from an aqueous pre-lyophilized formulation comprising an immunoglobulin in a buffer having a neutral or acidic pH (about 5.5 to about 6.5), sucrose, and a polysorbate.

[0060] In a preferred embodiment, the immunoglobulin is present in the pre-lyophilized formulation at a concentration of about 30 to about 60 mg/ml, more preferably about 40 to about 50 mg/ml, and even more preferably about 40 mg/ml. A preferred immunoglobulin is an IgG antibody, more preferably an IgG4 antibody, even more preferably a humanized recombinant IgG4 antibody, and most preferably natalizumab.

[0061] A buffer of pH 5.5 about to about 6.5 is used in the pre-lyophilized formulation. Preferably, the pH is about 6.0. Examples of suitable buffers include histidine, succinate (such as sodium succinate), gluconate, citrate and other organic acid buffers. A preferred pre-lyophilized formulation contains histidine, preferably about 1 to about 12 mM histidine. A even more preferred pre-lyophilized formulation contains about 6 mM histidine.

[0062] The pre-lyophilized formulation also comprises sucrose. Suitable concentrations of sucrose are in the range of about 20 to about 50 mg/ml, preferably about 41 mg/ml.

[0063] The pre-lyophilized formulation also comprises a polysorbate, such as polysorbate 20 or polysorbate 80 (i.e. Tween 20 and Tween 80, respectively) and poloxamer (e.g. poloxamer 188). In a preferred embodiment, the polysorbate is polysorbate 80. The polysorbate is preferably present at a weight per volume concentration of about 0.02 to about 0.08%, more preferably about 0.04%.

[0064] The weight ratio of immunoglobulin to sucrose in the pre-lyophilized formulation is preferably in the range of about 2:1 to about 0.5:1, more preferably about 1:1. The molar ratio of immunoglobulin to sucrose is about 300:1 to about 500:1, preferably about 400:1 to 500:1, more preferably about 450:1.

[0065] A bulking agent that provides good lyophilized cake properties, such as serine, glycine, and mannitol, can be optionally added to the present composition. These agents also contribute to the tonicity of the formulations and may provide protection to the freeze-thaw process and improve long-term stability. In addition, tonicity modifiers can be added to the formulation to control osmotic pressure. The formulation may further comprise one or more preservatives.

[0066] A preferred pre-lyophilized formulation is a formulation comprising about 40 mg/ml natalizumab, about 6 mM histidine (pH about 6), about 0.04% polysorbate 80, and about 41 mg/ml sucrose. The above pre-lyophilized formulation is lyophilized to form a dry, stable powder, which can be easily reconstituted to a particle-free solution suitable for administering to humans.

[0067] Lyophilization is a freeze drying process that is often used in the preparation of pharmaceutical products to preserve their biological activity. The liquid composition is prepared, then lyophilized to form a dry cake-like product. The process generally involves drying a previously frozen sample in a vacuum to remove the ice, leaving the non-water components intact, in the form of a powdery or cake-like substance. The lyophilized product can be stored for prolonged periods of time, and at elevated temperatures, without loss of biological activity, and can be readily reconstituted into a particle-free solution by the addition of an appropriate diluent. An appropriate diluent can be any liquid which is biologically acceptable and in which the lyophilized powder is completely soluble. Water, particularly sterile, pyrogen-free water, is a preferred diluent, since it does not include salts or other compounds which may affect the stability of the antibody. The advantage of lyophilization is that the water content is reduced to a level that greatly reduce the various molecular events which lead to instability of the product upon long-term storage. The lyophilized product is also more readily able to withstand the physical stresses of shipping. The reconstituted product is particle free, thus it can be administered without prior filtration.

[0068] The pre-lyophilized formulation of the present invention can be lyophilized using appropriate freezing and drying parameters. For example, parameters may include a pre-freeze to holding at about 10° C. to about −10° C. for about 10-30 minutes. Freezing parameters may include freezing for −50° C. to −70° C. over a period of about 45 minutes to about 75 minutes. Parameters for the additional freeze step may include freezing at −40° C. to about −60° C. Drying parameters may include a primary drying phase temperature of about −10° C. to −30 C and pressure between about 40 mTorr to about 120 mTorr; and a secondary drying phase at about 10° C. to about 25° C., using pressure between about 40 mTorr to 120 mTorr. A preferred total cycle time is about 60 to 100 hours. A preferred Lyophilization cycle may include a pre-freeze step, a freeze step, a primary drying step, and secondary drying step. Considerations for a lyophilization cycle include freeze temperature, pressure, primary drying, secondary drying, and cycle time.

[0069] For example, preferred lyophilization cycle parameters may be as follows:

[0070] First, pre-freeze, holding at 0° C. for 15 minutes.

[0071] For freezing, ramp to −60° C. over 60 minutes. Hold at −60° C. for 60 minutes.

[0072] In an additional freeze step, ramp to −50° C. and hold for 30 minutes.

[0073] For primary drying, ramp to −15° C. over 45 minutes with a pressure drop to 50 mTorr. Hold for 54 hours at −15° C. and 50 mT pressure.

[0074] For secondary drying, ramp to 20° C. over 35 minutes and hold for 24 hours.

[0075] The total cycle time is 82 hours.

[0076] This lyophilized product retains the stability of immunological activity of the immunoglobulin, and prevents the immunoglobulins intended for administration to human subjects from physical and chemical degradation in the final product.

[0077] The lyophilized product is rehydrated at the time of use in a diluent (e.g., sterile water or saline) to yield a particle-free solution. The reconstituted antibody solution is particle-free even after prolonged storage of the lyophilized cake at ambient temperature. The reconstituted solution can be administered parenterally, preferably intramuscularly or subcutaneously, to the subject.

[0078] An important characteristic of the lyophilized product is the reconstitution time or the time taken to rehydrate the product. To enable very fast and complete rehydration, it is important to have a cake with a highly porous structure. The cake structure is a function of a number of parameters including the protein concentration, excipient type and concentration, and the process parameters of the lyophilization cycle. Generally the reconstitution time increases as the protein concentration increases, and thus, a short reconstitution time is an important goal in the development of high concentration lyophilized antibody formulations. A long reconstitution time can deteriorate the product quality due to the longer exposure of the protein to a more concentrated solution. In addition, at the user end, the product cannot be administered until the product is completely rehydrated. This is to ensure that the product is particulate-free, the correct dosage is administered, and its sterility is unaffected. Thus, quick rehydration, such as a rehydration time of less than ten minutes, offers more convenience to the patients and the physicians.

[0079] In lyophilized products, the desired dosage can be obtained by lyophilizing the formulation at the target protein concentration and reconstituting the product with the same volume as that of the starting fill volume. The desired dosage

can also be obtained by lyophilizing a larger volume of a diluted formulation, and reconstituting it with a less volume. For example, if a desired product dosage is 100 mg of protein in 1 mL of the formulation, the formulations can be lyophilized with the following liquid configurations: 1 mL of 100 mg/mL, 2 mL of 50 mg/ml, or 4 mL of 25 mg/mL protein formulation. In all cases, the final product can be reconstituted with 1 mL diluent to obtain the target protein concentration of 100 mg/mL. However, as the protein concentration in the pre-lyophilized formulation is reduced, the fill volume increases proportionately. This correspondingly increases the length of the lyophilization cycle (especially the primary drying time), and thus significantly adds to the cost of the product. For example, if 1 mL fill volume (1 mm height in vial) of frozen material takes approximately 1 hour to sublimate its free water, then 10 mL fill volume (10 mm height) of frozen product will take approximately 10 hours of primary drying time. Therefore, it is advantageous to have a concentrated pre-lyophilized formulation (with immunoglobulin concentration about 40 mg/ml to about 50 mg/ml) such that the lyophilization process will be more efficient.

[0080] The present invention provides a highly concentrated pre-lyophilized immunoglobulin formulation (about 40 mg/ml to about 50 mg/ml), which is lyophilized efficiently and effectively to a dry formulation that retains the biological, physical and chemical stability of the immunoglobulin. The dry formulation is stable for storage at least for 3 months, preferably 6 months, at room temperature. The dry formulation can be reconstituted within a short time of less than ten minutes to a particle-free solution containing about 80 mg/ml to about 160 mg/ml immunoglobulin. Such highly concentrated antibody solution is ready for parenteral administration such as intravenous, intramuscular, intraperitoneal, or subcutaneous injection.

[0081] A preferred reconstituted product comprises about 80 mg/ml to about 160 mg/ml natalizumab, more preferably about 120 mg/ml natalizumab; about 123 mg/ml sucrose; about 0.12% polysorbate 80; and about 18 mM histidine at about pH 6.0.

3. Analytical Methods

[0082] Analytical methods for evaluating the product stability include size exclusion chromatography (SEC), dynamic light scattering test (DLS), differential scanning calorimetery (DSC), iso-asp quantification, potency, UV at 340 nm, UV spectroscopy, and FTIR. SEC (J. Pharm. Scien., 83:1645-1650, (1994); Pharm. Res., 11:485 (1994); J. Pharm. Bio. Anal., 15:1928 (1997); J. Pharm. Bio. Anal., 14:1133-1140 (1986)), which measures percent monomer in the product and gives information of the amount of soluble aggregates. The potency or bioidentity of an antibody can be measured by its ability to bind to its antigen. The specific binding of an antibody to its antigen can be quantitated by any method known to those skilled in the art, for example, an immunoassay, such as ELISA (enzyme-linked immunosorbant assay). There methods are merely exemplary of methods for evaluating product stability well known to one of skill in the art. By way of example, UV at 340 nm measures scattered light intensity at 340 nm and gives information about the amounts of soluble and insoluble aggregates. UV spectroscopy measures absorbance at 278 nm and gives information of protein concentration. FTIR (Eur. J. Pharm. Biopharm., 45:231 (1998); Pharm. Res., 12:1250 (1995); J. Pharm. Scien., 85:1290 (1996); J. Pharm. Scien., 87:1069 (1998)) measures IR spectrum in the amide one region, and gives information of protein secondary structure. Particular analytical methods are further set forth in the experimental section, supra.

4. Use of the Reconstituted Formulations

[0083] The reconstituted immunoglobulin formulations of the present invention may be administered to a mammal in need of treatment with the immunoglobulin, in accordance with known methods. These methods may include, but are not limited to intravenous administration as a bolus or by continuous infusion over a period of time, by intramuscular, intraperitoneal, intracerobrospinal, subcutaneous, intra-articular, intrasynovial, intrathecal, oral, topical, or inhalation routes. In preferred embodiments, the immunoglobulin formulation is administered to the mammal by intramuscular or subcutaneous administration. A typical daily dose may range from about 1 μg/kg to about 200 mg/kg subject weight or more, more preferably from about 0.01 mg/kg to about 150 mg/kg subject weight, more preferably, from about 0.1 mg/kg to about 100 mg/kg subject weight, more preferably about 1 mg/kg to about 75 mg/kg subject weight, and most preferably about 3 mg/kg to about 6 mg/kg subject weight. Typically, the physician will administer immunoglobulin until a dosage is reached that achieves the desired effect. The progress of this therapy may be easily monitored by conventional methods and assays.

[0084] The appropriate dosage of the immunoglobulin will depend, for example, on the condition to be treated, the severity and course of the condition, whether the immunoglobulin is administered for preventive or therapeutic purposes, previous therapy, the patient's clinical history and response to the immunoglobulin, the type of immunoglobulin used, and the discretion of the attending physician. Typically, the clinician will administer immunoglobulin until a dosage is reached that achieves the desired effect. The progress of this therapy can be easily monitored by conventional assays.

[0085] The immunoglobulin is suitably administered to the patient at one time or over a series of treatments and may be administered to the patient at any time from diagnosis onwards. The immunoglobulin may be administered as the sole treatment or in conjunction with other drugs or therapies useful in treating the condition in question. As used herein, two (or more) agents are said to be administered in combination when the two agents are administered simultaneously or are administered independently in a fashion such that the agents will act contemporaneously. For example, natalizumab formulations of this invention can be administered in combination with other therapeutic agents or physical therapies for the treatment of rheumatoid arthritis, multiple sclerosis (MS), Crohn's Disease, and other alpha-4 mediated diseases.

[0086] The invention is illustrated further by the following examples, which are not to be construed as limiting the invention in scope of the specific procedures described in them.

EXAMPLES

Example 1

[0087] A comparative study of high concentration reconstituted lyophilized and liquid formulations of natalizumab was performed in cynomolgus monkeys. The results of the study showed the reconstituted lyophilized formulation of

natalizumab produced expected pharmacokinetic and pharmacodynamic profiles very similar to the liquid formulation.

[0088] High concentration liquid and reconstituted lyophilized formulations of natalizumab were evaluated to compare their respective pharmacokinetic/pharmacodynamic profiles, relative bioavailability, and local tolerability following subcutaneous (SC) and intramuscular (IM) dosing. Both the liquid (150 mg/mL) and reconstituted lyophilized (120 mg/mL) high concentration formulations were administered by each extravascular route on Day 1 and their pharmacokinetic/pharmacodynamic profiles were evaluated through Day 36. A single 30 mg dose of commercial liquid natalizumab was also administered on Day 1 to determine the relative bioavailability of the high concentration formulations. Animals in the SC and IM dose groups were administered a second injection on Day 36 and injection site biopsies were performed on Day 39 to assess local tolerability.

[0089] The test articles, commercial liquid natalizumab, liquid high concentration natalizumab and lyophilized high concentration natalizumab were supplied by Biogen Idec. The reconstituted lyophilized natalizumab reconstitution fluid, Sterile Water for Injection, was supplied as an aqueous solution. Fresh vials of the stock test articles were used on each dosing day and were formulated to yield dosing solutions at the appropriate concentrations.

[0090] Thirty experimentally naive cynomolgus monkeys (15 males and 15 females) were assigned to five dose groups as shown in the following table 1:

TABLE 1

Group No.	Number of M/F	Route.	Test Article Formulation	Dose Level (mg/animal)	Dose Volume (mL/animal)	Dose Solution Conc. (mg/ml)
1	3/3	IV	Liquid*	30	1.5	20
2	3/3	SC	Liquid**	150	1.0	150
3	3/3	IM	Liquid**	150	1.0	150
4	3/3	SC	Lyophilized***	120	1.0	120
6	3/3	IM	Lyophilized***	120	1.0	120

*Commercial liquid natalizumab;
**Liquid high concentration natalizumab;
***Reconstituted lyophilized high concentration natalizumab
IV = intravenous;
SC = subcutaneous;
IM = intramuscular;
M/F = male/female

[0091] Pharmacologic-related increases in peripheral blood lymphocytes (and to a lesser extent, eosinophils, basophils, and unclassified cells) compared to prestudy baseline values were noted in all groups and considered an expected pharmacodynamic effect of the test article. Increased levels of affected white blood cells generally persisted longer in duration in individual animals receiving the higher SC and IM doses of natalizumab (e.g., from Day 8 through Day 36) versus the lower IV dose of the commercial formulation (typically Day 8 through Day 15). However, there were no consistent or apparent differences in magnitude or duration of response as a function of liquid versus lyophilized high concentration formulations of the test article, sex, or route of administration.

[0092] Mean T_{max} was achieved most rapidly for the commercial liquid IV dose group, and more rapidly for IM groups than the SC groups across high concentration formulations. Mean C_{max} values were less than dose proportional across routes when compared to the commercial liquid IV dose group and were consistent across high concentration formulations when administered extravascularly. The mean t½ values were consistent across all dose groups irrespective of route.

[0093] Both mean AUC_{last} and AUC_{inf} were greater than dose proportional in the SC and IM dose groups irrespective of formulation indicating complete absorption (i.e. relative bioavailability of 100%), and were also quite consistent across formulations when administered extravascularly.

[0094] Expected test article-related increases in circulating lymphocyte counts, and to a lesser extent, eosinophil, basophil and unclassified cell counts were seen, as compared to prestudy baselines present in all dose groups. These results were consistent with a 4-integrin saturation profiles and were attributed to the pharmacologic effects of the natalizumab. The duration of the increases in affected white blood cell counts was dose-dependent and typically greater for the liquid high concentration natalizumab and lyophilized high concentration natalizumab-treated groups (e.g., from Day 8 up to Day 36) compared to the group receiving the commercial liquid formulation intravenously (typically Day 8 to Day 15). There were no consistent differences observed relative to the changes in these white blood cell populations between the high concentration liquid and reconstituted lyophilized formulations of natalizumab, or any difference that was considered related to the route of administration (subcutaneous or intramuscular injection) or the sex of the animals.

[0095] In summary, reconstituted lyophilized high concentration natalizumab formulations following subcutaneous and intramuscular injections in cynomolgus monkeys at doses of 120 mg (reconstituted lyophilized formulation) were well tolerated and produced expected pharmacologic-related increases in peripheral blood lymphocyte counts that were comparable to, but of slightly greater persistence than after a single 30 mg intravenous dose of the commercial liquid formulation.

Example

[0096] Natalizumab is currently delivered as an IV infusion over a period of 1 to 2 hours. This requires the patient to visit a hospital or specialized infusion center. In order to make delivery of natalizumab more convenient, a subcutaneous administration is desired. It was advantageous to develop a lyophilized formulation from a bulk drug substance at a lower concentration that could then be reconstituted at a higher

concentration. The present study described here was designed to screen the effect of various starting and final protein concentrations on stability using sucrose as an excipient (Study A). The second part of the study was designed to screen other well-known lyo-protectants and excipients for their effects on the protein stability (Study B). Efforts were also made to examine solutions that would be feasible with regards to manufacturability in terms of fill volumes and reconstitution volumes.

[0097] In Study A, four formulations were prepared to examine the effect of the starting and final protein concentration on real time and accelerated stability for both the pre-lyophilized bulk and the lyophilized cake. All four of the pre-lyophilized formulations exhibited sufficient stability to be used as pre-lyophilized bulks for hold times of up to 6 months at 5° C. Two lyophilized formulations exhibited sufficient formulation characteristics and stability to be considered as candidates for further formulation development. One of these formulations consisted of a starting concentration of 40 mg/mL and a reconstituted concentration of 100 mg/mL with a 1:1 weight ratio of protein to sucrose. The second candidate formulation contained a 50 mg/mL starting concentration and a reconstitution concentration of 200 mg/mL with a 2:1 weight ratio of protein to sucrose. Both formulations contained a histidine buffer and polysorbate 80.

[0098] In addition, a high concentration liquid formulation with the same excipients profile as the current natalizumab (Tysabri™) formulation was prepared. At 5° C. this formulation demonstrated sufficient stability to aggregate formation to be considered a candidate for further development, although the rate of deamidation was more rapid than in the lyophilized formulations. At accelerated temperatures this formulation showed a tendency to form low molecular weight degradation products, which were not observed to the same extent in the lyophilized formulations.

Experimental Design

Materials

[0099] Natalizumab used for these studies was prepared from natalizumab supplied by Biogenldec, manufactured on February 2003. This material had been formulated and vialed, therefore the material needed to be pooled and the polysorbate 80 removed prior to use in these formulation studies. Briefly, this was accomplished by diafiltration into a low ionic strength, high pH (10 mM tris, 10 mM NaCl, pH 8.5) buffer. The material was bound to a DEAE-Sepharose column under these conditions and then eluted using 10 mM sodium phosphate, 140 mM NaCl, at pH 6. The column eluate was then diafiltered into 6 mM histidine, pH 6 and concentrated to between 70 and 100 mg/mL prior to further formulation.

Chemicals and Reagents

[0100] All chemicals and reagents used in this study, except as noted were purchased from VWR and were ACS grade or better. USP grade reagents were used as excipients when available. Polysorbate 80 was purchased from Sigma (Cat # P6474), and was vegetable derived and low peroxide.

Formulations for Study A

[0101] The following formulations were prepared by diluting stock solutions of the excipients and active to the desired concentrations as indicated in Table 2: Study A formulation parameters. All formulations were prepared at pH 6.

TABLE 2

Study A formulation parameters.

Formulation ID	Pre-lyo Concentrations	Reconstituted Concentrations
3944-18A	20 mg/mL Ab, 20 mg/mL sucrose, 6 mM his, 0.02% PS80	100 mg/mL Ab, 100 mg/mL sucrose, 30 mM his, 0.1% PS80
3944-18B	40 mg/mL Ab, 40 mg/mL sucrose, 6 mM his, 0.02% PS80	100 mg/mL Ab, 100 mg/mL sucrose, 15 mM his, 0.05% PS80
3944-18C	50 mg/mL Ab, 25 mg/mL sucrose, 6 mM his, 0.02% PS80	200 mg/mL Ab, 100 mg/mL sucrose, 24 mM his, 0.08% PS80
3944-18D	75 mg/mL Ab, 40 mg/mL sucrose, 6 mM his, 0.02% PS80	225 mg/mL Ab, 120 mg/mL sucrose, 18 mM his, 0.06% PS80
3944-18L	100 mg/mL, 10 mM sodium phosphate, 140 mM NaCl, pH 6, .02% PS80	NA

Abbreviations:

Ab = antibody,

his = histidine,

PS80 = polysorbate 80

Formulations for Study B

[0102] The following formulations were prepared by diluting stock solutions of the excipients and active to the desired concentrations as shown in Table 3: Study B formulation parameters. All formulations were at pH 6.

TABLE 3

Study B formulation parameters.

Formulation ID	Pre-lyo Concentrations	Reconstituted Concentrations
3976-4C	50 mg/mL Ab, 25 mg/mL sucrose, 6 mM his, 0.02% PS80	200 mg/mL Ab, 100 mg/mL sucrose, 24 mM his, 0.08% PS80
3976-4G	50 mg/mL Ab, 25 mg/mL sucrose, 15 mM NaCl, 6 mM his, 0.02% PS80	200 mg/mL Ab, 100 mg/mL sucrose, 60 mM NaCl, 24 mM his, 0.08% PS80
3976-4H	50 mg/mL Ab, 25 mg/mL sucrose, 6 mM his, 0.02% PS20	200 mg/mL Ab, 100 mg/mL sucrose, 24 mM his, 0.08% PS20
3976-4I	50 mg/mL Ab, 25 mg/mL trehalose, 6 mM his, 0.02% PS80	200 mg/mL Ab, 100 mg/mL trehalose, 24 mM his, 0.08% PS80
3976-4K	40 mg/mL Ab, 25 mg/mL sucrose, 6 mM his, 0.02% PS80	160 mg/mL Ab, 100 mg/mL sucrose, 24 mM his, 0.08% PS80

Abbreviations:
Ab = antibody,
his = histidine,
PS80 = polysorbate 80

Methods

Preparation of Formulations

[0103] The solutions were sterile filtered and filled as indicated into sterile glass vials. All samples for pre-lyophilized analysis and 3944-18L were filled at 0.5 mL into 2 cc vials, stoppered and capped. Formulas to be lyophilized were filled at the following volumes into 5 cc Kimble vials: Formulation 3944-18A—2.5 mL, Formulation 3944-18B—1.25 mL, Formulation 3944-18C—2 mL, Formulation 3944-18D—1.5 mL. All formulations for Study B were filled at 2 mL in 5 cc Kimble vials.

Lyophilization Cycles

[0104] For Study A, the vials were frozen at −20° C. The lyophilizer malfunctioned and the temperature was dropped to −70° C. for the weekend. Subsequent attempts to restart the lyophilization cycle resulted in the temperature rising to 3-4° C. prior to re-freezing. The lyophilizer was restarted and the cycle continued. Primary drying was performed at −20° C. for 20 hours with 100 mTorr vacuum. The temperature was then ramped to 20° C. over 3 hours and held for 30 hours at 100 mTorr for secondary drying.

[0105] For Study B, the vials were frozen at −50° C. for 2 hours to ensure uniform freezing. The temperature was then taken to −40° C. for 20 min under vacuum of 100 mTorr. Then the temperature was ramped to −25° C. over 20 minutes with 100 mTorr vacuum and primary drying proceeded for 20 hours. The shelf temperature was ramped slowly to 20° C. over 10 hours to begin secondary drying at 100 mTorr, and then held at 20° C. for 4 hours.

Study Set-Up

[0106] Vials of pre-lyophilized liquid, the high concentration liquid control, and lyophilized cakes were placed at 5, 30 and 40° C. Samples stored at 40° C. were assayed at 2, 4, 8 and 12 weeks. Samples stored at 30° C. were assayed at 3, 6, 9, and 12 weeks. Samples stored at 5° C. were assayed at 4, 8, and 12 weeks. Additional vials at 30° and 5° C. were analyzed at 6 months and 1 year for some formulations. All formulations were assayed pre- and post-lyophilization at time zero.

Assays

[0107] The samples were assayed by the following methods. Not all assays were performed at all time points. With the exception of the zero time point for pre-lyophilized samples, duplicate vials were sampled for each assay.

Appearance by Visual Examination

[0108] All samples were examined visually and their appearance recorded. Lyophilized cakes were examined for color, uniformity, robustness and evidence of meltback. Liquid and reconstituted samples were examined for color, clarity and presence of particulates.

Residual Moisture and Reconstitution Time

[0109] Lyophilized cakes were assayed for residual moisture using Karl Fischer at the zero time point (BOP 000-01290). Reconstitution time was measured by adding the appropriate volume of DI water, followed by gentle swirling. The time for the cake to completely dissolve was recorded (EOP 000-01292).

Concentration

[0110] The concentration of all samples was measured. Samples were diluted to 1 mg/mL using natalizumab placebo. The UV absorbance was scanned from 400 to 240 nm using a Varian 300Bio Spectrophotometer and 1 cm pathlength cuvette at 200 nm/minute. The absorbance at lambda max was recorded and the concentration was determined by dividing that value by 1.498 (the absorptivity coefficient for natalizumab) and adjusting by the appropriate dilution.

Turbidity

[0111] The absorption from 300 to 400 nm of a neat sample was measured using a 10 mm small volume cuvette (Starna Cells Inc. Cat #16.160-Q-10\Z20). The value recorded at 360 nm was reported.

Size Exclusion Chromatography

[0112] The amount of monomer, high molecular weight species, dimer and low molecular weight species were determined using a modification of Biogen SOP 22d.505. The samples were loaded to the column neat and the load volume was adjusted to allow a mass of approximately 400 μg on the column. The mass of the reference material load was also adjusted to be comparable. Detection was recorded at both 215 and 280 nm, however the main peak was off scale at 215 nm, so the 280 nm trace was used for calculations reported here.

Cation Exchange Chromatography

[0113] Cation exchange chromatography was performed. Due to differences in the chromatography system, the gradient was modified slightly to allow the main peak to elute between 9 and 12 minutes. Since the system used was a binary pump the high salt wash was only performed after each set of analyses. There was no evidence in the high salt wash of any peaks eluting with late retention times. Since the high salt wash was not performed after each sample, the re-equilibration time was shortened to 7 minutes.

Potency

[0114] The potency of selected samples was analyzed by the VCAM lysate assay (AAM 001-00965) and by the Jurkat cell assay (AAM 001-00700).

Results of Study A

[0115] This study was designed as a screening study to examine the effect of both the initial protein concentration and the final protein concentration on lyophilized cake parameters, reconstitution time and stability. Preliminary studies had shown that sucrose provided sufficient short-term lyo-protectant properties to natalizumab, while mannitol did not. For this reason, initial screening was performed using sucrose as a lyo-protectant. Early studies had also shown that the optimal pH for natalizumab, was pH 6. Phosphate, citrate, and histidine buffers are most commonly used for buffering at this pH. Phosphate buffer is not optimal for use in lyophilization of proteins due to its pH shift upon freezing. Citrate buffer has been implicated in pain on injection in some subcutaneous formulations. Consequently, histidine was chosen as the preferred buffer species. The initial concentration was fixed at 6 mM for ease of preparation of formulations and to maintain the final concentration at or below 30 mM after reconstitution. For Study 3A, the polysorbate 80 concentration was maintained at 0.02% in the pre-lyophilized solutions as this had been shown to give sufficient protection to the protein and also to maintain final concentrations at or below 0.1%. The sucrose concentration was selected to maintain between a 1:1 and 2:1 weight ratio of protein to sugar while still maintaining a final solution that would be close to isotonic.

Pre-Lyophilized and Liquid Formulations

[0116] The tables in the appendix contain all results recorded for all formulations. On visual examination, all formulations appeared colorless and clear to opalescent, without any visual particulates. As expected the opalescence increased somewhat with increasing protein concentration. None of the samples showed a change in protein concentration within the variation of the analysis and no trend was observed. The turbidity, as measured by absorbance at 360 nm, showed no change at 5° C. over 6 months or at 30° C. over 12 weeks of the study. The 40° C. pre-lyophilized samples showed a slight increase of turbidity with time for the samples at 40, 50 and 75 mg/mL. The 20 mg/mL pre-lyophilized sample and high concentration liquid did not demonstrate this trend in the 40° C. samples.

[0117] The formation of dimer, high molecular weight aggregate and low molecular weight species was monitored for all formulations. The tabular results are shown in the tables in the appendix. FIGS. **1** and **2** show the formation of high molecular weight species at 30° and 40° C. At 5° C. there was no change in the level of high molecular weight species in any formulation for the 6 months of storage.

[0118] The 5° C. data is shown herein. The results at 30° C. (FIG. **1**) showed no trend in formation of high molecular weight species for any of the pre-lyophilized formulations after 12 weeks of storage. The high concentration liquid formulation showed a definite increase in high molecular weight species over the 6 month storage period at 30° C.

[0119] At 40° C., the formation of high molecular weight species did not appear to begin until after 4 weeks of storage in the pre-lyophilized formulations. Then the amount of high molecular weight species continues to increase. The high concentration liquid formulation at high ionic strength shows lower starting percentage of high molecular weight species, but the amount appears to increase at a constant rate over the 3 month study at 40° C.

[0120] FIGS. **3** and **4** show the formation of low molecular weight species at 30 and 40° C. in the pre-lyophilized solutions. There was only a very small change in the level of low molecular weight species at 30° C. during 3 months of storage, but a definite upward trend was seen. Only the high concentration liquid was assayed at 6 months. At that time there was a considerable amount of low molecular weight species present, almost 6%.

[0121] There was a definite trend of formation of low molecular weight species during storage at 40° C. The rate of formation at this temperature appears to be somewhat concentration dependent as the higher concentration samples show a more rapid formation. Also, the formation of low molecular weight species at 30° and 40° C. appears to precede at a faster rate than the formation of high molecular weight species making this an important degradation pathway in the liquid samples.

[0122] There was very little change in the percentage of low molecular weight species over a 6 month time period for the samples stored at 5° C. This data is shown in the appendices, but not graphed here. All of the pre-lyophilized formulations went from an initial level of approximately 0.6-0.9% to 0.15% at 6 months. The high concentration liquid did not show any low molecular species even after 6 months of storage at 5° C.

[0123] FIGS. **5**, **6** and **7** show the total loss of monomer at each temperature due to formation of both high and low molecular weight species. At 2-8° C. there was essentially no change in the percent monomer. This would indicate that any of these formulations would be suitably stable as a pre-lyophilized formulation for storage up to 6 months at 2-8° C. The high concentration liquid formulation also shows no change at 2-8° C. The 30° C. samples show a very slight decrease in monomer. This change is due to formation of the low molecular weight species. This also indicates that any of these for-

mulations would exhibit sufficient stability at ambient temperatures to allow for processing. The high concentration liquid shows a loss of monomer that is concurrent with the increase in low molecular weight species at 6 months. All formulations showed loss of monomer at 40° C. over the three-month period tested. The rate of loss appears to correlate roughly with the protein concentration with the liquid at 100 mg/mL and the 75 mg/mL pre-lyophilized formulations showing the most rapid rate of loss. Further investigation into the mechanism of degradation due to formation of the low molecular weight species could provide better stabilization to this route of degradation.

[0124] Selected samples were analyzed by cation exchange chromatography. In all cases the results showed a shift towards a more acidic species (deamidation) with storage based on time and temperature. There was no difference among the various pre-lyophilized formulations. Since deamidation is generally influenced by pH, ionic strength and certain buffer species, this result would be expected. The degradation of the high concentration liquid formulation was not significantly different from the pre-lyophilized formulations at 5° C. However, it showed significantly faster degradation at both 30 and 40° C. This is most likely due to the high ionic strength and the presence of phosphate buffer.

Lyophilized Formulations

[0125] Tables 5-12 show the results for the stability of the samples stored as lyophilized formulations at 5, 30 and 40° C. All formulations were stored at 40° C. for 12 weeks, 30 and 5° C. for 6 months. In addition, Formulations 3944-18B and 3944-18C were analyzed after 1 year at 30 and 5° C.

[0126] The formulations were analyzed at the initial time point for residual moisture. The residual moisture was higher than desired, probably due to the problems experienced during the lyophilization cycle. The residual moisture was in the 5-6% range for these samples.

[0127] The time for reconstitution was measured and was directly correlated with the starting and final protein concentration. The cakes that were lyophilized from 75 mg/mL protein solutions took an average of 15-20 minutes to reconstitute. Samples lyophilized from 50 mg/mL took an average of 6-7 minutes, from 40 mg/mL took 5-6 minutes and from 20 mg/mL took 4-5 minutes. The values were variable but did not show any trend with regard to storage time or temperature.

[0128] The reconstituted vials were examined for appearance. All samples were clear to opalescent, colorless and free of particles. Two formulations that were stored at 30° C. for 1 year showed some slight yellow color. Turbidity was measured as a function of absorbance at 360 nm. All formulations showed a rise in turbidity when stored at 40° C. over a 12-week period. All formulations showed a less significant rise in turbidity when stored at 30° C. for up to 12 months. All formulations showed a slight rise in turbidity when stored at 5° C. for up to a year, except Formulation 3944-18C. (See tables in Appendix E-H). No change in protein concentration was observed outside the normal variation inherent in hand filling and reconstitution of the material.

[0129] The reconstituted samples were analyzed by size exclusion chromatography for formation of both low molecular and high molecular weight degradation products. Low molecular weight degradation was apparent at some time points, but there did not seem to be a trend for formation. The amount at all time points was lower than 0.2% in any sample, which is considered the limit of detection for the assay by Biogenldec. The main pathway of degradation was through formation of dimer and higher order aggregates. The loss of monomer with time is shown in FIGS. **8**, **9** and **10**. At 40° C. storage there is some loss of monomer with the most rapid loss in Formulations 3944-18D and 3944-18C. Formulations 39944-18B and 3944-18A show a much less pronounced downward trend. The same order of trending is seen in the 30° C., with 3944-18D and 3944-18C showing a more rapid loss of monomer. None of the formulations show a loss of monomer at 5° C. for up to 6 months for 3944-18A and 3944-18D, and up to a year for 3944-18B and 3944-18C.

[0130] Selected samples were analyzed by cation exchange chromatography. There did not appear to be any differences among the formulations. At 5° C. there was a shift from 71% main peak to 66% main peak. The percent of acid peaks remained fairly constant over time, but the percent of basic peaks increased with time from 8-10% at the initial time point to 14-15% after one year. The 30 and 40° C. samples exhibited the same trend with the percent basic peak reaching 18-19% after one year at 30° C. and 22-26% after 3 months at 40° C. Additional work would be needed to characterize this reaction pathway and to determine the origin of the degradation species.

Results of Study B

Selection of Formulations

[0131] Study B was set up to study the effect of excipients in addition to sucrose on the stability of natalizumab and to verify results seen in Study A. Based on the results from Study A it was determined that a starting concentration of 40-50 mg/mL was optimal for both good cake formation and reconstitution characteristics. The protein to sugar ratio was fixed at 2:1 weight ratio, with an initial concentration of 50 mg/mL and the reconstitution concentration target was 200 mg/mL. In addition, one formulation was examined with a starting concentration of 40 mg/mL and a target reconstitution concentration of 160 mg/mL. This formulation also had a protein to sugar ratio of 1.6:1 weight ratio.

[0132] Formulation 3976-4C contained the same formulation as 3944-18C in Study A. The stability of the pre-lyophilized solution was examined in study A and not repeated for B. Reports from the literature have indicated that a low level of sodium chloride added to high concentration protein solutions could help reduce the viscosity of these solutions. Formulation 3976-4G had 15 mM NaCl added to the pre-lyophilization formula to examine the effect of NaCl. Polysorbate 20 (PS20) is frequently used in protein formulations instead of polysorbate 80 (PS80). In formulation 3976-4H, the 0.02% PS80 was replaced with an equal amount of PS20. In formulation 3976-4I, an equal amount of trehalose was substituted for the sucrose.

Pre-Lyophilized Formulations

[0133] The pre-lyophilized formulations were analyzed for appearance. No significant changes to the appearance occurred for any of the solutions regardless of temperature of storage. They were all colorless and slightly opalescent with no appearance of particulates. There was no change in the protein concentration in any of the formulations. The turbidity was measured at all time points. For formulation 3976-4G, the initial turbidity measurement was high, but remained fairly constant at subsequent time points. No trend towards change in turbidity was observed in any of the formulations,

although the value measured for 3976-4G continued to be higher at all temperatures than the other formulations.

[0134] Loss of monomer due to formation of dimer and higher molecular weight aggregates and due to low molecular fragments was monitored. As seen previously, there was no change in the percent monomer for any of the samples up to 3 months at 5° C. Formulation 3976-4K was also analyzed at 6 months at 5° C. and showed no change in percent monomer. FIGS. **11** and **12** show the formation of low molecular weight species for each formulation at 30 and 40° C., respectively. As seen previously, there was substantial formation of low molecular weight species at 40° C. in all formulations with the rate of formation slightly lower in the 3976-4K, which had a lower protein concentration. These results were comparable to those seen in Study A. Otherwise there seemed to be no effect of excipients on this reaction. At 30° C., there was a slight rise in low molecular weight species. This rate was also comparable to that seen previously in Study 3A reaching between 0.2 to 0.4% after 12 weeks.

[0135] There was a slight increase in high molecular weight species at 40° C. for all the formulations except 3976-4H, which contained PS20 (FIG. **13**). There was no change in high molecular weight for any formulations at the other temperatures. It appeared that all formulations were stable to formation of aggregate, and the major degradation pathway was formation of low molecular weight species at elevated temperature. Any of these formulations would be sufficiently stable for further development as a pre-lyophilized bulk drug.

[0136] Cation exchange chromatography was performed on all formulations at the initial time point, but only on 3976-4K after 6 months at 5° C. storage. As seen in Study A, there was a shift to more acidic species on storage. This degradation is driven by pH and temperature.

Lyophilized Formulations

[0137] All samples were analyzed for moisture, cake appearance and reconstitution time at the initial time point. The cake appearance for all cakes was acceptable. The moisture levels were slightly lower than in Study A, generally between 3 and 4%, except for formulation 3976-4I, which had 5.4% moisture. Reconstitution time for all samples at all time points and temperatures were generally acceptable and below 10 minutes with a few exceptions taking between 10 and 14 minutes. Formulation 3976-4K, which had the lowest starting protein concentration also showed more rapid reconstitution times. Upon reconstitution all samples were colorless and slightly opalescent to opalescent for up to 12 weeks at all temperature with the exception of 3976-4I and 3976-4G. At 40° C. and 12 weeks, 3976-4I was very opalescent. Beginning at 6 weeks at 30° C. and 8 weeks for 5 and 40° C., 3976-4G was very opalescent. The addition of the NaCl did seem to reduce the viscosity of the formulation as seen by a tendency to less foaming and bubble formation during reconstitution, however, it also showed a significant increase in the opalescence of the solution. Formulation 3976-4C was analyzed at 6 months and 1 year at 5° C. At 5° C. after one year, 3976-4C showed a slight yellow color. Formulation 3976-4K was analyzed at 6 months and 1 year at 5 and 30° C. Formulation 3976-4K showed a slight yellow color at 30° C. after 6 months of storage, but not after 1 year at 5° C.

[0138] Samples were analyzed by size exclusion chromatography for up to 3 months at 40° C. At 5 and 30° C. samples were analyzed up to 3 months, and then an analysis was done at the one-year time point. In addition, formulations 3976-4C and 3976-4K were analyzed at 6 months as well. The amount of low molecular weight species was less than 0.2% in all samples. The major pathway of degradation was due to the formation of dimer and higher molecular weight species. FIGS. **14**, **15** and **16** show the loss of monomer due to formation of aggregate for each temperature. It is apparent at all the temperatures that the loss of monomer in Formulation 3976-4I, which contains trehalose, is more rapid than the other formulations. The formulations containing PS20 and NaCl showed comparable degradation to the formulations containing sucrose with PS80. Formulation 3976-4K showed the least rapid loss of monomer at all temperatures. This formulation had a lower starting protein concentration, a lower reconstitution concentration and a higher sucrose to protein ratio.

[0139] Selected samples were analyzed by cation exchange chromatography. The results from this assay were somewhat variable, but all formulations appeared to remain stable to changes in charge distribution at 5° C. At 40° C. all formulations showed a decrease in the main peak and increases in both the acidic and basic species. This trend was also observed in the samples from Formulation 3976-4K, which were analyzed after 1 year storage at 30° C.

[0140] Formulation 3976-4K stored at 5 and 40° C. was analyzed at the 8 week time point in both the VCAM lysate and the Jurkat cell assays for potency. The results are shown in the Table.

TABLE 4

	Potency Assay Results	
Sample/Assay	VCAM lysate	Jurkat
3976-4K - 5° C.	126%	98.2

Formation Screening Studies for Development of a High Concentration Lyophilized Formulation for Natalizumab

[0141]

3976-4K - 40° C.	124.3%	104%

Conclusions

Pre-Lyophilized Bulk Formulation

[0142] In the high concentration liquid formulation there was no loss of monomer for up to 6 months at 5° C., however, there was an increase in acidic species probably due to deamidation. For 6 months at 30° C. and 3 months at 40° C., this formulation showed loss of monomer through formation of both high and low molecular weight degradation species. A high protein concentration liquid in the current formulation may not exhibit sufficient long-term stability to be suitable as a commercial formulation without further optimization.

[0143] None of the pre-lyophilized formulations showed any significant loss of monomer when stored at 5° C. for 3 to 6 months. The change in the amount of deamidation for these formulations was comparable to that seen in the high concentration liquid. The formulations stored at 30° C. showed little or no increase in dimer and high molecular weight aggregates for up to 3 months, however there was an increase in the

amount of low molecular weight fragmentation species formed. At 40° C., the increase in low molecular weight species was more rapid than the increase in high molecular weight species. The rate of increase of the low molecular weight species appeared to be correlated with the protein concentration.

[0144] In general, formulations containing a protein concentration of 50 mg/mL or less with histidine, sucrose, and PS80 appeared to demonstrate sufficient stability for pre-lyophilized bulk.

Lyophilized Formulations

[0145] Formulations that were lyophilized from 50 mg/mL or less and reconstituted to 100 to 200 mg/mL showed good cake formation and acceptable reconstitution times at all temperatures and time points. Formulations containing histidine, sucrose, and PS80 had no loss of monomer up to one year at 5° C. Some of these formulations showed a slight increase in basic species after storage for a year; however, this increase is hard to quantitate given the variability in the assay. The major route of degradation of the protein at elevated temperatures was formation of dimer and higher molecular weight aggregates. Addition of NaCl decreased the viscosity but resulted in increased turbidity of the solution. Substitution of PS20 for PS80 appeared to have no effect on the stability, while substitution of trehalose for sucrose increased the rate of formation of aggregate.

[0146] A lyophilized formulation containing sucrose, histidine, and polysorbate 80 with natalizumab demonstrates sufficient stability to move into pre-clinical and early clinical studies. Additional studies will be performed to optimize the starting protein concentration, the sucrose to protein ratio, the reconstituted protein concentration and the lyophilization cycle. In addition the stability of the reconstituted samples will be examined.

TABLE 5

Pre-Lyo
20 mg/mL Natalizumab, 20 mg/mL Sucrose, 6 mM Histidine, 0.02% PS-80
Manufactured:
Testing Start Date: 0.5 mL fill

Time Point/ Temp.	Vial	Appearance	Conc. (mg/mL)	Turbidity A360 nm	% Monomer	% Dimer	% Aggregate	% LMW	SEC Ref Std & Avg. area count	% Acidic % Main % Basic
0	1	N/A	21.0	0.041	98.29	1.01	0.63	0.06	RS007-001 3448	18.1 69.6 12.4
	2	N/A	21.0			1.02	0.63	0.06		18.6 70.6 10.9
4 wk, 5 C.	1	clear, v. sl opal, colorless	N/A	0.035	98.43	0.99	0.49	0.09	RS007-001 33690	N/A
	2	clear, v. sl opal, colorless		0.037	98.44	0.98	0.49	0.09		
8 wk, 5 C.	1	clear, colorless	N/A	0.021	98.43	0.98	0.47	0.11	RS007-001 33245	N/A
	2	clear, colorless		0.020	98.50	0.97	0.45	0.07		
12 wk, 5 C.	1	clear, colorless	20.7	0.025	98.48	1.01	0.42	0.09	RS007-001 33881	N/A
	2	clear, colorless	20.9	0.027	98.48	1.01	0.43	0.08		
6 mo, 5 C.	1	clear, colorless	20.5	0.035	98.49	1.01	0.36	0.14	REF025 (RS007-001) 33759	24.0 63.9 63.9
	2	clear, colorless	20.5	0.033	98.47	1.01	0.37	0.15		23.9 63.9 12.2
					30° C.					
0	1	N/A	21.0	0.041	98.29	1.01	0.63	0.06	RS007-001 3448	18.1 69.6 12.4
	2	N/A	21.0		98.30	1.02	0.63	0.06		18.6 70.6 10.9
3 wk, 30 C.	1	clear, v. sl opal, colorless	N/A	0.029	98.46	0.93	0.48	0.13	RS007-001 33707	N/A
	2	clear, v. sl opal, colorless		0.044	98.48	0.93	0.48	0.12		
6 wk, 30 C.	1	clear, colorless	N/A	0.028	98.40	0.94	0.49	0.17	RS007-001 33758	N/A
	2	clear, colorless		0.027	98.42	0.95	0.48	0.16		
9 wk, 30 C.	1	clear, colorless	N/A	0.034	98.45	0.93	0.43	0.19	RS007-001 33757	N/A
	2	clear, colorless		0.031	98.45	0.93	0.43	0.19		
12 wk, 30 C.	1	clear, colorless	21.0	0.018	98.37	0.99	0.39	0.24	RS007-001 33897	N/A
	2	clear, colorless	20.8	0.024	98.38	0.99	0.40	0.23		
					40° C.					
0	1	N/A	21.0	0.041	98.29	1.01	0.63	0.06	RS007-001 3448	18.1 69.6 12.4

TABLE 5-continued

Pre-Lyo
20 mg/mL Natalizumab, 20 mg/mL Sucrose, 6 mM Histidine, 0.02% PS-80
Manufactured:
Testing Start Date: 0.5 mL fill

Time Point/ Temp.	Vial	Appearance	Conc. (mg/mL)	Turbidity A360 nm	% Monomer	% Dimer	% Aggregate	% LMW	SEC Ref Std & Avg. area count	% Acidic % Main % Basic
	2	21.0	98.30		0.63	0.06	21.0	98.30		18.6 70.6 10.9
2 wk, 40 C.	1	clear, v. sl opal, colorless	N/A	0.060	98.33	0.96	0.49	0.22	RS007-001 33834	N/A
	2	clear, v. sl opal, colorless		0.045	98.34	0.95	0.49	0.22		
4 wk, 40 C.	1	clear, v. sl opal, colorless	N/A	0.040	98.20	1.00	0.45	0.35	RS007-001 33690	N/A
	2	clear, v. sl opal, colorless		0.043	98.03	1.04	0.49	0.44		
8 wk, 40 C.	1	clear, colorless	N/A	0.060	93.93	1.61	0.65	3.81	33693	N/A
	2	clear, colorless		0.057	94.15	1.57	0.64	3.63		
12 wk, 40 C.	1	clear, colorless	20.8	0.068	91.12	2.01	1.04	5.83	RS007-001 33891	63.6 20.7 15.8
	2	clear, colorless	20.5	0.055	92.00	1.76	1.03	5.22		64.7 19.2 16.1

TABLE 6

Pre-Lyo
40 mg/mL Natalizumab, 40 mg/mL Sucrose, 6 mM Histidine, 0.02% PS-80
Manufactured:
Testing Start Date: 0.5 mL fill

Time Point/ Temp.	Vial	Appearance	Conc. (mg/mL)	Turbidity A360 nm	% Monomer	% Dimer	% Aggregate	% LMW	SEC Ref Std & Avg. area count	% Acidic % Main % Basic
0	1	NIA	40.1	0.053	98.26	1.02	0.65	0.07	RS007-001 3448	19.0 70.9 10.0
	2	N/A	40.1		98.26	1.02	0.64	0.07		18.5 71.1 10.4
4 wk, 5 C.	1	clear, sl opal, colorless	N/A	0.054	98.38	0.99	0.52	0.10	RS007-001 33690	N/A
	2	clear, sl opal, colorless		0.054	98.37	0.99	0.53	0.11		
8 wk, 5 C.	1	sl opal, colorless	N/A	0.050	98.42	1.01	0.48	0.09	RS007-001 33245	N/A
	2	sl opal, colorless		0.038	98.44	0.98	0.46	0.11		
12 wk, 5 C.	1	v. sl opal, colorless	39.3	0.059	98.43	1.05	0.42	0.10	RS007-001 338881	21.4 69.1 9.4
	2	v. sl opal, colorless	39.5	0.043	98.45	1.02	0.44	0.09		21.5 70.0 8.4
6 mo, 5 C.	1	v. sl opal, colorless	39.1	0.055	98.47	1.01	0.37	0.15	REF025 (RS007-001) 33759	25.2 62.8 11.9
	2	v. sl opal, colorless	39.5	0.052	98.71	0.95	0.34	—		25.5 63.0 11.5
					30° C.					
0	1	NIA	40.1	0.053	98.26	1.02	0.65	0.07	RS007-001 3448	19.0 70.9 10.0
	2	N/A	40.1		98.26	1.02	0.64	0.07		18.5 71.1 10.4

TABLE 6-continued

Pre-Lyo
40 mg/mL Natalizumab, 40 mg/mL Sucrose, 6 mM Histidine, 0.02% PS-80
Manufactured:
Testing Start Date: 0.5 mL fill

Time Point/ Temp.	Vial	Appearance	Conc. (mg/mL)	Turbidity A360 nm	% Monomer	% Dimer	% Aggregate	% LMW	SEC Ref Std & Avg. area count	% Acidic % Main % Basic
3 wk, 30 C.	1	clear, v. sl opal, colorless	N/A	0.042	98.45	0.95	0.46	0.13	RS007-001 33707	N/A
	2	clear, v. sl opal, colorless		0.055	98.45	0.95	0.46	0.13		
6 wk, 30 C.	1	clear, colorless	N/A	0.056	98.41	0.96	0.47	0.17	RS007-001 33758	N/A
	2	clear, colorless		0.053	98.42	0.96	0.46	0.16		
9 wk, 30 C.	1	sl opal, colorless	N/A	0.058	98.38	0.99	0.41	0.22	RS007-001 33757	N/A
	2	sl opal, colorless		0.060	98.40	0.98	0.40	0.22		
12 wk, 30 C.	1	v. sl opal, colorless	39.6	0.042	98.33	1.04	0.36	0.26	RS007-001 33897	46.3 8.0 45.7
	2	v. sl opal, colorless	40.7	0.042	98.33	1.03	0.37	0.26		45.8 46.5 7.7
					40° C.					
0	1	NIA	40.1	0.053	98.26	1.02	0.65	0.07	RS007-001 3448	19.0 70.9 10.0
	2	N/A	40.1		98.26	1.02	0.64	0.07		18.5 71.1 10.4
2 wk, 40 C.	1	clear, v. sl opal, colorless	N/A	0.071	98.30	0.97	0.48	0.25	RS007-001 33834	N/A
	2	clear, v. sl opal, colorless		0.062	98.30	0.97	0.48	0.25		
4 wk, 40 C.	1	clear, sl opal, colorless	N/A	0.065	97.92	1.04	0.47	0.58	RS007-001 33690	N/A
	2	clear, sl opal, colorless		0.065	97.90	1.05	0.47	0.58		
8 wk, 40 C.	1	sl opal, colorless	N/A	0.084	93.68	1.41	0.68	4.22	RS007-001 33693	N/A
	2	sl opal, colorless		0.080	93.56	1.36	0.72	4.36		
12 wk, 40 C.	1	v. sl opal, colorless	38.8	0.100	89.97	1.76	1.20	7.07	RS007-001 33891	69.2 16.5 14.4
	2	v. sl opal, colorless	39.1	0.103	90.02	1.83	1.47	6.69		69.2 17.2 13.6

TABLE 7

Pre-Lyo
40 mg/mL Natalizumab, 40 mg/mL Sucrose, 6 mM Histidine, 0.02% PS-80
Manufactured:
Testing Start Date: 0.5 mL fill

Time Point/ Temp.	Vial	Appearance	Conc. (mg/mL)	Turbidity A360 nm	% Monomer	% Dimer	% Aggregate	% LMW	SEC Ref Std & Avg. area count	% Acidic % Main % Basic
0	1	N/A	52.1	0.074	98.19	1.03	0.71	0.07	RS007-001 3448	18.6 71.0 10.4
	2	N/A	51.5		98.18	1.03	0.71	0.08		18.4 71.2 10.4
4 wk, 5 C.	1	clear, sl opal, colorless	N/A	0.070	98.31	1.01	0.57	0.10	RS007-001 33690	N/A
	2	clear, sl opal, colorless		0.068	98.33	1.01	0.56	0.10		
8 wk, 5 C.	1	sl opal, colorless	N/A	0.062	98.40	1.00	0.50	0.09	RS007-001 33245	N/A
	2	sl opal, colorless		0.056	98.37	1.01	0.52	0.10		

TABLE 7-continued

Pre-Lyo
40 mg/mL Natalizumab, 40 mg/mL Sucrose, 6 mM Histidine, 0.02% PS-80
Manufactured:
Testing Start Date: 0.5 mL fill

Time Point/ Temp.	Vial	Appearance	Conc. (mg/mL)	Turbidity A360 nm	% Monomer	% Dimer	% Aggregate	% LMW	SEC Ref Std & Avg. area count	% Acidic % Main % Basic
12 wk, 5 C.	1	sl opal, colorless	50.3	0.054	98.42	1.04	0.45	0.09	RS007-001 33881	21.9 66.2 11.9
	2	sl opal, colorless	50.6	0.057	98.41	1.04	0.46	0.09		22.2 68.2 9.6
6 mo, 5 C.	1	sl opal, colorless	51.9	0.064	98.44	1.03	0.38	0.14	REF025 (RS007-001) 33759	26.1 62.2 11.7
	2	sl opal, colorless	50.6	0.060	98.44	1.03	0.38	0.15		26.1 61.9 12.0
					30° C.					
0	1	N/A	52.1	0.074	98.19	1.03	0.71	0.07	RS007-001 3448	18.6 71.0 10.4
	2	N/A	51.5		98.18	1.03	0.71	0.08		18.4 71.2 10.4
3 wk, 30 C.	1	clear, sl opal, colorless	N/A	0.057	98.42	0.96	0.49	0.13	RS007-001 33707	N/A
	2	clear, sl opal, colorless		0.058	98.40	0.98	0.49	0.14		
6 wk, 30 C.	1	clear, colorless	N/A	0.059	98.55	0.93	0.44	0.08	RS007-001 33758	N/A
	2	clear, colorless		0.067	98.37	0.99	0.46	0.17		
9 wk, 30 C.	1	sl opal, colorless	N/A	0.064	98.34	0.99	0.41	0.26	RS007-001 33757	N/A
	2	sl opal, colorless		0.063	98.35	0.99	0.41	0.25		
12 wk, 30 C.	1	sl opal, colorless	52.6	0.052	98.21	1.05	0.37	0.36	RS007-001 33897	48.5 44.4 7.1
	2	sl opal, colorless	50.1	0.055	98.21	1.06	0.37	0.36		48.2 44.2 7.6
					40° C.					
0	1	N/A	52.1	0.074	98.19	1.03	0.71	0.07	RS007-001 3448	18.6 71.0 10.4
	2	N/A	51.5		98.18	1.03	0.71	0.08		18.4 71.2 10.4
2 wk, 40 C.	1	clear, sl opal, colorless	N/A	0.081	98.16	1.01	0.48	0.35	RS007-001 33834	N/A
	2	clear, sl opal, colorless		0.080	98.18	0.99	0.48	0.35		
4 wk, 40 C.	1	clear, sl opal, colorless	N/A	0.071	95.11	1.08	0.47	3.34	RS007-001 33690	N/A
	2	clear, sl opal, colorless		0.080	95.33	1.08	0.48	3.11		
8 wk, 40 C.	1	sl opal, colorless	NIA	0.095	91.46	1.36	0.89	6.29	RS007-001 33693	N/A
	2	sl opal, colorless		0.095	91.44	1.35	0.89	6.33		
12 wk, 40 C.	1	sl opal, colorless	49.8	0.116	86.90	1.64	1.86	9.60	RS007-001 33891	73.7 14.8 11.5

(v. = very, sl = slightly, opal = opalescent)

TABLE 8

Pre-Lyo
75 mg/mL Natalizumab, 40 mg/mL Sucrose, 6 mM Histidine, 0.02% PS-80
Manufactured:
Testing Start Date: 0.5 mL fill

Time Point/Temp	Vial	Appearance	Conc. (mg/mL)	Turbidity A360 nm	% Monomer	% Dimer	% Aggregate	% LMW	SEC Ref Std & Avg. area count	% Acidic % Main % Basic
0	1	N/A	77.2	0.097	97.23	1.53	1.15	0.09	RS007-001 3448	18.5 72.3 9.2
	2	N/A	77.6		97.23	1.53	1.14	0.09		17.9 71.9 10.1
4 wk, 5 C.	1	clear, sl opal, colorless	N/A	0.089	97.46	1.51	0.90	0.13	RS007-001 33690	N/A
	2	clear, sl opal, colorless		0.089	97.47	1.51	0.89	0.12		
8 wk, 5 C.	1	sl opal, colorless	N/A	0.071	97.54	1.51	0.83	0.13	RS007-001 33245	N/A
	2	sl opal, colorless		0.071	97.55	1.51	0.81	0.12		
12 wk, 5 C.	1	sl opal, colorless	73.1	0.072	97.58	1.56	0.75	0.11	RS007-001 33881	N/A
	2	sl opal, colorless	75.4	0.070	97.58	1.56	0.75	0.11		
6 mo, 5 C.	1	sl opal, colorless	75.9	0.081	97.72	1.53	0.59	0.15	REF025 (RS007-001) 33759	26.2 62.0 11.8
	2	sl opal, colorless	75.9	0.078	97.73	1.53	0.59	0.15		25.9 62.4 11.7
					30° C.					
0	1	N/A	77.2	0.097	97.23	1.53	1.15	0.09	RS007-001 3448	18.5 72.3 9.2
	2	N/A	77.6		97.23	1.53	1.14	0.09		17.9 71.9 10.1
3 wk, 30 C.	1	clear, sl opal, colorless	N/A	0.071	97.65	1.44	0.73	0.17	RS007-001 33707	N/A
	2	clear, sl opal, colorless		0.089	97.67	1.44	0.73	0.17		
6 wk, 30 C.	1	v. sl opal, colorless	N/A	0.077	97.64	1.45	0.70	0.21	RS007-001 33758	N/A
	2	v. sl opal, colorless		0.070	97.63	1.45	0.70	0.21		
9 wk, 30 C.	1	sl opal, colorless	N/A	0.084	97.90	1.36	0.56	0.18	RS007-001 33757	N/A
	2	sl opal, colorless		0.083	97.91	1.36	0.56	0.17		
12 wk, 30 C.	1	sl opal, colorless	79.7	0.072	97.42	1.53	0.55	0.51	RS007-001 33897	N/A
	2	sl opal, colorless	75.6	0.081	97.41	1.53	0.54	0.52		
					40° C.					
0	1	N/A	77.2	0.097	97.23	1.53	1.15	0.09	RS007-001	18.5
0	1	N/A	77.2	0.097	97.23	1.53	1.15	0.09	RS007-001 3448	18.5 72.3 9.2
	2	N/A	77.6		97.23	1.53	1.14	0.09		17.9 71.9 10.1
2 wk, 40 C.	1	clear, sl opal, colorless	N/A	0.092	97.31	1.46	0.73	0.51	RS007-001 33834	N/A
	2	clear, sl opal, colorless		0.111	97.33	1.46	0.72	0.50		
4 wk, 40 C.	1	clear, sl opal, colorless	N/A	0.104	93.12	1.53	0.70	4.66	RS007-001 33690	N/A
	2	clear, sl opal, colorless		0.098	93.00	1.51	0.71	4.79		
8 wk, 40 C.	1	sl opal, colorless	N/A	0.136	88.74	1.83	1.37	8.06	RS007-001	N/A
	2	sl opal, colorless		0.135	88.57	1.80	1.33	8.29	33498	

TABLE 8-continued

Pre-Lyo
75 mg/mL Natalizumab, 40 mg/mL Sucrose, 6 mM Histidine, 0.02% PS-80
Manufactured:
Testing Start Date: 0.5 mL fill

Time Point/Temp	Vial	Appearance	Conc. (mg/mL)	Turbidity A360 nm	% Monomer	% Dimer	% Aggregate	% LMW	SEC Ref Std & Avg. area count	% Acidic % Main % Basic
12 wk, 40 C.	1	sl opal, colorless	79.4	0.165	83.49	2.09	2.85	11.57	RS07-001 33891	68.2 17.1 14.6
	2	sl opal, colorless	84.1	0.174	86.55	1.26	1.78	10.41		68.6 13.7 17.7

TABLE 9

Reconstituted
100 mg/mL Natalizumab, 100 mg/mL Sucrose, 30 mM Histidine, 0.1% PS-80
Manufactured:
Testing Start Date: 0.5 mL fill

Time Point/ Temp.	Vial	Appearance	Recon Time (min.)	KF % Moisture	Conc. (mg/mL)	Turbidity A360 nm	% Monomer	% Dimer	% Aggregate	% LMW	SEC Ref Std & Avg. area count	% Acidic % Main % Basic
0	1	clear, sl opal	4.0	4.7	95.7	0.111	98.24	0.97	0.78	—	RS007-001 3448	19.1 70.8 10.1
	2	clear, sl opal	3.5		96.7	0.100	98.23	0.98	0.79	—		19.3 72.2 8.6
4 wk, 5 C.	1	clear, sl opal	5.1	N/A	N/A	0.146	98.41	0.90	0.70	—	RS007-001 33720	N/A
	2	clear, sl opal	5.2			0.164	98.41	0.89	0.69	—		
8 wk, 5 C.	1	opal, colorless	4.4	N/A	N/A	0.136	98.40	0.91	0.69	—	RS007-001 33245	N/A
	2	opal, colorless	6.1			0.138	98.41	0.91	0.68			
12 wk, 5 C.	1	opal, colorless	3.2	N/A	94.2	0.135	98.04	1.10	0.77	0.09	RS007-001 33881	N/A
	2	opal, colorless	5.0		96.1	0.134	98.07	1.08	0.76	0.08		
6 mo, 5 C.	1	opal, colorless	6.9	N/A	96.3	0.150	98.35	1.01	0.64	—	REF025 (RS007-001) 33759	21.1 66.8 12.1
	2	opal, colorless	6.2		96.2	0.153	98.33	1.02	0.66	—		21.2 66.6 12.2
						30° C.						
0	1	clear, sl opal	4.0	4.7	95.7	0.111	98.24	0.97	0.78	—	RS007-001 3448	19.1 70.8 10.1
	2	clear, sl opal	3.5		96.7	0.100	98.23	0.98	0.79	—		19.3 72.2 8.6
3 wk, 30 C.	1	clear, sl opal, colorless	3.5	N/A	N/A	0.143	98.35	0.98	0.53	—	RS007-001 33707	N/A
	2	clear, sl opal, colorless	6.0			0.151	98.36	0.98	0.51	—		
6 wk, 30 C.	1	sl opal, colorless	3.2	N/A	N/A	0.148	98.44	1.03	0.54	—	RS007-001 33758	N/A
	2	sl opal, colorless	4.0			0.132	98.42	1.04	0.54	—		
9 wk, 30 C.	1	opal, colorless	5.1	N/A	N/A	0.156	98.22	1.12	0.65	—	RS007-001 33757	N/A
	2	opal, colorless	6.3			0.161	98.24	1.10	0.66	—		

TABLE 9-continued

Reconstituted
100 mg/mL Natalizumab, 100 mg/mL Sucrose, 30 mM Histidine, 0.1% PS-80
Manufactured:
Testing Start Date: 0.5 mL fill

Time Point/ Temp.	Vial	Appearance	Recon Time (min.)	KF % Moisture	Conc. (mg/mL)	Turbidity A360 nm	% Monomer	% Dimer	% Aggregate	% LMW	SEC Ref Std & Avg. area count	% Acidic % Main % Basic
12 wk, 30 C.	1	opal, colorless	4.5	N/A	97.6	0.142	97.85	1.36	0.73	0.07	RS007-001 33897	N/A
	2	opal, colorless	3.3		98.6	0.140	97.86	1.35	0.72	0.07		
6 mo, 30 C.	1	opal, colorless	4.2	N/A	96.0	0.169	97.86	1.87	0.27	—	REF025 (RS007-001) 33774	21.6 64.0 14.4
	2	opal, colorless	3.6		97.3	0.175	97.83	1.53	0.64	—		21.6 64.4 14.0
						40° C.						
0	1	clear, sl opal	4.0	4.7	95.7	0.111	98.24	0.97	0.78	—	RS007-001 3448	19.1 70.8 10.1
	2	clear, sl opal	3.5		96.7	0.100	98.23	0.98	0.79	—		19.3 72.2 8.6
2 wk, 40 C.	1	clear	3.8	N/A	N/A	0.153	97.83	1.33	0.79	0.06	RS007-001 33791	N/A
	2	clear	3.1			0.181	97.82	1.34	0.79	0.05		
4 wk, 40 C.	1	clear, sl opal	3.5	N/A	N/A	0.160	98.07	1.28	0.65	—	RS007-001 33720	N/A
	2	clear, sl opal	4.2			0.159	98.04	1.30	0.67	—		
8 wk, 40 C.	1	opal, colorless	3.2	N/A	N/A	0.168	97.86	1.48	0.65	—	RS007-001 33693	N/A
	2	opal, colorless	4.9			0.210	97.79	1.57	0.64	—		
12 wk, 40 C.	1	opal, colorless	5.7	N/A	95.5	0.230	97.19	2.43	0.26	0.11	RS007-001 33891	N/A
	2	opal, colorless	3.7		96.2	0.238	97.16	2.45	0.27	0.12		

(v. = very, sl = slightly, opal = opalescent)

TABLE 10

Reconstituted
100 mg/mL Natalizumiab, 100 mg/mL, Sucrose, 15 mM Histidine, 0.05% PS-80
Manufactured:
Testing Start Date: 0.5 mL fill

Time Point/ Temp	Vial	Appearance	Recon Time (min.)	KF % Moisture	Conc. (mg/mL)	Turbidity A360 nm	% Monomer	% Dimer	% Aggregate	% LMW	SEC Ref Std & Avg. area count	% Acidic % Main % Basic
0	1	clear, sl opal	3.8	5.9	96.0	0.095	98.10	1.04	0.79	0.08	RS007-001 3448	18.9 71.0 10.1
	2	clear, sl opal	3.3		95.9	0.109	98.10	1.07	0.75	0.08		19.5 69.8 10.6
4 wk, 5 C.	1	clear, sl opal	5.8	N/A	N/A	0.139	98.44	0.93	0.63	—	RS007-001 33720	N/A
	2	clear, sl opal	2.2			0.133	98.46	0.91	0.64	—		
8 wk, 5 C.	1	opal, colorless	7.9	N/A	N/A	0.126	98.46	0.92	0.62	—	RS007-001 33245	N/A
	2	opal, colorless	6.2			0.114	98.46	0.92	0.63	—		
12 wk, 5 C.	1	opal, colorless	5.9	N/A	93.1	0.115	98.13	1.07	0.71	0.08	RS007-001 33881	19.3 68.9 11.8
	2	opal, colorless	2.7		93.1	0.138	98.01	1.24	0.67	0.09		19.4 68.7 11.8

TABLE 10-continued

Reconstituted
100 mg/mL Natalizumiab, 100 mg/mL, Sucrose, 15 mM Histidine, 0.05% PS-80
Manufactured:
Testing Start Date: 0.5 mL fill

Time Point/ Temp	Vial	Appearance	Recon Time (min.)	KF % Moisture	Conc. (mg/mL)	Turbidity A360 nm	% Monomer	% Dimer	% Aggregate	% LMW	SEC Ref Std & Avg. area count	% Acidic % Main % Basic
6 mo, 5 C.	1	opal, colorless	6.2	N/A	93.5	0.127	98.39	1.01	0.60	—	REF025 (RS007-001) 33759	21.3 66.7 12.0
	2	opal, colorless	6.1		93.4	0.132	98.40	1.01	0.60	—		21.1 66.8 12.0
12 mo, 5 C.	1	opal, colorless	7.5	N/A	93.3	0.125	98.34	1.00	0.67	—	REF025 (RS007-001) 36185	20.4 65.5 14.1
	2	opal, colorless	8.1		92.8	0.126	98.33	0.99	0.68	—		19.7 66.2 14.2
						30° C.						
0	1	clear, sl opal	3.8	5.9	96.0	0.095	98.10	1.04	0.79	0.08	RS007-001 3448	18.9 71.0 10.1
	2	clear, sl opal	3.3		95.9	0.109	98.10	1.07	0.75	0.08		19.5 69.8 10.6
3 wk, 30 C.	1	clear, sl opal, colorless	5.0	N/A	N/A	0.137	98.37	1.01	0.62	—	RS007-001 33707	N/A
	2	clear, sl opal colorless	8.4			0.123	98.33	1.05	0.62	—		
6 wk, 30 C.	1	sl opal, colorless	4.6	N/A	N/A	0.121	98.13	1.35	0.52	—	RS007-001 33758	N/A
	2	sl opal, colorless	6.8			0.123	98.14	1.36	0.50	—		
9 wk, 30 C.	1	opal, colorless	2.3	N/A	N/A	0.160	98.08	1.34	0.58	—	RS007-001 33757	N/A
	2	opal, colorless	4.5			0.147	97.99	1.42	0.58	—		
12 wk, 30 C.	1	opal, colorless	8.2	N/A	89.7	0.159	96.62	3.04	0.24	0.10	RS007-001 33897	23.5 66.3 10.2
	2	opal, colorless	7.5		90.4	0.126	97.58	1.69	0.65	0.08		22.6 68.3 9.1
6 mo, 30 C.	1	opal,	7.2	N/A	95.7	0.188	97.45	2.14	0.25	0.16	REF025 (RS007-001) 33774	22.7 15.1 23.0
	2	opal, colorless	6.2		94.0	0.195	97.33	2.25	0.25	0.16		62.0 15.0
12 mo, 30 C.	1	opal, slightly yellow	7.6	N/A	93.0	0.230	96.82	2.27	0.76	0.15	REF025 (RS007-001) 36185	22.9 58.1 19.0
	2	opal, slightly yellow	7.8		93.9	0.226	96.90	2.24	0.73	0.14		22.9 58.4 18.7
						40° C.						
0	1	clear, sl opal	3.8	5.9	96.0	0.095	98.10	1.04	0.79	0.08	RS007-001 3448	18.9 71.0 10.1
	2	clear, sl opal	3.3		95.9	0.109	98.10	1.07	0.75	0.08		19.5 69.8 10.6
2 wk, 40 C.	1	clear	5.4	N/A	N/A	0.142	96.96	2.77	0.20	0.07	RS007-001 33791	N/A
	2	clear	7.3			0.149	97.53	1.73	0.69	0.06		
4 wk, 40 C.	1	clear, sl opal	6.8	N/A	N/A	0.189	97.14	1.95	0.70	0.2	RS007-001 33720	N/A
	2	clear, sl opal	5.3			0.195	97.33	1.82	0.67	0.18		
8 wk, 40 C.	1	opal, colorless	6.5	N/A	N/A	0.227	96.94	2.76	0.11	0.20	RS007-001 33693	N/A
	2	opal, colorless	6.0			0.226	97.07	2.16	0.57	0.20		

TABLE 10-continued

Reconstituted
100 mg/mL Natalizumiab, 100 mg/mL, Sucrose, 15 mM Histidine, 0.05% PS-80
Manufactured:
Testing Start Date: 0.5 mL fill

Time Point/ Temp	Vial	Appearance	Recon Time (min.)	KF % Moisture	Conc. (mg/mL)	Turbidity A360 nm	% Monomer	% Dimer	% Aggregate	% LMW	SEC Ref Std & Avg. area count	% Acidic % Main % Basic
12 wk, 40 C.	1	opal, colorless	3.9	N/A	94.2	0.161	96.80	2.87	0.23	0.10	RS007-001 33891	21.0 55.1 24.0
	2	opal, colorless	4.1		91.9	0.173	96.96	2.69	0.24	0.10		21.8 55.8 22.4

(v. = very, sl = slightly, opal = opalescent)

TABLE 11

Reconstituted
200 mg/mL Natalizumiab, 100 mg/mL Sucrose, 24 mM Histidine, 0.08% PS-80
Manufactured:
Testing Start Date: 0.5 mL fill

Time Point/ Temp	Vial	Appearance	Recon Time (min.)	KF % Moisture	Conc. (mg/mL)	Turbidity A360 nm	% Monomer	% Dimer	% Aggregate	% LMW	SEC Ref Std & Avg. area count	% Acidic % Main % Basic
0	1	clear, sl opal	9.5	5.8	172.0	0.095	97.96	1.10	0.86	0.08	RS007-001 3448	19.7 71.8 8.5
	2	clear, sl opal	10.5		173.2	0.106	97.96	1.10	0.86	0.08		19.1 70.9 10.0
4 wk, 5 C.	1	clear, sl opal	4.8	N/A	N/A	0.157	97.91	1.16	0.79	0.13	RS007-001	N/A
	2	clear, sl opal	5.8			0.153	97.89	1.18	0.80	0.13	33720	
8 wk, 5 C.	1	opal, colorless	6.5	N/A	N/A	0.141	98.18	1.10	0.72	—	RS007-001	N/A
	2	opal, colorless	7.5			0.152	98.21	1.13	0.66	—	33245	
12 wk, 5 C.	1	opal, colorless	6.0	N/A	154.5	0.154	97.90	1.25	0.76	0.08	RS007-001 33881	18.6 63.8 17.7
	2	opal, colorless	5.6		170.6	0.150	97.88	1.27	0.77	0.09		19.9 68.9 11.1
6 mo, 5 C.	1	opal, colorless	7.3	N/A	174.9	0.167	98.07	1.28	0.66	—	REF025 (RS007-001) 33759	21.2 66.4 12.4
	2	opal, colorless	6.6		175.3	0.167	98.08	1.26	0.66	—		21.0 66.6 12.4
12 mo, 5 C.	1	opal, colorless	6.7	N/A	178.1	0.156	97.86	1.40	0.73	—	REF025 (RS007-001) 36185	20.0 65.5 14.5
	2	opal, colorless	3.8		172.2	0.152	97.93	1.33	0.74	—		19.4 65.6 14.9
						30° C.						
0	1	clear, sl opal	9.5	5.8	172.0	0.095	97.96	1.10	0.86	0.08	RS007-001 3448	19.7 71.8 8.5
	2	clear, sl opal	10.5		173.2	0.106	97.96	1.10	0.86	0.08		19.1 70.9 10.0
3 wk, 30 C.	1	clear, sl opal, colorless	4.2	N/A	N/A	0.165	97.79	1.48	0.73	—	RS007-001 33707	N/A
	2	clear, sl opal, colorless	4.3			0.169	97.77	1.50	0.73	—		
6 wk, 30 C.	1	v. sl opal, colorless	7.1	N/A	N/A	0.157	97.74	1.68	0.58	—	RS007-001 33758	N/A
	2	sl opal, colorless	5.9			0.163	97.77	1.65	0.59	—		

TABLE 11-continued

Reconstituted
200 mg/mL Natalizumiab, 100 mg/mL Sucrose, 24 mM Histidine, 0.08% PS-80
Manufactured:
Testing Start Date: 0.5 mL fill

Time Point/ Temp	Vial	Appearance	Recon Time (min.)	KF % Moisture	Conc. (mg/mL)	Turbidity A360 nm	% Monomer	% Dimer	% Aggregate	% LMW	SEC Ref Std & Avg. area count	% Acidic % Main % Basic
9 wk, 30 C.	1	opal, colorless	4.0	N/A	N/A	0.186	97.52	1.78	0.70	—	RS007-001 33757	N/A
	2	opal, colorless	3.8			0.185	97.41	1.89	0.70	—		
12 wk, 30 C.	1	opal, colorless	4.9	N/A	174.5	0.178	96.88	2.23	0.80	0.09	RS007-001 33897	20.0 59.0 21.0
	2	opal, colorless	5.4		177.6	0.183	96.93	2.20	0.79	0.08		19.9 58.1 22.0
6 mo, 30 C.	1	opal, colorless	6.0	N/A	173.2	0.237	96.16	3.45	0.39	—	REF025 (RS007-001) 33774	21.8 63.3 15.0
	2	opal, colorless	4.9		174.1	0.227	96.13	3.47	0.40	—		21.8 63.3 15.0
12 mo, 30 C.	1	opal, slightly yellow	7.0	N/A	171.2	0.221	95.35	3.56	1.09	—	REF025 (RS007-001) 36185	20.9 61.1 17.9
	2	opal, slightly yellow	6.5		168.8	0.220	95.26	3.60	1.14	—		20.8 61.2 18.0
						40° C.						
0	1	clear, sl opal	9.5	5.8	172.0	0.095	97.96	1.10	0.86	0.08	RS007-001 3448	19.7 71.8 8.5
	2	clear, sl opal	10.5		173.2	0.106	97.96	1.10	0.86	0.08		19.1 70.9 10.0
2 wk, 40 C.	1	clear	8.3	N/A	N/A	0.180	96.93	2.17	0.84	0.06	RS007-001 33791	N/A
	2	clear	3.9			0.166	96.89	2.20	0.85	0.07		
4 wk, 40 C.	1	clear, sl opal	3.6	N/A	N/A	0.196	96.37	2.62	0.88	0.14	RS007-001 33720	N/A
	2	clear, sl opal	2.4			0.203	96.34	2.62	0.89	0.15		
8 wk, 40 C.	1	opal, colorless	4.6	N/A	N/A	0.214	95.68	3.27	0.93	0.12	RS007-001 33693	N/A
	2	opal, colorless	6.2			0.208	95.98	3.18	0.84	—		
12 wk, 40 C.	1	opal, colorless	7.6	N/A	167.6	0.229	94.92	3.94	1.05	0.10	RS007-001 33891	19.9 53.5 26.6
	2	opal, colorless	4.8		167.0	0.241	94.90	3.94	1.06	0.09		20.5 54.6 24.9

TABLE 12

Reconstituted
225 mg/mL Natalizuniab, 120 mg/mL Sucrose, 18 mM Histidine, 0.06% PS-80
Manufactured:
Testing Start Date: 0.5 mL fill

Time Point/ Temp	Vial	Appearance	Recon Time (min.)	KF % Moisture	Conc. (mg/mL)	Turbidity A360 nm	% Monomer	% Dimer	% Aggregate	% LMW	SEC Ref Std & Avg. area count	% Acidic % Main % Basic
0	1	clear, sl opal	6.2	19.0	194.7	0.093	96.90	1.63	1.39	0.08	RS007-001 3448	19.7 70.3 10.0
	2	clear, sl opal		20.5	184.1	0.097	96.88	1.64	1.39	0.09		17.8 73.3 8.9
4 wk, 5 C.	1	clear, sl opal	14.3	N/A	N/A	0.136	96.82	1.72	1.32	0.14	RS007-001 33720	N/A
	2	clear, sl opal	18.0			0.143	96.87	1.67	1.33	0.13		

TABLE 12-continued

Reconstituted
225 mg/mL Natalizuniab, 120 mg/mL Sucrose, 18 mM Histidine, 0.06% PS-80
Manufactured:
Testing Start Date: 0.5 mL fill

Time Point/ Temp	Vial	Appearance	Recon Time (min.)	KF % Moisture	Conc. (mg/mL)	Turbidity A360 nm	% Monomer	% Dimer	% Aggregate	% LMW	SEC Ref Std & Avg. area count	% Acidic % Main % Basic
8 wk, 5 C.	1	opal, colorless	16.3	N/A	N/A	0.143	96.94	1.69	1.25	0.12	RS007-001 33245	N/A
	2	opal, colorless	18.8			0.142	96.91	1.69	1.28	0.11		
12 wk, 5 C.	1	opal, colorless	15.3	N/A	224.7	0.145	96.82	1.85	1.23	0.10	RS007-001 33881	
	2	opal, colorless	27.0		222.3	0.134	96.88	1.80	1.24	0.08		
6 mo, 5 C.	1	opal, colorless	15.5	N/A	196.9	0.149	97.10	1.81	1.09	—	REF025 (RS007-001) 33759	20.9 66.6 12.5
	2	opal, colorless	17.1		197.1	0.152	97.13	17.9	1.08	—		20.8 66.7 12.5
						30° C.						
0	1	clear, sl opal	19.0	6.2	194.7	0.093	96.90	1.63	1.39	0.08	RS007-001 3448	19.7 70.3 10.0
	2	clear, sl opal	20.5		184.1	0.097	96.88	1.64	1.39	0.09		17.8 73.3 8.9
3 wk, 30 C.	1	clear, sl opal, colorless	8.3	N/A	N/A	0.173	96.48	2.12	1.29	—	RS007-001 33707	N/A
	2	clear, sl opal, colorless	12.9			0.168	96.49	2.11	1.28	—		
6 wk, 30 C.	1	sl opal, colorless	11.9	N/A	N/A	0.143	96.41	2.28	1.16	0.14	RS007-001 33758	N/A
	2	sl opal, colorless	27.6			0.166	96.04	2.67	1.15	0.14		
9 wk, 30 C.	1	opal, colorless	21.6	N/A	N/A	0.178	95.91	2.84	1.25	—	RS007-001 33757	N/A
	2	opal, colorless	22.4			0.170	96.39	2.40	1.21	—		
12 wk, 30 C.	1	opal, colorless	19.3	N/A	211.6	0.174	95.81	2.83	1.26	0.09	RS007-001 33897	N/A
	2	opal, colorless	16.8		223.5	0.173	95.86	2.80	1.26	0.09		
6 mo, 30 C.	1	opal, colorless	24.4	N/A	181.3	0.238	95.10	3.57	1.33	—	REF025 (RS007-001) 33774	21.6 63.3 15.2
	2	opal, colorless	22.9		183.7	0.225	95.16	3.57	1.27	—		21.6 63.4 15.0
						40° C.						
0	1	clear, sl opal	19.0	6.2	194.7	0.093	96.90	1.63	1.39	0.08	RS007-001 3448	19.7 70.3 10.0
	2	clear, sl opal	20.5		184.1	0.097	96.88	1.64	1.39	0.09		17.8 73.3 8.9
2 wk, 40 C.	1	clear	14.5	N/A	N/A	0.161	95.17	3.40	1.36	0.07	RS007-001 33791	N/A
	2	clear	15.0			0.153	95.87	2.74	1.33	0.06		
4 wk, 40 C.	1	clear, sl opal	13.4	N/A	N/A	0.180	95.26	3.19	1.39	0.16	RS007-001 33720	N/A
	2	clear, sl opal	19.0			0.179	95.23	3.22	1.40	0.15		
8 wk, 40 C.	1	opal, colorless	18.3	N/A	N/A	0.210	94.86	3.77	1.37	—	RS007-001 33693	N/A
	2	opal, colorless	15.9			0.211	94.10	4.34	1.41	0.15		
12 wk, 40 C.	1	opal, colorless	20.8	N/A	194.2	0.248	93.87	4.54	1.52	0.07	RS007-001 33891	N/A
	2	opal, colorless	16.4		215.4	0.235	94.12	4.31	1.47	0.10		

TABLE 13

Pre-Lyo
50 mg/mL Natalizumab, 25 mg/mL Sucrose, 6 mM Histidine, 15 mM NaCl, 0.02% PS-80
Prepared:
Testing Start Date: 0.5 mL fill

Time Point/ Temp	Vial	Appearance, pH	Conc. (mg/mL)	Turbidity A360 nm	% Monomer	% Dimer	% Aggregate	% LMW	SEC Ref Std & Avg. area count	% Acidic % Main % Basic
0	1	clear, sl opal, colorless	50.0 50.7	0.181	98.31	1.04	0.57	0.07	RS007-001 33834	20.8 68.0 11.3
4 wk, 5 C.	1	sl opal, colorless	N/A	0.105	98.31	1.04	0.54	0.11	RS007-001 33626	N/A
	2	sl opal, colorless		0.093	98.31	1.04	0.54	0.12		
8 wk, 5 C.	1	sl opal, colorless	50.0	0.103	98.59	0.96	0.45	—	RS007-001 33670	N/A
	2	sl opal, colorless	50.0	0.098	98.60	0.96	0.44	—		
12 wk, 5 C.	1	sl opal, colorless	N/A	0.098	98.36	1.07	0.47	0.10	REF025 (RS007-001)	N/A
	2	sl opal, colorless		0.107	98.35	1.07	0.47	0.11	33608	

30° C.

Time Point/ Temp	Vial	Appearance	Conc. (mg/mL)	Turbidity A360 nm	% Monomer	% Dimer	% Aggregate	% LMW	SEC Ref Std & Avg. area count	% Acidic % Main % Basic
0	1	clear, sl opal, colorless	50.0 50.7	0.181	98.31	1.04	0.57	0.07	RS007-001 33834	20.8 68.0 11.3
3 wk, 30 C.	1	sl opal, colorless	N/A	0.038	98.54	0.95	0.15	0.06	RS007-001 33758	N/A
	2	sl opal, colorless		0.034	98.38	0.99	0.45	0.14		
6 wk, 30 C.	1	sl opal, colorless	N/A	0.109	98.54	0.95	0.41	0.10	RS007-001 33506	N/A
	2	sl opal, colorless		0.108	98.53	0.95	0.42	0.10		
9 wk, 30 C.	1	sl opal, colorless	N/A	0.104	98.50	0.99	0.35	0.16	RS007-001 33775	N/A
	2	sl opal, colorless		0.102	98.50	0.99	0.35	0.16		
12 wk, 30 C.	1	sl opal, colorless	N/A	0.102	98.04	1.12	0.37	0.47	REF025 (RS007-001)	N/A
	2	sl opal, colorless		0.106	98.05	1.10	0.38	0.47	33586	

40° C.

Time Point/ Temp	Vial	Appearance	Conc. (mg/mL)	Turbidity A360 nm	% Monomer	% Dimer	% Aggregate	% LMW	SEC Ref Std & Avg. area count	% Acidic % Main % Basic
0	1	clear, sl opal, colorless	50.0 50.7	0.181	98.31	1.04	0.57	0.07	RS007-001 33834	20.8 68.0 11.3
2 wk, 40 C.	1	clear, sl opal, colorless	N/A	0.105	98.05	1.01	0.46	0.48	RS007-001 33732	N/A
	2	clear, sl opal, colorless		0.109	98.05	1.01	0.46	0.48		
4 wk, 40 C.	1	sl opal, colorless	N/A	0.147	95.23	1.08	0.43	3.25	RS007-001 34124	N/A
	2	sl opal, colorless		0.106	95.20	1.08	0.42	3.30		
8 wk, 40 C.	1	sl opal, colorless	52.0	0.121	89.74	1.34	0.62	8.29	RS007-001 33852	N/A
	2	sl opal, colorless	54.0	0.116	89.53	1.22	0.65	8.59		

TABLE 13-continued

Pre-Lyo
50 mg/mL Natalizumab, 25 mg/mL Sucrose, 6 mM Histidine, 15 mM NaCl, 0.02% PS-80
Prepared:
Testing Start Date: 0.5 mL fill

12 wk, 40 C.	1	sl opal, colorless	N/A	0.128	86.74	1.47	1.39	10.41	REF025 (RS007-001)	N/A
	2	sl opal, colorless		0.131	86.46	1.47	1.35	10.72	33590	

TABLE 14

Pre-Lyo
50 mg/mL Natalizumab, 25 mg/mL Sucrose, 6 mM Histidine, 0.02% PS-20
Prepared:
Testing Start Date: 0.5 mL fill

Time Point/ Temp	Vial	Appearance, pH	Conc. (mg/mL)	Turbidity A360 nm	% Monomer	% Dimer	% Aggregate	% LMW	SEC Ref Std & Avg. area count	% Acidic % Main % Basic
0	1	clear, sl opal, colorless, 6.11	53.7 51.7	0.050	98.22	1.06	0.65	0.07	RS007-001 33834	21.0 67.9 11.1
4 wk, 5 C.	1	v. sl opal, colorless	N/A	0.058	98.38	1.00	0.59	0.03	RS007-001 33626	N/A
	2	v. sl opal, colorless		0.065	98.39	0.99	0.58	0.03		
8 wk, 5 C.	1	sl opal, colorless	50.1	0.060	98.59	0.95	0.46	—	RS007-001 33670	N/A
	2	sl opal, colorless	49.8	0.068	98.59	0.96	0.45	—		
12 wk, 5 C.	1	sl opal, colorless	N/A	0.066	98.31	1.08	0.50	0.12	REF025 (RS007-001)	N/A
	2	sl opal, colorless		0.065	98.31	1.08	0.49	0.12	33608	

30° C.

Time Point/ Temp	Vial	Appearance,	Conc. (mg/mL)	Turbidity A360 nm	% Monomer	% Dimer	% Aggregate	% LMW	SEC Ref Std & Avg. area count	% Acidic % Main % Basic
0	1	clear, sl opal, colorless, 6.11	53.7 51.7	0.050	98.22	1.06	0.65	0.07	RS007-001 33834	21.0 67.9 11.1
3 wk, 30 C.	1	v. sl opal, colorless	N/A	0.029	98.31	1.01	0.49	0.16	RS007-001 33758	N/A
	2	v. sl opal, colorless	N/A	0.019	98.31	1.02	0.52	0.16		
6 wk, 30 C.	1	sl opal, colorless	N/A	0.063	98.51	0.95	0.44	0.10	RS007-001 33506	N/A
	2	sl opal, colorless		0.061	98.33	1.00	0.47	0.21		
9 wk, 30 C.	1	sl opal, colorless	N/A	0.054	98.24	1.05	0.39	0.32	RS007-001 33775	N/A
	2	sl opal, colorless		0.046	98.25	1.05	0.39	0.32		
12 wk, 30 C.	1	sl opal, colorless	N/A	0.061	98.14	1.07	0.39	0.40	REF025 (RS007-001)	N/A
	2	sl opal, colorless		0.060	98.13	1.07	0.39	0.41	33586	

40° C.

Time Point/ Temp	Vial	Appearance	Conc. (mg/mL)	Turbidity A360 nm	% Monomer	% Dimer	% Aggregate	% LMW	SEC Ref Std & Avg. area count	% Acidic % Main % Basic
0	1	clear, sl opal, colorless, 6.11	53.7 51.7	0.050	98.22	1.06	0.65	0.07	RS007-001 33834	21.0 67.9 11.1

TABLE 14-continued

Pre-Lyo
50 mg/mL Natalizumab, 25 mg/mL Sucrose, 6 mM Histidine, 0.02% PS-20
Prepared:
Testing Start Date: 0.5 mL fill

2 wk, 30 C.	1	v. sl opal, colorless	N/A	0.102	98.06	1.03	0.48	0.43	RS007-001 33732	N/A
	2	v. sl opal, colorless	N/A	0.098	98.08	1.02	0.47	0.43		
4 wk, 40 C.	1	sl opal, colorless	N/A	0.099	95.41	1.09	0.47	0.10	RS007-001 34124	N/A
	2	sl opal, colorless		0.081	95.25	1.11	0.45	3.18		
8 wk, 40 C.	1	sl opal, colorless	53.5	0.104	90.07	1.37	0.80	7.76	RS007-001 33852	N/A
	2	sl opal, colorless	53.9	0.097	89.83	1.29	0.73	8.15		
12 wk, 40 C.	1	sl opal, colorless	N/A	0.101	89.27	0.82	1.02	8.89	REF025 (RS007-001)	N/A
	2	sl opal, colorless		0.097	89.09	0.80	0.98	9.12	33590	

TABLE 15

Pre-Lyo
50 mg/mL Natalizumab, 25 mg/mL Trehalose, 6 mM Histidine, 0.02% PS-80
Prepared:
Testing Start Date: 0.5 mL fill

Time Point/ Temp	Vial	Appearance, pH	Conc. (mg/mL)	Turbidity A360 nm	% Monomer	% Dimer	% Aggregate	% LMW	SEC Ref Std & Avg. area count	% Acidic % Main % Basic
0	1	clear, sl opal, colorless, 6.13	51.0 51.5	0.035	98.19	1.06	0.68	0.07	RS007-001 33834	19.7 69.3 11.0
4 wk, 5 C.	1	v. sl opal, colorless	N/A	0.056	98.26	1.05	0.60	0.10	RS007-001 33626	N/A
	2	v. sl opal, colorless		0.050	98.44	0.99	0.53	0.03		
8 wk, 5 C.	1	sl opal, colorless	52.7	0.076	98.59	0.96	0.45	—	RS007-001 33670	N/A
	2	sl opal, colorless	50.1	0.093	98.58	0.97	0.46	—		
12 wk, 5 C.	1	sl opal, colorless	N/A	0.063	98.35	1.08	0.48	0.10	REF025 (RS007-001)	N/A
	2	sl opal, colorless		0.057	98.34	1.08	0.48	0.11	33608	

30° C.

Time Point/ Temp.	Vial	Appearance	Conc. (mg/mL)	Turbidity A360 nm	% Monomer	% Dimer	% Aggregate	% LMW	SEC. Ref Std & Avg. area count	% Acidic % Main % Basic
0	1	clear, sl opal, colorless, 6.13	51.0 51.5	0.035	98.19	1.06	0.68	0.07	RS007-001 33834	19.7 69.3 11.0
3 wk, 30 C.	1	sl opal, colorless	N/A	0.006	98.33	1.00	0.51	0.15	RS007-001 33758	N/A
	2	sl opal, colorless		0.010	98.33	1.01	0.51	0.15		
6 wk, 30 C.	1	sl opal, colorless	N/A	0.061	98.32	1.00	0.47	0.21	RS007-001 33506	N/A
	2	sl opal, colorless	N/A	0.060	98.51	0.95	0.44	0.11		
9 wk, 30 C.	1	sl opal, colorless	N/A	0.059	98.21	1.08	0.38	0.32	RS007-001 33775	N/A
		sl opal, colorless	0.056	98.23	1.05	0.40	0.32			

TABLE 15-continued

Pre-Lyo
50 mg/mL Natalizumab, 25 mg/mL Trehalose, 6 mM Histidine, 0.02% PS-80
Prepared:
Testing Start Date: 0.5 mL fill

12 wk, 30 C.	2	sl opal, colorless	0.069	98.12	1.08	0.39	0.41	REF025 (RS007-001)	N/A N/A
		sl opal, colorless	0.067	98.06	1.15	0.38	0.42	33586	

40° C.

Time Point/ Temp.	Vial	Appearance	Conc. (mg/mL)	Turbidity A360 nm	% Monomer	% Dimer	% Aggregate	% LMW	SEC. Ref Std & Avg. area count	% Acidic % Main % Basic
0	1	clear, sl opal, colorless, 6.13	51.0 51.5	0.035	98.19	1.06	0.68	0.07	RS0007-001 33834	19.7 69.3 11.0
2 wk, 40 C.	1	clear, sl opal, colorless	N/A	0.065	98.07	1.03	0.48	0.42	RS0007-001 33732	N/A
	2	clear, sl opal, colorless		0.069	98.08	1.02	0.48	0.42		
4 wk, 40 C.	1	sl opal, colorless	N/A	0.061	95.49	1.09	0.48	2.94	RS0007-001 34124	N/A
	2	v. sl opal, colorless		0.060	95.37	1.09	0.46	3.08		
8 wk, 40 C.	1	sl opal, colorless	52.9 (potency =	0.085	89.95	1.32	0.82	7.91	RS0007-001 33852	N/A
	2	sl opal, colorless	78.1%)	0.081	89.89	1.27	0.81	8.04		
12 wk, 40 C.	1	sl opal, colorless	53.4	0.099	87.14	1.56	1.51	9.78	REF025 (RS007-001)	N/A
	2	sl opal, colorless	N/A	0.110	86.16	1.63	1.49	10.72	33590	

TABLE 16

Pre-Lyo
40 mg/mL Natalizumab, 25 mg/mL Sucrose, 6 mM Histidin, 0.02% PS-80
Prepared:
Testing Start Date: 0.5 mL fill

Time Point/ Temp	Vial	Appearance, pH	Conc. (mg/mL)	Turbidity A360 nm	% Monomer	% Dimer	% Aggregate	% LMW	SEC. Ref Std & Avg. area count	% Acidic % Main % Basic
0	1	clear, sl opal, colorless, 6.11	41.8 41.8	0.035	98.41	0.98	0.60	—	RS007-001 33834	19.4 69.1 11.5
4 wk, 5 C.	1	v. sl opal, colorless	N/A	0.049	98.45	0.98	0.53	0.03	RS007-001 33626	N/A
	2	v. sl opal, colorless		0.049	98.45	0.99	0.53	0.03		
8 wk, 5 C.	1	sl opal, colorless		0.051	98.61	0.95	0.44	—	RS007-001	N/A
	2	sl opal, colorless		0.057	98.59	0.96	0.45	—	33670	
12 wk, 5 C.	1	sl opal, colorless		0.054	98.37	1.06	0.46	0.11	REF025	N/A
	2	sl opal, colorless		0.052	98.39	1.06	0.46	0.10	(RS007-001) 33608	
6 mo, 5 C.	1	sl opal, colorless		0.065	98.39	1.07	0.39	0.16	REF025 (RS007-001) 33633	26.4 62.5 11.0
	2	sl opal, colorless		0.076	98.39	1.05	0.40	0.16		26.3 62.8 11.0

TABLE 16-continued

Pre-Lyo
40 mg/mL Natalizumab, 25 mg/mL Sucrose, 6 mM Histidin, 0.02% PS-80
Prepared:
Testing Start Date: 0.5 mL fill

30° C.

Time Point/ Temp	Vial	Appearance, pH	Conc. (mg/mL)	Turbidity A360 nm	% Monomer	% Dimer	% Aggregate	% LMW	SEC. Ref Std & Avg. area count	% Acidic % Main % Basic
0	1	clear, sl opal, colorless, 6.11	41.8 41.8	0.035	98.41	0.98	0.60	—	RS007-001 33834	19.4 69.1 11.5
3 wk, 30 C.	1	sl opal, colorless	N/A	0.018	98.39	0.99	0.51	0.14	RS007-001 33758	N/A
	2	sl opal, colorless		0.013	98.37	0.99	0.49	0.14		
6 wk, 5 C.	1	sl opal, colorless	N/A	0.060	98.54	0.93	0.43	0.10	RS007-001 33506	N/A
	2	sl opal, colorless		0.067	98.55	0.93	0.42	0.10		
9 wk, 5 C.	1	sl opal, colorless	N/A	0.047	98.28	1.03	0.40	0.29	RS007-001 33775	N/A
	2	sl opal, colorless		0.054	98.25	1.07	0.38	0.30		
12 wk, 30 C.	1	sl opal, colorless	N/A	0.074	98.13	1.12	0.37	0.38	REF025 (RS007-001)	N/A
	2	sl opal, colorless	N/A	0.063	98.16	1.09	0.38	0.37	33586	N/A

40° C.

Time Point/ Temp	Vial	Appearance, pH	Conc. (mg/mL)	Turbidity A360 nm	% Monomer	% Dimer	% Aggregate	% LMW	SEC. Ref Std & Avg. area count	% Acidic % Main % Basic
0	1	clear, sl opal, colorless, 6.11	41.8 41.8	0.035	98.41	0.98	0.60	—	RS007-001 33834	19.4 69.1 11.5
2 wk, 40 C.	1	clear, sl opal, colorless	N/A	0.058	98.14	1.00	0.48	0.38	RS007-001 33732	N/A
	2	clear, sl opal, colorless		0.054	98.39	0.93	0.45	0.24		
4 wk, 40 C.	1	sl opal, colorless	N/A	0.054	96.06	1.07	0.47	2.40	RS007-001 34124	N/A
	2	v. sl opal, colorless		0.055	95.90	1.06	.044	2.60		
8 wk, 40 C.	1	sl opal, colorless	41.3 (potency = 80.0%)	0.065	91.64	1.23	0.72	6.41	RS007-001 33852	N/A
	2	sl opal, colorless	43.1	0.064	91.75	1.26	0.70	6.30		
12 wk, 40 C.	1	sl opal, colorless	N/A	0.081	89.51	1.58	1.35	7.55	REF025 (RS007-001)	N/A
	2	sl opal, colorless		0.083	89.66	1.61	1.38	7.35	33590	

TABLE 17

Reconstituted
200 mg/mL Natalizumab, 100 mg/mL Sucrose, 24 mM Histidine, 0.08% PS-80
Reconstitute with 0.45 mL DI water to get 0.5 mL total volume
Prepared:
Lyophilization Complete:
Testing Start Date:

Time Point/ Temp.	Vial	Appearance, pH	Recon Time (min.)	KF % Moisture	Conc. (mg/mL)	Turbidity A360 nm	% Monomer	% Dimer	% Aggregate	% LMW	SEC Ref Std & Avg. area count	% Acidic % Main % Basic
Pre-lyo	1	clear, sl opal, 6.08	N/A	N/A	50.0 51.5	0.028	98.28	1.04	0.60	0.07	RS007-001 33834	20.7 68.1 11.3

TABLE 17-continued

Reconstituted
200 mg/mL Natalizumab, 100 mg/mL Sucrose, 24 mM Histidine, 0.08% PS-80
Reconstitute with 0.45 mL DI water to get 0.5 mL total volume
Prepared:
Lyophilization Complete:
Testing Start Date:

0	1	clear	13.5	4.0	183.2	0.160	98.14	1.11	0.69	0.06	RS007-001 33791	20.4 69.0 10.7
	2	clear	4.7		169.8	0.134	98.14	1.10	0.69	0.07		20.1 64.7 15.2
4 wk, 5 C.	1	sl opal, colorless	8.5	N/A	N/A	0.131	98.03	1.16	0.69	0.12	RS007-001 33626	N/A
	2	sl opal, colorless	8.3			0.140	98.03	1.16	0.69	0.12		
8 wk, 5 C.	1	opal, colorless	6.0	N/A	180.0	0.131	98.32	1.10	0.58	—	RS007-001 33670	22.1 63.9 14.0
	2	opal, colorless	4.1		185.4	0.135	98.33	1.09	0.58	—		22.9 62.9 14.2
12 wk, 5 C.	1	opal, colorless	4.7	N/A	N/A	0.144	97.99	1.28	0.64	0.10	REF025 (RS007-001)	N/A
	2	opal, colorless	5.5			0.147	97.99	1.28	0.64	0.10	33608	
6 mo 5 C.	1	opal, colorless	9.8	N/A	176.0	0.133	98.24	1.25	0.51	—	REF025 (RS007-001) 33633	21.8 66.2 12.0
	2	opal, colorless	7.8		172.6	0.157	98.19	1.28	0.53	—		21.8 66.2 12.0
*12 mo, 5 C.	1	opal, slightly yellow	13.2	N/A	222.8	0.113	97.76	1.46	0.68	0.10	REF025 (RS007-001) 36188	20.5 65.3 14.2

30° C.

Time Point/ Temp.	Vial	Appearance	Recon Time (min.)	KF % Moisture	Conc. (mg/mL)	Turbidity A360 nm	% Monomer	% Dimer	% Aggregate	% LMW	SEC Ref Std & Avg. area count	% Acidic % Main % Basic
0	1	clear, sl opal	13.5	4.0	183.2	0.160	98.14	1.11	0.69	0.06	RS007-001 33791	20.4 69.0 10.7
	2	clear, sl opal	4.7		169.8	0.134	98.14	1.10	0.69	0.07		20.1 64.7 15.2
3 wk, 30 C.	1	sl opal, colorless	3.3	N/A	N/A	0.165	97.50	1.68	0.68	0.14	RS007-001 33758	N/A
	2	sl opal, colorless	4.2			0.169	97.53	1.64	0.69	0.14		
6 wk, 30 C.	1	opal, colorless	4.4	N/A	N/A	0.175	97.31	1.88	0.68	0.13	RS007-001 33506	N/A
	2	opal, colorless	5.8			0.168	97.31	1.89	0.67	0.13		
9 wk, 30 C.	1	opal, colorless	6.5	N/A	N/A	0.181	96.94	2.71	0.24	0.11	RS007-001 33775	N/A
	2	opal, colorless	4.1			0.169	96.91	2.75	0.25	0.10		
12 wk, 30 C.	1	opal, colorless	6.8	N/A	N/A	0.175	96.68	2.49	0.73	0.11	REF025 (RS007-001)	N/A
	2	opal, colorless	5.6			0.184	96.71	2.47	0.72	0.09	33586	

40° C.

Time Point/ Temp.	Vial	Appearance	Recon Time (min.)	KF % Moisture	Conc. (mg/mL)	Turbidity A360 nm	% Monomer	% Dimer	% Aggregate	% LMW	SEC Ref Std & Avg. area count	% Acidic % Main % Basic
0	1	clear, sl opal	13.5	4.0	183.2	0.160	98.14	1.11	0.69	0.06	RS007-001 33791	20.4 69.0 10.7

TABLE 17-continued

Reconstituted
200 mg/mL Natalizumab, 100 mg/mL Sucrose, 24 mM Histidine, 0.08% PS-80
Reconstitute with 0.45 mL DI water to get 0.5 mL total volume
Prepared:
Lyophilization Complete:
Testing Start Date:

	2	clear, sl opal	4.7		169.8	0.134	98.14	1.10	0.69	0.07		20.1 64.7 15.2
2 wk, 40 C.	1	clear, sl opal	3.3	N/A	N/A	0.179	96.83	2.30	0.71	0.16	RS007-001 33732	N/A
	2	clear, sl opal	3.2			0.165	96.88	2.27	0.70	0.15		
4 wk, 40 C.	1	sl opal, colorless	9.5	N/A	168.0	0.172	96.21	2.80	0.85	0.15	RS007-001 34124	N/A
	2	sl opal, colorless	9.4		162.6	0.184	96.17	2.84	0.84	0.15		
8 wk, 40 C.	1	opal, colorless	9.5	N/A	179.0	0.203	95.82	3.94	0.25	—	RS007-001 33852	24.6 55.6 19.8
	2	opal, colorless	5.1		179.4	0.214	95.80	3.38	0.82	—		26.5 58.8 14.7

*Only 1 vial available for analysis at 12-month time point. Also, cake appeared to be double in size, so reconstituted with double the diluent.

TABLE 18

Reconstituted
200 mg/mL Natalizumab, 100 mg/mL Sucrose, 24 mM Histidine, 60 mM NaCl,
0.08% PS-80 Reconstitute with 0.45 mL DI water to get 0.5 mL total volume
Prepared:
Lyophilization Complete:
Testing Start Date:

Time Point/ Temp.	Vial	Appearance	Recon Time (min.)	KF % Moisture	Conc. (mg/mL)	Turbidity A360 nm	% Monomer	% Dimer	% Aggregate	% LMW	SEC Ref Std & Avg. area count	% Acidic % Main % Basic
0	1	clear	4.6	3.3	184.2	0.269	98.21	1.10	0.61	0.08	RS007-001 33791	18.1 65.7 16.2
	2	clear	7.0		182.0	0.273	98.20	1.11	0.61	0.08		20.7 62.4 16.8
4 wk, 5 C.	1	sl opal, colorless	8.6	N/A	N/A	0.291	98.16	1.13	0.61	0.10	RS007-001 33626	N/A
	2	Opal, colorless	8.2			0.510	98.14	1.16	0.62	0.08		
8 wk, 5 C.	1	v. opal, colorless	3.2	N/A	183.7	0.287	98.37	1.09	0.54	—	RS007-001 33670	22.6 63.1 14.3
	2	v. opal, colorless	6.8		184.0	0.509	98.35	1.09	0.55	—		22.0 64.0 14.0
12 wk, 5 C.	1	v. opal, colorless	5.7	N/A	N/A	0.471	98.06	1.26	0.58	0.10	REF025 (RS007-001)	N/A
	2	v. opal, colorless	4.8			0.485	98.05	1.26	0.58	0.11	33608	
12 mo, 5 C.	1 2	N/A	N/A	N/A	N/A	N/A	97.86 97.66	1.45 1.65	0.60 0.58	0.10 0.12	REF025 (RS007-001) 36412	N/A

30° C.

Time Point/ Temp.	Vial	Appearance	Recon Time (min.)	KF % Moisture	Conc. (mg/mL)	Turbidity A360 nm	% Monomer	% Dimer	% Aggregate	% LMW	SEC Ref Std & Avg. area count	% Acidic % Main % Basic
0	1	clear	4.6	3.3	184.2	0.269	98.21	1.10	0.61	0.08	RS007-001 33791	18.1 65.7 16.2
	2	clear	7.0		182.0	0.273	98.20	1.11	0.61	0.08		20.7 62.4 16.8

TABLE 18-continued

Reconstituted
200 mg/mL Natalizumab, 100 mg/mL Sucrose, 24 mM Histidine, 60 mM NaCl,
0.08% PS-80 Reconstitute with 0.45 mL DI water to get 0.5 mL total volume
Prepared:
Lyophilization Complete:
Testing Start Date:

3 wk, 30 C.	1	opal, colorless	6.6	N/A	N/A	0.376	97.65	1.61	0.62	0.12	RS007-001 33758	N/A
	2	opal, colorless	5.8			0.444	97.60	1.66	0.63	0.12		
6 wk, 30 C.	1	v. opal, colorless	6.0	N/A	N/A	0.436	97.24	2.00	0.65	0.10	RS007-001 33506	N/A
	2	v. opal, colorless	7.2			0.373	97.31	1.95	0.64	0.10		
9 wk, 30 C.	1	v. opal, colorless	6.2	N/A	N/A	0.443	97.07	2.20	0.59	0.14	RS007-001 33775	N/A
	2	v. opal, colorless	12.4			0.402	97.07	2.19	0.59	0.14		
12 wk, 30 C.	1	v. opal, colorless	6.2	N/A	N/A	0.401	96.91	2.34	0.64	0.11	REF025 (RS007-001)	N/A
	2	v. opal, colorless	8.1			0.460	96.75	2.47	0.67	0.11	33586	
12 mo 30 C.	1	N/A	N/A	N/A	N/A	N/A	94.99	3.98	0.90	0.13	REF025 (RS007-001)	N/A
	2						95.19	3.74	0.93	0.14	36412	

40° C.

Time Point/ Temp.	Vial	Appearance	Recon Time (min.)	KF % Moisture	Conc. (mg/mL)	Turbidity A360 nm	% Monomer	% Dimer	% Aggregate	% LMW	SEC Ref Std & Avg. area count	% Acidic % Main % Basic
0	1	clear	4.6	3.3	184.2	0.269	98.21	1.10	0.61	0.08	RS007-001 33791	18.1 65.7 16.2
	2	clear	7.0		182.0	0.273	98.20	1.11	0.61	0.08		20.7 62.4 16.8
2 wk, 40 C.	1	clear, sl opal	5.2	N/A	N/A	0.322	96.97	2.23	0.66	0.13	RS007-001 33732	N/A
	2	clear, sl opal	7.3			0.328	97.06	2.17	0.64	0.13		
4 wk, 40 C.	1	sl opal, colorless	8.9	N/A	169.0	0.428	96.32	2.75	0.79	0.15	RS007-001 34124	N/A
	2	sl opal, colorless	4.4		174.2	0.332	96.53	2.62	0.73	0.12		
8 wk, 40 C.	1	v. opal, colorless	9.8	N/A	164.6	0.339	96.21	3.09	0.70	—	RS007-001 33852	22.6 59.3 18.1
	2	v. opal, colorless	12.2		180.0	0.364	95.55	3.62	0.83	—		24.0 51.5 24.5
12 wk 40 C.	1	opal, colorless	6.5	N/A	N/A	0.359	94.92	4.03	0.93	0.12	REF025 (RS007-001)	N/A
	2	opal, colorless	11.2			0.397	94.31	4.51	1.08	0.11	33590	

TABLE 19

Reconstituted
200 mg/mL Natalizumab, 100 mg/mL Sucrose, 24 mM Histidine, 0.08% PS-20
Reconstitute with 0.45 mL DI water to get 0.5 mL total volume
Prepared:
Lyophilization Complete:
Testing Start Date:

Time Point/ Temp.	Vial	Appearance	Recon Time (min.)	KF % Moisture	Conc. (mg/mL)	Turbidity A360 nm	% Monomer	% Dimer	% Aggregate	% LMW	SEC Ref Std & Avg. area count	% Acidic % Main % Basic
0	1	clear	5.1	4.3	173.3	0.169	98.04	1.12	0.78	0.07	RS007-001 33791	19.4 69.5 11.1

TABLE 19-continued

Reconstituted
200 mg/mL Natalizumab, 100 mg/mL Sucrose, 24 mM Histidine, 0.08% PS-20
Reconstitute with 0.45 mL DI water to get 0.5 mL total volume
Prepared:
Lyophilization Complete:
Testing Start Date:

	2	clear	5.8		165.4	0.161	98.05	1.12	0.77	0.06		20.7 62.9 16.4
4 wk, 5 C.	1	v. sl opal, colorless	8.2	N/A	N/A	0.143	97.95	1.16	0.78	0.11	RS007-001 33626	N/A
	2	v. sl opal, colorless	11.4			0.184	97.92	1.17	0.79	0.13		
8 wk, 5 C.	1	opal, colorless	6.0	N/A	180.0	0.160	98.25	1.11	0.64	—	RS007-001 33670	24.2 61.1 14.7
	2	opal, colorless	6.7		178.5	0.154	98.24	1.11	0.65	—		23.5 62.3 14.2
12 wk, 5 C.	1	opal, colorless	5.5	N/A	N/A	0.154	97.89	1.29	0.73	0.09	REF025 (RS007-001)	N/A
	2	opal, colorless	4.6			0.163	97.90	1.28	0.72	0.10	33608	
12 mo, 5 C.	1 2	N/A	N/A	N/A	N/A	N/A	97.69 97.68	1.47 1.45	0.74 0.77	0.10 0.10	REF025 (RS007-001) 36412	N/A

30° C.

Time Point/ Temp.	Vial	Appearance	Recon Time (min.)	KF % Moisture	Conc. (mg/mL)	Turbidity A360 nm	% Monomer	% Dimer	% Aggregate	% LMW	SEC Ref Std & Avg. area count	% Acidic % Main % Basic
0	1	clear	5.1	4.3	173.3	0.169	98.04	1.12	0.78	0.07	RS007-001 33791	19.4 69.5 11.1
	2	clear	5.8		165.4	0.161	98.05	1.12	0.77	0.06		20.7 62.9 16.4
3 wk, 30 C.	1	sl opal, colorless	>10*	N/A	N/A	0.162	97.65	1.40	0.81	0.14	RS007-001 33758	N/A
	2	sl opal, colorless	5.3			0.175	97.41	1.68	0.79	0.13		
6 wk, 30 C.	1	opal, colorless	8.5	N/A	N/A	0.176	97.18	1.91	0.78	0.12	RS007-001 33506	N/A
	2	opal, colorless	6.9				0.202	97.12	1.96	0.79	0.13	
9 wk, 30 C.	1	opal, colorless	4.7	N/A	N/A	0.196	97.15	2.14	0.71	—	RS007-001 33775	N/A
	2	opal, colorless	3.8			0.195	97.04	2.25	0.71	—		
12 wk, 30 C.	1	opal, colorless	5.9	N/A	N/A	0.203	96.55	2.54	0.82	0.09	REF025 (RS007-001)	N/A
	2	opal, colorless	6.1			0.195	96.64	2.45	0.81	0.10	33586	
12 mo, 30 C.	1	N/A	N/A	N/A	N/A	N/A	94.62	3.99	1.26	0.13	REF025 (RS007-001)	N/A
	2						94.67	4.08	1.16	0.10	36412	

40° C.

Time Point/ Temp.	Vial	Appearance	Recon Time (min.)	KF % Moisture	Conc. (mg/mL)	Turbidity A360 nm	% Monomer	% Dimer	% Aggregate	% LMW	SEC Ref Std & Avg. area count	% Acidic % Main % Basic
0	1	clear	5.1	4.3	173.3	0.169	98.04	1.12	0.78	0.07	RS007-001 33791	19.4 69.5 11.1
	2	clear	5.8		165.4	0.161	98.05	1.12	0.77	0.06		20.7 62.9 16.4
2 wk, 40 C.	1 2	clear, sl opal clear, sl opal	6.6 4.5	N/A	N/A	0.185 0.184	96.80 96.82	2.25 2.24	0.81 0.81	0.14 0.13	RS007-001 33732	N/A

TABLE 19-continued

Reconstituted
200 mg/mL Natalizumab, 100 mg/mL Sucrose, 24 mM Histidine, 0.08% PS-20
Reconstitute with 0.45 mL DI water to get 0.5 mL total volume
Prepared:
Lyophilization Complete:
Testing Start Date:

4 wk, 40 C.	1	v. sl opal, colorless	5.1	N/A	165.6	0.187	96.12	2.76	0.97	0.15	RS007-001 34124	N/A
	2	v. sl opal, colorless	6.1		151.5	0.189	96.13	2.76	0.97	0.14		
8 wk, 40 C.	1	opal, colorless	5.9	N/A	177.3	0.228	95.83	3.28	0.89	—	RS007-001 33852	23.2 57.7 19.2
	2	opal, colorless	7.1		175.2	0.217	95.84	3.28	0.88	—		22.8 58.8 18.5
12 wk, 40 C.	1	opal, colorless	6.5	N/A	N/A	0.257	94.71	4.06	1.14	0.10	REF025 (RS007-001)	N/A
	2	opal, colorless	6.5			0.255	94.77	4.01	1.12	0.10	33590	

*Vial had crack

TABLE 20

Reconstituted
200 mg/mL Natalizumab, 100 mg/mL Trehalose, 24 mM Histidine, 0.08% PS-80
Reconstitute with 0.45 mL DI water to get 0.5 mL total volume
Prepared:
Lyophilization Complete:
Testing Start Date:

Time Point/ Temp.	Vial	Appearance	Recon Time (min.)	KF % Moisture	Conc. (mg/mL)	Turbidity A360 nm	% Monomer	% Dimer	% Aggregate	% LMW	SEC Ref Std & Avg. area count	% Acidic % Main % Basic
0	1	Clear	6.5	5.4	167.2	0.152	98.03	1.14	0.77	0.07	RS007-001 33791	20.8 63.5 15.6
	2	Clear	8.9		157.4	0.150	98.05	1.14	0.76	0.06		20.5 64.4 15.2
4 wk, 5 C.	1	v. sl opal, colorless	7.9	N/A	N/A	0.142	97.86	1.25	0.79	0.11	RS007-001 33626	N/A
	2	v. sl opal, colorless	9.7			0.140	97.89	1.23	0.77	0.11		
8 wk, 5 C.	1	opal, colorless	6.4	N/A	180.0	0.156	98.17	1.20	0.64	—	RS007-001 33670	22.4 63.3 14.3
	2	opal, colorless	5.5		183.4	0.151	98.16	1.21	0.63	—		23.2 62.2 14.5
12 wk, 5 C.	1	opal, colorless	6.5	N/A	N/A	0.160	97.80	1.39	0.70	0.10	REF025 (RS007-001)	N/A
	2	opal, colorless	3.5			0.171	97.82	1.38	0.70	0.10	33608	
12 mo, 5 C.	1 2	N/A	N/A	N/A	N/A	N/A	97.39 97.38	1.75 1.75	0.73 0.76	0.13 0.11	REF025 (RS007-001) 36412	N/A

30° C.

Time Point/ Temp.	Vial	Appearance	Recon Time (min.)	KF % Moisture	Conc. (mg/mL)	Turbidity A360 nm	% Monomer	% Dimer	% Aggregate	% LMW	SEC Ref Std & Avg. area count	% Acidic % Main % Basic
0	1	Clear	6.5	5.4	167.2	0.152	98.03	1.14	0.77	0.07	RS007-001 33791	20.8 63.5 15.6
	2	clear	8.9		157.4	0.150	98.05	1.14	0.76	0.06		20.5 64.4 15.2

TABLE 20-continued

Reconstituted
200 mg/mL Natalizumab, 100 mg/mL Trehalose, 24 mM Histidine, 0.08% PS-80
Reconstitute with 0.45 mL DI water to get 0.5 mL total volume
Prepared:
Lyophilization Complete:
Testing Start Date:

3 wk, 30 C.	1	sl opal, colorless	10.2	N/A	N/A	0.177	96.87	2.19	0.82	0.13	RS007-001 33758	N/A
	2	sl opal, colorless	6.3			0.173	96.88	2.18	0.81	0.13		
6 wk, 30 C.	1	opal, colorless	8.9	N/A	N/A	0.219	96.44	2.62	0.81	0.13	RS007-001 33506	N/A
	2	opal, colorless	7.6			0.200	96.41	2.66	0.80	0.13		
9 wk, 30 C.	1	opal, colorless	8.5	N/A	N/A	0.227	95.79	3.22	0.87	0.12	RS007-001 33775	N/A
	2	opal, colorless	10.4			0.240	95.71	3.29	0.87	0.13		
12 wk, 30 C.	1	opal, colorless	9.5	N/A	N/A	0.255	95.21	3.74	0.95	0.10	REF025 (RS007-001)	N/A
	2	opal, colorless	7.7			0.268	95.19	3.74	0.97	0.10	33586	
12 mo, 30 C.	1	N/A	N/A	N/A	N/A	N/A	91.45	6.75	1.69	0.11	REF025 (RS007-001)	N/A
	2						91.53	6.74	1.62	0.11	36412	

40° C.

Time Point/ Temp.	Vial	Appearance	Recon Time (min.)	KF % Moisture	Conc. (mg/mL)	Turbidity A360 nm	% Monomer	% Dimer	% Aggregate	% LMW	SEC Ref Std & Avg. area count	% Acidic % Main % Basic
0	1	clear	6.5	5.4	167.2	0.152	98.03	1.14	0.77	0.07	RS007-001 33791	20.8 63.5 15.6
	2	clear	8.9		157.4	0.150	98.05	1.14	0.76	0.06		20.5 64.4 15.2
2 wk, 40 C.	1	clear, sl opal	10.1	N/A	N/A	0.239	95.50	3.45	0.89	0.15	RS007-001 33732	N/A
	2	clear, sl opal	12.2			0.245	95.41	3.54	0.92	0.13		
4 wk, 40 C.	1	sl opal, colorless	7.5	N/A	164.1	0.295	93.80	4.85	1.19	0.15	RS007-001 34124	N/A
	2	sl opal, colorless	7.2		175.0	0.301	93.91	4.72	1.24	0.14		
8 wk, 40 C.	1	opal, colorless	6.7	N/A	173.2 (potency = 122.4%)	0.424	92.75	5.95	1.30	—	RS007-001 33852	28.9 49.9 21.1
	2	opal, colorless	7.0		171.7	0.428	92.70	5.96	1.34	—		26.9 53.8 19.3
12 wk, 40 C.	1	v. opal, colorless	7.9	N/A	N/A	0.546	90.63	7.44	1.82	0.11	REF025 (RS007-001)	N/A
	2	v. opal, colorless	9.7			0.580	90.67	7.43	1.79	0.11	33590	

TABLE 21

Reconstituted
160 mg/mL Natalizumab, 100 mg/mL Sucrose, 24 mM Histidine, 0.08% PS-80
Reconstitute with 0.45 mL DI water to get 0.5 mL total volume
Prepared:
Lyophilization Complete:
Testing Start Date:

Time Point/ Temp.	Vial	Appearance	Recon Time (min.)	KF % Moisture	Conc. (mg/mL)	Turbidity A360 nm	% Monomer	% Dimer	% Aggregate	% LMW	SEC Ref Std & Avg. area count	% Acidic % Main % Basic
0	1	clear	2.8	3.7	119.3	0.186	98.11	1.08	0.73	0.08	RS007-001 33791	19.2 69.2 11.6

TABLE 21-continued

Reconstituted
160 mg/mL Natalizumab, 100 mg/mL Sucrose, 24 mM Histidine, 0.08% PS-80
Reconstitute with 0.45 mL DI water to get 0.5 mL total volume
Prepared:
Lyophilization Complete:
Testing Start Date:

	2	clear	3.6		124.5	0.153	98.11	1.08	0.74	0.08		21.0 63.4 15.6
4 wk, 5 C.	1	v. sl opal, colorless	2.7	N/A	N/A	0.138	98.00	1.12	0.74	0.14	RS007-001 33626	N/A
	2	v. sl opal, colorless	2.4			0.149	98.00	1.12	0.74	0.14		
8 wk, 5 C.	1	opal, colorless	3.0	N/A	154.7 (potency = 133%)	0.146	98.38	1.03	0.59	—	RS007-001 33670	22.1 65.3 12.5
	2	opal, colorless	4.7		150.7	0.163	98.39	1.03	0.58	—		22.6 63.7 13.7
12 wk, 5 C.	1	opal, colorless	3.3	N/A	N/A	0.160	98.04	1.20	0.67	0.09	REF025 (RS007-001)	N/A
	2	opal, colorless	2.9			0.158	98.02	1.21	0.68	0.09	33608	
6 mo, 5 C.	1	opal, colorless	3.9	N/A	147.9	0.168	98.21	1.19	0.59	—	REF025 (RS007-001) 33633	21.9 66.2 11.9
	2	opal, colorless	3.1		155.2	0.164	98.20	1.21	0.59	—		21.9 66.2 11.9
12 mo, 5 C.	1	opal, colorless	3.4	N/A	145.6	0.155	98.13	1.23	0.64	—	REF025 (RS007-001) 36188	20.9 65.2 13.9
	2	opal, colorless	2.7		142.9	0.154	98.09	1.25	0.65	—		20.2 65.6 14.2

30° C.

Time Point/ Temp.	Vial	Appearance	Recon Time (min.)	KF % Moisture	Conc. (mg/mL)	Turbidity A360 nm	% Monomer	% Dimer	% Aggregate	% LMW	SEC Ref Std & Avg. area count	% Acidic % Main % Basic
0	1	clear	2.8	3.7	119.3	0.186	98.11	1.08	0.73	0.08	RS007-001 33791	19.2 69.2 11.6
	2	clear	3.6		124.5	0.153	98.11	1.08	0.74	0.08		21.0 63.4 15.6
3 wk, 30 C.	1	sl opal, colorless	2.1	N/A	N/A	0.176	97.97	1.38	0.65	—	RS007-001 33758	N/A
	2	sl opal, colorless	1.6			0.141	97.58	1.51	0.74	0.18		
6 wk, 30 C.	1	opal, colorless	3.1	N/A	N/A	0.195	97.80	1.56	0.64	—	RS007-001 33506	N/A
	2	opal, colorless	2.9			0.175	97.76	1.59	0.64	—		
9 wk, 30 C.	1	opal, colorless	3.3	N/A	N/A	0.188	97.23	1.94	0.71	0.12	RS007-001 33775	N/A
	2	opal, colorless	3.8			0.204	97.55	1.80	0.65	—		
12 wk, 30 C.	1	opal, colorless	3.9	N/A	N/A	0.188	97.33	2.41	0.27	—	REF025 (RS007-001)	N/A
	2	opal, colorless	3.5			0.180	97.32	2.41	0.27	—	33586	
6 mo, 30 C.	1	opal, slightly yellow	2.6	N/A	144.6	0.252	96.63	3.03	0.35	—	REF025 (RS007-001) 33633	22.1 63.7 14.2
	2	opal, slightly yellow	3.2		143.9	0.259	96.60	3.01	0.39	—		22.2 63.6 14.2
12 mo, 30 C.	1	opal, slightly yellow	6.0	N/A	140.8	0.218	96.07	2.99	0.94	—	REF025 (RS007-001) 36188	21.0 62.6 16.5

TABLE 21-continued

Reconstituted
160 mg/mL Natalizumab, 100 mg/mL Sucrose, 24 mM Histidine, 0.08% PS-80
Reconstitute with 0.45 mL DI water to get 0.5 mL total volume
Prepared:
Lyophilization Complete:
Testing Start Date:

	2	opal, slightly yellow	4.5		145.0	0.203	96.08	2.98	0.94	—	21.0 61.7 17.4

40° C.

Time Point/ Temp.	Vial	Appearance	Recon Time (min.)	KF % Moisture	Conc. (mg/mL)	Turbidity A360 nm	% Monomer	% Dimer	% Aggregate	% LMW	SEC Ref Std & Avg. area count	% Acidic % Main % Basic
0	1	clear	2.8	3.7	119.3	0.186	98.11	1.08	0.73	0.08	RS007-001 33791	19.2 69.2 11.6
	2	clear	3.6		124.5	0.153	98.11	1.08	0.74	0.08		21.0 63.4 15.6
2 wk, 40 C.	1	clear, sl opal,	1.6	N/A	N/A	0.198	97.29	1.88	0.71	0.12	RS007-001	N/A
	2	clear, sl opal,	2.3			0.171	97.32	1.87	0.70	0.12	33732	
4 wk, 40 C.	1	sl opal, colorless	3.1	N/A	149.7	0.195	96.70	2.30	0.82	0.18	RS007-001 34124	N/A
	2	sl opal, colorless	1.8		146.5	0.185	96.72	2.30	0.81	0.17		
8 wk, 40 C.	1	opal, colorless	3.9	N/A	145.5 (potency = 144%)	0.228	96.63	3.12	0.25	—	RS007-001 33852	23.6 58.7 17.7
	2	opal, colorless	2.1		148.0	0.202	96.66	3.12	0.23	—		23.5 59.2 17.3
12 wk, 40 C.	1	opal, colorless	3.4	N/A	N/A	0.225	95.69	3.27	0.94	0.10	REF025 (RS007-001)	N/A
	2	opal, colorless	2.5			0.220	95.70	3.27	0.94	0.09	33590	

Example 3

[0147] As demonstrated below, three formulations with slightly different initial protein concentrations were successfully lyophilized and showed excellent stability when stored at 5° C. for 6 months. Stability of these formulations when stored at 40° C. for 8 weeks was comparable to stability seen previously. Stability of the pre-lyophilized formulations stored for 6 months at 5° C. and reconstituted solutions stored at either 5° or 25° for one week was also excellent. A starting concentration of 40 mg/mL showed slightly better stability and better reconstitution characteristics than the other formulations. However, reconstitution of this formulation did allow a deliverable dose of 1 mL at 150 mg/mL.

Materials

[0148] The following table lists the materials and their source.

TABLE 22

Item	Manufacturer
Bulk Natalizumab (77.4 mg/mL)	Elan
Sucrose (96 mg/mL)	Elan
1% PS80	Elan

TABLE 22-continued

Item	Manufacturer
60 mM Histidine	Elan
6 mM Histidine	Elan
0.22-micron Cellulose Acetate Filter	Corning
5 cc Vials	Kimble
Grey Butyl 20 mm Lyo Stoppers, 2 leg	Kimble
20 mm Tear-Off Aluminum Seals	Wheaton

TABLE 23

Equipment
HPLC
HPLC
Uv-Vis Spectrophotometer
Karl Fischer Coulometric Titrator
pH Meter

Natalizumab

[0149] Natalizumab used for this study was the same as that used in Study 3A and Study 3B (AQS-2190). Natalizumab used for these studies was prepared from natalizumab supplied by Biogenldec. The polysorbate 80 included in this material, which had been formulated and vialed, was removed prior to use in this formulation study. Briefly, material was subjected to diafiltration into a low ionic strength, high pH (10 mM tris, 10 mM NaCl, pH=8.5) buffer. The material was bound to a DEAE-Sepharose column under these conditions and then eluted using 10 mM sodium phosphate, 140 mM NaCl, pH 6. The column eluate was then diafiltered into 6 mM histidine, pH 6 and concentrated to between 70 and 100 mg/mL prior to further formulation.

Chemicals and Reagents

[0150] All chemicals and reagents used in this study, except as noted were purchased from VWR and were ACS grade or better. USP grade reagents were used as excipients when available. Polysorbate 80 was purchased from Sigma (Cat # P6474); and was vegetable derived and low peroxide.

Formulations

[0151] The following formulations were prepared by diluting stock solutions of the excipients and active to the desired concentrations. All formulations were at pH 6.

TABLE 24

Study 4 formulation parameters

Formulation ID	Pre-lyo Concentrations	Target Reconstituted Concentration
4089-iL	40 mg/mL Ab, 24 mg/mL sucrose, 6 mM his, 0.02% PS80	150 mg/mL Ab, 90 mg/mL sucrose, 24 mM his, 0.08% PS80
4089-1M	45 mg/mL Ab, 24 mg/mL sucrose, 6 mM his, 0.02% PS80	
4089-1N	50 mg/mL Ab, 24 mg/mL sucrose, 6 mM his, 0.02% PS80	

Abbreviations:
Ab = antibody,
his = histidine,
PS80 = polysorbate 80 2.2

Methods

Preparation of Formulations

[0152] The sample formulations were sterile filtered and filled as indicated into sterile glass vials. All samples for pre-lyophilized analysis were filled at 0.5 mL into 3 cc vials, stoppered and capped. Formulas to be lyophilized were filled at 4.0 mL into 5 cc Kimble vials.

Lyophilization Cycle

[0153] During the freezing phase, the vials containing the samples were first cooled to 5° C. and held for 30 minutes. The temperature was then ramped to −5° C. over 20 minutes and held at −5° C. for 60 minutes. For the final stage of freezing, the vials were ramped to −40° C. over 45 minutes, held at this temperature for 2 hours, of which the last 20 minutes had a 100 mTorr vacuum applied. Primary drying was then performed as the temperature was taken to −25° C. over 20 min under vacuum of 100 mTorr and held there for 34 hours. The shelf temperature was ramped slowly to 20° C. over 10 hours to begin secondary drying at 100 mTorr, and then held at 20° C. for 6 hours.

Study Set-Up

[0154] Vials of pre-lyophilized liquid and lyophilized cakes were placed at 5 and 40° C. Samples stored at 40° C. were assayed at 2, 4 and 8 weeks. Samples stored at 5° C. were assayed at 4 weeks and 6 months. At the 4 week time point, 4 vials from each storage temperature were reconstituted, after which 2 vials were placed at 5° C. and 2 vials were placed at 25° C., for 1 week of reconstitution stability. All formulations were assayed pre- and post-lyophilization at time zero.

Assays

[0155] The samples were assayed by the following methods and the results are presented in tables 27-30. Not all assays were performed at all time points. With the exception of the zero time point for pre- and post-lyophilized samples, duplicate vials were sampled for each assay.

Appearance by Visual Examination

[0156] All samples were examined visually and their appearance recorded. Lyophilized cakes were examined for color, uniformity, robustness and evidence of meltback. Liquid and reconstituted samples were examined for color, clarity and presence of particulates.

Residual Moisture and Reconstitution Time

[0157] Lyophilized cakes were assayed for residual moisture using Karl Fischer Colorimetric Titrator at the zero time point. Reconstitution time was measured by adding the appropriate volume of DI water, followed by gentle swirling. The time for the cake to completely dissolve was recorded.

Concentration

[0158] The concentration of all samples was measured diluting the samples to 1 mg/mL using natalizumab placebo. The UV absorbance was scanned from 400 to 250 nm using a Varian Cary 300Bio and 10 mm pathlength cuvette at 200 nm/min. The absorbance at lambda max was recorded and the concentration was determined by dividing that value by 1.498 (the absorptivity coefficient for natalizumab) and adjusting by the appropriate dilution.

Turbidity

[0159] The absorption from 300 to 400 nm was measured of a neat sample using a 10 mm small volume cuvette (Starna Cells Inc. Cat #16.160-Q-10\Z20). The value recorded at 360 nm was reported.

Size Exclusion Chromatography

[0160] The amount of monomer, high molecular weight aggregates, dimer and low molecular weight species in the samples were determined by size exclusion chromatography. Briefly, the samples were loaded onto the column neat and the load volumes adjusted to allow a mass of approximately 400 μg on the column. The mass of a reference material load was also adjusted to be comparable. Detection was recorded at both 215 and 280 nm, however the main peak was off scale at

215 nm, so the 280 nm trace was used for calculations. The results are presented in tables 27-30

Results

[0161] Pre-Lyophilized Formulations

[0162] Tables 27-30 contain results recorded for all formulations. On visual examination, all formulations appeared colorless and slightly opalescent, without any visual particulates. The appearance did not change over time at 5° or 40° C. None of the samples showed a change in protein concentration within the variation of the analysis and no trend was observed. The turbidity of all formulations, as measured by absorbance at 360 nm, showed a slight increase after 6 months at 5° C. The 40° C. pre-lyophilized samples showed an increase of turbidity with time for all three formulations.

[0163] The formation of dimer, high molecular weight (aggregate) and low molecular weight species was monitored for all formulations. The results are shown in the tables and FIGS. **17-19**.

[0164] FIG. **17** shows the formation of high molecular weight species at 40° C. The formation of high molecular weight species did not appear to begin until after 4 weeks of storage in the pre-lyophilized formulations. At 8 weeks a small increase in high molecular weight species were apparent.

[0165] At 5° C. there was no change in the level of high molecular weight species in any formulation for the 6 months of storage. This data is shown in the appendices but not graphed here.

[0166] FIG. **18** shows the formation of low molecular weight species at 40° C. There was a definite trend in formation of low molecular weight species during storage at 40° C. Also, the formation of low molecular weight species appeared to proceed at a faster rate than the formation of high molecular weight species, making this an important degradation pathway in the liquid samples.

[0167] There was very little change in the percentage of low molecular weight species over a 6 month time period for the samples stored at 5° C. This data is shown in the appendices, but not graphed here. All of the pre-lyophilized formulations went from an initial level of approximately 0.11% to 0.18% at 6 months. BiogenIdec have shown the lower limit of quantitation for this assay to be 0.2%. Values below that the level are reported for trending information only.

[0168] FIG. **19** shows the total loss of monomer at 40° C. due to formation of both high and low molecular weight species. At 5° C., there was essentially no change in the percent monomer. This would indicate that any of these formulations would be suitably stable as a pre-lyophilized formulation for storage up to 6 months at 2-8° C.

[0169] Selected samples were analyzed by cation exchange chromatography. In all cases the results showed a shift towards a more acidic species (deamidation) with storage based on time and temperature. There was no difference among the various pre-lyophilized formulations. Since deamidation is generally influenced by pH, ionic strength and certain buffer species, this result would be expected. This data is shown in the tables below.

[0170] All three pre-lyophilized formulations showed results similar to the pre-lyophilized formulations in Study 3A and 3B.

Lyophilized Formulations

[0171] Table 25 below shows the reconstitution volumes tested in order to reach a protein concentration of 150 mg/mL. The reconstitution volumes determined to be closest to the target concentration were then used for the remainder of the study. The concentration was checked after each sample was completely dissolved. The reconstitution volumes used for 4089-1L, 4089-1M and 4089-1N, were 0.85, 1.0 and 1.1 mL, respectively.

TABLE 25

Reconstitution volumes

Formulation	Vial	Reconstitution Volume (mL)	Concentration (mg/mL)
4089-iL	1	0.8	156.7
	2	0.9	143.9
	3	0.85	151.8
4089-1M	1	0.8	168.2
	2	0.9	162.5
	3	1.0	158.5
4089-1N	1	0.9	179.4
	2	1.1	146.1
			159.9
			154.4
			153.5
	3	1.1	160.9
			156.8

[0172] Table 26 below shows the ability to remove a 1 mL dose from the reconstituted samples. This was only possible with 4089-1N, which was reconstituted with 1.1 mL. These data indicate that to produce a final deliverable volume of 1 mL at 150 mg/mL, a fill volume of 4 mL with a protein concentration of 50 mg/mL would be necessary.

TABLE 26

Evaluation of a 1 mL dose

Formulation	Reconstitution Volume (mL)	Needle Size	Vial	Volume Removed (mL)
4089-1L	0.85	21 gauge, 1½ inch	1	0.75
			2	0.75
			3	0.85
4089-1M	1.0	21 gauge, 1½ inch	1	0.9
			2	0.8
			3	0.85
4089-1N	1.1	20 gauge, 1½ inch	1	1.0
			2	1.0
			3	1.0

Stability

[0173] On visual examination, all formulations appeared to have acceptable lyophilized cakes, verifying that a 4 mL volume could be successfully lyophilized in a 5 mL vial. After reconstitution, all formulations appeared colorless and slightly opalescent, without any visible particulates. The appearance did not change over time at 5° or 40° C. None of the samples showed a change in protein concentration within the variation of the analysis and no trend was observed. The turbidity of all formulations, as measured by absorbance at 360 nm, showed a slight increase after 6 months at 5° C., from approximately 0.099-0.104 to 0.111-0.116. The 40° C. pre-lyophilized samples showed an increase of turbidity with time for all formulations.

[0174] The percent moisture of the lyophilized cakes ranged from 4.3 to 5.6 as measured by a Karl Fischer cou-

lometer titrator. The average percent moisture for 4089-1L, 4089-1M and 4089-1N, was 4.5, 5.2 and 4.9, respectively. The moisture was relatively high in these samples.

[0175] The reconstitution times for this study were all below 17 minutes. FIG. **4** shows the reconstitution times at 40° C. There appears to be a slight trend toward increasing reconstitution times upon storage at 40° C. The samples with higher starting protein concentration also show a trend towards longer reconstitution times. This was also noted in earlier studies (Study A and B)

[0176] The formation of dimer, high molecular weight aggregate and low molecular weight species was monitored for all formulations. The tabular results are shown in the following tables.

[0177] FIG. **5** shows the formation of high molecular weight species at 40° C. There is a definite trend of formation of high molecular weight species during storage at this temperature. The rate of formation of the aggregate appeared to be slightly slower in formulation 4089-1L. Without wishing to be bound by theory, this could be due to either the lower protein concentration of the starting formulation or the slightly higher sucrose to protein ratio.

[0178] At 5° C. there was no change in the level of high molecular weight species in any formulation for the 6 months of storage which display the % HMW at various times.

[0179] FIG. **6** shows the formation of low molecular weight species at 40° C. In contrast to the pre-lyophilized samples, which exhibited a rapid increase in the formation of low molecular weight species, the lyophilized samples showed no change over 8 weeks. There was no change in the percentage of low molecular weight species over a 6 month time period for the samples stored at 5° C. This data is shown in the appendices, but not graphed here.

[0180] FIG. **7** shows the total loss of monomer at 40° C. due to formation of both high and low molecular weight species. At 5° C., there was essentially no change in the percent monomer. This would indicate that any of these formulations would be suitably stable as a lyophilized formulation for storage up to 6 months at 2-8° C. and longer.

[0181] Samples were also analyzed by cation exchange chromatography. In all cases the results showed a shift towards a more basic species after 8 weeks at 40° C. There is very little change in the charge distribution within the variability of the assay. Select samples also showed a slight shift towards a more acidic species at that time point. This data is shown in the tables below, in the final column as % Acidic, % Main and % Basic.

Reconstituted Stability

[0182] After 4 weeks of storage at either 5° or 40° C., samples were reconstituted and then placed at 5° and 25° C. for 1 week of reconstituted stability. Testing was performed at the initial time point and at 1 week. The tables in the appendices contain all results recorded for all formulations. On visual examination, all formulations appeared colorless and slightly opalescent. All but two samples appeared free of particulates. The two vials containing "fluffy" white particulates had been stored at 40° C. prior to reconstitution and then stored at 25° C. for 1 week. The analyst may have contaminated these vials when they were opened for initial time point testing. None of the samples showed a change in protein concentration within the variation of the analysis and no trend was observed. The turbidity of all formulations, as measured by absorbance at 360 nm, did not show a change, within the variation of the analysis, after 1 week at either 5° or 25° C.

[0183] The formation of dimer, high molecular weight (aggregate) and low molecular weight species was monitored for all formulations. The results are shown in the tables below. There was no change in the level of high molecular weight species in any formulation after reconstituted and placed at 5° or 25° C. for 1 week. The level of low molecular weight species appeared to increase slightly upon storage at 25° C. after reconstitution and essentially remained the same after 5° C. reconstituted storage. These results show that all formulations would remain stable if reconstituted and then placed at 5° or 25° C. for 1 week.

[0184] Samples stored at 5° C. for reconstituted stability were also analyzed by cation exchange chromatography. The results for all three formulations showed a slight increase in more acidic species after 1 week, regardless of their storage temperature prior to reconstitution. The samples that had been stored at 5° C. prior to reconstitution also showed a slight shift towards a more basic species after 1 week of storage. The samples stored at 40° C. prior to reconstitution showed less of a shift towards more basic species after 1 week of storage at 5° C. These changes are very minor and may be more indicative of assay variability than actual changes to the protein.

Conclusions

[0185] The foregoing Study 4 has shown that a 4 mL volume can be successfully lyophilized in a 5 mL Kimble vial and have acceptable cake structure.

[0186] The reconstitution volumes determined to give the target protein concentration of 150 mg/mL, was 0.85 mL for 4089-1L (40 mg/mL pre-lyophilized concentration), 1.0 mL for 4089-1M (45 mg/mL pre-lyophilized concentration) and 1.1 mL for 4089-1N (50 mg/mL pre-lyophilized concentration). 4089-1N was the only formulation able to deliver a 1 mL dose, showing that 1.1 mL of water was the minimum reconstitution volume required. These results can be used to guide the final presentation developed with regards to fill volume, total solids and reconstitution volume. In general, samples with a lower initial protein concentration and higher sucrose to protein ratio showed shorter reconstitution times and slightly better stability with respect to loss of monomer. Based on fill volume and reconstitution volume, this indicates that a lower final protein concentration may give a more desirable product.

[0187] The reconstitution stability showed that all formulations were stable upon storage at 5° and 25° C. for 1 week, with no loss of monomer.

[0188] All three pre-lyophilized formulations remained stable at 5° C. over 6 months. However, upon storage at 40° C., all formulations showed a trend toward increasing amounts of low molecular weight species. The formation of low molecular weight species appears to be an important degradation pathway in the liquid samples given its fast rate of formation.

[0189] The lyophilized formulations also proved to be stable up to 6 months at 5° C. Upon storage at 40° C., there was a definite trend toward increasing amounts of high molecular weight species, while the amount of low molecular weight species remained the same. This shows that the formation of high molecular weight species is a more important degradation pathway in lyophilized samples. Additional optimization of the residual moisture levels and sucrose to protein ratios should improve the stability.

TABLE 27

Pre-Lyo
40 mg/mL Natalizumab, 24 mg/mL Sucrose, 6 mM Histidine and 0.02% PS-80
Prepared:
Testing Start Date: 0.5 mL fill

Time Point/ Temp.	Vial	Appearance/pH	Conc. (mg/mL)	Turbidity A360mn	% Monomer	% Dimer	% Aggregate	% LMW	SEC Ref Std (Avg. area count)	% Acidic % Main % Basic
0	1	sl opal, colorless/ 6.07	40.9	0.036	98.03	1.23	0.63	0.11	REF025 (33849)	20.9 67.9 11.2
2 wk, 40 C.	1	very sl opal, colorless	42.2	0.047	97.75	1.16	0.45	0.64	REF025 (33582)	39.7 51.5 8.8
	2	very sl opal, colorless	40.4	0.051	97.75	1.15	0.44	0.66		42.1 49.4 8.5
4 wk, 40 C.	1	very sl opal, colorless	43.0	0.070	93.84	1.19	0.45	4.52	REF025 (33610)	N/A
	2	very sl opal, colorless	43.4	0.072	94.19	1.21	0.47	4.12		
8 wk, 40 C.	1	very sl opal, colorless	42.3	0.091	90.31	1.36	0.82	7.51	REF025 (33838)	N/A
	2	very sl opal, colorless	41.4	0.091	90.33	1.36	0.91	7.40		
6 mo, 5 C.	1	very sl opal, colorless	41.1	0.057	98.11	1.25	0.47	0.18	REF025 (33851)	25.9 60.5 13.6
	2	very sl opal, colorless	40.9	0.058	98.10	1.25	0.47	0.18		26.1 61.2 12.8

TABLE 28

Pre-Lyo
40 mg/mL Natalizumab, 24 mg/mL Sucrose, 6 mM Histidine and 0.02% PS-80
Prepared:
Testing Start Date: 0.5 mL fill

Time Point/ Temp.	Vial	Appearance/pH	Conc. (mg/mL)	Turbidity A360 mn	% Monomer	% Dimer	% Aggregate	% LMW	SEC Ref Std (Avg. area count)	% Acidic % Main % Basic
0	1	sl opal, colorless/ 6.07	48.3	0.041	98.02	1.23	0.63	0.11	REF025 (33849)	22.6 64.5 12.9
2 wk, 40 C.	1	very sl opal, colorless	48.6	0.058	97.66	1.16	0.44	0.74	REF025 (33582)	41.5 44.2 14.3
	2	very sl opal, colorless	45.5	0.063	97.67	1.18	0.43	0.73		41.3 50.1 8.5
4 wk, 40 C.	1	very sl opal, colorless	49.0	0.081	93.41	1.22	0.48	4.89	REF025 (33610)	N/A
	2	very sl opal, colorless	49.2	0.079	93.64	1.22	0.47	4.67		
8 wk, 40 C.	1	very sl opal, colorless	48.2	0.108	90.14	1.43	1.11	7.32	REF025 (33838)	N/A
	2	very sl opal, colorless	50.0	0.161	90.46	1.43	1.11	7.00		
6 mo, 5 C.	1	very sl opal, colorless	46.1	0.066	98.09	1.25	0.48	0.18	REF025 (33851)	26.2 60.8 13.0
	2	very sl opal, colorless	46.0	0.068	98.11	1.25	0.47	0.16		26.3 60.6 13.1

TABLE 29

Pre-Lyo
50 mg/mL Natalizumab, 24 mg/mL Sucrose, 6 mM Histidine and 0.02% PS-80
Prepared:
Testing Start Date: 0.5 mL fill

Time Point/ Temp.	Vial	Appearance/pH	Conc. (mg/mL)	Turbidity A360 mn	% Monomer	% Dimer	% Aggregate	% LMW	SEC Ref Std (Avg. area count)	% Acidic % Main % Basic
0	1	sl opal, colorless/ 6.08	52.6	0.053	98.01	1.24	0.63	0.12	REF025 (33849)	21.7 67.6 10.8
2 wk, 40 C.	1	very sl opal, colorless	55.9	0.062	97.61	1.17	0.43	0.79	REF025 (33582)	44.3 47.9 7.8
	2	very sl opal, colorless	54.5	0.062	97.60	1.17	0.43	0.80		44.0 48.4 7.5
4 wk, 40 C.	1	very sl opal, colorless	55.8	0.087	93.60	1.25	0.55	4.60	REF025 (33610)	N/A
	2	very sl opal, colorless	55.9	0.084	93.04	1.22	0.48	5.27		
8 wk, 40 C.	1	very sl opal, colorless	55.3	0.118	89.19	1.42	1.13	8.26	REF025 (33838)	N/A
	2	very sl opal, colorless	53.9	0.128	88.61	1.40	1.14	8.86		
6 mo, 5 C.	1	very sl opal, colorless	51.9	0.072	98.08	1.26	0.48	0.19	REF025 (33851)	26.5 60.6 13.0
	2	very sl opal, colorless	52.3	0.067	98.08	1.25	0.48	0.19		26.6 61.1 12.4

TABLE 30

Lyophilized
150 mg/mL Natalizumab, 90 mg/mL Sucrose, 24 mM Histidine and 0.08% PS-80, pH 6
Reconstitute with 0.85 mL DI water to get 0.75-0.85 mL total volume
Prepared:
Lyophilization Complete:
Testing Start Date:

Time Point/ Temp.	Vial	Appearance	Recon Time (min.)	KF % Moisture	Conc. (mg/mL)	Turbidity A360 nm	% Monomer	% Dimer	% Aggregate	% LMW	SEC Ref Std (Avg. area count)	% Acidic % Main % Basic
0	1	sl opal, colorless	2.2	4.5	164.8	0.102	97.87	1.38	0.61	0.14	REF025 (33709)	21.1 65.1 13.8/
	2	sl opal, colorless	2.2	4.6	164.5	0.099	97.87	1.38	0.61	0.13		21.4 65.1 13.5
	3	sl opal, colorless	3.4	4.3	153.7	0.103	97.89	1.37	0.61	0.13		21.4 65.0 13.6
2 wk, 40 C.	1	sl opal, colorless	4.4	N/A	161.9	0.109	96.99	2.19	0.60	0.21	REF025 (33582)	19.7 63.5 16.9
	2	sl opal, colorless	3.7		157.2	0.111	97.00	2.18	0.60	0.23		20.1 68.3 11.6
4 wk, 40 C.	1	sl opal, colorless	3.9	N/A	159.2	0.136	96.50	2.63	0.63	0.24	REF025 (33610)	20.2 67.4 12.5

TABLE 30-continued

Lyophilized
150 mg/mL Natalizumab, 90 mg/mL Sucrose, 24 mM Histidine and 0.08% PS-80, pH 6
Reconstitute with 0.85 mL DI water to get 0.75-0.85 mL total volume
Prepared:
Lyophilization Complete:
Testing Start Date:

Time Point/ Temp.	Vial	Appearance	Recon Time (min.)	KF % Moisture	Conc. (mg/mL)	Turbidity A360 nm	% Monomer	% Dimer	% Aggregate	% LMW	SEC Ref Std (Avg. area count)	% Acidic % Main % Basic
	2	sl opal, colorless	5.7		159.1	0.135	96.56	2.60	0.63	0.20		20.2 67.2 12.5
8 wk, 40 C.	1	sl opal, colorless	3.8	N/A	166.4	0.156	95.76	3.39	0.69	0.16	REF025 (33838)	23.9 58.1 18.0
	2	sl opal, colorless	2.9		164.1	0.155	95.78	3.37	0.67	0.17		21.8 60.0 18.2
6 mo, 5 C.	1	sl opal, colorless	9.3	N/A	153.7	0.113	97.83	1.47	0.59	0.15	REF025 (33851)	21.0 65.8 13.2
	2	sl opal, colorless	7.4		152.3	0.113	97.83	1.47	0.59	0.16		21.0 65.7 13.2

TABLE 31

RECON STABILITY: SAMPLES STORED 4 WEEKS AT 40 C. PRIOR TO RECONSTITUTION.

Storage After Recon	Time point	Vial	Appearance	Recon Time (min.)	Conc. (mg/mL)	Turbidity A360 nm	% Monomer	% Dimer	% Aggregate	% LMW	SEC Ref Std (Avg. area count)	% Acidic % Main % Basic
5 C.	Initial	1	sl opal, colorless	3.9	159.2	0.136	96.50	2.63	0.63	0.24	REF025 (33610)	20.2 67.4 12.5
		2	sl opal, colorless	5.7	159.1	0.135	96.56	2.60	0.63	0.20		20.2 67.2 12.5
	1 wk	1	sl opal, colorless	N/A	154.6	0.132	96.57	2.60	0.60	0.23	REF025 (33604)	23.0 66.4 10.6
		2	sl opal, colorless		159.2	0.132	96.61	2.56	0.60	0.24		22.4 69.0 8.6
25 C.	Initial	3	sl opal, colorless	4.9	N/A	0.137	96.55	2.61	0.63	0.20	REF025 (33610)	N/A
		4	sl opal, colorless	4.4		0.135	96.52	2.64	0.63	0.21		
	1 wk	3	sl opal, colorless, "fluffy" white particulates	N/A	150.1	0.150	96.72	2.44	0.56	0.29	REF025 (33604)	20.6 69.6 9.8
		4	sl opal, colorless		153.6	0.125	96.70	2.47	0.56	0.27		20.3 70.2 9.5

TABLE 32

RECON STABILITY: SAMPLES STORED 4 WEEKS AT 5 C. PRIOR TO RECONSTITUTION.

Storage After Recon	Time point	Vial	Appearance	Recon Time (min.)	Conc. (mg/mL)	Turbidity A360 nm	% Monomer	% Dimer	% Aggregate	% LMW	SEC Ref Std (Avg. area count)	% Acidic % Main % Basic
5 C.	Initial	1	sl opal, colorless	6.0	160.9	0.106	97.78	1.40	0.63	0.19	REF025 (33620)	20.2 69.2 10.7
		2	sl opal, colorless	3.8	161.7	0.106	97.77	1.39	0.63	0.21		19.8 69.5 10.7
	1 wk	1	sl opal, colorless	N/A	150.6	0.107	97.80	1.39	0.60	0.22	REF025 (33604)	22.6 60.2 17.2
		2	sl opal, colorless		157.6	0.109	97.79	1.39	0.60	0.23		23.5 64.4 12.1
25 C.	Initial	3	sl opal, colorless	4.9	N/A	N/A	N/A	N/A	N/A	N/A	N/A	N/A
		4	sl opal, colorless	7.4								
		3	sl opal, colorless	N/A	162.8	0.109	97.83	1.36	0.55	0.25	REF025 (33604)	20.8 60.5 18.7
	1 wk	4	sl opal, colorless		153.9	0.112	97.80	1.38	0.55	0.27		20.1 62.0 18.0

Lyophilized
150 mg/mL Natalizumab, 90 mg/mL Sucrose, 24 mM Histidine and 0.08% PS-80, pH 6
Reconstitute with 1.0 mL DI water to get 0.8-0.9 mL total volume

Prepared:
Lyophilization Complete:
Testing Start Date:

Time Point/ Temp.	Vial	Appearance	Recon Time (min.)	KF % Moisture	Conc. (mg/mL)	Turbidity A360 nm	% Monomer	% Dimer	% Aggregate	% LMW	SEC Ref Std (Avg. area count)	% Acidic % Main % Basic
0	1	sl opal, colorless	2.6	4.8	162.5	0.099	97.85	1.39	0.61	0.14	REF025 (33709)	21.0 65.0 14.0
	2	sl opal, colorless	6.5	5.3	152.0	0.102	97.86	1.39	0.61	0.14		21.1 65.1 13.8
	3	sl opal, colorless	3.7	5.6	159.7	0.104	97.85	1.40	0.61	0.14		21.7 68.1 10.2
2 wk, 40 C.	1	sl opal, colorless	4.7	N/A	151.4	0.109	96.76	2.43	0.60	0.21	REF025 (33582)	19.9 67.9 12.2
	2	sl opal, colorless	4.8		155.2	0.112	96.74	2.41	0.60	0.24		20.1 67.7 12.2
4 wk, 40 C.	1	sl opal, colorless	5.4	N/A	160.8	0.137	96.12	3.03	0.66	0.19	REF025 (33610)	19.8 63.2 17.0
	2	sl opal, colorless	3.8		159.6	0.132	96.22	2.94	0.66	0.19		20.2 67.4 12.4
8 wk, 40 C.	1	sl opal, colorless	5.5	N/A	160.7	0.154	95.19	3.92	0.73	0.16	REF025 (33838)	23.7 57.2 19.1
	2	sl opal, colorless	7.3		160.2	0.155	95.18	3.91	0.73	0.17		21.7 58.9 19.4
6 mo, 5 C.	1	sl opal, colorless	5.8	N/A	146.3	0.111	97.78	1.52	0.60	0.15	REF025 (33851)	21.1 65.6 13.3
	2	sl opal, colorless	7.0		147.3	0.116	97.77	1.53	0.59	0.16		21.1 65.0 14.0

TABLE 33

RECON STABILITY: SAMPLES STORED 4 WEEKS AT 40 C. PRIOR TO RECONSTITUTION

Storage After Recon	Time point	Vial	Appearance	Recon Time (min.)	Conc. (mg/mL)	Turbidity A360 nm	% Monomer	% Dimer	% Aggregate	% LMW	SEC Ref Std (Avg. area count)	% Acidic % Main % Basic
5 C.	Initial	1	sl opal, colorless	5.4	160.8	0.137	96.12	3.03	0.66	0.19	REF025 (33610)	19.8 63.2 17.0
		2	sl opal, colorless	3.8	159.6	0.132	96.22	2.94	0.66	0.19		20.2 67.4 12.4
	1 wk	1	sl opal, colorless	N/A	153.7	0.131	96.16	2.97	0.62	0.24	REF025 (33604)	22.5 62.7 14.8
		2	sl opal, colorless		152.2	0.131	96.27	2.88	0.62	0.24		22.7 68.3 9.0
25 C.	Initial	3	sl opal, colorless	4.0	N/A	0.136	96.11	3.02	0.67	0.19	REF025 (33610)	N/A
		4	sl opal, colorless	4.1		0.138	96.17	2.96	0.66	0.21		
	1 wk	3	sl opal, colorless, "fluffy" white particulates	N/A	148.9	0.132	96.30	2.84	0.58	0.2	REF025 (33604)	20.1 70.5 9.4
		4	sl opal, colorless		147.5	0.130	96.37	2.78	0.57	0.28		19.8 70.4 9.8

TABLE 34

RECON STABILITY: SAMPLES STORED 4 WEEKS AT 5 C. PRIOR TO RECONSTITUTION.

Storage After Recon	Time point	Vial	Appearance	Recon Time (min.)	Conc. (mg/mL)	Turbidity A360 nm	% Monomer	% Dimer	% Aggregate	% LMW	SEC Ref Std (Avg. area count)	% Acidic % Main % Basic
5 C.	Initial	1	sl opal, colorless	4.5	150.1	0.108	97.79	1.40	0.62	0.18	REF025 (33620)	20.3 68.8 10.9
		2	sl opal, colorless	4.8	149.2	0.106	97.78	1.41	0.62	0.19		19.9 70.4 9.7
	1 wk	1	sl opal, colorless	N/A	145.2	0.112	97.80	1.40	0.59	0.21	REF025 (33604)	23.8 59.6 16.6
		2	sl opal, colorless		145.8	0.111	97.79	1.40	0.59	0.22		22.6 60.8 16.6
25 C.	Initial	3	sl opal, colorless	3.3	N/A	N/A	N/A	N/A	N/A	N/A	N/A	N/A
		4	sl opal, colorless	3.1								
	1 wk	3	sl opal, colorless	N/A	141.8	0.112	97.84	1.37	0.55	0.25	REF025 (33604)	20.8 66.9 12.3
		4	sl opal, colorless		140.0	0.111	97.84	1.37	0.54	0.25		20.2 61.8 18.0

TABLE 35

Lyophilized
150 mg/mL Natalizumab, 90 mg/mL Sucrose, 24 mM Histidine and 0.08% PS-80,
pH 6 Reconstitute with 1.1 mL DI water to get 1.0 mL total volume
Prepared:
Lyophilization Complete:
Testing Start Date:

Time Point/ Temp.	Vial	Appearance	Recon Time (min.)	KF % Moisture	Conc. (mg/mL)	Turbidity A360 nm	% Monomer	% Dimer	% Aggregate	% LMW	SEC Ref Std (Avg. area count)	% Acidic % Main % Basic
0	1	sl opal, colorless	6.6	4.7	161.3	0.099	97.84	1.41	0.62	0.14	REF025 (33709)	21.3 64.8 13.9
	2	sl opal, colorless	5.8	4.7	168.6	0.100	97.84	1.41	0.62	0.14		21.3 64.7 14.0
	3	sl opal, colorless	3.3	5.3	170.3	0.099	97.84	1.41	0.61	0.14		21.6 64.8 13.6
2 wk, 40 C.	1	sl opal, colorless	11.6	N/A	164.0	0.116	96.56	2.62	0.62	0.21	REF025 (33582)	19.8 68.1 12.1
	2	sl opal, colorless	6.9		159.3	0.115	96.54	2.63	0.62	0.21		20.0 63.7 16.2
4 wk, 40 C.	1	sl opal, colorless	5.6	N/A	163.3	0.135	95.87	3.25	0.69	0.19	REF025 (33610)	20.8 62.2 17.0
	2	sl opal, colorless	7.2		159.6	0.135	95.90	3.21	0.69	0.20		20.1 62.5 17.5
8 wk, 40 C.	1	sl opal, colorless	7.9	N/A	162.7	0.157	94.79	4.26	0.78	0.17	REF025 (33838)	23.8 56.9 19.2
	2	sl opal, colorless	16.1		166.5	0.155	94.79	4.25	0.78	0.18		23.7 56.8 19.5
6 mo, 5 C.	1	sl opal, colorless	6.0	N/A	149.1	0.115	97.75	1.56	0.60	0.15	REF025 (33851)	20.9 65.7 13.3
	2	sl opal, colorless	9.7		149.1	0.114	97.76	1.55	0.60	0.15		21.1 64.9 14.0

TABLE 36

RECON STABILITY: SAMPLES STORED 4 WEEKS AT 40 C. PRIOR TO RECONSTITUTION.

Storage After Recon	Time point	Vial	Appearance	Recon Time (min.)	Conc. (mg/mL)	Turbidity A360 nm	% Monomer	% Dimer	% Aggregate	% LMW	SEC Ref Std (Avg. area count)	% Acidic % Main % Basic
5 C.	Initial	1	sl opal, colorless	5.6	163.3	0.135	95.87	3.25	0.69	0.19	REF025 (33610)	20.8 62.2 17.0
		2	sl opal, colorless	7.2	159.6	0.135	95.90	3.21	0.69	0.20		20.1 62.5 17.5
	1 wk	1	sl opal, colorless	N/A	159.1	0.133	95.92	3.19	0.64	0.24	REF025 (33604)	22.8 66.6 10.5
		2	sl opal, colorless		155.9	0.132	95.97	3.16	0.64	0.23		23.2 67.2 9.6

TABLE 36-continued

RECON STABILITY: SAMPLES STORED 4 WEEKS AT 40 C. PRIOR TO RECONSTITUTION.

Storage After Recon	Time point	Vial	Appearance	Recon Time (min.)	Conc. (mg/mL)	Turbidity A360 nm	% Monomer	% Dimer	% Aggregate	% LMW	SEC Ref Std (Avg. area count)	% Acidic % Main % Basic
25 C.	Initial	3	sl, opal, colorless	8.6	N/A	0.136	95.86	3.23	0.69	0.22	REF025 (33610)	N/A
		4	sl opal, colorless	6.7		0.136	95.87	3.25	0.69	0.19		
	1 wk	3	sl opal, colorless	N/A	150.5	0.131	96.06	3.05	0.59	0.31	REF025 (33604)	20.4 70.0 9.6
		4	sl opal, colorless		149.9	0.128	96.07	3.05	0.59	0.29		20.1 70.5 9.4

TABLE 37

RECON STABILITY: SAMPLES STORED 4 WEEKS AT 5 C. PRIOR TO RECONSTITUTION.

Storage After Recon	Time point	Vial	Appearance	Recon Time (min.)	Conc. (mg/mL)	Turbidity A360 nm	% Monomer	% Dimer	% Aggregate	% LMW	SEC Ref Std (Avg. area count)	% Acidic % Main % Basic
5 C.	Initial	1	sl opal, colorless	7.1	162.0	0.107	97.72	1.43	0.62	0.22	REF025 (33620)	20.3 69.1 10.5
		2	sl opal, colorless	6.1	164.7	0.105	97.74	1.44	0.63	0.19		20.4 69.0 10.6
	1 wk	1	sl opal, colorless	N/A	162.3	0.114	97.75	1.42	0.59	0.23	REF025 (33604)	23.6 59.7 16.7
		2	sl opal, colorless		161.8	0.109	97.72	1.42	0.60	0.26		22.8 61.4 15.8
25 C.	Initial	3	sl opal, colorless	4.6	N/A	N/A	N/A	N/A	N/A	N/A	N/A	N/A
		4	sl opal, colorless	5.1								
	1 wk	3	sl opal, colorless	N/A	155.0	0.111	97.80	1.40	0.55	0.26	REF025 (33604)	21.2 61.9 16.9
		4	sl opal, colorless		153.4	0.109	97.80	1.40	0.55	0.25		20.4 62.5 17.25

Natalizumab Reformulation Development

	Pre-Lyophilization Amounts			
Name	Antegren (mg/mL)	Sucrose (mg/mL)	Histidine (mM)	PS-80 (%)
A	40	27.7	6	0.04
B	40	46.2	6	0.04
C	40	9.2	6	0.04

TABLE 38

Name	Target Post-Lyophilization Amounts: Antegren (mg/mL)	Sucrose (mg/mL)	Histidine (mM)	PS-80 (%)
A1	160	110.8	24	0.16
A2	100	69.3	15	0.1
B3	160	184.8	24	0.16
B4	40	46.2	6	0.04
AS	100	69.3	15	0.1
A6	40	27.7	6	0.04
C7	100	23.0	15	0.1
C8	40	9.2	6	0.04
C9	160	36.8	24	0.16
A10	100	69.3	15	0.1
B11	100	115.5	15	0.1

Example 4

[0190] The purpose of this study was to use the design of experiments to determine the effect of final protein concentration and the optimal protein to sucrose ratio for lyophilization of natalizumab to prevent and minimize aggregate formation.

Experimental Design Parameters

[0191] The final protein concentrations from 40 mg/mL to 160 mg/mL were examined with a protein to sucrose ratio of 1:100 to 1:500. The polysorbate 80 level was held constant at an amount of 0.01% per 10 mg/mL protein, and the histidine will be held constant at 10 mM per 40 mg/mL protein. Starting protein concentration (pre-lyophilization) will be 40 mg/mL. Vials were filled at a 2 mL fill, and then reconstituted to the desired final protein concentration.

[0192] Short term stability was examined at 0, 2, 4 and 6 weeks at 40 degrees Celcius.

Procedure:

[0193] 1. Diafilter the current formulation against one of the following buffers. Then ultrafilter to a protein concentration of >40 mg/mL. Measure the protein concentration and dilute to 40 mg/mL.

[0194] a. Formulation SA: 100:1 sucrose:protein ratio—final formulations 7, 8, 9

[0195] b. Formulation SB: 300:1 sucrose:protein ratio—final formulations 1, 2, 5, 6, 10

[0196] c. Formulation SC: 500:1 sucrose:protein ratio—final formulations 3, 4, 11

[0197] 2. 20 vials of each formulation will be filled at 2 mL/vial. This allows 10 vials for stability at 40 deg and addition vials for Tg, moisture, FTIR analysis, osmolality, etc. Amounts needed:

[0198] a. Formulation SA: 120 mL

[0199] b. Formulation SB: 200 mL

[0200] c. Formulation SC: 120 mL

[0201] 3. Vials are lyophilized using a conservative cycle to decrease moisture and reconstituted to the desired protein concentration

[0202] a. Formulations 4, 6, 8—reconstitute with 2 mL for a final concentration of 40 mg/mL

[0203] b. Formulations 1, 2, 5, 6, 10—reconstitute with 0.8 mL to give a final concentration of 100 mg/mL

[0204] c. Formulations 1, 3.9—reconstitute with 0.5 mL to give a final concentration of 160 mg/mL

[0205] 4. Stability is examined at 2, 4 and 6 weeks at 40 deg. by turbidity, concentration, appearance, SEC. Additional assay may be run at time 0 and 6 weeks, such as IEX, non-reduced SDS-PAGE and oxidation.

TABLE 39

Formulation Number: Final	Initial	final proten	protein:sucrose	Recon volume
1	A	160	300	1
2	A	100	300	1.6
3	B	160	500	1
4	B	40	500	4
5	A	100	300	1.6
6	A	40	300	4
7	C	100	100	1.6
8	C	40	100	4
9	C	160	100	1
10	A	100	300	1.6
11	B	100	500	1.6

Formulation A: 40 mg/mL protein, 6 mM histidine, 0.04% PS80, 27.7 mg/mL	Used 5 formulations
Formulation B: 40 mg/mL protein, 6 mM histidine, 0.04% PS80, 46.2 mg/mL	Used for 3 formulations
Formulation C: 40 mg/mL protein, 6 mM histidine, 0.04% PS80, 9.2 mg/mL	Used for 3 formulations
Fill each vial at 4 ml = 160 mg/vial	Reconstitute to desired volume as above
Total protein used = 4 mL * 40 mg/mL * 11 formulations * 30 vials 52800	350 vials
Form A 600 mL 80 vials DF vs 3 It	
Form B 360 48 vials DF vs 2 It	
Form C 360 48 vials DF vs 2 It	
UF to approx ½ volume	

TABLE 40

160 mg/mL Antegren, 110.8 mg/mL Sucrose, 24 mM Histidine, 0.16% PS-80
1 vial tested per time point.
Prepared:
Lyophilization Co Complete
Testing Start Date:
At T = 0 reconstituted with 1.0 mL., all other time points reconstituted with 0.8 mL.

2-8 C.

Time Point	Appearance, pH	Recon Time (min.)	KF % Moisture	Conc. (mg/mL)	Turbidity A360 nm	% Monomer	% Dimer	% Aggregate	% LMW	SEC Total Peak Area Count	% Acidic % Main % Basic
0	IV, Colorless	3.8	3.4	126.9	0.126	99.50	0.50	—	—	33274	15.8 66.7 17.6

TABLE 40-continued

160 mg/mL Antegren, 110.8 mg/mL Sucrose, 24 mM Histidine, 0.16% PS-80
1 vial tested per time point.
Prepared:
Lyophilization Co Complete
Testing Start Date:
At T = 0 reconstituted with 1.0 mL., all other time points reconstituted with 0.8 mL.

4 wk	III, Colorless	4.5	N/A	150.3	0.101	99.27	0.55	0.10	0.07	39516	13.6 71.2 15.2
8 wk	IV, BY7 6.37	4.7	N/A	159.5	0.110	99.22	0.68	—	0.10	41343	14.9 70.5 14.7
12 wk	1V, BY7	6.3	N/A	141.4	0.108	99.21	0.71	—	0.08	40153	15.2 70.5 14.3

25 C.

Time Point	Appearance, pH	Recon Time (min.)	Conc. (mg/mL)	Turbidity A360 nm	% Monomer	% Dimer	% Aggregate	% LMW	SEC Total Peak Area Count	% Acidic % Main % Basic
4 wk	IV, Colorless	4.7	151.7	0.111	98.89	1.03	—	0.07	39584	14.5 70.3 15.2
6 wk	1V, BY7	2.8	152.4	0.132	98.79	1.13	—	0.08	39933	14.6 69.6 15.8
8 wk	IV, BY6 6.27	3.7	153.3	0.116	98.64	1.25	—	0.11	39826	15.0 69.9 15.1
12 wk	IV, BY7	4.4	142.8	0.119	98.52	1.40	—	0.08	39447	15.2 68.9 15.9

40 C.

Time Point	Appearance	Recon Time (min.)	Conc. (mg/mL)	Turbidity A360 nm	% Monomer	% Dimer	% Aggregate	% LMW	SEC Total Peak Area Count	% Acidic % Main % Basic
2 wk	IV, Colorless	4.1	1543	0.124	98.52	1.48	—	—	39011	15.1 66.4 185
4 wk	IV, BY7	4.1	130.7	0.113	97.81	2.10	—	0.09	34892	14.9 63.9 21.1
6 wk	IV, BY7	4.1	151.8	0.113	97.28	2.41	0.21	0.10	39626	14.8 65.9 19.3

TABLE 41

100 mg/mL Antegren, 69.3 mg/mL Sucrose, 15 mM Histidine, 0.1% PS-80
1 vial tested per time point.
Prepared:
Lyophilization Complete:
Testing Start Date:
At T = 0 reconstituted with 1.6 mL, all other time points reconstituted with 1.3 mL.

2-8 C.

Time Point	Appearance, pH	Recon Time (min.)	KF % Moisture	Conc. (mg/mL)	Turbidity A360 nm	% Monomer	% Dimer	% Aggregate	% LMW	SEC Total Peak Area Count	% Acidic % Main % Basic
0	IV, Colorless	2.7	2.7	85.8	0.095	99.49	0.51	—	—	36736	15.7 67.6 16.8

TABLE 41-continued

100 mg/mL Antegren, 69.3 mg/mL Sucrose, 15 mM Histidine, 0.1% PS-80
1 vial tested per time point.
Prepared:
Lyophilization Complete:
Testing Start Date:
At T = 0 reconstituted with 1.6 mL, all other time points reconstituted with 1.3 mL.

4 wk	III, Colorless	2.4	N/A	106.6	0.111	99.28	0.55	0.10	0.06	35806	14.0 71.0 15.0
8 wk	III, BY7 6.36	2.7	N/A	104.1	0.107	99.25	0.67	—	0.08	35381	15.3 70.7 14.0
12 wk	III, BY7	4.2	N/A	97.1	0.107	99.21	0.72	—	0.07	35037	15.3 70.4 14.2

25 C.

Time Point	Appearance, pH	Recon Time (min.)	Conc. (mg/mL)	Turbidity A360 nm	% Monomer	% Dimer	% Aggregate	% LMW	SEC Total Peak Area Count	% Acidic % Main % Basic
4 wk	III, Colorless	3.0	106.2	0.101	98.90	1.02	—	0.08	35825	14.7 70.8 14.5
6 wk	IV, BY7	4.8	103.8	0.106	98.81	1.12	—	0.07	35581	14.7 69.8 15.5
8 wk	III, BY7 6.34	4.2	102.3	0.101	98.67	1.23	—	0.09	35055	14.9 69.3 15.8
12 wk	III, BY7	3.9	96.9	0.105	98.55	1.38	—	0.08	34771	15.4 68.9 15.6

40 C.

Time Point	Appearance	Recoil Time (min.)	Conc. (mg/mL)	Turbidity A360 nm	% Monomer	% Dimer	% Aggregate	% LMW	SEC Total Peak Area Count	% Acidic % Main % Basic
2 wk	III, Colorless	3.3	105.0	0.106	98.53	1.47	—	—	35468	15.5 66.5 18.0
4 wk	III. BY7	2.8	104.7	0.110	97.76	2.16	—	0.08	35751	15.3 64.2 20.5
6 wk	IV, BY7	2.7	104.5	0.111	97.32	2.38	0.21	0.09	35788	15.1 66.5 18.4

TABLE 42

160 mg/mL Antegren, 184.8 mg/mL Sucrose, 24 mM Histidine, 0.16%. PS-80
1 vial tested per time point.
Prepared:
Lyophilization Complete:
Testing Start Date:
At T = 0 reconstituted with 1.0 mL, all other time points reconstituted with 0.8 mL.

2-8 C.

Time Point	Appearance, pH	Recon Time (min.)	KF % Moisture	Conc. (mg/mL)	Turbidity A360 nm	% Monomer	% Dimer	% Aggregate	% LMW	SEC Total Peak Area Count	% Acidic % Main % Basic
0	IV, Colorless	3.4	2.3	121.4	0.112	99.55	0.45	—	—	31624	15.3 67.2 17.5

TABLE 42-continued

160 mg/mL Antegren, 184.8 mg/mL Sucrose, 24 mM Histidine, 0.16%. PS-80
1 vial tested per time point.
Prepared:
Lyophilization Complete:
Testing Start Date:
At T = 0 reconstituted with 1.0 mL, all other time points reconstituted with 0.8 mL.

4 wk	III, Colorless	5.4	N/A	148.1	0.124	99.37	0.46	0.10	0.07	37676	13.7 71.3 15.0
8 wk	III. BY7 6.36	4.1	N/A	145.3	0.105	99.34	0.57	—	0.10	37764	14.9 70.8 14.3
12 wk	III, BY7	7.3	N/A	138.2	0.116	99.32	0.60	—	0.09	37653	15.1 70.6 14.3

25 C.

Time Point	Appearance, pH	Recon Time (min.)	Conc. (mg/mL)	Turbidity A360 nm	% Monomer	% Dimer	% Aggregate	% LMW	SEC Total Peak Area Count	% Acidic % Main % Basic
4 wk	III Colorless	4.0	144.2	0.093	99.22	0.70	—	0.07	37807	14.7 70.9 14.4
6 wk	III, BY7	6.7	142.6	0.109	99.18	0.75	—	0.07	37627	14.7 70.6 14.7
8 wk	III, BY6 6.37	6.0	140.8	0.099	99.11	0.80	—	0.09	37563	15.2 70.1 14.8
12 wk	IV, BY7	6.9	123.4	0.118	99.10	0.82	—	0.08	36746	15.4 69.9 14.6

40 C.

Time Point	Appearance, pH	Recon Time (min.)	Conc. (mg/mL)	Turbidity A360 nm	% Monomer	% Dimer	% Aggregate	% LMW	SEC Total Peak Area Count	% Acidic % Main % Basic
2 wk	IV. Colorless	5.2	143.7	0.107	99.23	0.77	—	—	37128	15.6 66.6 17.9
4 wk	III, B Y7	4.0	141.1	0.102	98.84	1.08	—	0.08	37428	15.4 65.9 18.8
6 wk	III, BY7	3.5	141.0	0.114	98.65	1.27	—	0.08	37649	15.1 68.9 16.0

TABLE 43

40 mg/mL Antegren, 46.2 mg/mL Sucrose, 6 mM Histidine, 0.04% PS-80
1 vial tested per time point
Prepared:
Lyophilization Complete:
Testing Start Date:
At T = 0 reconstituted with 4.0 mL, all other time points reconstituted with 3.9 mL.

2-8 C.
A360 nm

Time Point	Appearance pH.	Recon Time (min.)	KF % Moisture	Conc. (mg/mL)	Turbidity A360 nm	% Monomer	% Dimer	% Aggregate	% LMW	SEC Total Peak Area Count	% Acidic % Main % Basic
0	III, Colorless	1.9	2.5	36.8	0.054	99.56	0.44	—	—	33960	15.9 67.5 16.6
4 wk	II, Colorless	2.7	N/A	38.0	0.041	99.35	0.46	0.13	0.06	34758	14.0 71.1 14.9
8 wk	II, BY7 6.37	3.9	N/A	38.2	0.046	99.34	0.58	—	0.07	35571	15.2 70.5 14.3

25 C.

Time Point	Appearance, pH	Recon Time (min.)	Conc (mg/mL)	Turbidity A360 nm	% Monomer	% Dimer	% Aggregate	% LMW	SEC Total Peak Area Count	% Acidic % Main % Basic
4 wk	II, Colorless	2.2	38.1	0.040	99.22	0.72	—	0.06	34667	14.8 71.1 14.1
6 wk	II, Colorless	2.8	38.6	0.044	99.19	0.75	—	0.06	35075	14.9 70.6 14.5
8 wk	II, BY7 6.35	3.0	38.3	0.053	99.12	0.80	—	0.08	34925	15.4 70.2 14.4
12 wk	II, Colorless	2.6	38.8	0.052	99.10	0.83	—	0.07	35107	15.5 70.0 14.5

40 C.

Time Point	Appearance	Recon Time (min.)	Conc (mg/mL)	Turbidity A360 nm	% Monomer	% Dimer	% Aggregate	% LMW	SEC Total Peak Area Count	% Acidic % Main % Basic
2 wk	II, Colorless	2.8	37.4	0.046	99.22	0.78	—	—	34308	15.5 66.9 17.6
4 wk	II, Colorless	1.9	37.7	0.052	98.82	1.11	—	0.07	35035	15.3 66.2 18.5
6 wk	II, Colorless	5.9	38.5	0.043	98.68	1.25	—	0.07	34997	15.3 68.9 15.8

TABLE 44

100 mg/mL Antegren, 69.3 mg ml. Sucrose, 15 mM Histidine, 0.1% PS-80
1 vial tested per time point.
Prepared:
Lyophilization Complete: Testing Start Date:
At T = 0 reconstituted with 1.6 mL, all other time points
reconstituted with 1.3 mL

2-8 C.

Time Point	Appearance, pH	Recon Time (min.)	KF % Moisture	Conc. (mg/mL)	Turbidity A360 nm	% Monomer	% Dimer	% Aggregate	% LMW	SEC Total Peak Area Count	% Acidic % Main % Basic
0	IV, Colorless	2.5	N/A	85.2	0.100	99.49	0.51	—	—	36262	15.9 67.0 17.1
4 wk	III. Colorless	3.6	N/A	107.5	0.112	99.27	0.55	0.11	0.07	36429	14.2 71.2 14.6
8 wk	IV, BY7 6.36	3.7	N/A	104.0	0.107	99.24	0.67	—	0.08	35154	15.3 70.6 14.1
12 wk	III, BY7	4.1	N/A	100.4	0.105	99.22	0.72	—	0.06	35247	15.5 70.4 14.1

25 C.

Time Point	Appearance, pH	Recon Time (min.)	Conc. (mg/mL)	Turbidity A360 nm	% Monomer	% Dimer	% Aggregate	% LMW	SEC Total Peak Area Count	% Acidic % Main % Basic
4 wk	III, Colorless	2.1	105.3	0.106	98.91	0.91	0.11	0.07	35903	14.9 70.7 14.4
6 wk	III, BY7	4.4	105.9	0.104	98.80	1.12	—	0.07	35374	14.9 69.8 15.4
8 wk	III, BY6 6.33	5.6	103.3	0.108	98.67	1.24	—	0.10	35697	15.3 69.7 15.0
12 wk	III, BY7	5.5	95.2	0.123	98.53	1.39	—	0.08	34222	15.4 69.1 15.5

40 C.

Time Point	Appearance	Recon Time (min.)	Conc. (mg/mL)	Turbidity A360 nm,	% Monomer	% Dimer	% Aggregate	% LMW	SEC Total Peak Area Count	% Acidic % Main % Basic
2 wk	III, Colorless	3.0	105.5	0.112	98.55	1.45	—	—	35690	15.4 66.8 17.8
4 wk	III, BY7	2.7	105.3	0.123	97.79	2.13	—	0.08	35694	15.4 64.5 20.1
6 wk	IV, BY7	3.4	105.0	0.115	97.29	2.61	—	0.09	35504	15.0 66.6 18.3

TABLE 45

40 mg/mL Antegren, 27.7 mg/mL Sucrose, 6 mM Histidine,
0.04% PS-80
1 vial tested per time point
Prepared:
Lyophilization Complete:
Testing Start Date:
At T = 0 reconstituted with 4.0 mL, all other time points
reconstituted with 3.9 mL.

2-8 C.

Time Point	Appearance. pH	Recon Time (min.)	KF % Moisture	Conc. (mg/mL)	Turbidity A360 nm	% Monomer	% Dimer	% Aggregate	% LMW	SEC Total Peak Area. Count	% Acidic % Main % Basic
0	III, Colorless	1.8	2.6	37.6	0.047	99.32	0.58	—	0.09	35322	16.0 67.5 16.5
4 wk	II, Colorless	3.5	N/A	39.1	0.042	99.28	0.54	0.11	0.06	35887	14.1 71.3 14.6
8 wk	II, BY7 6.34	2.6	N/A	39.6	0.064	99.28	0.54	0.11	0.06	36694	15.0 70.1 14.9
12 wk	II, Colorless	2.0	N/A	40.2	0.045	99.24	0.69	—	0.07	35619	15.3 70.5 14.2

25 C.

Time Point	Appearance, PH	Recon Time (min.)	Conc. (mg/mL)	Turbidity A360 nm	% Monomer	% Dimer	% Aggregate	% LMW	SEC Total Peak Area Count	% Acidic % Main % Basic
4 wk	II, Colorless	2.3	38.9	0.040	98.90	0.92	—	0.07	35695	14.8 70.8 14.4
6 wk	II, Colorless	3.6	39.5	0.046	98.79	1.14	—	0.07	35977	14.8 69.8 15.3
8 wk	II, BY7 6.35	2.8	40.1	0.054	98.79	1.14	—	0.07	36710	15.6 69.4 15.0
12 wk	II, Colorless	2.7	37.9	0.046	98.54	1.39	—	0.07	35784	15.5 69.1 15.4

40 C.

Time Point	Appearance, PH	Recon Time (min.)	Conc. (mg/mL)	Turbidity A360 nm	% Monomer	% Dimer	% Aggregate	% LMW	SEC Total Peak Area Count	% Acidic % Main % Basic
2 wk	III, Colorless	2.1	39.0	0.046	98.16	1.45	—	0.11	35830	15.5 66.3 18.2
4 wk	II, Colorless	2.6	38.3	0.048	97.77	2.14	—	0.08	35603	15.3 64.2 20.6
6 wk	II, Colorless	2.6	38.8	0.046	97.35	2.36	0.20	0.09	35888	15.0 66.7 18.3

TABLE 46

100 mg/nth Antegren, 23.0 mg mL Sucrose, 15 mM Histidine, 0.1% PS-80
1 vial tested per time point.
Prepared:
Lyophilization Complete:
Testing Start Date:
At T-0 reconstituted with 1.6 mL, all other time points reconstituted with 1.3 mL.

2-8 C.

Time Point	Appearance. pH	Recon Time (min.)	KF % Moisture	Conc. (mg/mL)	Turbidity A360 nm	% Monomer	% Dimer	% Aggregate	% LMW	SEC Total Peak Area. Count	% Acidic % Main % Basic
0	IV. Colorless	4.9	5.7	85.8	0.109	99.22	0.76	0.03	—	36747	15.5 67.2 17.2
4 wk	III, Colorless	2.6	NIA	107.9	0.120	98.94	0.99	—	0.07	36245	14.4 70.8 14.8
8 wk	IV, BY7 6.42	4.9	N/A	102.9	0.134	98.83	1.10	—	0.08	35153	15.1 69.4 15.4
12 wk	IV, BY7	6.7	N/A	103.3	0.201	98.78	1.17	—	0.05	35780	15.5 69.6 14.9

25 C.

Time Point	Appearance, PH	Recon Time (min.)	Conc. (mg/mL)	Turbidity A360 nm	% Monomer	% Dimer	% Aggregate	% LMW	SEC Total Peak Area Count	% Acidic % Main % Basic
4 wk	IV, Colorless	2.3	106.8	0.129	97.57	2.17	0.17	0.09	35755	15.1 68.9 16.0
6 wk	IV, BY7	5.1	107.5	0.148	97.20	252	0.19	0.09	35963	14.8 67.2 18.0
8 wk	IV, BY6 6.33	3.8	106.5	0.124	96.71	−2.95	0.25	0.09	35546	15.7 65.7 18.6
12 wk	III, BY7	5.9	99.7	0.122	96.22	3.39	0.28	0.10	35334	15.4 65.9 18.7

40 C.

Time Point	Appearance	Recon Time (min.)	Conc. (mg/mL)	Turbidity A360 nm	% Monomer	% Dimer	% Aggregate	% LMW	SEC Total Peak Area Count	% Acidic % Main % Basic
2 wk	IV, Colorless	2.5	105.9	0.133	95.76	3.93	0.30	—	35826	15.5 59.6 24.9
4 wk	IV, BY7	3.8	106.1	0.132	93.46	5.80	0.63	0.10	36136	145 55.0 30.5
6 wk	IV, Colorless	5.6	108.3	0.139	91.91	7.09	0.89	0.11	36007	14.7 57.8 27.4

TABLE 47

40 mg/mL Antegren, 9.2 mg/mL Sucrose, 6 mM Histidine, 0.04% PS-80
1 vial tested per time point.
Prepared;
Lyophilization Complete:
Testing Start Date:.
At T = 0 reconstituted with 4.0 mL, all other time points reconstituted with 3.9 mL.

2-8 C.

Time Point	Appearance, pH	Recon Time (min.)	KF % Moisture	Conc. (mg/mL)	Turbidity A360 nm	% Monomer	% Dimer	% Aggregate	% LMW	SEC Total Peak Area Count	% Acidic % Main % Basic
0	III, Colorless	2.2	5.0	36.6	0.082	99.24	0.76	—	—	34010	15.8 67.4 16.9
4 wk	II, Colorless	2.8	N/A	38.8	0.053	98.92	1.01	—	0.07	35211	14.4 71.1 14.5
8 wk	II, Colorless 6.38	2.6	N/A	39.3	0.052	98.84	1.09	—	0.07	36176	15.1 69.9 15.0
12 wk	II, Colorless	1.9	N/A	40.8	0.069	98.75	1.18	—	0.07	35825	15.4 69.7 14.9

25 C.

Time Point	Appearance, pH	Recon Time (min.)	Conc. (mg/mL)	Turbidity A360 nm	% Monomer	% Dimer	% Aggregate	% LMW	SEC Total Peak Area Count	% Acidic % Main % Basic
4 wk	II, Colorless	2.1	38.5	0.046	97.58	2.14	0.19	0.08	35236	15.0 68.9 16.1
6 wk	II, Colorless	3.4	38.6	0.053	97.22	2.48	0.21	0.09	34993	14.8 67.4 17.8
8 wk	III, BY7 6.30	3.0	39.0	0.063	96.73	2.91	0.25	0.11	35998	15.1 66.9 18.0
12 wk	II, Colorless	2.1	39.1	0.049	96.25	3.37	0.29	0.10	35465	15.5 65.9 18.6

40 C.

Time Point	Appearance	Recon Time (min.)	Conc. (mg/mL)	Turbidity A360 nm	% Monomer	% Dimer	% Aggregate	% LMW	SEC Total Peak Area Count	% Acidic % Main % Basic
2 wk	II, Colorless	2.1	38.5	0.052	95.52	3.99	0.32	0.17	35285	15.3 59.3 25.3
4 wk	II, Colorless	3.3	38.4	0.047	93.58	5.71	0.61	0.10	35716	14.7 58.6 26.7
6 wk	III. Colorless	43	38.7	0.055	92.17	6.90	0.84	0.10	35585	14.8 58.9 26.3

TABLE 48

160 mg/mL Antegren, 36.8 mg/mL Sucrose, 24 mM Histidine, 0.16% PS-80
1 vial tested per time point.
Prepared.
Lyophiliiation Complete
Testing Start Date:
At T = 0 reconstituted with 1.0 mL, all other time points reconstituted with 0.8 mL.

2-8 C.

Time Point	Appearance, PH	Recon Time (min.)	KF % Moisture	Conc. (mg/mL)	Turbidity A360 nm	% Monomer	% Dimer	% Aggregate	% LMW	SEC Total Peak Area Count	% Acidic % Main % Basic
0	IV, Colorless	6.0	5.5	128.8	0.162	99.23	0.77	—	—	33210	16.0 66.5 17.5
4 wk	IV, Colorless	7.8	N/A	153.4	0.140	98.90	1.02	—	0.08	40638	14.5 70.6 14.9
8 wk	IV, BY7 6.43	8.0	N/A	153.4	0.150	98.79	1.14	—	0.08	40900	15.6 69.4 15.0
12 wk	IV, BY7	6.4	N/A	143.9	0.163	98.72	1.21	—	0.07	40819	15.4 69.7 14.9

25 C.

Time Point	Appearance, PH	Recon Time (min.)	Conc. (mg/mL)	Turbidity A360 nm	% Monomer	% Dimer	% Aggregate	% LMW	SEC Total Peak Area Count	% Acidic % Main % Basic
4 wk	IV. Colorless	5.6	153.1	0.144	97.53	2.20	0.18	0.09	40260	15.2 69.0 15.8
6 wk	IV, BY7	7.6	156.6	0.179	97.15	2.56	0.20	0.09	40334	14.9 67.3 17.8
8 wk	IV, BY6 6.35	5.7	153.3	0.155	96.67	2.96	0.26	0.11	40584	15.3 67.6 17.1
12 wk	IV, BY7	9.8	131.7	0.136	96.16	3.44	0.29	0.10	40606	15.4 66.0 18.6

40 C.

Time Point	Appearance	Recon Time (min.)	Conc. (mg/mL)	Turbidity A360 nm	% Monomer	% Dimer	% Aggregate	% LMW	SEC Total Peak Area Count	% Acidic % Main % Basic
2 wk	IV. Colorless	8.7	156.8	0.163	95.67	4.02	0.30	—	40618	15.0 59.8 25.2
4 wk	IV, BY7	7.9	151.2	0.157	93.42	5.82	0.65	0.11	40641	14.5 55.1 30.4
6 wk	IV, BY7	9.1	156.0	0.152	91.75	7.21	0.93	0.11	40735	14.9 57.7 27.4

100 mg mL Antegren. 69.3 mg/m.. Sucrose, 15 mM Histidine, 0.1% PS-80

TABLE 49

100 mg/mL Antegren, 69.3 mg/mL Sucrose, 15 mM Histidine, 0.1% PS-80
1 vial tested per time point.
Prepared.
Lyophiliiation Complete
Testing Start Date:
At T = 0 reconstituted with 1.6 mL, all other time points
reconstituted with 1.3 mL.

2-8 C.

Time Point	Appearances, pH	Recon Time (min.)	Conc. (mg/mL)	Turbidity A360 nm	% Monomer	% Dimer	% Aggregate	% LMW	SEC Total Peak Area Count	% Acidic % Main % Basic
4 wk	III, Colorless	3.0	106.1	0.098	98.91	1.02	—	0.07	35758	15.2 70.7 14.1
6 wk	III, Colorless	5.2	103.3	0.100	98.80	1.14	—	0.07	35025	15.2 69.9 14.9
8 wk	IV, BY6 6.35	4.0	103.5	0.108	98.67	1.24	—	0.09	34972	14.9 69.9 15.2
12 wk	III, BY7	4.5	100.9	0.101	98.55	1.37	—	0.08	35358	15.6 69.1 15.2

40 C.

Time Point	Appearances, pH	Recon Time (min.)	Conc. (mg/mL)	Turbidity A360 nm	% Monomer	% Dimer	% Aggregate	% LMW	SEC Total Peak Area Count	% Acidic % Main % Basic
2 wk	III, Colorless	2.7	105.0	0.102	98.54	1.46	—	—	35940	15.6 66.7 17.7
4 wk	III, BY7	2.6	85.4	0.097	97.82	2.10	—	0.08	29414	15.3 64.0 20.8
6 wk	III, Colorless	2.9	106.3	0.100	97.33	2.36	0.21	0.09	35794	15.4 66.4 18.2

TABLE 50

100 mg/mL Antegren, 115.5 mg/mL Sucrose, 15 mM Histidine, 0.1% PS-80
1 vial tested per time point.
Prepared.
Lyophiliiation Complete
Testing Start Date:
At T = 0 reconstituted with 1.6 mL, all other time points
reconstituted with 1.3 mL.

2-8 C.

0	IV, Colorless	2.9	N/A	72.6	0.089	99.48	0.52	—	—	36877	15.5 67.1 17.4
4 wk	III, Colorless	3.4	N/A	104.7	0.100	99.28	0.55	0.11	0.06	35319	14.8 71.3 13.9
8 wk	III, BY7 6.42	4.7	N/A	102.3	0.106	99.23	0.68	—	0.08	34784	15.6 70.1 14.2
12 wk	III, BY7	5.8	N/A	100.5	0.104	99.21	0.72	—	0.07	35667	15.6 70.6 13.8

TABLE 50-continued

100 mg/mL Antegren, 115.5 mg/mL Sucrose, 15 mM Histidine, 0.1% PS-80
1 vial tested per time point.
Prepared.
Lyophiliiation Complete
Testing Start Date:
At T = 0 reconstituted with 1.6 mL, all other time points reconstituted with 1.3 mL.

Time Point	Appearances, pH	Recon Time (min.)	KF % Moisture	Conc. (mg/mL)	Turbidity A360 nm	% Monomer	% Dimer	% Aggregate	% LMW	SEC Total Peak Area Count	% Acidic % Main % Basic
0	IV, Colorless	6.7	2.0	82.0	0.090	99.54	0.46	—	—	35236	15.4 67.6 17.0
4 wk	III, Colorless	3.9	N/A	100.6	0.085	99.37	0.46	0.11	0.06	34035	14.8 71.5 13.7
8 wk	III, BY7 6.44	6.7	N/A	97.3	0.096	99.33	0.58	—	0.09	33404	15.5 70.9 13.6
12 wk	III, BY7	8.7	N/A	100.5	0.092	99.34	0.58	—	0.08	34370	15.7 70.7 13.6

Time Point	Appearances, pH	Recon Time (min.)	Conc. (mg/mL)	Turbidity A360 nm	% Monomer	% Dimer	% Aggregate	% LMW	SEC Total Peak Area Count	% Acidic % Main % Basic
					25 C.					
4 wk	III, Colorless	3.6	100.9	0.096	99.22	0.71	—	0.06	34149	15.3 71.2 13.5
6 wk	III, Colorless	3.4	100.1	0.088	99.18	0.75	—	0.06	34039	15.3 70.6 14.1
8 wk	III, BY6 6.37	4.9	99.0	0.097	99.14	0.76	—	0.07	33713	15.8 70.1 14.2
12 wk	III, BY7	4.4	94.5	0.100	99.09	0.83	—	0.07	33713	15.8 70.1 14.2
					40 C.					
2 wk	III, Colorless	3.8	98.1	0.089	99.22	0.78	—	—	33705	15.8 67.1 17.0
4 wk	III, BY7	3.1	97.5	0.092	98.81	1.11	—	0.08	34307	15.5 66.3 18.2
6 wk	III, Colorless	7.4	102.4	0.091	98.68	1.25	—	0.07	34449	15.6 69.1 15.3

TABLE 51

	A	B	C
	% HMW		
0	0.49	0.39	0.43
8	0.5	0.49	0.51
12	0.5	0.49	0.50

TABLE 51-continued

	A	B	C
	% LMW		
0	0.09	0	0.00
8	0.08	0.08	0.07
12	0.07	0.07	0.06
	% Monomer		
0	99.42	99.61	99.57
8	99.43	99.43	99.42
12	99.43	99.44	99.43

TABLE 52

					Lyo 40 C.						
	A1	A2	B3	B4	A5	A6	C7	C8	C9	A10	B11
					% HMW						
0	0.50	0.51	0.45	0.44	0.51	0.58	0.79	0.76	0.77	0.52	0.46
2	1.48	1.47	0.77	0.78	1.45	1.45	4.23	4.31	4.32	1.46	0.78
4	2.10	2.16	1.08	1.11	2.13	2.14	6.43	6.32	6.47	2.10	1.11
6	2.62	2.59	1.27	1.25	2.61	2.56	7.98	7.74	8.14	2.57	1.25
					% LMW						
0	0.00	0.00	0.00	0.00	0.00	0.09	0.00	0.00	0.00	0.00	0.00
2	0.00	0.00	0.00	0.00	0.00	0.11	0.00	0.17	0.00	0.00	0.00
4	0.09	0.08	0.08	0.07	0.08	0.08	0.10	0.10	0.11	0.08	0.08
6	0.10	0.09	0.08	0.07	0.09	0.09	0.11	0.10	0.11	0.09	0.07
					% Monomer						
0	99.50	99.49	99.55	99.56	99.49	99.32	99.22	99.24	99.23	99.48	99.54
2	98.52	98.53	99.23	99.22	98.55	98.16	95.76	95.52	95.67	98.54	99.22
4	97.81	97.76	98.84	98.82	97.79	97.77	93.46	93.58	93.42	97.82	98.81
6	97.28	97.32	98.65	98.68	97.29	97.35	91.91	92.17	91.75	97.33	98.68

TABLE 53

					Lyo 25 C.						
	A1	A2	B3	B4	A5	A6	C7	C8	C9	A10	B11
					% HMW						
0	0.50	0.51	0.45	0.44	0.51	0.58	0.79	0.76	0.77	0.52	0.46
4	1.03	1.02	0.70	0.72	1.02	0.92	2.34	2.33	2.38	1.02	0.71
6	1.13	1.12	0.75	0.75	1.12	1.14	2.71	2.69	2.76	1.14	0.75
8	1.25	1.23	0.80	0.80	1.24	1.27	3.20	3.16	3.22	1.24	0.76
12	1.40	1.38	0.82	0.83	1.39	1.39	3.67	3.66	3.73	1.37	0.83
					% LMW						
0	0.00	0.00	0.00	0.00	0.00	0.09	0.00	0.00	0.00	0.00	0.00
4	0.07	0.08	0.07	0.06	0.07	0.07	0.09	0.08	0.09	0.07	0.06
6	0.08	0.07	0.07	0.06	0.07	0.07	0.09	0.09	0.09	0.07	0.06
8	0.11	0.09	0.09	0.08	0.10	0.08	0.09	0.11	0.11	0.09	0.10
12	0.08	0.08	0.08	0.07	0.08	0.07	0.10	0.10	0.10	0.08	0.07
					% Monomer						
0	99.50	99.49	99.55	99.56	99.49	99.32	99.22	99.24	99.23	99.48	99.54
4	98.89	98.90	99.22	99.22	98.91	98.90	97.57	97.58	97.53	98.91	99.22
6	98.79	98.81	99.18	99.19	98.80	98.79	97.20	97.22	97.15	98.80	99.18
8	98.64	98.67	99.11	99.12	98.67	98.65	96.71	96.73	96.67	98.67	99.14
12	98.52	98.55	99.10	99.10	98.53	98.54	96.22	96.25	96.16	98.55	99.09

TABLE 54

					Lyo 25 C.						
	A	A2	B3	B4	A5	A6	C7	C8	C9	A10	B11
					% HMW						
0	0.50	0.51	0.45	0.44	0.51	0.58	0.79	0.76	0.77	0.52	0.46
4	0.65	0.65	0.56	0.59	0.66	0.65	0.99	1.01	1.02	0.66	0.57

TABLE 54-continued

	Lyo 25 C.										
	A	A2	B3	B4	A5	A6	C7	C8	C9	A10	B11
8	0.68	0.67	0.57	0.58	0.67	0.67	1.10	1.09	1.14	0.68	0.58
12	0.71	0.72	0.60	0.58	0.72	0.69	1.17	1.18	1.21	0.72	0.58
					% LMW						
0	0.00	0.00	0.00	0.00	0.00	0.09	0.00	0.00	0.00	0.00	0.00
4	0.07	0.06	0.07	0.06	0.07	0.06	0.07	0.07	0.08	0.06	0.06
8	0.10	0.08	0.10	0.07	0.08	0.07	0.08	0.07	0.08	0.08	0.09
12	0.08	0.07	0.09	0.07	0.06	0.07	0.05	0.07	0.07	0.07	0.08
					% Monomer						
0	99.50	99.49	99.55	99.56	99.49	99.32	99.22	99.24	99.23	99.48	99.54
4	99.27	99.28	99.37	99.35	99.27	99.28	98.94	98.92	98.90	99.28	99.37
8	99.22	99.25	99.34	99.34	99.24	99.25	98.83	98.84	98.79	99.23	99.33
12	99.21	99.21	99.32	99.35	99.22	99.24	98.78	98.75	98.72	99.21	99.34

TABLE 55

	Pre-Lyo A
5 C.	
	Pre-Lyo B
5 C.	
	Pre-Lyo C.
5 C.	
	A1
5 C.	Stayed IV, changed to BY7 at 8 wk
25 C.	Stayed IV, changed to BY7 at 6 wk
40 C.	Stayed IV, changed to BY7 at 4 wk
	A2
5 C.	Stayed III, changed to BY7 at 8 wk
25 C.	Stayed III, changed to BY7 at 6 wk
40 C.	Changed to IV at 6 wk, changed to BY7 at 4 wk
	B3
5 C.	Stayed III, changed to BY7 at 8 wk
25 C.	Changed to IV at 12 wk, changed to BY7 at 6 wk
40 C.	Stayed III, changed to BY7 at 4 wk
	B4
5 C.	No major changes, all stayed at II, colorless
25 C.	
40 C.	

TABLE 55-continued

	A5
5 C.	
25 C.	
40 C.	
	A6
5 C.	
25 C.	
40 C.	
	C7
5 C.	
25 C.	
40 C.	
	C8
5 C.	
25 C.	
40 C.	
	C9
5 C.	
25 C.	
40 C.	
	A10
5 C.	
25 C.	
40 C.	
	B11
5 C.	
25 C.	
40 C.	

TABLE 56

No major changes seen in turbidity at any temperature.

	A1	A2	B3	B4	A5	A6	C7	C8	C9	A10	B11
					40 C.						
0	0.126	0.095	0.112	0.054	0.100	0.047	0.109	0.082	0.162	0.089	0.090
2	0.124	0.106	0.107	0.046	0.112	0.046	0.133	0.052	0.163	0.102	0.089
4	0.113	0.110	0.102	0.052	0.123	0.048	0.132	0.047	0.157	0.097	0.092
6	0.113	0.111	0.114	0.043	0.115	0.046	0.139	0.055	0.152	0.100	0.091

TABLE 56-continued

No major changes seen in turbidity at any temperature.											
					25 C.						
0	0.126	0.095	0.112	0.054	0.100	0.047	0.109	0.082	0.162	0.089	0.090
4	0.111	0.101	0.093	0.040	0.106	0.040	0.129	0.046	0.144	0.098	0.096
6	0.132	0.106	0.109	0.044	0.104	0.046	0.148	0.053	0.179	0.100	0.088
8	0.116	0.101	0.099	0.053	0.108	0.054	0.124	0.063	0.155	0.108	0.097
12	0.119	0.105	0.118	0.052	0.123	0.046	0.122	0.049	0.136	0.101	0.100
					5 C.						
0	0.126	0.095	0.112	0.054	0.100	0.047	0.109	0.082	0.162	0.089	0.090
4	0.101	0.111	0.124	0.041	0.112	0.042	0.120	0.053	0.140	0.100	0.085
8	0.110	0.107	0.105	0.046	0.107	0.064	0.134	0.052	0.150	0.106	0.096
12	0.108	0.107	0.116	0.051	0.105	0.045	0.201	0.069	0.163	0.104	0.092

	Pre-Lyo 5 C		
	A	B	C
0	0.044	0.041	0.041
8	0.053	0.040	0.041
12	0.041	0.044	0.043

[0206] Also refer to Examples 25A, B, C, and D.

TABLE 57

Recon Stability					
4 wks at 40 C. 4089-1L % monomer			4 wks at 5 C 4089-1L % monomer		
5 C.	0	96.5	5 C.	0	97.78
	0	96.56		0	97.77
	1	96.57		1	97.8
	1	96.61		1	97.79
25 C.	0	96.55	25 C.	0	
	0	96.52		0	
	1	96.72		1	
	1	96.7		1	

4 wks at 40 C. 4089-1N % monomer		
5 C.	0	95.87
	0	95.90
	1	95.92
	1	95.97
25 C.	0	95.86
	0	95.87
	1	96.06
	1	96.07

Example 5

[0207] The formulation described herein is a lyophilized cake containing natalizumab, sucrose, histidine and polysorbate 80. The pre-lyophilized bulk drug substance contains 40 mg/mL antibody, 41 mg/mL sucrose, 0.04% polysorbate 80 and 6 mM histidine HCl, pH 6.0. This was filled at 4 mL per vial lyophilized, reconstituted with 1.0 mL water to 120 mg/mL, 123 mg/mL sucrose, 0.12% polysorbate 80 and 18 mM histidine HCl, pH 6.0.

[0208] Pre-lyophilized natalizumab composition was provided by BiogenIdec. It was formulated into phosphate buffered saline and was processed into an ammonium sulfate solution. This material was then diafiltered into the formulation buffer (without polysorbate) and concentrated to 40 mg/mL. The appropriate amount of polysorbate 80 was then added, the material was sterile filtered into polypropylene bottles and stored at 2-8° C. for 4 weeks prior to filling and lyophilization. Filling and lyophilization were performed in a non-GMP suite using a written batch record. The suite was sanitized prior to filling and all filling operations were performed under a laminar flow hood. Lyophilization was performed using a Virtis Gensis 25 EL lyophilizer.

[0209] The stability study consists of three arms, one examined the stability of the pre-lyophilized natalizumab composition for up to one year at the recommended storage temperature (2-8° C.) and up to 6 months at an accelerated temperature of 25° C. The lyophilized composition vials stored for 12 months at the recommended storage temperature (2-8° C.), 6 months at 25° C. and 3 months at 40° C. Vials at various timepoints from the 2-8° C. arm were reconstituted and stored for 1 week at both 2-8° C. (recommended temperature) and 25° C. (accelerated).

[0210] Quality control stability tests were performed with regard to appearance, A280, pH, non-reduced and reduced SDS-PAGE, cation exchange chromatography, and size exclusion chromatography.

Material, Methods and Testing Time Points

[0211] The following samples will be tested

TABLE 58

Sample Configuration	
Batch/Lot	Description
Pre-lyophilized BiogenIdec Lot #: LYO121504	2 mL fill in polypropylene vials
Lyophilized vials Lot# K65001 containing 160 mg of active/vial	5 mL vials containing lyophilized cake with butyl rubber stopper and Flip-off cap. Vials to be reconstituted with 1 mL of WFI or other purified water.

TABLE 59

Study Methods

Method Number	Title	Volume Needed
EOP 000-01291	Determination of Appearance of Lyophilized Vials	2 vials*
EOP 000-01291	Moisture	2 vials
EOP 000-01292	Determination of Time for Reconstitution	2 vials*
AAM 001-00141	Determination of the Appearance of Antegren and Matching Placebo Final Container**	2 vials*
AAM 001-00143	Determination of pH of Antegren Drug Substance, Final Container and Placebo for Antegren	1 mL*
AAM 001-00380	Non-Reduced SDS-Page and Reduced SDS-PAGE**	50 μL
EOP 001-01198	Determination of Charge Distribution of Antegren Drug Substance and Final Container by Weak Cation Exchange Chromatography**	50 μL

TABLE 59-continued

Study Methods

Method Number	Title	Volume Needed
EOP 001-01205	Size Exclusion Chromatography**	50 μL
AAM 001-00025	Concentration of Drug Substance, Final Container, and Placebo for Antegren by A280**	200 μL

*Non-destructive, use vial for subsequent testing.
**Modification to method required, see Section 3.3 below.

TABLE 60

Study Methods

Method Number	Title	Volume Needed
160a.213	VCAM Lysate	1 vial**
22d.530	Reducing Gel Chip CE	1 vial**
22d.596	Non-reducing Gel Chip CE	1 vial**
22d.544b and 22d.552a	Methionine Oxidation	1 vial**
22d.84	Particulates in Small Volume Parenterals	1 vial**

**One vial used for all 5 assays

TABLE 61

Stability Tests and Time points for Pre-Lyophilized Bulk

		1 Month		2 Month		3 Month		6 Month		12 Month or EOS
Test Methods	Initial	2-8	25	2-8	25	2-8	25	2-8	25	2-8
Appearance (AAM 001-00141)	X	X	X	X	X	X	X	X	X	X
Protein Concentration by A280	X	X	X	X	X	X	X	X	X	X
Size Exclusion Chromatography (SEC)	X	X	X	X	X	X	X	X	X	X
Cation Exchange Chromatography (CEX)	X	X	X	X	X	X	X	X	X	X
SDS-PAGE: reduced	X	X	X	X	X	X	X	X	X	X
SDS-PAGE: non-reduced	X	X	X	X	X	X	X	X	X	X
pH	X	X	X	X	X	X	X	X	X	X
VCAM Lysate*	X					X	X			X
Reducing Gel Chip*	X					X	X			X
Non-reducing Gel Chip CE*	X					X	X			X
Methionine oxidation*	X					X	X			X
Number of samples to pull per time point per condition at Elan	1	1	1	1	1	1	1	1	1	1

TABLE 62

Stability Tests and Time points for Lyophilized Vials

		1 Month			2 Month			3 Month			6 Month		12 Month or EOS
Test Methods	Initial	2-8	25	40	2-8	25	40	2-8	25	40	2-8	25	2-8
Appearance of cake	X	X	X	X	X	X	X	X	X	X	X	X	X
Time for reconstitution	X	X	X	X	X	X	X	X	X	X	X	X	X
Moisture	X										X	X	X
Appearance of reconstituted solution	X	X	X	X	X	X	X	X	X	X	X	X	X
Protein Concentration by A280	X	X	X	X	X	X	X	X	X	X	X	X	X
Size Exclusion Chromatography (SEC)	X	X	X	X	X	X	X	X	X	X	X	X	X
Cation Exchange Chromatography (CEX)	X	X	X	X	X	X	X	X	X	X	X	X	X
SDS-PAGE: reduced	X	X	X	X	X	X	X	X	X	X	X	X	X
SDS-PAGE: non-reduced	X	X	X	X	X	X	X	X	X	X	X	X	X
pH	X	X	X	X	X	X	X	X	X	X	X	X	X
VCAM Lysate*	X								X	X	X	X	X
Reducing Gel Chip*	X								X	X	X	X	X
Non-reducing Gel Chip*	X								X	X	X	X	X
Methionine oxidation*	X								X	X	X	X	X
SVP Particulates*	X								X	X	X	X	X
Number of vials to pull per time point per condition at Elan	2	2	2	2	2	2	2	2	2	2	2	2	2

[0212] Reconstituted Stability

[0213] At the following time points, 4 vials were pulled from 2-8° C., reconstituted and then placed at 2-8° C. and 25° C. for one week to examine the stability of the reconstituted material. For ease of use of analytical equipment and time, these samples were pulled one week before the scheduled timepoint, reconstituted, placed at the desired temperature and then assayed along side the other samples.

TABLE 63

Stability Tests and Time points for Reconstituted Vials

		3 Month		6 Month		12 Month or EOS
Test Methods	Initial	2-8	25	2-8	25	2-8
Appearance (AAM 001-00141)	X	X	X	X	X	X
Protein Concentration by A280	X	X	X	X	X	X
Size Exclusion Chromatography (SEC)	X	X	X	X	X	X
Cation Exchange Chromatography (CEX)	X	X	X	X	X	X
SDS-PAGE: reduced	X	X	X	X	X	X

TABLE 63-continued

Stability Tests and Time points for Reconstituted Vials

		3 Month		6 Month		12 Month or EOS
Test Methods	Initial	2-8	25	2-8	25	2-8
SDS-PAGE: non-reduced	X	X	X	X	X	X
pH	X	X	X	X	X	X
VCAM Lysate*		X	X			X
Reducing Gel Chip*		X	X			X
Non-reducing Gel Chip CE*		X	X			X
Methionine oxidation *		X	X			X
Number of samples to pull per time point per condition at Elan	2	2	2	2	2	2

Note:

Vials will be pulled from 2-8° C. at the listed time points, reconstituted and then stored at either 2-8° C. or 25° C. for one week and assayed as above.

Data

APPENDIX A

Total Number of Vials to be Placed at Each Condition. Note: 2-8° Numbers Include Initial Time Point Testing as Necessary

[0214]

TABLE 64

Pre-Lyophilized bulk sample requirements

Temperature	# vials required for Elan testing	Vial Overage	Total Required
5° C.	6	5	11 vials
25° C./60% RH	4	4	8 vials
Total 5° C. and 25° C./60% RH studies			19 vials

TABLE 65

Lyophilized sample requirements (including for reconstitution)

Temperature	# vials required for Elan testing	Vial Overage	Total Required
5° C.	24	12	36 vials
25° C./60% RH	8	5	13 vials
40° C./75% RH	6	4	10 vials
Total 5° C. and 25° C./60% RH studies			59 vials

Material, Methods and Testing Time Points

[0215]

TABLE 66

Study Methods

Method Number	Title	Volume Needed
EOP 000-01291	Determination of Appearance of Lyophilized Vials	2 vials*
EOP 000-01290+ or EOP 03201299**	Moisture	2 vials
EOP 000-01292	Determination of Time for Reconstitution	2 vials*
AAM 001-00141	Determination of the Appearance of Antegren and Matching Placebo Final Container**	2 vials*
AAM 001-00143	Determination of pH of Antegren Drug Substance, Final Container and Placebo for Antegren	1 mL*
AAM 001-00380	Non-Reduced SDS-Page and Reduced SDS-PAGE**	50 μL
EOP 001-01198	Determination of Charge Distribution of Antegren Drug Substance and Final Container by Weak Cation Exchange Chromatography**	50 μL
EOP 001-01205	Size Exclusion Chromatography**	50 μL
AAM 001-00025	Concentration of Drug Substance, Final Container, and Placebo for Antegren by A280**	200 μL

*Non-destructive use vial for subsequent testing.

**Modification to method required, see Section 3.3 below.

+Appropriate SOP to be determined, see text.

TABLE 67

Study Methods

Method Number	Title	Volume Needed
22d.394+	Karl Fisher	2 vials
160a.213	VCAM Lysate	1 vial**
22d.530	Reducing Gel Chip CE	1 vial**
22d.596	Non-reducing Gel Chip CE	1 vial**
22d.544b and 22d.552a	Methionine Oxidation	1 vial**
22d.84	Particulates in Small Volume Parenterals	1 vial**

**One vial used for all 5 assays.

+Appropriate SOP to be determined, see text.

Modifications Required to Assays

[0216] Size Exclusion chromatography is modified to include that the data collection should be made at the A280 nm wavelength.

[0217] Justification: The increased mass on the column from approximately 40 μg to 400 μg necessitates the use of the less sensitive wavelength.

[0218] Section 3.5 Table 5: The table will be modified to indicate that a total of 4 vials are necessary for the initial time point testing, at 3 months and at 12 months or end of study.

[0219] Justification: This table neglected to take into account the 2 additional vials needed at these time points for moisture testing. This testing is destructive and therefore the contents of the vials cannot be recovered for additional use.

TABLE 68

Stability Tests and Time points for Lyophilized Vials

		1 Month			2 Month			3 Month			6 Month		12 Month or EOS
Test Methods	Initial	2-8	25	40	2-8	25	40	2-8	25	40	2-8	25	2-8
Appearance of cake	X	X	X	X	X	X	X	X	X	X	X	X	X
Time for reconstitution	X	X	X	X	X	X	X	X	X	X	X	X	X
Moisture	X										X	X	X
Appearance of reconstituted solution	X	X	X	X	X	X	X	X	X	X	X	X	X
Protein Concentration by A280	X	X	X	X	X	X	X	X	X	X	X	X	X
Size Exclusion Chromatography (SEC)	X	X	X	X	X	X	X	X	X	X	X	X	X
Cation Exchange Chromatography (CEX)	X	X	X	X	X	X	X	X	X	X	X	X	X
SDS-PAGE: reduced	X	X	X	X	X	X	X	X	X	X	X	X	X
SDS-PAGE: non-reduced	X	X	X	X	X	X	X	X	X	X	X	X	X
pH	X	X	X	X	X	X	X	X	X	X	X	X	X
VCAM Lysate*	X							X	X	X	X	X	X
Reducing Gel Chip*	X							X	X	X	X	X	X
Non-reducing Gel Chip*	X							X	X	X	X	X	X
Methionine oxidation*	X							X	X	X	X	X	X
SVP Particulates*	X								X	X	X	X	X
Number of vials to pull per time point per condition at Elan	4	2	2	2	2	2	2	2	2	2	4	4	4

TABLE 69

Natalizumab, Pre-Lyophilized Bulk Stability Results

Product: Natalizumab, Lyophilized, 160 mg/vial	Mfr. Bulk Lot No: N/A	Control No: K65001 AQS: 2071
Mfr. Date: Pre-Lyophilized Bulk	Strength: 40 mg/mL	Stability Initiation Date:
Storage Conditions: 5° C. ± 3° C. Upright	Description: 5 mL fill in polypropylene vials	Mfr. Lot No: LYO121504

Test Performed

				Cation Exchange Chromatography (CEX)			SDS-PAGE Report value			Size Exclusion Chromatography		
		Conc						Non-Reduced		Report value		
Time	Appearance	Report	pH	Report value				MW			% Impurity	
point (months)	Report Observation	value (mg/mL)	Report value	% Lower Isoforms	% Higher Isoforms	% Peak 4	Reduced % IgG	comparable to Ref Std	% Half Antibody	% purity	% Oligomer	% LMW2
0	Colorless, slightly opalescent. Particles: 1	41	6.0	17.0	13.4	69.6	99.5	Conforms	11.0	99.7	0.2	0.1
1	Colorless, slightly opalescent. Particles: 1	41	6.1	15.8	14.8	69.4	99.2	Conforms	9.6	99.7	0.2	0.1
2	Colorless, slightly opalescent. Particles: 0	41	6.1	17.2	12.1	70.8	99.5	Conforms	9.1	99.7	0.2	0.1
3	Colorless, slightly opalescent. Particles: 0	40	6.2	18.2	12.4	69.4	99.4	Conforms	8.3	99.7	0.2	0.1

TABLE 69-continued

Natalizumab, Pre-Lyophilized Bulk Stability Results												
6	Colorless, slightly opalescent. Particles: 0	41	6.1	16.9	14.2	68.9	99.4	Conforms	8.3	99.7	0.3	0.0
12	Colorless, slightly opalescent. Particles: 0	41	6.1	17.9	11.9	70.2	100.0	Conforms	9.7	99.7	0.3	0.1

TABLE 70

Natalizumab, Pre-Lyophilized Bulk Stability Results

Product: Natalizumab, Lyophilized, 160 mg/vial	Mfr. Bulk Lot No: N/A	Control No: K65001 AQS: 2071
Mfr. Date: Pre-Lyophilized Bulk	Strength: 40 mg/mL	Stability Initiation Date:
Storage Conditions: 25° C. ± 2° C./60% RH + 5% RH Upright	Description: 5 mL fill in polypropylene vials	Mfr. Lot No: LYO121504

				Test Performed								
				Cation Exchange Chromatography (CEX)			SDS-PAGE Report value			Size Exclusion Chromatography		
		Conc						Non-Reduced		Report value		
Time	Appearance	Report	pH	Report value				MW			% Impurity	
point (months)	Report Observation	value (mg/mL)	Report value	% Lower Isoforms	% Higher Isoforms	% Peak 4	Reduced % IgG	comparable to Ref Std	% Half Antibody	% purity	% Oligomer	% LMW2
0	Colorless, slightly opalescent. Particles: 1	41	6.0	17.0	13.4	69.9	99.5	Conforms	11.0	99.7	0.2	0.1
1	Colorless, slightly opalescent. Particles: 1	41	6.1	17.3	14.1	68.6	99.1	Conforms	9.1	99.6	0.3	0.1
2	Colorless, slightly opalescent. Particles: 0	41	6.1	20.5	10.4	69.2	99.5	Conforms	9.9	99.6	0.3	0.1
3	Colorless, slightly opalescent. Particles: 0	41	6.1	23.6	10.2	66.2	99.1	Conforms	8.6	99.6	0.3	0.1
6	Colorless, slightly opalescent. Particles: 0	42	6.1	27.7	11.3	61.0	98.8	Conforms	8.6	99.6	0.4	

TABLE 71

Natalizumab, Lyophilized Stability Results

Product: Natalizumab, Lyophilized, 160 mg/vial Mfr. Date: Storage Conditions: 5° C. ± 3° C. Upright	Mfr. Bulk Lot No: N/A Strength: 120 mg/mL Description: 5 mL vials containing lyophilized cake with butyl rubber stopper and Flip-off cap. Vials to be reconstituted with 1 mL of WFI or other purified water	Control No: K65001 AQS: 2071 Stability Initiation Date: Mfr. Lot No: LYO121504

Test Performed

	Appearance		Conc.	Moisture	pH	Time of Reconstitution	CationExchang Chromatography(CEX) Report value		
Time point	Report Observation		Report value	Report	Report	Time of	% Lower	% Higher	
(months)	Cake	Solution	(mg/mL)	value	value	Reconstitution	Isoforms	Isoforms	% Peak 4
0	White 1 Cake	Colorless, slightly opalescent. Particles	136	0.3%	6.0	11 m 29 s 7 m 38 s	17.2	13.4	69.4
1	White 1 Cake	Colorless, slightly opalescent. Particles:	127	NR	6.1	7 m 18 s 6 m 41 s	16.1	14.5	69.4
2	White 1 Cake	Colorless, slightly opalescent. Particles:	135	NR	6.1	6 m 47 s 7 m 08 s	17.2	12.3	70.5
3	White 1 Cake1	Colorless, slightly opalescent. Particles 1 and 0	127	NR	6.2	5 m 22 s 4 m 16 s	17.8	12.7	69.5
6	White 1 Cake	Colorless, slightly opalescent. Particles: 0, 1, 0, 03	126	0.2	6.1	4 m 57 s 4 m 40 s 4 m 15 s	15.9	15.2	68.8
12	White 1 Cake	Colorless, slightly opalescent. Particles: 0, 0	132	0.8	6.2	6 m 36 s 8 m 17 s	16.9	12.6	70.5

	SDS-PAGE Report Value			Size Exclusion Chromatography Report Value		
		Non-Reduced			% Impurity	
Time point (months)	Reduced % IgG	MW comparable to Ref Std	% Half Antibody	% Purity	% Oligomer	% LMW2
0	99.52	Conform	10.7	99.6	0.3	0.1
1	99.9	Conform	8.1	99.5	0.3	0.1
2	99.5	Conform	10.6	99.5	0.3	0.1
3	99.7	Conform	9.0	99.3	0.3	0.3
6	99.7	Conform	7.8	99.5	0.4	0.1
12	100.0	Conform	8.5	99.5	0.4	0.1

1Refer to Analytical Summary for more detail description.

2 The initial OOT result was determined to be laboratory error (see LIR# 05-007 for more information.)

NR = test not required at time point according to protocol.

3 See QIR# G1-05-033.

TABLE 72

Natalizumab, Lyophilized Stability Results

Product: Natalizumab, Lyophilized, 160 mg/vial Mfr. Date: Storage Conditions: 25° C. ± 2° C./60% RH ± 5% RH Upright	Mfr. Bulk Lot No: N/A Strength: 120 mg/mL Description: 5 mL vial containing lyophilized cake with butyl rubber stopper and Flip-off cap. Vials to be reconstituted with 1 mL of WFI or other purified water	Control No: K65001 AQS: 2071 Stability Initiation Date: Mfr. Lot No: LYO121504

Test Performed

	Appearance		Conc.	Moisture	pH	Time of Reconstitution	Caution Exchange Chromatography(CEX) Report value		
Time point	Report Observation		Report value	Report	Report	Time of	% Lower	% Higher	
(months)	Cake	Solution	(mg/mL)	value	value	Reconstitution	Isoforms	Isoforms	% Peak 4
0	White 1 Cake	Colorless, slightly opalescent. Particles 1'	136	0.3%	6.01	11 m 29 s 7 m 38 s	17.2	13.4	69.4
1	White 1 Cake	Colorless, slightly opalescent. Particles: 1	126	NR	6.1	7 m 18 s 6 m 41 s	16.1	14.7	69.2
2	White 1 Cake	Colorless, slightly opalescent. Particles: 1	140	NR	6.1	6 m 32 s 6 m 09 s	17.0	12.5	70.6
3	White 1 Cake1	Colorless, slightly opalescent. Particles 0	117	NR	6.2	6 m 17 s 5 m 41 s	17.9	12.6	69.5
6	White 1 Cake	Colorless, slightly opalescent. Particles: 0, 0, 1, 0[3]	135	0.5	6.1	4 m 37 s 4 m 45 s 6 m 27 s[3]	16.7	15.0	68.3

	SDS-PAGE Report Value			Size Exclusion Chromatography Report Value		
		Non-Reduced			% Impurity	
Time point (months)	Reduced % IgG	MW comparable to Ref Std	% Half Antibody	% Purity	% Oligomer	% LMW2
0	99.52[2]	Conform[2]	10.7	99.6	0.3	0.1
1	99.8	Conform	9.1	99.3	0.6	0.1
2	99.5	Conform	10.3	99.2	0.7	0.1
3	99.7	Conform	8.2	99.1	0.8	
6	99.6	Conform	8.4	98.8	1.0	0.1

1Refer to Analytical Summary for more detail description.
[2]The initial OOT result was determined to be laboratory error (see LIR# 05-007 for more information.)
NR = test not required at time point according to protocol.
[3]See QIR# G1-05-033.

TABLE 73

Natalizumab, Lyophilized Stability Results

Product: Natalizumab, Lyophilized, 160 mg/vial Mfr. Date:	Mfr. Bulk Lot No: N/A Strength: 120 mg/mL Description: 5 mL vial containing lyophilized	Control No: K65001 AQS: 2071 Stability Initiation Date: Mfr. Lot No: LYO121504

TABLE 73-continued

Natalizumab, Lyophilized Stability Results

Storage Conditions: 40° C. ± 2° C./75% RH ± 5% RH Upright	cake with butyl rubber stopper and Flip-off cap. Vials to be reconstituted with 1 mL of WFI or other purified water

Test Performed

	Appearance		Conc.	Moisture	pH	Time of Reconstitution	Caution Exchange Chromatography(CEX) Report value		
Time point	Report Observation		Report value	Report	Report	Time of	% Lower	% Higher	
(months)	Cake	Solution	(mg/mL)	value	value	Reconstitution	Isoforms	Isoforms	% Peak 4
0	White 1 Cake	Colorless, slightly opalescent. Particles 1'	136	0.3%	6.0	11 m 29 s 7 m 38 s	17.2	13.4	69.4
1	White 1 Cake	Colorless, slightly opalescent. Particles: 1	125	NR	6.1	5 m 30 s 4 m 40 s	16.2	15.0	68.8
2	White 1 Cake	Colorless, slightly opalescent. Particles: 1	131	NR	6.1	5 m 40 s 5 m 38 s	17.2	13.2	69.5
3	White 1 Cake1	Colorless, slightly opalescent. Particles 0	129	NR	6.2	4 m 38 s 6 m 30 s	18.4	12.9	68.6

	SDS-PAGE Report Value			Size Exclusion Chromatography Report Value		
		Non-Reduced			% Impurity	
Time point (months)	Reduced % IgG	MW comparable to Ref Std	% Half Antibody	% Purity	% Oligomer	% LMW2
0	99.5[2]	Conform[2]	10.7	99.6	0.3	0.1
1	99.6	Conform	9.6	98.7	1.2	0.1
2	99.5	Conform	9.8	98.3	1.6	0.2
3	99.4	Conform	8.2	97.7	2.0	

1Refer to Analytical Summary for more detail description.

[2]The initial OOT result was determined to be laboratory error (see LIR# 05-007 for more information.

NR = test not required at time point according to protocol.

TABLE 74

Natalizumab, Reconstituted Vials Stability Results

Product: Natalizumab,	Mfr. Bulk Lot No: N/A	Control No: K65001 AQS: 2071
Lyophilized, 160 mg/vial	Strength: 120 mg/mL	Stability Initiation Date:
Reconstituted Vials	Description: 5 mL, type I glass vial	Mfr. Lot No: LYO121504
Mfr. Date:		
Storage Conditions: 5° C. ± 3° C. Upright		

TABLE 74-continued

Natalizumab, Reconstituted Vials Stability Results

Test Performed

Time point (months)	Appearance Report Observation Cake	Appearance Report Observation Solution	Conc. Report value (mg/mL)	pH Report value	Time of Reconstitution Time of Reconstitution	Caution Exchange Chromatography(CEX) Report value % Lower Isoforms	% Higher Isoforms	% Peak 4
0	White 1 Cake	Colorless, slightly opalescent. Particles 1'	132	6.0	NR	16.9	13.7	69.4
3	White 1 Cake	Colorless, slightly opalescent. Particles: 0	134	6.1	5 m 17 s 4 m 27 s	18.1	12.4	69.5
6	White 1 Cake	Colorless, slightly opalescent. Particles: 0, 1	133	6.1	4 m 13 s 6 m 03 s	16.9	14.1	69.0
12	White 1 Cake1	Colorless, slightly opalescent. Particles 0, 1	137	6.2	5 m 59 s 6 m 18 s	17.1	12.5	70.5

	SDS-PAGE Report Value			Size Exclusion Chromatography Report Value		
		Non-Reduced			% Impurity	
Time point (months)	Reduced % IgG	MW comparable to Ref Std	% Half Antibody	% Purity	% Oligomer	% LMW2
0	99.5	Conform	11.5	99.6	0.3	0.1
3	99.7	Conform	8.1	99.3	0.3	0.4
6	99.7	Conform	8.4	99.5	0.4	0.1
12	100.0	Conform	10.5	99.5	0.5	

1Refer to Analytical Summary for more detail description
NR = test not required at time point according to protocol.

TABLE 75

Natalizumab, Reconstituted Vials Stability Results

Product: Natalizumab, Lyophilized, 160 mg/vial Reconstituted Vials	Mfr. Bulk Lot No: N/A	Control No: K65001 AQS: 2071
Mfr. Date:	Strength: 120 mg/mL	Stability Initiation Date:
Storage Conditions: 25° C. ± 2° C./60% RH ± 5% RH Upright	Description: 5 mL, type I glass vial	Mfr. Lot No: LYO121504

TABLE 75-continued

Natalizumab, Reconstituted Vials Stability Results

Test Performed

Time point (months)	Appearance Report Observation Cake	Appearance Report Observation Solution	Conc. Report value (mg/mL)	pH Report value	Time of Reconstitution Time of Reconstitution	Caution Exchange Chromatography(CEX) Report value % Lower Isoforms	% Higher Isoforms	% Peak 4
0	NR	Colorless, slightly opalescent. Particles 1'	132	6.0	NR	16.9	13.7	69.4
3	White 1 Cake	Colorless, slightly opalescent. Particles: 0	141	6.1	7 m 16 s 5 m 15 s	18.7	11.9	69.5
6	White 1 Cake	Colorless, slightly opalescent. Particles: 0, 1	137	6.1	4 m 12 s 5 m 57 s	17.4	13.9	69.5

	SDS-PAGE Report Value			Size Exclusion Chromatography Report Value		
		Non-Reduced			% Impurity	
Time point (months)	Reduced % IgG	MW comparable to Ref Std	% Half Antibody	% Purity	% Oligomer	% LMW2
0	99.5	Conform	11.5	99.6	0.3	0.1
3	99.5	Conform	7.9	99.2	0.4	0.4
6	99.5	Conform	7.9	99.2	0.4	0.1

1Refer to Analytical Summary for more detail description.
NR = test not required at time point according to protocol

1. A stable lyophilized formulation prepared by lyophilizing an aqueous formulation, wherein the aqueous formulation comprises:

(a) about 20 mg/ml to about 80 mg/ml natalizumab;

(b) a buffer having a pH of about 5.5 to about 6.5;

(c) about 20 mg/ml to about 80 mg/ml sucrose; and

(d) about 0.02 to about 0.08% polysorbate.

2. The stable lyophilized formulation of claim **1**, wherein said aqueous formulation comprises about 30 mg/ml to about 80 mg/ml natalizumab.

3. The stable lyophilized formulation of claim **2**, wherein said aqueous formulation comprises about 40 mg/ml natalizumab.

4. The stable lyophilized formulation of claim **1**, wherein said buffer has a pH of about 6.0.

5. The stable lyophilized formulation of claim **1**, wherein said buffer is histidine.

6. The stable lyophilized formulation of claim **5**, wherein said histidine is present in said aqueous formulation at a concentration of about 1 mM to about 12 mM.

7. The stable lyophilized formulation of claim **6**, wherein said histidine is present in said aqueous formulation at a concentration of about 6 mM.

8. The stable lyophilized formulation of claim **1**, wherein said sucrose is present in said aqueous formulation at a concentration of about 20 mg/ml to about 80 mg/ml.

9. The stable lyophilized formulation of claim **8**, wherein said sucrose is present in said aqueous formulation at a concentration of about 41 mg/ml.

10. The stable lyophilized formulation of claim **1**, wherein said polysorbate is polysorbate 80.

11. The stable lyophilized formulation of claim **10**, wherein said polysorbate 80 is present in said aqueous formulation at a concentration of about 0.02% to about 0.08%.

12. The stable lyophilized formulation of claim **11**, wherein said polysorbate 80 is present in said aqueous formulation at a concentration of about 0.04%.

13. The stable lyophilized formulation of claim **1**, wherein the weight ratio of natalizumab to sucrose in said aqueous formulation is about 0.5:1 to about 2:1.

14. The stable lyophilized formulation of claim **13**, wherein the weight ratio of natalizumab to sucrose in said aqueous formulation is about 1:1.

15. The stable lyophilized formulation of claim **1**, wherein the molar ratio of sucrose to natalizumab in said aqueous formulation is about 300:1 to about 500:1.

16. The stable lyophilized formulation of claim **15**, wherein the molar ratio of sucrose to natalizumab in said aqueous formulation is about 400:1 to about 500:1.

17. The stable lyophilized formulation of claim **16**, wherein the molar ratio of sucrose to natalizumab in said aqueous formulation is about 450:1.

18. The stable lyophilized formulation of claim **1**, wherein said aqueous formulation further comprises a bulking agent.

19. The stable lyophilized formulation of claim **1**, wherein said aqueous formulation further comprises a tonicity modifier.

20. The stable lyophilized formulation of claim **1**, wherein said aqueous formulation comprises:

(a) about 40 mg/ml natalizumab;

(b) about 6 mM histidine, pH about 6.0;

(c) about 41 mg/ml sucrose; and

(d) about 0.04% polysorbate 80.

21. A stable reconstituted formulation comprising:

(i) about 80 to about 160 mg/ml natalizumab;

(ii) about 18 mM histidine at a pH of about 6.0;

(iii) about 123 mg/ml sucrose; and

(iv) about 0.12% polysorbate 80; wherein:

the reconstituted formulation has been prepared from a stable lyophilized formulation prepared by lyophilizing an aqueous formulation comprising:

(a) about 40 mg/ml natalizumab;

(b) about 6 mM histidine, pH about 6.0;

(c) about 41 mg/ml sucrose; and

(d) about 0.04% polysorbate 80.

22. The stable reconstituted formulation of claim **21**, wherein said stable reconstituted formulation comprises about 120 mg/ml natalizumab.

23. A method for preparing a stable reconstituted formulation, comprising reconstitution of a lyophilized formulation that has been prepared by lyophilizing an aqueous formulation comprising:

(a) about 30 to about 60 mg/ml natalizumab;

(b) a buffer having a pH of about 5.5 to about 6.5;

(c) about 20 to about 50 mg/ml sucrose; and

(d) about 0.02 to about 0.08% polysorbate.

24. The method of claim **24**, wherein said aqueous formulation comprises about 40 mg/ml to about 50 mg/ml natalizumab.

25. The method of claim **25**, wherein said aqueous formulation comprises about 40 mg/ml natalizumab.

26. The method of claim **23**, wherein said buffer has a pH of about 6.0.

27. The method of claim **23**, wherein said buffer is histidine.

28. The method of claim **28**, wherein said histidine is present in said aqueous formulation at a concentration of about 1 mM to about 12 mM.

29. The method of claim **29**, wherein said histidine is present in said aqueous formulation at a concentration of about 6 mM.

30. The method of claim **23**, wherein said sucrose is present in said aqueous formulation at a concentration of about 20 mg/ml to about 50 mg/ml.

31. The stable lyophilized formulation of claim **31**, wherein said sucrose is present in said aqueous formulation at a concentration of about 40 mg/ml.

32. The method of claim **23**, wherein said polysorbate is polysorbate 80.

33. The method of claim **32**, wherein said polysorbate 80 is present in said aqueous formulation at a concentration of about 0.02% to about 0.08%.

34. The method of claim **33**, wherein said polysorbate 80 is present in said aqueous formulation at a concentration of about 0.04%.

35. The method of claim **23**, wherein the weight ratio of natalizumab to sucrose in said aqueous formulation is about 0.5:1 to about 2:1.

36. The method of claim **35**, wherein the weight ratio of natalizumab to sucrose in said aqueous formulation is about 1:1.

37. The method of claim **23**, wherein the molar ratio of sucrose to natalizumab in said aqueous formulation is about 300:1 to about 500:1.

38. The method of claim **37**, wherein the molar ratio of sucrose to natalizumab in said aqueous formulation is about 400:1 to about 500:1.

39. The method of claim **38**, wherein the molar ratio of sucrose to natalizumab in said aqueous formulation is about 450:1.

40. The method of claim **23**, wherein said aqueous formulation further comprises a bulking agent.

41. The method of claim **23**, wherein said aqueous formulation further comprises a tonicity modifier.

42. The method of claim **23**, wherein said aqueous formulation comprises:

(a) about 40 mg/ml natalizumab;

(b) about 6 mM histidine, pH about 6.0;

(c) about 41 mg/ml sucrose; and

(d) about 0.04% polysorbate 80.

43. A method for treating a subject, comprising administering to said subject a therapeutically effective amount of a stable reconstituted formulation according to claim **23**, wherein said subject has a disorder that can be treated by administering natalizumab.

* * * * *

Available online at www.sciencedirect.com
ScienceDirect
Advanced Drug Delivery Reviews 58 (2006) 686–706
Advanced DRUG DELIVERY Reviews
www.elsevier.com/locate/addr

Formulation and delivery issues for monoclonal antibody therapeutics☆

Ann L. Daugherty [a,*], Randall J. Mrsny [b,1]

[a] *Genentech, Inc., 1 DNA Way South San Francisco, CA 94080, USA*
[b] *Center for Drug Delivery/Biology, Welsh School of Pharmacy, Cardiff University, Redwood Building, King Edward VII Avenue, Cardiff CF10 3XF, UK*

Received 24 February 2006; accepted 6 May 2006
Available online 22 May 2006

Abstract

Antibodies can have exquisite specificity of target recognition and thus generate highly selective outcomes following their systemic administration. While antibodies can have high specificity, the doses required to treat patients, particularly for a chronic condition, are typically large. Fortunately, advances in production and purification capacities have allowed for the exceptionally large amounts of highly purified monoclonal antibodies to be produced. Additionally, genetic engineering of antibodies has provided a stable of antibody-like proteins that can be easier to prepare. Together, these advances have made antibody-based therapies one of the most commonly pursued pharmaceuticals in biotechnology pipelines. With this success, however, has come a series of technical challenges in the formulation of antibody-based materials to maintain sufficient stability in a variety of configurations and sometimes at particularly high concentrations. This review focuses on issues related to identifying and verifying stable antibody-based formulations.
© 2006 Elsevier B.V. All rights reserved.

Keywords: Antibody; Stability; Delivery; Formulation

Contents

1. Introduction 687
2. Antibody characteristics relevant for formulation and delivery 688
3. General concerns for antibody formulations 689

☆ This review is part of the Advanced Drug Delivery Reviews theme issue on "Engineered Antibody Therapeutics", Vol. 58/5–6, 2006.

* Corresponding author. Tel.: +1 650 225 2198.
E-mail addresses: masi@gene.com (A.L. Daugherty), mrsnyr@cardiff.ac.uk (R.J. Mrsny).
[1] Tel.: +44 29 2087 4159.

0169-409X/$ - see front matter © 2006 Elsevier B.V. All rights reserved.
doi:10.1016/j.addr.2006.03.011

4. Stability issues for antibody formulations . . . 690
4.1. Oxidation . . . 690
4.2. Deamidation . . . 691
4.3. Aggregation . . . 692
4.4. Fragmentation . . . 694
5. Strategies to stabilize antibody formulations . . . 694
5.1. Lyophilization . . . 694
5.2. Polymer delivery systems . . . 695
6. Formulation issues for alternative forms of antibody delivery . . . 696
6.1. Oral . . . 698
6.2. Respiratory tract . . . 698
6.3. Miscellaneous delivery sites of the body . . . 699
6.4. Intracellular targeting . . . 699
7. Other delivery issues . . . 699
7.1. Antibody fragments . . . 699
7.2. Immunoconjugates . . . 700
8. Conclusions — challenges and opportunities . . . 701
Acknowledgements . . . 702
References . . . 702

1. Introduction

Therapeutic and diagnostic antibodies have become the fastest growing area of biopharmaceutical applications. There are now 18 monoclonal antibodies on the market and over 100 in clinical trials, which highlights the significance of these therapeutics and the advances made in antibody engineering. Further, by 2008, engineered antibodies are projected to be the source of over a third of the revenues from biotechnology [1,2].

A few seminal events have led to the current and projected prominence of antibodies as biopharmaceuticals include the identification of methods to generate murine monoclonal versions of antibodies [3], the cloning of human antibody sequences to allow for humanization of murine monoclonal antibodies through complementary-determining region (CDR) grafting [4] and even the establishment of fully humanized systems to generate monoclonal antibodies [5]. With the sequential identification of these technological advances, antibodies for therapeutic and prophylactic indications have moved from fully murine, to partially murine (mostly human) to completely human constructions. Added to these events, dramatic advances in production have led to the ability to prepare monoclonal antibodies at scales that can provide sufficient material at costs that make this area appealing to pharmaceutical companies. One important outcome of these various advances is a greater potential to use antibody drugs in chronic settings, tremendously expanding their biopharmaceutical applications.

The majority of currently approved antibody drugs address previously unmet medical needs in the areas of cancer and inflammation. These indications came from practical considerations related to earlier forms of murine and partially murine antibody therapeutics; the first monoclonal to be approved (OKT-3®, muromonab-CD3) was approved in 1986 for a single treatment regimen to protect from life-threatening tissue rejection following kidney transplant [6]. Adverse reactions due to acute immunogenicity problems due to delivery of a non-self protein limited the use of OKT-3® to only acute application [7,8]. Subsequent partially murine antibodies such as Panorex® (17-1A), Zevalin® (ibritumomab tiuxetan) and Bexxar® (tositumomab) were approved for a limited number of administrations to cancer patients who had failed frontline therapies [2]. With the advent of fully humanized antibodies, chronic therapeutic or prophylactic applications for infectious agents have become a realistic clinical option [2]. Another critical aspect to the success of antibodies as therapeutic agents involves improved methods to express, purify and characterize these proteins [9]. In general, antibody therapeutics are

large (typically >150 kDa), complex in nature (most are glycosylated) and must be administered in stoichiometric rather than catalytic quantities (nearly a gram per dose is required for many antibodies to be effective). Production and purification scales have thus reached levels of production that were previously assumed impossible in biotech companies [10]. Novel concerns then related to the development of stable formulations and delivery strategies for such large amounts of a complex molecule. Understanding product instability with regard to physicochemical and thermodynamic events becomes more and more critical to ensure market success [11]. The required high concentrations of antibodies in these formulations reduced the need to add a carrier protein, as is the case where serum albumin is commonly added in formulations of highly potent proteins such as erythropoietin alpha (Epogen®) and Factor VIII (Kogenate®) to enhance stability and reduce loss to vial surfaces. Simultaneously, the large amounts of an antibody protein used in these formulations allowed degradation products to be more readily detectable particularly when using the highly sensitive methods designed for evaluating hormone biotherapeutics.

Finally, the ability to prepare large quantities of an antibody that could be administered for chronic therapy resulted in a plethora of new and novel applications [9,10] involving the delivery of chemotherapeutics, radionuclides and imaging agents — to name a few. New issues, related to identifying stable formulations such as high concentration formulations that might reduce the volume of antibody administrations, arose in the move from intravenous infusions to the realm of subcutaneous injection strategies. In some cases the combination of agents with antibodies produced conflicting stability profiles. Additionally, potential new indications for antibody drugs increased the desire to find novel methods for sustained release, intracellular targeting [12] or delivery via methods not involving an injection. Thus, as is the case in most scientific advances, technological advances opened up possibilities for therapeutic opportunities that were not possible previously as well as a totally new set of problems that required solving. In this review we have attempted to identify the major issues associated with formulating and delivering antibody drugs, to recognize challenges already identified accompanied when possible by solutions, as well as to discuss concerns that will need to be addressed in the future as the use of antibody drugs continues to evolve.

2. Antibody characteristics relevant for formulation and delivery

The human body produces several classes of antibodies that appear to perform specific functions under different conditions and at discrete anatomic sites. Most of the currently approved antibody-based drugs are of the IgG1 class [13] and are glycosylated on the Fc (fragment crystallizable) domain. Glycosylation has been shown to participate in specific cell response events mediated by antibodies [14–16]: antibody-dependent cell-mediated cytotoxicity (ADCC) and complement-dependent cell-mediated cytotoxicity (CDCC) through receptor recognition events. Individual glycoforms of antibodies can provide improved efficacies for certain clinical outcomes [17]. In general, IgG1 and IgG3 antibodies are effective at initiating ADCC while IgG2 readily fixes complement but is poor at inducing ADCC. IgG4 appears to be inefficient at both ADCC and CDCC [13]. Interestingly, antibodies can be re-engineered to increase their capacity to recruit complement [18] or to adjust their affinities to the various classes of Fc receptors and thus ADCC function through mutation of specific amino acids within the Fc domain [19]. Molecular engineering has also provided a spectrum of new antibodies (Fig. 1). Other chapters in this issue delve deeply into the many characteristics of antibodies that make them remarkable and diversely applicable treatment agents: ligand binding properties, effector functions and potential for modification in their design. Other chapters will also address applications of newly engineered antibody-like molecules that move beyond the realm of intact, full-length IgG antibodies. In the current review, attention will be focused primarily on IgG1 since this is where the majority of published information exists for antibody drug formulation and delivery.

Antibodies, due to their large size (being greater than the filtration cut-off size of the kidney) and their ability to be sequestered for periods of time from the blood, via interactions with FcRn receptors present on

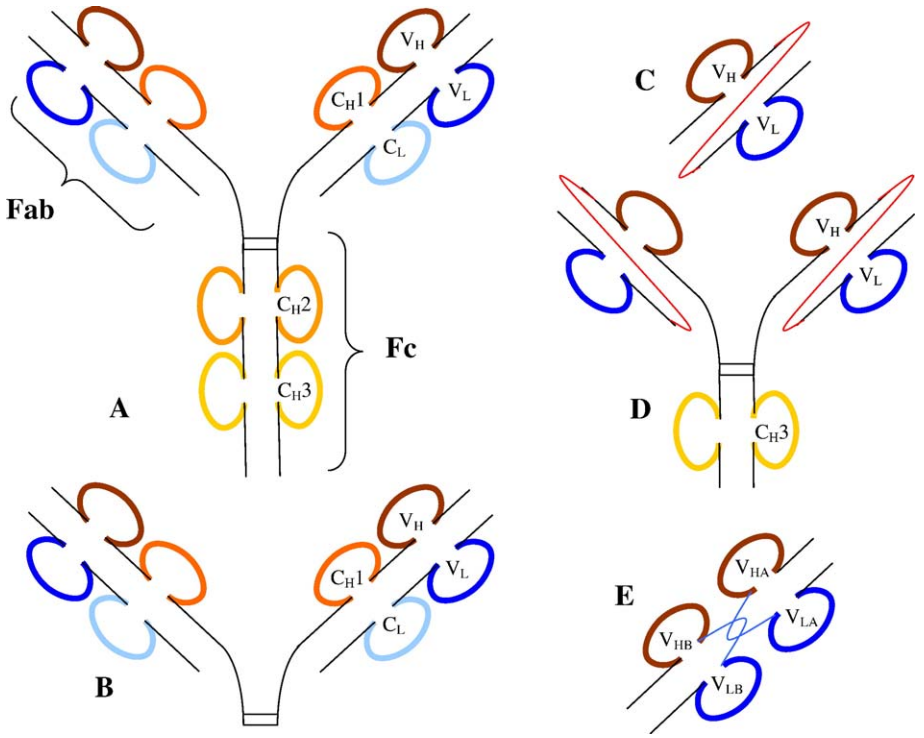


Fig. 1. General antibody structure and some antibody-based protein constructions. A) Human antibodies have a common framework that can be described as Fc (fragment crystallizable) and Fab (fragment antigen binding) domains that are derived from the folded structure of heavy (H) and light (L) chain proteins. Multiple constant (C) regions on both the H and L chain proteins are donated as are the variable (V) segments involved in antigen-specific recognition. B) Removal of the Fc domain produces a F(ab)2 structure. C) Single chain structures of the antigen binding region (scFv) can be prepared by themselves or D) in a construct that includes Fc domain elements. E) Bi-specific antibody elements (diabodies) can be prepared to bring two different antigens into close proximity. C_H, heavy chain constant regions; C_L, light chain constant region; V_H, heavy chain variable region; V_L, light chain variable region.

endothelial cells, can have extended serum profiles in the range of weeks. A number of engineered antibody-like molecules are now being examined for therapeutic applications [20]. Some engineered fragments, such as diabodies and minibodies, are much smaller than intact, full-length IgG1 and have very different properties of systemic distribution and clearance. Additionally, methods to prepare other antibody types such as dimeric secretory IgA [21] and methods to prepare antibodies using non-mammalian cell systems, such as plants [22], from the eggs of chimeric chickens [23] and from transgenic animals [24], are now being explored by academic and industrial groups. As these new approaches gain prominence, more information will be acquired about their unique requirements for successful formulation and delivery. At present, however, there is little information on formulation approaches for antibodies produced using these production processes.

3. General concerns for antibody formulations

Due to their proteinacous nature, antibodies present generic formulation issues that are similar for most protein therapeutics [11]. Proteins, in general, can be degraded under conditions when they are exposed to heat, freezing, light, pH extremes, agitation, sheer-stress, some metals and organic solvents. With ever advancing analytical technologies, the ability to assess the physicochemical and thermodynamic instability of antibody drugs has also led to the identification of several events that are more specific to the unique nature of this particular class of proteins: variations in

Fc glycosylation, partial heavy chain C-terminal Lys processing, Fc methionine oxidation, hinge-region cleavage and glycation of Lys residues [25]. In addition to these issues is the difficulty of preparing dosing materials that might have protein concentrations in the range of 100 mg/ml or greater. Since early preclinical assessment is so critical to successful identification of a new biotherapeutic product, general pre-formulation strategies are usually employed for initial studies with new antibody drugs. An initial formulation effort will likely employ an isotonic, non-hemolytic, slightly acidic solution that can be administered by intravenous infusion or subcutaneous injection in studies employing a relevant animal model. In some cases, some stability information for the antibody drug can be obtained from initial in silico and in vivo testing during this pre-clinical phase that aids in the selection of a formulation that is used in clinical trials [26].

Since most early pre-clinical studies attempt to emulate the delivery strategy that will be used in the clinic, initial studies frequently identify problems with either the initial pre-formulation approach and/or stability issues with the antibody drug itself. In the case of the formulation, protein precipitation can occur with refrigerated storage or with repeated freeze–thaw cycles; events that may be facilitated by an inappropriate pH or buffer selection. Analysis of antibody drugs stored in this initial pre-formulation system may also identify unstable sites within the protein or its linkage to attached molecules (chemotherapeutics, imagining agents, etc.). In the case of the antibody, this information is frequently evaluated to determine if re-engineering of the protein could be performed, for example, to provide greater thermodynamic stability or folding efficiency [27]. Such changes in the Fc region are typically conservative, but might act to modify Fc receptor binding properties to provide a different biological outcome [28,29]. Amino acid substitutions can also be made within the Fv region to improve thermal stability [30], but such changes might also alter antigen binding specificity [31].

4. Stability issues for antibody formulations

If one examines the amino acid sequences for currently approved IgG1-based antibody drugs, it becomes quite clear that only a small segment of these proteins are dramatically different from one another, being the Fv segments that are involved in antigen binding. It should be pointed out, however, that there are some minor differences in conserved regions as well. A priori, one might assume that by finding a stable formulation for one of these antibody drugs, that such a formulation would be good for most if not all, similar antibodies. If this were borne out by experience, there would be no need for a review such as this. Instead, each antibody seems to have a unique personality related to its requirements for stability; a phenomenon derived from the fact that the small differences between these antibodies are focused on surface-exposed amino acid differences that stipulate antigen specificity. Thus, the interfacial surface of each antibody drug is unique and thus requires specific formulation components to provide maximal stability and retention of activity.

Probably the most important aspect of identifying a successful antibody drug formulation is in the identification of truly detrimental alterations rather than all of the modifications that might occur. Although, from a regulatory standpoint, it may be beneficial to understand all of the potential degradation events associated with an antibody formulation, it is the recognition of a stability-indicating parameter (or several parameters) that allows the formulation scientist to focus in on what is critical to development of a successful product. Here, a series of physico-chemical and bioanalytical assays can be used to identify these parameters [32]. Although in vivo bioassays may ultimately be required to validate a stability-indicating formulation parameter, the most critical tools at the disposal of the formulation scientist are rapid and reproducible assays to measure protein changes due to oxidation, deamidation, aggregation, fragmentation and other forms of chemical modification that could lead to a loss of function of the antibody drug.

4.1. Oxidation

Methionine and cysteine residues are frequently a site of oxidation in protein drugs and this is also the case for antibody drugs [33]. In the case of antibody-based drugs, specific methionine residues within the Fc domain may be prone to oxidation, resulting in the

production of methionine sulfoxide [25]. While cysteines are present in the Fc framework as disulfide pairs, unpaired cysteines in the variable region may also be sites of oxidation. Besides methionine and cysteine residues, oxidation of histidine, tyrosine, tryptophan and phenylalanine residues can also occur [34]. A number of methods can be used to monitor oxidation of amino acid residues. As a starting point, the number of reactive protein thiols can be monitored using reagents such as 5,5′-dithionitrobenzoic acid or iodoacethyl dansylcadaverine [35], providing a simple readout on the number of protein thiols per protein. Total amino acid analysis can also be used to monitor reductions in methionine, tyrosine and phenylalanine residues. Tryptic digestion and peptide separation by liquid chromatography followed by mass spectroscopy analysis (LC-MS) can be used to identify specific sites of amino acid oxidation.

A careful study of methionine oxidation has been performed for the humanized monoclonal antibody that recognizes the her2/neu gene product. For this protein it was determined that a methionine at position 255 in at heavy chain of the Fc region was the primary site of oxidation and that a methionine at position 431 could also oxidize under more aggressive conditions. In this study, a chromatography assay was used to detect oxidation events following papain digestion to separate Fab and Fc segments of the antibody [36]. Another study on the stability of this same protein provides a valuable template for dealing with antibody oxidation: identification of a critical oxidation event, validation of a robust assay for monitoring that event and comparison of formulation parameters to determine conditions that facilitate oxidation. Addition of antioxidants or stoichiometric levels of free methionine or thiosulfate were found to reduce the extent of oxidation in formulations of this antibody [37].

Issues associated with administration of oxidized forms of an antibody may extend beyond concerns of reduced efficacy. Systemic lupus erythematosus (SLE) is a disease characterized by the induction of anti-double-stranded DNA antibodies. Studies have shown that increased levels of markers of protein oxidation, including those of methionine sulfoxide and 3-nitrotyrosine, correlated with SLE disease activity [38]. Additionally, oxidative modifications of antibodies isolated from synovial fluid samples collected from patients with rheumatoid arthritis suggested alteration of histidine, methionine, tyrosine and cysteine residues [39]. While no direct causal association is shown or implied, these observations bring attention to the issue that we do not fully understand the clinical impact of antibody oxidation events.

4.2. Deamidation

Glutamine and asparagine residues show a propensity for deamidation [40]. Both light and heavy chains of antibodies can undergo deamidation of these amino acids [41] and deamidation events are considered to be one of the major sources of charge heterogeneity of monoclonal antibodies [42]. Deamidation events appear to be highly selective events for individual antibodies. For example, analysis of several monoclonal antibodies that bind the her2/neu gene product demonstrated asparagine 30 deamidation on one or both light chains and asparagine 55 on the heavy chain [43]. Deamidation events lead to more acidic forms of the antibody through the acquisition of additional carboxylic acid groups. Conversely, aspartic acid residues can also undergo modification to a succinimide moiety that results in a basic antibody isoform of the antibody by removal of a carboxylic acid group [43]. In general, deamidation events appear to be relatively slow but are accelerated by unfolding of the antibody [44]. Initial detection of deamidation in antibody preparations is typically identified by differences in charge distribution or content using methods such as isoelectric focusing (IEF) or high-performance cation-exchange chromatography [43].

High performance chromatography can then be used to separate succinimide, isoaspartic and aspartic acid isoforms of tryptic digest fragments of the antibody which can be unambiguously characterized by tandem mass spectroscopy (MS). Correlation between tryptic digest tandem MS results and some other more readily accessible method, such as IEF, can provide a rapid format to follow antibody deamidation events. Using these techniques, asparagine deamidation events residues appears to occur more frequently than glutamine deamidation and specific asparagine residues appear to be selectively targeted for this event [33]. Deamidation of asparagine is frequently associated with rearrangement

events that lead to the formation of isoaspartic acid [42] and this outcome is correlated to amino acids adjacent to the asparagine prone for deamidation [44] that provide a method for prediction of potential deamidation sites (BOX). In particular, asparagine–glycine sequences can demonstrate accelerated deamidation rates since glycine residues lack a side-chain structure that would otherwise act to decreased conformation interference for backbone-associated isoaspartyl formation [45].

Box 1

Amino acid* sequences predicted to deamidate
SNG, LNG, LNN and ENN
(Note these have a following amino acid of G or N)
and those that are less prone to deamidation
GNT, GNS, GNV, TNY, SNY, SNF, SNT, SNK, SNL,
WNS, WNS, FNW, FNS, FNR HNA, HNH, LNW,
CNV, NNF, DNA, and YNP
*standard single amino acid letter nomenclature.

Non-enzymatic parameters of asparagine and glutamine deamidation in proteins have been defined in detail for factors such as pH, temperature and ionic strength [46,47]. The primary sequence dependence of these deamidation events can be explained by a simple steric and catalytic model [46,47]. Prediction of deamidation events based upon three-dimensional structures have also been described but the data set for these studies is not yet sufficient to produce a general model [48]. That asparagine and glutamine deamidation appear to be a constant phenomenon of proteins and correlate with their turnover provides the basis for the hypothesis that the presence and distribution of these amino acids within a protein can act as a molecular clock for its biological turnover [49,50]. For the formulation scientist, empiric assessment of factors such as pH and ionic strength provide the best strategy to identify a formulation that minimizes deamidation events. In general, deamidation does not result in a decrease in potency and deamidation may be hard to detect as the charge difference is small. At times, however, there can be a detrimental effect on potency through the introduction of an unfavorable negative charge that can have further ramification on biological function, particularly when deamidation occurs in the binding regions [51]. As particularly reactive residues are identified, it may be possible to have the antibody engineered to remove the problematic amino acid or to change adjacent residues to reduce its reactivity.

4.3. Aggregation

Liquid formulations of protein therapeutics frequently exhibit a decrease in concentration due to adsorptivity to container walls at low concentration and can show aggregation events at high concentrations. Initial preparations of antibody drugs were administered in acute situations by IV infusion that could allow for medium protein concentration (1–10 mg/ml) formulations not dramatically affected by adherence or aggregation losses. As antibody-based drugs became more widely used in chronic care, high concentration formulations that would allow for clinically acceptable SC injection volumes became desirable and aggregation became an important concern for designing formulations. Along with aggregation events, protein solutions at concentrations > 50 mg/ml may become sufficiently viscous as to no longer readily pass through the gauge of a needle that would be comfortable for patients' use. Some antibodies demonstrate high concentration viscosity issues while others do not. For example, the anti-respiratory syncytial viral antibody Synagis® is formulated at 100 mg/ml protein and is administered successfully by IM injection. Thus, addressing viscosity, adsorptive loss and aggregation in any specific antibody formulation will likely be performed on a case-by-case basis.

As protein–protein contact frequency increases at high concentrations, the opportunity for stable aggregate formation increases proportionally. Proteins are folded in such a way as to internalize hydrophobic domains and surface-expose more hydrophilic domains in a thermodynamically stable situation. As folded proteins undergo normal molecular motion transient surface exposure of hydrophobic domains can lead to protein–protein contacts that hide these

surfaces in a more energetically favorable manner. The outcome of these events is the stabilization of these protein–protein contacts with the ultimate outcome of dimerization, trimerization and so on — leading to extended aggregation events [52]. As protein concentration and temperature goes up, so does the probability of energetically favorable contacts leading to aggregation with increased frequency and duration of reversible protein–protein contacts leading to a greater extent of stable (even irreversible) aggregation events. Aggregation (covalent, non-covalent, dissociable, non-dissociable) must be considered a likely degradation event for high concentration antibody formulations.

For some antibodies reduced temperatures can incite reversible self-associations; these molecules are known as cryoimmunoglobulins [53]. IgG3 cryoimmunoglobulins have been shown to self-associate through sugar structures of the Fc domain [54]. Self-association events involving IgG1 antibodies seem to occur primarily through weak ionic and hydrophobic interactions [55]. More recent studies have examined kinetic and thermodynamic aspects of antibody solution dimerization using a recombinant human monoclonal antibody that recognizes vascular endothelial growth factor (rhMab-VEGF) as a model [56]. It was found that for this IgG1 class antibody, aggregation rates were greater in slightly alkaline (pH 7.5–8.5) compared to slightly acidic (pH 6.5–7.5) conditions. A high salt environment (1 M NaCl) also enhanced dimerization. Not surprisingly, self-association events were accelerated as the storage temperature was increased. One of the most striking aspects of these dimerization studies on rhMab-VEGF is that trastuzumab, another geneticall-ly engineered antibody with the same IgG1 framework and a 92% sequence homology with rhMab-VEGF, fails to demonstrate aggregation events under the same conditions.

A number of additives have been identified that can reduce the rate of protein aggregation [52,57]. A rather wide spectrum of agents can reduce protein aggregation rates: urea, guanidinium chloride, amino acids (in particular glycine and arginine), various sugars, polyalcohols, polymers (including polyethylene glycol and dextrans), surfactants and even antibodies themselves. Studies have shown that different proteins benefit from different types of anti-aggregating factors, consistent with the notion that the interfacial surfaces that drive interactions leading to aggregation are protein-specific. Conceptually, anti-aggregating agents might fall into one of two categories: small agents that fit into channels or grooves and large agents that might interact with lower-curvature surfaces of the protein. In essence, the small agents would act to stabilize a protein from acquiring a conformation that might be more reactive toward aggregation while a large agent might act to reduce the frequency of surface contacts that lead to an aggregation event. In the case of antibody formulation, either or both may be important. As we will discuss, agents found to effectively protect an antibody from aggregation may differ for various stress conditions; antibodies in solution that are undergoing agitation and thermal stress may differ from those of the same antibody as it undergoes lyophilization and reconstitution.

Protection from aggregation can be limited in antibody formulations by the addition of surface-active agents such as detergents, both charged and uncharged. As an interesting aside, such surface-active agents can help reduce protein loss due to adherence to surfaces that can occur with low concentration protein formulations. Polysorbate 20 and 80 (now available from a vegetal source) are examples of detergents that are widely used to reduce the rate of protein aggregation in high concentration antibody drug formulations. A precautionary note must be sounded, however, as detergents perform this function optimally at low concentrations (0.01% to 0.05%) and can act detrimentally to participate in protein unfolding at higher concentrations, e.g., 1%.

That antibody aggregation can be accelerated by several physical conditions provides the potential for multiple methods to determine if a particular antibody drug is prone to aggregation and to rapidly test formulations for their ability to impede aggregation. Agitation studies are done, in addition to thermal stability studies, to determine if aggregation can occur in a given formulation. Different test methods are used, employing a shaker or a stirring apparatus. In one study done on an IgG1 antibody found sizes of aggregates produced by the two methods were comparable [58]. They concluded that a higher throughput test could be constructed using stirring analyzed by absorbance measurement. In their work,

the stirred samples exhibited much higher absorbance and second particle species in DLS, indicating that stirring stress produces a higher amount of smaller protein aggregates. While Mahler found polysorbate 80 protects against aggregation, the stirred samples had an increase in turbidity and more aggregate products were detected by DLS as compared to a surfactant-free formulation. Polysorbate 80 stabilizes small aggregates and prevents further progress in the aggregation process.

4.4. Fragmentation

Intact, full-length antibodies are composed of several segments that have natural flexure sites. One site, in particular, exists at the flexure point between the Fc and Fv domain. Cleavage at this hinge region is a common concern when assessing antibody drug stability [25]. Molecular sizing methods such as sodium dodecyl sulphate polyacrylamide gel electrophoresis (SDS-PAGE) and size-exclusion high performance liquid chromatography (SE-HPLC) can be used to rapidly identify fragmentation events in antibody drugs [59]. Fragmentation of full-length antibody drugs is a common occurrence and invariably affects their function. In general, cleaved forms are present in such low amounts that it is likely that little change in efficacy would be seen [60]. At the very least, the antibody drug may have some small reduction in efficacy following fragmentation or may be more prone to proteases, degradation and clearance events that would limit the duration of its efficacy. At the worst, a fragmented antibody preparation may result in a different biodistribution and thus a different safety profile. This can be of particular concern if the antibody is being used to delivery a cytotoxic chemotherapeutic agent. Fortunately, the extent of fragmentation in an antibody can be easily limited in the formulated product.

5. Strategies to stabilize antibody formulations

While liquid antibody formulations are less expensive, faster to develop and generally easier to prepare for administration than alternative formulation approaches, liquid antibody formulations are prone to oxidation, deamidation, aggregation and fragmentation as discussed above. In each of these events, water is the common culprit: water mediates electron transfer during oxidation and deamidation events and its required addition across a peptide bond can be a critical step in fragmentation. The thermodynamic stresses that lead to protein aggregation are caused by hydrophobic protein surfaces being exposed to water and trying to find a lower energy state by non-native protein–protein interactions. Thus, water is a big problem for stabilizing antibody-based drugs. Lyophilization or introduction into hydrophobic polymer systems can reduce the impact of water on antibody drug formulations.

5.1. Lyophilization

Although some antibodies have demonstrated a propensity to undergo precipitation as they are cooled from 37 °C [53], antibodies are typically robust to freeze/thaw cycles [61]. Early studies reported that antibodies were stable to the freeze-drying (lyophilization) process in the absence of excipients that function as cryoprotectants [62], however, with the technical advancement of certain analytical methodologies, became evident that antibodies are generally damaged in some way as a result of lyophilization as demonstrated by extensive formation of insoluble aggregates [61]. More recently, studies have shown that freeze-drying antibodies to a specific percent of residual water (usually between 1 and 8%) allows for optimal stabilization in the dry state and stability during reconstitution [63]. Higher moisture content in lyophilized antibody preparations correlates with increased aggregation (as seen by SEC) and asparagine deamidation and isomerization (as measured by HIC). Studies have also been performed to identify optimized lyophilization schedules where the secondary drying phase is performed at an elevated temperature [64]. This technique allows the lyophylized cake to achieve optimum moisture content, allowing the final product to be conformationally stable (as measured by DSC) during extended storage. Solid-state structural studies can be used to monitor conformational changes and aggregation events during the storage of a lyophilized monoclonal antibody preparation [65]. Improved native-like structure and a reduction in aggregation can be obtained by incorporation of a carbohydrate excipient in sufficient

quantities to fulfill the hydrogen bonding requirements on the protein surface, suggesting a critical role for non-water molecules to act as placeholders for water molecules during drying and in the dry state. That the addition of excess carbohydrate failed to improve the stabilizing function of this excipient, reaffirms the conclusion that antibodies have a limited number of sites that must be protected in this fashion [65]. A variety of carbohydrates or polyol compounds such as sucrose, trehalose and mannitol have been shown to provide this stabilizing function [66,67].

The rate of rehydration when water is reintroduced during reconstitution of lyophilized formulations is a critical parameter. As water is removed during the different drying stages of the lyophilization cycle and replaced by a shell of non-water excipients, the antibody drug can undergo structural modifications that result in a non-native conformation as may be seen by differential scanning calorimetry [63]. If the rate of rehydration is sufficiently slow to allow recovery of native conformation as water replaces non-water excipient molecules, reconstitution will typically provide a satisfactory outcome for the antibody. If, however, the antibody does not have sufficient time or capacity to recover its native state during reconstitution, extensive aggregation can result. Efforts to protect monoclonal antibodies from the rigors of freeze-drying and reconstitution have been aided by a number of analytical methods that can examine protein modifications. In the solid state, circular dichroism (CD) and Fourier transform infrared (FTIR) spectroscopy may be used to evaluate the protein; after reconstitution in the liquid phase, SEC or SDS-PAGE have been utilized to gather information from lyophilization studies [68,69]. A microscopic apparatus to visually monitor freeze-drying events has even been described [70]. Excipients that have been reported to slow the reconstitution rate and thereby preventing such changes in the rehydrated antibody are glycerol [71,72] and polymeric materials such as polyethylene glycol [73].

Pharmaceutical scientists frequently use increased temperatures for accelerated formulation stability studies. Although such studies can be used to assess formulation parameters such as pH and ionic strength, antibodies lyophilized in the presence of a cryoprotective sugar excipient provide a more complicated picture. Lyophilized amorphous solids composed of a monoclonal antibody and a sugar cryoprotectant material such as sucrose or trehalose form glassy structures, liquids that are too viscous to flow. That antibody-excipient complexes exhibit a glass transition temperature (Tg) provides the basis for observations showing that these materials have unique properties above and below this value. Thus, in predicting shelf life in accelerated degradation studies, it is important to use testing temperatures that do not exceed the Tg threshold of the complex [67]. In general, lyophilized formulations containing trehalose may likely show less tendency toward antibody aggregation than those with sucrose, since trehalose preparations have a higher Tg [67]. With this in mind, a promising approach to assess secondary structural parameters in evaluating antibody formulation stability is the use of amide I band Raman spectroscopy. This method demonstrates a good correlation between structural protein perturbations immediately after lyophilization and the rate of aggregation during long-term storage under accelerated conditions [74].

5.2. Polymer delivery systems

Removal of water from antibody preparations, either by lyophilization or spray freeze-drying, provides a provides a starting point for incorporation of this dried material into a hydrophobic polymer matrix such as polylactide-co-glycolide (PLGA) that can be made into microspheres generated through a solid-in-oil-in-water (S/O/W) encapsulation process [75]. Although both mannitol and trehalose can stabilize human IgG during spray freeze-drying, the double-emulsion solvent evaporation method used to load spray freeze-dried human IgG into PLGA microspheres has been shown to produce extensive antibody aggregation [75]. Such an outcome is likely the result of thermodynamic stress experienced at the water/organic solvent interface and a variety of process methods and excipients can be use to minimize this concern [76].

One feature of PLGA microparticle preparations is their recognition by immune elements and their capacity to stimulate immunization against incorporated proteins [77–79]. While this has clear advantages for vaccines, it poses a serious concern for therapeutic protein delivery. Hydrophobic microparticles have been reported to incite local inflammation

at subcutaneous injection sites [80], events that may be partially mediated through macrophage recruitment [81]. Not only is the potential for antibody formation increased with local inflammation, the resulting injection site reaction may be clinically unacceptable.

In spite of some serious caveats, polymeric microspheres and delivery systems can be successful antibody formulations if administered to the appropriate sites, using certain types of polymers or preparing microspheres or polymeric formulations by methods that are more protective of the antibody. An example of a certain delivery site that may have less proclivity towards an inflammatory response is reported, where PLGA microspheres loaded with an anti-VEGF antibody were injected into the intravitreal humor of the eye, an immune-privileged site, for the treatment of age related macular degeneration (AMD) [82]. Resorbable polymers that show less potential to incite inflammation, e.g., have smoother surface characteristics, might be used to deliver antibodies in a sustained manner. Direct, local delivery of antibodies using carboxymethylcellulose aqueous gels can be an effective post-surgical anti-infective strategy [83]. Antibodies covalently coupled to a biodegradable hyaluronic acid hydrogel through a labile hydrazone linkage have been used for the sustained delivery of antibodies to sites within the central nervous system [84]. Introduction of dry powder IgG into ethylene–vinyl acetate copolymer (EVAc) has also been examined as a potential polymer-based antibody delivery system [85]. Similar to PLGA systems, EVAc microspheres can extend the time course of IgG release. This property makes polymers loaded with antibodies interesting opportunities for injectable sustained release delivery formats but also for topical application at mucosal surfaces. For example, long-term vaginal delivery of an antibody can be achieved in a mouse model using polymer vaginal rings [86,87]. Formulations of a biomedical grade polyurethane hydrogel with an antibody coating have also been prepared and shown to release bioactive protein [88]. It is important to note that one complicating aspect of many of these approaches is the requirement of a polymer solubilization step using a solvent, such as methylene chloride or isopropanol, which can compromise protein drug stability. Sustained release formulation approaches such as microspheres prepared using water, such as the PROMAXX microspheres (Epic Therapeutics) or crystallization of proteins [89] can bypass the use of solvents that are incompatible with proteins and antibodies.

6. Formulation issues for alternative forms of antibody delivery

To date, antibody development has focused primarily on injectable routes of administration: intravenous (IV), intramuscular (IM) and subcutaneous (SC). A long history of IV antibody infusions exists [90] and the advantages are clear for antibody-based drugs that are used in cancer treatments in order to reach tumor sites that may be diffuse or not otherwise accessible. In fact, the majority of the approved antibody-based drugs are administered by IV infusion (Table 1) with the total dose administered approaching one gram of protein per treatment in some cases. For many antibody-based therapies a critical safety concern involves the onset of acute or delayed systemic reactions following infusion [91,92]. Parameters and characteristics of the "infusion reaction" as well as treatment protocols have been well described with acute events commonly occurring within 10 min to 4 h and delayed events occurring 24 h to 4 days post dosing [93]. Although formation of antibodies to the administered antibody drug appear to be a risk factor for infusion reaction events [94], infusion reactions can occur following the initial exposure [93] and these reactions do not appear to be due to IgE responses or mast cell activation [95]. Most importantly for the patient, there appear to be treatment protocols to provide re-treatment of patients even after an infusion reaction event [93] with concomitant administration of immunomodulation molecules [94]. There are many unanswered questions about the mechanism and prevention of adverse infusion reaction events associated with IV infusion of antibody drugs. Certainly, one method is to explore IM and SC delivery when possible, although these delivery approaches may also have confounding aspects of tissue response and volume limitations.

Other routes are also amenable to antibody delivery. The increased number of antibody therapeutics on the market and the greater exploration of non-life threatening indications being treated by antibodies, drive efforts to deliver these agents by routes other than IV

Table 1
Formulations of approved products

Antibody product; company	Generic name; description	Delivery route	Formulation concentration	Buffer components; pH[a]	*Excipients*
Othroclone OKT3®; J & J-Ortho Biotech	Muromonab-CD3; Murine IgG2a, anti-CD3	IV	1 mg/ml	Na,K phosphate; pH 7	NaCl, polysorbate 80
Reopro®; Centocor-Lilly	Abciximab; Chimeric IgG1, anti-GPIIb/IIIa, Fab	IV	2 mg/ml	Na phosphate; pH 7.2	NaCl, polysorbate 80
Rituxan®; Idec-Genentech	Rituximab; Chimeric IgG1, anti-CD20	IV	10 mg/ml	Na citrate; pH 6.5	NaCl, polysorbate 80
Zenapax®; Roche	Daclizimab; Humanized IgG1, anti-CD25	IV	5 mg/ml	Na phosphate; pH 6.9	NaCl, polysorbate 80
Simulect; Novartis[b]	Basilixamab; Chimeric IgG, anti-CD25	IV	4 mg/ml	Na,K phosphate, glycine	NaCl, sucrose, mannitol, polysorbate 80
Synagis®; MedImmune[b]	Palivizumab; Humanized IgG1, anti-RSV	IM	100 mg/ml	Histidine, glycine	Mannitol
Remicade®; Centocor[b]	Infliximab; Chimeric IgG1, anti-TNFα	IV	10 mg/ml	Na phosphate; pH 7.2	Sucrose, polysorbate 80
Herceptin®; Genectech[b]	Trastuzumab; Humanized IgG1, anti-HER2	IV	21 mg/ml	Histidine; pH 6	Trehalose, polysorbate 20, benzyl alcohol[c]
Mylotarg®; Wyeth[b]	Gemtuzumab ozogamicin; Humanized IgG4, anti-CD33, immunotoxin	IV	4 mg/ml	Na phosphate	NaCl, sucrose, dextran 40
Campath®-1H; Millennium-ILEX	Alemtuzumab; Humanized IgG1, anti-CD52	IV	Unclear — 30 mg /vial	Na,K-phosphate pH 7	NaCl, KCl, NaEDTA, polysorbate 80
Zevalin®; Biogen Idec	Ibritumomab tiuxetan; Murine IgG1, anti-CD20; radiolabeled (^{90}Y or ^{111}In)	IV[d]	1.6 mg/ml	Na Acetate, Na, K-phosphate pH 7	NaCl, human albumin
Humira®; Abbott	Adalimumab; Human IgG1, anti-TNFα	IV	50 mg/ml	Na phosphate, Na Citrate; pH 5.2	Mannitol, polysorbate 80
Xolair®; Genentech[b]	Omalizumab; Humanized IgG1, anti-IgE	SC	125 mg/ml	Histidine	Sucrose, polysorbate 20
Bexxar®; Corixam-GSK	Tositumomab-I131; Murine IgG2a, anti-CD20, radiolabeled (^{131}I)	IV	14 mg/ml	Na phosphate; pH 7.2	NaCl, maltose
Raptiva®; Genentech	Efalizumab; Humanized IgG1, anti-CD11a	SC	100 mg/ml	Histidine; pH 6.2	Sucrose, polysorbate 20
Erbitux®; Imclone Systems	Cetuximab; Chimeric IgG1, anti-EGFR	IV	2 mg/ml	Na phosphate; pH 7.2	NaCl
Avasatin®; Genentech	Bevacizumab; Humanized IgG1, anti-VEGF	IV	25 mg/ml	Na phosphate; pH 6.4	Trehalose, polysorbate 20
Tysabri; Biogen Idec	Natalizumab; Humanized IgG4, anti-4α-integrin	IV	20 g/ml	Na phosphate; pH 6.1	NaCl; polysorbate 80

Ordered by approval dates in the US.
Abbreviations: RSV=respiratory syncytial virus; TNFα=tumor necrosis factor alpha; EGFR=epidermal growth factor receptor; VEGF=vascular endothelial growth factor; NaEDTA=sodium edentate.
[a] Some lyophilized formulations do not stipulate a pH (or range) following reconstitution.
[b] Lyophlized product, concentration, pH, etc. values are obtained after reconstitution.
[c] Added as a preservative to generate a multi-dose vial configuration.
[d] Kit where components are mixed just prior to administation.

infusion. These routes may be more effective, less invasive, provide easier delivery, permit self-administration and thereby be more convenient and possibly have lower costs if less active agent can be used, as in the case where the alternate route of administration delivers the therapeutic agent to the intended site directly. Interestingly, some studies have suggested that antibodies administered by IV infusion are more

susceptible to proteolysis than via IM injection [59] and sucrose-stabilized immunoglobulins have been associated with acute renal failure following IV infusion [96]. The antibody used to protect neonates from respiratory syncytial viral (RSV) infection (Synagis®) is one example of an antibody administered by IM injection. For reasons discussed above, the majority of antibody-based drugs have moved toward SC delivery with formulations efforts being focused to this end. Based upon the desired actions for a number of antibody-based drugs, however, routes of administration other than IV, IM or SC may be desirable. These alternative routes can provide unique formulation and stability issues.

6.1. Oral

Uptake of antibodies from the intestinal lumen can occur through fetal Fc receptors (FcRn) expressed at the apical surface of enterocytes [97]. This natural antibody uptake mechanism was initially identified in the gastrointestinal (GI) tract of neonatal rodents and its expression shown to vanish following "closure" of the intestine after weaning. It was only recently that the continued expression of this receptor in the adult intestine was demonstrated and this finding has prompted efforts to examine this receptor system as a means of delivery antibodies after oral administration. Although this pathway appears to be a viable route for the delivery of therapeutic antibodies, issues associated with antibody stability in the GI tract [98] and competition from endogenous antibodies can dramatically reduce the efficiency of uptake after oral delivery. Outside of this specific mechanism, no other transcellular mechanism of efficient antibody transport across epithelial cell of the GI tract has been demonstrated to date. Topical application of antibodies to produce a desired clinical outcome have been shown, however, with the oral delivery of a chicken-derived (IgY) antibodies for treating and preventing infectious diseases of the GI tract [98–100]. It should be noted that IgY antibodies have been shown to not bind to (or be transported by) FcRn [97].

6.2. Respiratory tract

Intranasal and pulmonary administration of protein therapeutics has shown more promising clinical outcomes than oral delivery. While the surfaces of both the respiratory tract and the gastrointestinal tracts are readily accessible, the respiratory tract is a far less hostile environment for an administered protein therapeutic. Nonetheless there are physical clearance mechanisms in place to remove foreign particles which act to reduce residence time dramatically following administration. In the case of nasal administration the use of a cream emulsion and a polymer delivery system has been shown to significantly decrease the clearance rate for a monoclonal antibody when applied to the nasal mucosa [101]. This study provides one approach for the topical application of a therapeutic antibody designed to provide clinical benefit at the mucosal surface. It does not, however, suggest that an appreciable amount of an antibody might be absorbed into the systemic circulation from this site. The nasal mucosa affords only a small absorptive surface area compared to the epithelial linings of the lung.

Aerosol delivery of antibodies to the lung has been explored as either a liquid or dry powder formulation, where in both cases the droplets or particles must be of sufficiently small size that they are respirable perhaps to the level of the deep lung but large enough that they are not readily exhaled or just impact the back of the throat [102]. The sizes of particles that provide this performance have a mass mean aerodynamic diameter and density such that they enter the alveoli and remain in the lung. This size window has been reported to be between 1 to 5 μm depending on the formulation used and in one case, far larger, 20 μm where the particles are dense (<0.4 g/cm^3) and highly porous [102].

Formulation efforts were made for producing fine dry powder particles of an anti-IgE monoclonal antibody (E25) in the size range desired for delivery to the lung [103]. These studies showed that sodium phosphate was capable of extending the usefulness of mannitol as a protective excipient in spray-dried antibody formulations and that mannitol can play a role both in maintaining protein stability as well as producing a suitable aerosol preparation. Further studies to assess carbohydrate excipients for spray-dried aerosol E25 formulations showed that excipient to protein ratios were critical. Degradation issues involved not only protein aggregation but also protein glycation or lactosylation, a protein modification

event where a reducing sugar can add covalently at a free amine [104]. The ability to formulate and delivery an antibody-based drug to the lung provides the potential for systemic delivery of that protein via uptake through the FcRn expressed at this mucosal surface. Elegant studies showing the distribution and function as well as the application of this transport route for systemic deliver of an Fc-containing protein chimera has been demonstrated [105,106]. Thus, the potential or systemic delivery of antibody-based drugs via the respiratory tract looks promising.

6.3. Miscellaneous delivery sites of the body

Unique aspects of antibody–polymer formulations designed for intravitreal injection [82] or topical vaginal delivery [86,87] have been discussed above. Additionally, antibody formulations using hyaluronic acid hydrogels for sustained brain delivery have been noted [84]. These methods focus on strategies to administer large amounts of an antibody at a specific site in order to provide a sustained level to improve efficacy and/or to minimize injection frequency. Other strategies have been described to deliver antibodies to miscellaneous sites throughout the body, For example, an anti-transferrin antibody (OX-26) has been described as a carrier for delivery of covalently attached therapeutic molecules across the blood–brain barrier following IV injection [107]. An anti-tumor necrosis factor antibody has been adsorbed onto cardiovascular stent wires for local neutralization of this cytokine in order to limit restenosis events following stent placement [108]. A CMC gel containing antibodies to prevent post-surgical infections has been administered to the intraperitoneal cavity [83].

6.4. Intracellular targeting

Some promising antibody drug targets are intracellular. Although techniques exist where a cell can synthesize an antibody and secrete it into the cell cytoplasm, successful use of this technology requires gene therapy. Instead, it is possible to chemically couple an antibody to a pH-sensitive polymer that functioned to disrupt membranes at acidic pH. Many antibodies are internalized by cells through a receptor-mediated uptake process that leads to their delivery into early and then late endosomes. During endosomal maturation after receptor–antibody internalization the pH of these vesicles will drop from near neutral to below pH 6. This approach was demonstrated in a format where the pH-responsive polymer poly(propylacrylic acid) was covalently attached to a monoclonal antibody to facilitate its delivery to the cytoplasm of target cells [12].

7. Other delivery issues

A wide range of novel drugs and drug conjugates are being developed using monoclonal antibodies and engineered antibody fragments [20]. For some of these novel therapeutic approaches to be successful, they require additional or non-traditional delivery strategies. A cursory discussion of some of these approaches as they relate to intracellular targeting, site placement and engineered antibodies fragments follows.

7.1. Antibody fragments

An entire spectrum of antibody fragments have been identified through protein engineering studies with many of these showing remarkable potential for unique and novel clinical opportunities [109]. These smaller recombinant antibody fragments, the monovalent antibody fragments, Fab and single chain Fv and the engineered variants, diabodies, triabodies, minibodies and single-domain antibodies are an emerging form of antibody therapy that are less costly to manufacture while still retaining the targeting specificity of full length antibodies. In fact some may have greater efficacy and more applications than whole monoclonal antibodies. It may be anticipated that this new subset of antibodies are posing new formulation challenges, however, to date, publications detailing stability studies and formulation development for these molecules are rare in the scientific literature so formulation data on antibody fragments is scant. The single V domains have been found to be poorly soluble and have a tendency to aggregate [109], but these problems are being overcome by the identification of mutants that minimize the hydrophobic interface and selected by phage display [110]. Five Fab molecules have been approved as of this writing with the one humanized

Fab (ranibizumab rhFab) awaiting approval in the very near future, but many are in early clinical trials and most in preclinical development. One study has been described that focused on Fab fragments. In general, the binding of an antibody to an effector protein does not necessarily inactivate that target's function [111]. When an antibody is effectively inactivating, however, the Fab fragments in the absence of an Fc domain can frequently function as highly potent binding agents capable of masking binding sites or enzymatic elements on macromolecules. For example, Fab fragments prepared from sheep anti-snake venom antibodies (Digibind, from GSK) can be an effective anti-venom. Storage of liquid formulations of such anti-venoms in sub-tropical countries where refrigeration may not be possible provides a significant formulation challenge. Although lyophilized products can perform well under these conditions, a pH 4.0 (acetate buffer) formulation was found to also be stable and potent for at least one year at room temperature [112], presumably room temperatures characteristic of the tropical and subtropical regions where the material would be used. Strikingly, this stable formulation did not require the presence of a protective carbohydrate excipient. To improve drug delivery, antibody fragments have been fused to many types of molecules, such as radionuclides, cytotoxic drugs, toxins, peptides and proteins, enzymes and liposomes [113]. An immunoliposome made with a Mab fragment is reported to deliver drugs to the brain as such a molecule is able to cross the formidable barrier of the blood brain barrier [114].

7.2. Immunoconjugates

Arming antibodies with materials useful for detection or cell killing has become a prominent approach to increase the utility of these proteins, reviewed by Wu and Senter, [20]. Antibodies provide a useful format for the production of radiopharmaceuticals for site- or tissue-specific localization using gamma scintigraphy [10,115] or for enhanced cell killing. There are currently three approved antibody–radionuclide drugs: two are murine radiolabeled Ab for B cell lymphomas ibritumomab tuixetan (^{90}Y, Zevalin) and tositumomab (^{131}I Bexxar) and the third is a humanized, gemtuzumab ozogamicin (calicheamicin, Mylotarg) for leukemia. The presence of a high energy emitting radionuclide, however, will compromise long-term stability of any antibody formulation; not only would the released energies act to damage the protein but there is strong preference to use short half-life isotopes for these procedures [116]. Thus, in these instances, a stable formulation based upon the principles discussed above can provide a product that can be radiolabeled and then used soon after this step. One example of this approach is a lyophilized antibody formulation that is reconstituted and prepared by a kit method prior to patient dosing [117].

Antibodies coupled with cytotoxins for targeted cell killing [118] are particularly useful in antibody-based cancer therapies [119]. Beyond the identification of a stable formulation for the antibody, such materials have several additional problems for the formulation scientist to solve: stability issues of the attached agent and stability of the linker used to join the attached agent to the antibody. In the case of a monoclonal antibody-vinca alkaloid conjugate, a pH range of 4.5–5.5 in a phosphate buffer showed improved solution stability compared to material stored at pH 6.5–7.4 as evidenced by antibody aggregation and hydrolysis of the chemical linker used to conjoin the alkaloid to the antibody [120]. In most cases, cytotoxic materials are coupled to antibodies using reversible chemistries to provide a release mechanism for maximal activity at the target site. Many of these antibody conjugates use a disulfide bond linkage that can be reduced by a novel redox enzyme present in endosomes and lysosomes of target cells [121]. Slightly oxidizing conditions that would provide added stability of this linker in the formulation could, over time, act to cause detrimental oxidation events in the antibody and/or the linked compound. Other conjugates use an acid-labile linker [122]. In this case, formulation pH must be restricted to either neutral or alkaline conditions. Enzymatic separation of antibody and a cytotoxic material could also be achieved by coupling the two through an amino acid linker that is recognized as a substrate by a specific protease or peptidase [123]. Formulation instability of this linker sequences can be corrected to some extent by selective changes of the amino acids used.

Thus, the challenges of immunoconjugates include maintaining both drug and antibody potency and stability. While some antibodies are efficacious by

themselves, many are much more therapeutically active after being armed with a toxin, drug and radionuclide [124]. These changes make the resulting product more difficult to prepare, stabilize and deliver. Yet, there is tremendous enthusiasm for these approaches as they provide the promise for some companies to transform their antibody into a potentially curative drug. For this reason many antibodies are combined with a generic delivery system, such as a liposome, that can be used to delivery a variety or even multiple agents simultaneously through antibody-directed targeting [125]. Examples of such an approach include studies performed using an antibody directed against the Her2/neu antigen to delivery liposomes containing a chemotherapeutic have been described [126], antibodies used to deliver cationic liposomes for the administration of nucleic acid material for gene therapy [127] and antibodies used in the targeted delivery of modified gelatin nanoparticles [128] that can be coupled through a disulfide linkage [129].

8. Conclusions — challenges and opportunities

As antibody-based drugs come to the forefront of therapeutics derived from biotechnology, they provide a range of new and exciting opportunities to treat a number of currently unmet medical needs. Successful clinical application of these novel agents requires the development of stable formulations that can be used for specific delivery methods. Antibodies, because of their endogenous nature, have built-in features that may pose problems for stability as biotherapeutics, that function in the normal clearance of these proteins from the body [40]. Thus, despite our best efforts to prepare stable antibody-based drug formulations, the ultimate stability of these products may be limited to inherent mechanisms of degradation pre-designed for the rate of clearance optimal for their function and turnover in the body. Protein engineering has led to significant advances in improving some of these parameters and the trend would predict that additional advances will be made in the near future (reviewed in [109]). Protein modifications can be engineered such that stability and efficacy can be improved in ways that cannot be achieved solely, if at all, with formulation alterations. While it is clear that more research is needed in the relatively new area of engineered antibody fragments for clinical use [109], they have great potential for diagnostic and therapeutic application.

In general, successful antibody formulation designs are simply the best compromise of minimizing several competing degradation pathways. One approach is to find a pH where the minimal amount of degradation events such as deamidation and oxidation will occur. Another is to identify a buffer system that can stabilize the formulation at that pH without damaging the antibody. One common tactic taken to reduce the rate of many of these chemical degradation events is to prepare lyophilized or freeze-dried antibody preparation but even these can be compromised by aggregation issues due to thermodynamic stress that occurs during freezing, drying and reconstitution. A number of protective excipients, mostly carbohydrates, can reduce the propensity of antibodies to aggregate during these stressful events. Another issue is to produce a formulation that is compatible with delivery — neither hypotonic — nor hypertonic solutions are well-tolerated upon injection. Added to this is the potential use of a surface active agent to help with liquid stability such as a non-ionic detergent at a low concentration [58] as well as the possible addition of preservatives required for multi-use systems [130].

The future of antibody based drugs is likely to include more complex systems than those currently approved for use in man. Possibly the most critical aspect of generating a pharmaceutically successful formulation for antibody based drugs is an understanding the critical aspects of stability for the protein or the materials associated with the protein. It has been known for some time that even a single amino acid change in the Fv region of an antibody can result in dramatic differences in antigen-binding specificity [31]. Also, alterations at specific amino acids in the Fc domain can dramatically change functional aspects of an antibody. Thus, these kinds of changes must be considered more important in the search for a successful formulation than those changes that do not appear to affect function. In the case of antibody or antibody-like agents being used to delivery a payload such as a toxin or chemotherapeutic, the stability of the material to be delivered and its continued association with the delivery antibody is crucial.

Acknowledgements

The authors wish to thank Reed Harris, Tom Patapoff and Nancy Valente for very insightful conversations and helpful suggestions. The review of the manuscript by Xanthe Lam, Brian Lobo and Chung Hsu is appreciated. The references cited in this review were not intended to inclusive of all of the seminal publications in the ever-expanding area of antibody stability and formulation. The relatively small numbers of references cited were selected to highlight specific aspects within the scope of this review. We regret that many excellent publications could not be cited that have made important contributions to this field.

References

[1] M. Baker, Upping the ante on antibodies, Nat. Biotechnol. 23 (2005) 1065–1072.
[2] J.M. Reichert, C.J. Rosensweig, L.B. Faden, M.C. Dewitz, Monoclonal antibody successes in the clinic, Nat. Biotechnol. 23 (2005) 1073–1078.
[3] G. Kohler, C. Milstein, Continuous cultures of fused cells secreting antibody of predefined specificity, Nature 256 (1975) 495–497.
[4] P.T. Jones, P.H. Dear, J. Foote, M.S. Neuberger, G. Winter, Replacing the complementarity-determining regions in a human antibody with those from a mouse, Nature 321 (1986) 522–525.
[5] N.C. Peterson, Advances in monoclonal antibody technology: genetic engineering of mice, cells, and immunoglobulins, ILAR J. 46 (2005) 314–319.
[6] L. Chatenoud, CD3-specific antibody-induced active tolerance: from bench to bedside, Nat. Rev., Immunol. 3 (2003) 123–132.
[7] S. Merluzzi, M. Figini, A. Colombatti, S. Canevari, C. Pucillo, Humanized antibodies as potential drugs for therapeutic use, Adv. Clin. Pathol. 4 (2000) 77–85.
[8] L.G. Presta, Engineering antibodies for therapy, Curr. Pharm. Biotechnol. 3 (2002) 237–256.
[9] L.H. Stockwin, S. Holmes, Antibodies as therapeutic agents: vive la renaissance!, Expert Opin. Biol. Ther. 3 (2003) 1133–1152.
[10] W.C. Bogard Jr., R.T. Dean, Y. Deo, R. Fuchs, J.A. Mattis, A.A. McLean, H.J. Berger, Practical considerations in the production, purification, and formulation of monoclonal antibodies for immunoscintigraphy and immunotherapy, Semin. Nucl. Med. 19 (1989) 202–220.
[11] E.M. Atkinson, W. Klum, Formulations strategies for biopharmaceuticals-ensuring success to market, IDrugs 4 (2001) 557–560.
[12] C.A. Lackey, O.W. Press, A.S. Hoffman, P.S. Stayton, A biomimetic pH-responsive polymer directs endosomal release and intracellular delivery of an endocytosed antibody complex, Bioconjug. Chem. 13 (2002) 996–1001.
[13] D.W. Grainger, Controlled-release and local delivery of therapeutic antibodies, Expert Opin. Biol. Ther. 4 (2004) 1029–1044.
[14] M. Imai, C. Landen, R. Ohta, N.K. Cheung, S. Tomlinson, Complement-mediated mechanisms in anti-GD2 monoclonal antibody therapy of murine metastatic cancer, Cancer Res. 65 (2005) 10562–10568.
[15] S. Siberil, C. de Romeuf, N. Bihoreau, N. Fernandez, J.L. Meterreau, A. Regenman, E. Nony, C. Gaucher, A. Glacet, S. Jorieux, P. Klein, M.P. Hogarth, W.H. Fridman, D. Bourel, R. Beliard, J.L. Teillaud, Selection of a human anti-RhD monoclonal antibody for therapeutic use: impact of IgG glycosylation on activating and inhibitory FcgammaR functions, Clin. Immunol. (2005).
[16] A. Wright, S.L. Morrison, Effect of altered CH2-associated carbohydrate structure on the functional properties and in vivo fate of chimeric mouse–human immunoglobulin G1, J. Exp. Med. 180 (1994) 1087–1096.
[17] R. Jefferis, Glycosylation of recombinant antibody therapeutics, Biotechnol. Prog. 21 (2005) 11–16.
[18] E.E. Idusogie, P.Y. Wong, L.G. Presta, H. Gazzano-Santoro, K. Totpal, M. Ultsch, M.G. Mulkerrin, Engineered antibodies with increased activity to recruit complement, J. Immunol. 166 (2001) 2571–2575.
[19] R.L. Shields, A.K. Namenuk, K. Hong, Y.G. Meng, J. Rae, J. Briggs, D. Xie, J. Lai, A. Stadlen, B. Li, J.A. Fox, L.G. Presta, High resolution mapping of the binding site on human IgG1 for Fc gamma RI, Fc gamma RII, Fc gamma RIII, and FcRn and design of IgG1 variants with improved binding to the Fc gamma R, J. Biol. Chem. 276 (2001) 6591–6604.
[20] A.M. Wu, P.D. Senter, Arming antibodies: prospects and challenges for immunoconjugates, Nat. Biotechnol. 23 (2005) 1137–1146.
[21] B. Corthesy, Recombinant secretory immunoglobulin A in passive immunotherapy: linking immunology and biotechnology, Curr. Pharm. Biotechnol. 4 (2003) 51–67.
[22] J.K. Ma, B.Y. Hikmat, K. Wycoff, N.D. Vine, D. Chargelegue, L. Yu, M.B. Hein, T. Lehner, Characterization of a recombinant plant monoclonal secretory antibody and preventive immunotherapy in humans, Nat. Med. 4 (1998) 601–606.
[23] L. Zhu, M.C. van de Lavoir, J. Albanese, D.O. Beenhouwer, P.M. Cardarelli, S. Cuison, D.F. Deng, S. Deshpande, J.H. Diamond, L. Green, E.L. Halk, B.S. Heyer, R.M. Kay, A. Kerchner, P.A. Leighton, C.M. Mather, S.L. Morrison, Z.L. Nikolov, D.B. Passmore, A. Pradas-Monne, B.T. Preston, V.S. Rangan, M. Shi, M. Srinivasan, S.G. White, P. Winters-Digiacinto, S. Wong, W. Zhou, R.J. Etches, Production of human monoclonal antibody in eggs of chimeric chickens, Nat. Biotechnol. 23 (2005) 1159–1169.
[24] N. Lonberg, Human antibodies from transgenic animals, Nat. Biotechnol. 23 (2005) 1117–1125.
[25] R.J. Harris, Heterogeneity of recombinant antibodies: linking structure to function, Dev. Biol. (Basel) 122 (2005) 117–127.
[26] R. Bazin, G. Boucher, G. Monier, M.C. Chevrier, S. Verrette, H. Broly, R. Lemieux, Use of hu-IgG-SCID mice to evaluate

the in vivo stability of human monoclonal IgG antibodies, J. Immunol. Methods 172 (1994) 209–217.
[27] S. Ewert, A. Honegger, A. Pluckthun, Stability improvement of antibodies for extracellular and intracellular applications: CDR grafting to stable frameworks and structure-based framework engineering, Methods 34 (2004) 184–199.
[28] S.J. Demarest, J. Rogers, G. Hansen, Optimization of the antibody C(H)3 domain by residue frequency analysis of IgG sequences, J. Mol. Biol. 335 (2004) 41–48.
[29] J. Hodoniczky, Y.Z. Zheng, D.C. James, Control of recombinant monoclonal antibody effector functions by fc *N*-glycan remodeling in vitro, Biotechnol. Prog. 21 (2005) 1644–1652.
[30] H. Yasui, W. Ito, Y. Kurosawa, Effects of substitutions of amino acids on the thermal stability of the Fv fragments of antibodies, FEBS Lett. 353 (1994) 143–146.
[31] S. Rudikoff, A.M. Giusti, W.D. Cook, M.D. Scharff, Single amino acid substitution altering antigen-binding specificity, Proc. Natl. Acad. Sci. U. S. A. 79 (1982) 1979–1983.
[32] A.R. Mire-Sluis, Progress in the use of biological assays during the development of biotechnology products, Pharm. Res. 18 (2001) 1239–1246.
[33] D.J. Kroon, A. Baldwin-Ferro, P. Lalan, Identification of sites of degradation in a therapeutic monoclonal antibody by peptide mapping, Pharm. Res. 9 (1992) 1386–1393.
[34] H.R. Griffiths, Antioxidants and protein oxidation, Free Radic. Res. 33 (2000) S47–S58 (Suppl).
[35] G. Hasegawa, M. Kikuchi, Y. Kobayashi, Y. Saito, Synthesis and characterization of a novel reagent containing dansyl group, which specifically alkylates sulfhydryl group: an example of application for protein chemistry, J. Biochem. Biophys. Methods 63 (2005) 33–42.
[36] F.J. Shen, M.Y. Kwong, R.G. Keck, R.J. Harris, The application of tert-butylhydroperoxide oxidation to study sites of potential methionine oxidation in a recombinant antibody, Techniques in Protein Chemistry, vol. VII, Academic Press, Inc, 1996, p.^pp. Pages.
[37] X.M. Lam, J.Y. Yang, J.L. Cleland, Antioxidants for prevention of methionine oxidation in recombinant monoclonal antibody HER2, J. Pharm. Sci. 86 (1997) 1250–1255.
[38] P.E. Morgan, A.D. Sturgess, M.J. Davies, Increased levels of serum protein oxidation and correlation with disease activity in systemic lupus erythematosus, Arthritis Rheum. 52 (2005) 2069–2079.
[39] H.E. Jasin, Oxidative modification of inflammatory synovial fluid immunoglobulin G, Inflammation 17 (1993) 167–181.
[40] A.B. Robinson, J.H. McKerrow, P. Cary, Controlled deamidation of peptides and proteins: an experimental hazard and a possible biological timer, Proc. Natl. Acad. Sci. U. S. A. 66 (1970) 753–757.
[41] Y. Mimura, E.A. Kabat, T. Tanaka, M. Fujimoto, K. Takeo, K. Nakamura, Microheterogeneity of mouse antidextran monoclonal antibodies, Electrophoresis 16 (1995) 116–123.
[42] W. Zhang, M.J. Czupryn, Analysis of isoaspartate in a recombinant monoclonal antibody and its charge isoforms, J. Pharm. Biomed. Anal. 30 (2003) 1479–1490.
[43] R.J. Harris, B. Kabakoff, F.D. Macchi, F.J. Shen, M. Kwong, J.D. Andya, S.J. Shire, N. Bjork, K. Totpal, A.B. Chen, Identification of multiple sources of charge heterogeneity in a recombinant antibody, J. Chromatogr., B, Biomed. Sci. Appl. 752 (2001) 233–245.
[44] D. Chelius, D.S. Rehder, P.V. Bondarenko, Identification and characterization of deamidation sites in the conserved regions of human immunoglobulin gamma antibodies, Anal. Chem. 77 (2005) 6004–6011.
[45] J.L. Radkiewicz, H. Zipse, S. Clarke, K.N. Houk, Neighboring side chain effects on asparaginyl and aspartyl degradation: an ab initio study of the relationship between peptide conformation and backbone NH acidity, J. Am. Chem. Soc. 123 (2001) 3499–3506.
[46] N.E. Robinson, A.B. Robinson, Prediction of primary structure deamidation rates of asparaginyl and glutaminyl peptides through steric and catalytic effects, J. Pept. Res. 63 (2004) 437–448.
[47] N.E. Robinson, Z.W. Robinson, B.R. Robinson, A.L. Robinson, J.A. Robinson, M.L. Robinson, A.B. Robinson, Structure-dependent nonenzymatic deamidation of glutaminyl and asparaginyl pentapeptides, J. Pept. Res. 63 (2004) 426–436.
[48] N.E. Robinson, A.B. Robinson, Prediction of protein deamidation rates from primary and three-dimensional structure, Proc. Natl. Acad. Sci. U. S. A. 98 (2001) 4367–4372.
[49] N.E. Robinson, A.B. Robinson, Deamidation of human proteins, Proc. Natl. Acad. Sci. U. S. A. 98 (2001) 12409–12413.
[50] N.E. Robinson, A.B. Robinson, Molecular clocks, Proc. Natl. Acad. Sci. U. S. A. 98 (2001) 944–949.
[51] L. Huang, J. Lu, V.J. Wroblewski, J.M. Beals, R.M. Riggin, In vivo deamidation characterization of monoclonal antibody by LC/MS/MS, Anal. Chem. 77 (2005) 1432–1439.
[52] J.L. Cleland, M.F. Powell, S.J. Shire, The development of stable protein formulations: a close look at protein aggregation, deamidation, and oxidation, Crit. Rev. Ther. Drug Carr. Syst. 10 (1993) 307–377.
[53] C.R. Middaugh, B. Gerber-Jenson, A. Hurvitz, A. Paluszek, C. Scheffel, G.W. Litman, Physicochemical characterization of six monoclonal cryoimmunoglobulins: possible basis for cold-dependent insolubility, Proc. Natl. Acad. Sci. U. S. A. 75 (1978) 3440–3444.
[54] D.J. Panka, Glycosylation is influential in murine IgG3 self-association, Mol. Immunol. 34 (1997) 593–598.
[55] C.G. Hall, G.N. Abraham, Reversible self-association of a human myeloma protein. Thermodynamics and relevance to viscosity effects and solubility, Biochemistry 23 (1984) 5123–5129.
[56] J.M. Moore, T.W. Patapoff, M.E. Cromwell, Kinetics and thermodynamics of dimer formation and dissociation for a recombinant humanized monoclonal antibody to vascular endothelial growth factor, Biochemistry 38 (1999) 13960–13967.
[57] B.M. Baynes, B.L. Trout, Rational design of solution additives for the prevention of protein aggregation, Biophys. J. 87 (2004) 1631–1639.
[58] H.C. Mahler, R. Muller, W. Friess, A. Delille, S. Matheus, Induction and analysis of aggregates in a liquid IgG1-

antibody formulation, Eur. J. Pharm. Biopharm. 59 (2005) 407–417.
[59] M. Page, C. Ling, P. Dilger, M. Bentley, T. Forsey, C. Longstaff, R. Thorpe, Fragmentation of therapeutic human immunoglobulin preparations, Vox Sang. 69 (1995) 183–194.
[60] A.J. Cordoba, B.J. Shyong, D. Breen, R.J. Harris, Non-enzymatic hinge region fragmentation of antibodies in solution, J. Chromatogr., B, Anal. Technol. Biomed. Life Sci. 818 (2005) 115–121.
[61] J.M. Sarciaux, S. Mansour, M.J. Hageman, S.L. Nail, Effects of buffer composition and processing conditions on aggregation of bovine IgG during freeze-drying, J. Pharm. Sci. 88 (1999) 1354–1361.
[62] H.R. Friedli, Methodology and safety considerations in the production of an intravenous immunoglobulin preparation, Pharmacotherapy 7 (1987) S36–S40.
[63] E.D. Breen, J.G. Curley, D.E. Overcashier, C.C. Hsu, S.J. Shire, Effect of moisture on the stability of a lyophilized humanized monoclonal antibody formulation, Pharm. Res. 18 (2001) 1345–1353.
[64] X. Ma, D.Q. Wang, R. Bouffard, A. MacKenzie, Characterization of murine monoclonal antibody to tumor necrosis factor (TNF-MAb) formulation for freeze-drying cycle development, Pharm. Res. 18 (2001) 196–202.
[65] J.D. Andya, C.C. Hsu, S.J. Shire, Mechanisms of aggregate formation and carbohydrate excipient stabilization of lyophilized humanized monoclonal antibody formulations, AAPS PharmSci 5 (2003) E10.
[66] J.L. Cleland, X. Lam, B. Kendrick, J. Yang, T.H. Yang, D. Overcashier, D. Brooks, C. Hsu, J.F. Carpenter, A specific molar ratio of stabilizer to protein is required for storage stability of a lyophilized monoclonal antibody, J. Pharm. Sci. 90 (2001) 310–321.
[67] S.P. Duddu, P.R. Dal Monte, Effect of glass transition temperature on the stability of lyophilized formulations containing a chimeric therapeutic monoclonal antibody, Pharm. Res. 14 (1997) 591–595.
[68] H.R. Costantino, K.G. Carrasquillo, R.A. Cordero, M. Mumenthaler, C.C. Hsu, K. Griebenow, Effect of excipients on the stability and structure of lyophilized recombinant human growth hormone, J. Pharm. Sci. 87 (1998) 1412–1420.
[69] C.C. Hsu, C.A. Ward, R. Pearlman, H.M. Nguyen, D.A. Yeung, J.G. Curley, Determining the optimum residual moisture in lyophilized protein pharmaceuticals, Dev. Biol. Stand. 74 (1992) 255–270 (discussion 271).
[70] C.C. Hsu, A.J. Walsh, H.M. Nguyen, D.E. Overcashier, H. Koning-Bastiaan, R.C. Bailey, S.L. Nail, Design and application of a low-temperature Peltier-cooling microscope stage, J. Pharm. Sci. 85 (1996) 70–74.
[71] L.L. Chang, D. Shepherd, J. Sun, X.C. Tang, M.J. Pikal, Effect of sorbitol and residual moisture on the stability of lyophilized antibodies: implications for the mechanism of protein stabilization in the solid state, J. Pharm. Sci. 94 (2005) 1445–1455.
[72] K. Gekko, Mechanism of polyol-induced protein stabilization: solubility of amino acids and diglycine in aqueous polyol solutions, J. Biochem. (Tokyo) 90 (1981) 1633–1641.
[73] T. Arakawa, Y. Kita, J.F. Carpenter, Protein-solvent interactions in pharmaceutical formulations, Pharm. Res. 8 (1991) 285–291.
[74] S.U. Sane, R. Wong, C.C. Hsu, Raman spectroscopic characterization of drying-induced structural changes in a therapeutic antibody: correlating structural changes with long-term stability, J. Pharm. Sci. 93 (2004) 1005–1018.
[75] J. Wang, K.M. Chua, C.H. Wang, Stabilization and encapsulation of human immunoglobulin G into biodegradable microspheres, J. Colloid Interface Sci. 271 (2004) 92–101.
[76] A.J. Jones, S. Putney, O.L. Johnson, J.L. Cleland, Recombinant human growth hormone poly(lactic-co-glycolic acid) microsphere formulation development, Adv. Drug Deliv. Rev. 28 (1997) 71–84.
[77] R.K. Gupta, A.C. Chang, G.R. Siber, Biodegradable polymer microspheres as vaccine adjuvants and delivery systems, Dev. Biol. Stand. 92 (1998) 63–78.
[78] E.C. Lavelle, M.K. Yeh, A.G. Coombes, S.S. Davis, The stability and immunogenicity of a protein antigen encapsulated in biodegradable microparticles based on blends of lactide polymers and polyethylene glycol, Vaccine 17 (1999) 512–529.
[79] D.T. O'Hagan, D. Rahman, J.P. McGee, H. Jeffery, M.C. Davies, P. Williams, S.S. Davis, S.J. Challacombe, Biodegradable microparticles as controlled release antigen delivery systems, Immunology 73 (1991) 239–242.
[80] A.L. Daugherty, J.L. Cleland, E.M. Duenas, R.J. Mrsny, Pharmacological modulation of the tissue response to implanted polylactic-co-glycolic acid microspheres, Eur. J. Pharmacol. Biopharm. 44 (1997) 89–102.
[81] A. Luzardo-Alvarez, N. Blarer, K. Peter, J.F. Romero, C. Reymond, G. Corradin, B. Gander, Biodegradable microspheres alone do not stimulate murine macrophages in vitro, but prolong antigen presentation by macrophages in vitro and stimulate a solid immune response in mice, J. Control. Release 109 (2005) 62–76.
[82] J. Mordenti, K. Thomsen, V. Licko, L. Berleau, J.W. Kahn, R.A. Cuthbertson, E.T. Duenas, A.M. Ryan, C. Schofield, T.W. Berger, Y.G. Meng, J. Cleland, Intraocular pharmacokinetics and safety of a humanized monoclonal antibody in rabbits after intravitreal administration of a solution or a PLGA microsphere formulation, Toxicol. Sci. 52 (1999) 101–106.
[83] K.A. Poelstra, N.A. Barekzi, A.M. Rediske, A.G. Felts, J.B. Slunt, D.W. Grainger, Prophylactic treatment of gram-positive and gram-negative abdominal implant infections using locally delivered polyclonal antibodies, J. Biomed. Mater. Res. 60 (2002) 206–215.
[84] W.M. Tian, C.L. Zhang, S.P. Hou, X. Yu, F.Z. Cui, Q.Y. Xu, S.L. Sheng, H. Cui, H.D. Li, Hyaluronic acid hydrogel as Nogo-66 receptor antibody delivery system for the repairing of injured rat brain: in vitro, J. Control. Release 102 (2005) 13–22.
[85] C.H. Wang, K. Sengothi, T. Lee, Controlled release of human immunoglobulin G. 1. Release kinetics studies, J. Pharm. Sci. 88 (1999) 215–220.
[86] P.Y. Kuo, J.K. Sherwood, W.M. Saltzman, Topical antibody delivery systems produce sustained levels in mucosal tissue and blood, Nat. Biotechnol. 16 (1998) 163–167.

[87] W.M. Saltzman, J.K. Sherwood, D.R. Adams, P. Castle, P. Haller, Long-term vaginal antibody delivery: delivery systems and biodistribution, Biotechnol. Bioeng. 67 (2000) 253–264.
[88] I.A. Rojas, J.B. Slunt, D.W. Grainger, Polyurethane coatings release bioactive antibodies to reduce bacterial adhesion, J. Control. Release 63 (2000) 175–189.
[89] M.X. Yang, B. Shenoy, M. Disttler, R. Patel, M. McGrath, S. Pechenov, A.L. Margolin, Crystalline monoclonal antibodies for subcutaneous delivery, Proc. Natl. Acad. Sci. U. S. A. 100 (2003) 6934–6939.
[90] J.T. Sgouris, Studies on immune serum globulin (IgG) and its modification for intravenous administration, Prog. Immunobiol. Stand. 4 (1970) 104–113.
[91] N. Cook-Bruns, Retrospective analysis of the safety of Herceptin immunotherapy in metastatic breast cancer, Oncology 61 (Suppl 2) (2001) 58–66.
[92] W.V. Crandall, L.M. Mackner, Infusion reactions to infliximab in children and adolescents: frequency, outcome and a predictive model, Aliment. Pharmacol. Ther. 17 (2003) 75–84.
[93] A. Cheifetz, L. Mayer, Monoclonal antibodies, immunogenicity, and associated infusion reactions, Mt. Sinai J. Med. 72 (2005) 250–256.
[94] F. Baert, M. Noman, S. Vermeire, G. Van Assche, D.H.G., A. Carbonez, P. Rutgeerts, Influence of immunogenicity on the long-term efficacy of infliximab in Crohn's disease, N. Engl. J. Med. 348 (2003) 601–608.
[95] A. Cheifetz, M. Smedley, S. Martin, M. Reiter, G. Leone, L. Mayer, S. Plevy, The incidence and management of infusion reactions to infliximab: a large center experience, Am. J. Gastroenterol. 98 (2003) 1315–1324.
[96] S.A. Chapman, K.L. Gilkerson, T.D. Davin, M.R. Pritzker, Acute renal failure and intravenous immune globulin: occurs with sucrose-stabilized, but not with D-sorbitol-stabilized, formulation, Ann. Pharmacother. 38 (2004) 2059–2067.
[97] W.I. Lencer, R.S. Blumberg, A passionate kiss, then run: exocytosis and recycling of IgG by FcRn, Trends Cell Biol. 15 (2005) 5–9.
[98] R.M. Reilly, R. Domingo, J. Sandhu, Oral delivery of antibodies. Future pharmacokinetic trends, Clin. Pharmacokinet. 32 (1997) 313–323.
[99] K. Horie, N. Horie, A.M. Abdou, J.O. Yang, S.S. Yun, H.N. Chun, C.K. Park, M. Kim, H. Hatta, Suppressive effect of functional drinking yogurt containing specific egg yolk immunoglobulin on *Helicobacter pylori* in humans, J. Dairy Sci. 87 (2004) 4073–4079.
[100] Y. Mine, J. Kovacs-Nolan, Chicken egg yolk antibodies as therapeutics in enteric infectious disease: a review, J. Med. Food 5 (2002) 159–169.
[101] S. Walsh, J. Kokai-Kun, A. Shah, J. Mond, Extended nasal residence time of lysostaphin and an anti-staphylococcal monoclonal antibody by delivery in semisolid or polymeric carriers, Pharm. Res. 21 (2004) 1770–1775.
[102] D.A. Edwards, J. Hanes, G. Caponetti, J. Hrkach, A. Ben-Jebria, M.L. Eskew, J. Mintzes, D. Deaver, N. Lotan, R. Langer, Large porous particles for pulmonary drug delivery, Science 276 (1997) 1868–1871.
[103] H.R. Costantino, J.D. Andya, P.A. Nguyen, N. Dasovich, T.D. Sweeney, S.J. Shire, C.C. Hsu, Y.F. Maa, Effect of mannitol crystallization on the stability and aerosol performance of a spray-dried pharmaceutical protein, recombinant humanized anti-IgE monoclonal antibody, J. Pharm. Sci. 87 (1998) 1406–1411.
[104] J.D. Andya, Y.F. Maa, H.R. Costantino, P.A. Nguyen, N. Dasovich, T.D. Sweeney, C.C. Hsu, S.J. Shire, The effect of formulation excipients on protein stability and aerosol performance of spray-dried powders of a recombinant humanized anti-IgE monoclonal antibody, Pharm. Res. 16 (1999) 350–358.
[105] A.J. Bitonti, J.A. Dumont, S.C. Low, R.T. Peters, K.E. Kropp, V.J. Palombella, J.M. Stattel, Y. Lu, C.A. Tan, J.J. Song, A.M. Garcia, N.E. Simister, G.M. Spiekermann, W.I. Lencer, R.S. Blumberg, Pulmonary delivery of an erythropoietin Fc fusion protein in non-human primates through an immunoglobulin transport pathway, Proc. Natl. Acad. Sci. U. S. A. 101 (2004) 9763–9768.
[106] G.M. Spiekermann, P.W. Finn, E.S. Ward, J. Dumont, B.L. Dickinson, R.S. Blumberg, W.I. Lencer, Receptor-mediated immunoglobulin G transport across mucosal barriers in adult life: functional expression of FcRn in the mammalian lung, J. Exp. Med. 196 (2002) 303–310.
[107] A.C. Granholm, D. Albeck, C. Backman, M. Curtis, T. Ebendal, P. Friden, M. Henry, B. Hoffer, J. Kordower, G.M. Rose, S. Soderstrom, R.T. Bartus, A non-invasive system for delivering neural growth factors across the blood–brain barrier: a review, Rev. Neurosci. 9 (1998) 31–55.
[108] Q. Javed, N. Swanson, H. Vohra, H. Thurston, A.H. Gershlick, Tumor necrosis factor-alpha antibody eluting stents reduce vascular smooth muscle cell proliferation in saphenous vein organ culture, Exp. Mol. Pathol. 73 (2002) 104–111.
[109] P. Holliger, P.J. Hudson, Engineered antibody fragments and the rise of single domains, Nat. Biotechnol. 23 (2005) 1126–1136.
[110] L. Jespers, O. Schon, L.C. James, D. Veprintsev, G. Winter, Crystal structure of HEL4, a soluble, refoldable human V(H) single domain with a germ-line scaffold, J. Mol. Biol. 337 (2004) 893–903.
[111] Y. Kawade, Neutralization of activity of effector protein by monoclonal antibody: formulation of antibody dose-dependence of neutralization for an equilibrium system of antibody, effector, and its cellular receptor, Immunology 56 (1985) 497–504.
[112] I. Al-Abdulla, J.M. Garnvwa, S. Rawat, D.S. Smith, J. Landon, A. Nasidi, Formulation of a liquid ovine Fab-based antivenom for the treatment of envenomation by the Nigerian carpet viper (*Echis ocellatus*), Toxicon 42 (2003) 399–404.
[113] T. Nakamura, K.W. Peng, S. Vongpunsawad, M. Harvey, H. Mizuguchi, T. Hayakawa, R. Cattaneo, S.J. Russell, Antibody-targeted cell fusion, Nat. Biotechnol. 22 (2004) 331–336.

[114] A. Schnyder, J. Huwyler, Drug transport to brain with targeted liposomes, NeuroRx 2 (2005) 99–107.
[115] M. Tuncay, S. Calis, H.S. Kas, M.T. Ercan, I. Peksoy, A.A. Hincal, In vitro and in vivo evaluation of diclofenac sodium loaded albumin microspheres, J. Microencapsulation 17 (2000) 145–155.
[116] A.M. Zimmer, J.M. Kazikiewicz, D.I. Webber, B.A. Patel, R. Goldman-Leikin, J.A. Radosevich, W.G. Spies, S.M. Spies, S.T. Rosen, Stability of radioiodinated monoclonal antibodies: in vitro storage and plasma analysis, Int. J. Radiat. Appl. Instrum., B Nucl. Med. Biol. 16 (1989) 691–696.
[117] G. Ferro-Flores, J. Lezama-Carrasco, A freeze dried kit formulation for the preparation of 99mTc-EHDP-MoAb-IOR CEA1 complex, Nucl. Med. Biol. 21 (1994) 1013–1016.
[118] M. Dyba, N.I. Tarasova, C.J. Michejda, Small molecule toxins targeting tumor receptors, Curr. Pharm. Des. 10 (2004) 2311–2334.
[119] G.P. Adams, L.M. Weiner, Monoclonal antibody therapy of cancer, Nat. Biotechnol. 23 (2005) 1147–1157.
[120] A. Riggin, D. Clodfelter, A. Maloney, E. Rickard, E. Massey, Solution stability of the monoclonal antibody-vinca alkaloid conjugate, KS1/4-DAVLB, Pharm. Res. 8 (1991) 1264–1269.
[121] G. Saito, J.A. Swanson, K.D. Lee, Drug delivery strategy utilizing conjugation via reversible disulfide linkages: role and site of cellular reducing activities, Adv. Drug Deliv. Rev. 55 (2003) 199–215.
[122] B.M. Mueller, W.A. Wrasidlo, R.A. Reisfeld, Antibody conjugates with morpholinodoxorubicin and acid-cleavable linkers, Bioconjug. Chem. 1 (1990) 325–330.
[123] C. Heinis, P. Alessi, D. Neri, Engineering a thermostable human prolyl endopeptidase for antibody-directed enzyme prodrug therapy, Biochemistry 43 (2004) 6293–6303.
[124] L. Brannon-Peppas, J.O. Blanchette, Nanoparticle and targeted systems for cancer therapy, Adv. Drug Deliv. Rev. 56 (2004) 1649–1659.
[125] J.W. Park, C.C. Benz, F.J. Martin, Future directions of liposome- and immunoliposome-based cancer therapeutics, Semin. Oncol. 31 (2004) 196–205.
[126] J.W. Park, K. Hong, P. Carter, H. Asgari, L.Y. Guo, G.A. Keller, C. Wirth, R. Shalaby, C. Kotts, W.I. Wood, et al., Development of anti-p185HER2 immunoliposomes for cancer therapy, Proc. Natl. Acad. Sci. U. S. A. 92 (1995) 1327–1331.
[127] D.D. Stuart, G.Y. Kao, T.M. Allen, A novel, long-circulating, and functional liposomal formulation of antisense oligodeoxynucleotides targeted against MDR1, Cancer Gene Ther. 7 (2000) 466–475.
[128] S. Balthasar, K. Michaelis, N. Dinauer, H. von Briesen, J. Kreuter, K. Langer, Preparation and characterisation of antibody modified gelatin nanoparticles as drug carrier system for uptake in lymphocytes, Biomaterials 26 (2005) 2723–2732.
[129] N. Dinauer, S. Balthasar, C. Weber, J. Kreuter, K. Langer, H. von Briesen, Selective targeting of antibody-conjugated nanoparticles to leukemic cells and primary T-lymphocytes, Biomaterials 26 (2005) 5898–5906.
[130] S. Gupta, E. Kaisheva, Development of a multidose formulation for a humanized monoclonal antibody using experimental design techniques, AAPS PharmSci 5 (2003) E8.

Mohammad A. Tabrizi
Gadi G. Bornstein
Scott L. Klakamp *Editors*

Development of Antibody-Based Therapeutics

Translational Considerations

26

Springer

Contents

1 **Translational Strategies for Development of Antibody-Based Therapeutics: An Overview** 1
Mohammad Tabrizi, Gadi Gazit Bornstein and Scott L. Klakamp

2 **Discovery Process for Antibody-Based Therapeutics** 9
Heather H. Shih

3 **Technologies for the Generation of Human Antibodies** 33
Ramesh R. Bhatt, John S. Haurum and C. Geoffrey Davis

4 **Application of Antibody Engineering in the Development of Next Generation Antibody-Based Therapeutics** 65
Randall J. Brezski and Juan Carlos Almagro

5 **Biophysical Considerations for Development of Antibody-Based Therapeutics** 95
Andrew W. Drake and Giuseppe A. Papalia

6 **Considerations in Establishing Affinity Design Goals for Development of Antibody-Based Therapeutics** 141
Mohammad Tabrizi

7 **Bioanalytical Considerations for Development of Antibody-Based Therapeutics: Pharmacokinetics and Immunogenicity** 153
Cherryl B. Funelas and Scott L. Klakamp

8 **Preclinical Considerations for Development of Antibody-Based Therapeutics in Oncology** 183
Gregory Landes and Kathleen Elias

9 **Factors Impacting the Tumor Localization and Distribution of Antibody-Based Therapeutics in Oncology** 241
David C. Blakey

10 **Preclinical Safety Considerations for the Development of Antibody-Based Therapeutics** 255
Lolke de Haan

11 **Application of Pharmacokinetic/Pharmacodynamic Modeling in the Development of Antibody-Based Therapeutics** 285
Donald E. Mager

12 **Application of Population Pharmacokinetic-Pharmacodynamic Approaches in the Design of Translational Strategies for Development of Antibody-Based Therapeutics** 303
Feng Jin

13 **Translational Biomarkers: Essential Tools in Development of Antibody-Based Therapeutics** 331
Mohammad A. Tabrizi and Cherryl B. Funelas

14 **Translational Research in Alzheimer's Disease for Development of Antibody-Based Therapeutics** 341
Eric C. Yuen, Enchi Liu and Gene G. Kinney

15 **Considerations in Manufacturing Process Development for Antibody-Based Therapeutics** 355
Paula C. Miller and Peiling Xu

16 **Strategies for Development of Next Generation Antibody-Based Therapeutics** 375
Mohammad Tabrizi and Gadi Gazit Bornstein

17 **Immune Complex Therapies for Treatment of Immune Thrombocytopenia** 391
Rong Deng and Joseph P. Balthasar

18 Application of Bioinformatics Principles for Target Evaluation 405
Anthony Carvalloza, Mohammad Fallahi and Sahba Tabrizifard

19 Concluding Remarks 419
Mohammad Tabrizi, Gadi Gazit Bornstein and Scott L. Klakamp

Editors Biography 423

Index 425

Chapter 15
Considerations in Manufacturing Process Development for Antibody-Based Therapeutics

Paula C. Miller and Peiling Xu

Abstract Antibody-based therapeutics are a rapidly growing sector of new pharmaceutical drug candidates. As the therapeutic utility of monoclonal antibodies continues to grow, development of robust manufacturing processes has been a significant focus within the pharmaceutical industry. This chapter describes the work-processes, challenges, and opportunities for platform production of antibodies with a focus on production for use in human clinical trials and marketing applications.

Introduction

The use of monoclonal antibodies in research is widespread. Antibodies are used as therapeutic (Sekhon 2010) and diagnostic agents (Hagemeyer et al. 2009), as well as tools to identify targets for treatment of disease (Sioud 2007) and to research disease pathways. As the utility of monoclonal antibodies continues to grow, development of high-yielding, robust manufacturing processes to produce them has been a significant focus within the pharmaceutical industry.

Antibodies share a common structural framework over large regions of the protein sequence and therefore exhibit similar physiochemical properties (Wang et al. 2007). The similarities in structure and physiochemical properties render

P. C. Miller (✉) · P. Xu
Pfizer Pharmaceuticals, Biotherapeutics Pharmaceutical Sciences,
St. Louis, MO, USA
e-mail: paula.c.miller@pfizer.com

P. Xu
e-mail: peiling.xu@pfizer.com

M. A. Tabrizi et al. (eds.), *Development of Antibody-Based Therapeutics*,
DOI: 10.1007/978-1-4419-5955-3_15,
© Springer Science+Business Media New York 2012

antibodies ideal candidates for a platform approach for production and purification. Currently, most monoclonal antibodies are produced in mammalian cell culture since mammalian cells possess the requisite machinery capable of performing complex post-translational modifications (PTMs) that are often required for drug efficacy and stability (Jenkins et al. 2008). Comparative studies also indicate that expression titers and specific productivity are higher for antibodies produced in mammalian expression systems (Geisse et al. 1996).

First generation antibody therapeutics were murine derived, followed later by chimeric, and more recently, fully human antibodies are being developed as therapeutics. It has been suggested that relative to murine and chimeric antibodies, fully human antibodies minimize the potential to elicit an immunogenic response in humans (Lonberg 2008). Although antibodies as a class are well suited for developing platforms for production and purification, each candidate must be evaluated individually to assess whether the operations and conditions defined by a given platform will be suitable for production. The following sections describe the work-processes, challenges, and opportunities for platform production of antibodies, with a focus on production for use in human clinical trials.

Cell Line Development

Once a development candidate has been identified (Chap. 2), cell line development begins with transfection of a suitable expression vector into a host cell line. Mammalian expression systems predominate for the large-scale production of antibodies since they can perform complex PTMs that are important for correct protein folding, stability, multimer formation, and secretion into the medium (Jenkins et al. 2008). Chinese Hamster Ovary (Owyang et al. 2011) cell lines are some of the more commonly used host cell lines for antibody production and employ selectable markers based on dihydroxy folate reductase (DHFR) and glutamine synthetase that are available in suitable stable expression vectors for these cell lines (Bebbington et al. 1992). While strong promoters are used to drive product expression, selection markers are often driven by weaker promoters to increase selection stringency (Shukla and Thommes 2010). Cell line stability is another key consideration during development. Typically a good production cell line will be stable for 70–100 generations. The primary goal is to create a stable cell line with the appropriate growth properties and a high specific productivity (Q_p). The selection process is typically facilitated by automation technology such as Fluorescence Activated Cell Sorting since large numbers of clones are typically screened to identify a clone that exhibits the best profile with regard to stability, productivity, and protein quality.

The selection process typically begins in microtiter plates, for example 256- or 96-well plates, progressing to higher volumes and lower well numbers as the selection process proceeds. The selection process also includes evaluation of a subset of promising clones in shake flasks and small bioreactors to assess cell

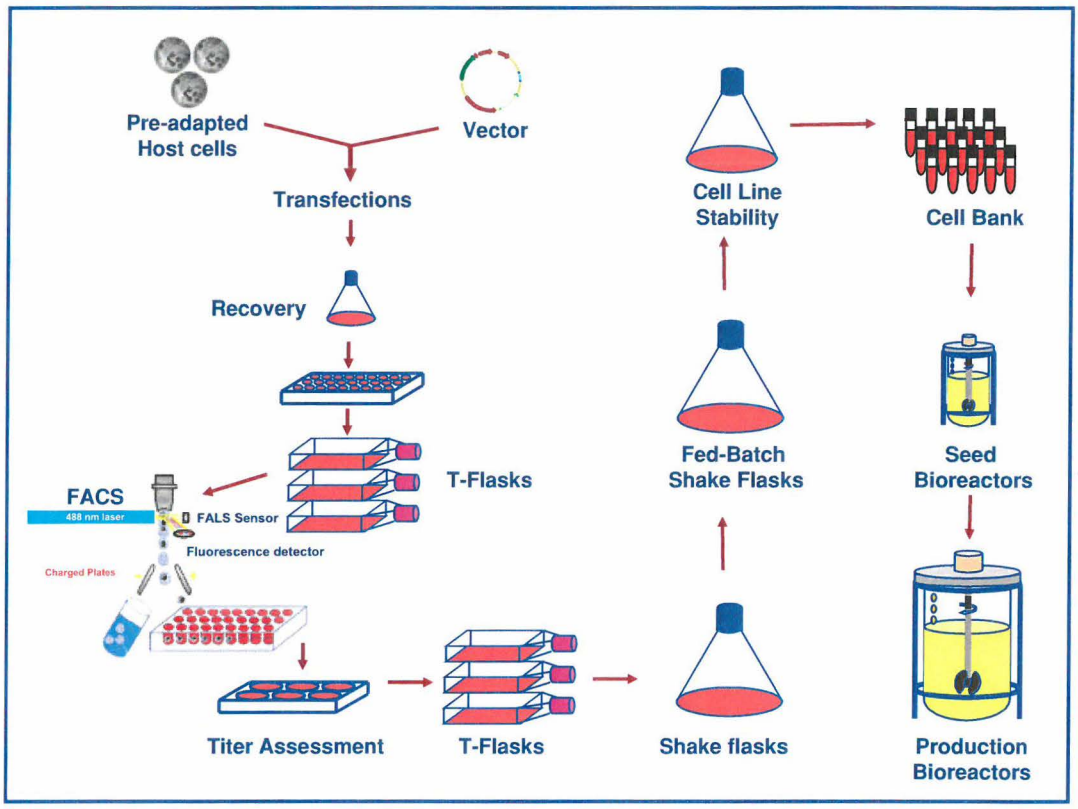


Fig. 15.1 Schematic of a generic cell line selection and production platform

viability and expression. During the selection process, the material that is produced is used to develop or confirm a suitable formulation, downstream processing methods, and to evaluate analytical platform methods. This material and material produced during subsequent cell culture process development are critical for an efficient and integrated strategy for production of clinical trial material. Once a clone is selected, a master cell bank (MCB) is prepared. The MCB, or a working cell bank (WCB) prepared from the MCB, is used in the scale-up and production of material for enabling regulatory toxicology studies and clinical trials (Fig. 15.1). It is worth noting that the MCB is prepared under GMP conditions and is used to generate all the antibody supplies for the lifetime of the product should the candidate be successful. Thus, the preparation of a MCB represents the earliest definition of the commercial process.

Cell Culture Process Development

Platform cell culture process development presents a number of challenges, including the need to adequately control for protein misfolding, aggregation, oxidation, deamidation, proteolysis, and glycosylation variants. Each of these

product-related impurities should be monitored and controlled under the platform conditions. In some cases the platform may need to be modified to address candidate-specific issues.

Scaling the process involves thawing vials from a MCB or WCB. This initial inoculum is expanded in shake flasks and small bioreactors and is then transferred to progressively larger seed reactors prior to transfer of the cell mass to the production bioreactor. There are two phases during process scaling. During the growth phase, the primary objective is to increase the viable cell mass, while during the protein production phase, cell growth slows and antibody expression and secretion ensues. A typical cycle-time in the bioreactor is 10–12 days. In traditional batch production, the media containing the required nutrients and additives is not replaced and production of cellular waste products limits the productivity of the cells. The more commonly employed fed-batch production involves replacing limiting components of the media during the growth and protein production phases (Shukla and Thommes 2010). Titers between 2 and 4 g/l have been attained using this technique and use of optimized media can increase titers further (Glynn et al. 2009). Perfusion technology employs various strategies to retain the cells in the bioreactor while continuously feeding new media to the trapped or immobilized cells. In these systems, high productivity can be maintained for months. The technology is as not widely employed in the pharmaceutical industry due to challenges in maintaining sterility over long periods of time and difficulties in maintaining a consistent product profile (Shukla and Thommes 2010; Kim 2007). Delivery of oxygen, pH, and temperature can impact cell productivity as well as protein quality and are, therefore, controlled during the cell culture process. The mass transfer of oxygen and carbon dioxide at the gas–liquid interface is directly affected by scale and is an important factor to control during scale-up of cell culture processes (Shukla and Thommes 2010).

Harvesting involves separating the cell culture from the growth medium or broth containing the desired antibody, and is accomplished using centrifugation, depth filtration, microfiltration, and various membrane filtrations. Centrifugation takes advantage of the density differences between the cells and the surrounding liquid and accelerates settling in the growth media. The cells are relatively fragile, so care must be taken to avoid excessive shear stresses during centrifugation that can result in cell lysis and the release of host proteins, DNA, and other impurities into the broth. Further removal of cellular debris is carried out using filtration based on size and charge. Depth filtration refers to the use of a porous medium that is capable of retaining debris from the broth throughout its matrix, rather than just on its surface. This can prevent fouling in subsequent membrane filtrations, and it has also been shown that depth filters are able to remove host cell protein contaminants from a recombinant monoclonal antibody process stream (Yigzaw 2006). Size-based membrane filtration is often the last step in the harvest process after which, the clarified broth is further processed through a number of chromatographic and virus removal steps in downstream purification.

Downstream Process Development

The common structural features of antibodies make them well suited to platform purification. Most if not all large-scale purification schemes incorporate Protein-A or MabSelect™ chromatography as the first downstream purification step. The Protein-A immobilized ligand binds to the Fc region of antibodies while host cell proteins (HCP), DNA, and other process related impurities flow through in the mobile phase. Typically Protein-A chromatography affords product in greater than 90% purity after elution from the column at low pH (Darcy et al. 2011).

Ion exchange chromatography is commonly used to further purify the antibody product from HCP, DNA, and other process and product-related impurities. Additional chromatography steps can be employed to address antibody-specific issues; for example, hydrophobic interaction chromatography (HIC) is often selected to remove high levels of aggregate (Shukla 2007). For mAbs, the trend has been to select either a 2- or 3-column downstream platform that efficiently purifies the majority of antibody candidates. In addition to Protein-A, three column platforms have employed anion (AEX) and cation (CEX) exchange steps. Protein-A followed by AEX chromatography using a weak partition mode, or Protein-A followed by CEX where the AEX column is replaced by a membrane are examples of 2-column platforms (Glynn et al. 2009; Shukla and Thommes 2010). Recent technological advances have made membranes an attractive addition, or a potential alternative, to traditional resin column chromatography. For example, the commercially available Sartobind Q membrane outperformed traditional AEX resins for DNA removal when compared side by side and could be reused up to 10 times without affecting its ability to remove DNA. The same membrane, however, is less effective than traditional resins when removing HCP (Yigzaw 2006).

Since antibodies are produced in mammalian cell culture that can harbor viruses harmful to humans, two orthogonal methods to remove viral particles are typically incorporated, in addition to the chromatography steps in the downstream process. These generally include a low pH viral inactivation step followed by viral filtration. Filter pore sizes of approximately 50 nm, capable of removing retroviral contaminates, have been used widely in the past; recently, however, filters designed for the smaller viruses ($\cong$20 nm) such as the Parvovirus, are being incorporated as a result of European Medicines Agency (EMA) requirements introduced in 2008 (EMA 2008). Often, the viral filters can be some of the more costly components in the purification process and smaller pore sizes are more susceptible to fouling, so they are often incorporated late in the platform when most other impurities have been removed. For clinical trials, it is necessary to demonstrate that the process is capable of clearing known and unknown viruses to appropriate levels. Typically this is accomplished using a panel of representative model viruses. The work is often outsourced to dedicated contract organizations due to the special precautions and culture methodology required to carry out this work in-house. In addition, demonstrating viral clearance may involve in-house development of a scaled-down model that mimics the downstream clearance steps

and uses viral mimetics to demonstrate viral clearance prior to outsourcing the clearance studies using live viruses. For First-In-Human (FIH) clinical trials it is generally acceptable to demonstrate clearance of two representative viruses, assayed once, using new resin; however, since subsequent trials in Europe would fall under the 2008 EMEA guidelines, and because viral clearance studies are expensive and time consuming, more and more companies are choosing to comply with the more recent EMEA guidelines in US trials even at early stages of development. Viral clearance validation for Phase 3 and Biologic License Application (BLA) filing is much more comprehensive including, but not limited to, demonstrating clearance for a minimum panel of four representative viruses, assayed in duplicate using new and recycled resins (Zhou and Tressel 2008).

The last downstream step is commonly ultrafiltration/diafiltration to reduce the volume, increase the protein concentration to an appropriate level for formulation, and to incorporate selected stabilizing excipients to facilitate storage and preparation of the fully formulated drug product. The Food and Drug Administration (FDA) defines a drug in part as "A substance intended for use in the diagnosis, cure, mitigation, treatment, or prevention of disease"(FDA 2012). This definition, along with others provided, serves to differentiate a drug substance from a drug product. The same drug substance can be found in multiple drug products (e.g. multiple strengths, formulations, or routes of delivery that all contain the same drug substance). For an antibody biotherapeutic, the drug substance refers to the antibody preparation after purification and addition of appropriate stabilizing agents. The drug product is the finished dosage form containing a specific strength of a drug substance, generally, but not necessarily, in association with additional active or inactive ingredients. The final drug product may also be incorporated into various delivery devices including pre-filled syringes and single or multiple use auto-injectors.

Production of clinical-grade material involves execution of multi-step processes and often multiple facilities to support manufacture of the drug substance, drug product, and the required analytical testing. In order to simplify logistics, it is often desirable to develop and define hold conditions for downstream process intermediates and storage conditions for the drug substance. Typical storage conditions are 2–8 °C and require supporting stability studies to define the use period for the stored drug substance. If an antibody is particularly unstable, even after including stabilizing excipients, the drug substance can be frozen to minimize degradation. In this case, however, it is additionally necessary to define and demonstrate drug substance freeze–thaw cycle conditions that do not negatively impact protein quality.

Formulation Development

Like other proteins, antibodies are subject to various degradation pathways. Degradation can occur during the process to prepare the drug substance or drug product and upon storage in the liquid, frozen, or solid state of either the drug

substance or drug product. The downstream process for production of the drug substance is designed to eliminate or reduce impurities and degradation products to within acceptable limits and to minimize formation during subsequent processing to confer a drug product with the appropriate quality. An understanding of the various degradation pathways is critical not only to minimize and remove impurities during production, but also to maintain the appropriate quality attributes of the final drug product post production, and for the duration of shipping and storage.

Degradation of antibodies can be generally categorized as either physical or chemical. Physical degradation includes surface adsorption, denaturation, and aggregation, while examples of chemical degradation include deamidation, oxidation, isomerization, fragmentation, and cross-linking (Chap. 4).

Proteins, including antibodies, can be readily adsorbed onto a variety of surfaces including storage containers, I.V. bags, tubing, etc. Surface adsorption, particularly at very low drug concentrations, can measurably reduce the concentration of antibody in solution and hence the drug available to the patient. In some cases, surface adsorption can be minimized by adding detergents or other surfactants (Doran 2006). Denaturation is another form of physical degradation and can occur as a result of shear, temperature changes, or lyophilization (Wang et al. 2007).

By far, the most significant form of physical degradation of antibodies is aggregation. As the demand for sub-cutaneous and intramuscular injection routes of administration to support patient focused delivery approaches increases, the ability to formulate antibodies at higher and higher concentrations has become a major focus in the pharmaceutical industry. These high concentrations present unique challenges, including the possibility for aggregation and high viscosity solutions that can be difficult to administer to patients. As concentration increases, hydrophilic and hydrophobic surfaces, transiently exposed during normal molecular motion, have an increased probability of interacting in an energetically favorable manner with exposed surfaces in other antibodies and forming stable aggregates (Daugherty 2010). Aggregation can be induced by sheer stress, shaking, temperature changes, freeze–thaw operations, long-term storage, and lyophilization. A variety of excipients including various sugars and surfactants are commonly employed to reduce or prevent aggregation. High concentration solutions can also present solubility and viscosity challenges. Typically high concentration solutions are necessary to deliver the required antibody dose as a single subcutaneous or intramuscular injection of 1–2 ml volume via a syringe. Precipitation and high viscosity can interfere with delivery via a syringe or other device. Screening for optimal pH as well as additives like sodium chloride or histidine have been used to decrease viscosity of antibody solutions (Wang et al. 2007).

Deamidation is one of the more prevalent forms of chemical degradation of antibodies and is a primary contributor to charge heterogeneity. Most deamidation proceeds via a succinimide intermediate and can be influenced by pH, steric effects, and primary sequence (Wang et al. 2007; Daugherty 2010). Typical strategies to control deamidation during processing and storage include screening

for optimal pH and the use of stabilizing buffering agents. Isomerization to afford isoaspartic acid species, often observed for antibodies, also occurs mostly via a succinimide intermediate and can be difficult to control. Since it does not require water to proceed, it can also occur in the solid state. Like other isomerization reactions and deamidation via a succinimide intermediate, steric factors and primary sequence can affect the rate of isomerization degradation pathways (Wang et al. 2007). Oxidation is another degradation pathway, although not as prevalent as deamidation. Methionine and cysteine are some of the more commonly oxidized residues, but oxidation of tyrosine, tryptophan, and histidine has also been observed (Daugherty 2010). Like deamidation, adjustment of the pH to minimize oxidation pathways is a common control strategy. Cross-linking via disulfide bond formation of unpaired cysteine residues or free thiol groups is a chemical degradation pathway that can lead to aggregation. Since antibodies contain several points of flexure within their framework, fragmentation is a common concern in addressing antibody stability. The hinge region between the Fc and Fv domains is one potential site of fragmentation that can affect the efficacy of the drug. The resulting fragments may be more susceptible to subsequent degradation or have a different bio-distribution and clearance profile than the intact monoclonal antibody. Typically optimization and control of pH, temperature, and process and handling conditions are sufficient to control fragmentation.

IgG antibodies produced in mammalian cells contain a biantennary complex attached to each of the two heavy chains within the Fc domain. When produced in CHO host cells these oligosaccharides are often fucosylated and microheterogeneous in nature. Although heterogeneity in glycosylation patterns is not unusual, proper glycosylation and distribution of variants may be critical for proper antibody function (Wang et al. 2007).

Although antibodies share a common framework, many of their degradation pathways are associated with specific primary sequences or the unique antigen binding regions (i.e. CDRs). Additionally, the rates of various degradation pathways for a single antibody differ for a specific set of conditions including pH, temperature, concentration, as well as processing and handling conditions. Therefore, determining the optimal formulation and storage conditions can be very compound specific. Most platform strategies strive to define a formulation or set of formulations that are suitable for the majority of candidates, but are not optimized for any specific candidate. This approach has been quite successful for antibodies, but does not eliminate the need to understand the degradation pathways for a specific compound and to document the selected formulation is suitable for a given antibody. This is particularly important for antibody drug candidates that ultimately become successful commercial products since the dose and dosage form generally evolves as development progresses from FIH studies to regulatory approval and launch.

Analytical Development

In the previous sections, a common theme is the importance of understanding how the production process, formulation, handling, and storage conditions affect the critical quality attributes of antibody drug candidates. Key to this understanding is the ability to monitor and measure the process and product-related impurities observed during development and production, and relate them to the efficacy and stability of a given candidate. A variety of methods can be used to identify, monitor, and quantify the various process and product-related impurities.

Of the various process related impurities, HCP, DNA, and endotoxins can have negative side effects on patients and are therefore of primary concern. Endotoxins, or pyrogenic lipopolysaccharides (LPS) are derived from Gram-negative bacteria such as *Escherichia coli*. In mammalian production hosts, endotoxins can be introduced into a process via raw materials. Endotoxin levels have been examined by the limulus amoebocyte lysate assay for the presence of LPS (GE 2007). HCPs are typically analyzed by Western blotting or 2D gel electrophoresis (GE 2007, Brass, 1996). DNA can be extracted and quantified by standard techniques, including qPCR. Additionally, a number of host cell specific ELISA-based assays to quantify HCP and DNA are also available (Glynn et al. 2009).

Product-related impurities are equally important to monitor and a variety of analytical methods have been employed to quantify the physical and chemical degradation pathways of antibodies. Physical degradation such as denaturation can be measured by various biophysical methods such as nuclear magnetic resonance spectroscopy, circular dichroism, or intrinsic fluorescence. Detecting aggregation can be challenging because aggregates can vary in size from simple dimers to complex multimers and can be soluble or precipitate out of solution. Size exclusion chromatography (SEC-HPLC) has become a standard method for detecting and quantitating aggregates but this method can underestimate high molecular mass species. Therefore, regulatory agencies often request an orthogonal method to confirm SEC-HPLC (Jenkins et al. 2008). Examples of other methods to detect aggregates include aggregate sensitive dyes or analytical ultracentrifugation. The latter method relies on the differences in sedimentation coefficients to separate species based on size. Since cross-linking via disulfide bonds can lead to formation of aggregates, measuring the total free thiol content by diagonal electrophoresis can provide an assessment of the propensity for cross-linking and intra- and intermolecular disulfide bond formation (Jenkins et al. 2008).

Chemical degradation, like fragmentation, can also be detected using methods that separate based on size. Deamidation is the primary source of charge heterogeneity and initial identification may involve detection of differences in charge distribution by isoelectric focusing or high performance cation exchange chromatography (Andya et al. 2001). Similar methods can be used to assess oxidative degradation. Further analyses to identify specific amino acid residues subject to deamidation, oxidative degradation, or other PTMs can be accomplished using

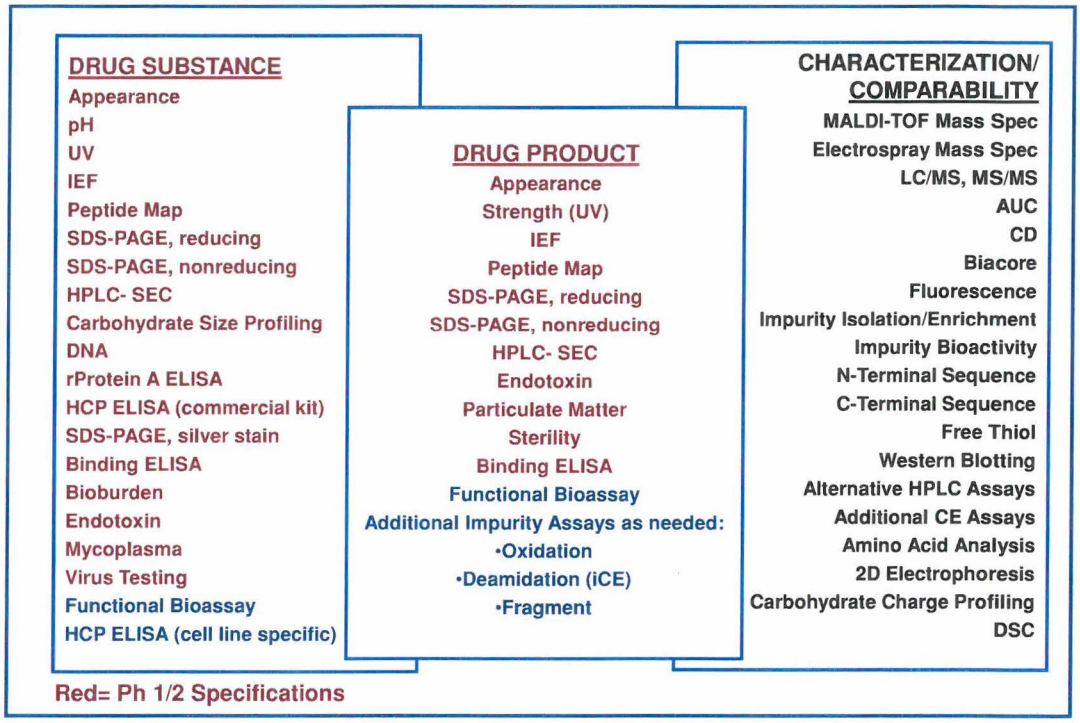


Fig. 15.2 Typical mAb analytical methods for release and characterization

amino acid sequencing, peptide mapping, tryptic digestion, HPLC, and mass spectrometry in various combinations.

Many of the methods described above are amenable to platform development for antibodies. Platform analytical methods are designed to detect and quantify the expected degradation pathways for antibodies, though the impurity profile for any specific antibody tends to be unique. Ultimately, however, for each candidate it is necessary to develop candidate-specific identity and bioassays. N-terminal sequencing and peptide mapping can serve as identity assays. Often simple binding ELISA-based (or Biacore) bioassays are initially developed for early clinical development. It is necessary, however, to develop a cell-based or functional bioassay for later stage clinical trials.

In addition, antibody preparations are evaluated or assayed for appearance, particulate matter, adventitious virus contamination and protein concentration; the latter usually by ultraviolet spectroscopy. Figure 15.2 illustrates a typical strategy for analytical release testing and characterization where methods (shown in red) are used for early Phase 1/2 analysis and additional methods (shown in blue) are added as development proceeds to Phase 3 and filing.

Project Management and Critical Path to Clinical Material

Production of clinical supplies requires close collaboration between multiple scientific disciplines. Often various teams, each with a different focus, are working in an integrated and iterative way during research, process development, and

manufacture with multiple hand-offs between these teams. More often than not, research, process development, and manufacture occur over multiple locations and long periods of time, where personnel move in and out of various roles on the teams. Furthermore, outsourcing some or all of the process development or manufacturing to contract manufacturing organizations (CMOs) is becoming increasingly common which brings with it additional complexity. The outsourced work typically requires a technology transfer and some level of oversight personnel to facilitate and act as technical consultants. The lead times to identify a CMO, conduct a quality audit, negotiate a contract, and schedule a slot for the work can cause delays if appropriate planning is not in place. Moreover, managing the contract and the payment schedule can require additional non-technical oversight. While the pharmaceutical industry's focus on speed to the clinic in recent years has fueled the development of platform process development for antibodies, the technical and business complexities have necessitated careful planning as well as project management to facilitate and streamline platform antibody production across scientific disciplines to ensure an appropriate balance between speed, cost, and quality.

Usually, the transfer of DNA or the appropriate expression vector for a specific candidate from the discovery team to the process development team is the first critical hand-off that initiates process development and manufacture of clinical supplies. For streamlined candidate development, it is also important to have representative protein material to enable early formulation screening and initial assessment of analytical methods. This material can come from the discovery team or can be prepared by the process development team after the hand-off from the discovery team. Within the process development team, cell line development, formulation development, and analytical method development all proceed in parallel. The cell culture development group continues to supply protein to the downstream purification group, and the downstream group supplies protein to the formulation scientists and analysts as process development proceeds. The analysts use this material to iteratively evaluate the capabilities of platform analytical methods to quantify impurities as the process and impurity profile changes during development. In addition to early screening of candidates to identify potential challenges, formulation scientists evaluate the impact of the platform formulation(s) on the selected candidate with regard to stability, storage, and handling. For these studies, it is preferable to use protein produced from the final or near final process to ensure the changes to the impurity profile during process development do not negatively affect the stability of the antibody in a given formulation. The selection of a formulation for the final drug product occurs before the drug substance manufacture begins. This is because some excipients defined in the final formulation are typically added during the last step of the drug substance manufacture to help stabilize the material for storage and for shipping to another facility where the drug product manufacture is completed. It is necessary, therefore, to define the final formulation before manufacture of the drug substance begins. This is different from small molecule development, where the manufacture of the drug substance can usually be decoupled from selection of a formulation that affords the

final drug product. Another difference between development of small molecules and biologics is that real-time stability studies to support clinical shelf-life are required for biologics, while for small molecules predictive stability is often sufficient. This is because proteins, with their associated tertiary structure, do not necessarily conform to Arrhenius-predicted degradation rates like their small molecule counterparts (Weiss et al. 2009). From a timing perspective, this means that after producing the clinical GMP material, a portion needs to be evaluated in a study to demonstrate that it is stable over time before it can be administered to patients. The need to perform real-time stability studies on the GMP clinical supplies can become a critical path to the clinic. Typically GLP material is prepared first to enable the regulatory toxicology studies and while the safety study is underway, the GMP clinical supplies are manufactured and evaluated for stability. The clinical supplies can be packaged and labeled for use while the stability studies proceed in parallel. The process development work and manufacture is documented in the CMC section of the Investigational New Drug or Investigational Medicinal Product Dossier submission and should demonstrate a robust process that consistently produces stable antibody preparations within the defined specifications.

In an accelerated development strategy, availability of representative protein generally defines the critical path to the clinic; first the material from cell culture development is used to enable the parallel development of the downstream purification process, analytical methods, and a suitable formulation; the GLP material is then used for a regulatory toxicology study, and finally, packaged GMP supplies with supporting stability studies are employed to enable clinical dosing. Since GMP supplies can be prepared while the regulatory toxicology is underway, from a production perspective, it is the process development and manufacture of GLP material for regulatory toxicology that is on the critical path to the clinic. Figure 15.3 illustrates the decrease in mAb cycle times for preparation of regulatory toxicology material over time. This graph demonstrates that platforms for antibody production along with careful planning, communication, and project management can afford increasingly fast cycle times.

Considerations for Biosimilar Development and Production

Biosimilars are generic versions of an "innovator" drug with the same amino acid sequence. Additionally, biosimilars are expected to demonstrate a high level of similarity to the innovator drug in a given indication even though they are produced from a different clone and manufacturing process. While generic small molecule drugs have been available for decades, biosimilars have only recently become available, and the first biosimilar antibodies are still in the development pipeline (Beck 2011; McCamish and Woollett 2011). The regulatory pathway for generic small molecules in the US was enabled by the Hatch-Waxman Amendments to the Drug Price Competition and Patent Term Restoration Act of 1984,

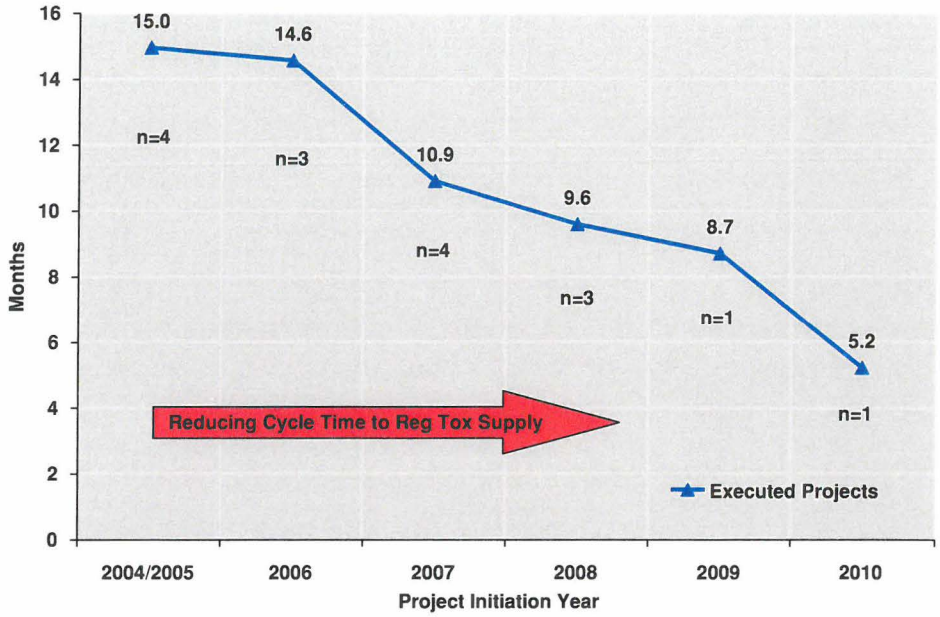


Fig. 15.3 Cycle times for fully executed platform monoclonal antibody development and manufacture of regulatory toxicology material over time (Pfizer Biotherapeutics)

which allowed an abbreviated New Drug Application as long as the generic sponsor could demonstrate bioequivalent safety and efficacy with the innovator drug. Additional clinical trials were not required by the generic sponsor as long as bioequivalence was demonstrated (FDA 1984). In comparison to small molecules, biotherapeutics are large, complex molecules that fold to incorporate specific tertiary structure and are subject to a variety of PTMs. As such, a biotherapeutic drug is a complex mixture of species and is nearly impossible to replicate in every detail.

Nevertheless, batch-to-batch variations are typically small during routine manufacture using the same clone and manufacturing process. Innovator manufacturing process changes, however, are frequently required after approval and during the product life cycle to meet changing demand and/or to decrease cost. Changes to increase productivity, scale of manufacturing, or in order to transfer the process to different manufacturing facilities are some common examples, and as previously discussed, such changes can result in a significant shift in quality attributes that can impact the safety and efficacy of the final drug. To address these concerns, regulatory agencies, and the pharmaceutical industry as a whole, have adopted a data-driven comparability approach where there is a direct comparison of the product before and after the manufacturing changes. Although it is necessary to demonstrate comparable safety and efficacy, these types of changes by the innovator rarely require additional clinical studies (McCamish and Woollett 2011).

Europe led the way in creating a pathway for the approval of biosimilars. In 2004, the European Medicines Agency (EMA) enacted legislation that granted their authority to approve biosimilar products that explicitly refer to a previously approved biotherapeutic for a given indication, based on a comparability approach

(EMEA 2004). For biosimilars, this typically means an abbreviated clinical strategy relative to a new drug, but it is not the same comparability exercise mentioned above- used to monitor product quality before and after manufacturing changes by the innovator- for which additional clinical trials are generally not required. Until recently, the FDA had lacked the authority to approve biosimilars, but in March 2010, as a part of the larger healthcare reform legislation, the Biologics Price Competition and Innovation Act (BPCIA) provided a path for the FDA to consider biosimilars, and furthermore, permits the FDA to designate interchangeability, an issue not addressed by the current EMA guidelines (FDA 2009). If a biosimilar is designated as interchangeable, then the biosimilar may be substituted for the innovator product without requiring prior consultation with the prescribing physician, and may, in turn, increase patient access to this important class of drugs. Currently there is no path to designate interchangeability in EU markets.

In highly regulated markets like the EU and US, a biosimilar is a compound that is "highly similar" to the innovator drug. In practice, determining what "highly similar" means for a given innovator drug can be challenging. The biosimilar sponsor may not rely on the innovator data or the published literature, but must determine the variability in the quality attributes of the innovator drug, preferably over a period of time, by obtaining and analyzing samples of commercial innovator reference product (McCamish and Woollett 2011). Furthermore, and in contrast to small molecule generics, the sponsor must carry out head-to-head clinical trials using both the innovator drug and the biosimilar. Obtaining innovator drug from multiple lots during the product life cycle can be difficult and expensive, but is necessary to define the so-called "goal posts" for the range of innovator quality attributes that define a "highly similar" compound. After defining the "goal posts", a sponsor can carry out iterative process development and analytical characterization to define the process parameters that afford a "highly similar" product. As the complexity of the innovator drug increases, so does the probability that multiple iterations will be required to be successful. The biosimilar sponsor may choose to narrow the quality target range in order to provide additional confidence that the quality attributes remain within the "goal posts" defined by the innovator product during the clinical development and approval process for a biosimilar. Having defined a "highly similar" candidate, the subsequent preclinical and clinical studies may be streamlined relative to a new biological entity. To complicate matters however, regulatory agencies generally require that the innovator reference product is approved and labeled in the local region. This makes a combined strategy for approval in the US and EU markets difficult and expensive. First-generation biosimilars introduced in the EU were "highly similar" to smaller, less complex recombinant innovator drugs like erythropoietin, somatropin, and insulin. The first mAb examples are currently in development (Beck 2011).

Selected Examples from the Literature

Immunogenicity: Hypersensitivity

Cetuximab (Erbitux), with annual sales over one billion US dollars, is a chimeric mouse-human IgG1 monoclonal antibody directed against the epidermal growth factor receptor, and is approved for use in colorectal cancer and squamous-cell carcinoma of the head and neck. A high prevalence of hypersensitivity reactions to cetuximab has been reported in some areas of the US (Chung et al. 2008).

Among 76 cetuximab-treated subjects, 25 exhibited a hypersensitivity reaction to the drug. IgE antibodies against cetuximab were found in *pretreatment* samples from 17 of these subjects, and only one of the 51 subjects who did not have a hypersensitivity reaction had such antibodies. The IgE antibodies were shown to be specific for an oligosaccharide, galactose-α-1,3-galactose, which is present within the Fab portion of the cetuximab heavy chain. Cetuximab is produced in the mouse cell line SP2/0, which expresses the gene for α-1,3-galactosyltransferase. A control study using cetuximab produced in CHO cells did not demonstrate the presence of the aforementioned glycosylation in the Fab region, and was thus not recognized by the preexisting IgE antibodies.

Monoclonal antibody glycosylation is important to the function and safety profile of the molecule and a detailed analysis of atypical glycosylation of monoclonal antibodies is important. An increasingly preferred approach is the use of CHO cells, which after extensive evaluation and experience in the pharmaceutical industry, have been shown to produce glycosylation patterns similar to those observed in humans. Another important consideration is post-market monitoring. In this case, the authors were able to identify preexisting antibodies from the control group, where no cetuximab was administered, and develop a post-market screen to identify the potential for a hypersensitivity reaction in certain patient populations.

Viral Contamination

Viral contamination may have a negative impact on the production process, and more importantly on patient safety. For these reasons, viral clearance continues to be a significant focus within the industry. This example describes Genentech's experience in dealing with two separate viral contaminations and a general approach for viral clearance and control. Additionally, polymerase chain reaction technology was first introduced here for the routine monitoring of viral contamination (Garnick 1996). In both cases of viral contamination, Minute Virus of Mice (MVM) was positively identified. MVM is a mouse-specific parvovirus. This virus is particularly resilient and can therefore be difficult to eradicate from colonies of laboratory animals. Although MVM has not been shown to infect humans,

parvoviruses from related families can cause disease in children and in immune-suppressed individuals (Heegaard and Brown 2002). In this case, the definitive source of the two contamination events was not conclusively identified, but the investigation suggested the contamination may have been introduced via raw materials used during the cell culture process.

In a second example, a DHFR mutant CHO K1 cell was used to produce an unnamed biotherapeutic—the culture was found to become rapidly acidic and widespread cell death was observed (Rabenau et al. 1993). Various methods were used to eliminate the possibility of bacterial, fungal or mycoplasma contamination. Using serum neutralization, electron microscopy, and RNA analysis, the authors identified the contamination as Epizootic Hemorrhagic Disease Virus, isolate 318 (EHDV-318). EHDV-318 was first isolated from a sentinel calf herd at the Khartoum University farm in Sudan, but at least 10 serotypes have been identified globally. The virus causes an often fatal hemorrhagic disease in North American white-tailed deer, but very little information is available about the impact of EHDV in domestic cattle and other ruminants. Thus far, transmission to humans has not been reported (Mohammed et al. 1996). A definitive source of the viral contamination in this case, however, was not determined due in large part to the multiple potential sources of contamination including the cell line, media supplements, inoculated/transfected materials, or laboratory staff.

Although mammalian expression systems like CHO offer advantages over bacterial expression systems, they may also harbor viruses that may be harmful to patients. In addition, viral contamination can have a significant negative impact on production and identifying the source of contamination poses a significant challenge due to the complex and multi-step nature of production processes. Because of the potential disruption of the production process and more importantly for patient safety, it is important to implement a clear quality assurance and control strategy to reduce the potential for viral contamination.

Concluding Remarks

The growth of the biotherapeutic pipeline within the pharmaceutical industry over the past 10 years, and specifically the growth of the monoclonal antibody sector, has fueled the development of platforms to more efficiently develop and manufacture these drugs. Moreover, antibodies are particularly well suited to platform process development and manufacture because they share a common structural framework over large portions of the protein sequence, and therefore exhibit similar physiochemical properties. This approach has been successful within the industry and typically relies on defining a set of development and production parameters that are designed to be suitable for the majority of antibody drug candidates, albeit not optimized for any specific candidate.

Further candidate-specific optimization, if required, can be deferred until the probability of commercial success merits the additional investment. Platforms for

process development and manufacture have also enabled progressively faster cycle times from candidate selection to the clinic. With increased speed, however, there is increased complexity as work proceeds across multiple teams and locations over long periods of time. The importance of project management to facilitate efficient and integrated development throughout the candidate and product life cycle cannot be understated.

While platforms for antibody production have been used to decrease cost and increase speed, it is still necessary to evaluate each candidate individually to assess whether the operations and conditions defined by a given platform will be suitable for production. This is particularly important for antibody drug candidates that ultimately become successful commercial products, since the production process generally evolves as development progresses from FIH studies to regulatory approval and launch. For biotherapeutics, product quality is inherently linked to the process by which the candidates are produced. This link is established early in the choice of a host cell line and clone selection, and continues in defining process parameters for cell culture fermentation and downstream purification. Formulation and drug storage conditions are equally important in maintaining the product quality attributes after manufacture.

Since manufacturing changes will likely be required during the life cycle of a successful product, a robust understanding of the process and the critical parameters that affect product quality is critical for the integration of these changes without disruption of product supply. Finally, as the patents on early biotherapeutics expire and some of the most profitable antibody drugs approach patent expiry, biosimilars are appearing in the marketplace. With regulatory paths for approval of biosimilars defined in both the EU and US markets, this is sure to be a growing segment of research and development. A fundamental understanding of the process parameters that impact product quality is an absolute requirement to develop a biosimilar that meets the "highly similar" standard when compared to the innovator product.

Lastly, the use of platforms to decrease cost and increase speed to the clinic, coupled with a robust understanding of the factors that affect product quality as the production process evolves over time, will ultimately decrease the cost of this important class of drugs, and more importantly, will greatly expand patient access to these life-saving medicines.

References

Andya JD, Shire SJ et al (2001) Identification of multiple sources of charge heterogeneity in a recombinant antibody. J Chromatogr B Biomed Sci Appl 752:233–245

Bebbington CR, Renner G et al (1992) High-level expression of a recombinant antibody from myeloma cells using a glutamine synthetase gene as an amplifiable selectable marker. Biotechnology (N Y) 10:169–175

Beck A (2011) Biosimilar, biobetter and next generation therapeutic antibodies. mAbs 3(2):107–110

Chung CH et al (2008) Cetuximab-induced anaphylaxis and IgE specific for galactose-α-1, 3-galactose. N Eng J Med 358(11):1109–1117

Darcy E, Leonard P et al (2011) Purification of antibodies using affinity chromatography. In: Walls D, Loughran ST (eds) Methods in molecular biology: protein chromatography, vol 681. Humana Press Inc., New York, pp 369–382

Daugherty AL, Mrsny RJ (2010) Formulation and delivery issues for monoclonal antibody therapeutics. In: Shire SJ, Gombotz W, Bechtold-Peters K, Andya J (eds) Current trends in monoclonal antibody development and manufacturing, Springer, New York, pp 103–129

Doran PM (2006) Loss of secreted antibody from transgenic plant tissue cultures due to surface adsorption. J Biotechnol 122(1):39–54

EMEA (2004) Directive 2004/27/EC of the European Parliament and of the Council of 31 March 2004 amending Directive 2001/83/EC on the Community code relating to medicinal products for human use

EMEA (2008) Evaluation of medicines for human use: guideline on virus safety evaluation of biotechnological investigational medicinal products. U. European Medicine Agency, London

FDA, w. F. g. (1984) Drug Price Competition and Patent Term Restoration Act of 1984, Hatch-Waxman Amendments

FDA, w. F. g. (2009) Biologics Price Competition and Innovation Act of 2009

FDA, w. F. g. (2012) Drugs@FDA Glossary of Terms, Food and Drug Administration

Garnick RL (1996) Experience with viral contamination in cell culture. Viral safety and evaluation of viral clearance from biopharmaceutical products. Dev Biol Stand 88:49–56

GE (2007) Pilot-scale capture of monoclonal antibody IgG4 on MabSelect Xtra with high purity and yield

Geisse S, Gram H et al (1996) Eukaryotic expression systems: a comparison. Protein Expr Purif 8(3):271–282

Glynn J, Hagerty T et al (2009) The development and application of a monoclonal antibody purification platform. BioPharm Int :16–20

Hagemeyer CE, von zur Muhlen C et al (2009) Single-chain antibodies as diagnostic tools and therapeutic agents. Thromb Haemost 101(6):1012–1019

Heegaard ED, Brown KE (2002) Human parvovirus B19. Clin Microbiol Rev :485–505

Jenkins N, Murphy L et al (2008) Post-translational modifications of recombinant proteins: significance for biopharmaceuticals. Mol Biotechnol 39:113–118

Kim LT, Yi-Chin Voldman, Joel Yu, Hanry (2007) A practical guide to microfluidic perfusion culture of adherent mammalian cells. Lab Chip 7(6):681–694

Lonberg N (2008) Fully human antibodies from transgenic mouse and phage display platforms. Curr Opin Immunol 20(4):450–459

McCamish M, Woollett G (2011) Worldwide experience with biosimilar development. mAbs 3(2):209–217

Mohammed MEH, Aradaib IE et al (1996) Application of molecular biological techniques for detection of epizootic hemorrhagic disease virus (EHDV-318) recovered from a sentinel calf in central Sudan. Vet Microbiol 52:201–208

Owyang AM, Issafras H et al (2011) XOMA 052, a potent, high-affinity monoclonal antibody for the treatment of IL-1beta-mediated diseases. MAbs 3(1):49–60

Rabenau H et al (1993) Contamination of genetically engineered CHO-cells by epizootic haemorrhagic disease virus (EHDV). Biologicals 21:207–214

Sekhon BS (2010) Biopharmaceuticals: an overview. Thai J Pharm Sci 34(1):1–19

Shukla AA, Thommes J (2010) Recent advances in large-scale production of monoclonal antibodies and related proteins. Trends Biotechnol 28(5):253–261

Shukla A et al (2007) Downstream processing of monoclonal antibodies—application of platform approaches. J Chromatogr B 848:28–39

Sioud M (2007) Main approaches to target discovery and validation. Methods Mol Biol 360(1): 1–12

Wang W, Singh S et al (2007) Antibody structure, instability, and formulation. J Pharm Sci 96(1):1–26

Weiss WF IV, Young TM et al (2009) Principles, approaches, and challenges for predicting protein aggregation rates and shelf life. J Pharm Sci 98(4):1246–1277

Yigzaw Y et al (2006) Exploitation of the adsorptive properties of depth filters for host cell protein removal during monoclonal antibody purification. Biotechnol Progr 22:288–296

Zhou JX, Tressel T (2008) Current practice and future strategies for viral clearance in mAb downstream production. Am Pharm Rev 11(1):109–110, 112, 114–121

Protein Science (1995), *4*:2073–2081. Cambridge University Press. Printed in the USA.
Copyright © 1995 The Protein Society

Destabilizing loop swaps in the CDRs of an immunoglobulin V_L domain



LARRY R. HELMS AND RONALD WETZEL

Macromolecular Sciences Department, SmithKline Beecham Pharmaceuticals, King of Prussia, Pennsylvania 19406

(RECEIVED May 15, 1995; ACCEPTED August 3, 1995)

Abstract

It is generally believed that loop regions in globular proteins, and particularly hypervariable loops in immunoglobulins, can accommodate a wide variety of sequence changes without jeopardizing protein structure or stability. We show here, however, that novel sequences introduced within complementarity determining regions (CDRs) 1 and 3 of the immunoglobulin variable domain REI V_L can significantly diminish the stability of the native state of this protein. Besides their implications for the general role of loops in the stability of globular proteins, these results suggest previously unrecognized stability constraints on the variability of CDRs that may impact efforts to engineer new and improved activities into antibodies.

Keywords: complementarity determining regions; hypervariable loops; immunoglobulin stability; protein stability; Stern–Volmer plots; unfolding

In the structures of antibody heavy and light chain variable domains, complementarity determining region (CDR) loops of diverse sequence and conformation project from β-sandwich frameworks to determine the affinity and specificity of antigen binding. These diverse sequences arise in the development of an antibody response via a complex combination of gene rearrangements and somatic mutations (Branden & Tooze, 1991). Protein engineers have transferred antigen binding activity from one framework to another by swapping hypervariable CDR loops between frameworks (Jones et al., 1986; Riechmann et al., 1988). In addition, totally artificial loop sequences have been introduced into variable domain frameworks to generate novel binding functions (Barbas et al., 1993; Fisch et al., 1994). This apparent tolerance of the immunoglobulin fold for both sequence diversity and loop swaps is consistent with the view that the major determinants of structural stability of globular proteins lie in the sequence-specific formation and packing of regular secondary structure elements (Shortle, 1992; Matthews, 1993), whereas surface loops are more forgiving of sequence changes (El Hawrani et al., 1994).

Although the CDR loops differ greatly in sequence, they are not infinitely variable in either sequence or conformation. Positions with highly conserved amino acids are found within many CDR sequences (Kabat et al., 1991). Further, X-ray crystallographic studies have demonstrated that only a limited number of "canonical structures" appear to be available for each CDR. For example, in an examination of the structural database available in 1989, only four different loop conformations were identified in the light chain crystallographic database for CDR1, and only three for CDR3 (Chothia et al., 1989). If these patterns do suggest constraints on the sequence variability of CDRs, however, it remains difficult from examination of evolved antibodies to either gauge the severity of these constraints or to understand their structural or functional basis.

In this report we describe the preparation of a number of mutants of the immunoglobulin light chain variable domain REI, in which wild-type CDR sequences were replaced by loops of differing sequence and length. These replacements cause dramatic reductions—and in some cases apparent elimination—of the net folding stability of the protein. The results have implications for the role of loops in determining the stabilities of immunoglobulins and other globular proteins and also suggest a folding stability constraint on the evolution of CDR structures.

Results

Figure 1 shows a ribbon diagram of the REI V_L domain highlighting its three CDRs. Figure 2 lists the mutants examined in this work and shows the CDR sequence changes carried out to produce the proteins. The RGD-containing sequences inserted into the REI CDRs are either derived from loop regions of the snake venom disintegrins kistrin (Dennis et al., 1989), barbourin (Scarborough et al., 1991), and echistatin (Gan et al., 1988) or (in REI-RGD18 and REI-RGD26) were designed, unnatural

Reprint requests to: Ronald Wetzel, Macromolecular Sciences Department, SmithKline Beecham Pharmaceuticals, 709 Swedeland Road, King of Prussia, Pennsylvania 19406; e-mail: wetzelrb%phvax.dnet@sb.com.

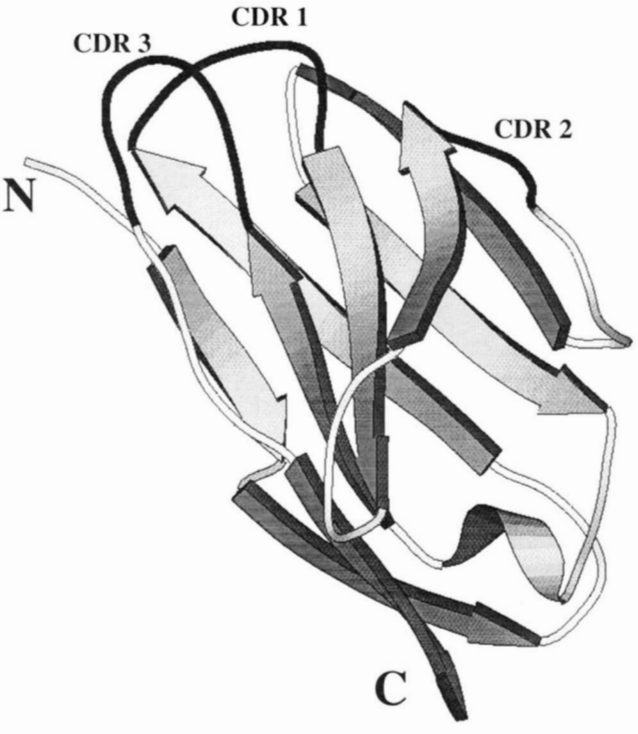


Fig. 1. Ribbon diagram of the REI V_L domain from the X-ray structural coordinates (structure 1REI from the Brookhaven protein structure database [Abola et al., 1987]) with the CDRs highlighted. Drawing produced using MOLSCRIPT (Kraulis, 1991).

sequences. Loop replacements were constructed in both CDR1 and CDR3, yielding domains that by several criteria appeared to be stably folded proteins. Thus, each mutant was stably expressed in *Escherichia coli* by secretion into the periplasm. In addition, the intradomain disulfide bonds of these mutants—like that of the wild type—form readily in the *E. coli* periplasm. Despite these indications of stability, however, and despite the solubility of these proteins in native buffer, further examination revealed significant destabilization in most of the mutants.

The folding integrity of an immunoglobulin domain can be assessed (Tsunenaga et al., 1987) by the intrinsic fluorescence of a conserved tryptophan, which is dramatically quenched in the folded state by the close proximity of the intradomain disulfide bond (Epp et al., 1974). Thus, the fluorescence of the wild-type domain in native buffer at RT is quite low compared to the fluorescence in 4 M guanidine hydrochloride (Gdn-HCl), where the protein is unfolded. Table 1 shows the fluorescence yield for WT REI V_L in native buffer is only 11% of the fluorescence in denaturant, and that some of the mutants (RGD12, RGD1, RGD34, RGD23, RGD18, RGD35, RGD32) also exhibit low fluorescence and are therefore also essentially completely folded in native buffer. In contrast, fluorescence ratios in Table 1 for the other mutants suggest they are substantially unfolded in native buffer under these conditions.

For the mutants that do exhibit folding stability in native buffer, stability was quantified by Gdn-HCl denaturation experiments to determine $\Delta\Delta G_{stab}$'s, the difference in free energy of stabilization between the wild-type sequence and each mutant. The wild-type domain at pH 7 exhibits an unfolding transition (Fig. 3), which gives a midpoint for Gdn-HCl unfolding (C_m) of 1.55 M and a corresponding free energy of stabilization of −6.8 kcal/mol (Table 1) (Hurle et al., 1994). These values are typical of globular proteins in this size range (Pfeil, 1981) and are also similar to values obtained for other V_L domains (Ahmad & Bigelow, 1986; Tsunenaga et al., 1987).

All of the loop insertion mutants examined prove to be substantially destabilized compared to the wild type (Fig. 3; Table 1). Some mutants, such as RGD1, RGD12, RGD23, and RGD34, are stably folded at pH 7 and RT in native buffer, but at the same time require significantly lower concentrations of Gdn-HCl, compared to wild type, to induce unfolding. Other mutants, such as RGD14, RGD17, and RGD22, are even more unstable, exhibiting significant fluorescence at pH 7 in native buffer at RT. Although it is difficult to rigorously determine the standard free energies of unfolding from the incomplete unfolding curves obtained for many of these proteins, because the na-

```
                                90                                  100
A REI-VL WT   ..YYCQQY------QSLP------YTFGQ...

  REI-RGD17   ..YYCQQYGTVSRVAKGDWNDDTSYTFGQ...
  REI-RGD4    ..YYCQ--GKISRIPRGDMPDDRS--FGQ...
  REI-RGD18   ..YYCQQ-----KGGRGDSGGK--YTFGQ...
  REI-RGD12   ..YYCQQY----RIPRGDMP----YTFGQ...
  REI-RGD26   ..YYCQ---KGGGGGRGDSK------FGQ...
  REI-RGD23   ..YYCQQ-----RIPRGDMP-----TFGQ...
  REI-RGD21   ..YYCQQ-----RIPRGDMP------FGQ...
  REI-RGD22   ..YYCQ------RIPRGDMP-----TFGQ...
  REI-RGD14   ..YYCQ------RIPRGDMP------FGQ...
  REI-RGD15   ..YYCQQY------PRGD------YTFGQ...

                  20                          40
B REI-VL WT   ..TITCQA---SQD---IIKYLNWYQQTP..

  REI-RGD35   ..TITCQASRIPRGDMPIIKYLNWYQQTP..
  REI-RGD32   ..TITCQAKRARGDDM-IIKYLNWYQQTP..
  REI-RGD34   ..TITCQARIPRGDMP-IIKYLNWYQQTP..
  REI-RGD37   ..TITCQAKIGRGDLV-IIKHLNWYQQKP..
  REI-RGD1    ..TITCQA---RGD---IIKYLNWYQQTP..
```

Fig. 2. Sequences of the loop swap mutants in this study. Residues underlined in the wild-type sequence indicate the CDR as defined by sequence homology within the immunoglobulin family (Kabat et al., 1991). Most of the RGD sequences introduced are derived from the active site loops of the snake venom disintegrins kistrin (Dennis et al., 1989) (RGD4, 12, 14, 15, 21, 22, 23, 34, and 35), echistatin (Gan et al., 1988) (RGD32), and barbourin (Scarborough et al., 1991) (RGD17). REI-RGD1 and RGD4 were described previously (Lee et al., 1993). Hyphens are included to accommodate the longest sequence in the lineup. **A:** Sequences of mutants derived from loop swaps in CDR3. **B:** Sequences of mutants derived from loop swaps in CDR1.

Table 1. *Properties of REI V_L-RGD hybrid proteins*

Name	Structure[a]	Δ Residues[b]	Fluorescence[c]	T_m (°C)[d]	C_m (M)[e]	$\Delta\Delta G_{unf}$[f]
RGD17	REI(Δ92-95/+GTVSRVAKGDWNDDTS)	+12	0.78		<0	>6.8
RGD4	REI(Δ90-97/+GKISRIPRGDMPDDRS)	+8	0.75	25	0	>6.8
RGD18	REI(Δ91-95/+KGGRGDSGGK)	+5	0.25		0.13	6.2
RGD12	REI(Δ92-95/+RIPRGDMP)	+4	0.12	37	0.40	5.1
RGD26	REI(Δ90-97/+KGGGGGRGDSK)	+3	0.85			>6.8
RGD23	REI(Δ91-96/+RIPRGDMP)	+2	0.25	33	0.28	5.6
RGD21	REI(Δ91-97/+RIPRGDMP)	+1	0.66			>6.8
RGD22	REI(Δ90-96/+RIPRGDMP)	+1	0.82			>6.8
RGD14	REI(Δ90-97/+RIPRGDMP)	0	0.84			>6.8
RGD15	REI(Δ92-95/+PRGD)	0	0.54		0	6.8
RGD35	REI(Δ27-28/+RIPRGDMP)	+6	0.21		0.20	5.9
RGD32	REI(Δ26-28/+KRARGDDM)	+5	0.22		0.32	5.4
RGD34	REI(Δ26-28/+RIPRGDMP)	+5	0.13	34	0.42	5.0
RGD1	REI(S26R/Q27G)	0	0.12		0.5	4.6
WT REI		–	0.11	55	1.55[e]	–

[a] Structural nomenclature for loop insertion mutants is as described by Wetzel (1988). Deleted wild-type residues are indicated on the left side of the slash, and the new sequence introduced into the gap is indicated to the right of the slash.
[b] Difference in REI length introduced by the loop swap.
[c] Intrinsic fluorescence at 350 nm upon excitation at 295 nm by a 4 μM protein solution at 25 °C relative to the signal in 4 M Gdn-HCl.
[d] Temperature for 50% unfolding as described in Figure 4.
[e] C_m for Gdn-HCl unfolding in 10 mM sodium phosphate, pH 7. The C_m value for REI WT is from Hurle et al. (1994).
[f] ΔG_{unf} for the mutant REI V_L minus ΔG_{unf} for the WT, calculated at the C_m of the WT; see the Materials and methods.

tive baseline is short or nonexistent, reasonable estimates for the amount of destabilization by the loop swaps range from 5 to greater than 7 kcal/mol (Table 1).

Although fluorescence can be sensitive to even small structural changes, the observed tryptophan fluorescence dequenching appears to be associated with a radical disorganization of the folded structure of REI. Unfolding curves such as those shown in Figure 3 are normally associated with global folding transitions. In addition, the unfolded states of REI V_L defined by fluorescence dequenching are nonnative when analyzed by other spectroscopic probes. CD (Fig. 4) of REI-RGD4, a mutant that is about 50% unfolded in native buffer at pH 7 and RT by fluorescence measurements, shows that the molecule's conforma-

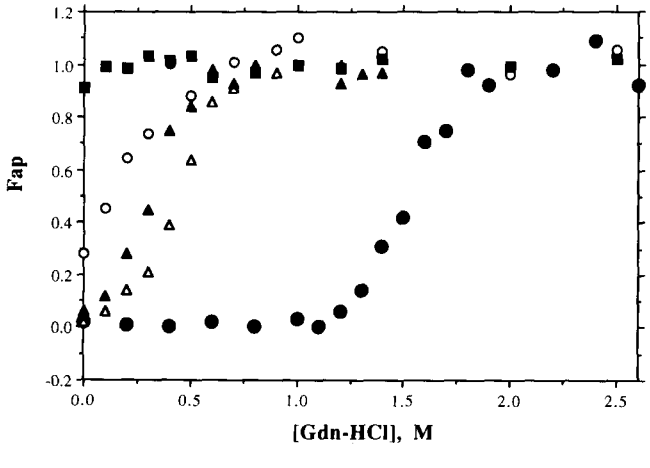


Fig. 3. Mole fraction of unfolded protein (Fap) versus Gdn-HCl concentration for denaturant unfolding of selected REI V_L sequence variants. ●, wild type; ■, RGD17; ○, RGD18; ▲, RGD32; △, RGD34. The data set for wild-type REI V_L is reproduced from Hurle et al. (1994).

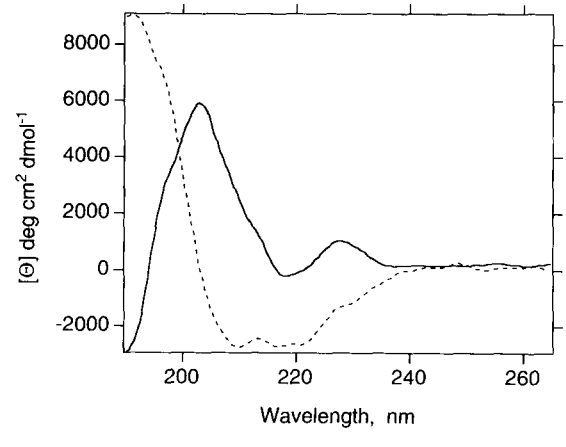


Fig. 4. CD spectra of WT (———) and RGD4 (– – – –) REI V_L. Measurements were made at 25 °C in 10 mM sodium phosphate, pH 7.4, on a Jasco model J-500-C spectropolarimeter equipped with a Macintosh computer-based data acquisition system. The wild-type data were collected on a sample of 0.7 mg/mL in a 0.02-cm-pathlength cell. REI-RGD4 mutant data were collected on a sample of 0.13 mg/mL in a 0.02-cm-pathlength cell. Each spectrum is presented as an average of 20 scans over the 265–190-nm range.

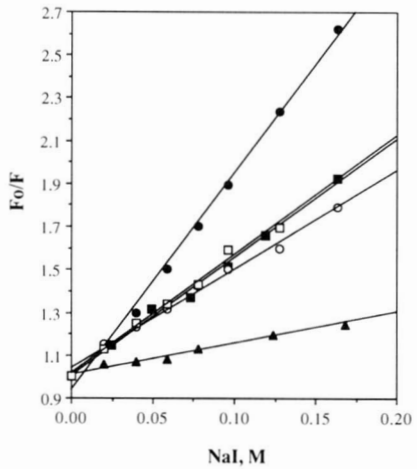


Fig. 5. Stern–Volmer plots of iodide quenching of the tryptophan in various REI V_L sequence variants. All samples were at 10 μg/mL in 10 mM sodium phosphate, 50 mM NaCl, pH 7.4. The wild-type sample also contained Gdn-HCl at 4 M. Fluorescence was read in a Perkin-Elmer MPF-66 spectrofluorometer in a thermostatted cell equilibrated at 22 °C. The $K_{S\text{-}V}$ values obtained for the REI V_L variants plotted are: ●, WT, 10.1; ▲, RGD4, 1.5; ○, RGD14, 4.6; □, RGD21, 5.5; ■, RGD22, 5.5.

tion under the same conditions, although not in statistical coil, is significantly different from the β-sheet conformation exhibited by the wild type (the spectrum of the *E. coli*-produced wild type matches well with the published spectrum of the REI V_L derived from Bence-Jones protein [Brahms & Brahms, 1980]).

It is possible that the observed fluorescence dequenching is due to misfolding into an alternatively packed structure in which Trp^{35} is no longer proximal to the disulfide bond. Stern–Volmer analysis was conducted on several of the REI V_L mutants to determine the accessibility of the Trp to a small molecule quencher. Figure 5 shows Stern–Volmer plots for WT REI V_L unfolded in 4 M Gdn-HCl and a number of apparently unfolded mutants in native buffer. (Because the Trp in the native folded structure is already quenched by the disulfide, it is not possible to derive a $K_{S\text{-}V}$ for Trp in the native state of REI.) This analysis shows that the tryptophan of the unfolded WT is fully accessible (Eftink & Ghiron, 1981) to iodide quenching, giving a $K_{S\text{-}V}$ of 10.1. The mutants RGD14, RGD21, and RGD22 are also sensitive to quenching, with $K_{S\text{-}V}$ values around 5. RGD4 is more resistant to iodide quenching, with a $K_{S\text{-}V}$ value of 1.5. A fully buried tryptophan would be expected to yield a $K_{S\text{-}V}$ value of 0.2 or less (Eftink & Ghiron, 1981). The accessibility of Trp^{35} to the large, charged iodide quencher supports the interpretation that these REI V_L variants are significantly unfolded or misfolded in native buffer.

In principle, inability to achieve a highly quenched fluorescent (native-like) state might be attributable to the absence of the intradomain disulfide bridge. Figure 6 shows an SDS-PAGE gel of a wild-type REI V_L and series of loop-swap mutants. The gel shows that, in general, a nonreduced, alkylated sample migrates more rapidly through the gel than a reduced, alkylated sample of the same protein. This is consistent with the existence of a disulfide in the nonreduced sample (Pollitt & Zalkin, 1983). Such mobility shifts can be difficult to observe in small proteins like REI V_L, and examination of Figure 6 shows the shifts to be small and variable. The absence of a shift in RGD14 probably simply reflects the limit of detection for this mutant. Other means were also used to confirm the existence of the disulfide in some of the mutant V_L domains. An alkylated sample of REI-RGD4 gives a parent ion in mass spectrometry consistent with molecular weight expected for the oxidized mutant and inconsistent with the alkylated molecule (L. Helms & D. McNulty, unpubl. result).

Although these proteins were purified by reverse-phase HPLC, in which they required acetonitrile concentrations for elution similar to that found for wild type, it is formally possible that some of the mutants exist as disulfide-linked dimers or oligomers that would likely exhibit alternate fluorescence characteristics. However, Figure 6 shows there are no disulfide-linked dimers or trimers in these preparations. Neither was there any Coomassie blue-stained material at higher molecular weights in the gel (not shown), consistent with the absence of larger covalent aggregates.

Noncovalent aggregation could in principle also compromise proper interpretation of the fluorescence data, by offering a competing "folding" pathway for the proteins and thus exaggerating their apparent instability as monitored by fluorescence dequenching. In fact, some REI V_L point mutants associated with light chain deposition disease exhibit substantial unfolding-related aggregation by gel-filtration analysis (L.R. Helms & R. Wetzel, unpubl.). However, gel filtration analysis indicates no large aggregates to be present in solutions of RGD 15 and RGD 21 (data not shown).

The destabilization of REI V_L variants assessed by denaturant unfolding was confirmed for some of the mutants by thermal unfolding studies. Figure 7B shows that the wild-type domain at pH 7 undergoes a cooperative thermal unfolding transition, as monitored by fluorescence, with a T_m of 55 °C. In contrast, RGD12, RGD23, and RGD34, three of the more stable of the

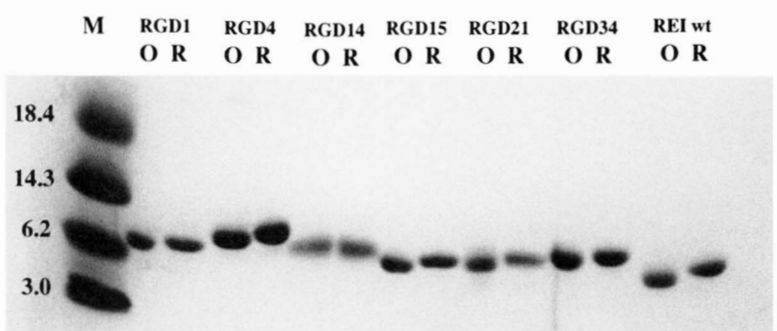


Fig. 6. Coomassie brilliant blue-stained, nonreducing SDS–polyacrylamide gel of various mutants of REI V_L. Reduced (R) samples were treated 30 min at 37 °C with 1 mM dithiothreitol in SDS-PAGE gel loading buffer, after which iodoacetic acid was added to 5 mM and incubated an additional 30 min. Nonreduced (O) samples were treated only with 5 mM iodoacetic acid. Samples were run on a 12% acrylamide gel (Laemmli, 1970).

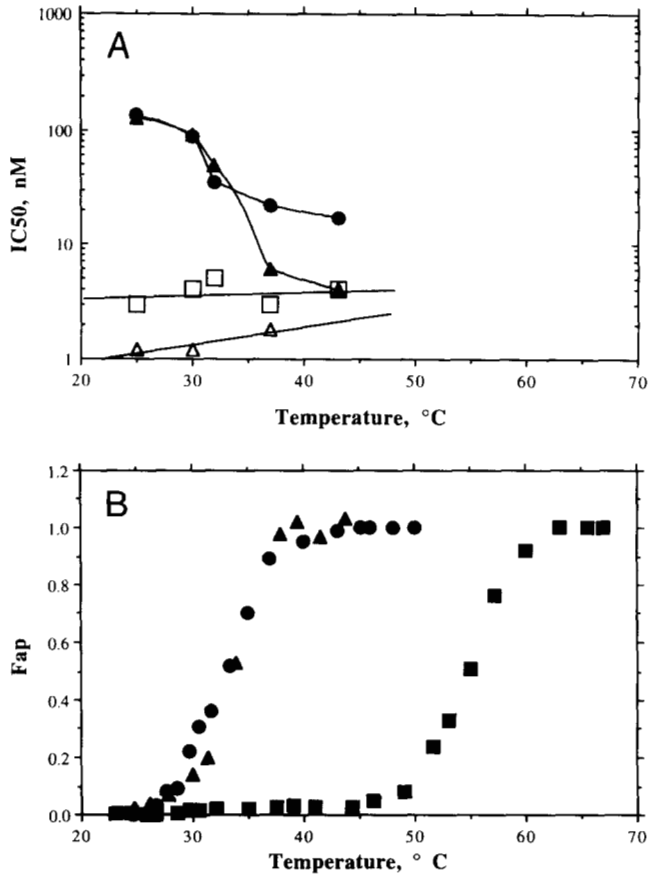


Fig. 7. Temperature dependence of binding and folding. ■, WT REI V_L; ●, REI-RGD23; ▲, REI-RGD34; □, SKF#106760; △, echistatin. **A:** Temperature dependence of IC_{50}'s for inhibition of binding of biotinylated fibrinogen to $\alpha_{IIb}\beta_3$. Assays were conducted as described (Lee et al., 1993), with all incubations done at 30 °C, except for the competition step, which was done at the temperatures indicated. Data points are the mean values of three or four independent determinations. The lack of significant temperature dependence to the inhibitory action of the peptide antagonist SKF#106760 (Samanen et al., 1991) and the snake venom disintegrin echistatin (Gan et al., 1988) show that the temperature dependence for RGD23 and RGD34 derives from a thermal effect on these REI mutants and not on the receptor. The wild-type REI V_L exhibits no binding at any temperature (Lee et al., 1993). Other destabilized RGD-containing mutants also exhibit thermal dependent binding (data not shown). **B:** Thermal unfolding curves for REI V_L domains.

loop replacement mutants, have T_m's that are at or below physiological temperature, about 20 °C lower than the WT (Fig. 7B; Table 1). Interestingly, the thermal unfolding transitions of these mutants are mirrored in the thermal sensitivity of their receptor binding. Figure 7A shows that these mutants are good antagonists of fibrinogen binding to the platelet receptor $\alpha_{IIb}\beta_3$ by virtue of their installed RGD sequences (Lee et al., 1993; Helms & Wetzel, 1994), but that binding affinity depends on assay temperature. The transitions in the temperature dependence of the IC_{50} values exactly follow the independently measured unfolding transitions. Because unrelated receptor antagonists do not exhibit temperature-dependent activity (Fig. 7A), the thermal dependence is not due to effects on the receptor.

The sequence RGD37 listed in Figure 2, containing the replacement of wild-type residues 26–28 with the sequence KIGRGDLV, was generated in an REI V_L sequence that contained two stabilizing mutations, Y32H (1.1 kcal/mol) and T39K (1.3 kcal/mol) (Frisch et al., 1994; H.-J. Fritz, pers. comm.). REI V_L with the two stabilizing mutations exhibited a C_m of 2.25 M Gdn-HCl, indicative of a $\Delta\Delta G$ with respect to WT of −3.1 kcal/mol. RGD37 exhibited a C_m of 0.55 M Gdn-HCl, for a $\Delta\Delta G$ with respect to REI(Y32H/T39K) of 7.0 kcal/mol destabilization. Thus, a sequence lacking prolines inserted into CDR1 is actually more destabilizing than is RIPRGDMP in both REI-RGD34 and REI-RGD35. Table 1 shows that another CDR1 insertion lacking prolines, KRARGDDM in REI-RGD32, is also highly destabilizing.

Discussion

We have been developing the immunoglobulin V_L domain REI for use as a "presentation scaffold" (Lee et al., 1993; Helms & Wetzel, 1994)—a small domain expected to hold an installed peptide sequence into a defined conformation and thus help elucidate the receptor-binding conformations of peptides. We chose the integrin receptor-binding motif Arg-Gly-Asp (RGD) for installation and study because of its small size and because of speculations on the importance of conformation in its receptor binding selectivity (Ruoslahti & Pierschbacher, 1987). We chose an immunoglobulin V_L domain as a scaffold, in part, based on the expectation that its CDRs should be particularly adept at accommodating sequence changes without incurring significant losses in folding stability.

The data presented here, however, suggest that sequence replacements in the CDR loops of immunoglobulin domains can be significantly destabilizing to the native structure of the domain. The destabilizing effects are observed for insertions in two separate CDRs and are seen for such changes as a single point mutation, a short replacement that leaves the loop length unchanged, and insertions that increase loop size to lengths equal to or greater than those known to be accommodated at these positions in immunoglobulins. The results have important implications for antibody engineering experiments as well as for the general perception that loops are particularly resilient parts of proteins that are capable of accommodating many sequence changes.

The nature of the nonnative state generated in destabilized REI V_L mutants

A number of experiments were conducted to investigate the degree of unfolding in the fluorescence dequenched state monitored in these studies. These proteins contain no large covalent or noncovalent aggregates, as assessed by nonreducing SDS-PAGE and native gel-permeation chromatography. The proteins contain the expected intramolecular disulfide bond, so that the absence of quenching of Trp in apparently unstable mutants cannot be ascribed to the absence of the disulfide. CD of the destabilized RGD4 in native buffer indicates secondary structure substantially different from the folded wild-type REI V_L, but not statistical coil. Whatever the structure of this nonnative state, it must be substantially reorganized from the native because the normally buried tryptophan is accessible to dynamic quenching by iodide. Further studies on the solution structures of the highly destabilized REI V_L mutants are warranted, especially because these molecules may hold important clues to the

partially unfolded states implicated in light chain amyloidosis and deposition disease (Hurle et al., 1994).

Loop swaps and destabilization

A number of mutagenesis studies have been conducted suggesting that loop sequences have relatively little effect on the thermodynamic stability of globular proteins (reviewed in El Hawrani et al., 1994). Our observation of significant destabilization by loop replacements is not unprecedented, however. Two *Staphylococcus* nuclease mutants constructed by replacing a five-residue β-turn with a β-turn sequence from concanavalin A were found to be destabilized by about 4.5 kcal/mol with a corresponding reduction in T_m of about 20 °C (Eftink et al., 1991). A mutant constructed by replacing the loop region of chymotrypsin inhibitor 2 with a nonapeptide sequence found in an α-helix in subtilisin Carlsberg is also significantly destabilized by about 8 kcal/mol (Osmark et al., 1993). In both of these cases, crystallographic analysis suggests that destabilization may be attributable to the loss of favorable long-range interactions in the WT between loop residues and residues elsewhere in the "host" structure (Hynes et al., 1989; Osmark et al., 1993).

The mechanism(s) by which the loop replacements described here destabilize REI V_L are not obvious. Most of the installed sequences are derived from the long, relatively disordered loops of the platelet antagonist disintegrins (Gould et al., 1990) and thus might be expected to be both relatively flexible and compatible with extended, solvated loop conformations. The RGD (or KGD) sequence itself, which is common to all of the inserted loops, would also be expected to be compatible with a solvated loop environment; in fact, the RGD sequence has been observed in a topologically similar loop to CDR3 in the fibronectin domain of several matrix proteins (Leahy et al., 1992; Main et al., 1992; Dickinson et al., 1994) as well as in the loops of disintegrins. The inserted loops vary considerably in length (leading to net changes in domain length of between 0 and +12 residues) and in the presence or absence of residues that increase (Gly) or decrease (Pro) peptide backbone configurational flexibility. Although many of the destabilizing replacements contain proline residues, two CDR1 mutants lacking prolines, REI-RGD32 (Table 1) and REI-RGD37 (Results), suffer destabilization equal to or greater than that of a mutant containing an insert of equal length and including prolines (REI-RGD34).

Two different CDRs—one between sheets (CDR1) and one within a sheet (CDR3)—were replaced with very similar effects on stability. In CDR3, different insertion points were explored, including points in the loop removed from any possible interaction with the body of the protein. In all cases, however, the destabilization was significant. For example, although the entire 90–97 sequence is within the CDR3 as defined by sequence homology (Fig. 2), it is possible that some replacements of residues 90, 91, and 97 may make altered packing interactions with framework residues, resulting in destabilization. However, replacements that leave residues 90, 91, 96, and 97 unchanged are also observed to destabilize the domain by 5 (RGD12) to 7 (RGD15) kcal/mol (Table 1).

As in the other examples of destabilizing loop replacements described previously (see above), interactions lost from the wild type in the process of replacement may account for some of the observed destabilization. Table 2 lists the hydrogen bonds found in the crystal structure of wild-type REI involving residues 26–29 and 90–97. There are only a few long-range H-bonds in each case. In CDR1, the serine side-chain OH is involved in several H-bonds thqat would be lost if Ser were replaced by another residue; however, REI-RGD35 retains this serine and is just as destabilized as the related REI-RGD34, which lacks this residue. The other long-range H-bonds, at residues 3–26 and 29–68, may be lost if the inserted loop occupies a conformation that brings atoms 26:N and 29:N out of position with respect to the wild-type structure.

Table 2 also lists a number of long-range H-bonds that may be lost in loop-swap mutants involving CDR3. The side chain of Gln 90 plays a very important role in orienting the wild-type loop, by lying in the loop plane and making H-bonds with residues 93, 95, and 97 (Table 2). This is a standard feature of CDR3 loops (Tramontano et al., 1989). This may be important in the destabilization of some of the mutants reported here, because even if Gln 90 is retained (as it is in many of the mutants), loops of different sizes compared with WT may not be able to adopt these H-bonds.

Although it is thus possible that lost H-bond contributions may account for some stability decrease in the mutants, further experiments and structural determination will be required to elucidate the mechanism of destabilization. X-ray crystal structure analysis of REI-RGD34, in progress, shows that the basic immunoglobulin fold is maintained in the folded state of this destabilized mutant (B. Zhao, L.R. Helms, E. Winborne, S. Abdel-Meguid, & R. Wetzel, unpubl. results).

Table 2. *Hydrogen bonds*[a] *in wild-type REI-*V_L

Donor	Acceptor	Molecule A	Molecule B
3:N	26:OG	3.24	–
26:N	3:O	3.27	3.23
26:OG	26:O	3.23	
26:OG	3:O		3.34
29:N	27:O	3.16	
29:N	28:OD2	3.02	2.98
29:N	68:O	3.29	3.14
30:N	28:OD2	2.75	2.48
90:N	97:O	3.31	3.36
90:NE2	1:OD2	3.16	–
90:NE2	93:O	3.14	–
90:NE2	95:O	3.02	–
90:NE2	97:OG1	3.21	–
91:N	32:O	3.29	3.22
91:N	90:OE1	3.32	–
92:N	90:OE1	2.88	–
93:OG	93:O	3.18	3.02
95:N	1:OD2	–	3.16
97:N	95:O	3.10	–
97:OG1	1:OD1	2.94	–
97:OG1	2:O	2.85	2.71
97:OG1	97:O	3.16	3.12
97:OG1	90:OE1	–	3.28

[a] Hydrogen bonds of acceptable bond lengths and geometries were identified in the coordinate set 1REI in the Brookhaven database (Bernstein et al., 1977; Abola et al., 1987) using Insight II™ (Biosym Technologies, San Diego, California). The independent data for Molecule A and Molecule B reflect the two independent monomers in the single dimer of the unit cell (Epp et al., 1974).

An important implication of these results is that there may be significant limitations on the allowed sequences and lengths of protein loops, including antibody hypervariable loops.

Thermal dependence of binding activity

The temperature dependence of receptor binding by these mutants confirms the ability of appropriately chosen scaffolds to control the conformation of an installed bioactive ligand (Wetzel, 1991). At the same time, the results underscore the importance of considering domain stability in the choice of a domain for a presentation scaffold. If the destabilizations of 5–7 kcal/mol found here and elsewhere for loop swaps prove to be somewhat general, it is clearly advantageous to choose a domain with a free energy of folding of significantly more than 7 kcal/mol for phage display and other scaffold experiments.

Stability of the immunoglobulin fold

Although immunoglobulin molecules are known to be highly stable proteins, relatively little is known about the properties of the fundamental immunoglobulin fold. Studies on wild-type V_L domains released by limited proteolysis of Bence-Jones proteins or expressed by recombinant DNA methods show that these immunoglobulin domains are about as stable as expected for proteins of about 100 amino acids, with ΔG^0_{stab} values around 3–9 kcal/mol (Ahmad & Bigelow, 1986; Tsunenaga et al., 1987; Hurle et al., 1994; Steipe et al., 1994; Stevens et al., 1995). Wild-type REI V_L falls within this range, with a ΔG^0_{stab} of about 6.5 kcal/mol (Hurle et al., 1994; Kolmar et al., 1994). As with other globular proteins, the folding stability of the V_L domain is sensitive to point mutations. Previously, we showed that single point mutations in framework residues of REI V_L can destabilize the domain by as much as 3 kcal/mol when transferred into REI V_L (Hurle et al., 1994). Similarly, Steipe et al. (1994) identified nonconserved residues in the framework sequences of the V_L domain of the antibody McPC603 and showed that conversion of these residues to the most common residues at these positions provided enhanced stability by up to 1.5 kcal/mol. Stabilizing point mutations for REI V_L have also been described (Frisch et al., 1994). The role of loop residues on immunoglobulin domain stability has not been investigated previously.

The work described here suggests that many loop sequences are not compatible with the variable domain framework, and thus that evolution of the natural repertoire of CDR sequences has occurred in the context of significant selective pressure against destabilizing sequences in the CDR positions. This is consistent with the observation of conserved residues (Kabat et al., 1991) and canonical structures (Chothia et al., 1989) in antibody CDR loops. Although canonical CDR structures are usually discussed in terms of the role of CDRs in antigen binding, our results suggest an additional important role of CDR sequence and structure: their contribution to domain stability. Given this possibility, it will be interesting to see the frequency with which new "canonical" CDR structures arise in antibodies generated through the emerging use of CDR sequence randomization methods (Barbas et al., 1993; Fisch et al., 1994).

V_L domains that possess poor stability might still be capable of forming functional antibodies, because additional stabilization energy is expected from the interaction between the folded V_H and V_L domains (Pantoliano et al., 1991) and would thus be expected to help rescue a V_L of impaired stability.

It remains to be seen whether viable antibodies containing poorly stable V_L domains can be produced; experiments are in progress to address this question. Even if it turns out that functional antibodies containing destabilized variable domains can be produced, they may nonetheless possess reduced net stabilities, which in turn might influence their temperature dependence of binding—as shown here for the $\alpha_{IIb}\beta_3$ interaction with REI V_L—as well as other properties such as immunogenicity and clearance. Furthermore, domain stability within the light chain itself has been suggested to play an important role in determining the metabolic fate of circulating light chains in amyloidosis (Hurle et al., 1994). Domain stability may also play an important role in immunoglobulin biosynthesis.

The unstable proteins described here were isolated from inclusion bodies (IBs) formed in the *E. coli* periplasm. Recently, Knappik and Plueckthun (1995) described amino acid replacements in the V_H domain of McPC603 that influence IB formation in *E. coli* expression of antibody fragments containing both V_L and V_H domains. Consistent with previous studies on the role of mutations in IB formation (Mitraki et al., 1993; Wetzel & Chrunyk, 1994), the authors described results suggesting that their mutations direct material into IBs by influencing folding rates rather than thermodynamic stability. Results of expression of REI V_L containing a variety of stabilizing and destabilizing mutations, both in framework regions (Hurle et al., 1994) and in CDRs (described here), suggest that, in contrast to these other systems, thermodynamic stability considerations may be sufficient to account for IB formation in the expression of the V_L domain. A formal analysis of REI V_L expression data from this point of view will be reported elsewhere (W. Chan, R. Wetzel, L.R. Helms, S. Ngola, & B. Maleeff, unpubl. results).

Materials and methods

Materials

Fibrinogen receptor $\alpha_{IIb}\beta_3$ isolated from human platelets was provided by Kyung Johanson (SmithKline). Cyclic RGD antagonist SKF#106760 was provided by James Samanen (SmithKline). *E. coli* MM294 was used for transformations and expression of REI V_L.

Production of REI V_L variants

Mutants were constructed from the WT coding sequence (Palm & Hilschmann, 1973) using cassette mutagenesis (Wells et al., 1985) and sequences confirmed by dideoxy nucleotide sequencing using Sequenase (USB) and established procedures (Sanger et al., 1977). All other recombinant DNA procedures were as described by Sambrook et al. (1989).

Proteins were expressed in *E. coli* under control of the *tac* promoter with a *pel B* leader sequence directing export to the periplasm of the cell. Cells were grown at 37 °C. Wild-type REI V_L was expressed solubly in the periplasm but most of the mutants accumulated in periplasmic IBs, presumably because of their decreased stabilities (W. Chan, L.R. Helms, & R. Wetzel, unpubl.). Despite their low stabilities, these proteins accumulated stably in the cell, presumably because IB formation protects them from proteolysis (Shortle & Meeker, 1989). These IBs contain protein

that is correctly processed (W. Chan, L.R. Helms, & R. Wetzel, unpubl.). These were solubilized in 8 M Gdn-HCl, then dialyzed into 1 M urea, 0.1% trifluoroacetic acid, and centrifuged to remove aggregated protein. Wild-type and solubilized mutants were all subjected to a final purification step of reverse-phase HPLC and analyzed for purity by HPLC and SDS-PAGE.

Denaturant and thermal unfolding studies

The integrity of the REI V_L fold was monitored by the fluorescence of the conserved immunoglobulin domain tryptophan, which is highly quenched in the native state due to its close proximity to the disulfide bond. Fluorescence was determined in a Perkin-Elmer MPF-66 spectrofluorometer with excitation at 295 nm and emission at 350 nm. The extent to which a mutant REI V_L is unfolded in native buffer at room temperature was initially estimated by determining the fluorescence of a 1 μM (monomer) sample in 10 mM sodium phosphate, pH 7.4 in the presence and absence of 4 M Gdn-HCl. The ratio of fluorescence in native buffer versus denaturant is low for a variant that is folded in native buffer (like the wild type, ratio = 0.11; see Table 1) and high for a variant that is substantially unfolded in native buffer (like RGD14, ratio = 0.84).

The degree of stability was confirmed and quantified by using fluorescence to determine the full Gdn-HCl denaturation curves. Samples of approximately 10 μg/mL (~1 μM, monomer) were incubated overnight at room temperature at various Gdn-HCl concentrations in 10 mM sodium phosphate, pH 7.4, and fluorescence was determined. Data were analyzed by nonlinear least-squares fitting to a two-state model using either NLIN (SAS Institute, Cary, North Carolina) or IGOR Pro (WaveMetrics) using the simultaneous baseline fitting method of Santoro and Bolen (1988) to generate fitted curves and values for transition midpoints (C_m's), transition slopes (A values), and free energies of unfolding (ΔG values). $\Delta\Delta G$ values were calculated from the C_m and A values with the WT curve as reference point, using the formula $\Delta\Delta G = \Delta G^{mut} - \Delta G^{WT} = A^{WT} * C_m^{mut} - A^{WT} * C_m^{WT}$, where $A^{WT} = -4.4$ kcal/mol/M (Gdn-HCl), determined experimentally.

Thermal stability was determined with samples of about 2 μM in REI V_L monomer in 10 mM sodium phosphate, pH 7.4, by monitoring fluorescence as a function of temperature. Temperature was controlled using a jacketed cell holder and a circulating water bath, with a temperature ramp rate of about 0.25 °C/min. Cell temperature was monitored using a thermocouple. As expected, fluorescence changed gradually with temperature until the thermal transition was reached, at which point fluorescence sharply increased. The slopes of the fluorescence variation with temperature outside the cooperative unfolding transition were determined and used to generate thermal Fap plots and T_m values.

Integrin receptor antagonist activity

The inhibition of the binding of biotinylated fibrinogen to the integrin receptor $\alpha_{IIb}\beta_3$ was determined by a microtiter assay as described previously (Lee et al., 1993), except the competition step was performed at the temperature indicated. The IC_{50} values were determined from a four-parameter fit using the software Softmax (Molecular Devices, Inc.), and the concentration of the inhibitor at 50% binding was recorded.

Acknowledgments

We thank Mark R. Hurle for helpful suggestions and for critical reading of the manuscript.

References

Abola E, Bernstein FC, Bryant SH, Koetzle TF, Weng J. 1987. Protein Data Bank. In: Allen FH, Bergerhoff G, Sievers R, eds. *Crystallographic databases – Information content, software systems, scientific applications*. Bonn/Cambridge/Chester: Data Commission of the International Union of Crystallography. pp 107–132.

Ahmad F, Bigelow CC. 1986. Estimation of the stability of globular proteins. *Biopolymers 25*:1623–1634.

Barbas CF III, Languino LR, Smith JW. 1993. High-affinity self-reactive human antibodies by design and selection: Targeting the integrin ligand binding site. *Proc Natl Acad Sci USA 90*:10003–10007.

Bernstein FC, Koetzle TF, Williams GJ, Meyer EJ, Brice MD, Rodgers JR, Kennard O, Shimanouchi T, Tasumi M. 1977. The Protein Data Bank: A computer-based archival file for macromolecular structures. *J Mol Biol 112*:535–542.

Brahms S, Brahms J. 1980. Determination of protein secondary structure in solution by vacuum ultraviolet circular dichroism. *J Mol Biol 138*: 149–178.

Branden C, Tooze J. 1991. *Introduction to protein structure*. New York: Garland.

Chothia C, Lesk AM, Tramontano A, Levitt M, Smith-Gill SJ, Air G, Sheriff S, Padlan EA, Davies D, Tulip WR, Colman PM, Spinelli S, Alzari PM, Poljak RJ. 1989. Conformations of immunoglobulin hypervariable regions. *Nature 342*:877–883.

Dennis MS, Henzel WJ, Pitti RM, Lipari MT, Napier MA, Deisher TA, Bunting S, Lazarus RA. 1989. Platelet glycoprotein iib-iiia protein antagonists from snake venoms: Evidence for a family of platelet-aggregation inhibitors. *Proc Natl Acad Sci USA 87*:2471–2475.

Dickinson CD, Veerapandian B, Dai XP, Hamlin RC, Xuong NH, Ruoslahti E, Ely KR. 1994. Crystal structure of the tenth type III cell adhesion module of human fibronectin. *J Mol Biol 230*:1079–1092.

Eftink MR, Ghiron CA. 1981. Fluorescence quenching studies with proteins [Review]. *Anal Biochem 114*:199–227.

Eftink MR, Ghiron CA, Kautz RA, Fox RO. 1991. Fluorescence and conformational stability studies of *Staphylococcus* nuclease and its mutants, including the less stable nuclease-concanavalin A hybrids. *Biochemistry 30*:1193–1199.

El Hawrani AS, Moreton KM, Sessions RB, Clarke AR, Holbrook JJ. 1994. Engineering surface loops of proteins – A preferred strategy for obtaining new enzyme function. *Trends Biotechnol 12*:207–211.

Epp O, Colman P, Fehlhammer H, Bode W, Schiffer M, Huber R, Palm W. 1974. Crystal and molecular structure of a dimer composed of the variable portions of the Bence-Jones protein REI. *Eur J Biochem 45*:513–524.

Fisch I, Griffiths A, Winter G. 1994. Generation of large phage antibody repertoires using in vivo recombination. *J Cell Biochem 18D*:T201.

Frisch C, Kolmar H, Fritz HJ. 1994. A soluble immunoglobulin variable domain without a disulfide bridge: Construction, accumulation in the cytoplasm of *E. coli*, purification and physicochemical characterization. *Biol Chem Hoppe-Seyler 375*:353–356.

Gan ZR, Gould RJ, Jacobs JW, Friedman PA, Polokoff MA. 1988. Echistatin. A potent platelet aggregation inhibitor from the venom of the viper, *Echis carinatus*. *J Biol Chem 263*:19827–19832.

Gould RJ, Polokoff MA, Friedman PA, Huang TF, Holt JC, Cook JJ, Niewiarowski S. 1990. Disintegrins: A family of integrin inhibitory proteins from viper venoms. *Proc Soc Exp Biol Med 195*:168–171.

Helms LR, Wetzel R. 1994. Proteolytic excision and in situ cyclization of a bioactive loop from an REI-VL presentation scaffold. *Protein Sci 3*:1108–1113.

Hurle MR, Helms LR, Li L, Chan W, Wetzel R. 1994. A role for destabilizing amino acid replacements in light chain amyloidosis. *Proc Natl Acad Sci USA 91*:5446–5450.

Hynes TR, Kautz RA, Goodman MA, Gill JF, Fox RO. 1989. Transfer of a beta-turn structure to a new protein context. *Nature 339*:73–76.

Jones PT, Dear PH, Foote J, Neuberger MS, Winter G. 1986. Replacing the complementarity-determining regions in a human antibody with those from a mouse. *Nature 321*:522–525.

Kabat EA, Wu TT, Perry HM, Gottesman KS, Foeller C. 1991. *Sequences of proteins of immunological interest*. Washington, D.C.: U.S. Department of Health and Human Services, Public Health Service, National Institutes of Health.

Knappik A, Plueckthun A. 1995. Engineered turns of a recombinant antibody improve its in vivo folding. *Protein Eng 8*:81–89.

Kolmar H, Frisch C, Kleeman G, Goetze K, Stevens FJ, Fritz HJ. 1994. Dimerization of Bence–Jones proteins: Linking the rate of transcription from an *Escherichia coli* promoter to the association constant of REIv. *Biol Chem Hoppe-Seyler 375*:61–70.

Kraulis PJ. 1991. MOLSCRIPT: A program to produce both detailed and schematic plots of protein structures. *J Appl Crystallogr 24*:946–950.

Laemmli UK. 1970. Cleavage of structural proteins during the assembly of the head of bacteriophage T4. *Nature 227*:680–685.

Leahy DJ, Hendrickson WA, Aukhil I, Erickson HP. 1992. Structure of a fibronectin type III domain from tenascin phased by MAD analysis of the selenomethionyl protein. *Science 258*:987–991.

Lee G, Chan W, Hurle MR, DesJarlais RL, Watson F, Sathe GM, Wetzel R. 1993. Strong inhibition of fibrinogen binding to platelet receptor αIIb-βIII by RGD sequences installed into a presentation scaffold. *Protein Eng 6*:745–754.

Main AL, Harvey TS, Baron M, Boyd J, Campbell ID. 1992. The three-dimensional structure of the tenth type III module of fibronectin: An insight into RGD-mediated interactions. *Cell 71*:671–678.

Matthews BW. 1993. Structural and genetic analysis of protein stability. *Annu Rev Biochem 62*:139–160.

Mitraki A, Danner M, King J, Seckler R. 1993. Temperature-sensitive mutations and second-site suppressor substitutions affect folding of the P22 tailspike protein in vitro. *J Biol Chem 268*:20071–20075.

Osmark P, Sorenson P, Poulson FM. 1993. Context dependence of protein secondary structure formation: The three-dimensional structure and stability of a hybrid between chymotrypsin inhibitor 2 and helix E from subtilisin Carlsberg. *Biochemistry 32*:11007–11014.

Palm W, Hilschmann N. 1973. Die Primaerstruktur einer kristallinen monoklonalen Immunglobulin-L-Kette vom k-Typ, Subgruppe I (Bence–Jones-Protein Rei.): Ein Beitrag zur Aufklaerung der dreidimensionalen Struktur der Immunglobuline. *Hoppe-Seyler's Z Physiol Chem 354*: 1651–1654.

Pantoliano MW, Bird RE, Johnson S, Asel ED, Dodd SW, Wood JF, Hardman KD. 1991. Conformational stability, folding, and ligand-binding affinity of single-chain Fv immunoglobulin fragments expressed in *Escherichia coli*. *Biochemistry 30*:10117–10125.

Pfeil W. 1981. The problem of the stability of globular proteins. *Mol Cell Biochem 40*:3–28.

Pollitt S, Zalkin H. 1983. Role of primary structure and disulfide bond formation in β-lactamase secretion. *J Bacteriol 153*:27–32.

Riechmann L, Clark M, Waldmann H, Winter G. 1988. Reshaping human antibodies for therapy. *Nature 332*:323–327.

Ruoslahti E, Pierschbacher MD. 1987. New perspectives in cell adhesion; RGD and integrins. *Science 238*:491–497.

Samanen J, Ali FE, Romoff T, Calvo R, Sorenson E, Vasko J, Storer B, Berry D, Bennett D, Strohasacker M, Powers D, Stadel J, Nichols A. 1991. Development of a small RGD peptide fibrinogen receptor antagonist with potent antiaggregatory activity *in vitro*. *J Med Chem 34*:3114.

Sambrook J, Fritsch EF, Maniatis T. 1989. *Molecular cloning: A laboratory manual*. Cold Spring Harbor, New York: Cold Spring Harbor Laboratory Press.

Sanger F, Nicklen S, Coulson AR. 1977. DNA sequencing with chain-terminating inhibitors. *Proc Natl Acad Sci USA 74*:5463–5468.

Santoro MM, Bolen DW. 1988. Unfolding free energy changes determined by the linear extrapolation method. I. Unfolding of phenylmethanesulfonyl α-chymotrypsin using different denaturants. *Biochemistry 27*: 8063–8074.

Scarborough RM, Rose JW, Hsu MA, Phillips DR, Fried VA, Campbell AM, Nannizzi L, Charo IF. 1991. Barbourin: A gpIIb-IIIa-specific integrin antagonist from the venom of *Sistrurus m. barbouri*. *J Biol Chem 266*: 9359–9362.

Shortle D. 1992. Mutational studies of protein structures and their stabilities. *Q Rev Biophys 25*:205–250.

Shortle D, Meeker AK. 1989. Residual structure in large fragments of staphylococcal nuclease: Effects of amino acid substitutions. *Biochemistry 28*:936–944.

Steipe B, Schiller B, Pluckthun A, Steinbacher S. 1994. Sequence statistics reliably predict stabilizing mutations in a protein domain. *J Mol Biol 240*:188–192.

Stevens PW, Raffen R, Hanson DK, Deng YL, Berrios-Hammond M, Westholm FA, Murphy C, Eulitz M, Wetzel R, Solomon A, Schiffer M, Stevens FJ. 1995. Recombinant immunoglobulin variable domains generated from synthetic genes provide a system for in vitro characterization of light chain amyloid proteins. *Protein Sci 4*:421–432.

Tramontano A, Chothia C, Lesk AM. 1989. Structural determinants of the conformations of medium-sized loops in proteins. *Proteins Struct Funct Genet 6*:382–394.

Tsunenaga M, Goto Y, Kawata Y, Hamaguchi K. 1987. Unfolding and refolding of a type kappa immunoglobulin light chain and its variable and constant fragments. *Biochemistry 26*:6044–6051.

Wells JA, Vasser M, Powers DB. 1985. Cassette mutagenesis: An efficient method for generation of multiple mutations at defined sites. *Gene 34*: 315–323.

Wetzel R. 1988. Commentary: Structure, function, nomenclature. *Protein Eng 2*:1–3.

Wetzel R. 1991. Commentary: Learning from the immune system; laboratory methods for creating and refining molecular diversity in polypeptides. *Protein Eng 4*:371–374.

Wetzel R, Chrunyk BA. 1994. Inclusion body formation by interleukin-1β depends on the thermal sensitivity of a folding intermediate. *FEBS Lett 350*:245–248.

Industria y Comercio SUPERINTENDENCIA

El futuro es de todos Gobierno de Colombia

BANDEJA DE ENTRADA >

NC2021/0003802 - NC Modificación a las reivindicaciones - Solicitado en Patente NC2018/0013689

Haga clic para expandir / contraer

Datos de la solicitud

Número de solicitud	NC2021/0003802
Referencia	184553
Fecha de radicación	25 mar. 2021
Estado	Presentada

Contacto

Apoderado

Número de identificación	Nombre(s)	Apellido(s)	Dirección (es)
79339809	JUAN CARLOS	CUESTA QUINTERO	Dirección Física : CLL 72 # 10 -07 OFC 603 BOGOTÁ D.C. (CO)

Solicitante

Número de identificación	Nombre(s)	Apellido(s)	Dirección (es)
		CELLTRION INC.	Dirección Física : 23, Academy-ro Yeonsu-gu Incheon 22014 22014 (KR)

Contacto de la solicitud

Número de identificación	Nombre	Dirección	Ciudad	Código postal	País	Tipo de dirección
79339809	JUAN CARLOS CUESTA QUINTERO	CLL 72 # 10 -07 OFC 603	BOGOTÁ		CO	Dirección Física

1 Solicitud (es)

Número de solicitud	Tipo de solicitud	Tipo de enlace	Título/Denominación	Fecha de radicación	Estado(s)	Titular
NC2018/0013689	Patente PCT	Vinculado	FORMULACIÓN FARMACÉUTICA LÍQUIDA ESTABLE	18 dic. 2018	Requerimiento de Examen de Fondo	CELLTRION INC.

Cra 13 No. 27-00 pisos 1, 3, 4, 5, 6, 7 y 10 PBX: (571)5870000 . Call center: (571)5920400 Línea gratuita nacional 018000-910165
www.sic.gov.co . e-mail: contactenos@sic.gov.co . Bogotá D.C. - Colombia.

Política de privacidad | Política editorial | Créditos | Webmaster: contactenos@sic.gov.co ::: Todos los derechos reservados 2008 - 2021

Cerrar

SUPERINTENDENCIA DE INDUSTRIA Y COMERCIO

NIT: 800.176.089-2

COMPROBANTE DE RECAUDO SISTEMA SIPI

Radicado: NC2021/0003802
Recibo: 21-31887
Fecha: 25/03/2021

JUAN CARLOS CUESTA QUINTERO
CC: 79.339.809
Pago PSE No: 517254
CUS: 933978020

NC Modificación a las reivindicaciones
Request on Patente PCT NC2018/0013689

Detalle del pago

Id.	Rentístico	Concepto y Servicio	Cant.	Val. Unit.	Subtotal
1	50005-01-03	Modificaciones / Correcciones al registro Patente PCT (DESCUENTO INTERNET)	1	$ 171,500	$ 171,500
		TOTAL			$ 171,500

Sede Centro: Carrera 13 No.27-00 Pisos 3,4,5 y 10 Bogotá D.C. - Colombia
Web: www.sic.gov.co e-mail:contactenos@sic.gov.co Conmutador:(571)5870000 Contact Center: (571)5920400